

H.-G. RAMMING and Z. KOWALIK



Numerical Modelling of Marine Hydrodynamics

Applications to Dynamic Physical Processes



ELSEVIER OCEANOGRAPHY SERIES

***Numerical Modelling of Marine
Hydrodynamics***
Applications to Dynamic Physical Processes

FURTHER TITLES IN THIS SERIES

- 1 J.L. MERO
THE MINERAL RESOURCES OF THE SEA
- 2 L.M. FOMIN
THE DYNAMIC METHOD IN OCEANOGRAPHY
- 3 E.J.F. WOOD
MICROBIOLOGY OF OCEANS AND ESTUARIES
- 4 G. NEUMANN
OCEAN CURRENTS
- 5 N.G. JERLOV
OPTICAL OCEANOGRAPHY
- 6 V. VACQUIER
GEOMAGNETISM IN MARINE GEOLOGY
- 7 W.J. WALLACE
THE DEVELOPMENT OF THE CHLORINITY/SALINITY CONCEPT
IN OCEANOGRAPHY
- 8 E. LISITZIN
SEA-LEVEL CHANGES
- 9 R.H. PARKER
THE STUDY OF BENTHIC COMMUNITIES
- 10 J.C.J. NIHOUL (Editor)
MODELLING OF MARINE SYSTEMS
- 11 O.I. MAMAYEV
TEMPERATURE-SALINITY ANALYSIS OF WORLD OCEAN WATERS
- 12 E.J. FERGUSON WOOD and R.E. JOHANNES
TROPICAL MARINE POLLUTION
- 13 E. STEEMANN NIELSEN
MARINE PHOTOSYNTHESIS
- 14 N.G. JERLOV
MARINE OPTICS
- 15 G.P. GLASBY
MARINE MANGANESE DEPOSITS
- 16 V.M. KAMENKOVICH
FUNDAMENTALS OF OCEAN DYNAMICS
- 17 R.A. GEYER
SUBMERSIBLES AND THEIR USE IN OCEANOGRAPHY AND OCEAN
ENGINEERING
- 18 J.W. CARUTHERS
FUNDAMENTALS OF MARINE ACOUSTICS
- 19 J.C.J. NIHOUL (Editor)
BOTTOM TURBULENCE
- 20 P.H. LEBLOND and L.A. MYSAK
WAVES IN THE OCEAN
- 21 C.C. VON DER BORCH (Editor)
SYNTHESIS OF DEEP-SEA DRILLING RESULTS IN THE INDIAN OCEAN
- 22 P. DEHLINGER
MARINE GRAVITY
- 23 J.C.J. NIHOUL
HYDRODYNAMICS OF ESTUARIES AND FJORDS
- 24 F.T. BANNER, M.B. COLLINS and K.S. MASSIE (Editors)
THE NORTH-WEST EUROPEAN SHELF SEAS: THE SEA BED AND THE
SEA IN MOTION
- 25 J.C.J. NIHOUL (Editor)
MARINE HYDRODYNAMICS — FORECASTING

Elsevier Oceanography Series, 26

Numerical Modelling of Marine Hydrodynamics

Applications to Dynamic Physical Processes

HANS-GERHARD RAMMING

*Institute of Oceanography
University of Hamburg
Hamburg, Germany (GFR)*

and

ZYGMUNT KOWALIK

*Institute of Meteorology
Gdynia, Poland*



ELSEVIER SCIENTIFIC PUBLISHING COMPANY
Amsterdam — Oxford — New York 1980

ELSEVIER SCIENTIFIC PUBLISHING COMPANY
335 Jan van Galenstraat
P.O. Box 211, 1000 AE Amsterdam, The Netherlands

Distributors for the United States and Canada:

ELSEVIER/NORTH-HOLLAND INC.
52, Vanderbilt Avenue
New York, N.Y. 10017

Library of Congress Cataloging in Publication Data

Ramming, Hans-Gerhard.

Numerical modelling of marine hydrodynamics
applications to dynamic physical processes.

(Elsevier oceanography series ; 26)

Bibliography: p.

Includes index.

1. Oceanography--Mathematical models.

2. Hydrodynamics--Mathematical models. I. Kowalik,

Zygmunt, joint author. II. Title.

GC203.R25 551.4'7'00184

79-24144

ISBN 0-444-41849-0

ISBN 0-444-41849-0 (Vol. 26)

ISBN 0-444-41623-4 (series)

© Elsevier Scientific Publishing Company, 1980

All rights reserved. No part of this publication may be reproduced, stored in a retrieval system or transmitted in any form or by any means, electronic, mechanical, photocopying, recording, or otherwise, without the prior written permission of the publisher, Elsevier Scientific Publishing Company, P.O. Box 330, 1000 AH Amsterdam, The Netherlands

Printed in The Netherlands

PREFACE

By invitation of the Polish Academy of Science - Institute of Hydroengineering - Dr. Hans-Gerhard Ramming, lecturer at the Institute of Oceanography of the University of Hamburg, had the opportunity to hold a twenty-hour seminar on 'Numerical Models and Their Applications in Shallow Water Areas' in April 1977 in Gdansk.

The scripts presented on that occasion, some theoretical additions and extensions were the basis of this work put forward by the authors.

The authors take pleasure in acknowledging the help and encouragement of many people who took part in the preparation of this book.

Special thanks are due to our friend Dr. M. Laska who initiated the idea of this book and whose help in the preparation of the English language version is greatly appreciated.

Great efforts were spent on the technical side. Here thanks are due in particular to Mrs. Agnes O'Kane, Dr. Philip O'Kane and Mr. Kurt Duwe for the final elaboration of the English language version, Mrs. Regina Hewer who typed the entire manuscript in a most efficient way looking for mathematical mistakes, and two Polish draughtswomen not known by name.

This Page Intentionally Left Blank

CONTENTS

Preface	V
Introduction	XI
I General Equations	1
1. The hydrodynamic differential equations of motion and continuity	2
2. The mass transport and free surface equations	9
3. One-dimensional motion	13
4. Frictional forces at the surface and the bottom	16
II Steady motion - numerical methods	23
1. Numerical approximation of steady phenomena	23
2. Convergence and choice of grid step	29
3. Boundary conditions	31
4. Some general properties of the differential operators	33
5. Numerical methods of solution of partial differential equations of steady state	35
6. Simple iteration method	37
7. Gauss-Seidel method	38
8. Line inversion method	39
9. Application of line inversion in the alternating-direction method	42
III Steady motion - oceanographical examples	45
1. Motion in channels - analytical solution	45
2. Wind-driven currents in a shallow sea	50
3. Ekman equations	51
4. The mass transport and stream function equations	52
5. Solution of the Dirichlet problem for elliptical equations in the multiply-connected domain	55
6. Determination of eddy viscosity	56
7. Some simplified models	57
8. Steady wind-driven circulation in the Baltic Sea	68
9. The influence of density stratification on the vertical distribution of current	78
10. The wind- and density-driven currents	83
11. Different methods to estimate the exchange of momentum in the Ekman layer	87

VIII

12. Dimensional analysis	89
13. Constant eddy viscosity	92
14. A statistical method based on the equation of turbulent energy b^2 and the scale length l	96
15. Shallow, horizontally unbounded sea	98
16. Two-layer model	101
17. A statistical method based on the equations of energy and dissipation	105
18. Influence of the density stratification	109
IV Unsteady motion - numerical methods	112
1. Principal equations and their difference form	113
2. Stability of the numerical solution	119
3. Stability of a system of equations	122
4. wave deformation	127
5. Physical and numerical solutions	130
6. Nonlinear equations	132
7. Numerical filtering in time and space	137
8. Boundary and initial conditions	144
9. The explicit numerical scheme	148
10. An implicit numerical scheme	154
11. Computational example to compare explicit and implicit properties	161
12. A numerical system with mixed explicit-implicit properties	161
13. Steady state processes from a point of view of numerical methods used for solving an unsteady problem	165
V Numerical treatment of tides	169
1. Introduction	169
2. A system of equations for the study of the tides	170
3. The boundary-value problem	175
4. The hydrodynamic-numerical method	178
5. Calculating the M_2 -tide in the Arctic Ocean - an example	182
6. The results of the computation of the tides in the Arctic Ocean	185
7. The energy balance equation	194
8. Numerical models to study the vertical distribution of velocity in the tide waves	197
9. A treatment of the boundary layer in the tide wave	201

VI	Models of shallow coastal areas and tidal rivers	206
	1. Some remarks on one-dimensional models	207
	2. River models	210
	3. A one-dimensional treatment of river flow: the multi-channel system	214
	4. A two-dimensional model of the River Elbe covering the area between Seemannshöft and Cuxhaven	221
	5. Approximation of the coast-line	223
	6. Modelling the flooding and uncovering of tidal flats	226
	7. A special treatment of the bottom friction in extremely shallow waters	232
	8. Residual currents	241
	9. The application of the grid refinement and the irregular grid	243
	10. Some results and conclusions derived from the nested model of the North Sea	249
	11. Some examples of the application of hydrodynamic-numerical models on coastal engineering	250
VII	The application of the transport equations	287
	1. Basic concepts	287
	2. Two-dimensional turbulent diffusion	291
	3. Numerical methods of solving the transport equation	297
	4. The application of the transport equation in a multi-channel model	302
	5. A comparison between an analytical and a numerical solution	308
	6. The turbidity zone of the River Elbe	313
	7. The transport of pollutants	318
VIII	Periodic motion	322
	1. Introduction	322
	2. The general properties of eigenvalues	326
	3. Eigenvalues in two-dimensional oscillations: The construction of a symmetrical matrix	328
	4. Galerkin's method and its application to the problem of eigenvalues and eigenvectors	331
	5. A method of resonance iterations	340
	6. A method of computing the longest period of free oscillation	345
	7. A method of computing a set of eigenperiods	347
	8. The influence of friction and small variations of frequency	351
	9. Numerical schemes describing frictionless motion	353
	List of figures	360
	Subject Index	364

This Page Intentionally Left Blank

INTRODUCTION

Knowledge of the motion of the ocean, adjacent and marginal seas and of estuarial waters has always been of great importance for sea-going people and for coastal zone dwellers.

Many attempts have been made to understand dynamic processes, such as tides, storm surges and ocean currents. Such considerations have to be based upon the results of observations and measurements.

Starting from the theory of hydrodynamics, the problem is to develop numerical methods which can be used to reproduce the observed or measured data. The numerical results of such a reproduction - or hindcasting - have to be compared with the results of measurements. If a close correlation demonstrates the validity of the theory, this hydrodynamic-numerical method may finally be used to forecast the dynamic processes of the sea, thus finding its practical application.

Frequently, the purpose of coastal engineering is to influence or to control the actual conditions of the motion in the sea. Here, the hydrodynamic theory delivers the necessary basic information for technical planning and helps to find the most effective solution to the problem.

Investigations have been carried out in many countries in order to solve the problems mentioned above. The main purpose of these investigations has been the development of methods which make possible a numerical simulation or physical reproduction of measured sea-levels and ocean currents and other physical phenomena of oceans and seas. In the following chapters, the progress of these investigations during the past years will be described.

Generally speaking three kinds of motion in the sea will be considered:

1. Steady motion caused by wind action or density gradients
2. Unsteady motion due to wind and tide-generating forces which vary in time and space
3. Stationary motion where the seiche-like phenomena will be described.

In addition the transport processes are analyzed and characterized in one chapter, since they play an important role in sea engineering. All these types of motion have been treated numerically. Therefore the numerical methods are discussed and presented in sufficient detail for the aims of this book. Of course it is not the purpose of this book to describe all the numerical problems but rather to give prac-

XII

tical methods and to discuss the salient and up-to-date aspects of the numerical approach.

The solved problems will start usually with the meso-scale motion in the adjacent sea (mainly the North Sea and the Baltic). After this problems of motion with smaller scales such as river inflows and shallow-water-phenomena will be considered.

It should be noted that, according to recent results, especially in shallow water areas, there is a strong nonlinear interaction between different types of motion, which can have such an influence that a separate treatment by simple superposition is not allowed anymore. The accuracy of the reproduction of the motion in the sea by means of the hydrodynamic theories can only be tested if measured sea-levels and current velocities are given for a comparison. To a certain degree the tides comply with this requirement. The harmonic tidal constituents for coastal stations and measurements of tidal currents in some places of the open sea are available. Sea-level data for storm surges have been recorded in the North Sea and in the Baltic which are suitable for a comparison with the results of the hydrodynamic-numerical method.

Measurements of currents, and especially those caused by density gradients, are not available in sufficient quantities to compare them with the results of the theory. For this type of motion only qualitative comparisons seem to be possible at present.

Chapter I GENERAL EQUATIONS

The system of hydrodynamic differential equations consists of four equations in four unknown functions, namely the three components of velocity and the pressure. These are functions of the three space-variables and of time. In its general form the system of equations is nonlinear. Uniquely determined solutions of this system can only exist if, in addition, boundary and initial values are specified.

Closed analytical solutions of this system of hydrodynamic differential equations in its general form have not yet been derived. Analytical solutions have only been obtained in special cases where extensive simplification and linearization of the equations has been introduced. When applying these hydrodynamic differential equations to problems of physical oceanography, one meets the following difficulties:

The geometry of the depth distribution and the coastline of the sea under consideration are part of the system of differential equations. Since the topography is in general very complicated, every effort should be made to represent these parameters analytically. For this reason, rectangles or channels of constant, linear or similarly simple depth distribution have always been used for the mathematical treatment of the problem.

Beside these simplifications of the geometry, the following assumptions have been made to bring the general system of hydrodynamic equations into a more manageable form:

- a) By vertical integration of the equations from the bottom to the surface of the sea, the number of independent variables and unknown functions can both be reduced by one. Consequently there remain the two horizontal components of mass transport or average velocity and the sea-level. The knowledge of these functions is sufficient to answer many practical questions.
- b) It is supposed that the velocity and the sea-level do not depend on time, i.e. the motion is steady. This supposition, of course, means a very strong restriction, but it will help us to investigate the three-dimensional distribution of current in the sea.
- c) When investigating oscillating processes, time can be eliminated from the equations by introducing an imaginary time factor. So the number of independent variables is reduced by one. This procedure is often applied in investigations of tides and other waves.

d) One-dimensional channels are investigated instead of two-dimensional areas.

All these simplifications restrict, of course, the generality of the solutions obtained. As is known today, the depth distribution and the coastline essentially influence the motion in the sea.

The results of geometrically simple models obviously do not present a satisfactory approximation of current velocities and sea-levels measured in natural areas. On the other hand the advantage of these simple models is evident for investigations of general principles and of the influence of single parameters on the motion in the sea. The solutions can be used to determine the accuracy of the numerical methods. For the representation of currents and sea-levels in nature they are of no use.

§1. The hydrodynamic differential equations of motion and continuity

Consider the space-time motion of the sea. We shall proceed with the help of the equations of the averaged turbulent motion on the rotating Earth (Proudman 1953; Defant 1961):

$$\frac{\partial u}{\partial t} + u \frac{\partial u}{\partial x} + v \frac{\partial u}{\partial y} + w \frac{\partial u}{\partial z} - fv = - \frac{1}{\rho} \frac{\partial p}{\partial x} + k \frac{\partial^2 u}{\partial z^2} + A \Delta u \quad (1.1)$$

$$\frac{\partial v}{\partial t} + u \frac{\partial v}{\partial x} + v \frac{\partial v}{\partial y} + w \frac{\partial v}{\partial z} + fu = - \frac{1}{\rho} \frac{\partial p}{\partial y} + k \frac{\partial^2 v}{\partial z^2} + A \Delta v \quad (1.2)$$

$$\frac{\partial w}{\partial t} + u \frac{\partial w}{\partial x} + v \frac{\partial w}{\partial y} + w \frac{\partial w}{\partial z} = - \frac{1}{\rho} \frac{\partial p}{\partial z} - g + k \frac{\partial^2 w}{\partial z^2} + A \Delta w \quad (1.3)$$

The equations are derived in a Cartesian coordinate system which is taken in such a way that the origin and the (x,y)-plane lie on the undisturbed water surface. (Fig. 1.) The x and the y-axes are directed to east and north respectively; the z-axis is vertically upwards. The velocity components in the direction of x, y and z are denoted by u, v and w respectively. Besides, in the equations of motion the following quantities appear:

t - time	f - Coriolis parameter ($2 \omega \sin \phi$)
ω - Earth's angular velocity (equal to 7.29×10^{-3})	
ϕ - latitude	ρ - sea water density
p - pressure	g - gravity acceleration
k - vertical eddy viscosity coefficient or coefficient of exchange of momentum in the vertical direction	

A - lateral eddy viscosity coefficient or coefficient of exchange of momentum in horizontal direction

$$\Delta = \frac{\partial^2}{\partial x^2} + \frac{\partial^2}{\partial y^2} \quad - \text{two-dimensional Laplace-operator.}$$

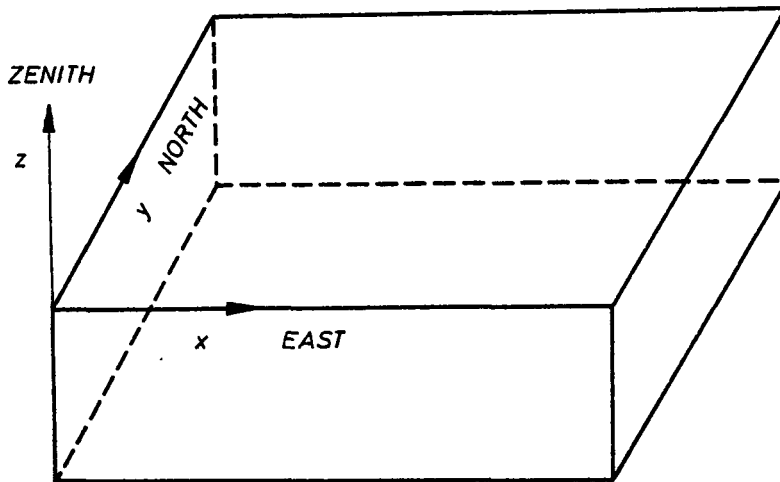


Fig. 1. CO-ORDINATE SYSTEM

The rectangular system of co-ordinates is appropriate for describing the motion in small basins where the curvature of Earth is very small. In other cases the spherical system of co-ordinates will be introduced.

Since sea water may be considered as an incompressible fluid we now add the continuity equation to the above system of equations in the form

$$\frac{\partial u}{\partial x} + \frac{\partial v}{\partial y} + \frac{\partial w}{\partial z} = 0 \quad (1.4)$$

The unknown quantities in equations (1.1) - (1.4) are three components of velocity and pressure. Density of the sea water (ρ) is

assumed to be known, for example, from the measurement of temperature and salinity. In case the thermohaline processes play an important role, an additional equation for density determination must be added.

In what will follow we shall use a compact form of the equations of motion by changing the variables to the column vectors

$$\vec{U} = \begin{bmatrix} u \\ v \\ w \end{bmatrix} \quad \vec{P} = \frac{1}{\rho} \begin{bmatrix} \frac{\partial p}{\partial x} \\ \frac{\partial p}{\partial y} \\ \frac{\partial p}{\partial z} + \rho g \end{bmatrix} \quad (1.5)$$

and the matrix

$$B = \begin{bmatrix} u \frac{\partial}{\partial x} + v \frac{\partial}{\partial y} + w \frac{\partial}{\partial z} - k \frac{\partial^2}{\partial z^2} - A, & -f, & 0 \\ f, & u \frac{\partial}{\partial x} + v \frac{\partial}{\partial y} + w \frac{\partial}{\partial z} - k \frac{\partial^2}{\partial z^2} - A, & 0 \\ 0, & 0, & u \frac{\partial}{\partial x} + v \frac{\partial}{\partial y} + w \frac{\partial}{\partial z} - k \frac{\partial^2}{\partial z^2} - A \end{bmatrix} \quad (1.6)$$

In this notation the system (1.1) - (1.3) is rewritten as one vector equation:

$$\frac{\partial \vec{U}}{\partial t} + B \vec{U} = -\vec{P} \quad (1.7)$$

We shall now discuss thoroughly the dynamical phenomena which will be of interest to us. In this way we shall derive from the general system of equations a simplified system in order to describe the currents and sea-level as functions of independent variables x , y , z , t . To calculate a current in any point of the sea, we first of all have to understand the phenomenon of momentum exchange in the vertical direction, which is usually characterized by the eddy viscosity coefficient k . On the other hand this knowledge is unnecessary in setting up the equation for the free surface. It is sufficient to have information on the values and directions of frictional stresses at the bottom and at the surface of the sea. This knowledge considerably simplifies the calculation of the free surface shape.

Bearing in mind these general remarks let us approach the detailed analysis of the equation of motion and continuity. As is usual in hydrodynamics we shall use dimensional analysis (Birkhoff, 1950) in order to obtain particular equations from the general equations.

To begin with, the characteristic values which describe the variables of the considered problem must be introduced. In the case of the Baltic or the North Sea the characteristic depth is $H \approx 100 \text{ m} = 10^4 \text{ cm}$ and the characteristic length $L \approx 10^3 \text{ km} = 10^8 \text{ cm}$. Before examining the equation of motion one can derive certain information from the equation of continuity (1.4). Rewriting (1.4) in a dimensional form

$$\frac{u}{L} + \frac{v}{L} + \frac{w}{H} = 0 \quad (1.8)$$

and taking $u = v = P$, we obtain

$$\left| \frac{w}{P} \right| = \frac{2H}{L} = 2 \times 10^{-4} \quad (1.9)$$

Hence in the seas being considered the vertical velocity (w) is small compared to the horizontal one, and we may conclude that in the equations the expressions with vertical velocity may be ignored. The conclusion, of course, is wrong in the case when dimensions of horizontal and vertical motion are of the same order.

With the above simplifications the equations (1.1) - (1.3) are

$$\frac{\partial u}{\partial t} + u \frac{\partial u}{\partial x} + v \frac{\partial u}{\partial y} - fv = -\frac{1}{\rho} \frac{\partial p}{\partial x} + k \frac{\partial^2 u}{\partial z^2} + A \Delta u \quad (1.10)$$

$$\frac{\partial v}{\partial t} + u \frac{\partial v}{\partial x} + v \frac{\partial v}{\partial y} + fu = -\frac{1}{\rho} \frac{\partial p}{\partial y} + k \frac{\partial^2 v}{\partial z^2} + A \Delta v \quad (1.11)$$

$$\frac{\partial w}{\partial t} = -\frac{1}{\rho} \frac{\partial p}{\partial z} - g \quad (1.12)$$

To proceed with the dimensional analysis, let us introduce the characteristic horizontal velocity $u = v = P = 100 \text{ cm/sec}$, vertical and horizontal eddy viscosity of $k = 10^3 \text{ cm}^2/\text{sec}$ and $A = 10^7 \text{ cm}^2/\text{sec}$ respectively. With these values we can evaluate the individual terms in the above equations as follows:

1. Nonlinear terms. Since the velocity and the horizontal dimensions are equal along the x and y directions, it is sufficient to analyse one of the nonlinear expressions only. Considering $u \frac{\partial u}{\partial x}$, then

$$u \frac{\partial u}{\partial x} = \frac{P^2}{L} = 10^{-4} \quad (1.13)$$

We can see that nonlinear terms are important when the velocity is changing within a very short horizontal distance (L).

2. Coriolis term

$$P = 10^{-4} \times 10^2 = 10^{-2} \quad (1.14)$$

3. Vertical friction term

$$k \frac{P}{H^2} = 10^3 \times 10^2 \times 10^{-8} = 10^{-3} \quad (1.15)$$

Again this term may be very big in very thin vertical layers, so-called friction layers.

4. Horizontal friction term

$$A \frac{P}{L^2} = 10^7 \times 10^3 \times 10^{-16} = 10^{-6} \quad (1.16)$$

5. Vertical acceleration term $\frac{\partial w}{\partial t}$.

To estimate its value we should know the characteristic time of the considered phenomenon. This time may be found by comparing the horizontal acceleration $\frac{P}{T}$ with any term in the equation of horizontal motion. If it is compared with the Coriolis term (1.14), then $T = 10^4$ sec. From this we may conclude that $\frac{\partial w}{\partial t} \ll g$, and the vertical acceleration may be ignored in (1.12).

Finally it is of definite interest to determine the horizontal dimensions of flow when the horizontal friction term is of the same order as the Coriolis term:

$$A \frac{P}{L^2} = Pf; \text{ and } L \approx 3.2 \text{ km} \quad (1.17)$$

Therefore the horizontal friction forces are important only in the narrow near-shore zone.

Dimensional analysis reveals that in the equations of motion the pressure gradient is balanced by the Coriolis force and the exchange of momentum in the vertical direction. Hence, the equations of motion are transformed to:

$$\frac{\partial u}{\partial t} - fv = -\frac{1}{\rho} \frac{\partial p}{\partial x} + k \frac{\partial^2 u}{\partial z^2} \quad (1.18)$$

$$\frac{\partial v}{\partial t} + fu = -\frac{1}{\rho} \frac{\partial p}{\partial y} + k \frac{\partial^2 v}{\partial z^2} \quad (1.19)$$

$$-\frac{1}{\rho} \frac{\partial p}{\partial z} - g = 0 \quad (1.20)$$

These equations describe motion in the horizontal plane only, since the equation for the vertical component of velocity is simplified to the hydrostatic state. It is important to underline that the frictional terms in the above equations are important only in the surface layer of the sea, down to a depth of approximately 100 m. Below this depth the currents may be described with the help of the geostrophic equation (Defant, 1961),

$$fv = \frac{1}{\rho} \frac{\partial p}{\partial x} \quad (1.21)$$

$$fu = - \frac{1}{\rho} \frac{\partial p}{\partial y} \quad (1.22)$$

when the Coriolis force is in a dynamic balance with the pressure gradient.

In the study which follows we shall mainly consider the steady current. This is due to certain difficulties, since firstly the computation of current in three dimensional space occupies a big part of operational computer memory and one additional variable (time) makes the computation very much more time consuming. Secondly, our knowledge on time variation of vertical momentum exchange is far from satisfactory.

Using (1.20) let us make a further transformation of the equations of motion. With this aim (1.20) is integrated from the arbitrary depth (z) up to the free surface ($z = \zeta$), assuming also that the free surface pressure is equal to the atmospheric pressure $p_a(x, y, t)$,

$$p = p_a + \rho g(\zeta - z) \quad (1.23)$$

Substituting (1.23) into (1.18) and (1.19) the new form of the equations for the horizontal components of current in an unstratified sea is obtained

$$\frac{\partial u}{\partial t} - fv = -g \frac{\partial \zeta}{\partial x} - \frac{1}{\rho} \frac{\partial p_a}{\partial x} + k \frac{\partial^2 u}{\partial z^2} \quad (1.24)$$

$$\frac{\partial v}{\partial t} + fu = -g \frac{\partial \zeta}{\partial y} - \frac{1}{\rho} \frac{\partial p_a}{\partial y} + k \frac{\partial^2 v}{\partial z^2} \quad (1.25)$$

These equations cannot be solved without suitable boundary and initial conditions. When studying the special problems we shall characterise the conditions in a more detailed way.

In the Baltic and North Sea two kinds of currents are observed - the current due to the wind stress and the density current caused by water exchange, mainly due to the horizontal salinity differences.

Generation of the wind-driven currents takes place at the free surface of the sea. Here the strongest currents of an order of 10 cm/sec to 100 cm/sec are observed.

Density-driven currents may appear in any layer of the sea. Their values are one or two orders of magnitude smaller than that of the wind-driven current. Assuming that the density ρ is an unknown variable we rearrange the equations of motion in such a way that the current due to the horizontal density stratification will appear. To obtain the new equations of motion we expand all dependent variables into series of the following form

$$\begin{aligned} p &= p_0 + p_1 + p_2 + \dots \\ \rho &= \rho_0 + \rho_1 + \rho_2 + \dots \\ u &= u_1 + u_2 + u_3 + \dots \\ v &= v_1 + v_2 + v_3 + \dots \end{aligned} \tag{1.26}$$

Here the basic state of the liquid is the hydrostatic one, described by p_0, ρ_0 .

Substituting (1.26) into (1.20), we have

$$\frac{\partial p}{\partial z} \approx \frac{\partial (p_0 + p_1)}{\partial z} = g (\rho_0 + \rho_1) \tag{1.27}$$

Assuming that the current due to density may be described by a term proportional to ρ_1 and rejecting all remaining terms as very small, we integrate equation (1.27) in the vertical direction from the arbitrary depth (z) to the sea surface ($z = \zeta$).

$$\int_p^p dp = -\rho_0 g \int_z^\zeta dz - g \int_z^\zeta \rho_1 dz \approx -\rho_0 g (\zeta - z) - g \int_z^\zeta \rho_1 dz$$

$$p = p_a + \rho_0 g (\zeta - z) + g \int_z^0 \rho_1 dz \tag{1.28}$$

Substituting (1.28) into the equations of motion (1.18) and (1.19) provides the equations, which describe the currents, in a density stratified sea.

$$\frac{\partial u}{\partial t} - fv = -\frac{1}{\rho} \frac{\partial p}{\partial x} a - \frac{\rho}{\rho_0} \cdot g \frac{\partial \zeta}{\partial x} - \frac{g}{\rho} \frac{\partial}{\partial x} \int_z^0 \rho_1 dz + k \frac{\partial^2 u}{\partial z^2} \quad (1.29)$$

$$\frac{\partial v}{\partial t} + fu = -\frac{1}{\rho} \frac{\partial p}{\partial y} a - \frac{\rho}{\rho_0} \cdot g \frac{\partial \zeta}{\partial y} - \frac{g}{\rho} \frac{\partial}{\partial y} \int_z^0 \rho_1 dz + k \frac{\partial^2 v}{\partial z^2} \quad (1.30)$$

In this system of equations four unknowns are present. Even when we add the continuity equation we still have only three equations. This is the consequence of our assumption that density is a variable and is unknown. There are two possible ways of solving this problem.

In the first case the density is taken to be known from the field measurements of salinity and temperature. Such a solution is admissible for the steady state problem or for very slow changes in time. Since measurements of density in time and space, with the speed and accuracy required for our problem, are practically impossible, this approach may not be used for dynamic problems.

In the second case the above system of equations is extended by adding the equation of density diffusion. This procedure introduces a great many mathematical obstacles (Sarkisyan, 1977).

§2. The mass transport and free surface equations

We shall now seek to develop the equations describing the geometrical shape of the free surface. The construction of these equations will be performed so that the process of momentum exchange will not affect the final result. To achieve this aim let us introduce instead of u and v the components of mass transport

$$M_x = \int_{-H}^{\zeta} \rho u dz; \quad M_y = \int_{-H}^{\zeta} \rho v dz \quad (1.31)$$

Substituting expression (1.23) for pressure in equations (1.10) and (1.11) and integrating them in the vertical direction from the bottom at $z = -H$ to the surface at $z = \zeta$ we find

$$\begin{aligned} & \frac{\partial M_x}{\partial t} + \frac{M_x}{H+\zeta} \cdot \frac{\partial M_x}{\partial x} + \frac{M_y}{H+\zeta} \cdot \frac{\partial M_x}{\partial y} - f M_y \\ & = -g(H+\zeta) \frac{\partial \zeta}{\partial x} - \frac{\partial p}{\partial x} a (H+\zeta) + \rho k \frac{\partial u}{\partial z} \Big|_{z=-H}^{z=\zeta} + A \Delta M_x \end{aligned} \quad (1.32)$$

$$\frac{\partial M_y}{\partial t} + \frac{M_x}{H+\zeta} \cdot \frac{\partial M_y}{\partial x} + \frac{M_y}{H+\zeta} \cdot \frac{\partial M_y}{\partial y} + f M_x$$

$$= -g(H+\zeta) \frac{\partial \zeta}{\partial y} - \frac{\partial p}{\partial y} a(H+\zeta) + \rho k \frac{\partial v}{\partial z} \Big|_{z=-H}^{z=\zeta} + A \Delta M_y \quad (1.33)$$

Since the components of stress at the lateral surface are expressed in the form

$$\tau(x) = \rho k \frac{\partial u}{\partial z}; \quad \tau(y) = \rho k \frac{\partial v}{\partial z} \quad (1.34)$$

the term $k \frac{\partial u}{\partial z}$ (and $k \frac{\partial v}{\partial z}$) may be written as $\tau(x)_{s(\text{surface})} - \tau(x)_{b(\text{bottom})}$. The values of the stresses are known from experiments but this problem will be discussed more closely, later on. The nonlinear (convective) terms in (1.32) and (1.33) are usually small if compared with other terms. Considering a flow in the sea basin we can disregard them except when shallow water regions are considered and where $\zeta \approx H$.

Since the equations of mass transport contain three dependent variables M_x, M_y, ζ , the additional equation is introduced through an integration, in the vertical direction, of the continuity equation (1.4);

$$\int_{-H}^{\zeta} \frac{\partial w}{\partial z} dz + \int_{-H}^{\zeta} \left(\frac{\partial u}{\partial x} + \frac{\partial v}{\partial y} \right) dz = 0 \quad (1.35)$$

The first term on the left side is the difference of vertical velocities at the surface and at the bottom

$$w(\zeta) - w(-H) \quad (1.36)$$

Taking, as before, the equation of the free surface in the form $z = \zeta(x, y, t)$ and differentiating it with respect to time, the value of the vertical velocity at the surface is defined as

$$w(z=\zeta) = \frac{d\zeta}{dt} = \frac{\partial \zeta}{\partial t} + \frac{\partial \zeta}{\partial x} u + \frac{\partial \zeta}{\partial y} v \quad (1.37)$$

The vertical velocity at the bottom is found in the same way by considering the equation of the bottom shape,

$$w(z=-H) = -\frac{dH}{dt} = -\frac{\partial H}{\partial x} u + \frac{\partial H}{\partial y} v \quad (1.38)$$

The second and third expressions on the left side of (1.35) are analogous and may be written as,

$$\int_{-H}^{\zeta} \frac{\partial u}{\partial x} dz = \frac{\partial}{\partial x} \int_{-H}^{\zeta} u dz - \frac{\partial \zeta}{\partial x} u(\zeta) - \frac{\partial H}{\partial x} u(-H) \quad (1.39)$$

$$\int_{-H}^{\zeta} \frac{\partial v}{\partial y} dz = \frac{\partial}{\partial y} \int_{-H}^{\zeta} v dz - \frac{\partial \zeta}{\partial y} v(\zeta) - \frac{\partial H}{\partial y} v(-H) \quad (1.40)$$

The final equation of continuity for the mass transport is obtained through the introduction of (1.36) - (1.40) into (1.35).

$$\frac{\partial M_x}{\partial x} + \frac{\partial M_y}{\partial y} + \rho \frac{\partial \zeta}{\partial t} = 0 \quad (1.41)$$

Further computations of free surface and mass transport variations in time and space will be performed with the help of (1.32), (1.33) and (1.41). It is possible, of course, on the basis of these equations, to build up one equation of higher order for ζ , but this way is rather difficult since the boundary conditions for the sea level are usually unknown. The above system of equations, on the other hand, has a very simple boundary condition, which in this case is that the component of mass transport normal to the coast equals zero.

Quite often in the oceanographic literature the equations presented above are formulated through another set of variables. One of them is the volume transport Q , whose components

$$Q_x = \int_{-H}^{\zeta} u dz; \quad Q_y = \int_{-H}^{\zeta} v dz \quad (1.42)$$

do not differ from the components of mass transport, since the density of the sea water $\rho \approx 1 \text{ g/cm}^3$.

More often the notion of mean velocity is used

$$U = \frac{1}{H + \zeta} \int_{-H}^{\zeta} u dz; \quad V = \frac{1}{H + \zeta} \int_{-H}^{\zeta} v dz \quad (1.43)$$

Let us arrange the equations of mass transport and continuity through the average velocity notion. Because

$$M_x = \int_{-H}^{\zeta} \rho u dz = \int_{-H}^{\zeta} u dz$$

therefore

$$U(H + \zeta) = M_x \quad \text{and} \quad V(H + \zeta) = M_y .$$

Introducing these quantities into (1.32), (1.33) and (1.41), we obtain

$$\frac{\partial U}{\partial t} + U \frac{\partial U}{\partial x} + V \frac{\partial U}{\partial y} - fV = -g\rho \frac{\partial \zeta}{\partial x} - \frac{\partial p}{\partial x} a + \frac{\tau_s^{(x)}}{H+\zeta} - \frac{\tau_b^{(x)}}{H+\zeta} + A \Delta U \quad (1.44)$$

$$\frac{\partial V}{\partial t} + U \frac{\partial V}{\partial x} + V \frac{\partial V}{\partial y} + fU = -g\rho \frac{\partial \zeta}{\partial y} - \frac{\partial p}{\partial y} a + \frac{\tau_s^{(y)}}{H+\zeta} - \frac{\tau_b^{(y)}}{H+\zeta} + A \Delta V \quad (1.45)$$

$$\frac{\partial \zeta}{\partial t} + \frac{\partial}{\partial x} (H + \zeta)U + \frac{\partial}{\partial y} (H + \zeta)V = 0 \quad (1.46)$$

In the process of deriving the equations of mass transport and mean velocities a number of simplifications and assumptions have been made. Now we shall discuss the implications of such procedures. It is quite clear that these simplifications are connected with the nonlinear terms. The question which remains is how to obtain from the term

$$u \frac{\partial u}{\partial x}$$

by integration in the vertical direction the terms

$$\frac{M_x}{H+\zeta} \cdot \frac{\partial M_x}{\partial x} \quad \text{and} \quad U \frac{\partial U}{\partial x} ?$$

In the first approach the situation is rather obvious. Average velocity U may be introduced into the nonlinear terms only when the vertical distribution of velocity is nearly constant, that is

$$U \approx \frac{1}{H+\zeta} \int_{-H}^{\zeta} u \, dz = u,$$

and when the average velocity does not differ much from the velocity at an arbitrary depth. This distribution is met in the sea only in special situations, namely, in the storm surge phenomena in a coastal zone (where nonlinear terms are important), and, as a general rule, in tidal waves.

Several attempts have been made to present the vertical distribution of velocity in such a special situation. Prandtl (1942) assumed a constant bottom friction and a linear change of the eddy viscosity coefficient k with depth,

$$k \frac{\partial u}{\partial z} = \tau = \text{const.}, \quad \text{when } k = \chi z.$$

From this result the so-called logarithmic velocity distribution follows

$$u(z) = u(z_0) + \frac{\tau}{\chi} \log \frac{z}{z_0} \quad (1.47)$$

where $\chi \approx 0.4$ is the Karman constant.

Another possible solution leads to the empirical potential law of velocity distribution,

$$u = u_0 \left(\frac{z}{z_0} \right)^{1/q} \quad (1.48)$$

An example of the velocity distribution approximated by the potential and logarithmic laws is plotted in fig. 2. Now with the fairly general potential law we may analyse the condition that $U \approx u$, by establishing the proper value of the exponent q and next comparing the empirical distribution of velocity and empirical magnitude of q . First of all let us rewrite (1.48) in the co-ordinate system from fig. 1, with the following conditions at the surface $z = \zeta$, $u = u_0$ and at the bottom $z = -H$, $u = 0$, thus,

$$u = u_0 \left(\frac{z + H}{H + \zeta} \right)^{1/q} \quad (1.49)$$

Integrating (1.49) from the bottom to the surface the mean velocity

$$U = \frac{u_0}{H + \zeta} \int_{-H}^{\zeta} \left(\frac{z + H}{H + \zeta} \right)^{1/q} dz \quad (1.50)$$

is expressed as a function of the surface velocity u_0 ,

$$U = u_0 \frac{q}{1+q} \quad (1.51)$$

The value of exponent q found from the empirical data varies from 5 to 7 (Dronkers, 1975). We may conclude here, with a good order of approximation, that $U \approx u_0$.

§3. One-dimensional motion

By one-dimensional motion we mean flow in straight channels and narrow seas. Directing the x co-ordinate along the axis of flow, instead of two equations (1.32) and (1.33) the following equation is written,

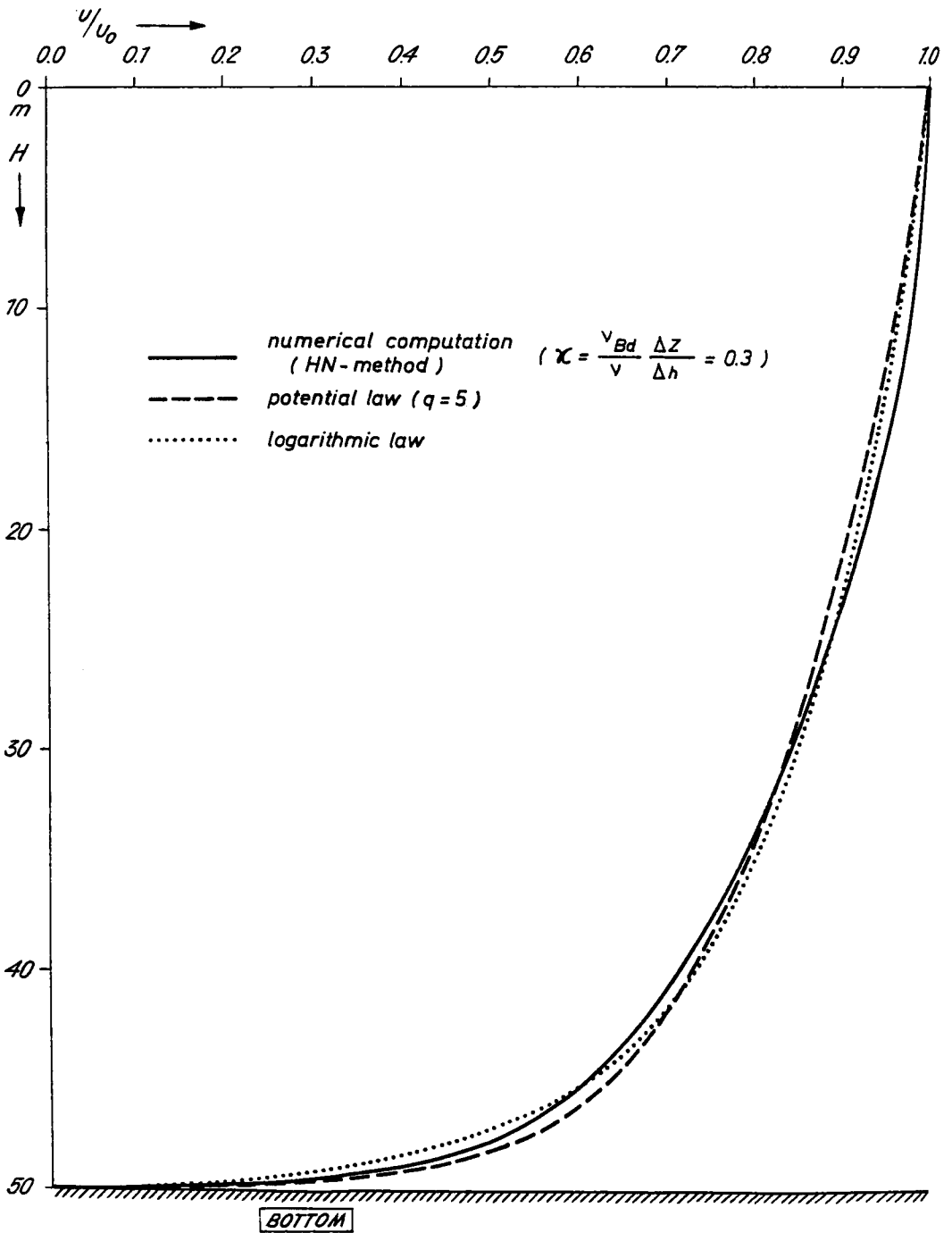


Fig. 2. COMPARISON OF THE OBSERVED CURRENT PROFILE IN THE TIDAL WAVI (CONTINUOUS LINE) WITH THE LOGARITHMIC LAW (BROKEN LINE) AND THE POTENTIAL LAW ($q = 5$) - ACCORDING TO SÜNDERMANN (1971).

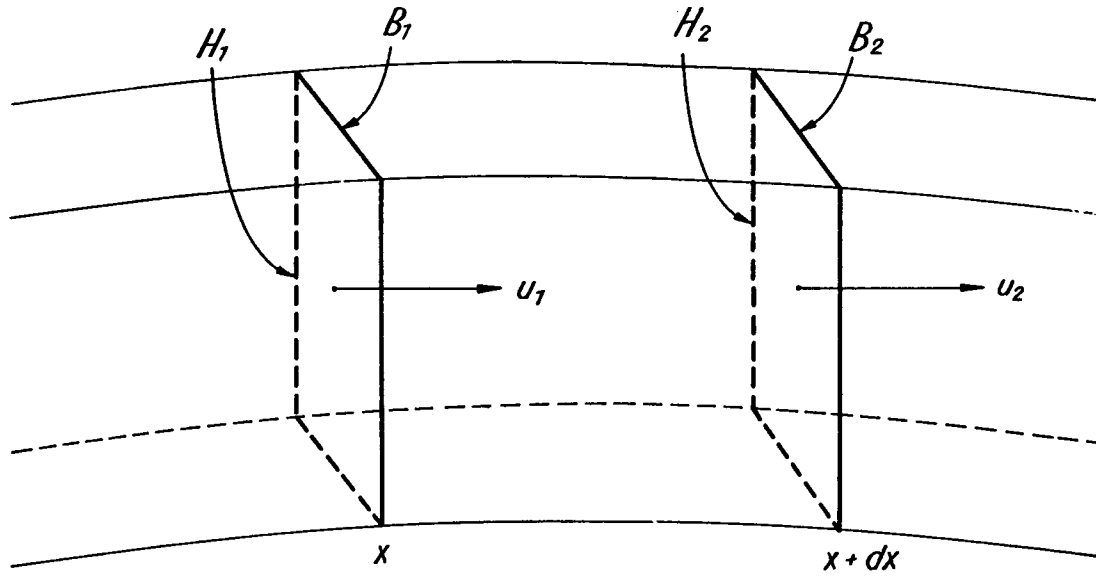


Fig. 3. FLOW GEOMETRY IN THE CHANNEL.

$$\frac{\partial M_x}{\partial t} + \frac{M_x}{H+\zeta} \frac{\partial M_x}{\partial x} = -\rho g(H+\zeta) \frac{\partial \zeta}{\partial x} + \tau_s^{(x)} - \tau_b^{(x)} + A \frac{\partial^2 M_x}{\partial x^2} \quad (1.52)$$

To this equation we may add the following comment; although we know that the meaning of eddy viscosity coefficient A in one-dimensional flow is not quite clear and that there is no data on its empirical value, we leave it in (1.52) since in the numerical forms the coefficient may improve the computational stability.

The continuity equation (1.41) could not be transformed as easily as the equation of motion. The co-ordinate perpendicular to the axis will be represented by the width of channel B (See fig. 3). To derive the equation of continuity let us consider two cross-sections in the channel. The distance between the sections is dx, the width of the first section is B_1 and of the second one B_2 . The depths are H_1 and H_2 respectively. The flow of mass through the first section in time dt equals $m_1 = \rho u_1 H_1 B_1 dt$. The flow through the second section in the same time is $m_2 = \rho u_2 H_2 B_2 dt$. If $m_2 < m_1$ the inflow of mass between the sections is observed, it will cause the free surface to change by $d\zeta$. Therefore the law of mass conservation can be written as

$$\begin{aligned} m_2 - m_1 &= B dx d\zeta = -dm = -dt(\rho u_2 H_2 B_2 - \rho u_1 H_1 B_1) \\ &= -\rho dt \frac{\partial (uHB)}{\partial x} dx \end{aligned} \quad (1.53)$$

In (1.53) the quantity ρuH expresses the mass transport M_x , and thus

$$\frac{\partial (M_x B)}{\partial x} + \rho B \frac{\partial \zeta}{\partial t} = 0 \quad (1.54)$$

An analogue of equation (1.41) is obtained only if the width of the channel is constant ($B = \text{constant}$)

$$\frac{\partial M_x}{\partial x} + \rho \frac{\partial \zeta}{\partial t} = 0 \quad (1.55)$$

In the following section we shall study one-dimensional motion with the help of equations (1.52), (1.54) and with appropriate boundary and initial conditions.

§4. Frictional forces at the surface and the bottom

The equations of motion include expressions which describe the

stresses at lateral surfaces due to external forces. On the sea surface wind stress causes a motion of the water but at the bottom the stress leads to decay of motion. Theoretically both have the same form

$$\rho k \frac{\partial u}{\partial z}$$

They depend on the eddy viscosity and the vertical gradient of velocity, but their empirical forms differ strongly. Investigations of bottom stress lead to quite different laws: one expresses the stress as a linear function of the average velocity; the other expresses a quadratic dependence. In the second case the equations of motion are nonlinear and their study is very complicated. The measurements of the bottom stress run already for many years under the different flow conditions. G.I. Taylor (1920) showed that the bottom stress is proportional to the square of the average velocity

$$\tau_b^{(x)} = rU(U^2 + V^2)^{1/2} \quad (1.56)$$

$$\tau_b^{(y)} = rV(U^2 + V^2)^{1/2}$$

The dimensionless friction coefficient r depends on many different factors, but mainly on the bottom roughness. In the enclosed table some measurements of this coefficient, obtained by different authors, are presented

author	place	method	$r \times 10^3$ range	$r \times 10^3$ mean value
Taylor (1918)	Irish Sea	a)	1.6 - 2.0	2.4
		b)		2.4
Grace (1936)	Bristol-Channel	c)	1.4 - 4.1	2.6
	(1937) English Channel	c)	2.4 - 21.3	9.3
Bowden and Fairbairn (1952)	Wharf Bay, Anglesey	d)	0.57- 2.04	1.8

A general mean value of r used in computation is usually taken as $r = 3.3 \times 10^{-3}$.

The various methods for the estimation of r may be subdivided as follows:

- a) Transference of a formula for the bottom friction on a river bed (Bazin) to a maritime basin
- b) Investigation of the amount of energy dissipated at the sea bottom
- c) Application of the equations of open-channel theory to the harmonic constants found by Doodson and Corkan and to the current velocities given by the tidal current tables
- d) Application of the simplified hydrodynamic equations of motion to measurements of water level and velocity in the open sea.

One of the simplest methods of stress determination is connected with the velocity distribution given by equation (1.47). Measuring the velocities at two depths z_1, z_2 and with help of equation (1.47) we get

$$u(z_1) = u(z_0) + \frac{\tau}{\chi} \log \frac{z_1}{z_0} \quad (1.58)$$

$$u(z_2) = u(z_0) + \frac{\tau}{\chi} \log \frac{z_2}{z_0} \quad (1.59)$$

Subtracting (1.59) from (1.58) the following expression for determining stress is easily obtained

$$\tau = \chi \frac{u(z_1) - u(z_2)}{\log z_2/z_1} \quad (1.60)$$

The logarithmic distribution of velocity allows us to calculate the friction coefficient as

$$r = \frac{1}{32} [\log (14.8H/z^*)]^{-2} \quad (1.61)$$

Here z^* is the roughness length equal to one thousand times the grain size.

In order to examine the characteristic magnitude of the friction term in the equations of motion τ_D/H , we calculate it for different velocities and depths.

U \ H	20	40	60	80	100 cm/sec
10 m	12	48	108	192	300×10^{-4} cm/sec
50 m	2	10	22	38	60×10^{-4} cm/sec
100 m	1	5	11	19	30×10^{-4} cm/sec

From this we conclude that the friction term is relatively unimportant in deep water, but for shallow water areas it has the same magnitude as the other terms of the integrated equations.

In hydraulics, instead of the coefficient r the coefficient of Chezy C is sometimes introduced

$$r = g C^{-2} \quad (1.62)$$

If in turn linear dependence on the mean velocity is taken

$$\tau_b^{(x)} = R U; \quad \tau_b^{(y)} = R V; \quad (1.63)$$

the friction coefficient R may be found as $r \sqrt{U^2 + V^2}$ or from the relation (Uusitalo, 1962)

$$R = \frac{k\pi}{4H} \quad (1.64)$$

Here k is eddy viscosity at the bottom. The value of R is in the range of 10^{-5} to 10^{-6} CGS units.

Generally speaking the coefficient of bottom friction is a variable parameter. Later on we shall present some solutions to this problem for the shallow water. Interesting ideas in this respect may be found in Kagan's works (1972).

The tangential stress at the sea surface is due to the wind. Experiments show that stress is a complicated function of wind velocity and the aerodynamic properties of the sea surface, namely

$$\tau_s = \rho_a C_z W_z^2 \quad (1.65)$$

where ρ_a is the air density, C_z the coefficient of aerodynamic resistance at a height z above the sea, and W_z the wind velocity at the same level.

The determination of the coefficient C_z constitutes one of the most important problems of sea dynamics (Kitajgorodski, 1970), since

the free surface is itself in motion. The results of many years' measurements obtained under different conditions and at different geographical locations have been gathered by Wilson (1960). The data show a big scattering and clear dependence on the wind velocity. Usually the wind measurements are performed at the level $z = 10$ m, therefore we shall use later this value as a subscript on the quantities C_{10} and W_{10} . Wilson showed that C_{10} for small and moderate winds (2 - 8 m/sec) is equal to 1.1×10^{-3} , and for strong winds (20 m/sec) C_{10} is equal to 2.6×10^{-3} . Using the data gathered by Wilson and his own new set of data, the dependence of C_{10} on wind speed is plotted in fig. 4.

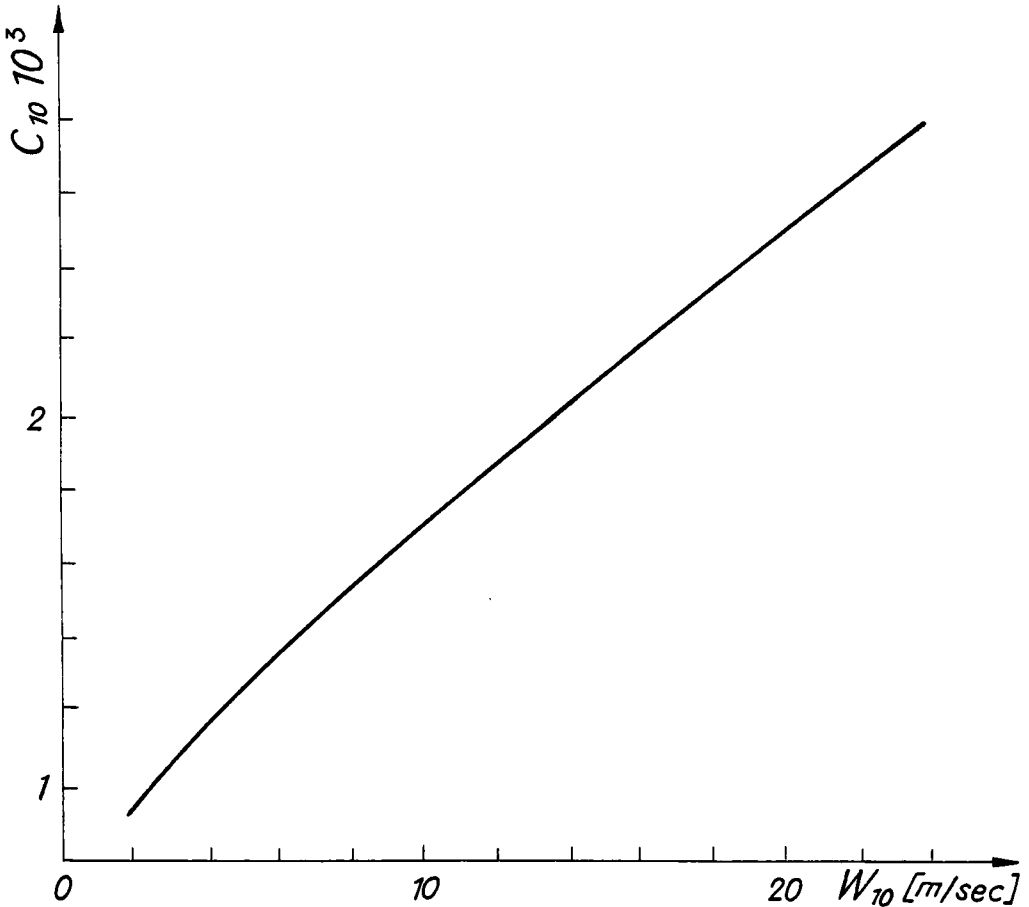


Fig. 4. COEFFICIENT OF AERODYNAMIC RESISTANCE C_{10} AT 10 m ABOVE SEA-LEVEL AGAINST WIND VELOCITY W_{10} .

Coefficient C_{10} in this figure is a linear function of wind

$$C_{10} = (0.9 + 0.08 \times 10^{-2} W) \times 10^{-3} \quad (1.66)$$

Here wind is given in cm/sec.

In the recent review of the drag coefficients over oceans and continents Garrat (1971) obtained

$$C_{10} = (0.75 + 0.067 \times 10^{-2} W) \times 10^{-3} \quad (1.67)$$

To calculate the wind stress at the sea surface with the help of equation (1.65) the wind velocity W_z is needed. Since measurements at sea of the true wind are rather scarce, charts of the pressure distribution over the sea are used instead as a practical expedient.

Very often the geostrophic wind which can be calculated from the isobaric charts is used. This is done by means of the formulae analogous to (1.21) and (1.22)

$$U_g = -\frac{1}{\rho_a f} \frac{\partial p_a}{\partial y} \quad (1.68)$$

$$V_g = \frac{1}{\rho_a f} \frac{\partial p_a}{\partial x} \quad (1.69)$$

whereby ρ_a and p_a are the density and pressure in the atmosphere. The geostrophic wind can be considered as a good approximation of the true wind at the sea surface. It has been shown, by meteorological investigations, that certain corrections should be made.

For instance according to Hasse and Wagner (1971) the relationship between surface and geostrophic wind may be classified as a function of a stability condition in the near water layer

unstable	$W = 0.56 W_g + 3.0$	(m/sec)	
near stable	$W = 0.56 W_g + 2.4$	(m/sec)	(1.70)
stable	$W = 0.56 W_g + 1.5$	(m/sec)	

Furthermore, often a correction for the wind direction is added, e.g. Duun-Christensen (1971) has used a value of 18° (counter-clockwise). Beside these corrections experiences obtained from the prediction of storm surges in Leningrad (Orlenko, 1971) indicated the influence of nongeostrophic deviations of the true wind.

So the different corrections though they complicate the final prediction of the wind field are worth-while, since the results of numerical computations are strictly related to the exactness of the meteorological data input.

REFERENCES

- Birkhoff, G., 1950. Hydrodynamics. Princeton.
- Bowden, K.F., Fairbairn, L.A., 1952. A Determination of the Friction Forces in a Tidal Current. Proc. Roy. Soc., A, v. 214: 371-392.
- Defant, A., 1961. Physical Oceanography. Pergamon Press, Oxford, vol. I, vol. II.
- Dronkers, J.J., 1975. Tidal Theory and Computations. Advances in Hydrosience. Academic Press, New York.
- Duun-Christensen, J.T., 1971. Investigations and Practical Use of the Hydrodynamic-Numeric Method for Calculating Sea Level Variations in the North Sea, the Skagerrak and Kategat. Deutsch. Hydr. Zeit., B. 24, H.5: 210-227.
- Garrat, J.R., 1977. Review of Drag Coefficients over Oceans and Continents. Month. Weat. Rev., N.7, v. 105: 915-929.
- Grace, S., 1936. Friction in the Tidal Currents of the Bristol-Channel. Geoph. Suppl. Mon. Not. R. Astr. Soc., v. 4.
- Grace, S., 1937. Tidal Friction in the Tidal Currents of the English Channel. Geoph. Suppl. Mon. Not. Roy. Astr. Soc., v. 4.
- Hasse, L., Wagner, V., 1971. On the Relationship between Geostrophic and Surface Wind at Sea. Month. Weath. Review, v. 99, N. 4: 255-260
- Kagan, B.A., 1962. On the Resistance Law in Tidal Flow. Atmosphere and Oceanic Physics, N. 8.
- Kitajgorodski, S.A., 1970. Physics of Air-Sea Interaction. Leningrad, Gidrometeoizdat.
- Krauss, W., 1966. Interne Wellen. Gebrüder Bornträger, Berlin.
- Orlenko, L.R., 1971. On the Accounting of Advection and Ageostrophic deviations when Calculating Wind and Tangent Strain over the Water Surface. Meteorologia i Hidrologia, N.7: 43-49.
- Prandtl, L., 1942. Führer durch die Strömungslehre. Braunschweig, Vieweg und Sohn.
- Proudman, J., 1953. Dynamical Oceanography. Methuen, London. Willey, New York.
- Sarkisyan, A.S., 1977. Numerical Analysis and Sea Current Prediction. Leningrad, Gidrometeoizdat.
- Taylor, G.I., 1919. Tidal Friction in the Irish Sea. Phil. Trans. Royal Soc. A, v. 220.
- Uusitalo, S., 1962. The Numerical Calculation of Wind Effect on Sea Level Elevations. In: Proceeding of Symposium on Mathematical-Hydrodynamic Methods of Physical Oceanography, Institut für Meereskunde der Universität Hamburg.
- Wilson, B.W., 1960. Note on Surface Wind Stress over Water at Low and High Wind Speeds. Journal of Geophysic Research, v. 65, N. 10: 3377 - 3382.

Chapter II STEADY MOTION – NUMERICAL METHODS

This chapter is devoted to the numerical treatment of a steady-in-time flow which is described by a stream function and the steady distribution of a substance which is characterized by the diffusion equation.

A general equation for this problem is the second order nonhomogeneous elliptical equation. The coefficients of the first derivatives vary in space, whereas the coefficients of the second derivatives are often very small. This creates the problem of proper numerical approximation up to the second order in space and leads frequently to the creation of additional terms in the difference equation which are not related to the differential form and are expressed as so-called numerical friction.

The construction of a difference equation on a given numerical grid provides a set of algebraic equations. Therefore when choosing a finite difference form we have to take into account the method which is to be used to solve the algebraic equations. Iterative methods are the most suitable with the space matrix which usually occurs in the problem of steady motion. The simplest methods of iteration are discussed in this chapter.

The criteria of convergence, in terms of the coefficients of the matrix, are given. The general properties of matrices and operators, especially the positive definite property which is very suitable in iterative schemes, are also discussed. From the many possible methods of solution of finite difference equations we discuss thoroughly the line inversion method. We believe that it has a great many applications and possesses useful properties such as convergence and self-correction. That is to say, any error appearing in the course of computation is suppressed by the use of this method.

§1. Numerical approximation of steady phenomena

Steady motion in the sea (Chapter III) and steady transport phenomena (Chapter VIII) are described by the second order differential equation

$$L \psi(x, y) = f(x, y) \quad (2.1)$$

where $L = L_1 + L_3$ and

$$L_1 = \frac{\partial}{\partial x} \left\{ r_1(x, y) \frac{\partial \cdot}{\partial x} \right\} + \frac{\partial}{\partial y} \left\{ r_2(x, y) \frac{\partial \cdot}{\partial y} \right\}$$

$$L_3 = a(x,y) \frac{\partial \cdot}{\partial x} + b(x,y) \frac{\partial \cdot}{\partial y} + c(x,y)$$

As the boundary condition we take

$$\psi(x,y) = 0 \quad (2.2)$$

for the problem of steady motion, and

$$\frac{\partial \psi}{\partial n} = 0 \quad (2.3)$$

for the transport problem, where n is the direction perpendicular to the boundary.

Here

$$r_1 > 0, r_2 > 0, |a| < C_1 < \infty, |b| < C_2 < \infty, |f| < C_3 < \infty \quad (2.4)$$

The quantities r , a , b , f are continuous and known functions in the closed domain \bar{D} , where $\bar{D} = (0 \leq x \leq l_1; 0 \leq y \leq l_2)$.

In the domain \bar{D} we introduce an equally spaced net (grid) with the step distance h . In this way the closed net space $\bar{D}_h = (x_j = jh; y_k = kh)$ is obtained. Here $j = 1, 2, 3, \dots, J$; $k = 1, 2, 3, \dots, K$. The boundary of domain \bar{D} is denoted as Γ and the boundary of \bar{D}_h as Γ_h . Now let us introduce the relationship between the difference and differential expressions for the first and second derivatives. This step is necessary for establishing the difference analog of differential equation (2.1) and its boundary condition (2.3). Using (a) the well known Taylor theorem for the arbitrary 2-point net of (j,k) and $(j+1,k)$ and (b) the fact that ψ is everywhere analytic in \bar{D} (Ref. to proof for 2nd order elliptic operators), we may write the forward difference of the function ψ in the x -direction as

$$\begin{aligned} \psi\{h(j+1),hk\} - \psi\{hj,hk\} &= \psi_{j+1,k} - \psi_{j,k} \\ &= \frac{\partial \psi}{\partial x} h + \frac{\partial^2 \psi}{\partial x^2} \frac{h^2}{2!} + \frac{\partial^3 \psi}{\partial x^3} \frac{h^3}{3!} + O(h^4) \end{aligned} \quad (2.5)$$

For the points j,k and $j-1,k$ in a similar way the backward difference in the x -direction is defined as

$$\psi_{j,k} - \psi_{j-1,k} = \frac{\partial \psi}{\partial x} h - \frac{\partial^2 \psi}{\partial x^2} \frac{h^2}{2!} + \frac{\partial^3 \psi}{\partial x^3} \frac{h^3}{3!} - O(h^4) \quad (2.6)$$

All analytical derivatives in (2.5) and (2.6) are taken at the point

(j,k). These differences allow us to describe three types of first order derivatives in the x-direction

a) Forward derivative

$$\psi_x = \frac{\psi_{j+1,k} - \psi_{j,k}}{h} = \frac{\partial \psi}{\partial x} + O(h) \quad (2.7)$$

b) Backward derivative

$$\psi_x^- = \frac{\psi_{j,k} - \psi_{j-1,k}}{h} = \frac{\partial \psi}{\partial x} + O(h) \quad (2.8)$$

c) Central derivative

$$\psi_x^* = \frac{\psi_{j+1,k} - \psi_{j-1,k}}{2h} = \frac{\partial \psi}{\partial x} + O(h^2) \quad (2.9)$$

The last formula was obtained by adding the expressions (2.5) and (2.6) and subsequent division by 2h. Subtracting (2.6) from (2.5) we derive an expression for the second order derivative in the form

$$\psi_{xx} = \frac{\psi_{j+1,k} + \psi_{j-1,k} - 2\psi_{j,k}}{h^2} + O(h^2) \quad (2.10)$$

In the above expressions $O(h)$ and $O(h^2)$ describe the order of the remaining terms (error) in the Taylor series in relation to the grid step h . The power of h indicates the order of approximation of the differential derivatives by the difference derivatives; where the power of h is highest, the best approximation or the greatest accuracy is obtained. It is seen from the Taylor approximation method that the accuracy can be increased by refining the net or by the consideration of more terms in the Taylor series. Now, for the arbitrary grid points of \overline{D}_h , the difference form of (2.1) may be written down. The selection of proper difference forms has to take into account not only the best order of approximation but also the convergence of the numerical solution to the analytical solution, and the properties of the numerical method chosen for the solution. If we introduce the iteration method of solution, the difference form of (2.1) must comply with the convergence criteria of the iterative method. A derivation of the full numerical form of (2.1) will proceed term by term. Firstly the operator

$$L_1 \psi = \frac{\partial}{\partial x} \left\{ r_1 \frac{\partial \psi}{\partial x} \right\} + \frac{\partial}{\partial y} \left\{ r_2 \frac{\partial \psi}{\partial y} \right\} \quad (2.11)$$

is considered with constant coefficients $r_1 = r_2 = r = \text{const}$. In this case (2.11) simplifies to

$$L_2 \psi = r \left\{ \frac{\partial^2 \psi}{\partial x^2} + \frac{\partial^2 \psi}{\partial y^2} \right\} \quad (2.12)$$

and its numerical form may be written down on the grid as

$$L_{2h} \psi = r \{ \psi_{xx} + \psi_{yy} \} \quad (2.13)$$

Substituting into (2.13) expression (2.10) for the second derivative along the x direction and the analogous formula for the y -co-ordinate we see that

$$|L_2 \psi - L_{2h} \psi| \leq R h^2 \quad (2.14)$$

where $R < \infty$, and does not depend on the grid step h .

In order for the condition $R < \infty$ to hold, we must assume that the fourth order derivatives of ψ exist and are bounded. This result is part of a general theorem due to Gershgorin (Collatz, 1955).

The approximation of L_1 (the differential equation (2.11)) with second order accuracy is carried out by means of an expression which possesses a spatial symmetry in relation to the term $\psi_{j,k}$

$$L_{1h} \psi = \frac{1}{h^2} \{ \text{RFX}(\psi_{j+1,k} - \psi_{j,k}) - \text{RBX}(\psi_{j,k} - \psi_{j-1,k}) \\ + \text{RFY}(\psi_{j,k+1} - \psi_{j,k}) - \text{RBY}(\psi_{j,k} - \psi_{j,k-1}) \} \quad (2.15)$$

where the coefficients are denoted by

$$\text{RFX} = \frac{r_{1,j+1,k} + r_{1,j,k}}{2}, \quad \text{RFY} = \frac{r_{2,j,k+1} + r_{2,j,k}}{2} \\ \text{RBX} = \frac{r_{1,j,k} + r_{1,j-1,k}}{2}, \quad \text{RBY} = \frac{r_{2,j,k} + r_{2,j,k-1}}{2} \quad (2.16)$$

The greatest problems occur in the approximation of the operator

$$L_3 \psi = a \frac{\partial \psi}{\partial x} + b \frac{\partial \psi}{\partial y} \quad (2.17)$$

because the coefficients a and b in the domain \bar{D} change their values in an arbitrary way from positive to negative. On the grid points in domain \bar{D}_h we shall write down the difference equation in such a way

that the forward or backward derivatives are chosen in agreement with the signs of coefficients a or b in order to comply with the convergence demands of the iteration process.

$$L_{3h}\psi = a^+\psi_x + \bar{a}\psi_{\bar{x}} + b^+\psi_y + \bar{b}\psi_{\bar{y}} \quad (2.18)$$

where

$$\begin{aligned} a^+ &= \frac{a + |a|}{2}; & \bar{a} &= \frac{a - |a|}{2} \\ b^+ &= \frac{b + |b|}{2}; & \bar{b} &= \frac{b - |b|}{2} \end{aligned} \quad (2.19)$$

Substituting into (2.18) the relations (2.7) and (2.8) we observe that, as $h \rightarrow 0$, the operator $L_{3h}\psi$ approximates the operator $L_3\psi$, and

$$|L_{3h} - L_3| \leq R_1 h \quad (2.20)$$

where $R_1 < \infty$, subject to the condition that the second derivatives $\frac{\partial^2 \psi}{\partial x^2}$ and $\frac{\partial^2 \psi}{\partial y^2}$ exist and are bounded.

In all, the expressions (2.15) and (2.18) approximate the differential equation (2.1) up to first-order accuracy. The second-order accuracy in this equation can be obtained with the difference scheme below. To avoid very long algebraic expressions we shall consider only the part of equation which is dependent on the variable x (the expression along the y -co-ordinate will be analogous)

$$\begin{aligned} & \frac{1}{h^2} \left\{ \sqrt{RFX} + \frac{ah}{4\sqrt{RFX}} \right\}^2 \{ \psi_{j+1,k} + \psi_{j,k} \} - \left\{ \sqrt{RBX} - \frac{ah}{4\sqrt{RBX}} \right\}^2 \{ \psi_{j,k} - \psi_{j-1,k} \} \\ &= \frac{1}{h^2} \{ RFX(\psi_{j+1,k} - \psi_{j,k}) - RBX(\psi_{j,k} - \psi_{j-1,k}) \} + \frac{a}{2h} (\psi_{j+1,k} - \psi_{j-1,k}) \\ & \quad + \frac{h^2 a^2}{16} \frac{\partial \psi}{\partial x} \left(\frac{1}{r_1} \cdot \frac{\partial \psi}{\partial x} \right) \end{aligned} \quad (2.21)$$

The above approximates the equation (2.1) with second-order accuracy in h , since the error is equal to

$$\frac{h^2 a^2}{16} \frac{\partial}{\partial x} \left\{ \frac{1}{r_1} \cdot \frac{\partial \psi}{\partial x} \right\} \quad (2.22)$$

but in this special case the error depends also on the parameter $\frac{h^2 a^2}{16r_1}$ and is of order $O(h^2)$ only if $\frac{a^2}{16r_1} < 1$.

In a steady motion r_1 plays the role of a bottom friction coefficient. Since usually $r_1 \approx 0$, we find

$$\frac{a^2}{16r_1} \gg 1 \quad (2.23)$$

This inequality shows that this difference scheme (2.21) does not provide a second order approximation and is not appropriate to study the steady current in the sea.

However, in two-dimensional transport processes the above inequality when expressed in terms of the coefficients of the governing differential equation (Chapter VII) takes the form

$$\frac{u^2}{16K_x} \ll 1 \quad (2.24)$$

In this case u is the horizontal velocity and K_x the eddy diffusion coefficient. Since the order of magnitude of u is 10^2 cm/sec and of K is 10^8 cm²/sec, it follows from (2.24) that (2.21) possesses second-order accuracy when used in the description of transport phenomena.

Finally let us consider the following problem connected with the question of accuracy. The approximation of (2.1) by means of expressions (2.12) and (2.18) leads to an error which is proportional to h . As h is finite that error may play an important role in the distortion of the solution. Taking the difference equation

$$r(\psi_{xx}^- + \psi_{yy}^-) + a^+ \psi_x + \bar{a} \psi_x^- + \bar{b} \psi_y^- + b^+ \psi_y = f_h \quad (2.25)$$

and introducing the derivatives from formulae (2.7), (2.8) and (2.9) we find

$$r\left\{\frac{\partial^2 \psi}{\partial x^2} + \frac{\partial^2 \psi}{\partial y^2}\right\} + \frac{|a|h}{2} \frac{\partial^2 \psi}{\partial x^2} + \frac{|b|h}{2} \frac{\partial^2 \psi}{\partial y^2} + a \frac{\partial \psi}{\partial x} + b \frac{\partial \psi}{\partial y} + O(h^2) = f(x, y) \quad (2.26)$$

Comparing expressions (2.1) and (2.26) it is obvious that in the latter case, besides the physical coefficient of friction r , there are two new coefficients

$$\frac{|a|h}{2} \quad \text{and} \quad \frac{|b|h}{2} .$$

These we shall call the coefficients of 'numerical friction'. They are a function of the space step and the coefficients a and b of the first derivatives. It is clear that in this case the order of approximation is increased, since the effects of 'numerical friction' will decay. But as the iteration processes involved are not always in the solution (due to the convergence criteria) higher approximation is possible. Let us evaluate the value of the numerical friction coefficient $\frac{h|a|}{2}$.

$$a = \frac{r}{H} \frac{\partial H}{\partial x} + \frac{f}{H} \frac{\partial H}{\partial y}$$

and because usually $r \ll f$, therefore we find that

$$a \approx \frac{f}{H} \frac{\partial H}{\partial y}.$$

The conclusion is that the effects of numerical friction occur in those parts of the domain \overline{D}_h where the depth H changes abruptly over very short horizontal distances and thereby distorts the computational results in a fundamental way.

§2. Convergence and choice of grid step

A proper approximation with high accuracy is an important step towards obtaining a solution. The study of the convergence of the numerical solution to the analytical solution is based on the method proposed by Gershgorin (Collatz, 1955). In this method it is assumed that the analytical solution exists together with its derivatives up to the fourth order.

To estimate the accuracy of the difference equation we introduce the error $z_h = \psi - \psi_h$. Here ψ is the analytical solution of the following problem

$$L\psi = f(x, y); \quad x, y \in \overline{D} \tag{2.27}$$

$$\psi = \text{Const.}; \quad x, y \in \Gamma$$

and ψ_h is the numerical solution of the problem

$$\begin{aligned} L_h \psi_h &= f_h; & x, y &\in \overline{D}_h \\ \psi_h &= C_h; & x, y &\in \Gamma_h. \end{aligned} \tag{2.28}$$

Subtracting (2.28) from (2.27) we find that the error z_h due to the approximation must satisfy

$$\begin{aligned} L_h z_h &= \psi_h; & x, y \in \bar{D}_h \\ z_h &= 0; & x, y \in \Gamma_h \end{aligned} \quad (2.29)$$

As an example, the error of approximation of the operator $L_3\psi$, considered above with the help of inequality (2.20), can be estimated as

$$L_h z_h = |L_{3h}\psi - L_3\psi| \leq R_1 h \quad (2.30)$$

But this expression provides an estimation for the operator which operates on z_h . We are more interested in the estimation of the error itself. Since we are dealing with an elliptical operator which has the positive definite property we may proceed from (2.30) straight to the error z_h (Young and Gregory, 1973). For equation (2.13) the error is equal to

$$|z_h| \leq \frac{h^2}{24} \frac{\partial^4 \psi}{\partial x^4} \rho^2 \quad (2.31)$$

where $\rho = \text{Max}(l_1, l_2)$ is the length which is equal to the maximum dimension of D_h . It is seen from (2.31) that the error is estimated by the fourth order analytical derivative. The derivative can, of course, be changed into a numerical one, but such a procedure seems to be dubious.

From a practical point of view we are interested in obtaining from this estimation some information on the choice of the grid distance h . The inequality (2.31) leads only to the information that $h < \rho$; this is not really very much. Of course, we may look for another way of solving this problem. Since we are dealing with a positive definite operator this property is fulfilled only with a grid distance chosen in such a way (Young and Gregory, 1973) that

$$0 < h \leq \text{Min}\left(\frac{2r}{|a|}, \frac{2r}{|b|}\right) \quad (2.32)$$

Again for the steady motion this inequality is somewhat disappointing, because $a \approx \frac{f}{H} \frac{\partial H}{\partial y}$. Therefore

$$h < \frac{2rH}{f} \frac{\partial y}{\partial H} \quad (2.33)$$

Replacing ∂y by h we obtain the condition for ∂H rather than for the grid distance, thus is $\partial H < \frac{2rH}{f}$. This means that for the solvability

of the problem the depth cannot change abruptly.

In contrast this information is very valuable for the transport phenomena in the horizontal plane. Since $r = K_x$ and $a = u$, we may write (2.32) as

$$h < \frac{2K_x}{u} = \frac{2 \times 10^8}{10^2} = 2 \times 10^6 \text{ cm} \quad (2.34)$$

This indicates that in the description of large scale diffusion processes a grid size smaller than 20 km should be chosen.

From the above we may conclude that the method of choosing a grid size in an elliptical problem so that it complies with a high order of accuracy in the numerical solution is not clear at all. A more practical way lies in comparing a simple analytical solution with a numerical one, and on this basis the final choice of h is made.

§3. Boundary conditions

In cases where the steady current is studied the boundary values of the stream function are known and there is no problem if all grid points lie exactly on an analytical boundary Γ . If the boundaries Γ and Γ_h do not coincide, one may use an interpolation formula to determine ψ at the net points which belong to the neighbourhood of Γ . Another solution to this problem consists in the introduction to the grid of different space steps in these parts of the domain D_h where Γ and Γ_h lie apart. Next the derivatives should be written on the new grid - see Collatz (1955).

Steady transport phenomena are characterized by a more complicated boundary condition, namely $\frac{\partial \psi}{\partial n} = 0$. This derivative is usually expressed on the right coast by forward differences and on the left coast by backward differences. In this way the derivatives have only first-order accuracy of approximation. We shall now present Samarski's (1971) useful method for increasing the order of approximation by retaining information from the differential equation. Again to simplify algebraic expressions we shall consider (2.1) along the x -axis only

$$\frac{\partial^2 \psi}{\partial x^2} + a_1 \frac{\partial \psi}{\partial x} = f_1(x, y) \quad (2.35)$$

$$\text{here } a_1 = \frac{a}{r_1}; \quad f_1 = \frac{f}{r_1}.$$

The boundary conditions are

$$\left. \frac{\partial \psi}{\partial x} \right|_{x=0} = 0; \quad \left. \frac{\partial \psi}{\partial x} \right|_{x=1} = 0 \quad (2.36)$$

The numerical form of the boundary condition on the left boundary is taken as a backward difference

$$\frac{\psi_1 - \psi_0}{h} = \frac{\partial \psi_0}{\partial x} + \frac{h}{2} \frac{\partial^2 \psi_0}{\partial x^2} + O(h^2) \quad (2.37)$$

The error of approximation in (2.37) is equal to $\frac{h}{2} \frac{\partial^2 \psi_0}{\partial x^2}$. If we subtract from the right side of (2.37) the term due to the error, the order of approximation will be proportional to h^2 . In order to achieve this aim, we rewrite condition (2.37) as

$$\frac{\psi_1 - \psi_0}{h} - \frac{\partial^2 \psi}{2 \partial x^2} = 0 \quad (2.38)$$

Via (2.35) we express $\frac{\partial^2 \psi_0}{\partial x^2}$ as $f_1 - a_1 \frac{\partial \psi_0}{\partial x}$, and introduce it into (2.38)

$$\frac{\psi_1 - \psi_0}{h} - \frac{h}{2} (f_1 - a_1 \frac{\partial \psi}{\partial x}) = 0 \quad (2.39)$$

Again, the analytical derivative $\frac{\partial \psi}{\partial x}$ in (2.39) can be altered to the difference form

$$\frac{\psi_1 - \psi_0}{h},$$

and finally the derivative with second-order accuracy is derived

$$\frac{\psi_1 - \psi_0}{h} \left(1 + \frac{ha_1}{2}\right) = \frac{hf_1}{2} \quad (2.40)$$

$$\frac{\psi_1 - \psi_0}{h} = \frac{hf_1}{2+ha_1}$$

The order of approximation obtained in the above formula is easily proved by the introduction of the difference form of $\frac{\partial \psi}{\partial x}$ from (2.37) and f_1 from (2.35). Then

$$\frac{\partial u}{\partial x} = 0 + O(h^2) \quad (2.41)$$

It is worth noting that the second order is obtained here with the directed (backward) derivative.

§4. Some general properties of the differential operators

Differential equation (2.1) may be solved numerically or analytically under fairly general conditions related to the coefficients of the equation. One of the most important properties of a differential operator is its positiveness. We shall call the operator (difference or differential) positive definite, if the scalar product of expressions $-L\vec{\psi}$ and $\vec{\psi}^*$ in domain \bar{D} is positive,

$$(-L\vec{\psi}, \vec{\psi})_{\bar{D}} = \iint_{\bar{D}} -L\vec{\psi} \cdot \vec{\psi}^* dx dy \geq 0 \quad (2.42)$$

In (2.24) $\vec{\psi}$ is the column vector and $\vec{\psi}^*$ is a transposed vector (that is a row vector). In the net domain the scalar product (2.42) acquires the form

$$(-L_h \psi_h, \psi_h)_{\bar{D}_h} = h^2 \sum_j \sum_k -L_h \psi_h \cdot \psi_h \geq 0 \quad (2.43)$$

Since the scalar product is considered in the closed domain \bar{D}_h it is important to take into account the boundary conditions at those points on the boundary.

We shall explain the notions of scalar product and positive operator on a very simple example. Let us take the homogeneous equation to describe one dimensional flow

$$-L \psi = -r \frac{d^2 \psi}{dx^2} - a \frac{d\psi}{dx} = 0 \quad (2.44)$$

To this we ascribe the following numerical form

$$-L_h \psi_h = -r \frac{\psi_{j+1} + \psi_{j-1} - 2\psi_j}{h^2} - a \frac{\psi_{j+1} - \psi_j}{h} = 0 \quad (2.45)$$

with the boundary conditions $\psi_0 = 0$, $\psi_J = 0$. The coefficients in the above equations are strictly positive.

The operator $-L_h \psi_h$ will be arranged in the form of a matrix A of coefficients and a column vector $\vec{\psi}$ which represents the values of the unknown function at the grid points.

$$\begin{bmatrix} 2r+ah & -r+ah & 0 & 0 \\ -r & 2r+ah & -r+ah & 0 \\ 0 & -r & 2r+ah & -r+ah \\ & & \cdot & \\ & & \cdot & \\ & & \cdot & \\ & -r & 2r+ah & \end{bmatrix} \begin{bmatrix} \psi_1 \\ \psi_2 \\ \psi_3 \\ \cdot \\ \cdot \\ \cdot \\ \psi_{J-1} \end{bmatrix} = \begin{bmatrix} 0 \\ 0 \\ 0 \\ \cdot \\ \cdot \\ \cdot \\ 0 \end{bmatrix} \quad (2.46)$$

First of all we may observe that the elements of the above matrix are not symmetrical on both sides of the main diagonal. Next, if we add the moduli of all elements of the matrix in any row or column (omitting a diagonal element), then it is clear that the modulus of the diagonal element is greater or equal to the sum of the moduli of the non-diagonal elements. Now we shall construct a scalar product $(-L\vec{\psi}, \vec{\psi}^*)$ in agreement with the multiplication rule of a matrix by a vector, thus

$$\begin{aligned}
 (-L\psi_h, \psi_h) &= (r + \frac{ah}{2})\psi_1^2 + (r + \frac{ah}{2})(\psi_1 - \psi_2)^2 \\
 &+ (r + \frac{ah}{2})(\psi_2 - \psi_3)^2 + \dots + (r + \frac{ah}{2})\psi_{J-1}^2 \quad (2.47)
 \end{aligned}$$

Since (2.47) is always positive we may state that the operator (2.45) is a positive definite one. In the case when the first derivative in (2.45) is chosen, not as a forward but as a backward or central difference, the positive property of the operator will not hold. Generally the positive definite property of an operator is strictly connected with the dominance of the main diagonal of coefficients in the matrix form of the difference equation. Sometimes the operator of an elliptical equation is called self-adjoint and then the equation (2.1) is written as (Young and Gregory, 1973)

$$\frac{\partial}{\partial x} (p \frac{\partial \psi}{\partial x}) + \frac{\partial}{\partial y} (q \frac{\partial \psi}{\partial y}) = f \quad (2.48)$$

subject to the condition that the coefficients in (2.1) are related as follows

$$a = \frac{\partial r_1}{\partial x}; \quad b = \frac{\partial r_2}{\partial y} \quad (2.49)$$

We have already written a numerical form (2.15) for equation (2.48). This is a numerical form of which the matrix of coefficients is

wholly symmetrical and therefore for such a matrix the required memory and amount of computation is greatly reduced. The self-adjoint operators and symmetrical matrices play a special role in the computational processes.

§5. Numerical methods of solution of partial differential equations of steady state

Let us again consider equation (2.1) in the next domain \bar{D}_h with boundary condition $\psi_{\Gamma_h} = 0$. The five-point difference equation is rearranged as follows

$$a_1\psi_{j+1,k} + a_2\psi_{j-1,k} + a_3\psi_{j,k+1} + a_4\psi_{j,k-1} - a_0\psi_{j,k} = f_{j,k} \quad (2.50)$$

Assuming that the number of internal grid points in \bar{D}_h is equal to N , and that in all points equation (2.1) has the form of (2.50) we come to N linear equations which we set in the matrix-vector form

$$A\vec{\psi} = \vec{c} \quad (2.51)$$

The matrix A contains only real quantities. On its diagonal the elements a_0 are nested; the vector $\vec{\psi}$ is a column vector with N elements (co-ordinates).

The methods of solution of this system may be subdivided into direct and iterative ones. The direct methods, such as the Gauss elimination procedure, give a solution in a finite number of steps, but they require big computer storage and are very time consuming (Ralston, 1965). The iterative methods contain simple algorithms which are easily repeated. They are very useful when applied to a sparse matrix like (2.46), where the elements are clustered around the main diagonal, but the solution is obtained as the limit of an iterative process.

In case the iterative method is applied, the equation (2.50) is rewritten as

$$\psi_{j,k}^{(n)} = \frac{a_1}{a_0}\psi_{j+1,k}^{(n-1)} + \frac{a_2}{a_0}\psi_{j-1,k}^{(n-1)} + \frac{a_3}{a_0}\psi_{j,k+1}^{(n-1)} + \frac{a_4}{a_0}\psi_{j,k-1}^{(n-1)} - \frac{f}{a_0} \quad (2.52)$$

where n denotes successive iterative steps. The simplified form of (2.52) in the matrix-vector notation is

$$\vec{\psi}^{(n)} = A\vec{\psi}^{(n-1)} + \vec{c} \quad (2.53)$$

The necessary and sufficient condition for the convergence of the iterative process (2.53) demands that the eigenvalues (proper numbers) of matrix A should be smaller than the modulus of unity (Faddeeva, 1959). Since, generally, the eigenvalues belong to the set of complex numbers we may state again the above condition in a geometrical form. Thus to fulfil the convergence condition, the eigenvalues should be confined within the unit circle in the plane of complex numbers. In what will follow the sufficient conditions described by the norm of a matrix or related conditions will be used. For the equation (2.50) and (2.52) the following inequalities should hold in order to fulfil the sufficient condition

$$a_0 \geq \sum_{m=1}^4 a_m \quad (2.54)$$

and

$$1 \geq \sum_{m=1}^4 a_m/a_0 \quad (2.55)$$

Therefore the diagonal elements of matrices A and A dominate the remaining elements in each row or column. Returning to the difference equation constructed in §1 of this chapter it is worth noticing that it was constructed in such a way as to retain the property of the dominant diagonal for the elements related to the function $\psi_{j,k}$. Although we ought to say that the study of the two-dimensional set of equations through the application of the vector-matrix notion is not obvious unlike the one-dimensional problem (2.46) which we have done already. A special way of indexing will be introduced in chapter VIII to effect the change from two-dimensional indexing j,k to one-dimensional indexing.

We can find a great number of iterative methods and procedures for accelerating the computations (Collatz, 1955; Ralston, 1965), but a theoretical basis has been worked out only for the simply connected domain of integration. In oceanographical problems where the domain is often multiply connected it is worth-while to start with simple iteration methods. In case the same problem has to be solved many times (for example with different external forces) as standard procedure, the method of acceleration is worth applying.

§6. Simple iteration method

The method is expressed by equation (2.53) and consists of constructing the sequence of column vectors which have N co-ordinates (components)

$$\begin{aligned}
 \vec{\psi}^{(1)} &= A\vec{\psi}^{(0)} + \vec{c} \\
 \vec{\psi}^{(2)} &= A\vec{\psi}^{(1)} + \vec{c} \\
 &\cdot \quad \quad \cdot \\
 &\cdot \quad \quad \cdot \\
 &\cdot \quad \quad \cdot \\
 \vec{\psi}^{(n)} &= A\vec{\psi}^{(n-1)} + \vec{c}
 \end{aligned} \tag{2.56}$$

Here the primes are omitted to make the notation simpler. If the elements of matrix A fulfil the sufficient condition (2.55), then the iteration process (2.56) converges to the analytical solution

$$\vec{\psi} = A\vec{\psi} + \vec{c} \tag{2.57}$$

For the arbitrary initial approximation $\vec{\psi}^{(0)}$ we shall find the condition for convergence of the iteration sequence to the analytical solution of (2.1). First we describe the error by the difference between the n-th iterative approximation $\vec{\psi}^{(n)}$ and the exact solution

$$\vec{v}^{(n)} = \vec{\psi} - \vec{\psi}^{(n)} \tag{2.58}$$

It is clear that $\vec{v}^{(n)}$ satisfies equation (2.52) with $f = 0$. Secondly we introduce the definition of the vector norm which we need for the following discussion (Faddeeva, 1959)

$$||\vec{v}^{(n)}|| = \text{Max}_{j,k} |v^{(n)}(j,k)| \tag{2.59}$$

Thus we may say that in this specific case it is the maximum modulus of the difference (2.58) taken over all points of the net. Generally this is a co-ordinate of a vector (in our case $\vec{v}^{(n)}$) with a maximum absolute value.

Denoting the elements of matrix A as $a_{j,k}$, where j stands for rows and k for columns, we define the matrix norm

$$||a_{j,k}|| = \text{Max}_j \sum_{k=1}^{N_j} |a_{j,k}| = \mu \tag{2.60}$$

Here N_1 denotes the number of columns in the matrix A .

We may say that by means of (2.60) the sum of the absolute values of the elements in the first row, next in the second row etc. is checked. The maximum sum is chosen to be a norm. For example the norm related to equation (2.52) is given by the expression

$$(|a_1| + |a_2| + |a_3| + |a_4|) / |a_0| \quad (2.61)$$

Returning to the convergence problem of the iterative sequence (2.56) we subtract (2.57) from the last equation in the sequence (2.56)

$$\vec{v}^{\rightarrow}(n) = \vec{v}^{\rightarrow}(n) - \vec{v}^{\rightarrow} = A(\vec{v}^{\rightarrow}(n-1) - \vec{v}^{\rightarrow}) = A\vec{v}^{\rightarrow}(n-1) \quad (2.62)$$

and applying the matrix and vector norms we obtain

$$||\vec{v}^{\rightarrow}(n)|| = ||A\vec{v}^{\rightarrow}(n-1)|| \leq ||A|| ||\vec{v}^{\rightarrow}(n-1)|| \leq \mu^n ||\vec{v}^{\rightarrow}(0)|| \quad (2.63)$$

If the norm of the initial value vector $\vec{v}^{\rightarrow}(0)$ is bounded

$$||\vec{v}^{\rightarrow}(0)|| = Q < \infty, \quad (2.64)$$

then convergence is based on the existence of the limit of the sequence (2.62)

$$\lim_{n \rightarrow \infty} ||\vec{v}^{\rightarrow}(n)|| \leq \lim_{n \rightarrow \infty} \mu^n Q \quad (2.65)$$

The iterative process (sequence) (2.56) is convergent if $\mu < 1$, that is to say the norm of matrix A has to be smaller than the modulus of unity. In the case of (2.52) the norm is expressed by (2.61). Therefore we may conclude that the condition $\mu < 1$ is analogous to the condition of dominance of diagonal elements in a matrix of coefficients.

§7. Gauss-Seidel method

The simple iterative method is based on the values of ψ computed during the previous step of the iteration. The central idea of the Gauss-Seidel method is to accelerate this process by using, in the course of the computation, the values recently derived during the same step. Thus at any grid point m , the values computed at the previous $m-1$ points are utilised. The Gauss-Seidel method of iteration is described by

$$\vec{\psi}^{(n)} = A_1 \vec{\psi}^{(n)} + A_2 \vec{\psi}^{(n-1)} \quad (2.66)$$

or in the developed form

$$\psi_j^{(n)} = \sum_{k=1}^{m-1} a_{jk} \psi_k^{(n)} + \sum_{k=m}^N a_{jk} \psi_k^{(n-1)} \quad (2.67)$$

Introducing matrix and vector norms in expression (2.66) we find

$$\|\vec{\psi}^{(n)}\| \leq \mu_1 \|\vec{\psi}^{(n)}\| + \mu_2 \|\vec{\psi}^{(n-1)}\| \quad (2.68)$$

where

$$\mu_1 = \|A_1\| = \max_j \sum_{k=1}^{m-1} |a_{jk}| \quad (2.69)$$

$$\mu_2 = \|A_2\| = \max_j \sum_{k=m}^N |a_{jk}| \quad (2.70)$$

The inequality (2.68) is easily transformed to

$$\|\vec{\psi}^{(n)}\| \leq \frac{\mu_2}{1-\mu_1} \|\vec{\psi}^{(n-1)}\| = \left[\frac{\mu_2}{1-\mu_1} \right]^n \|\vec{\psi}^{(0)}\| = \left[\frac{\mu_2}{1-\mu_1} \right]^n \cdot B \quad (2.71)$$

If the initial values are bounded $\|\vec{\psi}^{(0)}\| = B < \infty$ the convergence of the Gauss-Seidel iterative scheme is assured when

$$\frac{\mu_2}{1-\mu_1} < 1, \quad \mu_1 + \mu_2 < 1 \quad (2.72)$$

§8. Line inversion method

Although this method is best suited for solving ordinary differential equations of second order (Samarski, 1972), the method of splitting up the operator gives a new way of obtaining from the partial differential equation a system of ordinary differential equations (Marchuk, 1974; Janenko, 1967).

Let us therefore consider the ordinary differential equation

$$-L\psi = -\frac{d^2\psi}{dy^2} - p(y) \frac{d\psi}{dy} - q(y)\psi(y) = f(y) \quad (2.73)$$

with $q(y)$ positive and $p(y)$ to be defined later on.

Introducing the net with grid distance h , (2.73) may be written in the numerical form

$$\frac{2\psi_k - \psi_{k+1} - \psi_{k-1}}{h^2} - p_k \frac{\psi_{k+1} - \psi_{k-1}}{2h} - q_k \psi_k = f_k \quad (2.74)$$

The index k runs from 0 on the left boundary to N on the right one. It is important to understand that the approximation of the first derivative in the above equation is rather general. The real method of approximation depends here on many possibilities and the best situation arises when (2.73) is self-adjoint, when instead of

$$\frac{d^2\psi}{dy^2} + p \frac{d\psi}{dy}$$

one may write

$$\frac{d}{dy} \left(p_1 \frac{d\psi}{dy} \right).$$

This takes place only if $\frac{dp_1}{dy} = p$.

If it is not the case the appropriate results may give the expression (2.21). Either way the approximation should be written down to make the diagonal terms in the matrix of coefficients dominate over the nondiagonal terms.

To equation (2.73) we add the boundary conditions

$$\alpha_0 \psi_0 + \alpha_1 \frac{\psi_1 - \psi_0}{h} = A \quad (2.75)$$

on the left, and

$$\beta_0 \psi_N + \beta_1 \frac{\psi_N - \psi_{N-1}}{h} = B \quad (2.76)$$

on the right respectively.

Here A and B are known functions. $\alpha_0, \alpha_1, \beta_0, \beta_1$ are equal to zero or unity depending on what kind of boundary conditions are stated, i.e. the Dirichlet condition (given function), the Neumann condition (given derivatives of the function) and the mixed condition respectively.

We rearrange equation (2.74) to three-point form

$$-a_k \psi_{k-1} + b_k \psi_k - c_k \psi_{k+1} = d_k \quad (2.77)$$

In the following considerations we assume that $b_k > 0$, $a_k > 0$, $c_k > 0$. The diagonal dominance condition provides

They give the method for computing the coefficients s_k and e_k in all grid points starting from the left boundary value (2.75). This process is called forward elimination. The method is completed by a second process, backward elimination, whereby the values of ψ are calculated using expression (2.80) beginning from the right boundary condition (2.76).

In order to start this recurrence process it is necessary to find the initial coefficients s_1 and e_1 . From (2.75) ψ_0 is defined as

$$\psi_0 = \frac{Ah - \alpha_1 \psi_1}{\alpha_0 h - \alpha_1} \quad (2.86)$$

Next substituting ψ_0 into (2.77), written down on the grid point $k=1$

$$-a_1 \psi_0 + b_1 \psi_1 - c_1 \psi_2 = d_1 \quad (2.87)$$

we find a relationship between ψ_1 and ψ_2 . By comparing (2.87) and (2.81) at the grid point $k=1$, the coefficients required to start the recursion process may be defined in the following way

$$s_1 = \frac{c_1 (\alpha_0 h - \alpha_1)}{b_1 (\alpha_0 h - \alpha_1) + \alpha_1 a_1} \quad (2.88)$$

$$e_1 = \frac{d_1 (\alpha_0 h - \alpha_1) + a_1 Ah}{b_1 (\alpha_0 h - \alpha_1) + \alpha_1 a_1} \quad (2.89)$$

The method of line inversion has a very good computational property. First of all the iterative processes based on this method show the tendency to self-correction and they converge quite fast. The self-correction is related to the stability since any error introduced in the course of computation (say round-off error) is not amplified. The main condition to be fulfilled is formulated by (2.78). The method of line inversion was extended by Lindzen and Kuo (1969) to a wide class of ordinary and partial differential equations.

§9. Application of line inversion in the alternating-direction method

The line inversion method is applied to the elliptical equation in alternate directions. First the inversion is performed along the x-axis and then along the y-axis (or vice-versa). Each iteration step consists of two substeps. The method will be used to solve the equation (2.50).

Let us assume that the l -th iteration is already computed. In the first substep the function $\psi_{j,k}^{l+1/2}$ is evaluated

$$\begin{aligned} \psi_{j,k}^{l+1/2} = & \psi_{j,k}^l + \rho (a_1 \psi_{j+1,k}^{l+1/2} + a_2 \psi_{j-1,k}^{l+1/2} - \frac{a_0}{2} \psi_{j,k}^{l+1/2} - \frac{1}{2} f_{j,k}^{l+1/2}) \\ & + \rho (a_3 \psi_{j,k+1}^l + a_4 \psi_{j,k-1}^l - \frac{a_0}{2} \psi_{j,k}^l - \frac{1}{2} f_{j,k}^l) \end{aligned} \quad (2.90)$$

The line inversion method in this substep is applied to the j -co-ordinate. The unknown function $\psi_{j,k}^{l+1/2}$ is computed from known values of $\psi_{j,k}^l$. In the second substep the following algorithm is used

$$\begin{aligned} \psi_{j,k}^{l+1} = & \psi_{j,k}^{l+1/2} + \rho (a_1 \psi_{j+1,k}^{l+1/2} + a_2 \psi_{j-1,k}^{l+1/2} - \frac{a_0}{2} \psi_{j,k}^{l+1/2} - \frac{1}{2} f_{j,k}^{l+1/2}) \\ & + \rho (a_3 \psi_{j,k+1}^{l+1} + a_4 \psi_{j,k-1}^{l+1} - \frac{a_0}{2} \psi_{j,k}^{l+1} - \frac{1}{2} f_{j,k}^{l+1}) \end{aligned} \quad (2.91)$$

In this substep the inversion method is applied to the k -co-ordinate, and the function $\psi_{j,k}^{l+1}$ is calculated from the known function $\psi_{j,k}^{l+1/2}$. The quantity ρ is a positive constant called the iteration parameter. Its optimum choice is rather difficult, but if we observe that the iteration process is analogous to the equation which depends on time, then ρ is closely related to the time step T . To show this analogy let us introduce into (2.1) the time parameter then

$$\frac{\partial \psi}{\partial t} = r \Delta \psi + a \frac{\partial \psi}{\partial x} + b \frac{\partial \psi}{\partial y} - f \quad (2.92)$$

Here $r=r_1=r_2=\text{constant}$ and Δ is the Laplacian operator. Equation (2.92) with a suitable boundary condition gives the solution to the steady problem expressed by (2.1), when $t \rightarrow \infty$.

Using the methods described by Janenko (1967) we split up the equation (2.92) into a system of equations

$$\frac{1}{2} \frac{\partial \psi}{\partial t} = \frac{r}{2} \Delta \psi + \frac{a}{2} \frac{\partial \psi}{\partial x} + \frac{b}{2} \frac{\partial \psi}{\partial y} - \frac{f}{2} \quad (2.93a)$$

$$\frac{1}{2} \frac{\partial \psi}{\partial t} = \frac{r}{2} \Delta \psi + \frac{a}{2} \frac{\partial \psi}{\partial x} + \frac{b}{2} \frac{\partial \psi}{\partial y} - \frac{f}{2} \quad (2.93b)$$

Considering this system on two substeps l , $l+1/2$ and $l+1/2$, l it may be written down on the first substep as

$$\frac{\psi_{j,k}^{l+1/2} - \psi_{j,k}^l}{T} = \frac{r}{2} \frac{\partial^2 \psi_{j,k}^{l+1/2}}{\partial x^2} + \frac{a}{2} \frac{\partial \psi_{j,k}^{l+1/2}}{\partial x} - \frac{f_{j,k}^l}{2} + \frac{r}{2} \frac{\partial^2 \psi_{j,k}^l}{\partial y^2} + \frac{b}{2} \frac{\partial \psi_{j,k}^l}{\partial y} \quad (2.94)$$

and on the second substep as

$$\frac{\psi^{l+1} - \psi^{l+1/2}}{T} = \frac{r\partial^2\psi^{l+1}}{2\partial y^2} + \frac{b\partial\psi^{l+1}}{2\partial y} - \frac{f^{l+1}}{2} + \frac{r\partial^2\psi^{l+1/2}}{2\partial x^2} + \frac{a\partial\psi^{l+1/2}}{2\partial x} \quad (2.95)$$

It is clear from the above that equation (2.94) is related to equation (2.90) and (2.95) to (2.91), thus the iteration parameter is analogous with time in physical processes. The methods for choosing the time step T will be described in the course of analysing the unsteady phenomena (Chapter IV, §13).

REFERENCES

- Collatz, L., 1955. Numerische Behandlung von Differentialgleichungen. Springer-Verlag, Berlin.
- Faddeeva, V.N., 1959. Computational Methods of Linear Algebra. Dover Publication, New York.
- Forsythe, G.E. and Wasow, W.R., 1960. Finite Difference Methods for Partial Differential Equations. John Wiley and Sons Nnc., New York.
- Fox, L., 1962. Numerical Solution of Ordinary and Partial Differential Equations. Addison-Wesley Pub. Co., Reading, Mass.
- Janenko, N.N., 1967. The Small Steps Method of Solving the Mathematical Physics Problem (in Russian). Published by Nauka. Moscow.
- Lindzen, R.S. and Kuo, H.L., 1969. A Reliable Method of the Numerical Integration of a Large Class of Ordinary and Partial Differential Equations. Monthly Weather Review v.97, N. 10: 732-734
- Marchuk, G., 1974. Numerical Solution of Sea and Air Dynamic's Problems (in Russian). Published by Gidrometeoizdat, Leningrad.
- Ralston, A., 1965. A First Course in Numerical Analysis. Mc Graw-Hill, New York.
- Samarski, A.A., 1971. Introduction to the Theory of Difference Schemes (in Russian). Published by Nauka. Moscow.
- Young, D.M. and Gregory, R.T., 1973. A Survey of Numerical Mathematics. v.II, Addison-Wesley Pub. Co., Reading, Mass.

Chapter III STEADY MOTION – OCEANOGRAPHICAL EXAMPLES

In this chapter the system of equations (1.24) and (1.25) is applied to study steady currents ($\frac{\partial}{\partial t} \approx 0$), when the nonlinear phenomena are of no importance. Since the equations are now linear and if we take the bottom friction in the linear form (1.63), it is possible to obtain an analytical solution in a simple-shaped sea area. We shall briefly introduce such solutions here, since they play an important rôle in testing the numerical calculation.

The main part of this chapter is devoted to the numerical description of the three-dimensional current distribution in the sea. The current distribution in the vertical direction is solved using the superposition principle. The currents due to wind stress, sea-level variations and density distribution are found in a different way and afterwards are superposed. The central problem of this chapter is the elliptical nonhomogeneous equation for the stream function of mean current which results from the search for the current component due to sea-level variations.

The presented pattern of mean barotropic flow shows a clear dependence on the interaction between the wind stress and the bottom slope.

The interaction of the baroclinic component of flow with the bottom relief plays the main role in establishing the circulation when density stratification exists.

§1. Motion in channels - analytical solution

To construct an analytical solution in a channel in order to describe the steady flow we start from the system of equations (1.4), (1.24) and (1.25), assuming that

- a) the Coriolis force does not play any role,
- b) the depth H is constant,
- c) the transverse velocity v is very small, and
- d) $\frac{\partial \zeta}{\partial t} = \frac{\partial u}{\partial t} = 0$.

Then the equations take the form

$$-g \frac{\partial \zeta}{\partial x} + k \frac{\partial^2 u}{\partial z^2} = 0 \quad (3.1)$$

and

$$\frac{\partial u}{\partial x} + \frac{\partial w}{\partial z} = 0 \quad (3.2)$$

Since at the bottom, due to the friction, the velocity disappears, the following set of boundary conditions will be valid

$$u \Big|_{z=-H} = 0, \quad w \Big|_{z=-H} = 0 \quad (3.3)$$

At the sea surface the wind acts causing the stress

$$ku \Big|_{z=\zeta} = \tau_s^{(x)} \quad (3.4)$$

For the vertical velocity the kinematic condition (1.37) provides at the sea surface

$$w = \frac{d\zeta}{dt} = \frac{\partial \zeta}{\partial t} + u \frac{\partial \zeta}{\partial x} \quad (3.5)$$

Firstly the equation of motion (3.1) is integrated over z

$$uk = \frac{1}{2} g \frac{\partial \zeta}{\partial x} z^2 + az + b \quad (3.6)$$

The integration constants a and b can be determined from the boundary conditions (3.3) and (3.4). Therefore

$$u = \frac{1}{k} \frac{1}{2} g \frac{\partial \zeta}{\partial x} (z^2 - H^2) + (\tau_s^{(x)} - g\zeta \frac{\partial \zeta}{\partial x}) (z + H) \quad (3.7)$$

In the above $\frac{\partial \zeta}{\partial x}$ does not depend on the vertical co-ordinate z , but it is unknown. The usual way of solving this problem is to construct an additional equation by integrating (3.1) from the bottom $z=-H$ up to the surface $z = \zeta$

$$\tau_s^{(x)} = g (H + \zeta) \frac{\partial \zeta}{\partial x} \quad (3.8)$$

When $\zeta \ll H$, the sea-level along the x -axis is

$$\zeta = \zeta_0 + \frac{x\tau_s^{(x)}}{gH} \quad (3.9)$$

This simple formula says that the sea-level is proportional to the tangential wind stress $\tau_s^{(x)}$ and the path x , but inversely proportional to the depth. With constant depth and wind stress the free surface is a plane. We can see from this that even simple equations lead to convenient results that reproduce the natural conditions qualitatively. It is worth noticing that in (3.8) and (3.9) the sea-level does not

depend on the bottom stress, since the mass transport in one-dimensional steady flow is equal to zero.

Hansen (1950) presented a nonlinear equation relating the sea-level to the wind stress

$$H + \zeta = H + \zeta_0 \left[1 + \frac{3\tau_s(x)x}{g(H+\zeta_0)^2} \right]^{1/2} \quad (3.10)$$

For the large depths we may develop the squareroot according to the Taylor series and write approximately

$$H + \zeta = H + \zeta_0 + \frac{3}{2} \frac{\tau_s(x)}{2g(H+\zeta_0)} \quad (3.11)$$

We shall proceed with the analysis of the action of a steady wind acting in a channel. In the case of a shallow water channel with a constant depth (3.8) may be rewritten in a special form

$$(H+\zeta) \frac{d\zeta}{dx} = \frac{\tau_s(x)}{gH} = \text{constant} = c \quad (3.12)$$

and its solution is

$$\zeta = -H + \sqrt{2c\sqrt{x - L_0}} \quad \text{if } x > L_0 \quad (3.13)$$

$$\zeta = -H \quad \text{if } x \leq L_0$$

Here L_0 is the co-ordinate of the water line which consists of the boundary between the areas covered and uncovered by water (Fig. 5). The value of L_0 is found from the statement of the profile

$$\int_{L_0}^L (H + \zeta) dx = HL \quad (3.14)$$

which can be rearranged in the form

$$L_0 = L - \left[\frac{3}{2\sqrt{2c}} \frac{HL}{L} \right]^{2/3} \quad \text{if } L_0 > 0 \quad (3.14a)$$

The following figures present a comparison between the analytical and numerical solutions under different wind and depth conditions in a channel of 36 km length. The difference, as plotted in the figures, can be interpreted as a measure of the accuracy of the numerical method used in the computation.

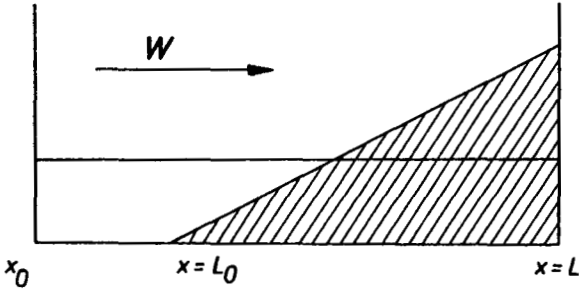


Fig. 5. SEA-LEVEL VARIATIONS UNDER THE ACTION OF WIND W IN ONE-DIMENSIONAL GEOMETRY.

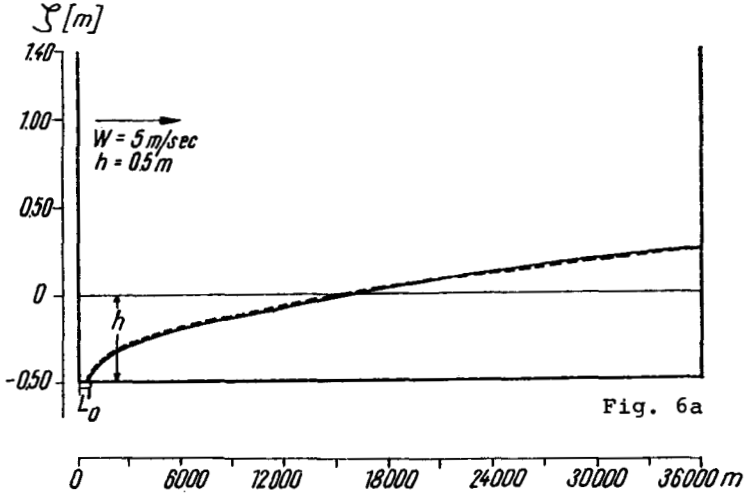


Fig. 6a

----- ANALYTICAL SOLUTION _____ NUMERICAL RESULT

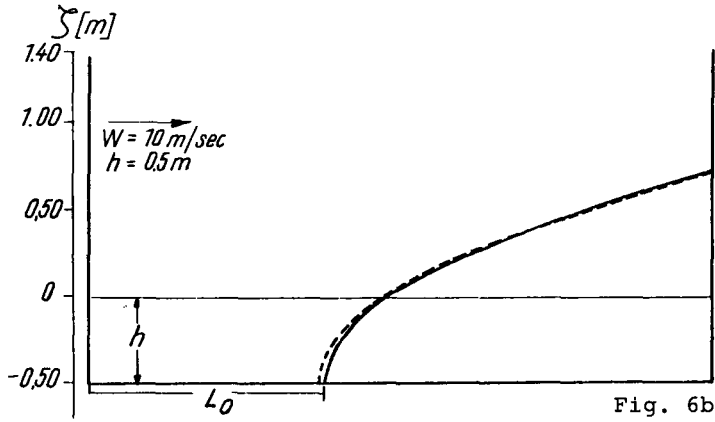


Fig. 6b

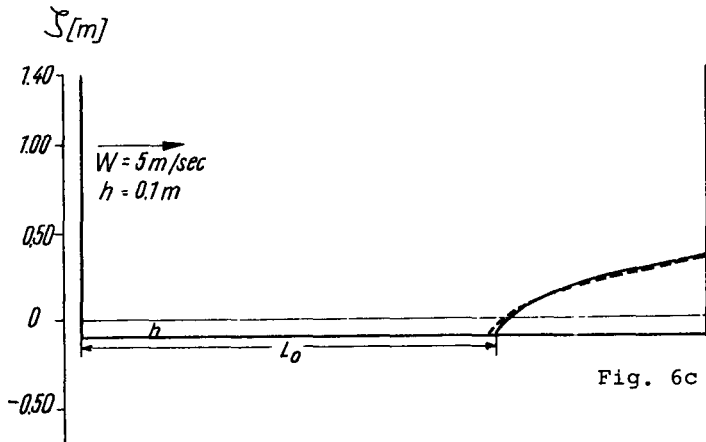


Fig. 6c

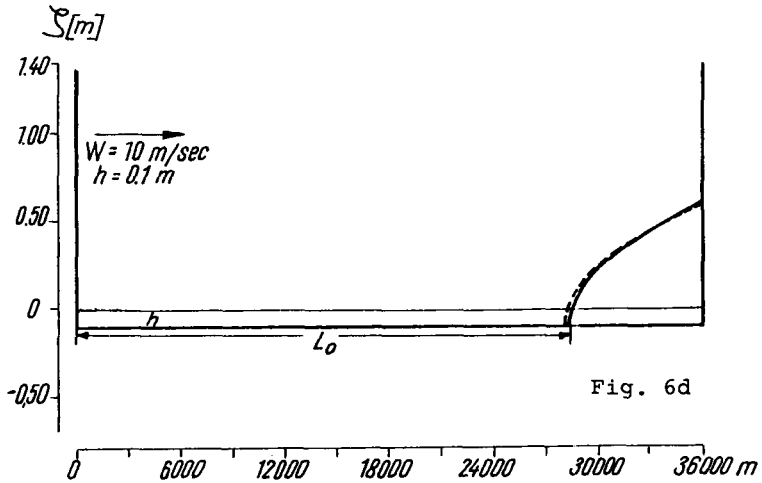


Fig. 6d

Figs. 6. SLOPE OF THE SEA SURFACE UNDER THE ACTION OF A HOMOGENEOUS AND CONSTANT WIND.

§2. Wind-driven currents in a shallow sea

We have just studied the wind-driven motion in a simplified physical situation. Now let us approach the three-dimensional motion. Although this kind of motion can be described by means of several dynamic models that of Ekman (1905,1923) seems to have the most physically-sound base. The main external force, i.e. wind stress, will cause a drift current and a transfer of momentum in the vertical direction. At the same time the presence of the coast will change the level of the sea, and so the second type of current, due to the slope of the sea surface, is observed.

In the linear Ekman model the current is a simple superposition of the two types of current, that is the result of the superposition of the solutions of homogeneous and nonhomogeneous differential equations.

The current \vec{u} can be written as

$$\vec{u} = f_1(\vec{\tau}) + f_2(\nabla\zeta) \quad (3.15)$$

where $f_1(\vec{\tau})$ is the current due to the wind stress $\vec{\tau}$, and $f_2(\nabla\zeta)$ is the current due to the slope of the sea surface $\nabla\zeta$.

The first part of the solution is strictly defined because the wind stress is a known function of the wind speed and the direction across the sea. The second part is unknown, and an additional equation for the slope should be given. The difficulties which arise here fit into two categories; the first is connected with a compensation of the surface slope by the vertical gradient of density (this effect gives $\nabla\zeta = 0$ at a certain depth) and the second is due to the lack of sufficient knowledge about the vertical eddy viscosity coefficient being a function of depth, wind, etc. These difficulties usually force the use of the method of vertical integration of the horizontal current and lead to the computation of the mass transport instead of the current.

In a shallow sea where the baroclinic effect does not seem to be very important, the slope of the sea surface should not change with depth. The fulfilment of the above supposition clarifies our definition of a shallow sea. Thus in this chapter a shallow sea is a sea where the baroclinic effect is negligible. One can vertically integrate the Ekman equations for current and in this way obtain an additional equation for determining the slope. This allows us to obtain the current field through equation (3.15).

In many cases finding the slope of the sea surface from the differential equation of the water level variation is a rather difficult task, because the boundary conditions for this problem are not always clear. To overcome this obstacle one usually uses a stream function and looks for the solution of an elliptical differential equation for this stream function.

In a real sea, additional problems arise in connection with islands. The region of integration is changed from a simply- to a multiply-connected domain and auxiliary boundary conditions must be introduced to obtain values of the stream function inside the region. The ideas for such conditions can be found in the theory of elasticity but it seems that Kamenkovitch (1961) was the first to give such conditions for the dynamic problems in the sea. It should be added that the Ekman theory has undergone many changes and the works of Felzenbaum (1960), Saint-Guilly (1959, 1962) and Welander (1957) are of extreme importance in this connection.

§3. Ekman equations

The Ekman equations for steady wind-driven currents can be written on the basis of the equations (1.24) and (1.25)

$$-\rho f v = -\rho g \frac{\partial \zeta}{\partial x} + k \frac{\partial^2 u}{\partial z^2} \quad (3.16)$$

and

$$\rho f u = -\rho g \frac{\partial \zeta}{\partial y} + k \frac{\partial^2 v}{\partial z^2} \quad (3.17)$$

The boundary conditions are usually taken as follows: at the surface of the sea ($z = \zeta = 0$)

$$\tau_s(x) = k \frac{\partial u}{\partial z}; \quad \tau_s(y) = k \frac{\partial v}{\partial z} \quad (3.18)$$

and at the bottom ($z = -H$)

$$u = v = 0 \quad (3.19)$$

To find the solution of the system (3.16), (3.17) with boundary conditions (3.18), (3.19) one multiplies (3.17) by the complex number $i = \sqrt{-1}$ and adds (3.16) to (3.17). The solution of the resulting

differential equation is a sum of solutions of the homogeneous and nonhomogeneous equations

$$s = u + iv = \frac{\tau \sinh \alpha (H+z)}{\alpha k \cosh \alpha H} + \frac{Kg i}{f} \left\{ \frac{\cosh \alpha z}{\cosh \alpha H} + 1 \right\} \quad (3.20)$$

where

$$\alpha = \left\{ \frac{f}{2u} \right\}^{1/2} (1 + i); \quad \tau_s = \tau_s^{(x)} + i \tau_s^{(y)}; \quad -K = \frac{\partial \zeta}{\partial x} + i \frac{\partial \zeta}{\partial y}$$

Now, in equation (3.20) the part with the water level variation K is unknown. To find this component we assume that in a shallow sea water level variations are not compensated by the vertical gradient of density. In this case the value of K in (3.20) is taken as constant and does not depend on depth. With this assumption we involve the additional equation for obtaining the value of K by vertical integration of (3.16) and (3.17).

§4. The mass transport and stream function equations

Integrating equations (3.16) and (3.17) over the depth from the bottom $z = -H$ to the surface $z = \zeta$ one finds

$$-fM_y = -\rho g H \frac{\partial \zeta}{\partial x} + \tau_s^{(x)} - R_1 M_x \quad (3.21)$$

$$fM_x = -\rho g H \frac{\partial \zeta}{\partial y} + \tau_s^{(y)} - R_1 M_y \quad (3.22)$$

The bottom stress components $\rho k \frac{\partial u}{\partial z} \Big|_{z=-H}$ and $\rho k \frac{\partial v}{\partial z} \Big|_{z=-H}$ are taken in the linearized form as $R_1 M_x$ and $R_1 M_y$ respectively. The value of the frictional coefficient R_1 is assumed to be constant and will be given later, but it is related to the expression (1.63), since $R_1 = \frac{R}{H}$.

In obtaining the solution (3.20) and equations (3.21), (3.22) an additional assumption is involved, namely, the sea-level variations ζ have to be smaller than the depth of the sea H at a given point. This excludes the very shallow part of the sea from further consideration.

Equations (3.18) and (3.19) account for two boundary conditions, one at the surface and the other at the bottom. In addition, with the aid of the mass transport scheme, one can establish a boundary condition at the sea coast. The mass transport component normal to the coastline is taken as zero:

$$M_n = 0 \quad (3.23)$$

The principal aim in computing the field of current by means of equation (3.20) will be achieved if the components of the mass transport are known, since one can then obtain the components of the slope $\frac{\partial \zeta}{\partial x}$, $\frac{\partial \zeta}{\partial y}$ from (3.21) and (3.22). Now a new problem arises, that of finding the mass transport in the sea. First of all we observe that the continuity equation for the horizontal mass transport is valid

$$\frac{\partial M_x}{\partial x} + \frac{\partial M_y}{\partial y} = 0 \quad (3.24)$$

This equation is satisfied if we define the stream function by setting

$$M_x = \frac{\partial \psi}{\partial y}; \quad M_y = -\frac{\partial \psi}{\partial x} \quad (3.25)$$

From equations (3.21) and (3.22) by cross differentiation and by using (3.24) and (3.25) we can eliminate $\frac{\partial \zeta}{\partial x}$, $\frac{\partial \zeta}{\partial y}$ and come to the final equation (Kowalik, 1969)

$$R_1 \Delta \psi + \frac{f}{H} J(H, \psi) - \frac{R_1}{H} (\nabla H \nabla \psi) + \beta \frac{\partial \psi}{\partial x} = (\text{rot} \vec{\tau})_z + \frac{1}{H} \left(\frac{\partial H}{\partial x} \tau_s(y) - \frac{\partial H}{\partial y} \tau_s(x) \right) \quad (3.26)$$

where the symbols are defined as follows

$\Delta = \frac{\partial^2}{\partial x^2} + \frac{\partial^2}{\partial y^2}$	the two-dimensional Laplacian operator
$J(H, \psi) = \frac{\partial H \partial \psi}{\partial x \partial y} - \frac{\partial H \partial \psi}{\partial y \partial x}$	the Jacobian operator
$\nabla = \vec{i} \frac{\partial}{\partial x} + \vec{j} \frac{\partial}{\partial y}$	the two-dimensional nabla operator
$(\nabla H \nabla \psi)$	the two-dimensional scalar product
$(\text{rot} \vec{\tau})_z$	the vertical z-components of $\text{rot} \vec{\tau}$
$\beta = \frac{\partial f}{\partial y}$	the latitudinal variation in the Coriolis parameter f

The β -term will be neglected in subsequent calculations.

Boundary conditions for equation (3.26) can be found by assuming that the coast of the sea is described by an analytical curve $\Gamma_0(x, y)$. One can choose two directions, normal \vec{n} and tangential \vec{s} to this curve, as shown in fig. 7. With this assumption the boundary condition (3.23) becomes

$$M_n = \frac{\partial \psi}{\partial s} = 0; \quad \psi(s) \Big|_{\Gamma_0} = \text{const.} = c_0 \quad (3.27)$$

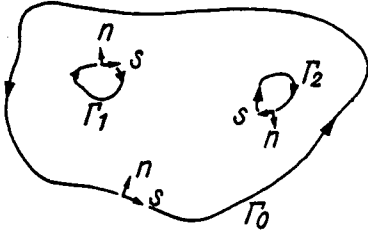


Fig. 7. INTEGRATION CONTOUR IN THE MULTIPLY-CONNECTED DOMAIN.

Thus the problem of finding the mass transport is transformed into the elliptical equation for the stream function (3.26) which, with boundary conditions (3.27), constitutes the Dirichlet problem. It appears that the task of computing the field of horizontal current is now formulated. We have proceeded through the sequence of equations beginning with equation (3.20) and ending with equation (3.26). But additional difficulties arise when island structures are to be incorporated into the solution. Let $\Gamma_1, \Gamma_2, \dots, \Gamma_n$ be the contours characterizing the islands inside the main contour Γ_0 as shown in fig. 7. Then the conditions (3.27) hold on every contour as

$$\psi \Big|_{\Gamma_1} = c_1; \quad \psi \Big|_{\Gamma_2} = c_2; \quad \dots; \quad \psi \Big|_{\Gamma_n} = c_n \quad (3.28)$$

At this point the problem is unspecified because the values of the integration constant are not known. When there are no islands (simply connected domain) one can take $\psi \Big|_{\Gamma_0} = c_0$ as zero and obtain the solution of equation (3.26). This is not the case for the multiply-connected domain. It is possible to assign a definite value to one of the arbitrary constants of integration c_0, c_1, \dots, c_n and for our later use we take the value c_0 on contour Γ_0 as zero. And thus we come to the problem of finding a solution for (3.26) in the multiply-connected domain with the following boundary conditions

$$\psi \Big|_{\Gamma_0} = 0; \quad \psi \Big|_{\Gamma_1} = c_1; \quad \dots; \quad \psi \Big|_{\Gamma_n} = c_n \quad (3.29)$$

§5. Solution of the Dirichlet problem for elliptical equations in the multiply-connected domain

Let us assume for the moment that the constants c_1, c_2, \dots, c_n are known. Equation (3.26) is linear and so are the boundary conditions (3.29). This gives us an opportunity to use the principle of superposition in constructing the solution of (3.26) as the sum of solutions of the nonhomogeneous equation (3.26) with homogeneous boundary conditions $c_0 = c_1 = \dots = c_n = 0$ and the homogeneous equation with nonzero boundary conditions $c_0 = 0, c_1 \neq 0$ or $c_2 \neq 0$ or ... or $c_n \neq 0$. In accordance with above the solution of (3.26) is

$$\psi = \psi_0 + \sum_{k=1}^n c_k \psi_k \quad (3.30)$$

where ψ_0 is the solution of (3.26) with homogeneous boundary conditions

$$\psi_0 \Big|_{\Gamma_0} = \psi_0 \Big|_{\Gamma_1} = \dots = \psi_0 \Big|_{\Gamma_n} = 0 \quad (3.31)$$

and ψ_k is the solution of the homogeneous part of equation (3.26) with boundary conditions

$$\psi_k \Big|_{\Gamma_k} = 1, \psi_j \Big|_{\Gamma_j} = 0 \quad \text{with } j \neq k, j = 1, \dots, n \quad (3.32)$$

When looking for the solution of the Dirichlet problem in the form of the sum (3.30), the boundary values on the contours $\Gamma_1, \Gamma_2, \dots, \Gamma_n$ are defined as 1; however, the values of the constants c_1, c_2, \dots, c_n are still unknown. In order to find them we introduce some auxiliary conditions connected with integration along a contour in a multiply-connected domain. Suppose we move along the closed contour Γ_k . On arriving at the same point we started from, we observe that the values of the field variables have not changed, since there is a steady state. Suppose for the stream function that $d\psi = 0$ along Γ_k , and for the level variations that $d\zeta = 0$. The last condition in the integral form is

$$\oint_{\Gamma_k} \frac{\partial \zeta}{\partial s} ds = \oint_{\Gamma_k} (\nabla \zeta ds) = 0 \quad (3.33)$$

The value of such an integral depends on the direction of motion along contour Γ_k , as shown in fig. 7. If one performs such an integration along every contour $\Gamma_1, \Gamma_2, \dots, \Gamma_n$, it transpires that there are n conditions for determining the n arbitrary constants c_1, c_2, \dots, c_n . For this reason one can rewrite equations (3.21) and (3.22) in vector form

$$\frac{1}{\rho g H} [\vec{f}\vec{M}] = -\nabla\zeta + \frac{\vec{\tau} - r\vec{M}}{\rho g H} \quad (3.34)$$

Multiplying (3.34) by $d\vec{s}$ using scalar products and integrating along the contour Γ_k one finds

$$\oint_{\Gamma_k} \left\{ \frac{1}{\rho g H} [\vec{f}\vec{M}] \right\} d\vec{s} = - \oint_{\Gamma_k} (\nabla\zeta \cdot d\vec{s}) + \oint_{\Gamma_k} \frac{1}{\rho g H} (\vec{\tau} - r\vec{M}) \cdot d\vec{s} \quad (3.35)$$

Taking into account the boundary condition for mass transport (3.23) and expression (3.33), equation (3.35) becomes

$$\oint_{\Gamma_k} \frac{\tau_s}{c^2} ds = \oint_{\Gamma_k} \frac{r}{c^2} M_s ds = \oint_{\Gamma_k} \frac{r}{c^2} \frac{\partial\psi}{\partial n} ds \quad (3.36)$$

where τ_s, M_s are the components of wind stress and transport in the \vec{s} direction and $c^2 = gH$

At last inserting (3.30) in (3.36) we obtain the final system of equations for defining the arbitrary constants c_1, c_2, \dots, c_n

$$\oint_{\Gamma_k} \frac{\tau_s}{c^2} ds = \oint_{\Gamma_k} \frac{r}{c^2} \left(\frac{\partial\psi_0}{\partial n} + \sum_{l=1}^n \frac{\partial\psi_l}{\partial n} \right) ds \quad (3.37)$$

where $k = 1, 2, \dots, n$.

§6. Determination of eddy viscosity

The most important parameter in the problem being considered is the eddy viscosity coefficient k . The knowledge of this coefficient as a function of wind speed W , density of water ρ , depth of the sea H and the Coriolis parameter f is essential for the calculation of the current (since it does not appear appropriate to develop an analytical solution). Later we take k from the range 1 to 10^3 CGS units to obtain the best agreement with observation.

The eddy viscosity coefficient's dependence on the above-stated parameters was published by Felzenbaum (1960). We will use two expressions:

1. for the shallow sea (in the Ekman sense), when the Coriolis force does not play a significant role*

$$v_1 = \frac{k_1}{\rho} = (0.54 \times 10^{-4}) WH \quad (3.38)$$

2. for the deep sea, when a current does not depend on depth

$$v_2 = \frac{k_2}{\rho} = (4.7 \times 10^{-8}) \frac{W^2}{f} = (4.7 \times 10^{-4}) W^2 \quad (3.39)$$

Equating (3.38) and (3.39) yields

$$H_1 = (8.7 \times 10^{-4}) \frac{W}{f} \quad (3.40)$$

the depth which separates the two regions for which (3.38) and (3.39) are developed. Thus, if the depth of the sea at a given point is H , one can use (3.38) or (3.39) according to the following criterion

$$\text{if } H_1 > H \text{ then } k = k_1; \text{ if } H_1 < H \text{ then } k = k_2 \quad (3.41)$$

In section 4 the constant R_1 was involved in connection with bottom stress. This constant for small depth can be calculated by means of the Ekman results (1905)

$$R_1 = \frac{\pi k}{4H^2} \approx \frac{k}{H^2} \quad (3.42)$$

The order of magnitude of R_1 is usually 10^{-4} to 10^{-6} CGS units. In this calculation we experimented with some values of R_1 over the range 10^{-5} to 10^{-6} CGS units and came to the same conclusion as Lauwerier (1962), that the small changes in R_1 do not play a serious role in the final value of mass transport.

§7. Some simplified models

To begin with let us take a rectangular sea with the sides $a=200$ km along the x -axis and $b=100$ km along the y -axis. Our purpose is to learn about current distributions in connection with different winds, bottom slopes and the presence of islands in the sea.

*Note that our original definition of the shallow sea is connected with the absence of a baroclinic effect.

A. Analytical solution

For simplified conditions - constant depth and a not very much complicated wind field - an analytical solution may be derived. Assuming a steady and uniform wind acting in the positive x-direction equation (3.26) takes the form

$$R_1 \Delta \psi = 0 \quad (3.43)$$

With the boundary condition (3.27) the mass transport components in the domain of integration are $M_x = 0$, $M_y = 0$ and the system of equations (3.21), (3.22) simplifies to

$$-gH \frac{\partial \zeta}{\partial x} + \tau_s(x) = 0 \quad (3.44)$$

From (3.44) the water elevation is described by

$$\zeta = \frac{\tau_s(x)}{gH} \left(\frac{a}{2} - x \right) \quad (3.45)$$

If one assumes a constant depth of $H = 50$ m and steady winds blowing in the positive x-direction but with speed varying along the y-axis (Fig. 8), the equation (3.26) for the stream function takes the form

$$R_1 \Delta \psi = \frac{\partial \tau_s(x)}{\partial y} \quad (3.46)$$

with boundary conditions

$$\psi(0, y) = \psi(x, 0) = \psi(a, y) = \psi(x, b) = 0 \quad (3.47)$$

Taking the wind speed $W = W_x = qy$, equation (3.46) can be rewritten as

$$\Delta \psi = k'y \quad (3.48)$$

where $k' = \frac{2yrg^2}{R_1}$. The solution of (3.48) has already been found in elasticity (see Kac, 1956) as

$$\psi = k' \frac{y}{3!} (y^2 - b^2) - k' \frac{2b}{\pi^3} \sum_{n=0}^{\infty} \frac{(-1)^n}{n^3} \sinh \frac{n\pi}{b} x \sinh \frac{n\pi}{b} y / \sinh \frac{n\pi}{b} a \quad (3.49)$$

At the same time a numerical solution of equation (3.46) can be found by transforming the equation into finite difference form with the help of expression (2.13)

$$\frac{R_1}{h^2}(\psi_{j+1,k} + \psi_{j-1,k} + \psi_{j,k+1} + \psi_{j,k-1} - 4\psi_{j,k}) = \frac{1}{2h}(\tau_{s,j,k+1}^{(x)} - \tau_{s,j,k-1}^{(x)}) \quad (3.50)$$

where $x = y = k$ is the mesh size and j, k the mesh point with the co-ordinates x and y respectively. The solution of equation (3.50) can be obtained by the iteration method if one takes (3.50) in the form

$$\psi_{j,k} = \frac{1}{4}(\psi_{j+1,k} + \psi_{j-1,k} + \psi_{j,k+1} + \psi_{j,k-1}) + \frac{h}{8R_1}(\tau_{s,j,k-1}^{(x)} - \tau_{s,j,k+1}^{(x)}) \quad (3.51)$$

This iteration scheme will be convergent since condition (2.55) is fulfilled here.

The results of the computation are plotted in fig. 8. The a-symmetry in the distribution of the streamlines is at once seen to be associated with the wind distribution along the y -axis.

Since the mass transport is known, we can now find $\frac{\partial \zeta}{\partial x}$ and $\frac{\partial \zeta}{\partial y}$ from equations (3.21) and (3.22). Inserting these values in equation (3.20) one obtains the current. The surface current, calculated in such a way, is given in fig. 9. Maximum values of current (up to 150 cm/sec) are observed in that part of the sea where the wind is strongest. The strong currents are not only due to the action of the wind, but also to the slope which is large. This can be seen at the bottom of fig. 9 where the currents appear to be due only to the slope, with values up to 70 cm/sec. The dependence of the current on depth is shown in fig. 10. This is at the point with co-ordinates $x = 120$ km and $y = 20$ km in fig. 8.

The vertical distribution of the current apparently has no connection with the Coriolis force. To complete this analysis we would like to stress the fact that such a strong curl of wind stress is rather unusual for steady state conditions in nature.

B. Constant wind stress and non-uniform depth

Assume that the depth of the sea is varying along the x -axis as $H = (2.5 \times 10^{-4})x + (25 \times 10^2)$ cm, and wind is blowing to the north with the constant speed of $W = W_y = 8$ m/sec. Equation (3.26) is now changed into

$$R_1 \Delta \psi + \frac{f \partial H \partial \psi}{H \partial x \partial y} - \frac{R_1 \partial H \partial \psi}{H \partial x \partial x} + \beta \frac{\partial \psi}{\partial x} = \frac{1 \partial H}{H \partial x} \tau_s^{(y)} \quad (3.52)$$

In this equation we retain for the moment expression $\beta \frac{\partial \psi}{\partial x}$ to show the well-known fact that the variations of the depth can give rise

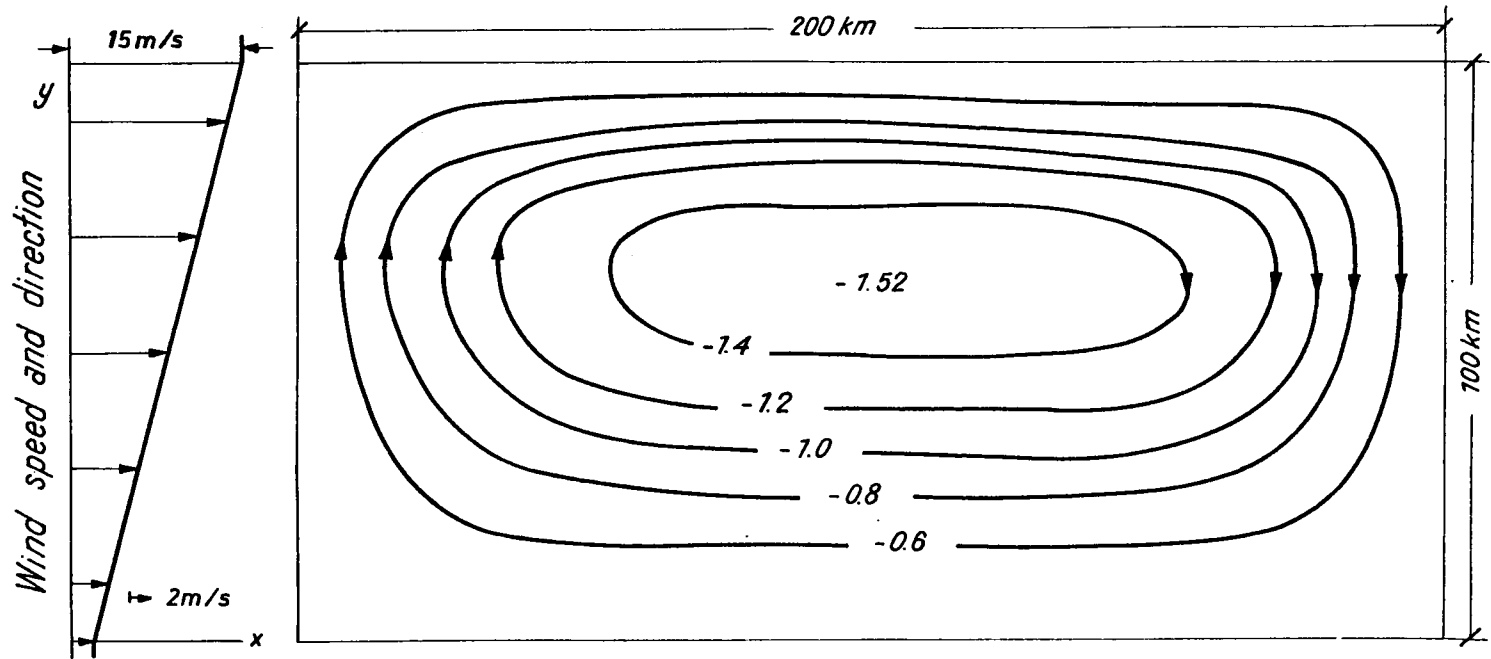


Fig. 8. STREAMLINES OF THE VERTICALLY INTEGRATED HORIZONTAL MASS TRANSPORT OF THE WIND-DRIVEN CIRCULATION IN A RECTANGULAR SEA WITH CONSTANT DEPTH. THE NUMBERS ARE IN MILLIONS OF TONS PER SECOND.

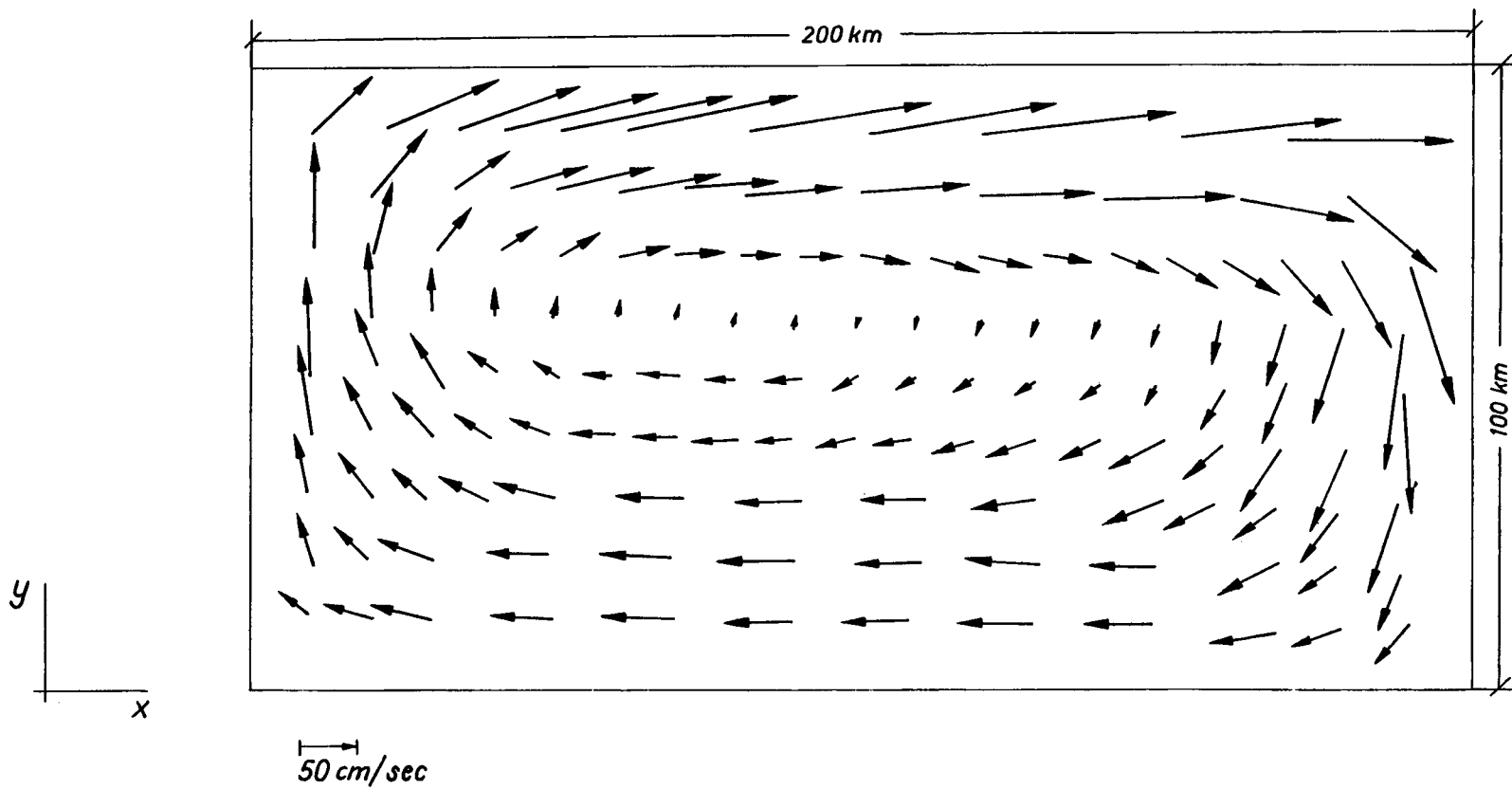


Fig. 9. SURFACE CURRENT CORRESPONDING TO THE WIND PATTERN IN FIG. 8.

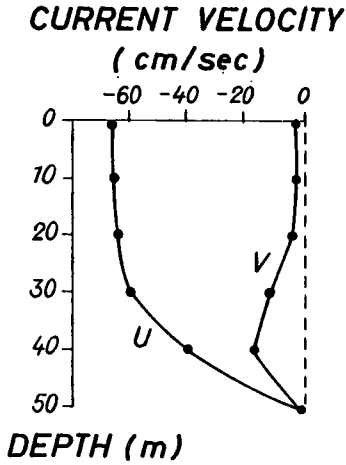


Fig. 10. CURRENT VELOCITY AS A FUNCTION OF DEPTH AT THE POINT $x = 120$ km, $y = 20$ km IN FIG. 9.

to an intensification of the current at the coast (Neumann, 1958; Garner et al., 1962). Stommel (1948) explained the western intensification by using $\beta \frac{\partial \psi}{\partial x}$, but from equation (3.52) it is seen that the β -effect can be compensated when

$$\beta \frac{\partial \psi}{\partial x} = \frac{R_1}{H} \frac{\partial H \partial \psi}{\partial x \partial x} \quad (3.53)$$

Thus if the depth is varying as $H = H_0 \exp(\frac{\beta x}{R_1})$ we should not observe any intensification of the current at the coast. Further on we will put $\beta \frac{\partial \psi}{\partial x} = 0$, and will study the a-symmetry in the flow due to the non-uniform depth.

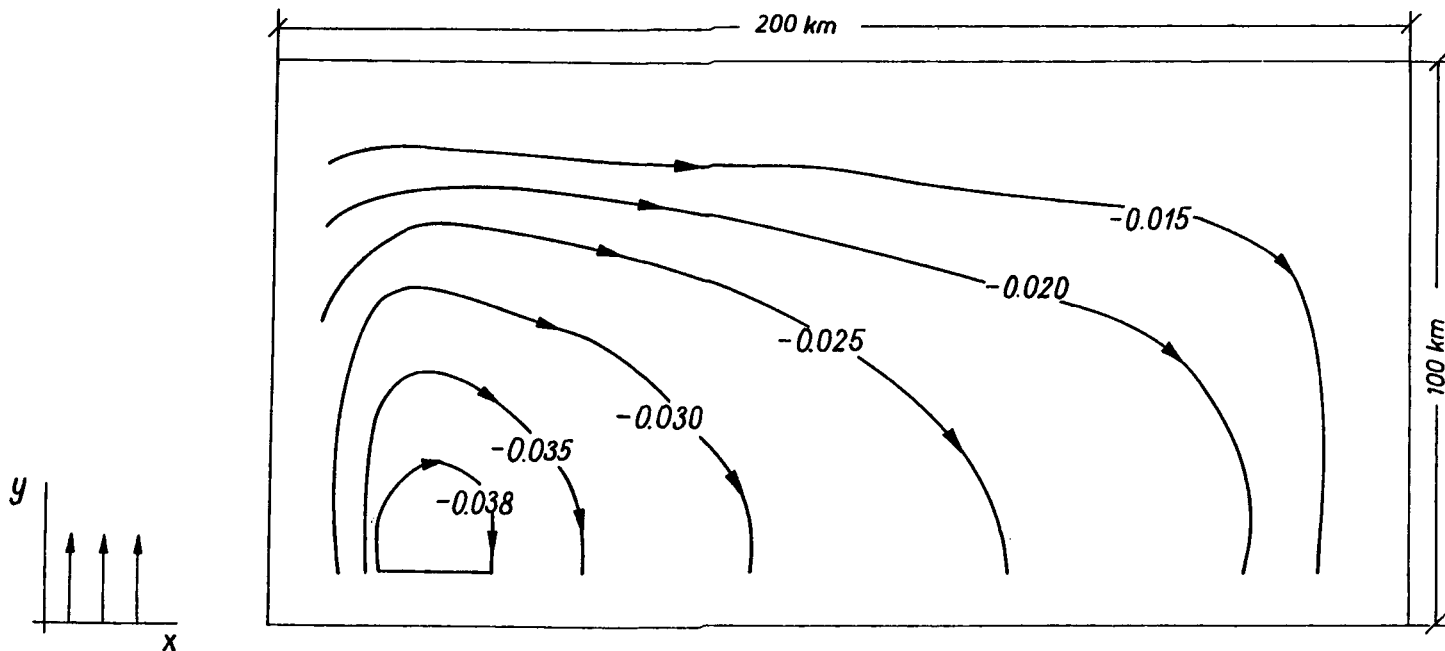


Fig. 11. STREAMLINES OF THE VERTICALLY INTEGRATED HORIZONTAL MASS TRANSPORT OF THE WIND-DRIVEN CIRCULATION IN THE SEA WITH NONUNIFORM DEPTH H , $H = 2500 + 0.00025x$ (cm). THE NUMBERS ARE GIVEN IN MILLIONS OF TONS PER SECOND.

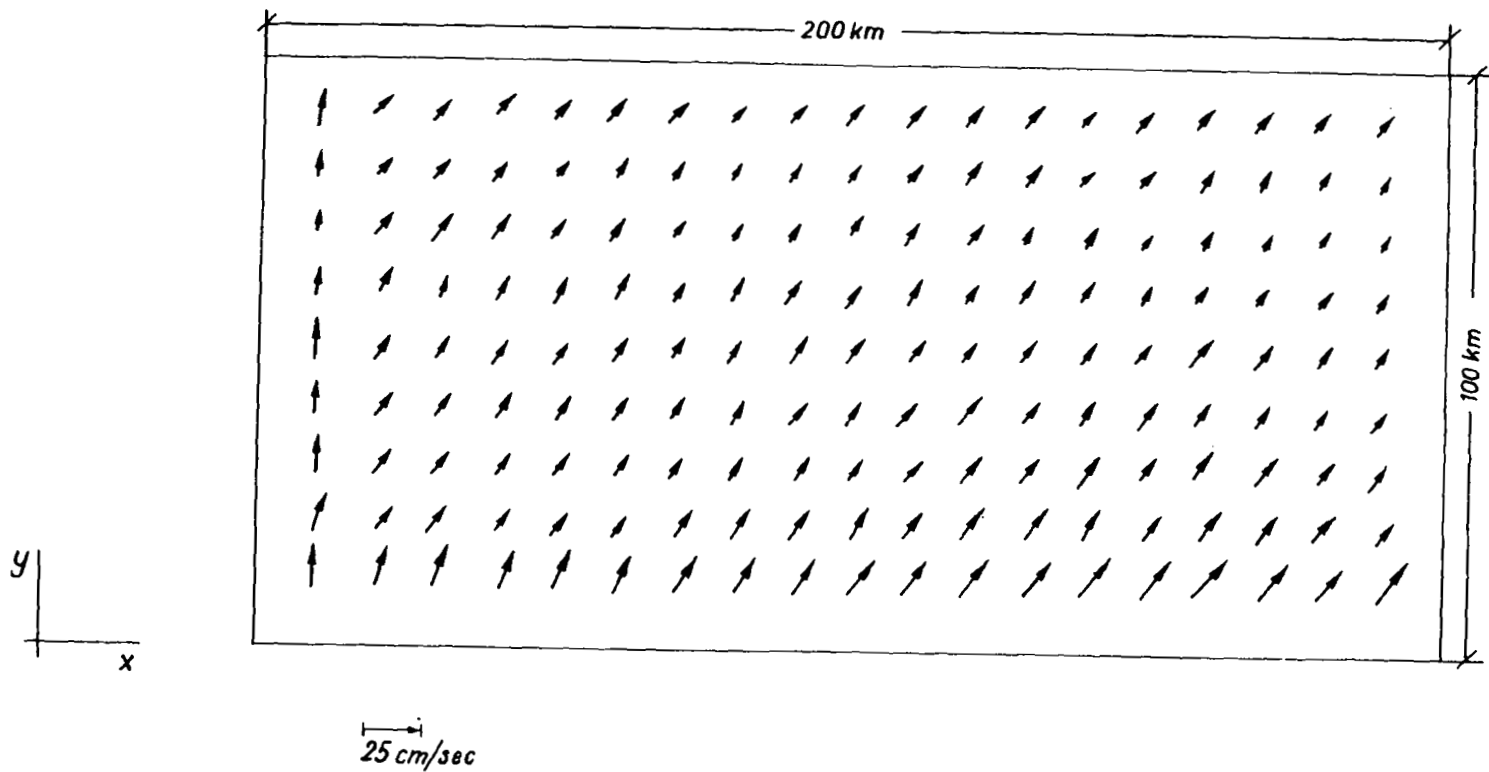


Fig. 12. SURFACE CURRENT CORRESPONDING TO THE WIND PATTERN IN FIG. 11.

It is observed also that in the equation (3.52) wind stress $\tau_s^{(y)}$ is coupled with bottom slope and so the sign of the forcing function is dependent on the bottom slope.

A difficulty arises at once if one wishes to obtain the solution of equation (3.52) by the iteration method, because the coefficients of the first derivatives are variable. We shall use here the method of forward-backward derivatives described by equation (2.18).

The computed stream function is given in figure 11. Since wind is constant one can combine the non-uniform distribution of the stream function with the bottom slope. In fig. 12 the surface current is shown. The intensification of the surface current is observed at the southern shore. At the same time a comparison of fig. 11 and fig. 12 shows how the direction of the surface current and the direction of the vertically-integrated flow differ from each other. This feature gives rise to the rapid change of the current direction with depth as shown in fig. 13 (at the point with co-ordinates $x = 120$ km, $y = 20$ km in figures 11 and 12).

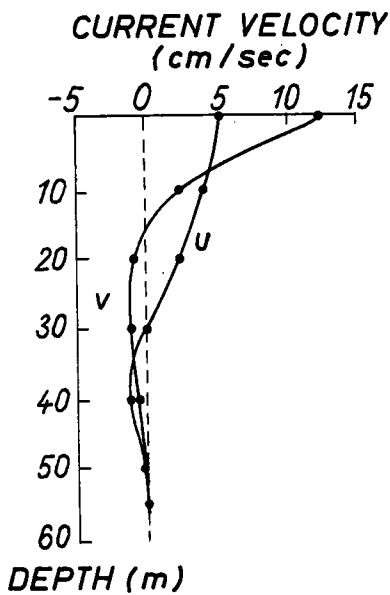


Fig. 13. CURRENT VELOCITY AS A FUNCTION OF DEPTH AT THE POINT $x = 120$ km, $y = 20$ km IN FIGS. 11,12.

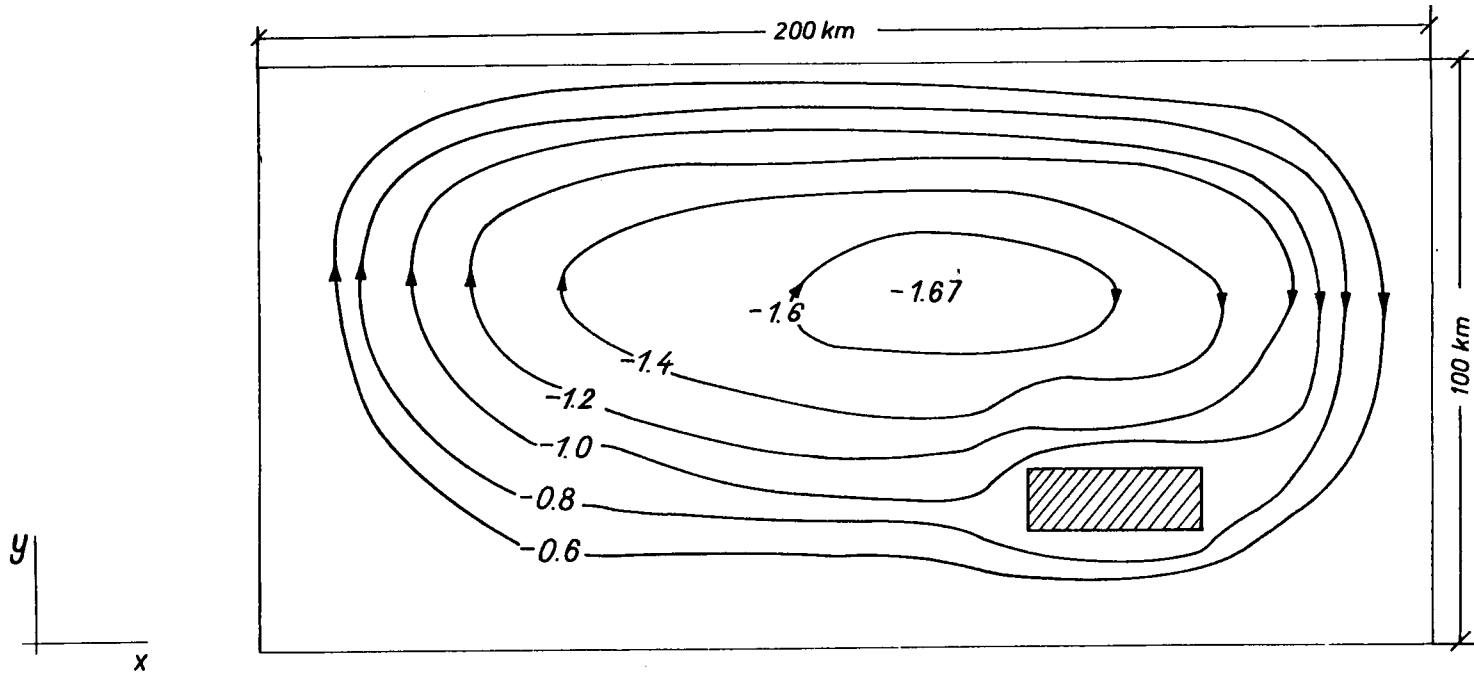


Fig. 14. STREAMLINES OF THE VERTICALLY INTEGRATED HORIZONTAL MASS TRANSPORT OF THE WIND-DRIVEN CIRCULATION IN THE SEA WITH AN ISLAND. WIND PATTERN AND DEPTH AS IN FIG. 8. THE NUMBERS ARE IN MILLIONS OF TONS PER SECOND.

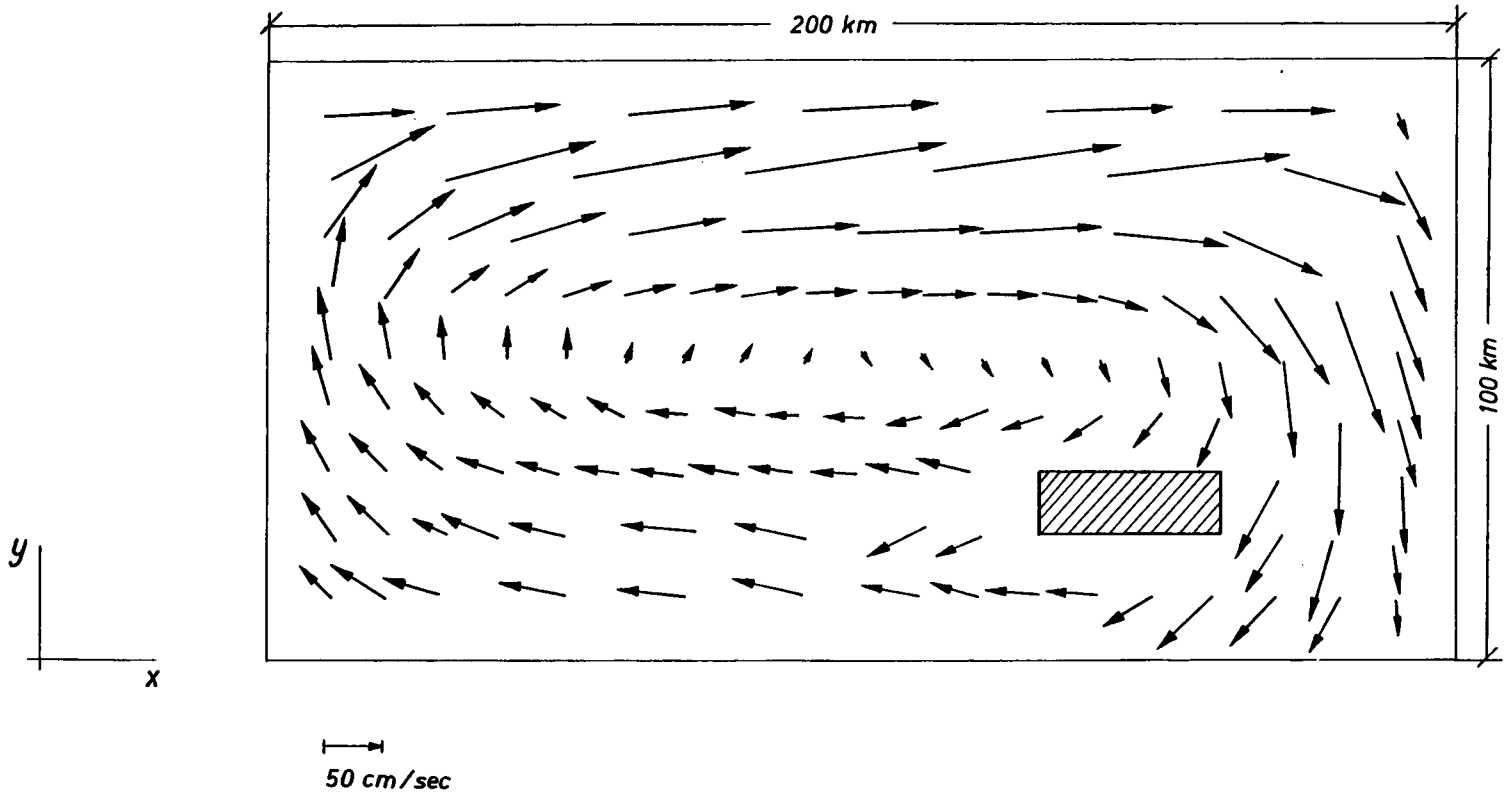


Fig. 15 SURFACE CURRENT IN THE SEA WITH AN ISLAND. WIND PATTERN AND DEPTH AS IN FIG.8.

C. Uniform depth, strong curl of the wind stress and the presence of an island

Here we take again case A but with an island introduced within the main contour (figs. 14 and 15). The domain of integration is no longer simply connected, and the solution of equation (3.46) is

$$\psi = \psi_0 + c_1 \psi_1 \quad (3.54)$$

where c_1 can be found from equation (3.37) as

$$\oint_{\Gamma_1} \frac{\tau_s}{c^2} ds = \oint_{\Gamma_1} \frac{R_1}{c^2} (\psi_0 + c_1 \psi_1) ds \quad (3.55)$$

The results of the computation of the stream function are shown in fig. 14. The flow is similar to that in fig. 8, but the island gives a certain local redistribution in pattern. Of particular interest is the pattern on the downcurrent side of the island. The change in the streamline pattern gives the change in direction and speed of the surface current around the island (fig. 15), and also gives the change in vertical distribution of current, as shown in fig. 16 (at the point with the co-ordinates $x = 120$ km, $y = 20$ km in figs. 14 and 15). This probably signifies a special type of flow around an island as was predicted by Stockman (1966).

§8. Steady wind-driven circulation in the Baltic Sea

Let us turn to the more realistic case and calculate currents in the Central and Southern Baltic (neglecting the Gulf of Bothnia). If we take a mesh size equal to 20 km, we will be able to take into account two islands: Bornholm (B) and Gotland (G) (figs. 17 and 18).

Two cases are examined, one for a constant wind of 10 m/sec blowing towards the east and a second with a constant wind of 10 m/sec blowing towards the south. In these cases for the nonhomogeneous part of equation (3.26) only the terms due to coupling between wind stress and bottom slope are present. The solution for the stream function of the horizontal mass transport is a sum of three terms

$$\psi = \psi_0 + c_1 \psi_1 + c_2 \psi_2 \quad (3.56)$$

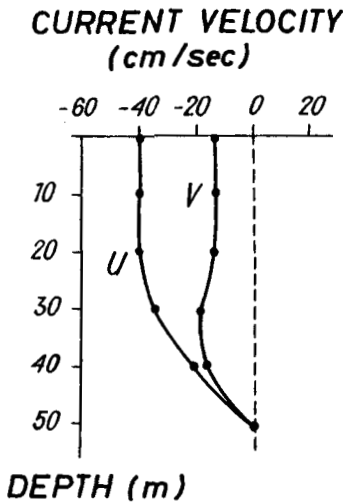


Fig. 16. CURRENT VELOCITY AS A FUNCTION OF DEPTH
AT THE POINT $x = 120$ km, $y = 20$ km IN FIG. 14.

Constants c_1 and c_2 can be found by the solution of two linear equations (see equation 3.37)

$$\oint_{\Gamma_1} \frac{\tau_s}{c^2} ds = \oint_{\Gamma_1} \frac{R_1}{c^2} (\psi_0 + c_1 \psi_1 + c_2 \psi_2) ds \quad (3.57a)$$

$$\oint_{\Gamma_2} \frac{\tau_s}{c^2} ds = \oint_{\Gamma_2} \frac{R_1}{c^2} (\psi_0 + c_1 \psi_1 + c_2 \psi_2) ds \quad (3.57b)$$

The main difference between solution (3.56) and the solutions obtained in section 7 is not only due to the presence of a second island, but also to the more complicated bottom slope. The bottom slope in the Baltic (and in every real sea) changes from positive to negative

Fig. 17. STREAMLINES OF VERTICALLY INTEGRATED MASS TRANSPORT OF THE WIND-DRIVEN CIRCULATION IN THE CENTRAL AND SOUTHERN BALTIC. A CONSTANT WIND IS BLOWING TOWARDS EAST ($W = 10$ m/sec). THE NUMBERS ARE IN MILLIONS OF TONS PER SECOND.

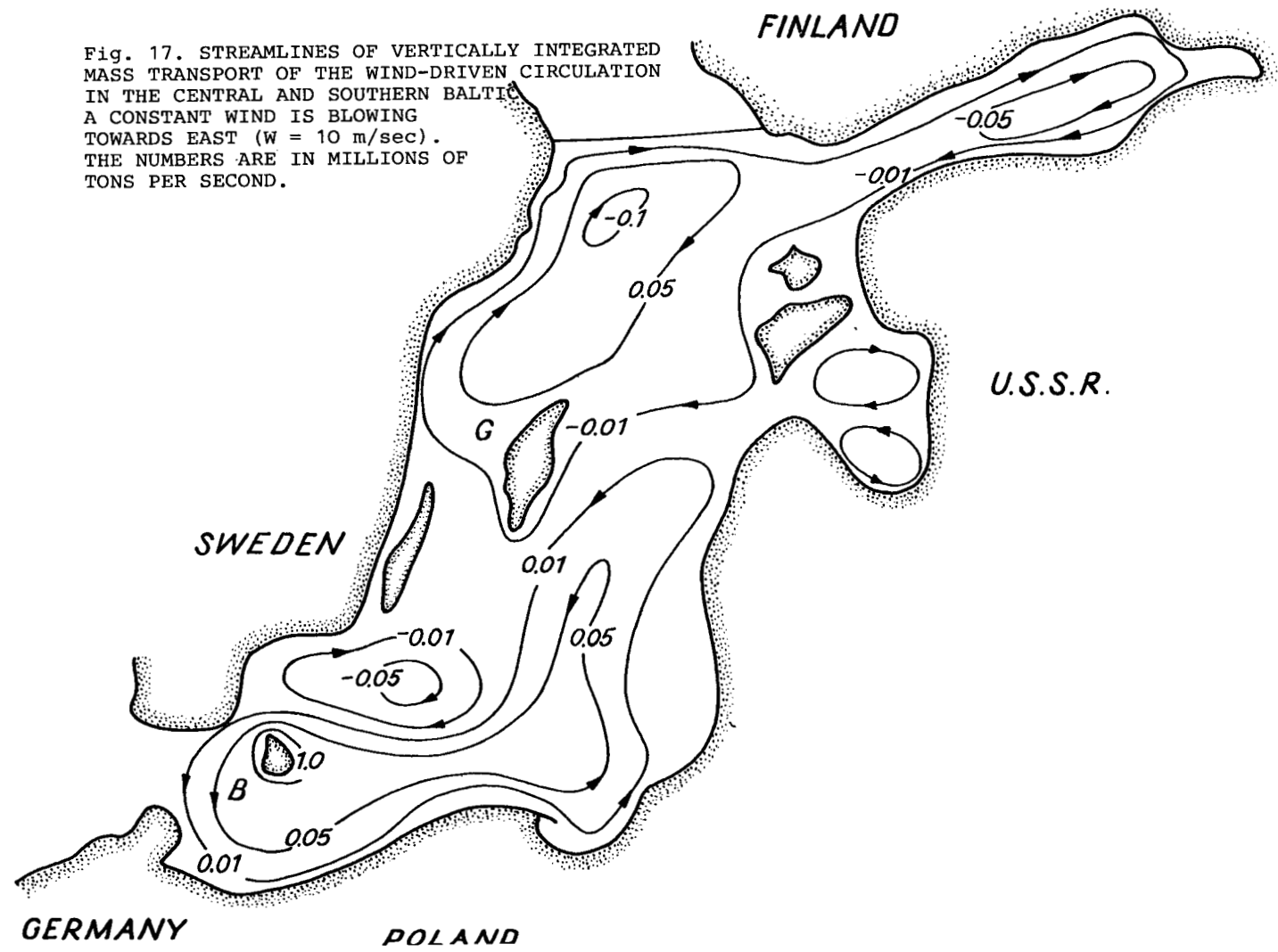
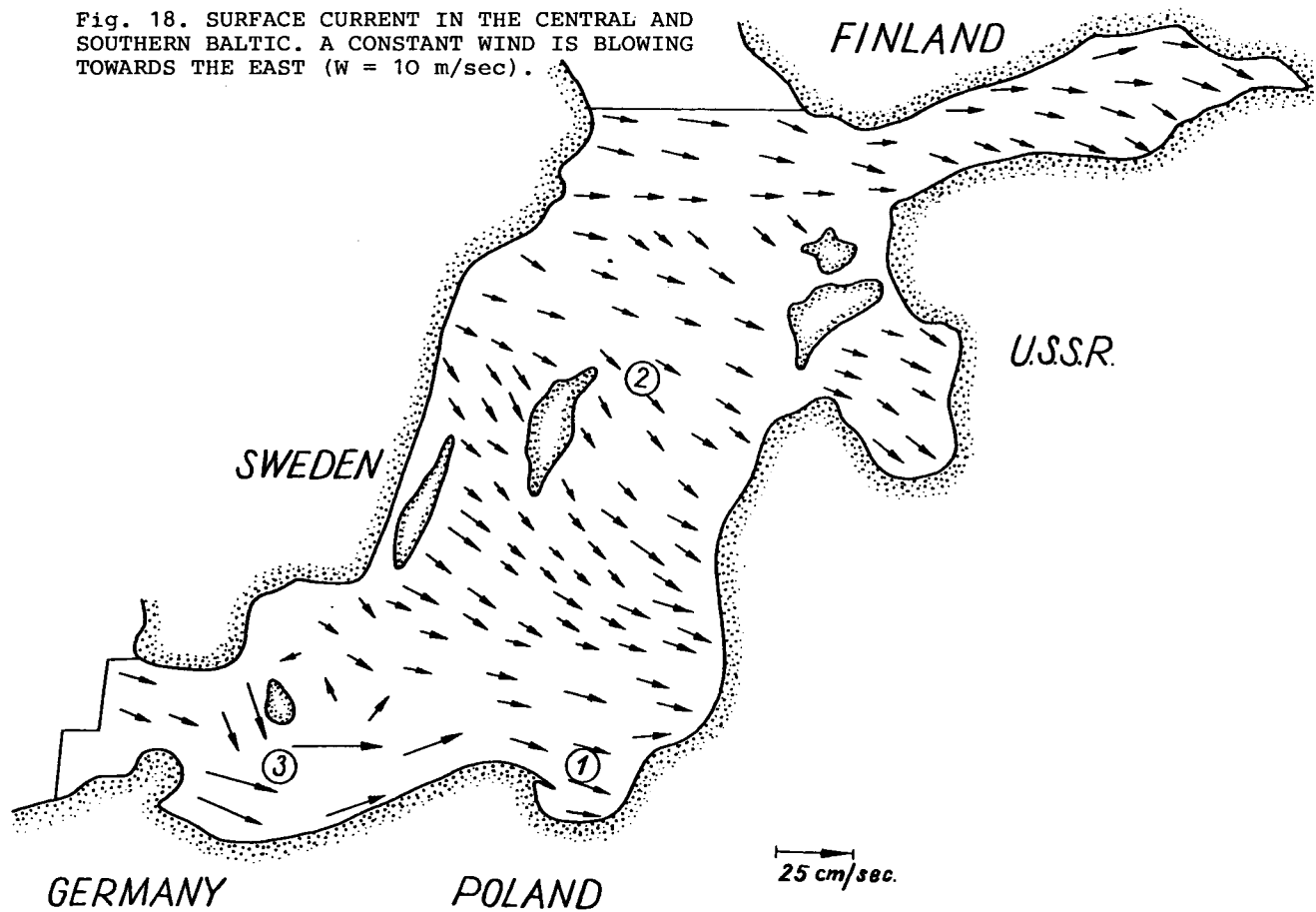


Fig. 18. SURFACE CURRENT IN THE CENTRAL AND SOUTHERN BALTIC. A CONSTANT WIND IS BLOWING TOWARDS THE EAST ($W = 10$ m/sec).



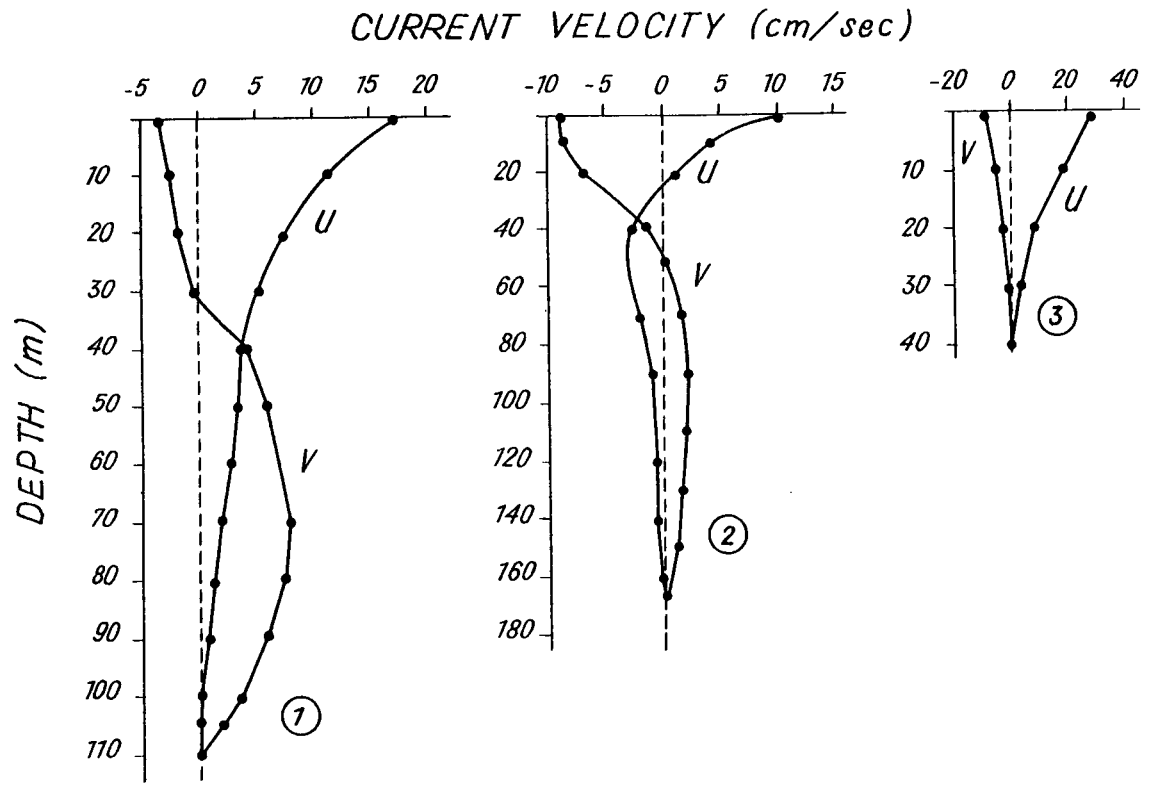


Fig. 19. CURRENT AGAINST THE DEPTH AT THE POINTS 1, 2, 3 IN FIG. 18.

values and coupling with the wind stress (see equation (3.26)) gives a complicated form for the solution of the equation for the stream function.

The coupling term in equation (3.26) has the form $\tau_s^{(x)} \frac{\partial H}{\partial y} \frac{1}{H}$, thus the sign of this term will depend on $\frac{\partial H}{\partial y}$. This can be seen in fig. 17, since, roughly speaking, the depth of the Baltic Sea is increasing towards Gotland Island from both the southerly and northerly directions. Close to the island $\frac{\partial H}{\partial y} = 0$, and thus there are two large gyres in fig. 17. The gyre in the northern part of the sea rotates in a clockwise direction and the other in the southern part rotates in an anti-clockwise direction. There are also small gyres connected with local changes in the bottom slope. Now that we have the value of the stream function we can compute the surface current by means of our usual method. The result is presented in fig. 18.

The magnitude of the current speed is generally in the range of 10 cm/sec to 20 cm/sec, but near to Bornholm Island and the southern coast of the Baltic one observes that the magnitude varies from 5 cm/sec to 40 cm/sec; here the directions of the velocity vectors indicate also an anti-clockwise circulation.

The vertical distribution of current (Fig. 19) at the points 1, 2 and 3 in fig. 18 shows additional features.

At the points 1 and 2 the strong variation in current direction and speed with depth is noted. This is probably caused by the difference in behaviour of the two current components (the current due to the wind stress is decaying faster with depth than the current due to the slope).

At point 3 where the water is shallow (40 m) the current direction does not change from the surface to the bottom.

Next the computation for the second case was carried out (wind blowing towards the south). Here the wind stress was coupled with the east-west component of the bottom slope $\frac{\partial H}{\partial x}$. Again two large gyres appeared (Fig. 20); one in the eastern part of the sea rotating in a clockwise direction and the other in the western part rotating in an anti-clockwise direction.

The flows around Bornholm Island and in the Gulf of Finland have a different appearance associated with the local changes in the bottom slope. The surface velocity is shown in fig. 21.

Again, in general, values of the current are in the range of 10cm/sec to 20 cm/sec, but in the Bornholm Basin they change from 5 cm/sec to 50 cm/sec. The current pattern indicates here a clockwise circulation.

Fig. 20. STREAMLINES OF THE VERTICALLY INTEGRATED HORIZONTAL MASS TRANSPORT OF THE WIND-DRIVEN CIRCULATION IN THE CENTRAL AND SOUTHERN BALTIC. A CONSTANT WIND IS BLOWING TOWARDS THE SOUTH ($W = 10$ m/sec). THE NUMBERS ARE IN MILLIONS OF TONS PER SECOND.

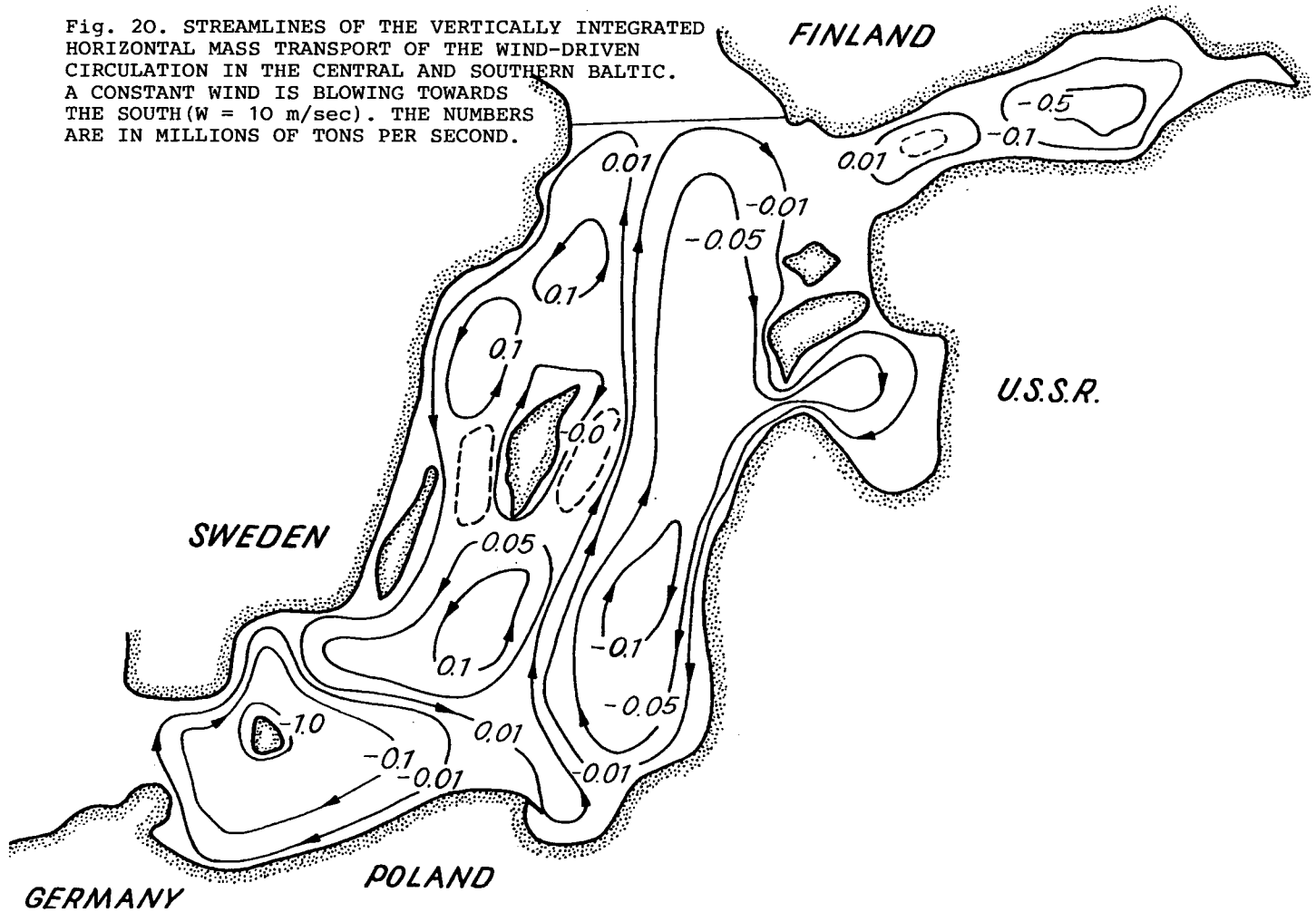
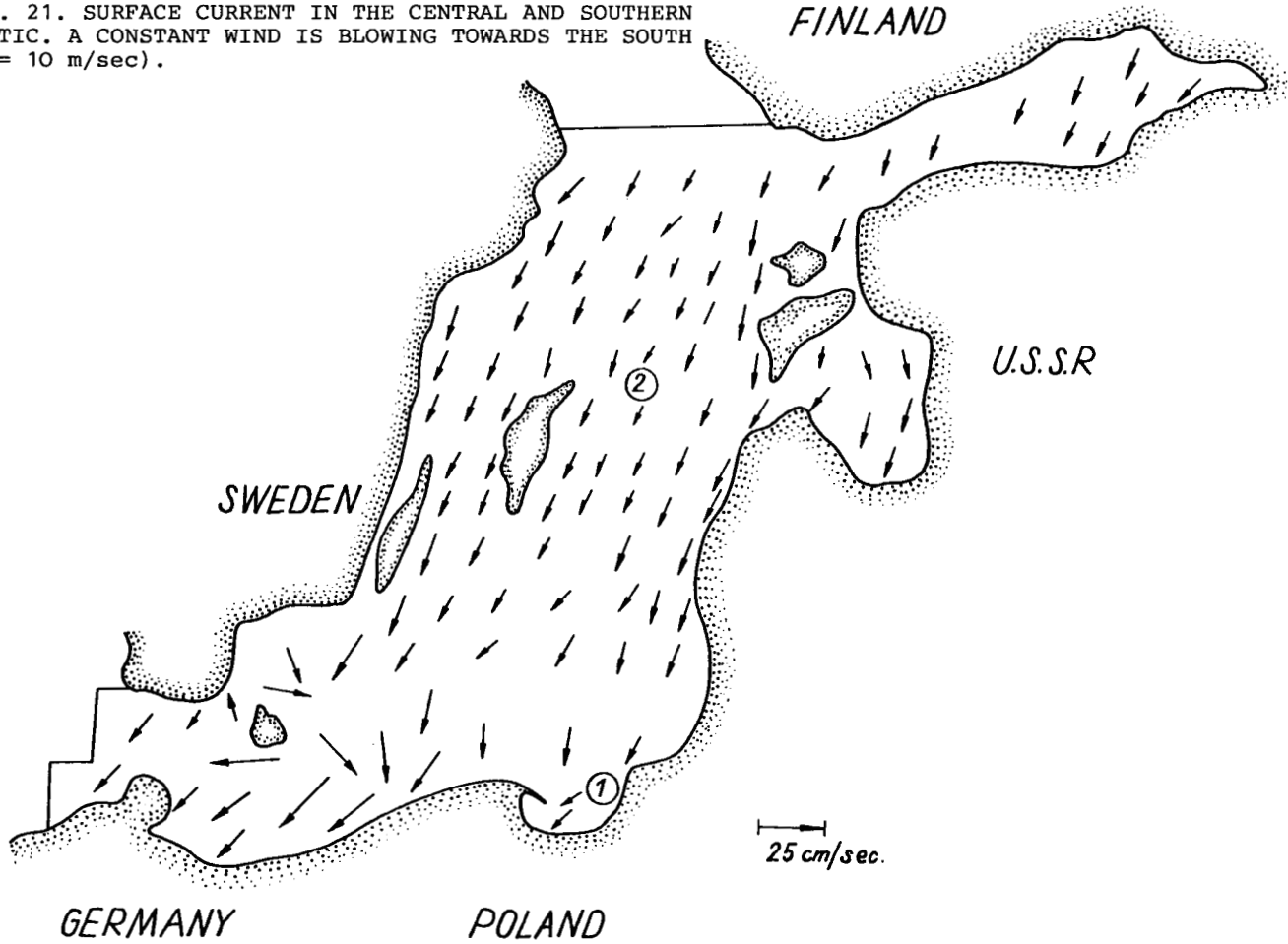


Fig. 21. SURFACE CURRENT IN THE CENTRAL AND SOUTHERN BALTIC. A CONSTANT WIND IS BLOWING TOWARDS THE SOUTH ($W = 10$ m/sec).



It should be mentioned that there may possibly be an abnormal flow around Bornholm, as may be seen from figs. 17 and 20, but our numerical results should be considered very carefully here, since the size of the island is near the chosen mesh size (20 km), and therefore the numerical evaluation of the contour integrals (3.57) may involve a considerable error.

To complete the above description, the vertical distribution of current is shown in fig. 22 (at the points 1 and 2 in fig. 21). As before the current undergoes large changes in direction and magnitude over the depth. To clarify this phenomenon we split the current into its two components, one due to the wind stress v_t and the other due to the surface slope v_s . Absolute values of these components are shown in fig. 23. We observe here the important feature of Ekman's theory, the existence of two boundary layers; one for the v_t component at the surface and the other for the v_s component at the bottom.

CURRENT VELOCITY (cm/sec)

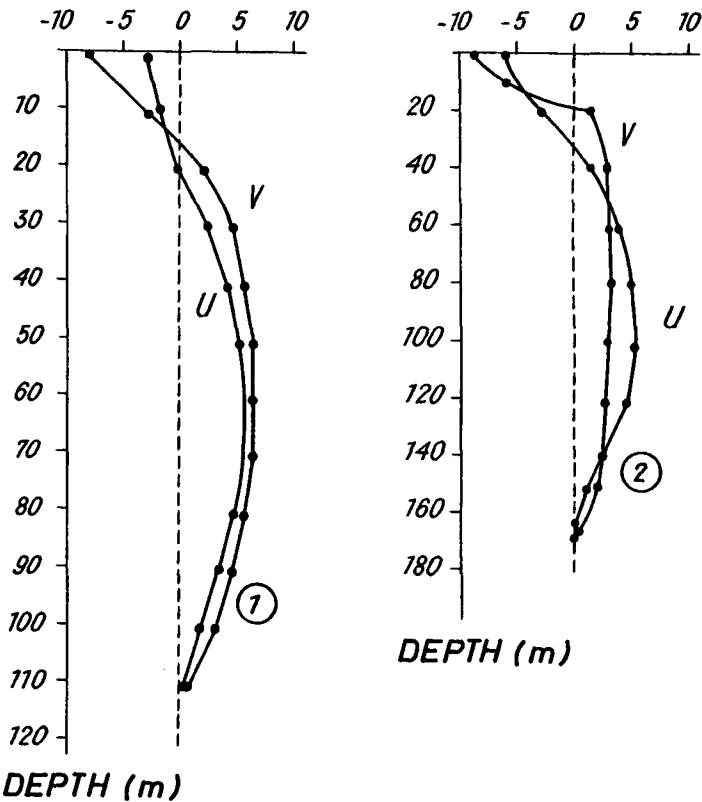


Fig. 22. CURRENT AGAINST THE DEPTH AT THE POINTS 1 AND 2 IN FIG. 21.

ABSOLUTE CURRENT VELOCITIES (cm/sec)

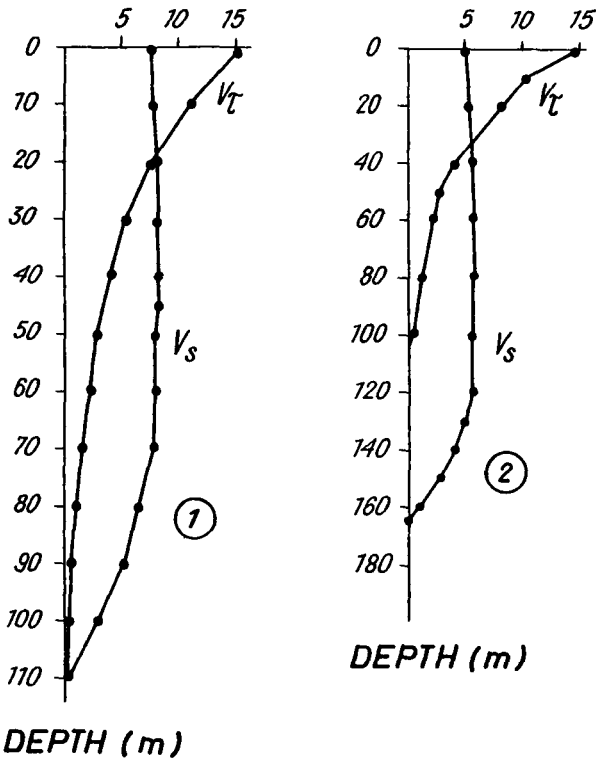


Fig. 23. ABSOLUTE VALUES OF CURRENT VELOCITIES AGAINST DEPTH AT THE POINTS 1 AND 2 IN FIG. 21.

It is worth-while noticing that the surface boundary layer in Ekman's theory is connected with friction depth D where

$$D = \left(\frac{2k}{\rho f} \right)^{1/2} \quad (3.58)$$

Since the depths H are 110 m and 165 m at points 1 and 2 respectively, and the wind speed is 10 m/sec, we can use expression (3.39) for determining the eddy viscosity coefficient k and find $D = 97$ m. At this depth the component v_T is practically negligible (see fig. 23).

The boundary layer at the bottom which governs the v_S component can be characterized by the 'bottom' friction depth. To find this friction depth by means of (3.58) one must know the eddy viscosity,

but to determine the eddy viscosity coefficient we need to know the wind speed (since the depth is already known). The wind speed can be determined through an experimental relation (see Ekman, 1905; Felzenbaum, 1960) between surface current velocity v and the wind speed above the sea W

$$\frac{v}{W} = 1.5 \times 10^{-2} \quad (3.59)$$

Now let us imagine for a moment that the current components due to the slope in fig. 23 were caused by a wind acting at the bottom of the sea and that the surface of the sea takes the rôle of the bottom. By this reversal of fig. 23 the value of the 'surface' current is 7 cm/sec at point 1. Therefore by (3.59) the wind speed is $W = 4.7$ cm/sec and the friction depth (3.58) is $D = 45$ m. At point 2 the value of the 'surface' current is 5 cm/sec which results in a friction depth of $D = 32$ m. These values of friction depth are in fair agreement with the v_s components in fig. 23.

§9. The influence of density stratification on the vertical distribution of current

To solve this problem we assume that the eddy viscosity coefficient is no longer a known and a priori given quantity but is an unknown factor to be found in the process of integration of a system of equations in which the equation of turbulent energy plays the central rôle. By means of this equation the influence of density stratification is also taken into account through the Archimedian force term. The density distribution for such a calculation is taken from the 'in situ' measurements. After the stream function (to compute the sea-level components $\frac{\partial \zeta}{\partial x}$ and $\frac{\partial \zeta}{\partial y}$) has been found, we still observe in equations (3.16) and (3.17) one unknown, and that is the eddy viscosity coefficient k . To find it we introduce first of all the equation of turbulent energy, for the case of the mean motion in the horizontal direction and the exchange of momentum in the vertical direction. This was presented by Phillips (1966) and Zilitinkievich (1970) as follows

$$-\frac{\partial}{\partial z} (k_b \frac{\partial b^2}{\partial z}) = k \left[\left[\frac{\partial u}{\partial z} \right]^2 + \left[\frac{\partial v}{\partial z} \right]^2 \right] + \frac{g}{\rho} k \frac{\partial \rho}{\partial z} - \epsilon \quad (3.60)$$

In (3.60) b^2 is a turbulent energy, ϵ denotes the dissipation term and k_b , k_ρ the coefficients of exchange of energy and the mass re-

spectively. In order to find the relationship of the unknown parameters k, k_b, k_ρ and ε , the Kolmogoroff hypothesis of similarity is used. In this way all unknowns are expressed by the turbulent energy b^2 and the scale of turbulence l .

When analysing the dimensions of the above parameters we obtain

$$k = c_0 l b; \quad K_\rho = \alpha_\rho k; \quad k_b = \alpha_b k; \quad \varepsilon = c_1 \frac{b^3}{l} \quad (3.61)$$

where $c_1, c_0, \alpha_\rho, \alpha_b$ are non-dimensional universal constants.

But again we have a new unknown l in equation (3.61). To find its magnitude the expression proposed by von Karman is used

$$l = - \chi \frac{b}{\rho} \frac{\partial}{\partial z} \left(\frac{b}{l} \right) \quad (3.62)$$

where $\chi \approx 0.4$.

In equation (3.60) the density of the sea water ρ plays an important rôle, and thus it influences the vertical current distribution. The density itself can be treated as unknown and then it can be found from the equation of diffusion with suitable boundary conditions. Or it can be taken as a known value from the 'in situ' measurements. The second case is considered in this work.

The values of the universal constants which appear in equation (3.60) were chosen by Zilitinkievich, Lajchtman and Monin (1967) as

$$c_1 = c_0^4 = c = 0.046; \quad \alpha_b = 0.73 \quad (3.63)$$

For obvious reasons the information about α_ρ is poor and its value is only known approximately. In our computations α_ρ takes four different values $\alpha_\rho = 0, 0.01, 0.1, 1$.

Now we add the relevant boundary conditions to the equations (3.60) and (3.62). The simplest boundary condition for equation (3.60) is that the decay of the flow of turbulent energy and mass occurs at the surface and at the bottom of the sea

$$\frac{\partial b^2}{\partial z} = 0; \quad \frac{\partial \rho}{\partial z} = 0 \quad (3.64)$$

According to the above condition equation (3.60) simplifies to

$$k \left[\left[\frac{\partial u}{\partial z} \right]^2 + \left[\frac{\partial v}{\partial z} \right]^2 \right] = c_0 c_1 \frac{b^4}{k} = (\tau_s^{(x)})^2 + (\tau_s^{(y)})^2 \frac{1}{k} \quad (3.65)$$

If the stresses at the bottom and the surface are known, the value of the turbulent energy at the boundaries can be found easily. For equation (3.62) the boundary condition results from the known fact that the scale of turbulence in the vicinity of the bottom is a linear function of the distance (Monin and Jaglom, 1965), and so we have at the bottom

$$l = \chi z_0 \quad (3.66)$$

where z_0 is a roughness parameter.

Thus we may say that the problem of a wind-driven circulation in a shallow sea is closed. To solve it we proceeded through a set of equations, where the main ones were (3.16) and (3.17) which are equations of motion with two unknowns: sea-level slope and eddy viscosity coefficient. In the first part we found the components of the sea-level slope by means of the mass transport equation. In the second part the equations (3.60) and (3.62) with suitable boundary conditions were introduced to find the eddy viscosity coefficient k . The integration of the system of equations developed in the second part was performed by the iteration method.

In order to initiate a computational process, the arbitrary value of $k = k(z)$ was taken and next the equations (3.16) and (3.17), and (3.62) were solved and a new value of k was obtained by means of (3.61). The iteration process runs until the following inequality takes place

$$\left| \frac{k_{j+1} - k_j}{k_{j+1}} \right| < 0.05$$

where j is the iteration index. The solution of the equations (3.16), (3.17) and (3.60) in the iteration process was performed by the line inversion method (Ch.II, §8). The nonlinear term in the energy equation $\epsilon = c_0 c_1 b^4 / k$ on every iteration step j was taken in a linearised form as

$$\epsilon_j = c_0 c_1 b_j^2 b_{j-1}^2 / k_j \quad (3.67)$$

Let us apply the equations developed above to find the vertical distribution of the horizontal current component in the Baltic at the position $\phi = 54^{\circ}50'$, $\lambda = 19^{\circ}12'$, where the depth is about 100 m.

We shall use our previous computation of mass transport for a southerly wind of 10 m/sec.

The current distribution is analysed as a function of water density and of the nondimensional parameter $\alpha_\rho = k_\rho/k$ which is the reciprocal of Richardson's parameter Ri .

For the density distribution at the point shown in fig. 24 a typical summer profile was chosen. As usual two layers of water are present here due to the horizontal water exchange with the North Sea. This density profile will be used later on for the computation of the expression $\frac{g\partial\rho}{\rho\partial z}$ in equation (3.60).

As in many computations of the wind-driven circulation the eddy viscosity coefficient is taken as constant. It seems reasonable to compare such a value with the results of the work presented here where the coefficient varies with depth.

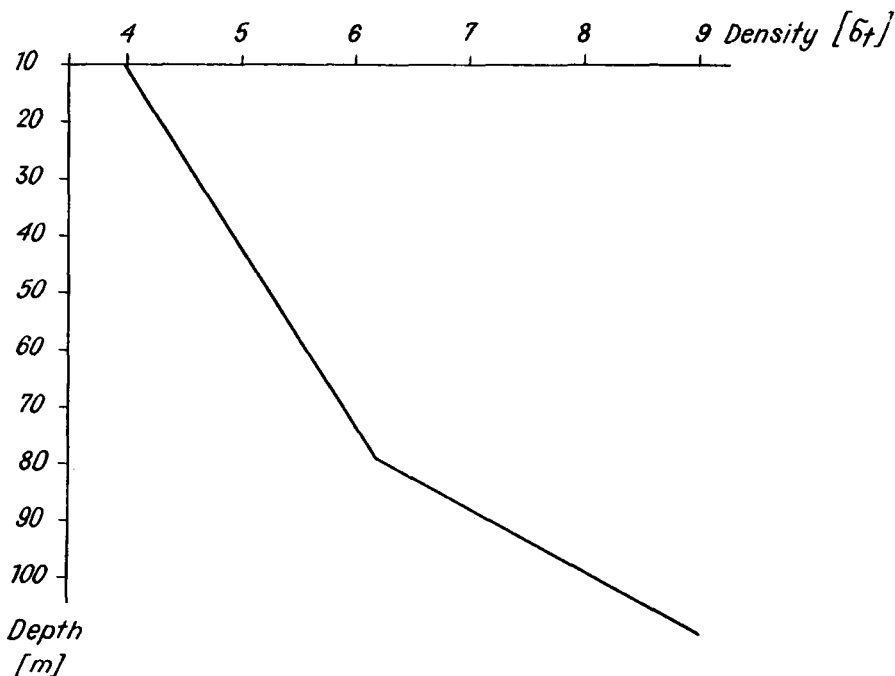


Fig. 24. A SIMPLIFIED SUMMER DENSITY DISTRIBUTION IN THE BALTIC SEA AT THE POINT WITH GEOGRAPHICAL CO-ORDINATES $\lambda = 19^{\circ}12'$, $\phi = 54^{\circ}50'$.

In fig. 25 the v component was computed with constant k equal to $470 \text{ cm}^2/\text{sec}$ (dashed line) and is compared with the v component for the case when $\alpha_\rho = 0.1$ (continuous line). In the figure a smooth curve for the velocity is observed when $k = 470 \text{ cm}^2/\text{sec}$. In the case where the velocity is computed by taking into account the turbulent processes of energy exchange instead of using a constant k strong gradients of velocity can be seen. Such a phenomenon in water masses is connected with the decay at a certain depth of the components of the drift current. The below distribution shows that in the case of a constant eddy viscosity coefficient the processes of turbulent exchange are taking place in the total water volume, i.e. from the surface to the bottom. In reality, these processes should decay at a certain depth, due to the action of the Archimedian force and revive anew in the very thin layer above the bottom. In conclusion it seems important to acknowledge the law of decay of the current in the boundary layer at the bottom. In the case of a constant coefficient linear decay is observed, whereas in the case of a variable coefficient the logarithmic law takes place. This last phenomenon is confirmed by laboratory experiments.

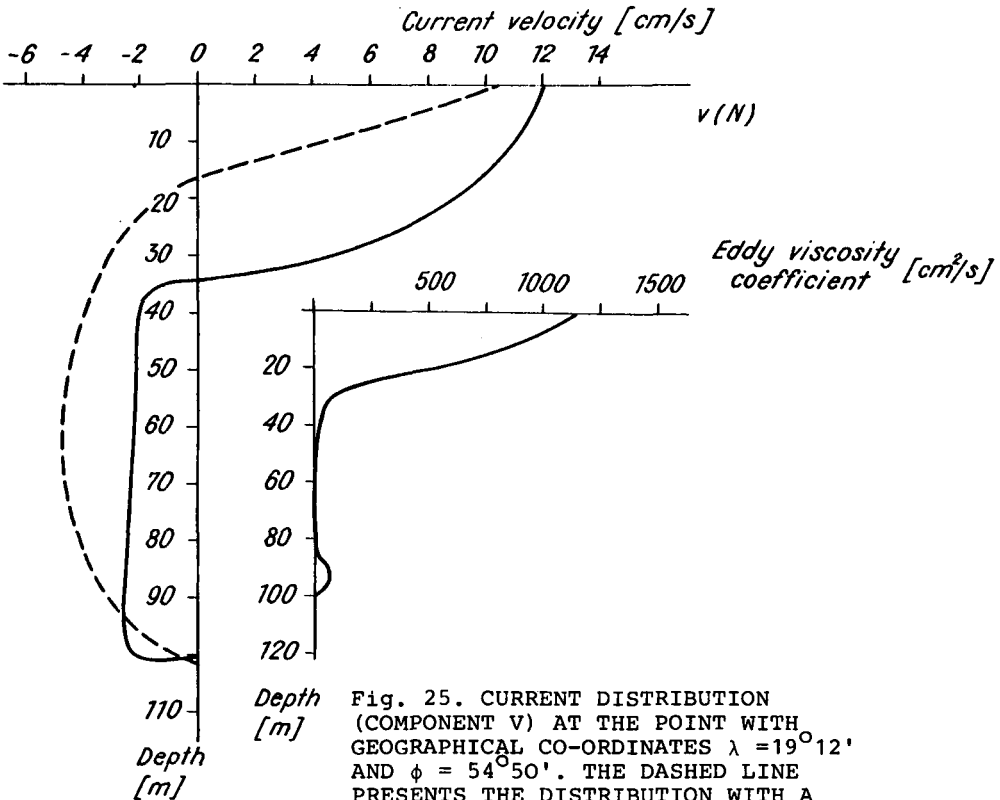


Fig. 25. CURRENT DISTRIBUTION (COMPONENT v) AT THE POINT WITH GEOGRAPHICAL CO-ORDINATES $\lambda = 19^\circ 12'$ AND $\phi = 54^\circ 50'$. THE DASHED LINE PRESENTS THE DISTRIBUTION WITH A KONSTANT EDDY VISCOSITY COEFFICIENT ($470 \text{ cm}^2/\text{sec}$), THE CONTINUOUS LINE RESULTS FROM A VARIABLE EDDY VISCOSITY DISTRIBUTION INDICATED BY AN ADDITIONAL DIAGRAM.

§10. The wind- and density-driven currents

When considering the interrelation of density- and wind-driven phenomena a natural question arises. Why did we previously consider the barotropic component only and reject the baroclinic one? The possibility of ignoring the baroclinic component in a shallow sea can be deduced simply from the time of development of the wind current and the baroclinic current. Drift currents develop in about two days whereas baroclinic currents require about 200 days for full development because of the non-uniform horizontal density distribution. This can be shown easily using dimensional analysis. Thus it is obvious that in a study of wind-driven currents for intervals of up to two days the baroclinic component can be ignored.

The purpose of the present model is to provide an approach when the wind-driven and the density currents can be treated as one conjoint phenomenon. However, considering that the interrelations between both, at the various time periods, are rather complicated, we shall here consider those currents that can be called the mean climatic ones.

Our aim is to investigate the Baltic water circulation during the summer season, from the averaged multi-year observations of a) atmospheric pressure fields at sea-level and b) the water density. As the water density distribution will depend on the cyclonic activity in the atmosphere, the pre-setting of average data on density in a stationary model involves the necessity to pre-set an appropriately averaged distribution of wind or atmospheric pressure.

Generally, we shall base our model on that presented by Sarkisyan (1966) and the computation performed by Kowalik and Staskiewicz (1976). Proceeding from the equations of motion (1.29) and (1.30) and assuming the steady state $\frac{\partial u}{\partial t} = 0$, $\frac{\partial v}{\partial t} = 0$ we set the following equations to describe the horizontal velocities in a stratified sea

$$-\rho_0 f v = -\rho_0 g \frac{\partial \zeta}{\partial x} - g \frac{\partial}{\partial x} \int_z^0 \rho_1 dz + \rho_0 k \frac{\partial^2 u}{\partial z^2} \quad (3.68)$$

$$\rho_0 f u = -\rho_0 g \frac{\partial \zeta}{\partial y} - g \frac{\partial}{\partial y} \int_z^0 \rho_1 dz + \rho_0 k \frac{\partial^2 v}{\partial z^2} \quad (3.69)$$

The wind acting at the surface will cause the stress

$$\tau_s^{(x)} = \rho_0 k \frac{\partial u}{\partial z}; \quad \tau_s^{(y)} = \rho_0 k \frac{\partial v}{\partial z} \quad (3.70)$$

At the bottom, due entirely to the friction, the velocity decays to zero

$$u = v = 0 \quad (3.71)$$

The solution of the stated problem is easily obtained in the complex form

$$S = u + iv = \frac{\tau}{k\alpha} \frac{\sinh\alpha(z+H)}{\cosh\alpha H} + \frac{Kgi}{f} \left(\frac{\cosh\alpha z}{\cosh\alpha H} + 1 \right) + F(z) + F \Big|_{z=-H} \frac{\cosh\alpha z}{\cosh\alpha H} - \frac{1}{\alpha} \frac{dF}{dz} \Big|_{z=0} \frac{\sinh\alpha(z+H)}{\cosh\alpha H} \quad (3.72)$$

In (3.72) the following notation is used

$$\tau = \tau_s^{(x)} + i\tau_s^{(y)}; \quad K = \frac{\partial\zeta}{\partial x} + i\frac{\partial\zeta}{\partial y};$$

$$F = \frac{1}{\alpha} \int_z^0 \frac{g}{\rho} \left(\frac{\partial}{\partial x} \int_{\eta}^0 \rho_1 dz + i \frac{\partial}{\partial y} \int_{\eta}^0 \rho_1 dz \right) \sinh\alpha(z-\eta) d\eta$$

As the sea-level slope K is unknown, in order to proceed further, we shall integrate (3.68) and (3.69) in the vertical direction to obtain the mass transport equations

$$-fM_y = -\rho g H \frac{\partial\zeta}{\partial x} + \tau_s^{(x)} - R_1 M_x - F_1 \quad (3.73)$$

$$fM_x = -\rho g H \frac{\partial\zeta}{\partial y} + \tau_s^{(y)} - R_1 M_y - F_2 \quad (3.74)$$

By cross differentiation of these equations and through the application of the continuity equation (3.24) we derive the equation of the stream function

$$R_1 \Delta\psi + \frac{R_1}{H} J(H, \psi) - \frac{R_1}{H} (\nabla H, \nabla\psi) + \beta \frac{\partial\psi}{\partial x} = -(\text{rot}\vec{\tau})_z + \frac{1}{H} (\tau_s^{(y)} \frac{\partial H}{\partial x} - \tau_s^{(x)} \frac{\partial H}{\partial y}) + \frac{1}{H} (F_1 \frac{\partial H}{\partial y} - F_2 \frac{\partial H}{\partial x}) + \frac{\partial F_2}{\partial x} - \frac{\partial F_1}{\partial y} \quad (3.75)$$

where

$$F_1 = g \int_{-H}^0 \left[\frac{\partial}{\partial x} \int_z^0 \rho_1 d\eta \right] dz; \quad F_2 = g \int_{-H}^0 \left[\frac{\partial}{\partial y} \int_z^0 \rho_1 d\eta \right] dz$$

In the computational model of the entire area of the basin, we pre-set the mean multiyear density distribution for the month of August (data elaborated by Kowalik and Taranowska (1974)) which is the most typical summer month. As boundary conditions we take that the normal component of mass transport taking into account the water exchange with the North Sea and the discharges of the main rivers is known.

The numerical solutions of (3.75) were performed by means of the Gauss-Seidel method (Ch. II, §7). The approximation problem was solved by the approach presented in Chapter II, §1. In the derived pattern of circulation a central rôle is played by the baroclinic component of the current interacting with the bottom shape. This is due partly to the rather small wind velocities during the period concerned (the maximum is around 5m/sec). In fig. 26 we present the distribution of sea-level height in the Baltic, since it can be used as a criterion to check the correctness of the computations.

The amplitude of the sea-level is equal to 17 cm. Generally speaking, the water level increases from the Danish Straits to the extreme limits of the Gulf of Finland. Some weak tendencies to form a closed circulation in the horizontal plane are observed only in the Bornholm Deep and the Gulf of Gdansk (anticyclonic gyre) and the Gotland Deep area (cyclonic gyre).

Since water level observations at coastal stations in the Baltic have been conducted for many years, it was possible to prepare, among others, the average monthly water level distributions along the coast. Fig. 27 presents the observed multi-year average distribution of sea-levels for the month of August (Lazarenko, 1961).

The water level calculated from our model largely coincides with the averaged measurement data from the coastal stations.

The horizontal current distributions were computed on 15 levels. An example in fig. 28 shows the current at the sea surface. The maximum speed is distributed as follows: at 0m - 9cm/sec, at 30 m - 5cm/sec, at 100 m - 3 cm/sec, at 140m - 2cm/sec and at 180 m - 1 cm/sec. Since the current caused entirely by the wind penetrates down to a depth of 100 m, we may conclude that the characteristic density-driven velocity is in a range of 1 to 3 cm/sec. This is in fairly good agreement with the values which can be derived from dimensional analysis.

The results presented enable us to say that the diagnostic model of climatic circulation, based upon measured density and wind fields (or the atmospheric pressure distribution) is a valuable tool for the description of real conditions.

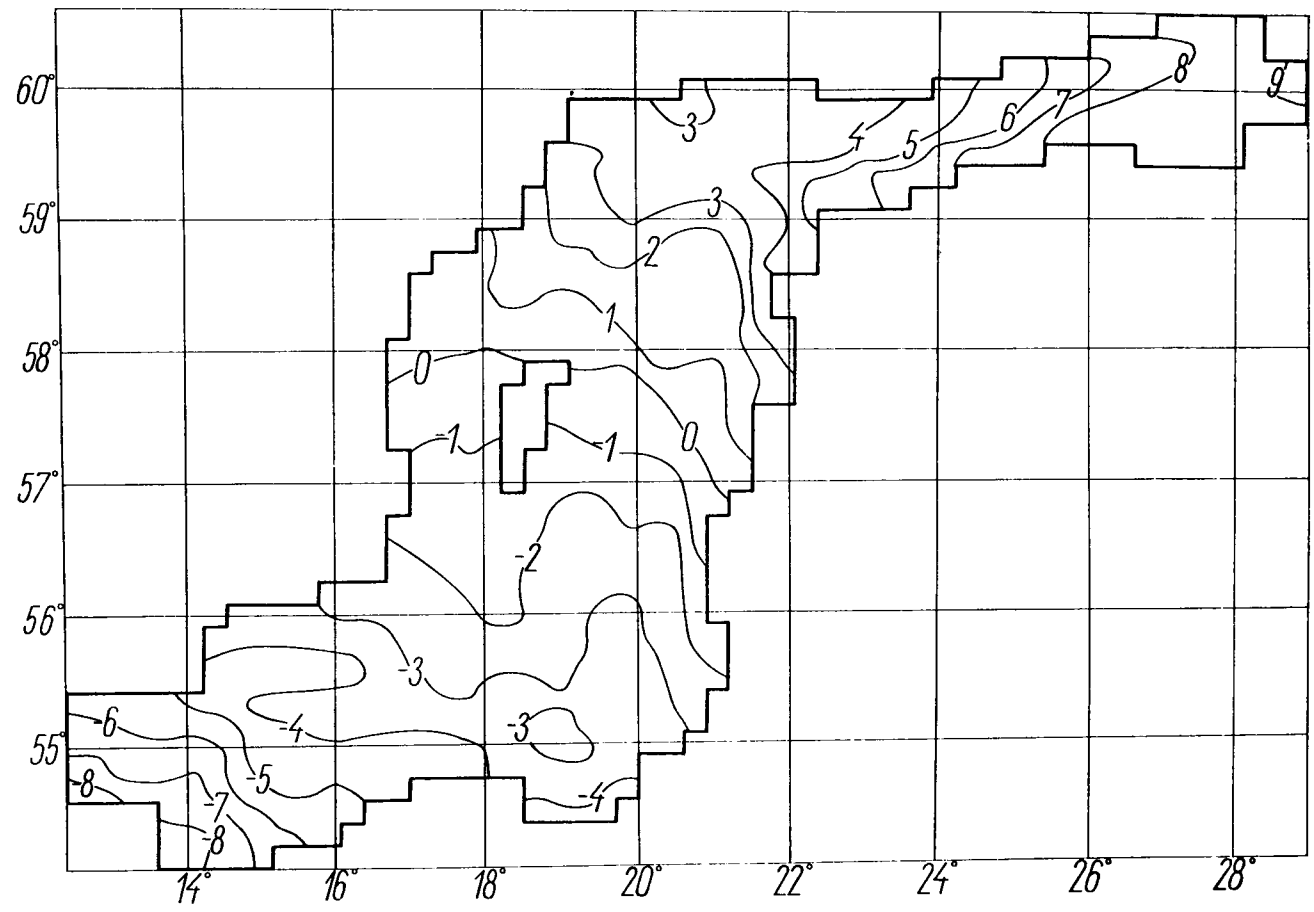


Fig. 26. CALCULATED SEA-LEVEL, THE NUMBERS ARE GIVEN IN CM.

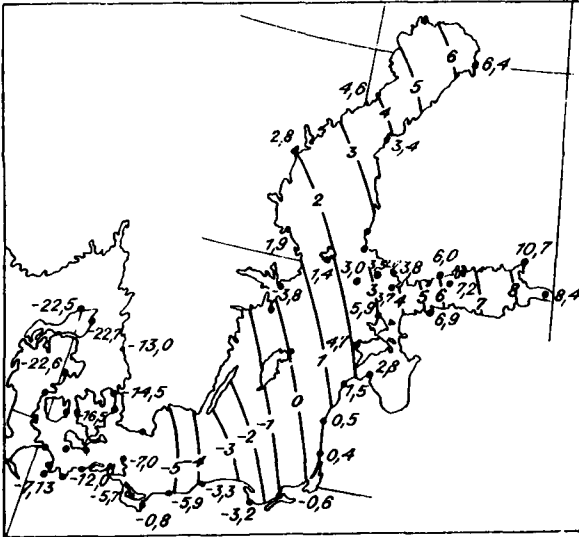


Fig. 27. OBSERVED SEA-LEVEL ACCORDING TO LAZARENKO (1960), THE NUMBERS ARE GIVEN IN CM.

§11. Different methods to estimate the exchange of momentum in the Ekman layer

The aim of the following paragraphs is to present systematically what knowledge exists on eddy viscosity as a decisive parameter in current computation.

In our search for the vertical distribution of the eddy viscosity coefficient we shall deal mainly with steady, uniform and horizontal flow in the absence of stratification in a horizontally infinite and vertically bounded layer of rotating fluid.

The different ways of description of eddy viscosity and their underlying hypotheses will be compared and studied.

The comparison concerns four methods:

- a) Eddy viscosity as a function of nondimensional parameters
- b) Constant eddy viscosity based on an empirical relation between the wind velocity and the surface current velocity

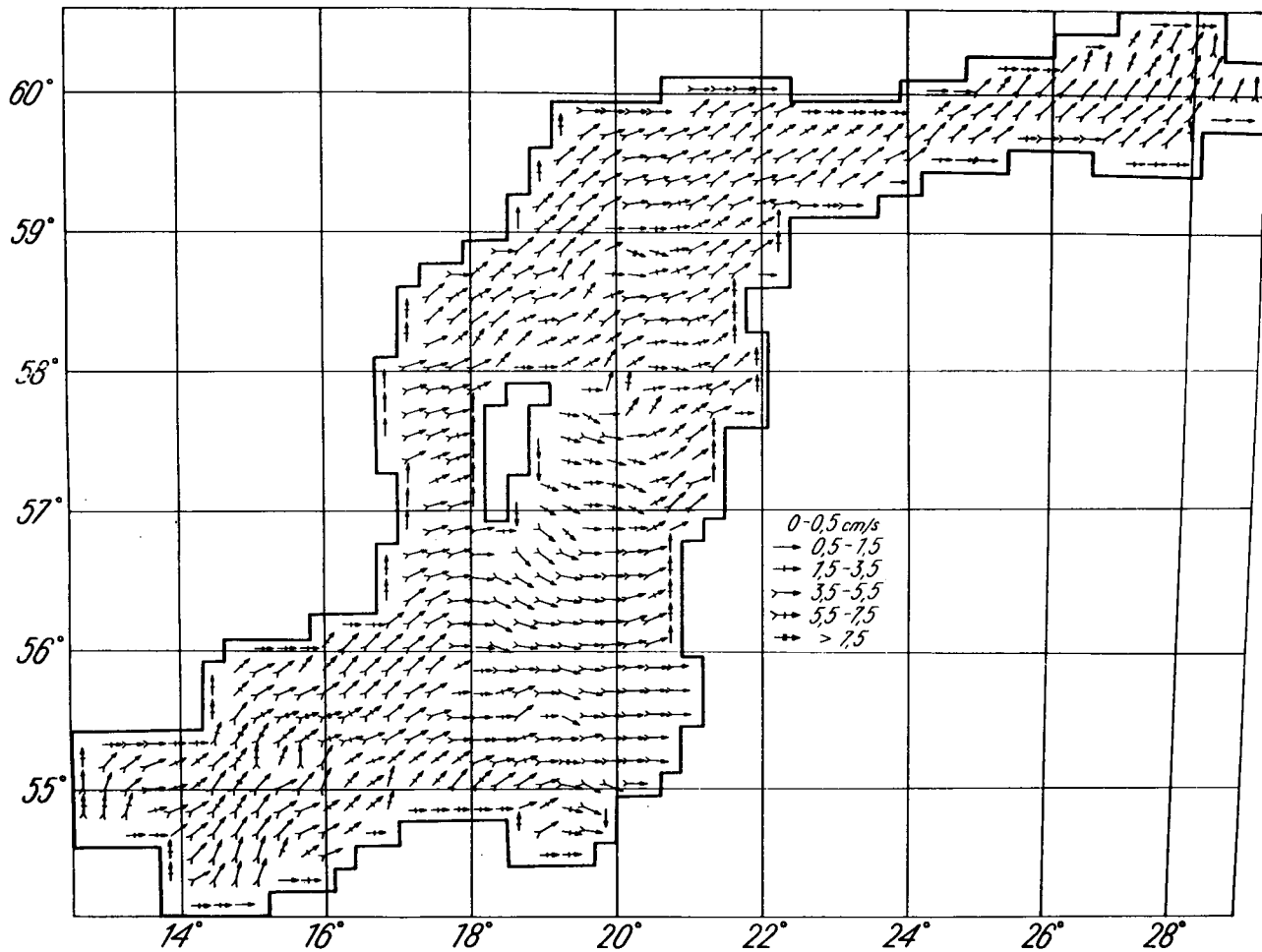


Fig. 28. WIND- AND DENSITY-DRIVEN CURRENTS AT THE SEA SURFACE.

- c) A statistical method based on the equations of turbulent energy and the scale length
- d) A statistical method based on the equations of turbulent energy and the dissipation function.

Numerical computations show certain differences between methods c) and d). They are related to the scale length definition at the larger distance from the sea surface. Method d), though the most promising, needs further elaboration with regard to the different boundary conditions, since the results derived by this method can be well apart from what has traditionally been anticipated.

When speaking about boundary layers in the sea we are dealing with two layers, one appears close to the bottom, and in this way reminds of flow types occurring in pipes or channels, the other exists at the sea surface, where often no analogy to pipe flow exists.

The consideration throughout will be usually related to a) shallow sea, i.e. the depth is small compared with the Ekman depth, accordingly bottom and surface boundary layers merge into one layer, b) deep sea, i.e. the depth is greater than the Ekman depth.

The different approaches to be studied will allow us to clarify and explain the different expressions derived for the eddy viscosity coefficient as given in §6 and §9.

§12. Dimensional analysis

Relating the properties of a turbulent boundary layer under neutral conditions to nondimensional parameters proved to be very successful in the past, see e.g. Csanady (1967), Blackadar and Tennekes (1968), Zilitinkevich (1970).

To apply the dimensional analysis one may state the following set of parameters which determine the flow within the planetary boundary layer:

V_*	= $\sqrt{\tau/\rho}$ friction velocity	z_0	roughness of the bounding surface
f	Coriolis parameter	ν	molecular kinematic viscosity
z	vertical co-ordinate.		

With these parameters it is possible to construct three independent, nondimensional numbers. To give a proper description of different portions of the flow in the boundary layer the numbers can be

constructed in different ways. First of all we may reject the molecular viscosity as a parameter by using the Reynolds number $Re = V_* z / \nu$. In natural flows $Re \gg 1$, therefore in agreement with the π -theorem (Kline, 1965) these flows do not depend on Re , and the molecular viscosity can be omitted from the set of defining parameters. This is, of course, true, except when $z \rightarrow 0$, or $V_* \rightarrow 0$, i.e. near bounding surfaces.

Beside the Reynolds number defined above a possibility exists to set a 'surface' Reynolds number as $Re_s = V_* z_0 / \nu$. Such a number seems to be more appropriate for the scaling of flow close to sea surface or bottom.

With the remaining dimensional parameters two nondimensional numbers can be constructed, i.e. the Rossby number $Ro = V_* / fz$, and the ratio z/z_0 . Again one may introduce a 'surface' Rossby number $Ro_s = V_* / fz_0$ to resolve the properties of the flow in the vicinity of the bounding surfaces.

Therefore, in general, the eddy viscosity k can be described by a function of two nondimensional parameters

$$k/V_* z = F(V_* / fz_0, z/z_0) \quad (3.76)$$

In further considerations the origin of our system of co-ordinates will be placed at the sea surface (since we shall deal predominantly with the surface boundary layer) and the z -axis will be directed towards the Earth's centre (left system of co-ordinates). Though in the whole book we prefer the right hand system of co-ordinates, we deviate from this convention now, since the values of co-ordinates related to the sea are negative (Fig. 1). Therefore, e.g., the Reynolds number should be written as $Re = -V_* z / \nu$. To avoid such a situation we shall change the direction of the z -axis; in all previously derived expressions one has to change z to $-z$ accordingly.

Let us first study an asymptote of (3.76) close to the sea surface, when $z \rightarrow 0$, thus $Ro \rightarrow \infty$ and

$$k/V_* z = F_1(z/z_0) \quad (3.77)$$

A careful analysis of the experimental data shows that in a very thin surface layer the molecular forces may play a substantial rôle in the exchange of momentum (Kitajgorodski, 1970). Since we do not intend to resolve that thin layer in which $z_0/z \approx 1$, we shall simply assume that beneath a molecular layer $z/z_0 \gg 1$, and from (3.77) we

get

$$k = C_s V_* z \quad (3.78)$$

where C_s denotes a constant.

From (3.78) follows that in the near surface layer the eddy viscosity coefficient is changing in a linear way with depth. This layer is commonly called a constant flux layer (constant flux of momentum). Since the stress τ is related to velocity by (1.34) the logarithmic dependence of velocity on depth in a surface layer follows from (3.78). The same holds for the bottom boundary layer.

In turn we may put $z \rightarrow \infty$, then from (3.76) follows

$$k = V_* z F_2(V_*/fz) \quad (3.79)$$

or, because $z \rightarrow \infty$,

$$k = C_d V_* z^2 f / V_* = C_d z^2 f \quad (3.80)$$

Assuming z in (3.80) as the depth of the Ekman layer D and defining the dependence of D on the Rossby number

$$D/z = F_3(V_*/fz) \quad (3.81)$$

the Ekman depth is obtained as

$$D = C_e V_* / f \quad (3.82)$$

By inserting (3.82) into (3.80) the eddy viscosity coefficient at the great depth is derived

$$k = C_d' V_*^2 / f \quad (3.83)$$

In (3.80), (3.82) and (3.83) the coefficients C_d , C_e and C_d' denote universal constants to be defined later on.

From the two derived asymptotes of the general law for the dependence of eddy viscosity on depth the following picture emerges: In the layers near the bottom and the free surface the exchange of momentum can be described by the eddy viscosity coefficient k which is a linear function of depth. The rest of the Ekman layer is characterized by the constant eddy viscosity coefficient.

It is easy to see that this general picture possesses the inherent flaws. On one hand in the layers situated close to the bounding surfaces the molecular forces may play a definite rôle, and on the other hand between the surface boundary layer, where the linear law prevails, and the 'outer' boundary layer of constant eddy viscosity a matching layer with an intermediate law should also exist.

§13. Constant eddy viscosity

Though this approach seems to be a step backward compared with the dimensional analysis it may serve two aims, on one side it sets a definite magnitude to the eddy viscosity and on the other side the vertical distribution of current can be derived in a comparatively simple way.

The approach we shall present here is the modified idea of Felzenbaum (1960); see also Kowalik (1969).

Our aim is to justify the expressions used in §6. To find the eddy viscosity distribution we shall base upon the Ekman solution (3.20) and on an empirical relation between the current velocity at the sea surface U_0 and the wind velocity W

$$\beta = U_0/W \quad (3.84)$$

The coefficient β is often called 'wind factor'. The knowledge of this factor is very obscure. The old data relating surface velocity and wind velocity are shortly summarized by Defant (1961). Theoretically from the Ekman solution for an unbounded ocean follows

$$U_0 = \tau / \sqrt{fk} \quad (3.85)$$

Assuming τ to be proportional to the wind velocity W

$$U_0 = \beta_1 W / \sqrt{\sin\phi} = W\beta \quad (3.86)$$

Thus (3.86) shows the variation of β along the geographical latitude ϕ . The data gathered by Krasiuk and Sauskan (1970) and the measurements performed by Tomczak (1964) display a dependence of β on wind speed. At small wind speeds $\beta \approx 0.015$; its magnitude grows up to 0.03 - 0.04 at 30 m/sec wind speed.

Based on available data we have set a tentative expression to take into account the dependence on the wind velocity at mean latitudes as

$$\beta = 0.013 + 7 \times 10^{-6} W \quad (\text{cm/sec}) \quad (3.87)$$

By introducing the velocity from (3.20) in (3.84) the implicit equation to define an unknown value k is obtained

$$(SS^*)^{1/2} = U_0 = W\beta \quad (3.88)$$

In (3.88) S^* is a complex conjugate of S .

A general implicit equation which follows from (3.88) was solved by Felzenbaum (1960). We approach the problem by notions of the deep and shallow sea, since these cases can be treated analytically.

A Shallow sea case ($H \rightarrow 0$, or equivalently $f \rightarrow 0$)

Equation (3.20) is simplified to the following form

$$u = \frac{1}{\rho k} \tau_s(x) (H - z) + \frac{g}{k} \frac{(H^2 - z^2)}{2} \frac{\partial \zeta}{\partial x} \quad (3.89)$$

$$v = \frac{1}{\rho k} \tau_s(y) (H - z) + \frac{g}{k} \frac{(H^2 - z^2)}{2} \frac{\partial \zeta}{\partial y} \quad (3.90)$$

Integrating (3.89) and (3.90) from the sea surface to the bottom and then introducing the stream function through (3.25) the sea slope components are obtained

$$\frac{\partial \zeta}{\partial x} = -\frac{3}{2\rho g H} \tau_s(x) + \frac{3k}{g H^3} \frac{\partial \psi}{\partial y} \quad (3.91)$$

$$\frac{\partial \zeta}{\partial y} = -\frac{3}{2\rho g H} \tau_s(y) - \frac{3k}{g H^3} \frac{\partial \psi}{\partial x} \quad (3.92)$$

The aim of the above procedure is to introduce the components of slope in (3.89) and (3.90) so that eventually the current at the free surface will be a function of stress and some other parameters but not of the slope, which is difficult to obtain.

An equation for the unknown function ψ in (3.91) and (3.92) is derived by cross-differentiation and subsequent subtraction of these equations

$$\frac{1}{2\rho} \left[\frac{\partial}{\partial y} (\tau_s(x)/H) - \frac{\partial}{\partial x} (\tau_s(y)/H) \right] = k \left[\frac{\partial}{\partial y} (H^{-3} \frac{\partial \psi}{\partial y}) + \frac{\partial}{\partial x} (H^{-3} \frac{\partial \psi}{\partial x}) \right] \quad (3.93)$$

In the case of $\tau_s^{(x)} = \text{const.}$, $\tau_s^{(y)} = \text{const.}$ and $H = \text{const.}$ (3.93) reduces to

$$\Delta\psi = 0 \quad (3.94)$$

The boundary condition for this problem follows from the impermeability of the coast

$$\psi = 0 \quad (3.95)$$

With such a condition the solution to (3.94) is $\psi = \text{constant}$. The slope components (3.91) and (3.92) are therefore

$$\frac{\partial \zeta}{\partial x} = -\frac{3}{2} \frac{1}{gH} \tau_s^{(x)} ; \quad \frac{\partial \zeta}{\partial y} = -\frac{3}{2} \frac{1}{gH} \tau_s^{(y)} \quad (3.96)$$

When (3.96) is introduced in (3.89) and (3.90) the components of the velocity at the free surface result in

$$u_o = \frac{H}{4\rho k} \tau_s^{(x)} ; \quad v_o = \frac{H}{4\rho k} \tau_s^{(y)} \quad (3.97)$$

Finally inserting (3.97) into (3.88)

$$U_o = W\beta = (u_o^2 + v_o^2)^{1/2} = \frac{H}{4\rho k} [\tau_s^{(x)2} + \tau_s^{(y)2}]^{1/2} \quad (3.98)$$

the eddy viscosity coefficient is expressed as

$$k = \frac{H}{4\rho\beta W} [\tau_s^{(x)2} + \tau_s^{(y)2}]^{1/2} = \frac{H}{4\rho\beta W} \tau_s \quad (3.99)$$

Assuming the dependence of τ_s on the wind W in the form

$$\tau_s = \gamma W^2 \quad (1.65)$$

the above expression can be rewritten as

$$k = \gamma WH/4\beta \quad (3.100)$$

In the case of a horizontally unbounded sea ($\frac{\partial \zeta}{\partial x} = 0$, $\frac{\partial \zeta}{\partial y} = 0$) the eddy viscosity coefficient is equal to

$$k = \gamma WH/ \beta \quad (3.101)$$

Comparing (3.101) with the previously derived expression (3.78) it is observed that the actual depth in (3.78) is superseded by the over-all depth H in (3.101), while the wind velocity W and friction velocity V_* remain for the same parameter. Therefore in principle the model with constant eddy viscosity can be applied to define the C_s constant in expression (3.78).

B. Deep sea case ($H \rightarrow \infty$)

In this case expression (3.20) is expressed as

$$u = \frac{1}{\alpha_1 k \sqrt{2}} \exp(-\alpha_1 z) \cdot [\tau_s^{(x)} \sin(\pi/4 - \alpha_1 z) + \tau_s^{(y)} \cos(\pi/4 - \alpha_1 z)] + \frac{g \partial \zeta}{f \partial y} \quad (3.102)$$

$$v = \frac{1}{\alpha_1 k \sqrt{2}} \exp(-\alpha_1 z) \cdot [-\tau_s^{(x)} \cos(\pi/4 - \alpha_1 z) + \tau_s^{(y)} \sin(\pi/4 - \alpha_1 z)] - \frac{g \partial \zeta}{f \partial x} \quad (3.103)$$

where

$$\alpha_1 = \sqrt{f/2k}$$

Again by integrating from the surface to the bottom and subsequently introducing the stream function the sea slope components are obtained

$$\frac{\partial \zeta}{\partial x} = - \frac{1}{\rho g H} \tau_s^{(x)} \frac{f}{g H} \frac{\partial \psi}{\partial x} \quad (3.104)$$

$$\frac{\partial \zeta}{\partial y} = - \frac{1}{\rho g H} \tau_s^{(y)} - \frac{f}{g H} \frac{\partial \psi}{\partial y} \quad (3.105)$$

Implying the cross-differentiation technique and solving as we did before an equation for the stream function in a basin of uniform depth the same result is obtained, i.e.

$$\frac{\partial \psi}{\partial x} = 0; \quad \frac{\partial \psi}{\partial y} = 0$$

Therefore the system (3.104), (3.105) reduces to

$$\frac{\partial \zeta}{\partial x} = -\frac{1}{\rho g H} \tau_s^{(x)} ; \quad \frac{\partial \zeta}{\partial y} = -\frac{1}{\rho g H} \tau_s^{(y)} \quad (3.106)$$

but in this case if (3.106) is inserted into (3.102) and (3.103) respectively, it will not give any input, because, when $H \rightarrow \infty$, the slope components (3.106) disappear.

The components of the current at the sea surface based on (3.102) and (3.103)

$$u_o = \frac{1}{2\alpha_1 k} (\tau_s^{(x)} + \tau_s^{(y)}); \quad v_o = \frac{1}{2\alpha_1 k} (\tau_s^{(y)} - \tau_s^{(x)}) \quad (3.107)$$

can therefore be introduced in (3.88)

$$(u_o^2 + v_o^2)^{1/2} = \beta W \quad (3.108)$$

In order to derive the eddy viscosity coefficient in the deep sea, we get then

$$k = (\gamma/\beta)^2 \cdot W^2 / f \quad (3.109)$$

Again (3.109) is quite similar to expression (3.83), though it is quite clear that c_D is not equal to the constant used in (3.109), because the underlying phenomena are of a different nature.

Expression (3.109) describes the exchange of momentum in the whole Ekman layer, while (3.83) does only hold in the outer portion of the same layer.

Since (3.100) holds in the shallow sea and (3.109) in the deep one, it is possible to compare both expressions and to find (Kowalik, 1969)

$$H_{cr} = 4(\gamma/\beta) \cdot W/f \quad (3.110)$$

the depth which divides the regions where (3.100) and (3.109) can be applied respectively. If $H < H_{cr}$, (3.100) should be used, if on the other hand $H > H_{cr}$, (3.109) is appropriate.

§14 A statistical method based on the equation of turbulent energy b^2 and the scale length l

The method is known as the closure of the set of equations of motion and continuity with the additional hypotheses which follow from the statistical theory of turbulence (Launder and Spalding, 1972).

At first we consider an equation for the turbulent energy. This equation like many others arises from the general transport equation for a scalar as a dependent variable. The aim is to include a wide range of turbulent processes in a simple equation with a certain number of unknown parameters which subsequently can be defined by experimental results. In all equations isotropy is usually assumed (Willebrand, 1974) and the flow conditions are set in close proximity to an equilibrium regime characterized by the inertial range of turbulent flow. An intermittent laminar-turbulent or an internal wave flow can be described by the transport equation but still some work is required to apply the postulates taken from the near-wall turbulence into oceanic conditions.

The general transport equation for the quantity Q can be written as

$$\frac{dQ}{dt} = \text{Production } (Q) - \text{Dissipation } (Q) + \text{Diff.}(Q) \quad (3.111)$$

From this simple principle the equations of energy dissipation are derived, see e.g. Daly and Harlow (1970), Nakayama (1970). The purpose of building an equation in the above form is not to learn something about detailed features of turbulence but to find possibly the quantities that are characteristic for the mean flow, i.e. the distribution of velocity and stresses. The idea behind equation (3.111) is to relate the local properties of mean turbulence to nonlocal effects such as diffusion and advection. The local hypotheses which are sufficient in describing the laminar motion and on which the idea of the virtual eddy viscosity is based are not adequate to describe the turbulent flow consisting of the broad spectra of eddies.

The basic equation for the kinetic energy b^2 of turbulent flow (3.60) we take in simplified form

$$k \left[\left(\frac{\partial u}{\partial z} \right)^2 + \left(\frac{\partial v}{\partial z} \right)^2 \right] + \frac{\partial}{\partial z} \left(k \frac{\partial b^2}{\partial z} \right) - \epsilon = 0 \quad (3.112)$$

It is usually considered together with the additional relationships which follow from the Kolmogorov hypothesis of similarity (3.61) and the scale of turbulence obtained from Karman's hypothesis (Kline, 1965)

$$1 = -2\chi \left[\left(\frac{\partial u}{\partial z} \right)^2 + \left(\frac{\partial v}{\partial z} \right)^2 \right] / \frac{\partial}{\partial z} \left[\left(\frac{\partial u}{\partial z} \right)^2 + \left(\frac{\partial v}{\partial z} \right)^2 \right] \quad (3.113)$$

If the x -axis is directed along the surface velocity, expression (3.113) takes the simplified form

$$l = -\chi \frac{\partial u}{\partial z} / \frac{\partial^2 u}{\partial z^2} \quad (3.114)$$

Omitting the diffusion term in (3.112) the length scale is also easily described by the energy

$$l = -2\chi b^4 / k^2 \cdot \frac{\partial}{\partial z} (b^4 / k^2) \quad (3.115)$$

Though the formula (3.114) is closing the system of equations, from the numerical point of view the second derivative in the denominator makes Karman's hypothesis useless; nevertheless, analytically still some consequences can be sought.

On the other hand in the derivation of (3.113) von Karman assumed steady flow and negligible molecular viscous effects (Kline, 1965). Therefore only under very stringent conditions formula (3.113) may be applied to an unsteady or oscillatory flow. To comply with the requirement of small viscous effects it is enough to deal with big Reynolds numbers

$$Re = vl / \nu \gg 1 \quad (3.116)$$

At the wall where $l \rightarrow 0$ and $\nu \rightarrow 0$ (3.116) cannot hold, thus at a small distance from the wall the similarity law developed by von Karman must be superseded by a different approximation.

Now we can add the relevant boundary conditions to the equations (3.112) and (3.113). These conditions are formulated by equations (3.64), (3.65) and (3.66).

The magnitudes of the universal constants in the similarity relationships (3.61) are usually determined by means of a hypothesis found by Blackadar (1962), the assumption of the neutral velocity profile, i.e. a distribution of velocity is related to a non-stratified fluid. Such an assumption leads to dependence (3.63). Some time ago Zilitinkevich et al. (1967) estimated c as 0.046, recent values obtained through the examination of tube flows give $c = 0.08$, therefore $c_0 = 0.532$ and $c_1 = 0.150$.

§15. Shallow, horizontally unbounded sea

By directing the x -axis along the wind and, as in the shallow sea $H \rightarrow 0$, the equation of motion with variable eddy viscosity reduces to

$$\frac{\partial}{\partial z} \left(k \frac{\partial u}{\partial z} \right) = \frac{\partial \tau}{\partial z} = 0 \quad (3.117)$$

The proper boundary conditions are set by (3.18). The equation of energy we shall use in a simplified form assuming the process of energy diffusion being of secondary importance. This allows us on one hand to solve the problem analytically, and on the other hand to explain the way of choosing the universal constants through the neutral velocity distribution as expressed by (3.63).

As a solution of (3.117) with boundary condition

$$-k\rho\frac{\partial u}{\partial z} = \tau_s \quad (3.118)$$

inserted into the energy equation

$$k\left(\frac{\partial u}{\partial z}\right)^2 - \epsilon = 0 \quad (3.119)$$

together with (3.61) we get

$$b = \sqrt{\tau_s / \rho \sqrt{c_0 c_1}} \quad (3.120)$$

Next, (3.114) together with (3.118) provides

$$\frac{dk}{dz} = -\chi c_0 b \quad (3.121)$$

thus

$$k = \chi c_0 b (H - z) = \chi c_0 \sqrt{\tau_s / \rho \sqrt{c_0 c_1}} \cdot (H - z) \quad (3.122)$$

Comparing (3.122) with the distribution in neutral flow (Blackadar, 1962)

$$k = \chi V_* (H - z) = \chi \sqrt{\tau_s / \rho} \cdot (H - z) \quad (3.123)$$

we find

$$c_0 / \sqrt[4]{c_0 c_1} = 1 \quad (3.124)$$

or denoting $c_0 c_1 = c$ it follows

$$c_0^4 = c \text{ and } c_0^3 = c_1 \quad (3.125)$$

From the above consideration it is clear that the neutral distribution is strongly based on the rejection of the diffusion term in (3.112).

We shall see later on that such a procedure is not quite valid.

The length scale from (3.122) and (3.61) is expressed as

$$l = k/c_0 b = \chi(H - z) \quad (3.126)$$

Finally, integrating (3.117) with the eddy viscosity given by (3.123) we arrive at

$$u = \frac{1}{\chi} \sqrt{\tau_s/\rho} \cdot \ln \frac{H-z}{z_0} \quad (3.127)$$

where z_0 denotes a bottom roughness parameter.

To our disposal we still have an empirical boundary condition, (3.88). It can be used to find a bottom roughness, or at least to clarify which z_0 should be used to derive the proper value of velocity (Kuftarkov and Felzenbaum, 1968).

Thus inserting (3.127) into (3.88) at $z = 0$ we obtain

$$z_0 = H \exp\left(-\frac{W\beta\chi}{\sqrt{\tau_s/\rho}}\right) = H \exp\left(-\frac{\beta\chi}{\sqrt{\gamma}}\right) \quad (3.128)$$

Setting in (3.128) $H = 500$ cm, $W = 10$ m/sec and $\tau = 2$ g/cmsec² the bottom roughness becomes equal to 1.75 cm.

The main conclusion from the formulae derived above is that in the shallow sea the turbulent energy is constant throughout depth. This leads to the linear dependence of the eddy viscosity and the scale length on depth and the logarithmic velocity distribution.

Now we shall turn to the complete case of the energy equation with the diffusion term included and we shall check our previous conclusions.

The system of equations (3.112) and (3.117) has now to be solved by a numerical method. To this we include the time term in (3.112) and integrate this equation in time together with the equations of motion until the steady state occurs. The nonlinear terms are approximated by the explicit numerical scheme

$$\frac{B^{l+1} - B^l}{T} = k^l \left[\left(\frac{\partial u}{\partial z}\right)^2 + \left(\frac{\partial v}{\partial z}\right)^2 \right]^l - c_0 c_1 \frac{(B^2)^l}{k^l} + \frac{\partial}{\partial z} \left(k \frac{\partial B^l}{\partial z} \right) \quad (3.129)$$

here

$B = b^2$ $T =$ time step of numerical integration

$t = lT$ $l = 1, 2, 3, \dots$

A difficulty appears, as we stated previously, in the numerical integration of (3.114). Therefore we take the scale length of turbulence as

$$l = C_1 z \quad (3.130)$$

with posteriori choice of C_1 from condition (3.84).

The eddy viscosity coefficient and the dissipation were calculated by (3.61). The results are plotted in fig. 29, here the value of energy b is constant throughout depth and the distribution of eddy viscosity is almost linear, while the development of the steady state solution is presented by plots after 5 min., 2 h and 5 h of integration. The results are compared with the previous analytical solution which is shown in fig. 29 by broken lines.

In both cases the distribution of velocity and energy is quite close, but in the pattern of eddy viscosity displays a pronounced difference, especially in the vicinity of the free surface.

The presence of the diffusion term involves therefore the definite difference in the solution.

§16. Two-layer model

From the above considerations emerges a notion of two layers with different laws of momentum exchange, i.e. a near surface layer and an outer layer. We shall explore the idea through the set of equations introduced in the previous paragraphs.

As before, the x -axis will be directed alongside the wind, so that the equation of motion in the surface boundary layer will simplify to (3.117) with boundary condition (3.118). At the bottom of the surface layer $z = \delta$ the continuity of velocity and stress holds. By assuming in the surface layer the linear law for the eddy viscosity and in the outer layer the constant eddy viscosity k_δ , the overall law can be represented as

$$k = k_\delta + \chi V_* (\delta - z) = k_\delta + \chi \sqrt{\tau_s / \rho} \cdot (\delta - z) \quad (3.131)$$

The solution of (3.117)

$$u = u_0 + \frac{1}{\chi} \sqrt{\tau_s / \rho} \cdot \ln \left[\frac{k_\delta + \chi \sqrt{\tau_s / \rho} (\delta - z)}{k_\delta + \chi \sqrt{\tau_s / \rho} \cdot \delta} \right] \quad (3.132)$$

is therefore a modified logarithmic law.

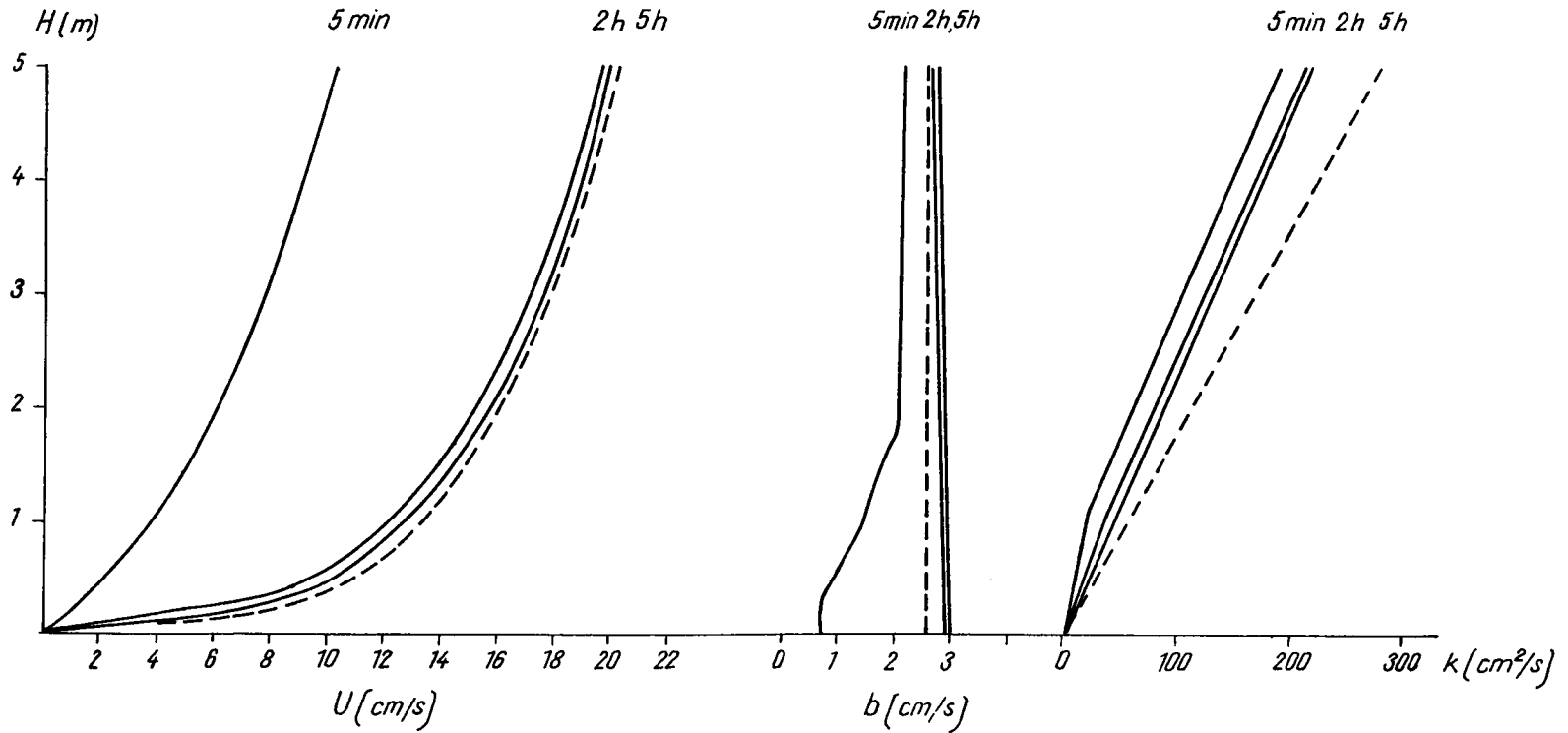


Fig. 29. DISTRIBUTION OF VELOCITY U , SQUARE ROOT OF ENERGY B AND EDDY VISCOSITY K AGAINST DEPTH H . THE DASHED LINE DENOTES THE ANALYTICAL SOLUTION, CONTINUOUS LINES DENOTE THE NUMERICAL SOLUTIONS. AT THE BOTTOM $K = 1 \text{ cm}^2/\text{sec}$, $z_0 = 1.7 \text{ cm}$.

Solving next the system (3.16) and (3.17) (with $\frac{\partial \zeta}{\partial x} = 0$, $\frac{\partial \zeta}{\partial y} = 0$) in the outer Ekman layer from $z = \delta$ to $z \rightarrow \infty$, we arrive at

$$u = u_{\delta} \exp[-\alpha_1(z-\delta)] \cos \alpha_1(z-\delta) \quad (3.133)$$

$$v = v_{\delta} \exp[-\alpha_1(z-\delta)] \sin \alpha_1(z-\delta)$$

In (3.133) u_{δ} is the velocity (3.132) at $z = \delta$.

Due to continuity of stress at $z = \delta$

$$\tau_s = \rho k \left[\left(\frac{\partial u}{\partial z} \right)^2 + \left(\frac{\partial v}{\partial z} \right)^2 \right]^{1/2} = \sqrt{fk\rho} u_{\delta} \quad (3.134)$$

one can calculate k_{δ} or u_{δ} .

In case the upper boundary layer is absent we have discussed above the way of calculating a constant eddy viscosity coefficient. Let us make therefore a proper modification of (3.109) to obtain the constant eddy viscosity in the outer Ekman layer. Since

$$k = (\gamma/\beta)^2 \cdot w^2/f = \gamma^2 w^4/U_o^2 f = \tau_s^2/U_o^2 f \quad (3.135)$$

one may think along the following lines; throughout the logarithmic surface layer the stress is constant, therefore at $z = \delta$ the stress is equal to the wind stress, but the surface current U_o in (3.135) at depth $z = \delta$ should be superseded by u_{δ} , therefore (3.135) can be rewritten as

$$k_{\delta} = \gamma^2 w^4/u_{\delta}^2 f = \tau_s^2/u_{\delta}^2 f \quad (3.136)$$

This expression follows, of course, straightforward from (3.134). Though (3.136) may help to understand the increase of exchange of momentum due to the presence of the logarithmic surface boundary layer ($u_{\delta} < U_o$, thus $k_{\delta} > k$), it does not take us nearer to the overall solution of the problem.

Introducing u_{δ} from (3.134) in (3.132) leads to

$$\tau_s / \sqrt{fk_{\delta}} = u_o + \frac{1}{\chi} \sqrt{\tau_s / \rho} \ln [k_{\delta} / (k_{\delta} + \chi \sqrt{\tau_s / \rho} \delta)] \quad (3.137)$$

at $z = \delta$. Here still two unknowns occur, i.e. the thickness of the logarithmic layer δ , and the eddy viscosity in the outer Ekman layer k_{δ} .

One possibility is to apply (3.61) to express the eddy viscosity coefficient as

$$k = c_0 \bar{l} \bar{b} \quad (3.138)$$

where \bar{l} and \bar{b} are the scale length and the energy averaged over the depth. The vertical integration will be carried out from $z = \delta$ to $z = H$, where $H - \delta = D$ is the Ekman depth.

First, taking for l von Karman's expression (3.114) we obtain

$$\bar{l} = \chi / \alpha_1 = \chi \sqrt{2k_\delta / f} \quad (3.139)$$

Secondly, by integrating (3.112) the energy is estimated as

$$\bar{b} = \frac{1}{\sqrt{c\pi}} \sqrt{\alpha_1 u_\delta k_\delta} \quad (3.140)$$

Finally, introducing (3.139) and (3.140) in (3.138) the eddy viscosity in the outer layer is obtained

$$k_\delta = \frac{1}{f\sqrt{c\pi}} c_0^2 \chi^2 \tau \sqrt{2} \quad (3.141)$$

This allows us together with (3.137) to find k_δ and δ . The values derived in this way are much in excess of what is usually anticipated for the wind $W = 10$ m/sec, $\tau = 2$; because $k_\delta = 2555$ cm²/sec and $\delta = 4176$ m. One may therefore conclude that the whole Ekman layer is included in the logarithmic layer.

The coefficient (3.141) compared with the case of constant eddy viscosity (3.135) gives a completely distorted picture of current distribution.

The most probable error is due to the length scale assumption; the von Karman's hypothesis - though useful in the surface boundary layer - is providing an overestimated length scale in the outer layer.

Such a conclusion can also be anticipated from the fact that the von Karman's relationship is based on the Reynolds number similarity (Kline, 1965), while the dynamics of the outer layer are governed by the Rossby number.

Another possibility is to apply a different hypothesis for the length scale. We shall assume here the expression of Mellor and Durbin (1975)

$$\bar{l} = 0.1 \cdot \frac{\int_\delta^H |z| b^2 dz}{\int_\delta^H b^2 dz} \quad (3.142)$$

Our choice follows from the actual fact that Mellor's and Durbin's (1975) formula for the eddy viscosity in a non-stratified fluid sets the coefficient 0.1 in (3.142) when compared with the formulae of constant eddy viscosity (3.101) or (3.109). Therefore we may assume that (in a non-stratified fluid) the approach taken by Mellor and Durbin is consistent with the approach of Felzenbaum (1960).

From (3.112), by means of (3.61) and (3.133), the turbulent energy distribution in the outer layer can be derived as

$$b^2 = \frac{\sqrt{2}}{\sqrt{c_0 c_1}} u_\delta k_\delta \alpha_1 \exp(-\alpha_1(z-\delta)) \quad (3.143)$$

Inserting (3.143) into (3.142) the length scale follows as

$$\bar{l} = \frac{0.1}{\alpha_1} \quad (3.144)$$

Taking (3.144) as the new length in (3.138) and next checking (3.139) we see that in (3.141) should be superseded by 0.1

$$k = \frac{1}{\sqrt{c\pi f}} c_0^2 (0.1)^2 \sqrt{2} \tau \quad (3.145)$$

For the wind $W = 10$ m/sec ($\tau = 2$) and $f = 10^{-4}$ sec $^{-1}$, the eddy viscosity is equal to 159.7 cm 2 /sec. The thickness of the logarithmic layer derived from (3.137)

$$\delta = \frac{k_\delta}{\chi \sqrt{\tau_s / \rho}} \left\{ \exp \left[-\frac{\chi}{\sqrt{\tau_s / \rho}} \left(\frac{\tau_s}{\sqrt{fk_\delta}} - U_0 \right) \right] - 1 \right\} \quad (3.146)$$

provides $\delta = 6.4$ m, while the Ekman depth calculated from the expression $\alpha_1 D = \pi$ is equal to 56.1 m.

The general picture is plotted in fig. 30. Here the results of a two-layer model (broken line) are compared with the model of a constant eddy viscosity coefficient (continuous line).

§17. A statistical method based on the equations of energy and dissipation

The weakness of the methods presented above lies mainly in the scale length notion. Therefore in this paragraph we shall explore shortly the possibility of closure through the turbulent dissipation equation. To the set of equations, instead of the scale length, the dissipation equation is adjoined (Jones and Launder, 1972)

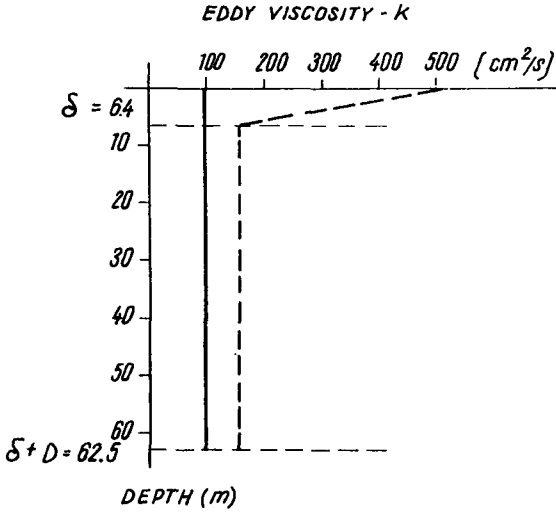


Fig. 30. DISTRIBUTION OF EDDY VISCOSITY IN THE TWO-LAYER MODEL (DASHED LINE) AND IN THE ONE-LAYER MODEL (CONTINUOUS LINE).

$$\frac{\partial}{\partial z} \left(k \frac{\partial \epsilon}{\partial z} \right) + c_2 k \frac{\epsilon}{b^2} \left[\left(\frac{\partial u}{\partial z} \right)^2 + \left(\frac{\partial v}{\partial z} \right)^2 \right] - c_\epsilon \frac{\epsilon^2}{b^2} = 0 \quad (3.147)$$

where

$$c_\epsilon = 2.0(1.0 - 0.3 \exp(-Re^2)) \quad (3.148a)$$

$$k = c_k 0.08 \frac{b^4}{\epsilon}; \quad c_k = \exp(-2.5/(1.0 + Re/50)) \quad (3.148b)$$

$$c_2 = 1.55 \quad (3.148c)$$

The local Reynolds number in (3.148) is estimated by

$$Re = \frac{\rho b^4}{k \epsilon} \quad (3.149)$$

Practically in natural flows the local Reynolds number is always large so that

$$c_\epsilon = 2.0; \quad c_k = 1.0 \quad (3.150)$$

result. Equation (3.147) was used to predict the near-wall boundary layer. Judging from our previous experience it may predict properly the logarithmic boundary layer in the sea.

To describe the whole Ekman layer a modification of the above equation is surely needed. To resolve the flow in the deep sea Marchuk et al. (1976) proposed

$$1.38k\frac{\epsilon}{2}\left[\left(\frac{\partial u}{\partial z}\right)^2 + \left(\frac{\partial v}{\partial z}\right)^2\right] + \frac{\partial}{\partial z}\left(k\frac{\partial \epsilon}{\partial z}\right) - 1.4\frac{\epsilon^2}{b^2} = 0 \quad (3.151)$$

We start again by solving the problem in the shallow sea by including the dissipation (3.147) in the set of equations. For the numerical solution of (3.147) we shall develop an explicit numerical scheme in the way it has been done for the energy equation (3.129). To start with the unknown equation, it is good to compare the results derived by (3.147) and the previous result from the scale length hypothesis. The main problem which arises is to formulate a proper set of boundary conditions. To comply with (3.61), energy and length should be specified at the bounding surfaces. The magnitude of energy can be estimated by (3.65), but one may have a quite difficult problem to define the scale length. In order to find at least in the family of solutions given by (3.147) one related to the hypotheses mentioned above, we fix in every numerical experiment the eddy viscosity at the free surface as $k_s = 211 \text{ cm}^2/\text{sec}$ and allow the eddy viscosity at the bottom to be variable. The numerical solutions for the velocity, the energy, the eddy viscosity and the dissipation are presented in fig. 31.

They show that also the energy and the eddy viscosity distribution is quite close to the results obtained by the energy scale method, although the velocity distribution is not completely identical.

Still, to close the overall problem, the surface boundary condition should be specified.

To equation (3.151) one may propose at the free surface

$$\frac{\partial \epsilon}{\partial z} = 0 \quad (3.152)$$

i.e. a decay in the flux of dissipation (whatever it may mean!). At the lower boundary in the sea which is deep enough

$$\epsilon \rightarrow 0 \quad (3.153)$$

In this somehow obscure way the overall problem is closed.

The method to choose the coefficients in (3.151) for the flow in the sea is neither clear nor fully proved through a comparison with observed data. Still much work on the experimental and the numerical

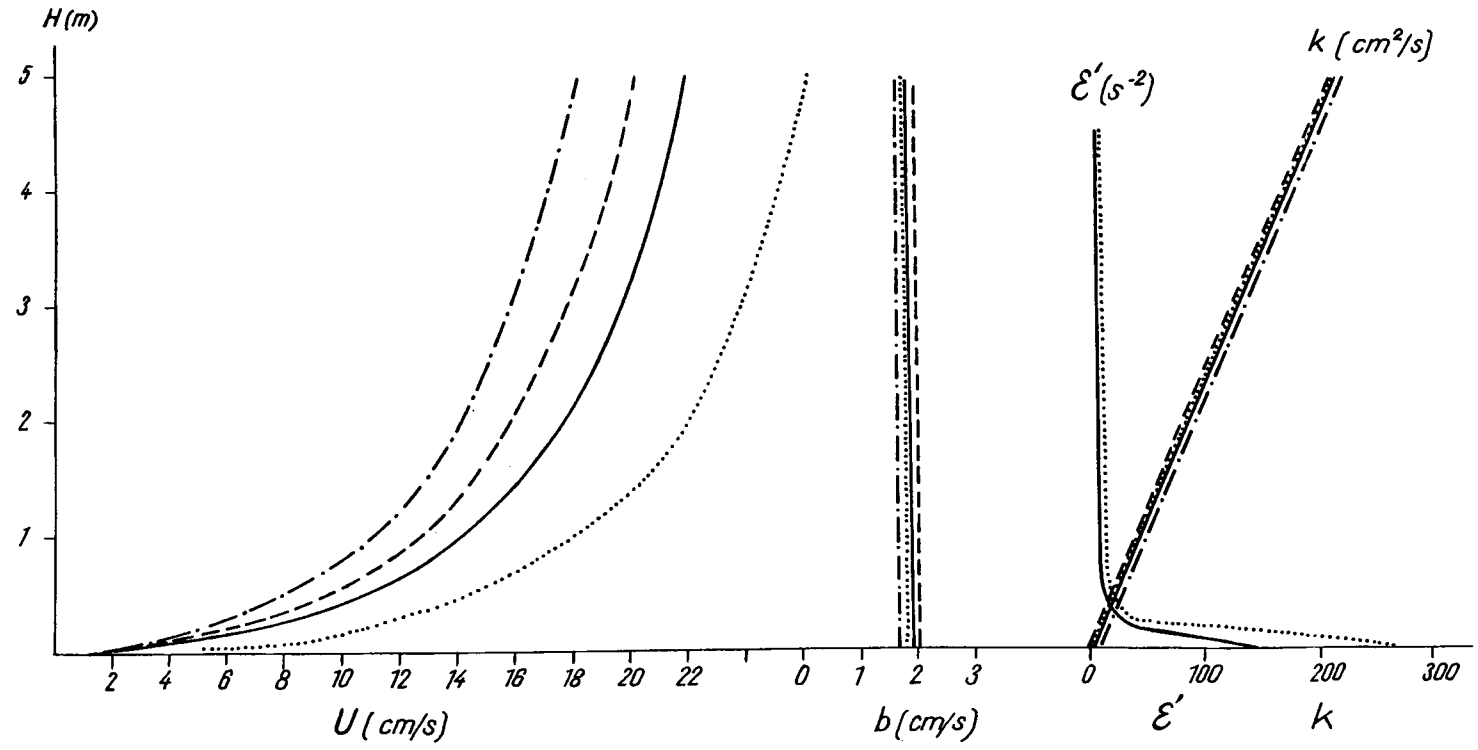


Fig. 31. DISTRIBUTION OF VELOCITY U , SQUARE ROOT OF ENERGY b , EDDY VISCOSITY k AND DISSIPATION ϵ' ($\epsilon' = \epsilon/\nu$), AGAINST THE DEPTH H . EDDY VISCOSITY AT THE BOTTOM IS DENOTED BY K_0 AND AT THE SEA SURFACE BY K_s .

- . . . - SOLUTION BY B- ϵ METHOD, $K_0=4.1 \text{ cm}^2/\text{sec}$, $K_s= 211 \text{ cm}^2/\text{sec}$
- SOLUTION BY B- l METHOD, $K_0=1.0 \text{ cm}^2/\text{sec}$, $K_s= 211 \text{ cm}^2/\text{sec}$
- SOLUTION BY B- ϵ METHOD, $K_0=2.0 \text{ cm}^2/\text{sec}$, $K_s= 211 \text{ cm}^2/\text{sec}$
- SOLUTION BY B- ϵ METHOD, $K_0=1.0 \text{ cm}^2/\text{sec}$, $K_s= 211 \text{ cm}^2/\text{sec}$

side is to be done. The results derived by (3.147) are far more interesting than those calculated by means of the linear length scale hypothesis.

When the flow is calculated by (3.147) with the slip condition at the bottom, neither the scale nor the eddy viscosity are linear functions of depth, they show a maximum inside the water column (Ignatova and Kvon, 1978).

§18. Influence of the density stratification

Finally, the possible way of solving the eddy viscosity problem in a density stratified fluid should shortly be mentioned. A general solution is possible with the set of equations presented above, including the effects of the Archimedian force.

This approach we have already explored in §9.

The nondimensional parameters' approach which may help to comprehend the physics is well developed in the description of near-surface dynamics of the atmosphere (Lajchtman, 1970; Turner, 1973). A theory of similarity related to the names of Monin and Obukchov (1954) is widely exploited there. Though the theory provides certain hints in understanding the steady motion, the treatment of nonsteady processes is still very unclear.

We can define a set of parameters to describe motion in the Ekman layer of a stratified sea in the way it has been done in §11. Here we may put aside of V_* , z, z_0 , f the additional parameters related to a flux of density $Q = -\rho'W$ and the Archimedian force $g\rho'/\rho$ (see eq. 1.27).

With these parameters we may construct the three nondimensional numbers

$$\frac{V_*}{fz}, \frac{1}{fV_*^2} \frac{Q}{\rho^2} g\rho', z_0/z \quad (3.154)$$

In the near-surface layer the number of parameters can be reduced to V_* , z , z_0 , $g\rho'/\rho$, Q , accordingly the flow is there governed by

$$z_0/z, z/L_{M-O} \quad (3.155)$$

Here L_{M-O} denotes the Monin-Obukchov length

$$L_{M-O} = V_*^3 / (g\rho'/\rho) \quad (3.156)$$

In case the influence of roughness is of secondary importance the flow is governed exclusively by z/L_{M-O} .

REFERENCES

- Blackadar, A.K., 1962. The Vertical Distribution of Wind and Turbulent Exchange in a Neutral Atmosphere. *Journ. Geoph. Res.* v.67,N.8: 3095-3102.
- Blackadar, A.K. and Tennekes, H., 1968. Asymptotic Similarity in Neutral Barotropic Boundary Layers. *Journ. Atm. Sciences* v. 25:1015-1020.
- Csanady, G.T., 1967. On the "Resistance Law" of a Turbulent Ekman Layer. *Journ. Atm. Sciences* v. 24:467-471.
- Daly, B.J. and Harlow, F.H., 1970. Transport Equations in Turbulence. *Phys. Fluids* v. 13, N. 11: 2634-2649
- Defant, A., 1961. *Physical Oceanography*. Per. Press v.1:729.
- Ekman, V.W., 1905. On the Influence of the Earth's Rotation on the Ocean Currents. *Arkiv. Mat. Fysik* v. 2, N.11.
- Ekman, V.W., 1923. Über Horizontalzirkulation bei winderzeugten Meeresströmungen. *Arkiv. Mat. Astron. Fysik* v. 17, N. 26.
- Felzenbaum, A.I., 1960. Theoretical Fundamentals and Methods of Calculating a Steady Sea Current. Publ. by Academy of Sciences, Moscow.
- Garner, D.M.; Neumann, G. and Pierson, W.T., 1962. Proc. of Symposium on Math.-Hydrod. Methods in Phys. Ocean., *Mitteilungen des Instituts für Meereskunde der Universität Hamburg* v. 1.
- Hansen, W., 1950. Triftstrom und Windstau. *Deutsch. Hydr. Zeit.* v.3: 303-313.
- Ignatova, G.Sh. and Kvon, V.I., 1978. On the Hydrodynamic Scheme of Sliding in a Turbulent Current. *Meteorologia and Hidrologia* N. 7: 50-54.
- Jones, W.P. and Launder, B.E., 1972. The Prediction of Laminarization with a Two-Equation Model of Turbulence. *Int. J. Heat Mass Transf.* v. 15: 301-314.
- Kao, A.M., 1956. *Elasticity Theory (in Russian)*. Moscow.
- Kamenkovitch, V.M., 1961. On the Integration of the Sea Current Equations in Multiply-Connected Space (in Russian). *Dokl. A.N. SSSR* N. 5.
- Kitajgorodski, S.A., 1970. *Physics of Atmosphere and Ocean Interaction*. Gidrometeoizdat, Leningrad.
- Kline, St.J., 1965. *Similitude and Approximation Theory*. Mc Graw-Hill Book Company, New York.
- Kowalik, Z., 1969. Wind-driven Circulation in a Shallow Sea with Application to the Baltic Sea. *Acta. Geoph. Polonica* v. XVII, N. 1: 13-37.
- Kowalik, Z. and Tarnowska, S., 1974. Density Currents in the Baltic. *Oceanologia* N. 3.
- Kowalik, Z. and Staśkiewicz, A., 1976. Diagnostic Model of the Circulation in the Baltic Sea. *Deutsch. Hydr. Zeit.* Band 29, Heft 6.
- Krasiuk, V.S. and Sauskan, F.M., 1970. On the Computation of the Wind Currents in the Ocean. *Meteorologia and Hidrologia* N. 9: 68-74.
- Kuftarkov, Y.M. and Felzenbaum, A.I., 1968. On the Application of the Energy Balance Equation in certain Simple Current Problems. *Morskoi Hidrofizicheski Inst. Sevastopol* 1968: 90-105.
- Lajchtman, D.L., 1970. *Physics of Atmospheric Boundary Layers*. Leningrad, Gidrometeoizdat.

- Launder, B.E. and Spalding, D.B., 1972. A Mathematical Model of Turbulence. Academic Press, London, New York.
- Lauwerier, H.A., 1962. Proc. of Symposium on Math.-Hydrod. Methods in Phys. Oc., Mitteilungen der Instituts für Meereskunde der Universität Hamburg, v. 1.
- Lazarenko, N.N., 1961. Sea Level Oscillations in the Baltic (in Russian). Trudy Gosudarstven. Okeanogr. Inst. N. 65.
- Marchuk, G.I.; Kochergin, V.P.; Klimok, V.I.; Sukhorukov, V.A., 1976. Mathematical Modelling of Surface Turbulence in the Ocean. Izv. Atmosph. Ocean Physics v. 12, N. 8: 841-849.
- Mellor, G.L. and Durbin, P.A., 1975. The Structure and Dynamics of the Ocean Surface Mixed Layer. Journ. Phys. Ocean. v. 5: 718-728.
- Monin, A.S. and Jaglom, A.M., 1965/66. Statistical Hydrodynamics v. 1 and v. 2, Nauka. Moscow.
- Monin, A.S. and Obukchow, A.M., 1954. Basic Laws of the Turbulent Mixing in the near Earth's Layer of Atmosphere. Trudy Geofiz. Inst. v. 24: 163-187.
- Nakayama, P.I., 1970. Turbulence Transport Equations and their Numerical Solution. A I A A Paper N. 70-3: 1-8.
- Neuman, G., 1958. On the Mass Transport of Wind-Driven Currents in a Baroclinic Ocean with Application to the North Atlantic. Zeit. für Meteorol. N. 12.
- Phillips, O.M., 1966. Dynamics of the Upper Ocean. London, Cambridge University Press.
- Ramming, H.-G., 1970. Investigation of Motion Processes in Shallow Water Areas. Report on the Symposium on Coastal Geodesy, Munich.
- Ramming, H.-G., 1973. Reproduktion physikalischer Prozesse in Küstengebieten, Die Küste Heft 22.
- Saint-Guilly, B., 1959. Sur la Solution du Problème d'Ekman. Deutsch. Hydr. Zeit. Band 12, Heft 6.
- Saint-Guilly, B., 1962. Proc. of Symposium on Math.-Hydrod. Methods in Phys. Oceanogr., Mitteilungen des Instituts für Meereskunde der Universität Hamburg v. 1.
- Sarkisyan, A.S., 1966. Theory and Computation of Oceanic Currents. Leningrad.
- Stockman, V.B., 1966. A Qualitative Analysis of the Cause of Abnormal Circulation Around Ocean Islands. Atm. and Ocean. Physics II, 11.
- Stommel, H., 1948. The Westward Intensification of Wind-Driven Ocean Currents. Trans. Am. Geoph. Union v. 29, N. 2.
- Tomczak, G., 1964. Investigations with Drift Cards to determine the Influence of the Wind on the Surface Currents. Studies in Oceanogr.: 129-139.
- Turner, J.S., 1973. Buoyancy Effects in Fluids. Cambridge University Press.
- Welander, P., 1957. Wind Action on a Shallow Sea: Some Generalizations of Ekman's Theory. Tellus N. 9.
- Willebrand, J., 1974. Parametrization of Heat and Momentum Flux in the Ekman Layer. Fellowship Lectures WHOI v. II: 148-158.
- Zilitinkevich, S.S.; Lajchtman, D.L.; Monin, A.S., 1967. Dynamics of the Atmospheric Boundary Layer. Atmosph. Ocean. Phys. v. 3, N. 3.
- Zilitinkevich, S.S., 1970. Dynamics of the Atmospheric Boundary Layer (in Russian), Leningrad.

Chapter IV UNSTEADY MOTION – NUMERICAL METHODS

Mathematical models represent a certain approximation of natural conditions. With this idealization, however, the modelling is not completed. It is usually found that the solution to these problems cannot be obtained in an analytical way. The reasons for this are, on the one hand, the nonlinearity of the basic equations and, on the other hand, the complicated topography of natural sea areas. Thus, one can either introduce further simplifications and schematizations (linearization of the equations, assumption of an elementary geometry) or solve the equations numerically. The first way leads to important basic insights. For practical applications only the second way is suitable. This last type of model is called a hydrodynamic-numerical model.

The first step in applying a numerical procedure is the discretization of the given continuum (for both, the space and time dimension). A numerical computation always produces only a finite amount of information at representative points of this continuum.

The discretization is, in principle, always carried out by covering the continuum under consideration (e.g. a tidal period in an estuary) with a space-time grid which is one-, two- or three-dimensional depending on the model. The grid is characterized by certain grid distances for this finite number of grid points: Δx , Δy , Δz , Δt . The unknown physical quantities are calculated for each point. In order to do this the governing basic equations in the continuous variables are transformed into difference equations (finite difference technique) or normal equations (finite element method).

This means that in each case a system of algebraic equations is derived with the physical properties at the grid points as the unknowns.

The solution to this system of algebraic equations is connected with new (mathematical) problems. The discretization leads unavoidably to approximation errors. This raises the question of the quality of a numerical solution.

In particular two mathematical questions have to be investigated:

- the agreement of the exact analytical solution and the exact solution of the corresponding system of algebraic equations,
- the agreement of the numerical solution of the system of algebraic equations and the exact solution of this system.

The first question concerns the approximation method, the second one the finite accuracy of the numerical calculation (round off

errors). There are two important quantitative measures for these errors: the rate of convergence and the numerical stability of the method.

The requirements of convergence and stability, when applied to the numerical solution of models, result in a series of criteria which interrelate the space distances and the time step. Generally, the discretization of the spatial and the time dimensions cannot be chosen independently. This restriction may increase the numerical efforts considerably.

The derivation of the stability criteria governing the difference equations is usually carried out by a Fourier-transformation of the discretized equations.

In discussing the numerical procedures, we distinguish between explicit and implicit methods. A method is called explicit if a new value at a certain grid point is calculated only from the known values at other grid points. This means that we always treat one equation at a time. A method is called implicit if some new unknown values are coupled by a set of equations which must be solved simultaneously. Both methods are fundamentally different with respect to the numerical procedure and stability. Explicit methods are unstable if the criteria of stability are not fulfilled. On the contrary implicit methods allow one to exceed the criteria, but at the expense of accuracy. Nevertheless, the latter is sometimes preferred due to the smaller computational effort.

§1. Principal equations and their difference form

The study of the sea level $\zeta(x,y,t)$ as a function of wind velocity and direction will be carried out with the help of a system of equations (1.32), (1.33) and (1.41), assuming that the convective terms and the exchange of momentum in the horizontal direction are negligible in relation to other terms

$$\frac{\partial M_x}{\partial t} - fM_y = -\rho gH \frac{\partial \zeta}{\partial x} + \tau_s^{(x)} - RM_x \quad (4.1)$$

$$\frac{\partial M_y}{\partial t} + fM_x = -\rho gH \frac{\partial \zeta}{\partial y} + \tau_s^{(y)} - RM_y \quad (4.2)$$

$$\frac{\partial M_x}{\partial x} + \frac{\partial M_y}{\partial y} + \rho \frac{\partial \zeta}{\partial t} = 0 \quad (4.3)$$

To simplify the notation we set everywhere the density of water as $\rho = 1 \text{ g/cm}^3$. The boundary condition to the above system is analogous to (3.23), i.e. the normal component of mass transport vanishes at the coast

$$M_n = 0 \quad (4.4)$$

To facilitate the following considerations we introduce again the vector-matrix notation which proved very useful

$$\vec{M} = \begin{bmatrix} M_x \\ M_y \\ \zeta \end{bmatrix}; \quad \vec{\tau} = \begin{bmatrix} \tau_s^{(x)} \\ \tau_s^{(y)} \\ 0 \end{bmatrix}; \quad B = \begin{bmatrix} R & -f & gH \frac{\partial}{\partial x} \\ f & R & gH \frac{\partial}{\partial y} \\ \frac{\partial}{\partial x} & \frac{\partial}{\partial y} & 0 \end{bmatrix} \quad (4.5)$$

With the help of (4.5) the system of equations takes the compact form

$$\frac{\partial \vec{M}}{\partial t} + B\vec{M} = \vec{\tau} \quad (4.6)$$

The solution of this system of equations with the boundary condition (4.4), for real anemometric situations and the real geometry of the basin, may be derived only by using the numerical approach. Introducing suitable time-space grids, with the step T along the time-axis and h along the x and y space directions, we obtain instead of continuous functions the set of discrete values given at the grid points (Fig. 32-34b). A discrete co-ordinate along the x -axis is set in the form $x_j = jh$, where j is an integer in the range $0 \leq j \leq J$. Similarly along the y -axis $y_k = kh$, $0 \leq k \leq K$, and along the t -axis $t_l = lT$, $0 \leq l \leq L$. When the grid step diminishes the numerical solution should approach the analytical one. Thus we first intend to give the measure of approximation of the analytical solution by the numerical one. Assume that the analytical solution of the above system $\zeta(x,y,t)$ and the numerical solution $\zeta_{j,k}^l$ are known. We relate the analytical values to the grid points j,k,l and denote them by $\zeta(j,k,l)$. The modulus of the difference $\zeta(j,k,l) - \zeta_{j,k}^l$ is a measure of the approximation of the analytical solution by the numerical one. For the quantitative description of the difference we shall apply the notion of a norm. Here the definition of a norm is analogous to that

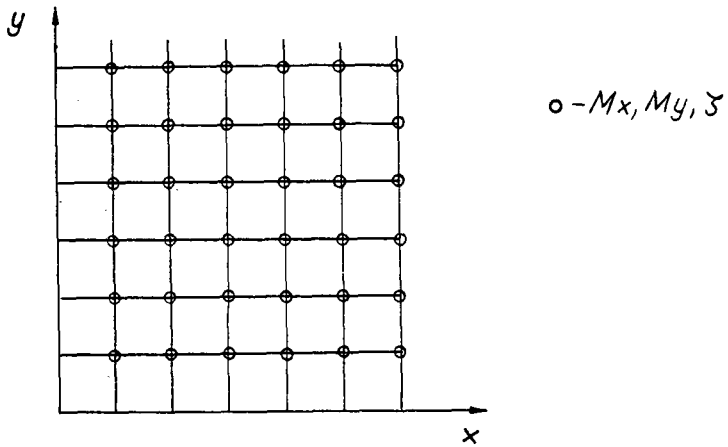


Fig. 32. A SYMMETRICAL COMPUTATIONAL GRID. IT IS SELDOM USED.

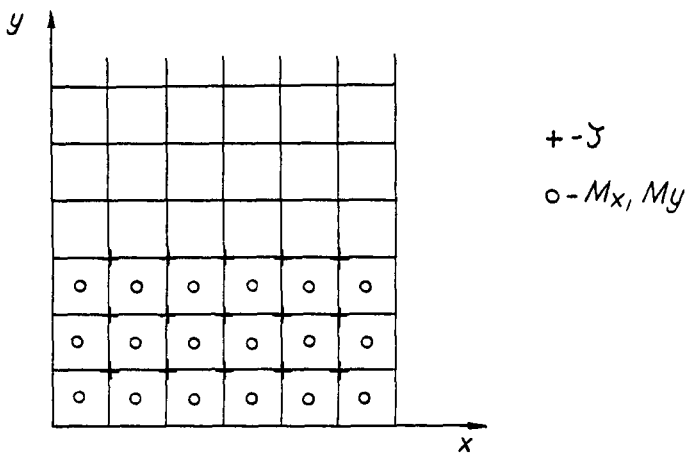


Fig. 33. STAGGERED COMPUTATIONAL GRID, CONVENIENT IN THE PRESENCE OF HORIZONTAL FRICTION.

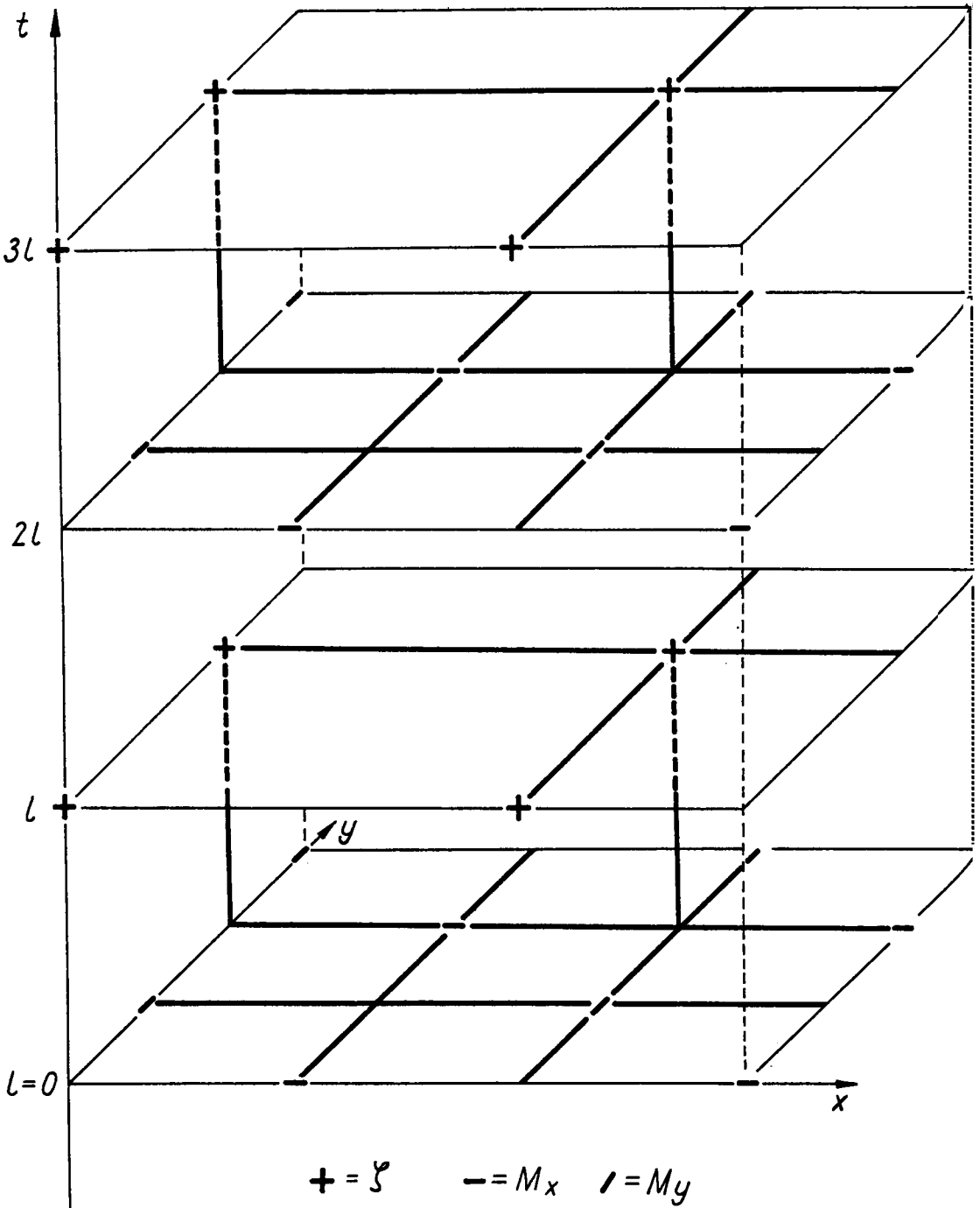


Fig. 34a. THE ORDER OF COMPUTATIONS IN TIME t ON THE STAGGERED NUMERICAL GRID. THE GRID IS CONVENIENT FOR THE BOUNDARY CONDITION $M_n = 0$.

presented already in expression (2.59). It is the maximum norm, i.e. the maximum value of the modulus of the difference taken over all grid points

$$||\zeta|| = \text{Max}_{j,k,l} |\zeta(j,k,l) - \zeta_{j,k}^1| \quad (4.7)$$

In the same way the norm which describes the order of the approximation of the differential operator B (4.6) by the difference operator $B_{j,k}^1$ is defined as

$$||B\zeta|| = \text{Max}_{j,k,l} |B\zeta(j,k,l) - B_{j,k}^1 \zeta_{j,k}^1| \quad (4.8)$$

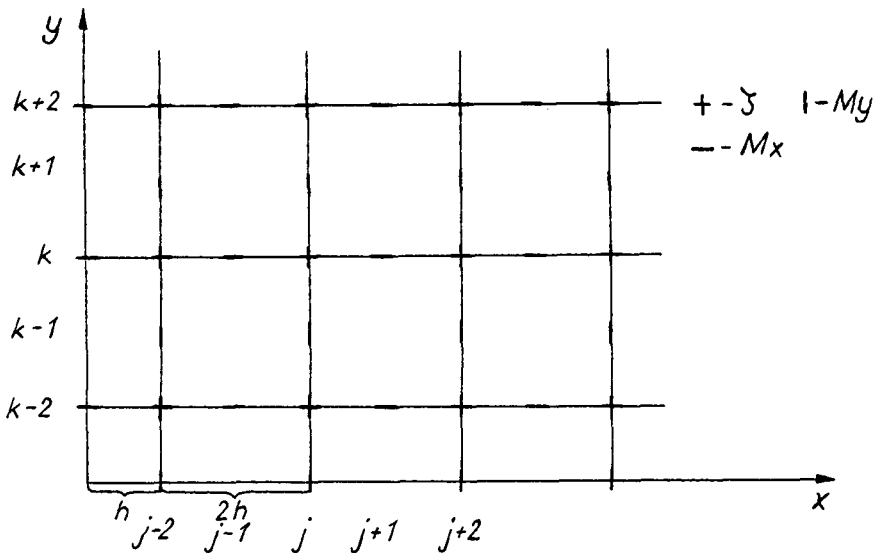


Fig. 34b. THE COMPUTATIONAL GRID FROM FIG. 34a PLACED IN THE x, y PLANE.

Now let us recall briefly the method of approximation of a differential equation by the difference equation (Forsythe and Wasow, 1960). Instead of the system (4.1) - (4.3) let us use for illustrative purposes the simplified set of equations which is obtained rejecting the external forces ($\tau_s = 0$) and the Coriolis force ($f = 0$), since the approximation of these terms does not present any problems.

$$\frac{\partial M_x}{\partial t} = -gH \frac{\partial \zeta}{\partial x} \quad (4.9)$$

$$\frac{\partial M_y}{\partial t} = -gH \frac{\partial \zeta}{\partial y} \quad (4.10)$$

$$\frac{\partial \zeta}{\partial t} = -\frac{\partial M_x}{\partial x} - \frac{\partial M_y}{\partial y} \quad (4.11)$$

The description of the differential derivatives in terms of finite differences will be done by using the Taylor series. The function ζ given at an arbitrary grid point j, k, l together with its derivatives is described at the adjacent point $j, k, l+1$ as follows

$$\zeta_{j,k}^{l+1} = \zeta_{j,k}^l + T \frac{\partial \zeta(j,k,l)}{\partial t} + \frac{T^2}{2!} \frac{\partial^2 \zeta(j,k,l)}{\partial t^2} + O(T^3) \quad (4.12)$$

In the same way the space derivatives along the x - and y -axes can be easily approximated with the help of expressions (2.7), (2.8) and (2.9). Finally, the system (4.9) - (4.11) can be written in the numerical form

$$\frac{M_{x,j,k}^{l+1} - M_{x,j,k}^l}{T} + O(T) = -gH \frac{\zeta_{j+1,k}^l - \zeta_{j,k}^l}{h} + O(h) \quad (4.13)$$

$$\frac{M_{y,j,k}^{l+1} - M_{y,j,k}^l}{T} + O(T) = -gH \frac{\zeta_{j,k+1}^l - \zeta_{j,k}^l}{h} + O(h) \quad (4.14)$$

$$\begin{aligned} \frac{\zeta_{j,k}^{l+1} - \zeta_{j,k}^l}{T} + O(T) + \frac{M_{x,j+1,k}^l - M_{x,j,k}^l}{h} \\ + \frac{M_{y,j,k+1}^l - M_{y,j,k}^l}{h} + O(h) = 0 \end{aligned} \quad (4.15)$$

When analysing the derived system of equations it is obvious that a first-order approximation only in space and time has been obtained.

Generally speaking, since the difference equations contain (implicitly) a certain method of solution, they should satisfy a number of requirements which seem to be essential, both for deriving a proper solution and for a sufficiently high order of approximation. Let us list some of these requirements

a) Consistency: if the mesh width h and the time step T vanish, the difference equations should approach the differential equations.

The deviation between the differential and difference equations is called the truncation error. For consistency, therefore, the truncation error should vanish when h and T vanish. This property is closely connected with the degree of approximation.

- b) Stability: inevitably errors are introduced into the computation by round-off and by truncation. A method is called stable if these errors do not grow with time.
- c) Convergence: even if the difference equations approach the differential equations for vanishing h and T (consistency), their solutions do not necessarily approach each other. If they do, the method is called convergent. Then the discretization error between the solutions of the difference and differential equations vanishes. The 'equivalence theorem' by Lax and Richtmyer (1956) states that consistency and stability are necessary and sufficient for convergence, when the initial value problem is properly posed and there are no turbulent discontinuities (Abbott, 1979). This means that a separate analysis of convergence is generally not necessary.

§2. Stability of the numerical solution

In order to ensure a proper order of approximation for hydrodynamic processes dependent on time it is not sufficient for the solution of the numerical problem to be close enough to the analytical solution. The question arises: if a small error is introduced during an arbitrary time step, will it be amplified (unstable system) or will it decay (stable system)? Stability of linear equations is usually studied by the Fourier method. O'Brien, Hyman and Kaplan (1951) implemented this method to study computational stability by observing the effect of an error. We shall proceed in the same way. We begin by assuming that at a moment in time t an error $\delta\vec{M}$ is imposed on the solution vector $\vec{M} = (M_x, M_y, \zeta)$. Such an error arises from truncation and rounding in a finite-word-length computer.

Let us present this error in the form of one harmonic wave (component) and study its behaviour from the moment t to $t + T$. Although the error should be presented as a sum of different component waves, the linearity of the equations and the principle of superposition allow us to consider only one wave. We can then apply the results to each wave component. The mathematical form of $\delta\vec{M}$ is

$$\delta\vec{M} = \vec{M}^* e^{i\omega t} \cdot e^{i\sigma_1 x} \cdot e^{i\sigma_2 y} \quad (4.16)$$

where \vec{M}^* is a column vector of amplitudes, ω denotes the frequency, and σ_1 and σ_2 are the wave numbers along the x- and y-axes respectively. In differential form, the domain of integration is discretized as $x_j = jh$, $y_k = kh$ and $t = lT$. Therefore (4.16) is described by

$$\delta \vec{M} = \vec{M}^* \lambda^{Tl} e^{i\sigma_1 jh} e^{i\sigma_2 kh} \quad (4.17)$$

where $\lambda = e^{i\omega}$ will often be called 'stability parameter'. In further considerations we shall omit δ in denoting the error. If at an arbitrary moment $|\lambda| < 1$, then it is evident that the error is not amplified with time. If on the other hand $|\lambda| > 1$, the growth of an error with time is observed and indicates the unstable behaviour of the numerical scheme. Let us give some examples of stability in the problems pertaining to sea dynamics.

The equation of the sea-level in a one-dimensional basin (Lamb, 1932)

$$\frac{\partial^2 \zeta}{\partial t^2} = gH \frac{\partial^2 \zeta}{\partial x^2} \quad (4.18)$$

may be solved numerically through the form

$$\frac{\zeta_j^{l+1} + \zeta_j^{l-1} - 2\zeta_j^l}{T^2} = gH \frac{\zeta_{j+1}^l + \zeta_{j-1}^l - 2\zeta_j^l}{h^2} \quad (4.19)$$

Since the same equation characterizes the error propagation we introduce here (4.17) and obtain the following expression for the stability parameter λ

$$\left(\lambda + \frac{1}{\lambda} - 2\right) = -g \frac{HT^2}{h^2} 4 \cdot \sin^2 \left(\frac{\sigma_1 h}{2}\right) \quad (4.20)$$

Rearranging (4.20) in a more convenient form

$$\lambda^2 + \lambda(\phi^2 - 2) + 1 = 0 \quad (4.21)$$

where ϕ^2 denotes the right side of (4.20). The roots are easily derived as

$$\lambda_{1,2} = \frac{1}{2} (2 - \phi^2 \pm \sqrt{(\phi^2 - 2)^2 - 4}) \quad (4.22)$$

The stability condition $|\lambda_{1,2}| \leq 1$ provides

$$\frac{1}{h^2} gHT^2 \leq 1 \quad (4.23)$$

and therefore the choice of time or space steps in the course of numerical computation should comply with this inequality.

Let us indicate a second method which in many cases can guarantee the stability of the numerical computation. In expression (4.19) the derivative along the x-axis is written at moment l ; this is the so-called explicit (in time) form. If the same derivative is set at moment $l+1$, we obtain an implicit form. Then, instead of (4.19) we find

$$\frac{\zeta_j^{l+1} + \zeta_j^{l-1} - 2\zeta_j^l}{T^2} = \frac{gH}{h^2} (\zeta_{j+1}^{l+1} + \zeta_{j-1}^{l+1} - 2\zeta_j^{l+1}) \quad (4.24)$$

The equation to derive the stability parameter takes the form

$$\lambda + \frac{1}{\lambda} - 2 = -\lambda\phi^2 \quad (4.25)$$

and its roots are

$$\lambda_{1,2} = \frac{1 \pm i\phi}{1 + \phi^2} \quad (4.26)$$

This result proves that $|\lambda|$ is always smaller than unity. Therefore the difference equation chosen in the described manner shows unconditional stability which allows us an arbitrary choice of time and space steps.

Let us consider in turn the diffusion equation (Chapter VII) in the simplest form

$$\frac{\partial c}{\partial t} = k \frac{\partial^2 c}{\partial x^2} \quad (4.27)$$

Here c denotes a concentration and k is the eddy diffusivity coefficient.

The difference analogue of (4.27) is written down in two different ways; the explicit

$$c_j^{l+1} - c_j^l = \frac{kT}{h^2} (c_{j+1}^l + c_{j-1}^l - 2c_j^l) \quad (4.28)$$

and the implicit

$$c_j^{l+1} - c_j^l = \frac{kT}{h^2} (c_{j+1}^{l+1} + c_{j-1}^{l+1} - 2c_j^{l+1}) \quad (4.29)$$

Introducing in (4.28) the expression for an error (4.17) yields

$$\lambda = 1 - \frac{4kT}{h^2} \sin^2\left(\frac{\sigma_1 h}{2}\right) \quad (4.30)$$

Since stability occurs when $|\lambda| \leq 1$, from (4.30) the following inequality is derived.

$$0 \leq \frac{kT}{h^2} \leq 1/2 \quad (4.31)$$

This shows again that in order to preserve numerical stability the time and space steps cannot be chosen in an arbitrary way but have to be within the limits imposed by (4.31).

The stability parameter for the implicit form (4.29) is found to be

$$\lambda = 1/[1 + \frac{4kT}{h^2} \sin^2\left(\frac{\sigma_1 h}{2}\right)] \quad (4.32)$$

Since there $|\lambda| \leq 1$, we find again that if the implicit expression is implemented unconditional stability is assured.

§3. Stability of a system of equations

The simple example of the stability problem given above was applicable to one equation with one dependent variable. Let us turn now to a system of difference equations. To analyse stability we shall use the theoretical works of Neuman, Lax, Richtmyer and Morton (1967) and many others who have contributed to this field. As previously stated the aim is to find out if a perturbation (error) introduced at an arbitrary moment of time into a system of equations will be amplified or dampened with increasing time. Since we shall deal with a system of equations the vector-matrix notation (4.6) will be used to facilitate further considerations. Let us start on the basis of (4.1) - (4.3) and consider the simplest system describing the propagation of long waves along the x-axis

$$\frac{\partial \mathbf{M}}{\partial t} = -gH \frac{\partial \zeta}{\partial x} \quad (4.33a)$$

$$\frac{\partial \zeta}{\partial t} = - \frac{\partial M_x}{\partial x} \quad (4.33b)$$

This system in the vector-matrix form is

$$\frac{\partial \vec{M}}{\partial t} + B_1 \vec{M} = 0 \quad (4.34)$$

A numerical solution of (4.33) will be realized through the algorithm

$$M_{x,j}^{l+1} - M_{x,j}^l = - \frac{gHT}{2h} (\zeta_{j+1}^l - \zeta_{j-1}^l) \quad (4.35a)$$

$$\zeta_j^{l+1} - \zeta_j^l = - \frac{T}{2h} (M_{x,j+1}^l - M_{x,j-1}^l) \quad (4.35b)$$

To this system the following vector-matrix form is ascribed

$$\vec{M}^{l+1} = B \vec{M}^l \quad (4.36)$$

where

$$\vec{M}^{l+1} = \begin{bmatrix} M_x^{l+1} \\ \zeta^{l+1} \end{bmatrix} \quad \vec{M}^l = \begin{bmatrix} M_x^l \\ \zeta^l \end{bmatrix}$$

$$B = \begin{bmatrix} 1 & -\frac{gHT}{h} i \sin \sigma_1 h \\ -\frac{T}{h} i \sin \sigma_1 h & 1 \end{bmatrix} \quad (4.37)$$

The matrix B is usually called the amplification matrix. The stability properties of a numerical equation depend on the eigenvalues λ_i of B.

According to Neuman the sufficient condition for stability is (Lax and Richtmyer, 1956)

$$|\lambda_i| \leq 1 + O(T) \quad (4.38)$$

The eigenvalues of B can be derived by the equation (see chapter VIII)

$$B - \lambda E = 0 \quad (4.39)$$

In (4.39) E denotes the unit matrix, that is the one which has units on the main diagonal and where the other elements are equal to zero.

Introducing B from (4.37) in (4.39) a determinant which specifies the eigenvalues is obtained

$$|B - \lambda E| = \begin{vmatrix} 1 - \lambda & -\frac{gHT}{h} i \sin\sigma_1 h \\ -\frac{T}{h} i \sin\sigma_1 h & 1 - \lambda \end{vmatrix} = 0 \quad (4.40)$$

In the ensuing work the study of stability will not be carried out by the above method, since it is often very difficult to build the amplification matrix B. Therefore we shall proceed by the straight introduction of expression (4.17) into a numerical system. In the case of (4.35) the system to derive λ is

$$(\lambda-1)M_x^* + \zeta^* \frac{gHT}{h} i \sin\sigma_1 h = 0 \quad (4.41a)$$

$$M_x^* \frac{T i}{h} \sin\sigma_1 h + (\lambda-1) \zeta^* = 0 \quad (4.41b)$$

The unique solution of this homogeneous system is only possible in the case where the determinant of this system becomes equal to zero. Thus for λ two values are given

$$\lambda_{1,2} = 1 \pm i \frac{T}{h} \sqrt{gH} \sin\sigma_1 h \quad (4.42)$$

The main result which allows us to use expression (4.17) is that the determinant of system (4.41) is analogous to the determinant (4.40). Therefore the examination of the error propagation in the system of equations is equivalent to the study of the amplification matrix.

Coming back to the result expressed by (4.42) it is clear that the absolute value of one root is always greater than unity and the system of equations (4.35) is always unstable.

As we know already the numerical form developed above is not the only one. Let us alter (4.35) to a somewhat different form, which is implicit

$$M_{x,j}^{l+1} - M_{x,j}^l = -\frac{gHT}{2h} (\zeta_{j+1}^{l+1} - \zeta_{j-1}^{l+1}) \quad (4.43a)$$

$$\zeta_j^{l+1} - \zeta_j^l = -\frac{T}{2h} (M_{x,j+1}^{l+1} - M_{x,j-1}^{l+1}) \quad (4.43b)$$

When (4.17) is introduced into (4.43) the values of λ are described by

$$\lambda_{1,2} = [1 \pm \frac{T}{h} \sqrt{gH} \sin \sigma_1 h] / [1 + (\frac{T}{h} \sqrt{gH} \sin \sigma_1 h)^2] \quad (4.44)$$

Therefore in (4.44) $|\lambda_{1,2}| \leq 1$ and the numerical system (4.43) is unconditionally stable. Analyzing both these algorithms we find in each case that the approximation is of second order with respect to space $O(h^2)$ and of first order with respect to time $O(T)$.

With this order of approximation appearing in the equations a certain systematic error exists and leads to the effect of numerical friction (2.26). The central derivatives may be used to obtain a second order approximation but such numerical schemes are usually unstable. One of the possible solutions to this problem is to split the system of equations into a more complicated one. In the above system we split the time step T into two substeps and instead of one equation we obtain two equations.

The equation of one-dimensional motion

$$\frac{\partial M_x}{\partial t} = -gH \frac{\partial \zeta}{\partial x} \quad (4.45)$$

can be split into

$$\frac{1}{2} \cdot \frac{\partial M_x}{\partial t} = -\frac{1}{2} gH \frac{\partial \zeta}{\partial x} \quad (4.46a)$$

$$\frac{1}{2} \cdot \frac{\partial M_x}{\partial t} = -\frac{1}{2} gH \frac{\partial \zeta}{\partial x} \quad (4.46b)$$

The continuity equation may be treated in the same way. Instead of time step $l, l+1$ we introduce two time steps $l, l+1/2$ and $l+1/2, l+1$. Finally, the system of equations (4.33) is set in the following numerical form

$$\frac{M_{x,j}^{l+1/2} - M_{x,j}^l}{T} = -gH \frac{1}{2} \frac{\zeta_{j+1}^l - \zeta_{j-1}^l}{2h} \quad (4.47a)$$

$$\frac{\zeta_j^{l+1/2} - \zeta_j^l}{T} = -\frac{1}{2} \frac{M_{x,j+1}^l - M_{x,j-1}^l}{2h} \quad (4.47b)$$

on the first time step $T/2$ and

$$\frac{M_{x,j}^{l+1} - M_{x,j}^{l+1/2}}{T} = - \frac{gH\zeta_{j+1}^{l+1} - \zeta_{j-1}^{l+1}}{2 \cdot 2h} \quad (4.48a)$$

$$\frac{\zeta_j^{l+1} - \zeta_j^{l+1/2}}{T} = - \frac{1}{2} \frac{M_{x,j+1}^{l+1} - M_{x,j-1}^{l+1}}{2h} \quad (4.48b)$$

on the second time step.

The investigation of the stability of (4.47) and (4.48) is performed by substituting $M_{x,j}^{l+1/2}$ and $\zeta_j^{l+1/2}$ from (4.47) into (4.48). Then for the parameter λ we obtain two values

$$\lambda_{1,2} = [1 - A \pm 2i\sqrt{A}]/[1 + A] \quad (4.49)$$

where

$$A = \left(\frac{T}{2h}\right)^2 gH \sin^2(\sigma_1 h) \quad (4.50)$$

Since $|\lambda_{1,2}| \leq 1$ the system is always stable and the approximation in space and time attains the second order. This result is due entirely to the splitting-method. It seems desirable to retain some general properties in the course of splitting (Marchuk, 1974).

Considering equation

$$\frac{\partial \phi}{\partial t} + L\phi = 0 \quad (4.51)$$

and allowing it to be split into the following system

$$\begin{aligned} \frac{1}{N} \frac{\partial \phi}{\partial t} + L_1 &= 0 \\ \frac{1}{N} \frac{\partial \phi}{\partial t} + L_2 &= 0 \\ &\vdots \\ &\vdots \\ &\vdots \\ \frac{1}{N} \frac{\partial \phi}{\partial t} + L_N &= 0 \end{aligned} \quad (4.52)$$

then the following properties are important (according to Marchuk, 1974):

1. The additive property of the operators

$$L = \sum_{i=1}^N L_i$$

2. If L is positive definite, $(L\phi, \phi) \geq 0$, then for every L_i the same property should hold, $(L_i\phi, \phi) \geq 0$.

Here, as usual, the parenthesis denotes scalar multiplication.

§4. Wave deformation

In this part we shall use, following Leendertse (1967), a practical approach to the description of a numerical system. The amplitude and phase of a wave as given by the analytical solution can be compared with the amplitude and phase of the same wave derived from the numerical solution.

Using this we can draw certain conclusions about wave deformation, as well as the properties of the system of finite difference equations. Let us again consider the system (4.33) which describes the simplified one-dimensional motion. The analytical solution (in an infinite domain) may be represented as a sum of elementary waves such as

$$\zeta = \zeta^* e^{i\omega t} e^{i\sigma_1 x} \quad (4.53a)$$

$$M_x = M_x^* e^{i\omega t} e^{i\sigma_1 x} \quad (4.53b)$$

Substituting this form of solution into (4.33) we obtain the expression

$$\omega/\sigma_1 = \pm\sqrt{gH} \quad (4.54)$$

which describes the celerity of long-wave propagation (phase velocity) in the positive and negative directions of the x -axis. Deriving a solution of the same problem using the finite difference analogue (4.43) we can rearrange (4.53) as

$$\zeta_j^1 = \zeta^* e^{i\omega_1 T} e^{i\sigma_1 jh} \quad (4.55a)$$

$$M_{x,j}^1 = M_x^* e^{i\omega_1 T} e^{i\sigma_1 jh} \quad (4.55b)$$

The eigenvalues have been determined already by (4.44) as

$$\lambda_{1,2} = e^{i\omega_{1,2} T} = \frac{1 \pm iA}{1 + A^2} = \cos\omega_{1,2} T + i \sin\omega_{1,2} T \quad (4.56)$$

Hereafter $\omega_{1,2}$ denotes the numerically computed frequency, whereas ω is given by the analytical consideration. The absolute value $|\lambda_{1,2}|$

is a measure of the amplification (or decay) of a wave when it propagates in time from moment l to $l+1$. The phase change we describe from (4.56) by

$$\tan \omega_{1,2} T = \pm A \quad (4.57)$$

whence

$$\omega_{1,2} T = \arctan (\pm A) \quad (4.58)$$

Now let us analyze (4.58) under the assumption that $A < 1$. Developing (4.58) in the series (taking $+A$) we obtain

$$\omega_{1,2} T = A - \frac{A^3}{3} + \frac{A^5}{5} - \frac{A^7}{7} + \dots \quad (4.59)$$

Taking into account the form of $A = \frac{1}{h} \sqrt{gH} T \sin \sigma_1 h$ we also develop $\sin \sigma_1 h$ as a series and arrive at

$$\omega_{1,2} = \sigma_1 \sqrt{gH} \left[1 - \frac{(\sigma_1 h)^2}{3!} + \frac{(\sigma_1 h)^4}{5!} - \dots \right] \left[1 - \frac{A^2}{3} + \frac{A^4}{5} - \frac{A^6}{7} + \dots \right] \quad (4.60)$$

Both series in (4.60) are smaller than unity and are equal to 1 when $h \rightarrow 0$ and $T \rightarrow 0$. Thus we may say that for all values of the parameter $\frac{T}{h} \sqrt{gH}$ the solution obtained from (4.43) has a frequency smaller than the frequency computed in the analytical way by (4.54). The celerity of wave propagation which is calculated numerically will be smaller than the real celerity. This is the phenomenon of wave deformation by the numerical system of difference equations.

Now let us briefly describe the wave amplitude's behaviour by means of the parameter $|\lambda_{1,2}|$. On the basis of (4.56) it follows that

$$|\lambda_{1,2}| = (1 + A^2)^{-1/2} \quad (4.61)$$

and the wave amplitude decays when it propagates in time from l to $l+1$. Only in the limiting case of $A \rightarrow 0$ will the amplitude be constant in time. The dampening of the amplitude in the implicit difference scheme (4.43) after N time steps is expressed by

$$|\lambda_{1,2}|^N = (1 + A^2)^{-N/2} \quad (4.62)$$

We observe from expressions (4.44) and (4.56) that for arbitrary values of the ratio T/h the numerical scheme is always stable (convergent). This feature is very important from the point of view of

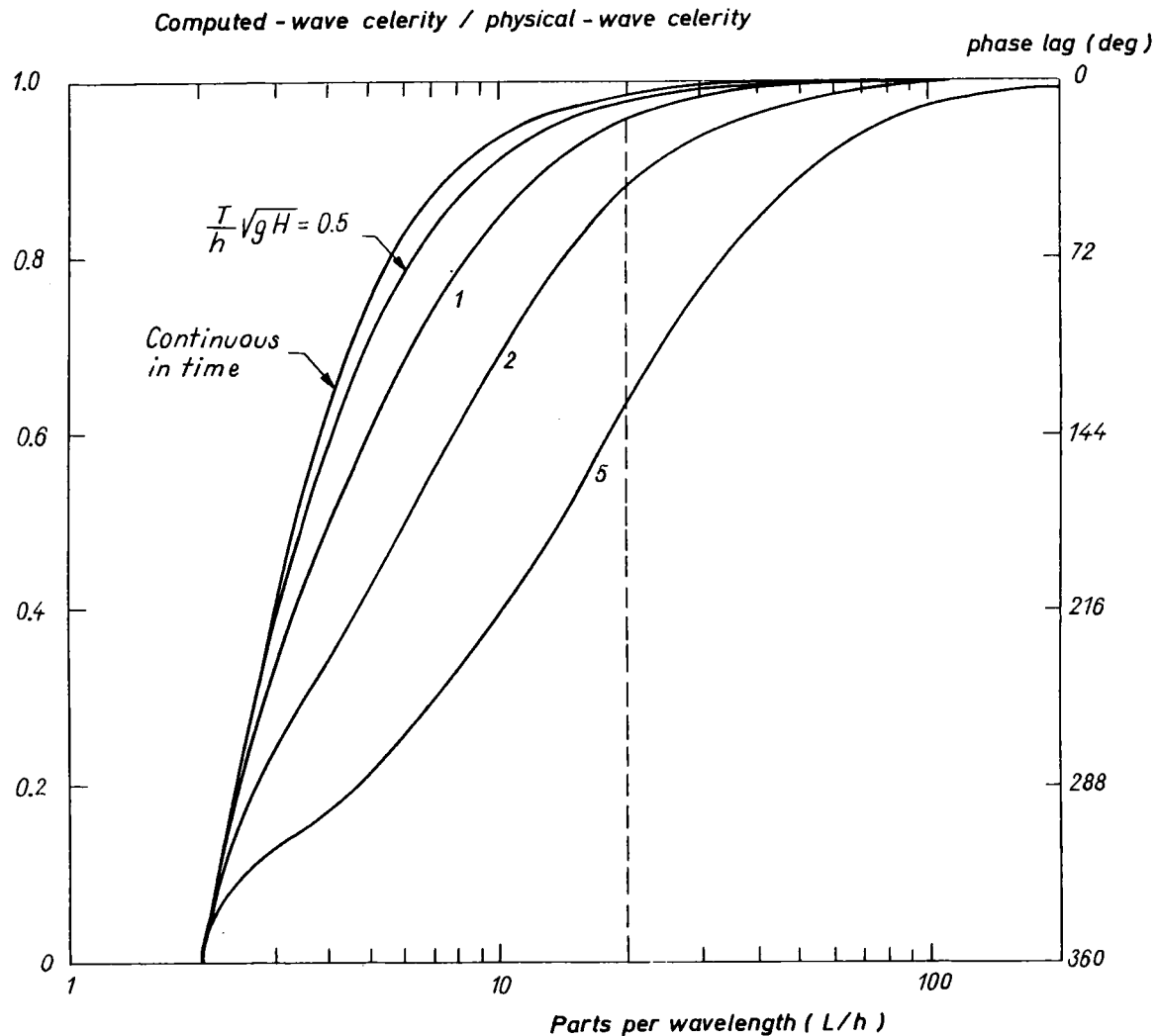


Fig. 35. CHARACTERISTICS OF IMPLICIT SCHEME ACCORDING TO LEENDERTSE (1967).

the practical application of numerical systems, especially implicit ones. However the real physical phenomena are only described in the same way by both the analytical and the numerical solutions when

$$\frac{T}{h}\sqrt{gH} < 1.$$

This feature we shall consider once more in §9 of this chapter. There the same physical process will be treated by both the explicit and implicit algorithms. The corresponding solutions will be obtained and compared. This feature can also be presented in a very illuminating graphical fashion, see fig. 35. If the wave length of a wave is denoted by L , then the quotient L/h indicates what sort of grid should be chosen for the true description of a wave with wave length L .

The other parameters introduced in fig. 35 express a) the relationship between the celerity derived from a numerical scheme and the analytical celerity and b) the phase difference (shift) between a wave calculated numerically and the corresponding analytical solution. From this figure we may draw the conclusion that, if $L/h < 10$ and $\frac{T}{h}\sqrt{gH} < 2$ the results from the numerical scheme will contain only errors which are inherent.

§5. Physical and numerical solutions

In certain numerical schemes parasitic solutions are observed. Together with solutions characterizing the physical processes we also find numerical (parasitic or false) solutions which have nothing to do with reality. Usually the numerical solutions are related to the symmetrical numerical systems. In such schemes the space derivatives are taken at the centre of the time interval. Let us start with the example of Miyakoda (1962) and consider the equation

$$\frac{\partial \zeta}{\partial t} = -U \frac{\partial \zeta}{\partial x} \quad (4.63)$$

Taking a symmetrical numerical scheme

$$\zeta_j^{1+1} - \zeta_j^{1-1} = -U \frac{T}{h} (\zeta_{j+1}^1 - \zeta_{j-1}^1) \quad (4.64)$$

we shall seek the solution in the form of

$$\zeta_j^1 = \lambda^1 \cdot e^{i\sigma_1 j h} \quad (4.65)$$

where λ is derived by introducing (4.65) into (4.64). Hence

$$\lambda = i\phi \pm \sqrt{1 - \phi^2} \quad (4.66)$$

and

$$\phi = U \frac{T}{h} \sin \sigma_1 h$$

The case $\phi \geq 1$ is unstable. On the other hand if $\phi < 1$ the two values of λ are

$$\lambda_1 = e^{-i\theta}; \quad \lambda_2 = -e^{i\theta} \quad (4.67)$$

where $\theta = \arcsin \phi$.

These values when substituted into (4.65) provide two solutions. The first one

$$\zeta_j^1 = e^{-i1\theta} e^{i\sigma_1 j h} \quad (4.68)$$

represents the wave which describes the physical process. The second solution

$$\zeta_j^1 = (-e^{-i\theta})^1 e^{i\sigma_1 j h} \quad (4.69)$$

represents the numerical wave. The main characteristic in (4.69) is the alternating sign showing whether 1 is odd or even. The same feature may be observed in the system (4.33) when written in the following numerical form

$$\frac{M_{x,j}^{1+1} - M_{x,j}^{1-1}}{2T} = -gH \frac{\zeta_{j+1}^1 - \zeta_{j-1}^1}{2h} \quad (4.70a)$$

$$\frac{\zeta_j^{1+1} - \zeta_j^{1-1}}{2T} = - \frac{M_{x,j+1}^1 - M_{x,j-1}^1}{2h} \quad (4.70b)$$

Analyzing the stability with the help of (4.17) we obtain the equation

$$\lambda^4 - 2\lambda^2 [1 - 2(T/h)^2 gH \sin^2 \sigma_1 h] + 1 = 0 \quad (4.71)$$

which has the following roots

$$\lambda_{1,2,3,4} = \pm [A \pm i\sqrt{1 - A^2}]^{1/2} \quad (4.72)$$

subject to the condition that $|A| \leq 1$ where

$$A = 1 - 2(T/h)^2 gH \sin^2 \sigma_{1h}.$$

As in equation (4.66) the numerical solutions in (4.72) are due to the roots λ with negative real part. Evidently these solutions could effect the computed solution, since during the computation the numerical (false) solution and physical solution may have common areas. Due to this fact the numerical scheme may provide the physical wave during a certain step and on the next step it may jump to the false solution. Generally speaking, this feature leads to erroneous solutions. We shall return to this problem later on, in the course of treating methods which remove the numerical (false) solutions by filtering.

§6. Nonlinear equations

The main obstacle in solving numerical problems is the nonlinearity of the equations. In the following consideration we shall start with one-dimensional movement described by the equations (1.52) and (1.55) where the nonlinear terms are due to advection and bottom stress.

$$\frac{\partial M_x}{\partial t} + \frac{M_x}{H} \frac{\partial M_x}{\partial x} = -gH \frac{\partial \zeta}{\partial x} + \tau_s(x) - \frac{r}{H^2} M_x |M_x| + A \frac{\partial^2 M_x}{\partial x^2} \quad (4.73)$$

$$\frac{\partial \zeta}{\partial t} + \frac{\partial M_x}{\partial x} = 0 \quad (4.74)$$

General methods for solving the nonlinear equations are still in a state of development, see e.g. Ames (1965).

In practical application the great number of different methods are met and this indicates that none of them is really good enough. One of the most useful approaches is based on the 'linearization' of the nonlinear terms. Usually such a term is altered so as to give a product of two terms which are related individually to different time steps. Let us consider only one nonlinear term pertinent to the above system, when the motion of water takes place under the influence of bottom friction alone. Then (4.73) simplifies to

$$\frac{\partial M_x}{\partial t} = - \frac{r}{H^2} |M_x| M_x \quad (4.75)$$

We apply to this equation the following numerical scheme

$$\frac{M_{x,j}^{l+1} - M_{x,j}^l}{T} = -\frac{r}{H^2} |M_x| M_{x,j}^l \quad (4.76)$$

$|M_x|$ can be taken at different moments in time $l-1, l, l+1$. In the course of stability analysis that value cannot be taken as explicit, since the methods applied in verifying the stability are essentially linear. We shall, therefore, set the expression $M_x r/H^2$ equal to a positive coefficient W .

From (4.76) we derive by using (4.17)

$$\lambda - 1 = -TW \quad (4.77)$$

whence $|\lambda| = |1 - TW|$ and the quantity WT is confined to the range

$$0 \leq WT \leq 2 \quad (4.78)$$

Unconditional stability for the arbitrary quantity WT is obtained in the numerical scheme when the right side of (4.76) is taken at $l+1$ time step, whence

$$|\lambda| = \left| \frac{1}{1 + WT} \right| < 1 \quad (4.79)$$

This method of linearization is often used in the iteration process, see e.g. (3.67).

Let us consider other problems which appear in (4.73). First of all it is not quite obvious how to approximate the advection term

$$\frac{M_x}{H} \frac{\partial M_x}{\partial x}$$

Even if M_x/H is treated as a coefficient of the first derivative it will vary in space and time, and in applying any stable method we ought to take into account this feature. Let us approach the solution of system (4.73), (4.74) using the Crank-Nicholson (1947) method. In this scheme the space derivatives are written as a sum of two expressions at two time steps, say $l, l+1$. In the nonlinear terms the additional time step $l + 1/2$ is also introduced. The equation of mass transport (4.73) in Crank-Nicholson notation becomes

$$\frac{M_x^{l+1} - M_x^l}{T} + \frac{M_x^{l+1/2}}{2H} \left[\frac{\partial M_x^{l+1}}{\partial x} + \frac{\partial M_x^l}{\partial x} \right] + \frac{gH}{2\partial x} \frac{\partial \zeta^{l+1}}{\partial x} + \frac{\partial \zeta^l}{\partial x} \frac{gH}{2} = \quad (4.80)$$

$$= -\frac{r}{2H^2} |M_x^{1+1/2}| (M_x^1 + M_x^{1+1}) + \frac{A}{2} \left[\frac{\partial^2 M_x^1}{\partial x^2} + \frac{\partial^2 M_x^{1+1}}{\partial x^2} \right]$$

and the continuity equation

$$\frac{\zeta^{1+1} - \zeta^1}{T} + \frac{1}{2} \left[\frac{\partial M_x^1}{\partial x} + \frac{\partial M_x^{1+1}}{\partial x} \right] = 0 \quad (4.81)$$

Assuming in (4.80) that $M_x^{1+1/2}$ is known, the stability of the system (4.80) and (4.81) may be investigated with the help of expression (4.17). Since $|\lambda| = 1$ we can draw the conclusion that the algorithm is unconditionally stable. The Crank-Nicholson scheme, in spite of second-order approximation and stability, is rather troublesome in practical applications. First of all the presented algorithm does not show the method of computation, since the variables at the $l+1/2$ time step remain unknown. Secondly, the method of computing these variables will surely influence the overall order of approximation. To understand the basis of the Crank-Nicholson approach we use the splitting method. Thus the equation of mass transport is splitted into

$$\frac{M_x^{1+1/2} - M_x^1}{T} = -g \frac{H \partial \zeta^1}{2 \partial x} - \frac{r}{2H^2} |M_x^1| M_x^1 + \frac{A}{2} \frac{\partial^2 M_x^1}{\partial x^2} \quad (4.82)$$

$$\begin{aligned} \frac{M_x^{1+1} - M_x^{1+1/2}}{T} + \frac{1}{2H} M_x^{1+1/2} \left[\frac{\partial M_x^1}{\partial x} + \frac{\partial M_x^{1+1}}{\partial x} \right] \\ = -g \frac{H \partial \zeta^{1+1}}{2 \partial x} - \frac{r}{2H^2} |M_x^{1+1/2}| M_x^{1+1} + \frac{A}{2} \frac{\partial^2 M_x^{1+1}}{\partial x^2} \end{aligned} \quad (4.83)$$

The continuity equation we leave in the previous (4.81) form.

The general idea of the above algorithm is to calculate from equation (4.82) $M_x^{1+1/2}$, in order to compute the nonlinear terms in (4.83). Since the value of $\zeta^{1+1/2}$ does not take part in the computation, we need only one equation for the sea-level.

In (4.83) ζ^{1+1} is an unknown but it may be expressed through (4.81) Thus substituting it into (4.83), the equation for the mass transports on the second substep becomes

$$\frac{M_x^{1+1} - M_x^{1+1/2}}{T} + \frac{M_x^{1+1/2}}{2H} \left[\frac{\partial M_x^1}{\partial x} + \frac{\partial M_x^{1+1}}{\partial x} \right] = \quad (4.84)$$

$$= -\frac{gH}{2} \left[\frac{\partial \zeta^1}{\partial x} - \frac{T}{2} \frac{\partial^2 M_x^1}{\partial x^2} + \frac{\partial^2 M_x^{1+1}}{\partial x^2} \right] - \frac{r}{2H^2} |M_x^{1+1/2}| M_x^{1+1} + \frac{A}{2} \frac{\partial^2 M_x^{1+1}}{\partial x^2}$$

The method for implementing the above equation at every time step is

1. Solve the explicit equation (4.82)
2. Solve the implicit equation (4.84)
3. Calculate ζ^{1+1} from (4.81)

The best approach for solving the implicit equation (4.84) is the method of factorisation (Ch. II, §8). For each iterative method (and time integration is fully analogous to an iterative process) the matrix of coefficients should satisfy the condition of diagonal predominance (2.78). In equation (4.84) the coefficients on the main diagonal are those with index j . Therefore the first derivative in the advective term cannot be taken as symmetrical (centred in space), but it ought to be altered to the directional derivative (backward or forward), as was explained in (2.18). Therefore we have

$$\frac{1}{2}(a + |a|)(M_{x,j}^{1+1} - M_{x,j-1}^{1+1}) + \frac{1}{2}(a - |a|)(M_{x,j+1}^{1+1} - M_{x,j}^{1+1}) \quad (4.85)$$

where

$$a = \frac{1}{2hH} M_x^{1+1/2}.$$

In (4.85), independently of the sign, the coefficient of $M_{x,j}^{1+1}$ is always positive and thus it strengthens the diagonal terms.

Now we introduce other methods of describing the nonlinear terms. The well-known Lax-Wendroff scheme (Richtmyer and Morton, 1967), when applied to a nonlinear equation of motion, provides good results only in one-dimensional motion. Therefore there is no need to analyse this method. Instead of that we introduce two other methods which are quite useful. Leaving only the terms pertinent to advection in the equation of motion, the following numerical algorithm based on central derivatives can be proposed

$$\frac{M_{x,j}^{1+1} - M_{x,j}^{1-1}}{2T} + \frac{M_x}{H} \frac{M_{x,j+1}^1 - M_{x,j-1}^1}{2h} = 0 \quad (4.86)$$

With the help of (4.17) the equation for finding the stability parameter is found to be

$$\lambda^2 + is\lambda - 1 = 0 \quad (4.87)$$

Here $|\lambda_{1,2}| = 1$, if the inequality $s = \frac{1}{hH} M_x T \sin \sigma_1 h < 1$ holds.

This is a scheme of second-order accuracy, but here we have to solve two problems

1. How to reject the numerical (false) solution, since as we know from previous consideration (Ch. IV, §5) one root of (4.87) provides an additional solution.
2. The overall algorithm has to be organised in such a way as to deliver the value of the coefficient M_x/H before starting the computation with (4.86).

The last method which we would like to present was proposed by Roberts and Weiss (1966). It is based on the notion of the angular derivative

$$\frac{M_{x,j}^{l+1} - M_{x,j}^l}{T} + \frac{M_x}{hH} \left[\frac{M_{x,j}^{l+1} + M_{x,j+1}^l}{2} - \frac{M_{x,j}^l + M_{x,j-1}^{l+1}}{2} \right] = 0 \quad (4.88)$$

The main idea of the method lies in the assumption that at the moment $l+1$ at grid point J the values of $M_{x,j}^l$ are known at the grid points with an index j which is smaller than J . The distribution of variables in space and time in (4.88) is presented in fig. 36.

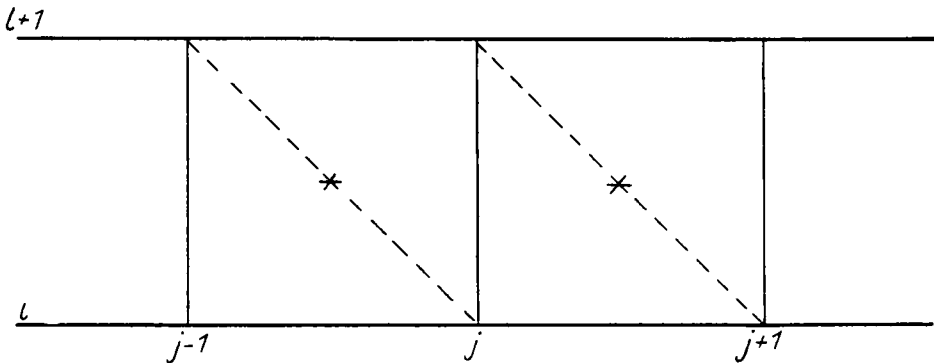


Fig. 36. THE METHOD TO CONSTRUCT THE ANGULAR DERIVATIVES.

It can be seen that the angular derivative is defined in the center of the rectangle, on its diagonal. Using (4.17) it is easily verified

that $|\lambda| = 1$ and there is no computational (false) solution in (4.88). The practical realisation of the algorithm with an angular derivative is usually performed in two steps as in the system (4.82) and (4.83). Since in the expression

$$\frac{M_x}{H} \frac{\partial M_x}{\partial x}$$

nonlinear interactions can give rise to an instability in the shortest waves, it is desirable to control the stability by representing the coefficient M_x/H as a filter in the form $\frac{1}{4H}(M_{x,j-1} + 2M_{x,j} + M_{x,j+1})$. This approach will lead (eventually) to a dampening of the shortest waves on a numerical grid.

§7. Numerical filtering in time and space

We have proved, in certain numerical schemes, the existence of numerical (false) solutions. This may lead to a splitting of the solution into two independent branches. These unwanted solutions will be removed by 'numerical filtering'.

Another problem arises when considering stability. As was shown by Phillips (1959) an instability is often related to the shortest waves whose wave length is equal to twice the grid-spacing.

Applying a numerical filter to the space of grid points separated by $2h$ leads to an improvement in the stability conditions. Computations performed in real basins show that such an instability is caused by the non-uniform coast-line, the bottom shape and especially by the nonlinearities. The general solution of these problems fits into three connected categories:

1. By using numerical filters for modifying the time-space characteristics of sea-level ζ and mass transport M .
2. By developing special forms of difference equations with the numerical filter incorporated directly in the equations of motion and continuity.
3. By introducing a pseudo-viscosity as an additional term in the equations in a manner analogous to the horizontal friction term.

A Numerical filter for the modification of variables in processes of time integration

The well-known three-point-filtering of a variable F which depends on time is expressed by (Shuman, 1957)

$$\bar{F}^l = F^l + 0.5\nu(F^{l-1} - 2F^l + F^{l+1}) \quad (4.89)$$

where ν denotes a filter parameter, and \bar{F} is the filtered value.

Assuming F is a periodically alternating function

$$F = e^{i\omega t} = e^{i\omega lT} \quad (4.90)$$

we define the response of filter R_C as

$$R_C = \frac{\bar{F}^l}{F^l} = 1 - \nu(1 - \cos\omega T) \quad (4.91)$$

It follows from (4.91) that only in the limiting cases, when $\nu \approx 0$, or $\omega T \rightarrow 0$, does the function remain unchanged after filtering. When the filtering is performed consecutively in time, at a time step l we already have at hand the filtered value at the $l-1$ time step. Therefore it is much simpler to use, instead of (4.89), the altered expression proposed by Asselin (1972)

$$\bar{F}^l = F^l + 0.5\nu(\bar{F}^{l-1} - 2F^l + F^{l+1}) \quad (4.92)$$

though the response function becomes more complicated

$$R_C = \frac{(2 - \nu)^2 + 2\nu^2(1 - \cos\omega T) e^{i\omega T}}{(2 - \nu)^2 + 4\nu(1 - \cos\omega T)} = R e^{i\delta} \quad (4.93)$$

Here R is the amplitude of the response function and δ expresses the phase shift. This sort of filtering acts on the amplitude of the wave and at the same time introduces a phase difference. The dependence of R and δ on the filter parameter and on $\cos T$ is plotted in figs. 37 and 38 according to Asselin (1972).

We shall study now the effect of a filter when used in conjunction with a symmetrical numerical scheme on the removal of the computational mode of solution.

To the differential equation

$$\frac{\partial F}{\partial t} = i\omega F \quad (4.94)$$

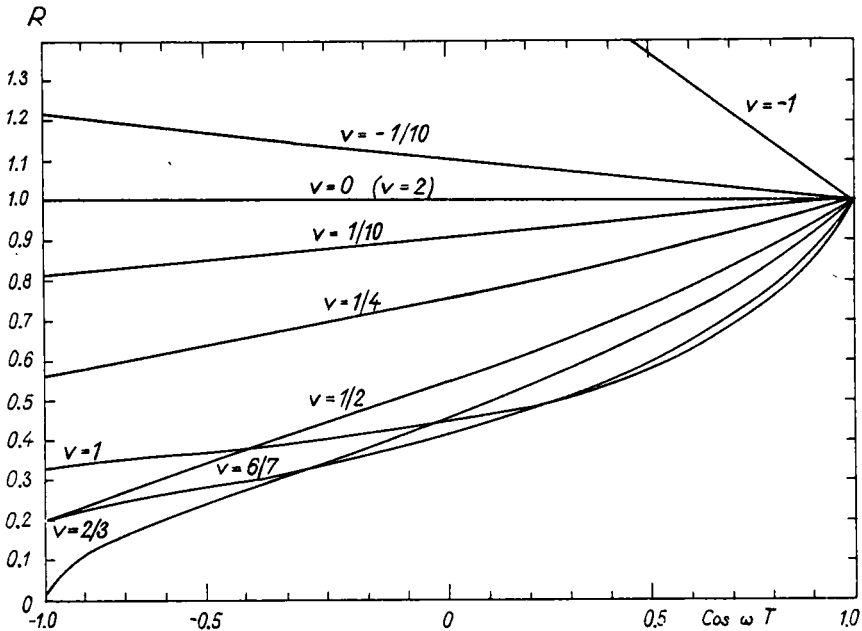


Fig. 37. AMPLITUDE RESPONSE DUE TO THE APPLICATION OF A TIME FILTER TO A PERIODIC FUNCTION FOR A FEW VALUES OF THE FILTER PARAMETER ν , ACCORDING TO ASSELIN (1972).

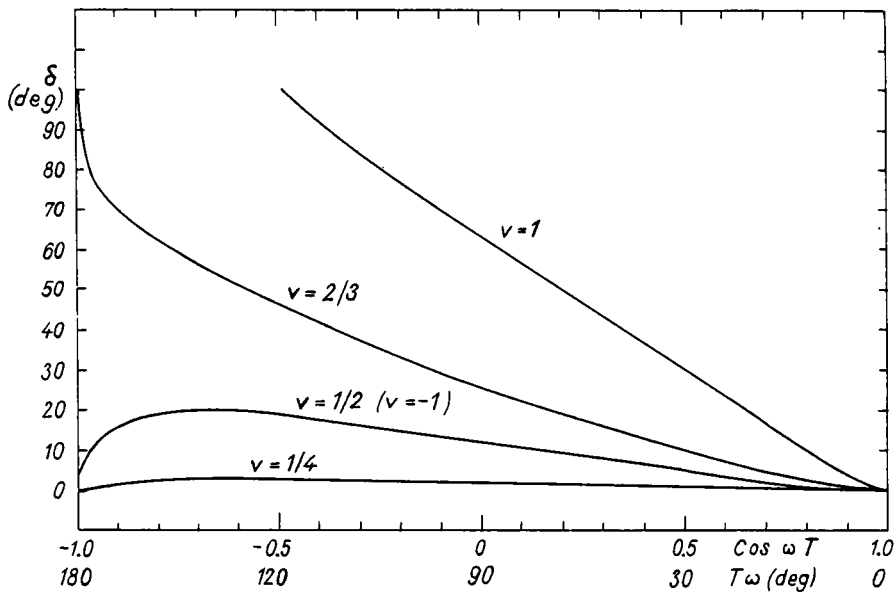


Fig. 38. PHASE SHIFT δ DUE TO THE APPLICATION OF A TIME FILTER TO A PERIODIC FUNCTION, ACCORDING TO ASSELIN (1972).

we ascribe the finite-difference analogue

$$\frac{F^{l+1} - F^{l-1}}{2T} = i\omega F^l \quad (4.95)$$

Analysing the stability of (4.95) using (4.17) we find

$$\lambda^2 - 2T\omega i\lambda - 1 = 0 \quad (4.96)$$

Two values of λ are derived as

$$\lambda_{1,2} = i\omega T \pm \sqrt{1 - T^2\omega^2} \quad (4.97)$$

Assuming $1 > (T\omega)^2$ the two different roots are

$$\lambda_1 = i\omega T + \sqrt{1 - (T\omega)^2}$$

which represents the physical mode of solution and

$$\lambda_2 = i\omega T - \sqrt{1 - (T\omega)^2}$$

which describes the computational mode.

Our aim is to choose the filter parameters in such a manner that $|\lambda_2| \rightarrow 0$. To this end let us take (4.95) with a built-in filter in order to control the computational and physical mode, thus

$$\frac{F^{l+1} - \bar{F}^{l-1}}{2T} = i\omega F^l \quad (4.98)$$

The filtered value \bar{F}^{l-1} in (4.98) is calculated from (4.92). If the amplification factor (or stability parameter) is defined as $\lambda = F^{l+1}/F^l$, then (4.98) yields

$$\lambda_{1,2} = v/2 + i\omega T \pm \sqrt{(1 - v/2)^2 - (\omega T)^2} \quad (4.99)$$

If $v = 0$, we return to the previous solution expressed by (4.97) and $|\lambda_{1,2}| = 1$. If $v \neq 0$ it follows that

$$|\lambda_1| = \{ [v/2 + \sqrt{(1 - v/2)^2 - (\omega T)^2}]^2 - (\omega T)^2 \}^{1/2} \quad (4.100)$$

$$|\lambda_2| = \{ [v/2 - \sqrt{(1 - v/2)^2 - (\omega T)^2}]^2 - (\omega T)^2 \}^{1/2} \quad (4.101)$$

whence $|\lambda_1| > |\lambda_2|$. The computational mode λ_2 always corresponds to the negative sign in (4.99). The introduction of a filter provides the following results

1. The computational and physical modes are differentiated, due to the fact that $|\lambda_1| \neq |\lambda_2|$
2. The computational mode is removed in the course of computation since $|\lambda_1| > |\lambda_2|$; see also fig. 39

Finally, it is important to stress that the above methods of numerical filtering may be used not only in time but also in space.

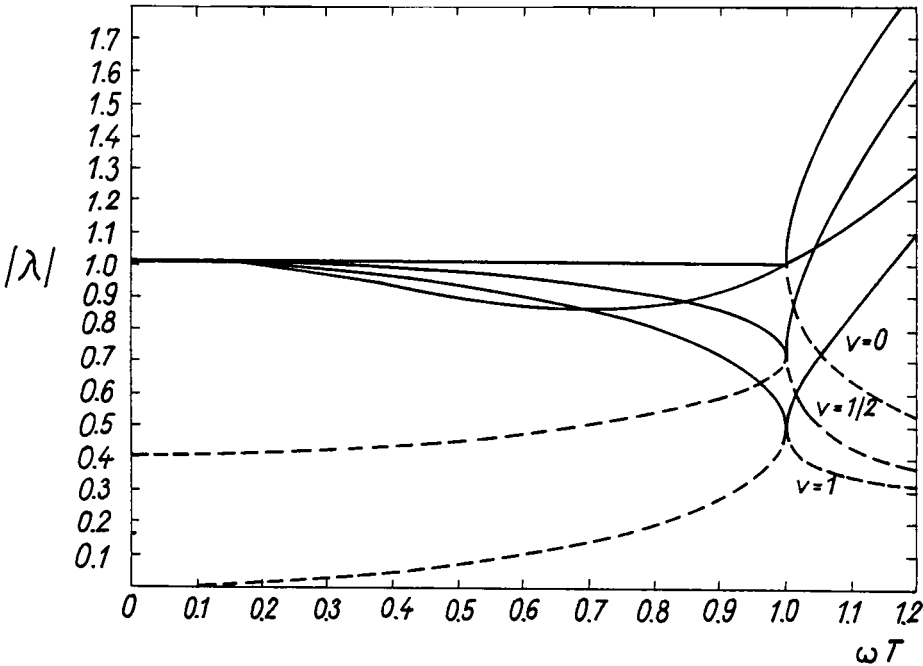


Fig. 39. AMPLIFICATION FACTOR λ FOR THE DIFFERENT FILTER PARAMETERS v . THE DASHED LINES DESCRIBE THE COMPUTATIONAL (FALSE) MODE OF SOLUTION, SINCE FOR THIS MODE $|\lambda| < 1$ THE APPLICATION OF SUCH A FILTER WILL SUPPRESS THE COMPUTATIONAL MODE.

B Difference equations with a built-in filter

Instead of filtering the data, the filter may be used in conjunction with the finite-difference equation itself. According to Shuman (1962) we consider a nonlinear equation

$$\frac{\partial u}{\partial t} + u \frac{\partial u}{\partial x} = 0 \quad (4.102)$$

With the notation

$$\bar{f}^x = 1/2 (f_{j+1/2} + f_{j-1/2}) \quad (4.103)$$

$$f_x = 1/h (f_{j+1/2} - f_{j-1/2}) \quad (4.104)$$

the difference form of (4.102) becomes

$$\bar{u}_t^t + \bar{u}^{xx} \bar{u}_x^x = 0 \quad (4.105)$$

The nonlinear term in (4.105) represents the smoothed function

$$\begin{aligned} \frac{1}{4} \bar{u}_x^x (u_{j+1} + 2u_j + u_{j-1}) &= \frac{1}{2h} (u_{j+1} - u_{j-1}) \frac{1}{4} (u_{j+1} + 2u_j + u_{j-1}) \\ &= \frac{1}{2h} (u_{j+1} - u_{j-1}) u_j^* \end{aligned} \quad (4.106)$$

Similar expressions can be constructed in a two-dimensional space for a function

$$\begin{aligned} f_{j,k}^* &= \frac{1}{4} (f_{j,k-1}^* + 2f_{j,k}^* + f_{j,k+1}^*) = \frac{1}{4} \left[\frac{1}{4} (f_{j-1,k-1} + 2f_{j,k-1} + f_{j+1,k-1}) \right. \\ &\quad \left. + \frac{2}{4} (f_{j-1,k} + 2f_{j,k} + f_{j+1,k}) + \frac{1}{4} (f_{j-1,k+1} + 2f_{j,k+1} + f_{j+1,k+1}) \right] \end{aligned} \quad (4.107)$$

and also for the derivatives

$$\frac{\partial \zeta_{j,k}^*}{\partial x} = \frac{1}{4} \left(\frac{\partial \zeta_{j,k+1}}{\partial x} + 2 \frac{\partial \zeta_{j,k}}{\partial x} + \frac{\partial \zeta_{j,k-1}}{\partial x} \right) \quad (4.108a)$$

$$\frac{\partial \zeta_{j,k}^*}{\partial y} = \frac{1}{4} \left(\frac{\partial \zeta_{j-1,k}}{\partial y} + 2 \frac{\partial \zeta_{j,k}}{\partial y} + \frac{\partial \zeta_{j+1,k}}{\partial y} \right) \quad (4.108b)$$

Substituting (4.107) and (4.108) into the equations of motion and continuity gives the following special form

$$\frac{M_{x,j,k}^{1+1} - M_{x,j,k}^{1-1}}{2T} = -gH \frac{\partial \zeta_{j,k}^*}{\partial x} + fM_{y,j,k}^* \quad (4.109)$$

$$\frac{M_{y,j,k}^{1+1} - M_{y,j,k}^{1-1}}{2T} = -gH \frac{\partial \zeta_{j,k}^*}{\partial y} - fM_{x,j,k}^* \quad (4.110)$$

$$\frac{\zeta_{j,k}^{l+1} - \zeta_{j,k}^{l-1}}{2\tau} = -\frac{\partial M_{x,j,k}^*}{\partial x} - \frac{\partial M_{y,j,k}^*}{\partial y} \quad (4.111)$$

To explain the action of a filter in conjunction with a difference scheme, we return to the scalar wave equation (4.102).

The numerical form of (4.102) when constructed with a central derivative and without filtering has the amplification factor (4.87) $|\lambda| = 1$, subject to the condition that the inequality

$$u \frac{\tau}{h} \sin \sigma_1 h < 1 \quad (4.112)$$

is fulfilled. Solving the same problem with the help of (4.105) we find $|\lambda| = 1$, but (4.112) changes to

$$u \frac{\tau}{h} \sin \sigma_1 h \cdot \frac{1}{2} (1 + \cos \sigma_1 h) < 1 \quad (4.113)$$

Only when $\sigma_1 h = \frac{2}{L} \pi h \rightarrow 0$ do we obtain (4.112). Such a situation arises for a very long wave. If the wave length L is comparable to the grid step h , then in the limiting case of the shortest wave $L=2h$

$$\frac{1}{2} (1 + \cos \sigma_1 h) = \frac{1}{2} (1 + \cos \frac{2\pi}{2h} h) = 0.$$

Therefore the additional expression in (4.113) alters the stability criterion only in the range of the shortest wave when L is close to $2h$.

C The introduction of viscosity

Real hydrodynamic processes which take place in the sea and in the ocean are influenced by the turbulent cascade of energy from the large-scale motion into motion on the smaller meso- and micro-scales. At the smallest scale the energy is dissipated into heat. This natural process when described numerically is distorted by the imposed grid system, especially at the shortest scale, since the length of the gridspacing h is usually much greater than the scale at which the dissipation takes place. In this way the possibility arises that in a numerical grid energy will tend to grow in the shortest waves which can be resolved by the grid.

A common procedure for removing this effect is the introduction of a so-called pseudo-viscosity (Richtmyer and Morton, 1967) which

smoothes the numerical solution imitating the sub-grid-scale dissipation. In our case we add the following viscosity terms to the left side of the equations

$$\frac{1}{4}(\alpha - 1) \frac{(21)^2}{2\Delta t} U = - A \Delta U \quad (4.114a)$$

$$\frac{1}{4}(\alpha - 1) \frac{(21)^2}{2\Delta t} V = - A \Delta V \quad (4.114b)$$

$$\frac{1}{4}(\alpha - 1) \frac{(21)^2}{2\Delta t} \zeta = - A \Delta \zeta \quad (4.114c)$$

where $0 < \alpha < 1$.

The same effect can be achieved with a proper choice of the horizontal eddy viscosity coefficients. By means of these coefficients the turbulent interaction is parameterised for the scales not represented by the average quantities (sub-grid interaction). This scale, of course, depends on the discretization due to the limited resolution of the adopted grid. This means that the eddy coefficients have to be chosen in relation to the grid distances. As was shown by Brettschneider (1967) the formula

$$A \approx 0.01 \frac{h^2}{T} \quad (4.115)$$

delivers a good approximation of the eddy viscosity coefficient for numerical computation. Sometimes valuable hints on the eddy viscosity problem may be found in the researches on the general circulation of the atmosphere, see e.g. Smagorinsky, Manabe and Holloway (1965).

§8. Boundary and initial conditions

Study of the motion and sea-level variations will be performed with the system of equations (4.1), (4.2) and (4.3). The proper boundary conditions for this system may be chosen depending on the practical situation

$$\begin{aligned} M_n &= 0 \quad \text{on land boundary} \\ M_n &= \phi_1(\Gamma) \quad \text{on water (open) boundary} \\ M_s &= 0 \quad \text{on land boundary} \\ \zeta(\Gamma) &= \phi_2(\Gamma) \quad \text{on water boundary} \end{aligned} \quad (4.116)$$

Here M_n and M_s denote the normal and tangential components of mass transport at the coast; $\phi_1(\Gamma)$ and $\phi_2(\Gamma)$ are known functions of space and time. At the initial moment the dependent variables are taken as zero in the whole domain of integration

$$\zeta(x, y, t=0) = M_x(x, y, t=0) = M_y(x, y, t=0) = 0 \quad x, y \in \bar{D} \quad (4.117)$$

Such conditions result from the lack of data with which to describe the sea-level and mass transport (or average velocity) in the whole of the studied basin at the initial moment. On the other hand it is easy to see that a solution of the presented system of equations does not depend on the initial conditions. To explain this feature we shall seek a solution which is periodical in space. We also set the external force $\tau_s^{(x)} = 0$, $\tau_s^{(y)} = 0$, since it is not pertinent to the problem under consideration. The assumption of space periodicity simplifies the algebra, because the solution obtained does not depend on the boundary conditions. Seeking a solution in the form of $\vec{M} = \vec{M}_1(t) \cdot \exp(i\alpha x + i\beta y)$ we obtain by virtue of (4.6)

$$\frac{\partial \vec{M}_1}{\partial t} + B_1 \vec{M}_1 = 0 \quad (4.118)$$

where the matrix B_1 becomes

$$B_1 = \begin{bmatrix} R & -f & \alpha g i H \\ f & R & \beta g i H \\ i\alpha & i\beta & 0 \end{bmatrix} \quad (4.119)$$

The operator B_1 may be described by the set of eigenvalues λ_j and related eigenfunctions $\vec{\phi}_j$.

We decompose the vector solution M_1 of equation (4.118) into a linear combination of the eigenfunctions $\vec{\phi}_k$

$$M_1 = \sum_{k=1}^{\infty} \vec{\phi}_k c_k \quad (4.120)$$

Here c_k are the unknown coefficients to be found.

Related to the operator B_1 there is a spectral problem which may be defined as (Ch. VIII)

$$B_1 \vec{\phi}_j = \lambda_j \vec{\phi}_j \quad (4.121)$$

We now seek a solution for the eigenvectors $\vec{\phi}_k$, since it is related to M_1 through (4.120).

Introducing (4.120) into (4.118) yields

$$\frac{\partial \vec{\phi}_k}{\partial t} + B_1 \vec{\phi}_k = 0 \quad \text{for every } k \quad (4.122)$$

Taking next into account (4.121) we find

$$\frac{\partial \vec{\phi}_k}{\partial t} + \lambda_k \vec{\phi}_k = 0 \quad \text{for every } k \quad (4.123)$$

therefore $\vec{\phi}_k \approx e^{-\lambda_k t}$.

This result provides a unique answer to the problem of the dependence of the solution on the initial conditions. Since it is obvious from (4.123) that if every eigenvalue λ_k possesses a positive real part then $\vec{\phi}_k$ will decay with time, and in such a situation the solution \vec{M} will be independent of the initial condition (after an appropriate span of time has elapsed). If on the other hand λ_k has a negative real part, the solution is strongly influenced by the initial condition (but is also unstable). This requirement related to the eigenvalues is easily verified by calculating all the eigenvalues of the matrix B_1 (4.119). The choice of proper boundary conditions from (4.116) depends on the type of equation used. Generally, we shall deal with the mixed type, but when the expressions with horizontal friction are present in the whole time-space domain, then the system of equations is usually a hyperbolic one. As was proved by Marchuk et al. (1972) a unique solution of the hyperbolic set of equations exists if the normal and tangential components of mass transport are given on the boundary (rigid or liquid). On the other hand when the equations show hyperbolic properties we ought to use the other type of boundary condition.

But first of all we present the method to prove the hyperbolic properties of a set of equations in domain $\bar{D}(x, y, t)$. First the simplified system of equations (4.9), (4.10) and (4.11) is set in the vector matrix form

$$\frac{\partial \vec{M}}{\partial t} + A \frac{\partial \vec{M}}{\partial x} + B \frac{\partial \vec{M}}{\partial y} = 0 \quad (4.124)$$

where

$$A = \begin{bmatrix} 0 & 0 & gH \\ 0 & 0 & 0 \\ 1 & 0 & 0 \end{bmatrix}; B = \begin{bmatrix} 0 & 0 & 0 \\ 0 & 0 & gH \\ 0 & 1 & 0 \end{bmatrix} \quad (4.125)$$

For the system (4.124) to be hyperbolic at a point $P(x, y, t)$ of the domain $\bar{D}(x, y, t)$ the eigenvalues λ of the linear combination $\alpha_1^2 A + \alpha_2^2 B$ (given that $\alpha_1^2 + \alpha_2^2 = 1$) should be real and different at the point $P \in \bar{D}$ (Courant and Hilbert, 1962). The eigenvalues of this linear combination are derived from the determinant

$$\text{Det}(\alpha_1 A + \alpha_2 B - \lambda E) = 0 \quad (4.126)$$

whence

$$\lambda_1 = 0; \lambda_{2,3} = \pm\sqrt{gH} \quad (4.127)$$

The number of boundary conditions required for a unique solution of the hyperbolic system is equal to the number of negative eigenvalues. It follows that for the problem defined by (4.124) one boundary condition already provides the solution.

In physical reality the overall situation is much more complicated. Generally, two problems are important:

1. Very often we require the operators in the equations to be positive-definite. This in turn strongly influences the possible choice of boundary conditions.
2. A sufficient number of boundary conditions is very difficult to acquire. Usually at the liquid boundaries the velocities are unknown (for example in the tidal problem), but the sea-level is known. With this sort of condition the solution of the parabolic problem is impossible. The practical approach is to solve the hyperbolic problem at grid points on the nearest line to the liquid boundary by using sea-level boundary conditions and then after deriving the mass transport (or mean velocities) to solve the parabolic problem in the whole domain.

Due to this and other problems as well the so-called staggered net is usually introduced for carrying out numerical calculations. The values of M_x , M_y and ζ are defined at different grid points (fig.34). The grid distance for the same variable is $2h$ and time step is $2T$. This allows us to overcome many obstacles, i.e. very often it is difficult to define sea-level at the coast. Then, as in fig.34, sea-level ζ may be computed at the distance h from the coast. On the

coast the velocity is defined, since the normal component vanishes there.

§9. The explicit numerical scheme

Equations (4.1), (4.2) and (4.3) are defined on the numerical grid as plotted in fig. 34 as follows

$$\begin{aligned} & \frac{M_{x,j+1,k}^{1+1} - M_{x,j+1,k}^{1-1}}{2T} - \frac{1}{4}f(M_{y,j+2,k+1}^{1-1} + M_{y,j,k+1}^{1-1} + M_{y,j,k-1}^{1-1} + M_{y,j+2,k-1}^{1-1}) \\ &= -\frac{g}{2h}H_{j+1,k}(\zeta_{j+2,k}^1 - \zeta_{j,k}^1) + \tau_{s,j+1,k}^{(x)} - R_{j+1,k}^{1-1}M_{j+1,k}^{1-1} \quad (4.128) \\ & + \frac{A}{4h^2}(M_{x,j+3,k}^{1-1} + M_{x,j-1,k}^{1-1} + M_{x,j+1,k+2}^{1-1} + M_{x,j+1,k-2}^{1-1} - 4M_{x,j+1,k}^{1-1}) \end{aligned}$$

$$\begin{aligned} & \frac{M_{y,j,k+1}^{1+1} - M_{y,j,k+1}^{1-1}}{2T} + \frac{1}{4}f(M_{x,j+1,k+2}^{1-1} + M_{x,j-1,k+2}^{1-1} + M_{x,j-1,k}^{1-1} + M_{x,j+1,k}^{1-1}) \\ &= -\frac{g}{2h}H_{j,k+1}(\zeta_{j,k+2}^1 - \zeta_{j,k}^1) + \tau_{s,j,k+1}^{(y)} - R_{j,k+1}^{1-1}M_{j,k+1}^{1-1} \quad (4.129) \\ & + \frac{A}{4h^2}(M_{y,j+2,k+1}^{1-1} + M_{y,j-2,k+1}^{1-1} + M_{y,j,k+3}^{1-1} + M_{y,j,k-1}^{1-1} - 4M_{y,j,k+1}^{1-1}) \end{aligned}$$

$$\begin{aligned} \frac{\zeta_{j,k}^{1+2} - \zeta_{j,k}^1}{2T} &= -\frac{1}{2h}(M_{x,j+1,k}^{1+1} - M_{x,j-1,k}^{1+1}) - \frac{1}{2h}(M_{y,j,k+1}^{1+1} - M_{y,j,k-1}^{1+1}) \\ & \quad (4.130) \end{aligned}$$

where

$$R = \frac{r}{H^2} \sqrt{(M_x^{1-1})^2 + (M_y^{1-1})^2} = \frac{r}{H^2} |M^{1-1}| \quad (4.131)$$

This algorithm is well known and was described by Fischer (1959) and Kagan (1970). The order of approximation differs for different terms, of course. For example the Coriolis force is derived as a mean value from the four surrounding grid points

$$\frac{1}{4}f(M_{Y,j+2,k+1}^{1-1} + M_{Y,j+2,k-1}^{1-1} + M_{Y,j,k+1}^{1-1} + M_{Y,j,k-1}^{1-1}) \quad (4.132)$$

If the exact value of this component is taken as

$$f M_{Y,j+1,k}^{1-1} \quad (4.133)$$

then the difference between (4.132) and (4.133) is equal to

$$0.5h^2 f \Delta M_Y + O(h^2) \quad (4.134)$$

In the same way the component along the y-axis may be analysed. It is obvious that (4.134) is in the limit equal to zero, but, since h is of finite magnitude in the difference scheme a numerical friction analogous to the physical friction is observed. It is worth underlining that the effects of horizontal friction which are physical and numerical play a secondary rôle in the storm surge phenomena (this conclusion follows from dimensional analysis).

The order of approximation of the Coriolis force may be improved according to Fischer (1965). To simplify the notation we shall draw attention only to the development of the scheme in time

$$\frac{M_x^{1+1} - M_x^{1-1}}{2T} - \frac{f}{2} M_y^{1+1} - \frac{f}{2} M_y^{1-1} = -gH \frac{\partial \zeta^1}{\partial x} + A \Delta M_x^{1-1} - R M_x^{1-1} \quad (4.135)$$

$$\frac{M_y^{1+1} - M_y^{1-1}}{2T} + \frac{f}{2} M_x^{1+1} + \frac{f}{2} M_x^{1-1} = -gH \frac{\partial \zeta^1}{\partial y} + A \Delta M_y^{1-1} - R M_y^{1-1} \quad (4.136)$$

$$\frac{\zeta^{1+2} - \zeta^1}{2T} + \frac{\partial M_x^{1+1}}{\partial x} + \frac{\partial M_y^{1+1}}{\partial y} = 0 \quad (4.137)$$

We rearrange the first equation in the form

$$M_x^{1+1} - fT M_y^{1+1} = F_1 \quad (4.138)$$

and the second equation as

$$M_y^{1+1} + fT M_x^{1+1} = F_2 \quad (4.139)$$

F_1 and F_2 denote all the terms which are related to the 1 and 1-1 time steps. From (4.138) and (4.139) we derive the components of

mass transport at the moment $l+1$

$$M_x^{l+1} = \frac{F_1 + F_2 fT}{1 + (fT)^2} \quad (4.140)$$

and

$$M_y^{l+1} = \frac{F_2 - F_1 fT}{1 + (fT)^2} \quad (4.141)$$

In the course of computation we calculate firstly F_1 and F_2 , and next M_x^{l+1} and M_y^{l+1} by (4.140) and (4.141), and finally from (4.137) the sea-level ζ^{l+2} at the instant $l+2$. In this way we by-pass all difficulties due to the implicit form of (4.135) and (4.136).

Let us study now the stability properties of the explicit form (4.128), (4.129) and (4.130).

Introducing an error array in the form of (4.17) into the system of equations the result is obtained in the matrix-vector form

$$\begin{bmatrix} \lambda^2 + a, & -b, & ic\lambda\sin\sigma_1h \\ b, & \lambda^2 + a, & ic\lambda\sin\sigma_2h \\ \frac{ic\sin\sigma_1h}{\sqrt{gH}}, & \frac{ic\sin\sigma_2h}{\sqrt{gH}}, & \lambda - 1/\lambda \end{bmatrix} \cdot \begin{bmatrix} M_x \\ M_y \\ \zeta \end{bmatrix} = \begin{bmatrix} 0 \\ 0 \\ 0 \end{bmatrix} \quad (4.142)$$

where

$$a = 2 RT - 1 + \frac{2TA}{h^2}(\sin^2\sigma_1h + \sin^2\sigma_2h)$$

$$b = 2 fT \cos\sigma_1h \cos\sigma_2h$$

$$c = \frac{2 T gH}{h}$$

A unique solution to the uniform equation (4.142) is obtained only if the determinant of the matrix is equal to zero which leads to an equation of sixth order for the parameter λ . The result obtained in this manner is very general and difficult to interpret. Therefore we consider at first a simplified system of equations when the friction and Coriolis forces are neglected ($R = 0$, $A = 0$, $f = 0$). As a result of this simplification the stability parameter λ is defined by the determinant in which $a = -1$, $b = 0$ and $c = \frac{gH}{h} \frac{2T}{h}$.

$$\begin{vmatrix} \lambda^2 - 1 & 0 & ic\lambda\sin\sigma_1h \\ 0 & \lambda^2 - 1 & ic\lambda\sin\sigma_2h \\ \frac{ic\sin\sigma_1h}{\sqrt{gH}} & \frac{ic\sin\sigma_2h}{\sqrt{gH}} & \frac{\lambda^2-1}{\lambda} \end{vmatrix} = 0 \quad (4.143)$$

from which we find a biquadratic equation for λ . Its roots are

$$\lambda_{1,2}^2 = \frac{1}{2}(2 - Q \pm i\sqrt{Q(4 - Q)}) \quad (4.144)$$

where

$$Q = \frac{gH}{h^2} (2T)^2 (\sin^2\sigma_1h + \sin^2\sigma_2h)$$

From (4.144) and inequality $Q < 4$ it follows that $|\lambda_{1,2}^2| = 1$. The inequality on the other hand relates time and space steps to the parameters of the difference equation

$$T^2 \leq \frac{h^2}{2gH} \quad (4.145)$$

This is the well-known Courant, Friedrich and Lewy condition. In one-dimensional flow this condition is described by (4.23). When Coriolis and friction forces in the equations of motion are of influence the analysis of the determinant is rather complicated. To omit the difficulty we assume, following Phillips(1959), that an instability is generated in the numerical system at the shortest wave length which can be resolved on the grid. On the grid plotted in fig. 34 the shortest wave is double the grid size, i.e. $4h$. Because the wave number along the x-axis is equal to $\sigma_1 = \frac{2\pi}{L}$ when the shortest wave length is introduced ($L_{\min} = 4h$), the arguments of the expressions in (4.142) become

$$\sigma_1h = \frac{2\pi}{2h}h = \frac{\pi}{2} = \sigma_2h \quad (4.146)$$

Therefore in (4.142) $\sin\sigma_1h$ and $\sin\sigma_2h$ equal unity; $\cos\sigma_1h$ and $\cos\sigma_2h$ both vanish and the determinant of (4.142) simplifies to

$$\begin{vmatrix} \lambda^2 + a' & 0 & ic\lambda \\ 0 & \lambda^2 + a' & ic\lambda \\ \frac{ic}{\sqrt{gH}} & \frac{ic}{\sqrt{gH}} & \frac{\lambda^2 - 1}{\lambda} \end{vmatrix} = 0 \quad (4.147)$$

where $a' = 2RT - 1 + \frac{4AT}{h^2}$

The determinant (4.147) may be rearranged as a biquadratic equation

$$(\lambda^2 + a') [(\lambda^2 + a')(\lambda^2 - 1) + 2\lambda^2 c^2 / \sqrt{gH}] = 0 \quad (4.148)$$

and from it one of the roots is easily derived as

$$\lambda^2 = -a' = 1 - 2RT - \frac{4AT}{h^2} \quad (4.149)$$

Its absolute value is

$$|\lambda| = \left| \sqrt{1 - 2RT - 4AT/h^2} \right| \leq 1 \quad (4.150)$$

This inequality states the criterion for the time step

$$T \leq 1/(R + 2A/h^2) \quad (4.151)$$

This somewhat strange condition, from a physical point of view, states that the stronger the friction in the system the smaller the time step that should be chosen in a difference scheme has to be. The remaining roots of (4.148) provide an additional criterion for the limits imposed on the time and space steps

$$\frac{T}{h} (2gH + \frac{2}{T} h^2 R + \frac{4}{T} A)^{1/2} \leq 1 \quad (4.152)$$

Summarising the results obtained from Phillips' conjecture on the generation of an instability at the shortest resolvable wave length it should be stressed that this is the most probable mechanism but the possibility cannot be excluded that an instability may appear at wave lengths $L > L_{\min}$.

The study of stability by the Neuman method is confined to an analysis of the properties of the difference equation inside the grid region. Additionally the stability is influenced by the boundary conditions and by the external forces. To study the action of the boundary conditions and the way of approximating these conditions we rely upon the definition of the positive definite operator in the closed domain $\bar{D}(x,y)$ (Ch. II, §4). That is, we shall take the boundary condition in such a manner as to comply with this definition.

The system of equations in vector-matrix form becomes

$$\frac{\partial \vec{M}}{\partial t} = -B\vec{M} + \vec{\tau}_s \quad (4.153)$$

The vector and the matrix in (4.153) are defined as

$$\vec{M} = \begin{bmatrix} M_x \\ M_y \\ \alpha \zeta \end{bmatrix}; \quad \vec{\tau}_s = \begin{bmatrix} \tau_s(x) \\ \tau_s(y) \\ 0 \end{bmatrix}; \quad B = \begin{bmatrix} R-A\Delta & -f & \alpha \frac{\partial}{\partial x} \\ f & R-A\Delta & \alpha \frac{\partial}{\partial y} \\ \alpha \frac{\partial}{\partial x} & \alpha \frac{\partial}{\partial y} & 0 \end{bmatrix} \quad (4.154)$$

where $\alpha = \sqrt{gH}$.

As always B will be called a positive-definite operator in the domain $\bar{D}(x,y)$ if the scalar product is positive

$$(\vec{M}, \vec{BM})_{\bar{D}}^* = \int_{\bar{D}} (\vec{M}, \vec{BM})^* d\bar{D} \geq 0 \quad (4.155)$$

Rearranging (4.155) in cartesian co-ordinates we find

$$\int_D [R^2(M_x^2 + M_y^2) - AM_x \Delta M_x - AM_y \Delta M_y + \alpha^2 (\frac{\partial M_x \zeta}{\partial x} + \frac{\partial M_y \zeta}{\partial y})] dx dy > 0 \quad (4.156)$$

It is obvious that the first expression under the integral is positive. The integral

$$- \int_D (M_x A \Delta M_x + M_y A \Delta M_y) dx dy \quad (4.157)$$

is equal to

$$-A \int_D [(\frac{\partial M_x}{\partial x})^2 + (\frac{\partial M_y}{\partial x})^2 + (\frac{\partial M_x}{\partial y})^2 + (\frac{\partial M_y}{\partial y})^2] dx dy \quad (4.158)$$

and is therefore also positive.

The last expression

$$c_1 = \int_D \alpha^2 [\frac{\partial (M_x \zeta)}{\partial x} + \frac{\partial (M_y \zeta)}{\partial y}] dx dy \quad (4.159)$$

may be altered into an integral along the boundary Γ . When the condition on a rigid boundary $M_n = 0$ (4.116) is given then $c_1 = 0$. If, on the other hand, part of the boundary is liquid then $c_1 \leq 0$. Therefore a possibility arises that the operator B will be negative-definite and the iteration process and time-integration do not converge. It should be underlined that condition (4.156) is an integral. Thus it is possible that the influence of an open boundary on the overall

solution is negligible when the ratio of the length of the liquid boundaries to the closed boundaries is small.

Nevertheless, the boundary condition at the liquid boundary should not be taken in an arbitrary way but in agreement with (4.155). In the case of numerical approximation the fulfilment of (4.156) has to be checked in every case. In a symmetrical lattice one can write (4.159) as

$$c_{1h} = h^2 \alpha^2 \sum_{jk} \frac{1}{2h} (\zeta_{j+1,k} M_{x,j+1,k} - \zeta_{j-1,k} M_{x,j-1,k}) \quad (4.160)$$

$$+ h^2 \alpha^2 \sum_{jk} \frac{1}{2h} (\zeta_{j,k+1} M_{y,j,k+1} - \zeta_{j,k-1} M_{y,j,k-1})$$

Therefore, with the condition $M_n = 0$, (4.160) does not vanish along the boundaries. In a-symmetrical lattices the vanishing can be achieved by a special combination of backward and forward differences.

§10. An implicit numerical scheme

An implicit form of difference equation is introduced to bring about the possibility of increasing the time step and saving computer time in this way. As usual the system of equations (4.1), (4.2) and (4.3) will be considered under the additional assumption that the horizontal friction term can be neglected $A = 0$. This simplification does not change the physics of the flow, because the horizontal friction term is at least one order of magnitude smaller than the other terms. But from the mathematical point of view we pass from the parabolic system of equations to a hyperbolic one. The boundary and initial conditions are taken from the set defined by (4.116) and (4.117). According to Sielecki (1968) and Kowalik (1975) we take the implicit difference scheme as

$$\frac{M_x^{l+1} - M_x^l}{T} = f M_y^{l+1} - g H \frac{\partial \zeta^{l+1}}{\partial x} + \tau_s^{(x)l+1} - R M_x^{l+1} \quad (4.161)$$

$$\frac{M_y^{l+1} - M_y^l}{T} = -f M_x^{l+1} - g H \frac{\partial \zeta^{l+1}}{\partial y} + \tau_s^{(y)l+1} - R M_y^{l+1} \quad (4.162)$$

$$\frac{\zeta^{l+1} - \zeta^l}{T} = - \frac{\partial M_x^{l+1}}{\partial x} - \frac{\partial M_y^{l+1}}{\partial y} \quad (4.163)$$

Although this system is unconditionally stable (as we shall demonstrate later on) it has to be solved at each time step by an iterative procedure due to its implicit structure. It is, of course, possible to consider a great number of methods, though the main problem is the fulfilment of sufficient criteria for the convergence of a chosen method. Let us consider first the above system without any alteration.

Introducing an index of iteration q we shall solve it through the following numerical scheme

$$q+1 M_x^{l+1} (1 + RT) = fT^q M_y^{l+1} - gHT \frac{q_{\partial \zeta}^{l+1}}{\partial x} + M_x^l + \tau_s^{(x)l+1} \quad (4.164)$$

$$q+1 M_y^{l+1} (1 + RT) = -fT^q M_x^{l+1} - gHT \frac{q_{\partial \zeta}^{l+1}}{\partial y} + M_y^l + \tau_s^{(y)l+1} \quad (4.165)$$

$$q+1 \zeta^{l+1} = \zeta^l - T \left\{ \frac{q_{\partial M_x}^{l+1}}{\partial x} + \frac{q_{\partial M_y}^{l+1}}{\partial y} \right\} \quad (4.166)$$

Forgetting for the time being the index $l+1$ we build the amplification matrix from an iteration step q to step $q+1$ (by introducing (4.17) and changing l to q)

$$\begin{bmatrix} 0 & fT/(1 + RT) & TgH i \sin \sigma_1 h / (h + hRT) \\ -fT/(1 + RT) & 0 & -TgH i \sin \sigma_2 h / (h + hRT) \\ -\frac{1}{h} T i \sin \sigma_1 h & -\frac{1}{h} T i \sin \sigma_2 h & 0 \end{bmatrix} \quad (4.167)$$

The eigenvalues λ of this matrix are given by the equation

$$-\lambda^3 + \lambda \{ [fT/(1+RT)]^2 + gH(\sin^2 \sigma_1 h + \sin^2 \sigma_2 h) \left(\frac{T}{h\sqrt{1+RT}} \right)^2 \} = 0 \quad (4.168)$$

Hence

$$\lambda_{1,2} = \pm \{ [fT/(1+RT)]^2 + gH(\sin^2 \sigma_1 h + \sin^2 \sigma_2 h) \left(\frac{T}{h\sqrt{1+RT}} \right)^2 \}^{1/2} \quad (4.169)$$

If we simplify the set of equations by neglecting the Coriolis term ($f = 0$) and frictional forces ($R = 0$), (4.169) becomes

$$\lambda_{1,2} = \frac{T}{h} \{ gH(\sin^2 \sigma_1 h + \sin^2 \sigma_2 h) \}^{1/2} \quad (4.170)$$

As has been shown in chapter II an iteration process is convergent when the modulus of its eigenvalues is less than or equal to unity.

$$\text{Thus } |\lambda_{2,3}| = T\sqrt{2gH}/h \leq 1 \quad (4.171)$$

expresses the well-known criteria for stability of an explicit scheme.

Generally one may say that there is no stability condition whatsoever which limits the time step in an implicit method. However, due to application of an iteration method (at each time step) and the requirements of the convergence criteria in the iteration process itself we arrive finally at an additional condition for the time-space step (see expression (4.171)).

Our aim is to find an iteration scheme which does not include such severe restrictions as (4.171). To do this we transform the general system of equations by introducing ζ^{1+1} from (4.163) into (4.161) and (4.162)

$$\frac{M_x^{1+1} - M_x^1}{T} = fM_y^{1+1} + gHT \left(\frac{\partial^2 M_x^{1+1}}{\partial x^2} + \frac{\partial^2 M_y^{1+1}}{\partial x \partial y} \right) - gH \frac{\partial \zeta^1}{\partial x} + \tau_s^{(x)1+1} - RM_x^{1+1} \quad (4.172)$$

$$\frac{M_y^{1+1} - M_y^1}{T} = -fM_x^{1+1} + gHT \left(\frac{\partial^2 M_y^{1+1}}{\partial y^2} + \frac{\partial^2 M_x^{1+1}}{\partial y \partial x} \right) - gH \frac{\partial \zeta^1}{\partial y} + \tau_s^{(y)1+1} - RM_y^{1+1} \quad (4.173)$$

Introducing space indices j, k these equations may be rearranged in a form suitable for computation by an iterative method

$$\begin{aligned} & (1 + RT + 2gHT^2/h^2)M_{x,j,k}^{1+1} - gHT^2/h^2 (M_{x,j+1,k}^{1+1} + M_{x,j-1,k}^{1+1}) \quad (4.174) \\ & = fTM_{y,j,k}^{1+1} + gHT^2/(4h^2) (M_{y,j+1,k+1}^{1+1} + M_{y,j-1,k-1}^{1+1} - M_{y,j-1,k+1}^{1+1} \\ & \quad - M_{y,j+1,k-1}^{1+1}) - gHT/(2h) (\zeta_{j+1,k}^1 - \zeta_{j-1,k}^1) + T\tau_s^{(x)1+1} + M_{x,j,k}^1 \end{aligned}$$

$$\begin{aligned} & (1 + RT + 2gHT^2/h^2)M_{y,j,k}^{1+1} - gHT^2/h^2 (M_{y,j,k+1}^{1+1} + M_{y,j,k-1}^{1+1}) \quad (4.175) \\ & = -fTM_{x,j,k}^{1+1} + gHT^2/(4h^2) (M_{x,j+1,k+1}^{1+1} + M_{x,j-1,k-1}^{1+1} - M_{x,j-1,k+1}^{1+1} \\ & \quad - M_{x,j+1,k-1}^{1+1}) - gHT/(2h) (\zeta_{j,k+1}^1 - \zeta_{j,k-1}^1) + T\tau_s^{(y)1+1} + M_{y,j,k}^1 \end{aligned}$$

The above equations are given on a symmetrical lattice, where ζ , M_x and M_y are computed at the same grid points (fig. 32). At each time step these equations can be solved by an arbitrary iterative

method. The computation will run until the proper accuracy is reached and then we proceed to the next time step. The application of an iterative method at each time step is evidently the result of the implicit notation, since the left side of (4.174) and (4.175) taken at the $l+1$ moment in time is a function of the right side which in turn also depends on the time step. Therefore during the computation both (4.174) and (4.175) have to be considered together. When (4.174) is solved its right side is assumed to be known from the previous iteration of (4.175) and vice-versa.

The factorisation method (Ch. II, §8) is best suited for the application. (4.174) is taken thereby along the x -axis and (4.175) along the y -axis. The convergence condition of an iterative method is fulfilled in D_h , since in the matrix of coefficients in (4.174) and (4.175) the diagonal element $1 + RT + 2gHT^2/h^2$ prevails over the sum of the non-diagonal elements $2gHT^2/h^2$.

The stability properties of the implicit system of equations (4.161), (4.162) and (4.163) will be analysed by inserting an array of errors (4.17) into the system. The result takes the form of a cubic equation in

$$\begin{aligned} & [\lambda(1+RT) - 1]^2(\lambda - 1) + \lambda^2(T/h)^2 gH(\sin^2\sigma_1 h + \sin^2\sigma_2 h) [\lambda(1+RT) - 1] \\ & + \lambda^2(\lambda - 1)(fT)^2 = 0 \end{aligned} \quad (4.176)$$

The Neuman criterion for numerical stability states that all roots of (4.176) should be inside or (and) on the unit circle in the complex plane. For further consideration let us represent (4.176) in a somewhat different form denoting

$$\gamma_1 = 1 + RT; \quad \gamma_2 = gH(T/h)^2 (\sin^2\sigma_1 h + \sin^2\sigma_2 h) \quad (4.177)$$

thus

$$\begin{aligned} & \lambda^3[\gamma_1^2 + \gamma_1\gamma_2 + (fT)^2] - \lambda^2[2\gamma_1 + \gamma_1^2 + \gamma_2 + (fT)^2] \\ & + \lambda(1 + 2\gamma_1) - 1 = 0 \end{aligned} \quad (4.178)$$

The parameters T , h , $\sin\sigma_1 h$ and $\sin\sigma_2 h$ may change over a wide range. The full solution or explicit derivation of λ is of course impossible in such a general case. Therefore let us consider some simplified cases:

A. Let $T \rightarrow 0$, $h < \infty$, then $\gamma_1 = 1$, $\gamma_2 = 0$, $fT = 0$ and equation (4.178) becomes

$$(\lambda - 1)^3 = 0 \quad (4.179)$$

B. Let $T \rightarrow \infty$, then using the properties of the roots of the cubic equation we obtain

$$\lambda_1 \lambda_2 \lambda_3 = \frac{1}{\gamma_1^2 + \gamma_1 \gamma_2 + (fT)^2} = 0 \quad (4.180)$$

$$\lambda_1 \lambda_2 + \lambda_1 \lambda_3 + \lambda_2 \lambda_3 = \frac{1 + 2\gamma_1}{\gamma_1^2 + \gamma_1 \gamma_2 + (fT)^2} = \frac{O(T)}{O(T^3)} = 0 \quad (4.181)$$

$$\lambda_1 + \lambda_2 + \lambda_3 = \frac{\gamma_1^2 + 2\gamma_1 + \gamma_2 + (fT)^2}{\gamma_1^2 + \gamma_1 \gamma_2 + (fT)^2} = \frac{O(T^2)}{O(T^3)} = 0 \quad (4.182)$$

$$\text{and hence } \lambda_1 = \lambda_2 = \lambda_3 = 0. \quad (4.183)$$

C. Let us consider for $0 < T < \infty$ the following parameter values $T = 10^3$ sec and 10^6 sec with $h = 10^6$ cm, $f = 10^{-4}$ sec $^{-1}$, $H = 10^4$ ca and $r = 10^{-6}$ sec $^{-1}$. The results are given in the following table

T	$1/2(\sin^2 \sigma_1 h + \sin^2 \sigma_2 h)$	λ_1	λ_2	λ_3
10^3	0	1	1	1
10^3	1	0.292	0.146-0.496i	0.146-0.496i
10^6	0	1	0	0
10^6	1	0	0.5	0

D. Since the instabilities usually start from the waves of minimum length ($L_{\min} = 2h$) on a numerical grid of spacing h , we find $\sigma_1 h = \sigma_2 h = \pi$, $\gamma_2 = 0$ and equation (4.178) takes the form

$$(\lambda \gamma_1 - 1)^2 (\lambda - 1) + \lambda^2 (\lambda - 1) (fT)^2 = 0 \quad (4.184)$$

Three roots of the equation are

$$\lambda_1 = 1; \quad \lambda_{2,3} = (\gamma_1 \pm ifT) / (\gamma_1^2 + (fT)^2) \quad (4.185)$$

As $\gamma_1 > 1$, we have always $|\lambda_{2,3}| < 1$.

To equation (4.178) we also apply the straightforward method for the analysis of the stability properties by proving the inequality $|\lambda| < 1$. Let us rewrite (4.178) as

$$\lambda^3 + a_1\lambda^2 + a_2\lambda + a_3 = 0 \quad (4.186)$$

where

$$a_1 = -\frac{2\gamma_1 + \gamma_1^2 + \gamma_2 + (fT)^2}{\gamma_1^2 + \gamma_1\gamma_2 + (fT)^2} < 0 \quad (4.187)$$

$$a_2 = \frac{1 + 2\gamma_1}{\gamma_1^2 + \gamma_1\gamma_2 + (fT)^2} > 0 \quad (4.188)$$

$$a_3 = -\frac{1}{\gamma_1^2 + \gamma_1\gamma_2 + (fT)^2} < 0 \quad (4.189)$$

By the substitution $\lambda = 1/u$ the polynomial (4.186) is transformed to

$$1 + a_1u + a_2u^2 + a_3u^3 = 0 \quad (4.190)$$

Next (4.190) is rearranged through the introduction of a new variable $u = \frac{1-v}{1+v}$. Therefore, if the root of the cubic equation (4.186) is a complex number, the root of (4.190) is also complex and its value is

$$u_1 = a + ib \quad (4.191)$$

or expressed through the new variable

$$v_1 = \frac{1 - a^2 - b^2 - 2ib}{1 + a^2 + b^2 + 2a} \quad (4.192)$$

Here we may conclude that if $|\lambda| < 1$, then $|u_1| > 1$ and since $u_1 = \sqrt{a^2 + b^2}$ the real part of (4.192) is in the negative half-plane, that is $\text{Re}(v_1) < 0$. Using this property we shall not proceed by the previous way, i.e. by solving equation (4.186). But instead we shall analyse the roots with the aim of showing that $|\lambda| \leq 1$. In this method it is sufficient to prove that all the roots of the polynomial have a negative real part. To find the roots with such properties we shall apply the Routh-Hurwitz condition to equation (4.186) (Gantmacher, 1959)

$$A_0v^3 + A_1v^2 + A_2v + A_3 = 0 \quad (4.193)$$

where

$$\begin{aligned}
 A_0 &= 1 - a_1 + a_2 - a_3 \\
 A_1 &= 3 - a_1 - a_2 + 3a_3 \\
 A_2 &= 3 + a_1 - a_2 - 3a_3 \\
 A_3 &= 1 + a_1 + a_2 + a_3
 \end{aligned}
 \tag{4.194}$$

The following determinant plays a central rôle. It is built from the coefficients of (4.194)

$$i = \begin{vmatrix}
 A_1 & A_3 & A_5 & & & & \\
 A_0 & A_2 & A_4 & & & & \\
 0 & A_1 & A_3 & & & & \\
 0 & A_0 & A_2 & & & & \\
 & & & \cdot & & & \\
 & & & & \cdot & & \\
 & & & & & \cdot & \\
 & & & & & & A_i
 \end{vmatrix}
 \tag{4.195}$$

The Routh-Hurwitz theorem states that the necessary and sufficient condition for the existence of roots with negative real parts in the polynomial (4.193) is the positiveness of the following subdeterminants

$$S_1 = A_1 > 0 \tag{4.196a}$$

$$S_2 = A_1 A_2 - A_0 A_3 > 0 \tag{4.196b}$$

$$S_3 = A_3 S_2 > 0 \tag{4.196c}$$

with the assumption

$$A_0 > 0 \tag{4.196d}$$

Introducing into (4.196) the values (4.187) to (4.189) we find that all inequalities hold. This in turn implies that all the roots of (4.186) are within the unit circle in the imaginary plane and the system of equations (4.161), (4.162) and (4.163) is unconditionally stable for an arbitrary time-space step.

§11. Computational example to compare explicit and implicit properties

Since the method of implicit time integration allows us to introduce an arbitrary time step, it should find frequent application.

To compare the results obtained by the explicit (M I) and the implicit method (M II) we consider a rectangular sea basin where the dimension along the x-axis is 200 km and along the y-axis is 100 km and with a complicated bottom shape. Wind of 10 m/sec acts parallel to the y direction from the moment $t = 0$ up to $t \rightarrow \infty$. The flow is studied in time until a steady state occurs (Kowalik, 1975). The results of the computation at the point P with co-ordinates $x = 60$ km and $y = 20$ km are presented in the form of a stream function ψ ,

$$M_y = \frac{\partial \psi}{\partial x}$$

$$M_x = -\frac{\partial \psi}{\partial y},$$

and plotted in fig. 40. Computations were performed by means of M I with constant time step $T = 60$ sec and by means of M II with different time steps from $T = 5 \times 10^2$ sec up to $T = 5 \times 10^4$ sec. As may be seen from these considerations the results of the implicit scheme depend on T and with the growth of the time step the absolute value of ψ diminishes.

When the time step in the implicit method is close to the time step of the explicit method, the results of both computations are comparable. Therefore we may say that the implicit method is stable for any time step, but the physical properties of the hydrodynamic processes limit the time step.

Nevertheless, increasing the time step T_i in an implicit method is possible in relation to the explicit time step T_e . As follows from our calculations it is possible over the range $T_i < 10T_e$.

§12. A numerical system with mixed explicit-implicit properties

A numerical system with mixed properties was developed by Leendertse (1967) and by Marchuk et al. (1969) for obtaining a high order of approximation. In the following we shall present the method proposed by Marchuk et al. To begin with we split the equation of motion into two similar parts

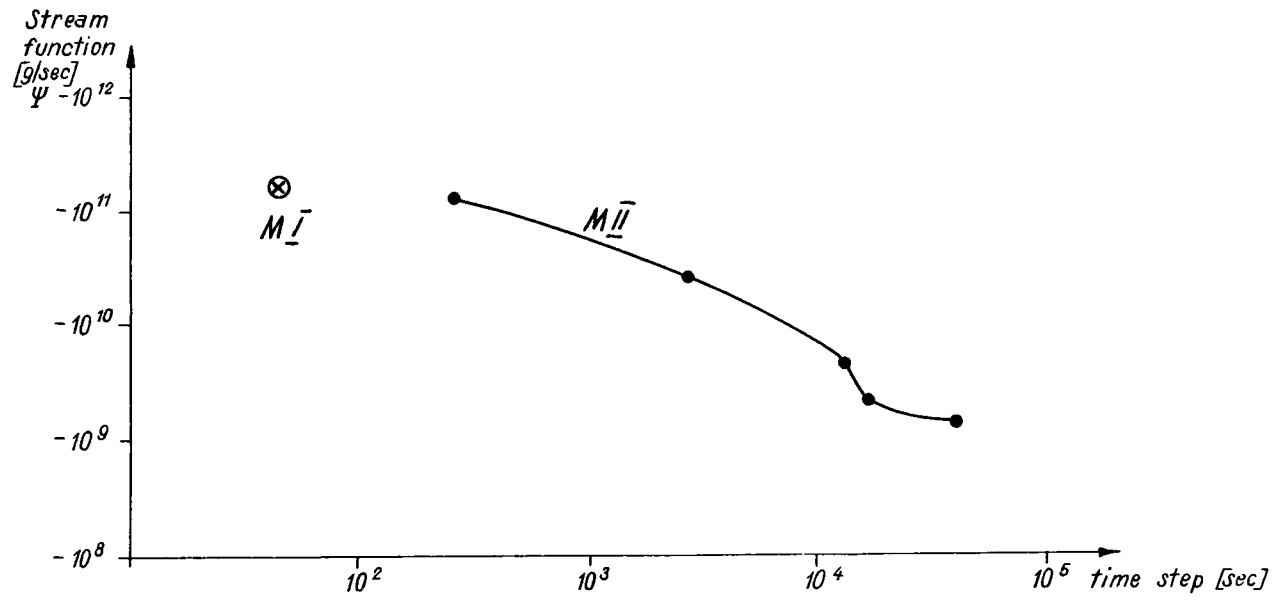


Fig. 40. STREAM FUNCTION COMPUTED BY THE EXPLICIT METHOD WITH TIME STEP $T = 60$ sec (M I) AND BY THE IMPLICIT METHOD WITH DIFFERENT TIME STEPS (M II).

$$\frac{1}{2} \frac{\partial M_x}{\partial t} - \frac{f}{2} M_y = -\frac{1}{2} gH \frac{\partial \zeta}{\partial x} - \frac{R}{2} M_x + \frac{A}{2} \Delta M_x \quad (4.197a)$$

$$\frac{1}{2} \frac{\partial M_y}{\partial t} + \frac{f}{2} M_x = -\frac{1}{2} gH \frac{\partial \zeta}{\partial y} - \frac{R}{2} M_y + \frac{A}{2} \Delta M_y \quad (4.197b)$$

Next introducing the half time step $T/2$ the following implicit numerical form is proposed

$$\frac{M_x^{1+1/2} - M_x^1}{T} = \frac{f}{2} M_y^1 - \frac{1}{2} gH \frac{\partial \zeta^1}{\partial x} - R^1 M_x^1 + \frac{A}{2} \left(\frac{\partial^2 M_x^1}{\partial x^2} + \frac{\partial^2 M_x^{1+1/2}}{\partial y^2} \right) \quad (4.198)$$

$$\frac{M_y^{1+1/2} - M_y^1}{T} = -\frac{f}{2} M_x^{1+1/2} - \frac{1}{2} gH \frac{\partial \zeta^1}{\partial y} - R^1 M_y^1 + \frac{A}{2} \left(\frac{\partial^2 M_y^{1+1/2}}{\partial x^2} + \frac{\partial^2 M_y^1}{\partial y^2} \right) \quad (4.199)$$

on the first substep and on the second substep

$$\begin{aligned} \frac{M_y^{1+1} - M_y^{1+1/2}}{T} = & -\frac{f}{2} M_x^{1+1/2} - \frac{1}{2} gH \frac{\partial \zeta^{1+1}}{\partial y} - R^{1+1/2} M_y^{1+1} \\ & + \frac{A}{2} \left(\frac{\partial^2 M_y^{1+1/2}}{\partial x^2} + \frac{\partial^2 M_y^{1+1}}{\partial y^2} \right) \end{aligned} \quad (4.200)$$

$$\begin{aligned} \frac{M_x^{1+1} - M_x^{1+1/2}}{T} = & \frac{f}{2} M_y^{1+1} - \frac{1}{2} gH \frac{\partial \zeta^{1+1}}{\partial x} - R^{1+1/2} M_x^{1+1} \\ & + \frac{A}{2} \left(\frac{\partial^2 M_x^{1+1}}{\partial x^2} + \frac{\partial^2 M_x^{1+1/2}}{\partial y^2} \right) \end{aligned} \quad (4.201)$$

In (4.200) and (4.201) the value of the sea-level is unknown, therefore we use the equation of continuity to express this variable.

The equation of continuity will be arranged in three different forms in order to do this.

A. To calculate ζ^{1+1} we use

$$\frac{\zeta^{1+1} - \zeta^1}{T} = -\left(\frac{\partial M_x^{1+1/2}}{\partial x} + \frac{\partial M_y^{1+1/2}}{\partial y} \right) \quad (4.202)$$

B. To calculate $\frac{\partial \zeta^{1+1}}{\partial x}$ we use

$$\frac{\zeta^{1+1} - \zeta^1}{T} = -\frac{1}{2} \left(\frac{\partial M_x^1}{\partial x} + \frac{\partial M_x^{1+1}}{\partial x} \right) - \frac{\partial M_y^{1+1/2}}{\partial y} \quad (4.203)$$

C. To calculate $\frac{\partial \zeta^{1+1}}{\partial y}$ we use

$$\frac{\zeta^{1+1} - \zeta^1}{T} = -\frac{\partial M_x^{1+1/2}}{\partial x} - \frac{1}{2} \left(\frac{\partial M_y^1}{\partial y} + \frac{\partial M_y^{1+1}}{\partial y} \right) \quad (4.204)$$

After calculating $\frac{\partial \zeta^{1+1}}{\partial x}$ from (4.203) we introduce it into (4.201) and in a similar way $\frac{\partial \zeta^{1+1}}{\partial y}$ from (4.204) is introduced into (4.200). The new form of equations (4.200) and (4.201) becomes

$$\begin{aligned} \frac{M_y^{1+1} - M_y^{1+1/2}}{T} = & -\frac{f}{2} M_x^{1+1/2} - \frac{1}{2} gH \left[\frac{\partial \zeta^1}{\partial y} - T \left(\frac{\partial^2 M_x^{1+1/2}}{\partial x \partial y} + \frac{1}{2} \frac{\partial^2 M_y^1}{\partial y^2} \right) \right] \quad (4.205) \\ & + \frac{A}{2} \frac{\partial^2 M_y^{1+1/2}}{\partial x^2} + \left[\frac{1}{2} \left(\frac{gHT}{2} + A \right) \frac{\partial^2}{\partial y^2} - R^{1+1/2} \right] M_y^{1+1} \end{aligned}$$

$$\begin{aligned} \frac{M_x^{1+1} - M_x^{1+1/2}}{T} = & \frac{f}{2} M_y^{1+1} - \frac{1}{2} gH \left[\frac{\partial \zeta^1}{\partial x} - T \left(\frac{\partial^2 M_y^{1+1/2}}{\partial x \partial y} + \frac{1}{2} \frac{\partial^2 M_x^1}{\partial x^2} \right) \right] \quad (4.206) \\ & + \frac{A}{2} \frac{\partial^2 M_x^{1+1/2}}{\partial x^2} + \left[\frac{1}{2} \left(\frac{gHT}{2} + A \right) \frac{\partial^2}{\partial x^2} - R^{1+1/2} \right] M_x^{1+1} \end{aligned}$$

The problem of deriving the mass transport and sea-level is solved with the help of equations (4.198), (4.199), (4.205), (4.206) and (4.202).

The equations of mass transport are integrated at each time step by the factorisation method.

In (4.198) the factorisation is performed for variable $M_x^{1+1/2}$ along the y direction and in (4.199) $M_y^{1+1/2}$ is factorised along the x direction, and so on.

Therefore, from this point of view the method of computation is an explicit one. The stability of the system depends on the stabilities of the two substeps. An analysis involves quite long algebraic expressions, but finally a criterion is found which is close to the well-known criterion for an explicit scheme $T < h/\sqrt{2gH}$.

Comparing these three different methods which are considered above, that is explicit, implicit and mixed one, we may conclude that

- A. The explicit method is the simplest in practical realisation.
- B. The best approximation, second order in time and space, is given by the mixed method.

§13. Steady state processes from a point of view of numerical methods used for solving an unsteady problem

The contents of this final paragraph are closely related to the discussion in chapter II. For a steady state process described by an equation

$$\Delta\psi = f(x,y); \quad x,y \in D \quad (4.207)$$

with boundary condition $\psi|_{\Gamma} = C$ we set up the related non-stationary problem

$$\frac{\partial\psi}{\partial t} = \Delta\psi - f; \quad \psi|_{\Gamma} = C_1 \quad (4.208)$$

The solution of (4.208) when $t \rightarrow \infty$ coincides with the solution of the problem stated by (4.207). Introducing a numerical scheme to integrate the unsteady problem we can obtain in the limit a distribution for ψ under steady state conditions. As an example of application of this method let us consider the one-dimensional problem

$$\frac{\psi_j^{l+1} - \psi_j^l}{T} = \frac{1}{h^2}(\psi_{j+1}^l + \psi_{j-1}^l - 2\psi_j^l) - f_j^l \quad (4.209)$$

Hence the stability condition from (4.17) provides the constraint on step size

$$0 \leq T/h^2 \leq 1/2 \quad (4.210)$$

Continuing from this partial result we return to the problems considered in chapter II, where the general method of solution was the iterative method. It is obvious that the iterative process is quite analogous to the above described method of deriving a steady state solution through an equation of unsteady motion.

Now, analysing the iterative solution on step l (of the iteration) and comparing it with the previous step we find in certain parts of the domain D the differences (errors) between the two steps. Our aim is to diminish this error, that is, to accelerate the convergence of the iterative scheme. Among the many acceleration methods proposed we present the method of Richardson (Thompson, 1961).

Denoting the difference between the iterative solution of (4.207)

at step 1 and the right side of (4.207) as

$$R^1 = \Delta^* \psi^1 - h^2 f \quad (4.211)$$

Richardson's algorithm is stated as follows

$$\psi^{1+1} = \psi^1 + \alpha (\Delta^* \psi^1 - h^2 f) \quad (4.212)$$

where

$$\Delta^* \psi^1 = \psi_{j+1}^1 + \psi_{j-1}^1 - 2\psi_j^1 \quad (4.213)$$

and α is an iterative parameter. The choice of the optimum value of an iterative parameter is a difficult but not a hopeless task as it was shown by Carré (1961) and O'Brien (1968).

We present here only the range of variability of α using the analogy with the unsteady problem. For equation (4.212) stability takes place when (compare with (4.210))

$$0 \leq \alpha \leq 1/2 \quad (4.214)$$

The two-dimensional operator in (4.212) provides

$$0 \leq \alpha \leq 1/4 \quad (4.215)$$

and finally in the three-dimensional case

$$0 \leq \alpha \leq 1/6$$

Therefore, we may apply Richardson's method of accelerating an iterative process by setting α to any value within these ranges of variability.

REFERENCES

- Ames, W.F., 1965. Nonlinear Partial Differential Equations in Engineering. Academic Press, New York, London.
- Asselin, R., 1972. Frequency Filter for Time Integrations. Monthly Weather Review v. 100, N. 6.
- Brettschnéider, G., 1967. Anwendung des hydrodynamisch-numerischen Verfahrens zur Ermittlung der M_2 -Mitschwingungszeit in der Nordsee. Mitteilungen des Instituts² für Meereskunde der Universität Hamburg, VII.

- Carré, B.A., 1961. The Determination of the Optimum Accelerating Factor for Successive Over-Relaxation. *Computer Journal*. v. 4, N.1.
- Courant, R. and Hilbert, D., 1962. *Methods of Mathematical Physics*. Interscience Publishers Inc., New York.
- Crank, J. and Nicholson, P., 1947. A Practical Method for Numerical Integration of Solutions of Partial Differential Equations of Heat Conduction Type. *Proc. Cambridge Phil. Soc.* 43, 50.
- Fischer, G., 1959. Ein numerisches Verfahren zur Errechnung von Windstau und Gezeiten in Randmeeren. *Tellus* v. II, N. 1.
- Fischer, G., 1965. On a Finite-Difference Scheme for Solving the Nonlinear Primitive Equations for a Barotropic Fluid with Application to the Boundary Current Problem. *Tellus* v. 17, N. 4.
- Forsythe, G.E. and Wasow, W.R., 1960. *Finite Difference Methods for Partial Differential Equations*. John Wiley and Son Inc., New York.
- Gantmacher, F.R., 1959. *The Theory of Matrices*. Chelsea Publishing Company, New York.
- Hansen, W., 1956. Theorie zur Errechnung des Wasserstandes und der Strömungen in Randmeeren nebst Anwendungen. *Tellus* v. 8, N. 3.
- Hansen, W., 1962. *Proc. of Symposium on Math.-Hydrod. Methods in Phys. Oceanogr.*, Mitteilungen des Instituts für Meereskunde der Universität Hamburg, I.
- Kagan, B.A., 1970. On the Features of Some Finite-Difference Schemes Used in Numerical Integration of Tidal Dynamics Equations. *Atmospheric and Oceanic Physics* N. 7.
- Kowalik, Z., 1975. On the Numerical Solution of a Steady Circulation in the Sea. *Acta Geophysica Polonica* N.4.
- Lamb, H. 1932. *Hydrodynamics*. Cambridge University Press.
- Lax, P.D. and Richtmyer, R.D., 1956. Survey of the Stability of Linear Finite-Difference Equations. *Communications on Pure and Applied Mathematics* v. IX: 267-293.
- Leendertse, J.J., 1967. *Aspects of a Computational Model for Long-Period Water-Wave Propagation*. Rand Corporation, California.
- Marchuk, G.I.; Kagan, B.A.; Tamsalu, R.E., 1969. Numerical Methods to Compute Tidal Motion in Adjacent Seas. *Atmospheric and Oceanic Physics* T. 5, N. 7.
- Marchuk, G.; Gordiejev, R.; Kagan, B.A.; Rivkind, W., 1972. Numerical Method to Solve Tidal Dynamics Equation and the Results of its Testing (in Russian). Published by Computational Centre, Novosibirsk.
- Marchuk, G., 1974. *Numerical Solution of Sea and Atmospheric Dynamics Problems*. Gidrometeoizdat, Leningrad.
- Miyakoda, K., 1962. Contribution to the Numerical Weather Prediction - Computation with Finite-Differences. *Japanese Journal of Geophysics* v. 3, N. 1.
- O'Brien, G.G.; Hyman, M.A.; Kaplan, S., 1951. A Study of the Numerical Solution of Partial Differential Equations. *Journal of Mathematics and Physics* v. 29, N.4.
- O'Brien, J.J., 1968. Comments on "The Over-Relaxation Factor in the Numerical Solution of the Omega Equation". *Monthly Weather Review* v. 96, N. 2.
- Phillips, N.A., 1959. *An Example of Nonlinear Computational Instability. The Atmosphere and Sea in Motion*. Rockefeller Ins. Press, New York.

- Richtmyer, R.D. and Morton, K.W., 1967. *Difference Methods for Initial Value Problems*. Interscience Publishers.
- Roberts, K.V. and Weiss, N.O., 1966. *Convective Difference Schemes*. *Mathematics of Computation* v. 20, N.94.
- Shuman, F.G., 1957. *Numerical Methods in Weather Prediction: II - Smoothing and Filtering*. *Monthly Weather Review* v. 85:357-361.
- Shuman, F.G., 1962. *Numerical Experiments with Primitive Equations*. *Proc. of the International Symposium on Numerical Weather Prediction in Tokyo, Nov. 7-13, 1960*. Meteorological Soc. of Japan, Tokyo.
- Sielecki, A., 1968. *An Energy-Conserving Difference Scheme for the Storm Surge Equations*. *Monthly Weather Review* v. 96, N. 3.
- Smagorinsky, J.; Manabe, S.; Holloway, J.L., 1965. *Numerical Results from a Nine-Level General Circulation Model of the Atmosphere*. *Monthly Weather Review* v. 93, N. 12.
- Sündermann, J., 1966. *Ein Vergleich zwischen der analytischen und der numerischen Berechnung winderzeugter Strömungen und Wasserstände in einem Modellmeer mit Anwendungen auf die Nordsee*. *Mitteilungen des Instituts für Meereskunde der Universität Hamburg*, IV.
- Thompson, P.D., 1961. *Numerical Weather Analysis and Prediction*. Macmillan Company, New York.

Chapter V NUMERICAL TREATMENT OF TIDES

§1. Introduction

The classical problem of the tides of the world ocean can be formulated as follows:

Determine the tides and tidal currents by means of the hydrodynamic equations, introducing only the tide-generating forces and the geometry of the bottom topography and coastline which are presumed to be known.

In principle, it is possible to compute quantitatively the tides and tidal currents at each point of the world ocean using the hydrodynamic differential equations without consulting measurements of tides and tidal currents, whether from the coast or from the open sea.

Since the times of Newton mathematicians and physicists, like Bernoulli, Laplace, Hough, Darwin, Poincaré and others, have studied the tidal problem. The goal of their efforts was to set up analytical solutions of the hydrodynamic differential equations. These could be found, however, only for geometrically simple oceans. The knowledge gained by these studies is summarized by Lamb (1945) and Defant (1961). Proceeding in this way it is impossible to seize quantitatively the phenomena in a natural basin. To obtain analytical solutions for such phenomena is extremely difficult. Even for the relatively simple example of a rectangular basin with Coriolis force and tidal stimulation, no closed solution exists. These difficulties lead to the search for a numerical solution to the tidal problem. It seems that Defant (1919, 1924, 1932) was the first to apply the numerical method to the so-called narrow-sea-problem where the domain of integration could be considered as a one-dimensional channel. The application of the numerical procedure (with the boundary condition $\zeta = 0$ on the open boundary and $U = 0$ at the closed boundary) allowed Defant to derive several solutions for elongated basins such as the Red Sea, the English Channel, the Mediterranean Sea and the Atlantic Ocean.

The first application of the two-dimensional set of equations is due to Hansen (1949). He applied them to the tide problem in the northern part of the Atlantic Ocean, and afterwards to the North Sea problem (Hansen, 1952).

Generally speaking, two different approaches to the tide problem are feasible. The first approach is based on the well-known fact that the harmonic (in time) boundary conditions generate harmonic motion and therefore all variables in the equations of motion and continuity may be set in the form $e^{i\omega t}$. Consequently the time variable can be

removed and the final equation of sea-level is obtained from the primary system of equations. This equation with proper boundary conditions is usually solved by iteration methods.

On the other hand, one can solve the system of primary equations by time-integration with the periodical boundary condition. The integration in time is continued until the stationary state occurs, i.e. the shape of the tidal curve is repeated in time without any distortion.

The latter method, although very valuable in the treatment of non-linear equations, needs more computer time than the former procedure. Accordingly, the first method has found widespread application when studying the distribution of the tides. It is very often called the boundary value method. For this reason it is very difficult to mention all the contributors to this approach. The most conspicuous results were obtained by Bogdanov et al. (1964) for the tides of the Pacific Ocean and for different basins of the World Ocean (Bogdanov, 1975). A slightly different approach to the boundary value problem has been presented by Pekeris and Accad (1967) who computed the M_2 -tide in the Atlantic Ocean.

The methods of solution are related here to the system of algebraic equations (see chapter II). The overall iteration process depends strongly on the bottom friction coefficient. This leads, in deep basins, to very slow convergence and sometimes to divergence of the solution.

On the other hand, the time dependent integration or the hydrodynamic method has also been initiated by Hansen (1956) and was subsequently developed by his colleagues. The best results with this approach obtained Zahel (1973, 1977). The system of equations is written on a staggered net in the explicit form (as demonstrated in chapter IV, §9).

Another form of an explicit scheme has been widely used by Heaps (1969, 1972) for the tide and storm surge problem in adjacent seas.

In the Soviet Union a group of people associated with Marchuk (see Marchuk et al. (1969)) has developed a semi-implicit method related to the small step method. This seems to be the only numerical scheme for the computation of the tide which has a second order approximation in space and time with the horizontal and vertical friction terms included. Application of this scheme yielded several interesting results for the main parts of the World Ocean (Marchuk and Kagan, 1977)

§2. A system of equations for the study of the tides

The problem of tide prediction is usually studied by the linearized form of equations (1.44) - (1.46)

$$\frac{\partial U}{\partial t} - fV + g \frac{\partial \zeta}{\partial x} + \frac{\tau_b^{(x)}}{H+\zeta} - A\Delta U = K_x \quad (5.1)$$

$$\frac{\partial V}{\partial t} + fU + g \frac{\partial \zeta}{\partial y} + \frac{\tau_b^{(y)}}{H+\zeta} - A\Delta V = K_y \quad (5.2)$$

$$\frac{\partial \zeta}{\partial t} + \frac{\partial}{\partial x}(HU) + \frac{\partial}{\partial y}(HV) = 0 \quad (5.3)$$

On the right hand side of the equations of motion, K_x and K_y describe the components of the tide generating force. This set of equations, with proper boundary conditions, can be applied to solve the tidal problem in an adjacent sea of small horizontal dimensions when the curvature of Earth can be neglected. If, on the other hand, the dimensions of the basin are big, the above equations can be formulated in the spherical system of co-ordinates

$$\frac{\partial U}{\partial t} - fV + \frac{g}{R \cos \phi} \frac{\partial \zeta}{\partial \lambda} + \frac{\tau_b^{(\lambda)}}{H+\zeta} + G_\lambda = K_\lambda \quad (5.4)$$

$$\frac{\partial V}{\partial t} + fU + \frac{g}{R} \frac{\partial \zeta}{\partial \phi} + \frac{\tau_b^{(\phi)}}{H+\zeta} + G_\phi = K_\phi \quad (5.5)$$

$$\frac{\partial \zeta}{\partial t} + \frac{1}{R \cos \phi} \frac{\partial (HU)}{\partial \lambda} + \frac{\partial (HV \cos \phi)}{\partial \phi} = 0 \quad (5.6)$$

Here λ denotes the geographical longitude, ϕ the geographical latitude and R Earth's radius. The horizontal eddy viscosity terms are expressed in the following way

$$G_\lambda = -A\{\Delta U + R^{-2}[-U(1 + \tan^2 \phi) - 2\frac{\tan \phi \partial V}{\cos \phi \partial \lambda}]\} \quad (5.7)$$

$$G_\phi = -A\{\Delta V + R^{-2}[-V(1 + \tan^2 \phi) + 2\frac{\tan \phi \partial U}{\cos \phi \partial \lambda}]\} \quad (5.8)$$

The components of the tide generating force K_λ and K_ϕ are related to the tide potential θ (Lamb, 1945) as

$$K_\lambda = \frac{1}{R \cos \phi} \frac{\partial \theta}{\partial \lambda}; \quad K_\phi = \frac{1}{R} \frac{\partial \theta}{\partial \phi} \quad (5.9)$$

The tide potential for the M_2 constituent (moon semidiurnal) depends on latitude and longitude, and becomes negligibly small at high latitudes

$$\theta = \frac{C}{2}R \cos^2\phi \cos(\sigma t + 2\lambda) \quad (5.10)$$

where

$$C = 0.761 \times 10^{-7}, \quad \sigma = 1.405 \times 10^{-4} \text{ sec}^{-1}$$

The quasistatic response of the free surface of the ocean to (5.10) is equal to

$$\zeta_s = \frac{C}{2}R \cos^2\phi \cos(\sigma t + 2\lambda) \quad (5.11)$$

Therefore the tide potential is related to the surface elevation in the following way

$$\frac{1}{g}\theta = \zeta_s \quad (5.12)$$

The elevation of the free surface due to tidal forcing is evaluated with respect to the fixed sea bottom. However, when the bottom itself is in a state of motion due to the elastic yielding of the solid Earth, the sea-level will also change for the same reason. The motion of the sea bottom arises from (Hendershott, 1977; Kagan, 1977)

- A. The attraction of the solid Earth by the Moon or/and the Sun,
- B. The pressure of the water column above the sea bottom,
- c. The attraction between the ocean and the solid Earth.

All these reasons should be accounted for in a redefinition of the tidal forces responsible for tidal motion in the ocean. We shall dwell only upon point A which seems to be the most important.

The total tidal potential θ^* containing the tidal potential θ and the additional gravitational potential due to the elastic yielding of the solid Earth can be written as

$$\theta^* = (1 + k)\theta \quad (5.13)$$

The bottom displacement γ , in term of the free surface variation ζ , is equal to

$$\delta = h \zeta \quad (5.14)$$

In (5.13) and (5.14) k and k denote Love's numbers and are equal to 0.302 and 0.612 respectively.

The total sea-level elevation ζ_0 should contain the sea-level variations relative to the bottom ζ and the bottom displacement δ . Such an approach causes a redefinition of all terms in the equations of motion and continuity which contain the sea-level. For example in equation (5.5) the pressure term $\frac{g\partial\zeta}{R\partial\phi}$ should be changed, in terms of the total sea-level ζ_0 , to $\frac{g}{R} \frac{\partial\zeta_0}{\partial\phi}$.

Since tide gauges record the value of ζ the expression is usually written in the form

$$\frac{g}{R} \frac{\partial\zeta_0}{\partial\phi} = \frac{g}{R} \left(\frac{\partial\zeta}{\partial\phi} + \frac{\partial\delta}{\partial\phi} \right) \quad (5.15)$$

If the solid Earth's tide is static in character, $\frac{\partial\delta}{\partial\phi}$ is related in a straightforward manner to the gravitational Earth potential by (5.14) and (5.12).

Therefore, leaving the left hand side of (5.4) and (5.5) unchanged, we introduce the factor $\gamma = 1 + k - h$ to account for the additional term due to ζ_0 and δ , and rewrite the expressions for the tidal force as

$$K_\lambda = \frac{\gamma}{R} \frac{\partial\theta}{\cos\phi\partial\lambda} \quad \text{and} \quad K_\phi = \frac{\gamma}{R} \frac{\partial\theta}{\partial\phi} \quad (5.16)$$

This result is easily obtained by introducing a) the total sea-level ζ_0 into (5.4) and (5.5) instead of ζ and b) the total potential θ^* instead of θ . Observe also that from (5.15) we find

$$\frac{\partial\zeta}{\partial\phi} = \frac{\partial\zeta_0}{\partial\phi} - \frac{\partial\delta}{\partial\phi} = \frac{1}{g} \frac{\partial\theta^*}{\partial\phi} - \frac{h}{g} \frac{\partial\theta}{\partial\phi} = \frac{(1 + k - h)}{g} \frac{\partial\theta}{\partial\phi} \quad (5.17)$$

It is evident that the system (5.4) - (5.6) can be integrated only in an area which excludes the Earth's pole (since there $\cos\phi = 0$). For hydrodynamic problems in polar regions it is necessary to write a new system of equations, the solution to which is unique in the polar region. To this end a stereographic projection can be applied. The projection is obtained by setting a plane Q (Fig. 41), which passes through the parallel of latitude ϕ_0 (usually $\phi_0 = 60^\circ$). That part of the spherical sheet above the latitude ϕ_0 is projected onto the surface Q. The new system of equations is written in the plane Q. Its form is similar to the one derived in the Cartesian system of co-ordinates with the scale factor m (see e.g. Kowalik and Nguyen Bich Hung, 1977):

$$\frac{\partial U}{\partial t} - fV + mg\frac{\partial \zeta}{\partial x} + \frac{\tau_b(x)}{H+\zeta} - m^2 A \Delta U = K'_x \quad (5.18)$$

$$\frac{\partial V}{\partial t} + fU + mg\frac{\partial \zeta}{\partial y} + \frac{\tau_b(y)}{H+\zeta} - m^2 A \Delta U = K'_y \quad (5.19)$$

$$\frac{\partial \zeta}{\partial t} + m\frac{\partial (HU)}{\partial x} + m\frac{\partial (HV)}{\partial y} = 0 \quad (5.20)$$

The new system of co-ordinates (x,y) has its origin at the north pole. The x-axis is directed along 0° longitude and y runs along 90° longitude.

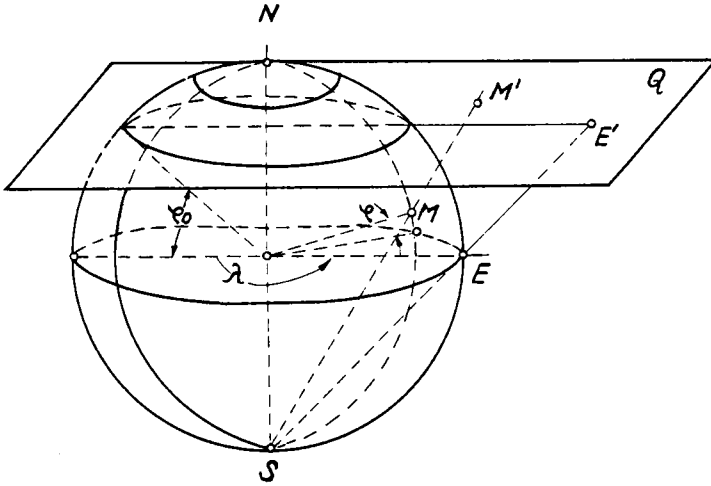


Fig. 41. STEREOGRAPHIC PROJECTION

The scale factor m for a map projection relates a surface area on the stereographic map to its image on a unit sphere

$$m = \frac{\Delta S(\text{map})}{\Delta S(\text{sphere})} = \frac{1 + \sin \phi_0}{1 + \sin \phi} \quad (5.21)$$

ϕ_0 is usually the 60° latitude and thus the magnitude of m in the polar regions is close to unity.

To obtain a unique solution to the above system of equations we shall specify, later on, the proper set of initial and boundary conditions. In deriving these conditions we shall follow the line presented in chapter IV, §8.

§3. The boundary-value problem

As we know already a solution to the tide problem in an adjacent sea can be sought using two different methods. On the one hand, it may be solved as an initial-value problem with prescribed boundary conditions on each time step. The numerical integration proceeds until a stationary oscillatory motion occurs in the domain of integration. On the other hand, since the phenomenon being considered is of an oscillatory character in time, one may assume that the dependent variables change with time in the following manner

$$\begin{aligned} U &= \bar{U}e^{-i\omega t} \\ V &= \bar{V}e^{-i\omega t} \\ \zeta &= \bar{\zeta}e^{-i\omega t} \end{aligned} \quad (5.22)$$

In the primary set of equations (5.1) - (5.3) we shall introduce certain simplifications. Firstly the bottom friction term is taken in the linear form (1.63). Secondly the lateral exchange of momentum is assumed to be negligible. The latter assumption, though generally true, is somewhat artificial in coastal zones, where big horizontal differences in the current velocity are present. The simplification is also motivated by the desire to obtain a final equation (5.27) of the elliptical type; if the Laplacian operator is left in equations (5.1) and (5.2), the final equation for the sea-level will be of the bi-harmonic type.

From now on we shall assume that the dependent variables \bar{U} , \bar{V} and $\bar{\zeta}$ are complex functions of x and y . Introducing (5.22) into the system (5.1) - (5.3) a new set of equations without the time variable is obtained

$$-i\omega\bar{U} - f\bar{V} = -g\frac{\partial\bar{\zeta}}{\partial x} - R_1\bar{U} \quad (5.23)$$

$$-i\omega\bar{V} + \bar{U}f = -g\frac{\partial\bar{\zeta}}{\partial y} - R_1\bar{V} \quad (5.24)$$

$$-i\omega\bar{\zeta} + \frac{\partial(H\bar{U})}{\partial x} + \frac{\partial(H\bar{V})}{\partial y} = 0 \quad (5.25)$$

where $R_1 = R/(H+\zeta)$.

Introducing \bar{U} and \bar{V} from the first and second equation into the third one, the equation which describes the sea-level $\bar{\zeta}$ is obtained. To explore such a possibility we compute the determinant on the basis of (5.23) and (5.24)

$$\begin{vmatrix} R_1 - i\omega & -f \\ f & R_1 - i\omega \end{vmatrix} = (R_1 - i\omega)^2 + f^2 = \overset{*}{\Delta} \quad (5.26)$$

In case (5.26) is equal to zero the transformation proposed above is impossible. It is clear that in a sufficiently deep sea $R_1 = \frac{R}{H+\zeta} \rightarrow 0$, and, if $\omega^2 = f^2$, the determinant $\overset{*}{\Delta}$ is equal to zero. This happens where the period of oscillation is equal to the pendulum period $\frac{2\pi}{f}$, i.e. on the so-called 'critical latitude'. For the M_2 -tide the 'critical latitude' is $74^\circ 30'$. From the above discussion the conclusion may be drawn that the proposed method is erroneous in the vicinity of the 'critical latitude'. Hence, to improve the situation at the 'critical latitude' the term describing the lateral exchange of momentum must be introduced into the set of equations.

The problem of the 'critical latitude' does not appear at all when the solution is derived by an analytical method (Stretensky, 1947; Racer-Ivanova, 1956). Two solutions are initially obtained, one valid for each side of the 'critical latitude'. These are then 'matched' together by ensuring that the continuity of the solution and its derivatives is satisfied at the 'critical latitude'.

Let us now return to the transformation proposed above. We shall apply it only outside the region of the 'critical latitude'. The final equation for sea-level oscillation then takes the form

$$-\Delta\zeta + \alpha \frac{\partial \zeta}{\partial x} + \beta \frac{\partial \zeta}{\partial y} + \gamma \zeta = 0 \quad (5.27)$$

(From now on we shall omit the bar over ζ),
where

$$\alpha = \frac{1}{H} \left[\frac{1}{(R_1 - i\omega)} \frac{\partial H}{\partial y} - \frac{\partial H}{\partial x} \right]$$

$$\beta = \frac{1}{H} \left[\frac{1}{(R_1 - i\omega)} \frac{\partial H}{\partial x} - \frac{\partial H}{\partial y} \right]$$

$$\gamma = \frac{i\omega}{gH} [(R_1 - i\omega)^2 + f^2] / (R_1 - i\omega)$$

The numerical solution to (5.27) was given by Hansen (1952) for the case where ζ is known on the whole boundary. If the boundary of an adjacent sea consists of Γ_1 part water and Γ_2 part land, the amplitude will be prescribed only on Γ_1

$$\zeta \Big|_{\Gamma_1} = \psi(x, y) \quad (5.28)$$

On Γ_2 the perpendicular component of velocity is equal to zero. Applying (5.23) and (5.24) we obtain (see also chapter VIII, equation 8.9)

$$[(R_1 - i\omega) \frac{\partial \zeta}{\partial x} + f \frac{\partial \zeta}{\partial y}] \cos \alpha + [(R_1 - i\omega) \frac{\partial \zeta}{\partial y} - f \frac{\partial \zeta}{\partial x}] \cos \beta = 0 \quad (5.29)$$

Here α and β are the angles between the direction perpendicular to the coast and the x- and y-axis respectively. Representing ζ as a sum of real ζ_r and imaginary ζ_i parts, we find two elliptic equations

$$-\Delta \zeta_r + a \frac{\partial \zeta_r}{\partial x} + b \frac{\partial \zeta_r}{\partial y} + c \zeta_r = F_1 \quad (5.30a)$$

$$-\Delta \zeta_i + a \frac{\partial \zeta_i}{\partial x} + b \frac{\partial \zeta_i}{\partial y} + c \zeta_i = F_2 \quad (5.30b)$$

with the pertinent boundary conditions

$$\zeta_r = \psi_r \quad (5.31a)$$

$$\zeta_i = \psi_i \quad (5.31b)$$

on Γ_1 , and on Γ_2

$$\left[\frac{\partial \zeta_r}{\partial x} + d \frac{\partial \zeta_r}{\partial y} \right] \cos \alpha + \left[\frac{\partial \zeta_r}{\partial y} - d \frac{\partial \zeta_r}{\partial x} \right] \cos \beta = d_1 \cos \alpha \frac{\partial \zeta_i}{\partial y} - d_1 \cos \beta \frac{\partial \zeta_i}{\partial x} \quad (5.32a)$$

$$\left[\frac{\partial \zeta_i}{\partial x} + d \frac{\partial \zeta_i}{\partial y} \right] \cos \alpha + \left[\frac{\partial \zeta_i}{\partial y} + d \frac{\partial \zeta_i}{\partial x} \right] \cos \beta = d_1 \cos \alpha \frac{\partial \zeta_r}{\partial x} + d_1 \cos \beta \frac{\partial \zeta_r}{\partial y} \quad (5.32b)$$

where

$$a = -\frac{1}{H} \left(\frac{\partial H}{\partial x} - \frac{fR_1}{R_1^2 - \omega^2} \frac{\partial H}{\partial y} \right)$$

$$b = -\frac{1}{H} \left(\frac{\partial H}{\partial y} + \frac{fR_1}{R_1^2 + \omega^2} \frac{\partial H}{\partial x} \right)$$

$$c = -\frac{\omega^2}{gH} (R_1^2 + f^2 + \omega^2) / (\omega^2 + R_1^2)$$

$$F(\zeta_i) = \frac{\omega}{H} (R_1^2 + \omega^2)^{-1} \left[f \left(\frac{\partial H \partial \zeta_i}{\partial x \partial y} - \frac{\partial H \partial \zeta_i}{\partial y \partial x} \right) + \frac{R_1}{g} (f^2 + R_1^2 + \omega^2) \right]$$

$$d = \frac{Rf}{R^2 + \omega^2}; \quad d_1 = \frac{\omega f}{R^2 + \omega^2}$$

To obtain $F(\zeta_r)$ in the above equation replace ζ_i with ζ_r .

The solution of the system (5.30) with boundary conditions (5.31) and (5.32) can be derived for natural basins by the numerical method only.

Because ζ_r in (5.30a) is dependent on ζ_i and the reverse situation occurs in (5.30b), both equations should be solved at the same time. This reminds us somewhat of the situation in the implicit set of equations (4.172) and (4.173). Therefore, we introduce a) a finite-difference grid with space step h and b) an iterative index n and c) the elliptical operator (5.30) L . We may state the following

$$L_h \zeta_r^{n+1} = F_1(\zeta_i^n) \quad (5.33a)$$

$$L_h \zeta_i^{n+1} = F_2(\zeta_r^n) \quad (5.33b)$$

Applying an iterative procedure to (5.33) consisting of successive approximations with a suitable convergence condition (Ch. II, §5), a solution to the system (5.30) can be derived.

In case the boundary conditions are given in terms of velocities it is possible to solve the above problem through the elimination of sea-level from the equations (5.23) - (5.25). The final set of steady state equations for the U and V components can again be solved by the iteration method.

§4. The hydrodynamic-numerical method

Integrating in time the set of nonlinear tide equations by means of the numerical method using the harmonic boundary condition has already found widespread application. The works of Hansen (1956) and others gradually disclosed the manifold problems, either related to numerical stability and convergence or to various hydrodynamic aspects such as the rôle of vertical and horizontal friction.

Frequently a numerical analogue of the differential equations, which was applied by Hansen, is formulated on the staggered grid shown in fig. 34. There U , V and ζ are calculated on different grid

points. An explicit numerical scheme defined on this grid was discussed extensively in chapter IV, §9. Therefore we shall not dwell upon such a numerical approach here.

Instead, let us consider a numerical grid as plotted in fig. 33. There, both velocity components are calculated on the same grid point but the sea-level is set apart. The aim of using different numerical grids is clear enough. They enable us to arrive at a better approximation of the equations and at the same time they can ease the formulation of boundary conditions, which, as we know from chapter IV, §8, are not a well-posed problem in the numerical formulation.

The grid in fig. 33 has been applied by Lauwerier and Damsté (1963) and subsequently by Heaps (1969, 1972) in the study of tides and storm surges.

We prescribe the following numerical analogue of the continuous system (5.1) - (5.3)

$$\frac{U_{j,k}^{l+1} - U_{j,k}^{l-1}}{2T} - fV_{j,k}^{l-1} = -\frac{g}{2} \frac{\zeta_{j+1,k+1}^l + \zeta_{j+1,k-1}^l - \zeta_{j-1,k+1}^l - \zeta_{j-1,k-1}^l}{2h}$$

$$- R_1^{l-1} U_{j,k}^{l-1} + \frac{A}{4h^2} (U_{j+2,k}^{l-1} + U_{j-2,k}^{l-1} + U_{j,k+2}^{l-1} + U_{j,k-2}^{l-1} - 4U_{j,k}^{l-1}) \quad (5.34a)$$

$$\frac{V_{j,k}^{l+1} - V_{j,k}^{l-1}}{2T} + fU_{j,k}^{l-1} = -\frac{g}{2} \frac{\zeta_{j+1,k+1}^l + \zeta_{j-1,k+1}^l - \zeta_{j+1,k-1}^l - \zeta_{j-1,k-1}^l}{2h}$$

$$- R_1^{l-1} V_{j,k}^{l-1} + \frac{A}{4h^2} (V_{j+2,k}^{l-1} + V_{j-2,k}^{l-1} + V_{j,k+2}^{l-1} + V_{j,k-2}^{l-1} - 4V_{j,k}^{l-1}) \quad (5.34b)$$

$$\frac{\zeta_{j-1,k-1}^{l+2} - \zeta_{j-1,k-1}^l}{2T} = -\frac{1}{4h} [(HU^{l+1})_{j,k} + (HU^{l+1})_{j,k-2} - (HU^{l+1})_{j-2,k}$$

$$- (HU^{l+1})_{j-2,k-2}] - \frac{1}{4h} [(HV^{l+1})_{j,k} + (HV^{l+1})_{j-2,k} - (HV^{l+1})_{j-2,k-2}$$

$$- (HV^{l+1})_{j,k-2}] \quad (5.34c)$$

The stability properties of the system (5.34) can be checked by taking all dependent variables in the form (4.17). The resulting set of equations for the amplitudes U^* , V^* , ζ^* is of homogeneous form

$$\begin{aligned}
 U^* (\lambda^2 - 1) - 2TfV^* + \frac{g_i T \lambda}{h} \zeta^* \cos \sigma_2 h \sin \sigma_1 h + R_1 2TU^* \\
 + V^* A \frac{2T}{h^2} (\sin^2 \sigma_1 h + \sin^2 \sigma_2 h) = 0
 \end{aligned} \tag{5.35a}$$

$$\begin{aligned}
 V^* (\lambda^2 - 1) + 2TfU^* + \frac{g_i T \lambda}{h} \zeta^* \sin \sigma_2 h \cos \sigma_1 h + R_1 2TV^* \\
 + V^* A \frac{2T}{h^2} (\sin^2 \sigma_1 h + \sin^2 \sigma_2 h) = 0
 \end{aligned} \tag{5.35b}$$

$$(\lambda^2 - 1) \zeta^* + \frac{T}{h} \lambda i H U^* \cdot \sin \sigma_1 h \cdot \cos \sigma_2 h + \frac{T}{h} \lambda i H V^* \cdot \sin \sigma_2 h \cdot \cos \sigma_1 h = 0 \tag{5.35c}$$

Therefore its solution is possible if the determinant of (5.35) is equal to zero. This condition leads to a characteristic equation for the parameter λ , which is of order of six

$$(\lambda^{2-1+a})^2 (\lambda^2 - 1) + \lambda^2 \alpha^2 (\lambda^{2-1+a}) + (\lambda^2 - 1) \beta^2 = 0 \tag{5.36}$$

where

$$a = 2R_1 T + \frac{2AT}{h^2} (\sin^2 \sigma_1 h + \sin^2 \sigma_2 h)$$

$$\alpha^2 = \frac{gHT^2}{h^2} (\sin^2 \sigma_1 h \cos^2 \sigma_2 h + \sin^2 \sigma_2 h \cos^2 \sigma_1 h)$$

$$\beta^2 = (2fT)^2$$

$$R_1 = \frac{R}{H + \zeta}$$

By changing, in (5.36), λ^2 to δ , a third order equation is obtained and in this way the method presented in chapter IV, equation (4.193), may be applied to study the properties of the roots of (5.36). The general solution is quite complicated. Essentially it involves certain restrictions on the magnitude of the coefficients in (5.36) through the inequalities (4.196).

Let us proceed by assuming an extremely simplified case of wave propagation in a frictionless medium with vanishing Coriolis force. The roots of the characteristic equation (5.36) are

$$\lambda_0 = 1 \quad \text{and} \quad \lambda_{1,2} = \frac{1}{2} (2 - p \pm \sqrt{p(p-2)}) \tag{5.37}$$

The value of (5.37) will lie within the unit circle in the complex plane

$$p < 2; \quad \alpha^2 \frac{gT^2}{h} < 2 \quad (5.38)$$

This is the basic condition which appears in all stability analyses of the explicit numerical scheme in chapter IV.

One may essentially improve the order of approximation of the Coriolis and bottom friction terms in system (5.34) by expressing the velocity as a sum over two time steps $\frac{1}{2}(V^{1+1} + V^{1-1})$ and $\frac{1}{2}(U^{1+1} + U^{1-1})$. Then the equations of motion (5.34a) and (5.34b) can be written in the following manner

$$U_{j,k}^{1+1}(1 + RT) - fTV_{j,k}^{1+1} = p^1 \quad (5.39)$$

$$V_{j,k}^{1+1}(1+RT) + fTU_{j,k}^{1+1} = Q^1$$

where

$$p^1 = ftV_{j,k}^{1-1} + TRU_{j,k}^{1-1} - \frac{gT}{2h}(\zeta_{j+1,k+1}^1 + \zeta_{j+1,k-1}^1 - \zeta_{j-1,k+1}^1 - \zeta_{j-1,k-1}^1) \\ + \frac{A}{4h^2}(U_{j+2,k}^{1-1} + U_{j-2,k}^{1-1} + U_{j,k+2}^{1-1} + U_{j,k-2}^{1-1} - 4U_{j,k}^{1-1})$$

$$Q^1 = -fTU_{j,k}^{1-1} + TRV_{j,k}^{1-1} - \frac{gT}{2h}(\zeta_{j+1,k+1}^1 + \zeta_{j-1,k+1}^1 - \zeta_{j+1,k-1}^1 - \zeta_{j-1,k-1}^1) \\ + \frac{A}{4h^2}(V_{j+2,k}^{1-1} + V_{j-2,k}^{1-1} + V_{j,k+2}^{1-1} + V_{j,k-2}^{1-1} - 4V_{j,k}^{1-1})$$

Solving the system (5.39) for the unknowns $U_{j,k}^{1+1}$ and $V_{j,k}^{1+1}$ yields

$$U_{j,k}^{1+1} = [p^1(1+RT) + fTQ^1]/[(1+RT)^2 + (fT)^2] \quad (5.40a)$$

$$V_{j,k}^{1+1} = [Q^1(1+RT) - fTp^1]/[(1+RT)^2 + (fT)^2] \quad (5.40b)$$

These expressions together with (5.34c) complete the system for calculating the velocities and the sea-level.

§5. Calculating the M_2 -tide in the Arctic Ocean - an example

In this paragraph we shall mainly follow the results presented by Kowalik and Untersteiner (1978). Our aim is to consider point by point as many questions as possible which are pertinent to the tide computation. When studying tidal motion in a system of spherical co-ordinates the difficulty arises in the proximity of the pole. Although an analytical solution can be constructed in such a region, a numerical solution is rather cumbersome and therefore we turn to the stereographic system of co-ordinates and apply the system (5.18) - (5.20).

To derive a unique solution of this system in the domain of integration, it is sufficient to set everywhere on the boundary the values of the normal and tangential mass transport equal to zero, as was proved by Marchuk et al. (1972).

Initially the dependent variables are taken as zero in the domain \bar{D}

$$\zeta(x,y,t=0) = U(x,y,t=0) = V(x,y,t=0) = 0 \quad (5.41)$$

In an adjacent sea connected to the ocean the boundary condition can be easily stated on an impermeable coast (Γ_c) due to the nonslip condition. But on the open boundary (Γ_o) usually only a sea-level distribution is known. With these boundary conditions, by virtue of the result derived by Marchuk et al. (1972), the solution to the above set of equations cannot be found. Therefore the numerical solution shall be constructed as follows. On the boundary between an adjacent sea and the ocean the hyperbolic problem (with the horizontal friction neglected, i.e. $\Delta U = 0$, $\Delta V = 0$) is solved, and the velocity distribution is found. With these data a new boundary is formed and the full system (the lateral friction included) of equations can be solved in the whole domain \bar{D} .

Such an approach is quite appropriate since the uniqueness of the solution to a hyperbolic problem is guaranteed when the sea-level is given as boundary condition (Ch. IV, §8). With the above restriction in mind, the boundary conditions pertinent to the system (5.18) - (5.20) can be stated as

$$U = V = 0 \quad \text{on } \Gamma_c \quad (5.42a)$$

and

$$\zeta = \zeta(t) \quad \text{on } \Gamma_o \quad (5.42b)$$

In addition conservation of mass is assumed in the domain \bar{D} . This property will be checked by an integral taken over the tidal period T_p and along the open boundary Γ_o

$$\int_0^{T_p} \int_0^L (UH\cos\alpha + VH\sin\alpha) ds dt \quad (5.43)$$

Here, α denotes an angle between the perpendicular direction to the boundary Γ_o and the x-axis; L is the length of Γ_o .

To derive a numerical solution to system (5.18) - (5.20) with the boundary conditions (5.42) the staggered space grid, as presented in fig. 34, is introduced and applied to the Arctic with a mesh size $h = 75$ km and time step $T = 62.1$ sec.

Before applying the proper numerical form to the basic equations it is worth noticing that each numerical scheme, due to the finite values of time and space steps, is distorting the physical parameters of the computed wave. The wave distortion by a numerical scheme may be estimated only in rather simple numerical schemes as was shown by Leendertse (see chapter IV, §4). To avoid the problem (at least partly) we solved the tidal problem by two different numerical methods with different approximations and, by comparing the results, we intended to find a possible source of error.

Firstly, the explicit numerical scheme analogous to the one discussed in chapter IV, §9, equations (4.128) - (4.130), is applied. The only difference which arose was due to the presence of the scale factor m in the system (5.18) - (5.20).

In the numerical system (4.128) - (4.130) the overall approximation in space and time is only of first order. This is clearly seen from the time index, that is to say on the right hand side of equation (4.128) where the horizontal friction term is set at the point in time $l-1$ and the sea surface slope at time l . Since the step sizes h and T possess finite magnitudes, the first order of approximation leads to numerical friction which is analogous to the horizontal friction in the equations. In the case of an unsuitable choice of grid size, this can cause wave distortion.

The stability of the above numerical scheme could be, of course, studied by the von Neumann method, but there is no need for that, because we may easily implement the results obtained in chapter IV, §9 and by Kowalik and Nguyen Bich Hung (1977). Under quite general conditions the time and space steps are related by the following stability criterion

$$T \leq h/\sqrt{2gH}m \quad (5.44)$$

If the friction and Coriolis forces play an important rôle, the formulation of a more general criterion is difficult. However, in the case of the shortest waves on the net, whose wave length is equal to double the space step and where instabilities usually start, by analogy with (4.151) we may write

$$T \leq 1/(R + \frac{2m^2A^2}{h^2}) \quad (5.45)$$

We shall not dwell upon the stability problems too long but it seems important to stress that the criteria which result from the application of the von Neumann method do not take into account the boundary conditions and nonlinear properties of the differential equations. Therefore inequalities (5.44) and (5.45) are only guidelines for establishing the magnitudes of the space and time step in order to preserve the stability of the numerical computation.

Now we shall turn to the second numerical scheme which was applied in computing the tides in the Arctic. The scheme presented in chapter IV, §12 will be used. It possesses a second-order approximation in space and time, and has mixed explicit-implicit properties.

To derive a unique solution of both numerical systems we adjoin the boundary conditions (5.42). Condition (5.42b) is prescribed on the open boundary between Northern Norway and Central Greenland. The complete set of data on the open boundary was established mainly on the basis of Nekrasov's work (1975)

$$\zeta_{j,k}^1 = H_{j,k} \cos(\sigma t - g_{j,k}^0) \quad (5.46)$$

where

$H_{j,k}$ and $g_{j,k}^0$ denote harmonic constants of the M_2 -constituent taken on the grid points situated at the open boundary

σ denotes the angular velocity of the M_2 -constituent, equal to $1.405 \times 10^{-4} \text{ sec}^{-1}$.

The computed results are presented in the next section. We shall not present individual results for the two methods, because they agree in amplitude to within a few millimeters; the greatest phase error was equal to 9° . From the comparison of the two methods with different degrees of approximation we may infer that wave deformation due to the numerical scheme is rather small.

§6. The results of the computation of the tides in the Arctic Ocean

The aim of this paragraph, though it is confined to the Arctic tide, is to accustom the reader to the variety of problems which arise and which can be clarified by relating the computed tide to local conditions.

The Arctic Ocean consists of a very deep basin ($H_{\max} = 5.1$ km) with a strong variation of bathymetry and the greatest shelf in the World Oceans. Therefore both, bottom and horizontal friction, play an important rôle. This concerns in a particular way the horizontal friction due to the presence of the critical latitude. In the course of different numerical experiments it was found that the stable picture of a tide wave appears with $A = 5 \times 10^8$ up to 10^9 cm²/sec.

The Arctic Ocean is almost permanently and completely covered by a layer of ice. Due to friction there exists a loss of energy against this layer, but it should be stressed that the ice cover does not effect the amplitude of a very long wave, as was shown by Kagan (1968).

When comparing the numerical results with gauge measurements one has to understand that many phenomena in relation to the tides, especially those in the coastal region, cannot be properly resolved, since the grid we use is unable to represent such features which belong to the subgrid scale.

To our understanding one of the most important phenomena, not included in the basic set of equations (5.1) - (5.3), is the density stratification. It not only influences the tides but also makes it possible for internal waves to be generated, thus causing a transfer of energy from tides to internal tides.

The results of computations for the Arctic Ocean in the form of co-tidal and co-range lines, obtained by the numerical schemes mentioned above, are plotted in figs. 42 and 43. The phase is referred to Greenwich and is expressed in degrees.

Since the amplitude of the equilibrium M_2 -tide is negligible in the Arctic Ocean, we may draw the conclusion from the above figures that the tide in question is the co-oscillating tide of the Atlantic Ocean.

The M_2 -wave penetrates the Arctic Ocean mainly through the Greenland Sea. It propagates and slowly decreases from around 40 cm at Spitzbergen down to 2 - 3 cm at the extremities of the East-Siberian and Chukchi Sea. At the same time, the tidal wave due to the rotation of the Earth undergoes certain modifications; the motion is no longer alternating but rotating. The set of co-tidal lines plotted in fig.42 show the rotation around the amphidromic point ($\phi = 81^{\circ}30'N$, $\lambda = 133^{\circ}W$), off the coast of Canada. This picture is typical for a standing Kelvin

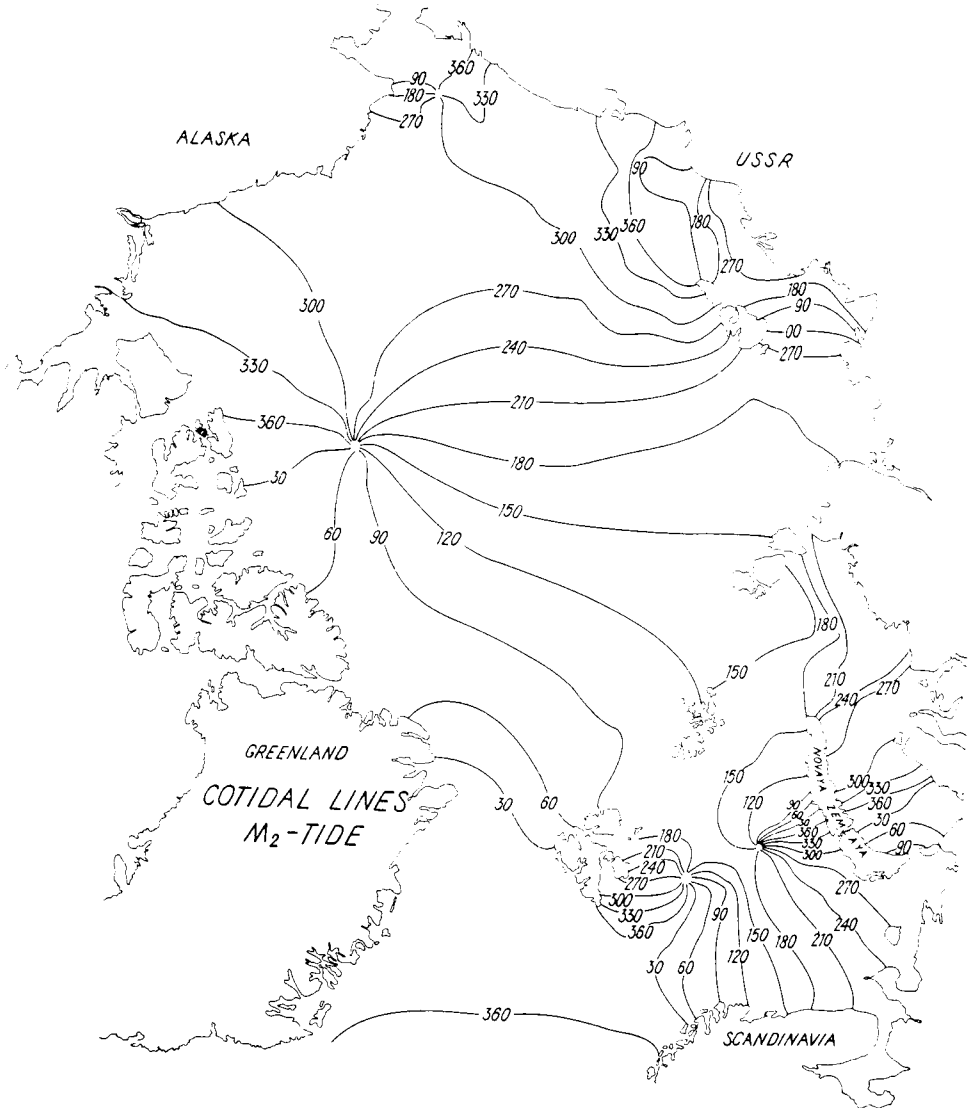


Fig. 42. CO-TIDAL LINES OF THE M_2 -TIDE IN THE ARCTIC OCEAN. PHASE ANGLES IN DEGREES ARE REFERRED TO GREENWICH (SOLAR TIME).

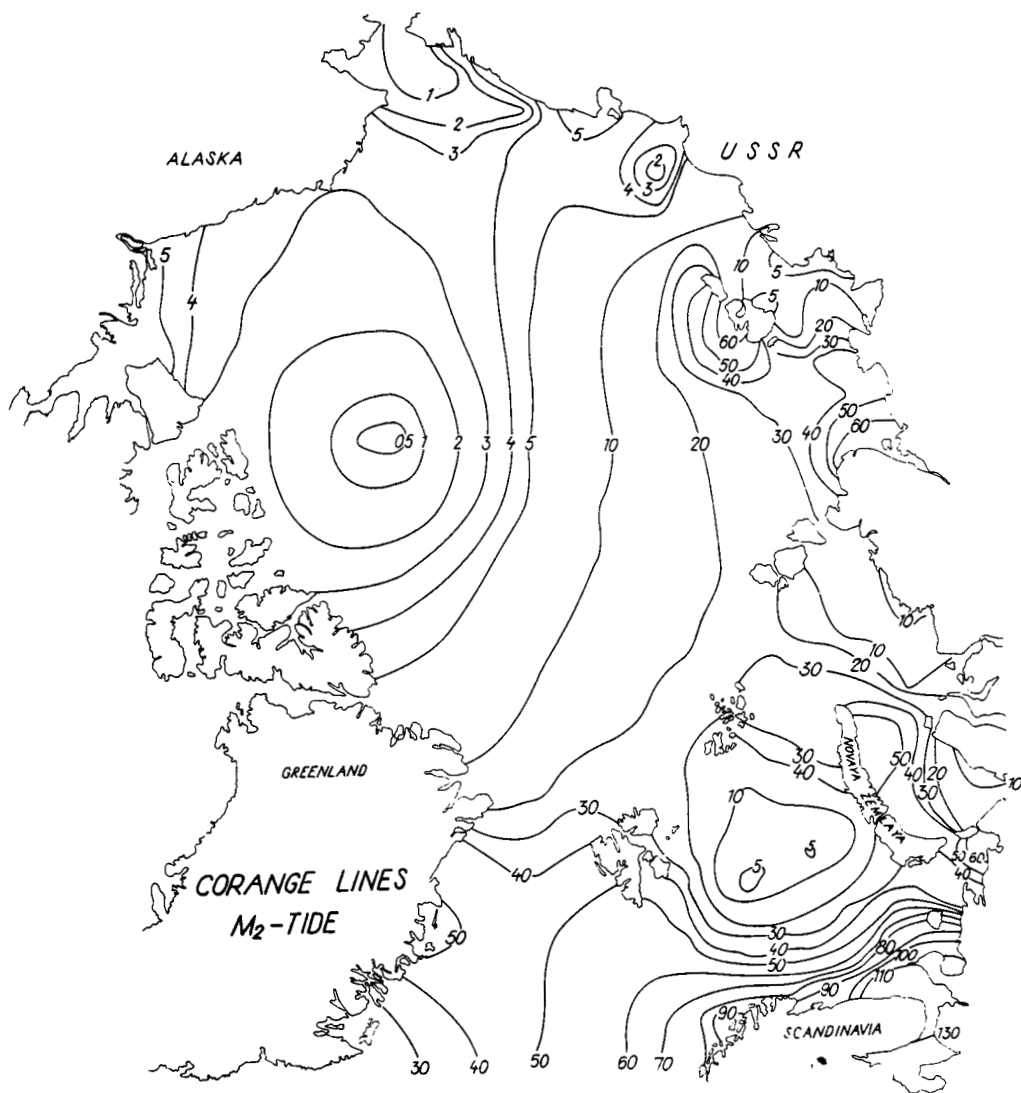


Fig. 43. CO-RANGE LINES OF THE M_2 -TIDE IN THE ARCTIC OCEAN, AMPLITUDES IN CM.

wave resulting from the superposition of an incident and reflected wave in a semi-enclosed channel - the way it was deduced by Taylor (1921). The general character of the M_2 -wave, if compared with the map of co-tidal lines from the Oceanographic Atlas (1958) and with Zahel's map (1977), is reproduced properly. However, one has to understand that the co-tidal lines plotted in the Oceanographic Atlas are to a large extent hypothetical, especially in the open waters. Due to the extreme difficulty in the development and maintenance of tide gauges in the polar seas, even today, the distribution of the amplitude and phase of the tide in these regions is still obscure.

When approaching the shelf zone of Siberia the co-tidal lines become parallel to the depth contour, as can be inferred from fig. 44. Instead of one-dimensional motion along the line of propagation, rotary motion is observed to the East of the North Siberian Islands. This type of motion was explained by Sverdrup (1926) through the introduction of waves on an unlimited rotating disc.

The wave which turns to the Siberian Shelf is obviously dissipated there to a large extent. It becomes clear by inspection of the wave amplitude (Fig. 43) on the shelf and in the coastal region; for example the amplitude is of the order of 10 - 15 cm at the entrance to the shelf and slowly decreases to 2 - 3 cm at the extremities of Siberia.

The other M_2 -tide entering the Polar Seas from the Atlantic Ocean between Spitzbergen and Norway produces the high tide in the southern part of the Barents Sea and in the White Sea, decreasing slowly in the direction of Novaya Zemlya. We were unable to reproduce the White Sea area exactly with our net. Therefore the tides in the western part of the Barents Sea and around Novaya Zemlya are somewhat distorted, as may be seen in table 5.1.

Nevertheless, these tides die out on the shelf around the Islands of Novaya Zemlya and they do not influence the general picture in the Arctic Ocean. This conclusion is inferred from the following two numerical experiments. In the first experiment the White Sea was closed and at the southern part of Novaya Zemlya the amplitude rose up to 2 m. The second computation with the White Sea present is shown in fig. 42 and fig. 43. It shows that the phase and amplitude off the shelf area in the proper Arctic Ocean remain unchanged in both experiments.

Below, we compare the data derived from the numerical computations with gauge observations published by the International Hydrographic Bureau in Monaco.

TABLE 5.1

Comparison of the data derived from the numerical computations with gauge observations published by the International Hydrographic Bureau at Monaco

<u>Location</u> $\phi =$, $\lambda =$	<u>Amplitude (cm)</u>		<u>Phase (deg.)</u>	
	observed	calculated	observed	calculated
Spitzbergen				
78°58'N, 12°06'E	49.9	48	26°	22°
80°00'N, 16°52'E	27.9	29	93,2°	70°
79°43'N, 10°52'E	41.5	41	45°	43°
Greenland				
82°11'N, 30°30'W	10.6	12	356°	20°
76°46'N, 18°46'W	50.8	53	307°	10°
83°40'N, 33°35'W	4.2	5	307°	50°
Norway (Tromsø)				
69°38.8'N, 18°52'E	87.6	84	39°	10°
SSSR				
69°55'N, 32°02'E	99.1	97	151°	145°
69°05'N, 36°18'E	130.8	125	220°	190°
Novaya Zemlya				
76°16'N, 63°03'E	15.2	30	283°	140°
Ayon Island				
69°52'N, 167°43'E	1.8	4	347°	340°
T-3 Island				
71°55'N, 160°20'W	4.5	3.3	311°	300°
Point Barrow				
71°18'N, 156°40'W	4.5	3.1	313°	305°

The set of equations (5.18) - (5.20) also presents the possibility of studying the velocity distribution of the M_2 -tide. The flow changes periodically with the tide, rotating slowly through an ellipse. The velocities along the major and minor axes of the ellipse are plotted in fig. 44. The major axis is usually parallel to the direction of

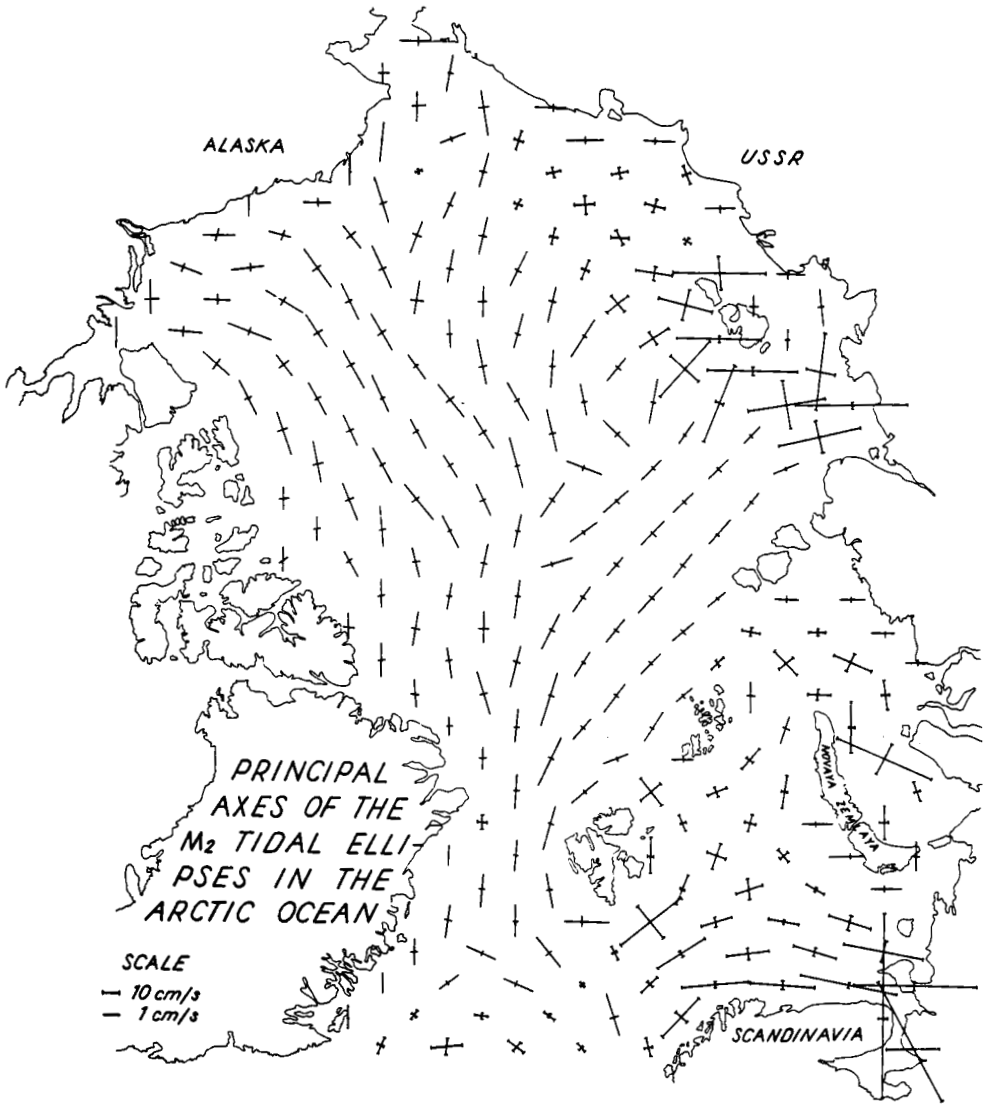


Fig. 44. PRINCIPAL AXES OF THE M_2 TIDAL ELLIPSES IN THE ARCTIC OCEAN.

propagation of the tidal wave in the basin. The greatest velocities are associated with the shelf areas of the Barents Sea and around the New Siberian Islands. The motion in the deep portion of the Arctic Ocean, when compared with the Norwegian and Chukchi Sea, is not only dampened out but also changes its character from alternating to rotating. Although we did not present the directions of rotation in fig.44, the feature is very valuable, because it helps to identify the type of wave.

Propagation over a long path without reflection is usually accompanied by a uniform direction of rotation; on the other hand, the reflected wave, when it couples with an incident wave, provides a very complicated pattern of rotation. In general, the properties of an ellipse can be expressed through the components U and V (e.g. Hansen, 1952). Defining U and V as

$$U = U_1 \cos \omega t + U_2 \sin \omega t \quad (5.47a)$$

$$V = V_1 \cos \omega t + V_2 \sin \omega t \quad (5.47b)$$

the length of the major and minor axes is equal to

$$A = \frac{1}{\sqrt{2}} \sqrt{U_1^2 + U_2^2 + V_1^2 + V_2^2 + \sqrt{(U_1^2 + U_2^2 + V_1^2 + V_2^2)^2 - 4(U_1 V_2 - U_2 V_1)}} \quad (5.48a)$$

$$B = \frac{1}{\sqrt{2}} \sqrt{U_1^2 + U_2^2 + V_1^2 + V_2^2 - \sqrt{(U_1^2 + U_2^2 + V_1^2 + V_2^2)^2 - 4(U_1 V_2 - U_2 V_1)}} \quad (5.48b)$$

The direction of rotation is defined by the sign of the magnitude $U_1 V_2 - U_2 V_1$. The positive sign indicates an anti-clockwise rotation. Likewise the negative sign is due to clockwise rotation. Zero means an absence of rotation of flow.

Since the Arctic Ocean is covered by ice, it is of interest to consider the possible action of tidal current on it. If a continuous and stationary ice cover occurs it is reasonable to assume that the tidal current does not affect the ice very much. If, on the other hand, the ice cover consists of ice floes one may suppose that due to the tidal current periodic variations in the ice distribution and compactness may occur. The study of such an action by the tides will be performed with the help of

$$\text{div } \vec{U} = \frac{\partial U}{\partial x} + \frac{\partial V}{\partial y}$$

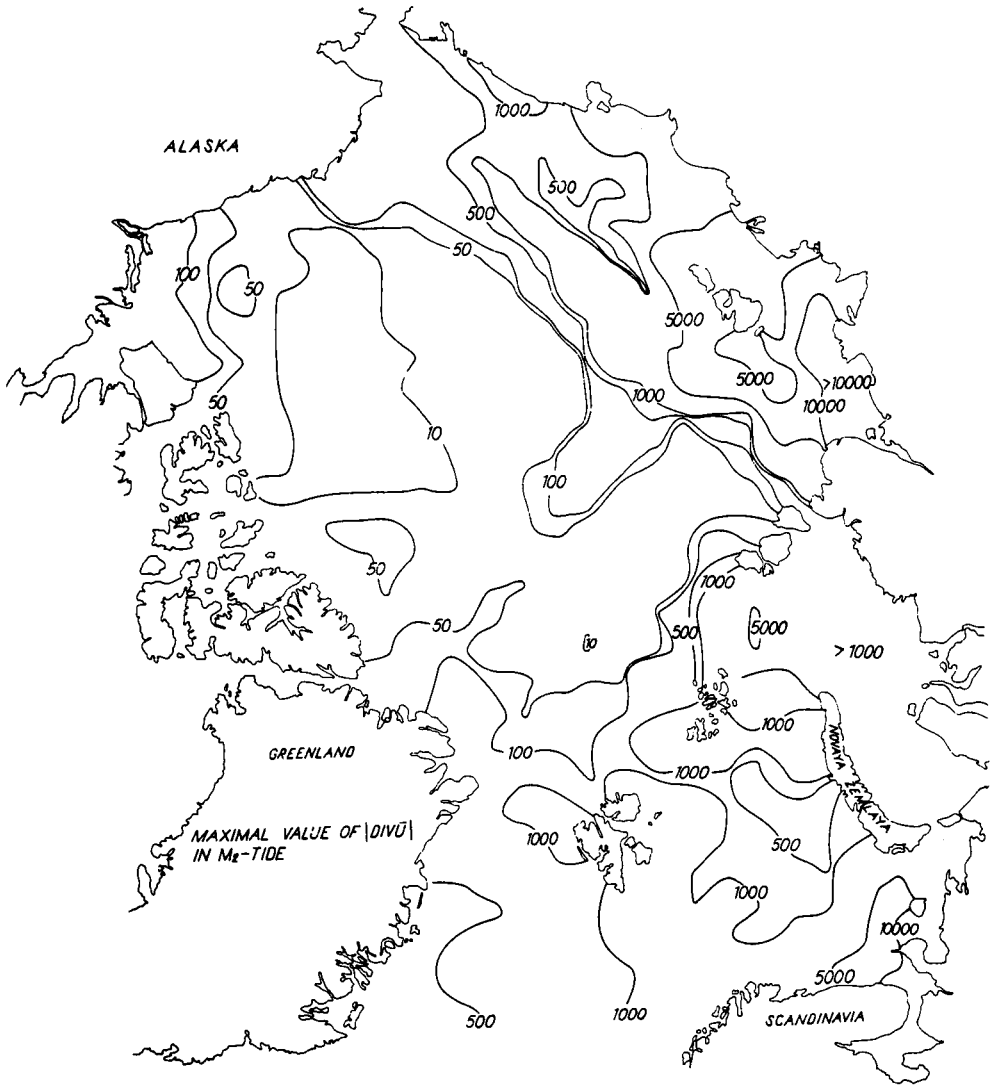


Fig. 45. MAXIMUM ABSOLUTE VALUES OF VELOCITY DIVERGENCE. TO DERIVE ACTUAL VALUES OF $\text{DIV } \vec{U}$, THE NUMBERS GIVEN SHOULD BE MULTIPLIED BY 10^{-11} $\text{DIV } \vec{U}$ IN SEC^{-1} .

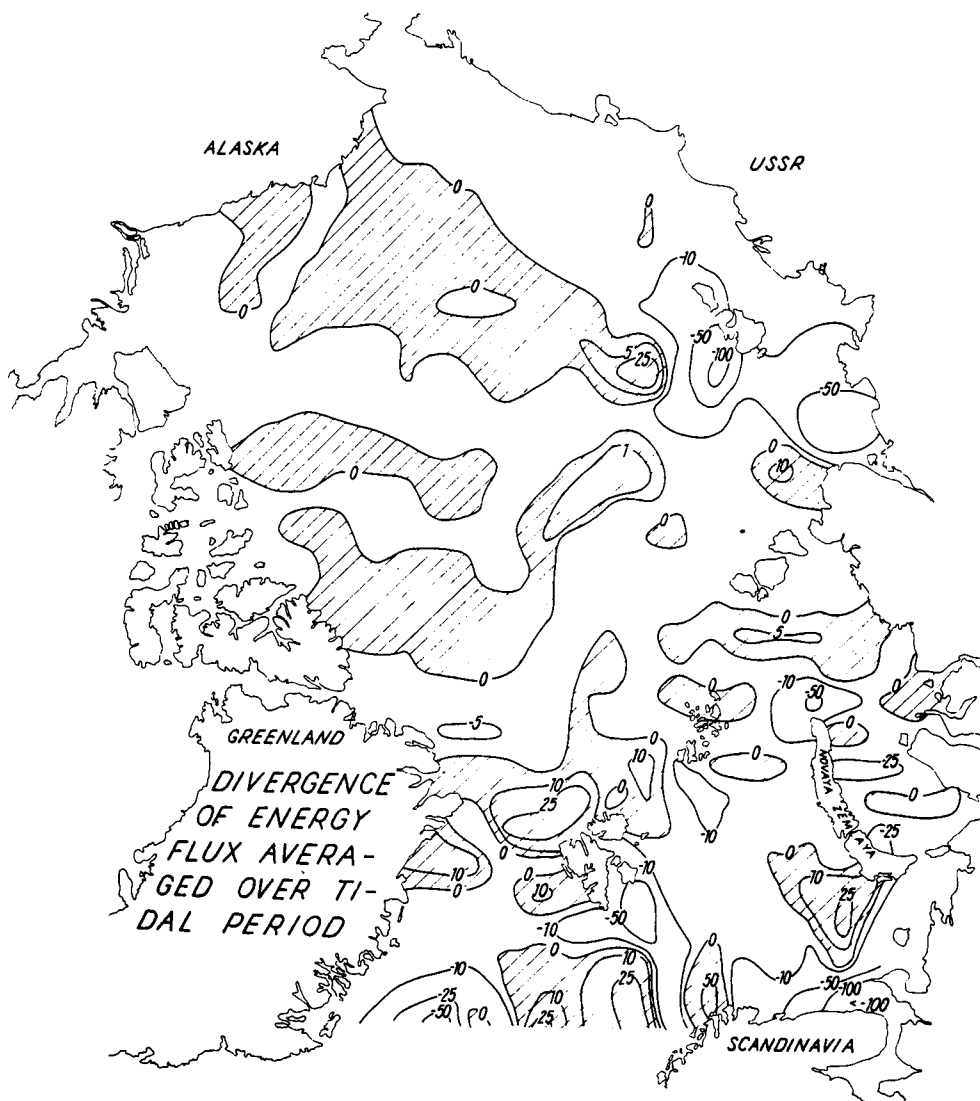


Fig. 46. DIVERGENCE OF HORIZONTAL ENERGY FLUX IN ERG/SEC, AVERAGED OVER ONE M_2 TIDAL PERIOD.

It is clear that $\text{div } \vec{U} < 0$ shows the zones of flow divergence and $\text{div } \vec{U} > 0$ indicates the reverse situation. At the same time, the ice floes will undergo a concentration in the case of $\text{div } \vec{U} < 0$ and will disperse if $\text{div } \vec{U} > 0$. Due to the tide's periodicity, alternating half periods of convergence and divergence are encountered. Therefore it is of interest to produce a map of the maximum value of the modulus of the divergence over one period (Fig. 45). In this way the areas of possibly pronounced horizontal motion can be specified. A short inspection of fig. 45 shows that the respective zones are confined to the Barents Sea, the Novaya Zemlya Islands and the New Siberian Islands.

§7. The energy balance equation

From the system of primary equations (5.1) - (5.3) we shall derive an equation for the energy balance of a tide wave in domain \bar{D} . Multiplying (5.1) by HU , (5.2) by HV and (5.3) by $g\zeta$, and adding the resulting equations side by side we find

$$\frac{1}{2} \frac{\partial (H\vec{U}^2)}{\partial t} + \frac{1}{2} g \frac{\partial \zeta^2}{\partial t} + \vec{\tau}_b \vec{U} + gV(H\vec{U}\zeta) - AH\vec{U}\Delta\vec{U} = H\vec{K}\vec{U} \quad (5.49)$$

In (5.49) the following vectors have been introduced

$$\vec{U} = (U, V), \quad \vec{\tau}_b = (\tau_b^{(x)}, \tau_b^{(y)}), \quad \vec{K} = (K_x, K_y).$$

Integrating (5.49) over the domain \bar{D} an equation for the energy balance is obtained

$$\frac{1}{2} \frac{\partial}{\partial t} \int_{\bar{D}} (H\vec{U}^2 + g\zeta^2) dD + \int_{\bar{D}} \vec{\tau}_b \vec{U} dD + g \int_{\bar{D}} V(H\vec{U}\zeta) dD - \int_{\bar{D}} AH\vec{U}\Delta\vec{U} dD = \int_{\bar{D}} H\vec{K}\vec{U} dD \quad (5.50)$$

Let us describe equation (5.50) term by term:

$$E_{\text{kin}} = \frac{1}{2} \frac{\partial}{\partial t} \int_{\bar{D}} H\vec{U}^2 dD \quad \text{denotes the kinetic energy of the tide wave}$$

$$E_{\text{pot}} = \frac{1}{2} \frac{\partial}{\partial t} \int_{\bar{D}} g\zeta^2 dD \quad \text{is the potential energy of the tide wave}$$

$$E_{D1} = \int_{\bar{D}} \vec{\tau}_b \vec{U} dD \quad \text{describes the dissipation of tidal energy due to bottom friction}$$

$$E_{D2} = \int_{\bar{D}} AH\vec{\Delta}\vec{U} dD \quad \text{the dissipation of tidal energy due to the exchange of momentum in the horizontal direction}$$

$$E_f = \int_{\bar{D}} g\nabla(\vec{U}H\zeta) dD \quad \text{is the horizontal flux of energy from the sources to the sinks}$$

$$E_{pr} = \int_{\bar{D}} H\vec{K}\vec{U} dD \quad \text{describes the production of tidal energy due to the tide generating force.}$$

If the domain \bar{D} is bounded by the contour Γ_C on which condition (5.42a) is fulfilled, the rate of production of tidal energy E_{pr} should be precisely balanced by the dissipation term.

This follows from the fact that, after averaging over tide period T_p ,

$$\frac{1}{T_p} \int_0^{T_p} E_{kin} dt = \frac{1}{T_p} \int_0^{T_p} E_{pot} dt \quad (5.51)$$

The horizontal flux of energy through the boundary is equal to zero,

$$E_f = \int_{\bar{D}} g\nabla(\vec{U}H\zeta) dD = \int_{\Gamma} g\zeta HU_n dD = 0, \quad (5.52)$$

due to the boundary condition (5.42a).

Therefore we obtain

$$\frac{1}{T_p} \int_0^{T_p} E_{D1} dt = \frac{1}{T_p} \int_0^{T_p} E_{pr} dt \quad (5.53)$$

In (5.53) E_{D2} is neglected since usually $E_{D1} \gg E_{D2}$.

If the domain D represents an adjacent sea then Γ consists of an impermeable part Γ_C and an open part Γ_O on which the boundary conditions (5.42) are prescribed. Since an adjacent sea is ordinarily of small area the energy-producing term E_{pr} is of negligible importance, but on the open boundary the flux of energy due to E_f appears

$$\frac{1}{T_p} \int_0^{T_p} g \left[\int_0^L \zeta U_n H dl \right] dt = E_f \quad (5.54)$$

where L denotes the length of Γ_O and U_n the component of velocity perpendicular to Γ_O . Assuming a simplified form of velocity $U_n = U_0 \cdot \cos(\sigma t - \alpha)$ and sea-level variation $\zeta = \zeta_0 \cos(\sigma t - \beta)$ along the boundary Γ_O , the time average in (5.54) leads to

$$E_f = \frac{L}{2} H U_0 \zeta_0 g \cos(\alpha - \beta) \quad (5.55)$$

In this case the energy flux through the open boundary Γ_0 is balanced by the dissipation due to the bottom friction.

From all the terms considered above, the tidal dissipation due to the bottom friction plays the most intricate rôle in an explanation of the secular decrease in the rate of rotation of the Earth. To estimate the mean energy dissipated in unit time we shall average E_{D1} over the tidal period T_p

$$\frac{1}{T_p} \int_0^{T_p} \int_D \vec{\tau}_b \cdot \vec{U} \, dD \, dt = \frac{1}{T_p} \int_0^{T_p} \int_D \frac{r}{H} \sqrt{U^2 + V^2} (U^2 + V^2) \, dD \, dt \quad (5.56)$$

Due to the depth in (5.56) the highest rate of dissipation is associated with the shallow coastal areas.

The first estimate of overall loss of energy on the shelf of the World Ocean was made by Jeffreys (1921) and Heiskanen (1921). Recently the problem has been reconsidered, see e.g. Kagan (1977) and Hendershot (1977).

The estimates reported in these papers are very different from each other and this is mainly because the knowledge of the tide distribution over open waters is still far from being complete.

We shall illustrate this with reference to the example of the Arctic. The magnitude of the energy dissipation in the Arctic area as computed by (5.56) is equal to 5.1×10^{17} erg/sec.

Since the Arctic M_2 -tide is considered to be co-oscillating, the general flow of wave energy is directed from the Atlantic to the Arctic Basin. In studying the flux of energy it is useful to calculate firstly

$$Fl = \frac{1}{T_p} \int_0^{T_p} \int_D g \nabla (H \vec{U} \zeta) \, dt \quad (5.57)$$

that is, the value of divergence of the horizontal energy flux related to an arbitrary point of domain D .

The map of Fl is presented in fig. 46. The most intense sinks of energy are found at the entrance to the White Sea and near the New Siberian Islands, where the tidal amplitudes are largest. According to the general reasoning the field of horizontal energy flux should show no sources. It must be assumed that the sources appearing in fig. 46 are the result of truncation errors inherent in the numerical schemes employed. The total horizontal flux of energy over the Arctic (7×10^{17} erg/sec) is comparable to the energy dissipated by the bottom friction.

§8. Numerical models to study the vertical distribution of velocity in the tide waves

Assuming that the distribution of velocity along the vertical axis can be calculated from the linear equations (1.24) and (1.25) (with atmospheric pressure $p_a = 0$), namely

$$\frac{\partial u}{\partial t} - fv = -g \frac{\partial \zeta}{\partial x} + k \frac{\partial^2 u}{\partial z^2} \quad (5.58a)$$

$$\frac{\partial v}{\partial t} + fu = -g \frac{\partial \zeta}{\partial y} + k \frac{\partial^2 v}{\partial z^2} \quad (5.58b)$$

It is seen from (5.58) that the velocity is a superposition of two components. One is due to the surface slope, which is completely independent of depth, and the other component is a function of the exchange of momentum in the vertical direction.

The overall surface slope in the tide wave's slope ζ_x is set as a difference $\zeta - \zeta_g$. Here ζ_g is the elevation due to the tidal force and is defined by (5.12).

Since the frictional force acts on the tide wave only at the bottom, the components of current due to the momentum exchange are confined to the bottom boundary layer only.

The equations (5.58) are linear and, applying the superposition principle, the system (5.58) can be split into

$$\frac{\partial u_1}{\partial t} - fv_1 = -g \frac{\partial \zeta_x}{\partial x} \quad (5.59a)$$

$$\frac{\partial v_1}{\partial t} + fu_1 = -g \frac{\partial \zeta_x}{\partial y} \quad (5.59b)$$

and

$$\frac{\partial u_2}{\partial t} - fv_2 = k \frac{\partial^2 u_2}{\partial z^2} \quad (5.60a)$$

$$\frac{\partial v_2}{\partial t} + fu_2 = k \frac{\partial^2 v_2}{\partial z^2} \quad (5.60b)$$

In (5.59) and (5.60) the components of velocity due to the surface slope are denoted by the subscript 1 and the velocity due to the turbulent stress by subscript 2.

The sea-level distribution in (5.59) can be derived through the solution of the tide problem, as presented in the previous paragraphs, and afterwards, a solution to (5.59) can be easily obtained. The real problem is posed by the system (5.60). As a boundary condition we assume at the free surface $z = H + \zeta$ a) that $u = u_1$, $v = v_1$ and b) that $u_2 = v_2 = 0$; at the bottom owing the nonslip condition $u = 0$, $v = 0$, thus $u_2 = -u_1$, $v_2 = -v_1$. Additionally, since at the free surface the horizontal stress vanishes, the relevant boundary conditions may be set as $\frac{\partial u}{\partial z} = 0$, $\frac{\partial v}{\partial z} = 0$.

We shall proceed further by implementing an explicit numerical analogue to (5.60), introducing the indices l for time and j for the z -co-ordinate

$$\frac{u_j^{l+1} - u_j^l}{T} - fv_j^l - \frac{k}{h^2}(u_{j+1}^l + u_{j-1}^l - 2u_j^l) = 0 \quad (5.61a)$$

$$\frac{v_j^{l+1} - v_j^l}{T} + fu_j^l - \frac{k}{h^2}(v_{j+1}^l + v_{j-1}^l - 2v_j^l) = 0 \quad (5.61b)$$

Setting the dependent variables in (5.61) as $\lambda^l e^{i\sigma_1 j h}$ (see e.g. 4.17), the stability of the numerical scheme is assured if

$$T < 2\phi k / [f^2 + (\phi k)^2] \quad (5.62)$$

where

$$\phi = \frac{4}{h^2} \sin^2 \sigma_1 \frac{h}{2} \quad (5.63)$$

In case the eddy viscosity coefficient k is a function of depth, a more appropriate numerical analogue of (5.60) is

$$\begin{aligned} \frac{u_j^{l+1} - u_j^l}{T} - fv_j^l - \frac{1}{h^2} \left[\frac{1}{2}(k_{j+1} + k_j)(u_{j+1}^l - u_j^l) - \frac{1}{2}(k_j + k_{j-1})(u_j^l - u_{j-1}^l) \right] \\ = 0 \end{aligned} \quad (5.64a)$$

$$\begin{aligned} \frac{v_j^{l+1} - v_j^l}{T} + fu_j^l - \frac{1}{h^2} \left[\frac{1}{2}(k_{j+1} + k_j)(v_{j+1}^l - v_j^l) - \frac{1}{2}(k_j + k_{j-1})(v_j^l - v_{j-1}^l) \right] \\ = 0 \end{aligned} \quad (5.64b)$$

If the turbulent motion is decaying ($k \rightarrow 0$), the inequality (5.62) can be difficult to fulfil. The time step which follows from it is so short that the overall time of computation may be unrealistic. Therefore a fully-implicit numerical scheme should be employed taking into consideration the discussion on this subject in chapter IV, §11.

Writing (5.60) in the implicit form

$$\frac{u_j^{l+1} - u_j^l}{T} - f v_j^{l+1} - \frac{k}{h^2} (u_{j+1}^{l+1} + u_{j-1}^{l+1} - 2u_j^{l+1}) = 0 \quad (5.65a)$$

$$\frac{v_j^{l+1} - v_j^l}{T} + f u_j^{l+1} - \frac{k}{h^2} (v_{j+1}^{l+1} + v_{j-1}^{l+1} - 2v_j^{l+1}) = 0 \quad (5.65b)$$

through the application of (4.17) one obtains the following root of the characteristic equation

$$|\lambda| = 1/\sqrt{(1 + \phi k T)^2 + (f T)^2} \quad (5.66)$$

From (5.66) we may conclude that (5.65) is stable for an arbitrary choice of the space and time step.

Both methods which have been presented, i.e. explicit and implicit, have only first-order approximation in time. Often better results can be attained with second-order approximation (but not always). We shall use a splitting method to build up a second-order scheme for (5.60). Instead of a time step T between the moments in time l and $l+1$, we consider two substeps $T/2$ related to the points in time l , $l+1/2$ and $l+1$, thus

$$\frac{u_j^{l+1/2} - u_j^l}{T} - \frac{f}{2} v_j^l - \frac{k}{2} \Delta u^l = 0 \quad (5.67a)$$

$$\frac{v_j^{l+1/2} - v_j^l}{T} + \frac{f}{2} u_j^{l+1/2} - \frac{k}{2} \Delta v^l = 0 \quad (5.67b)$$

$$\frac{v_j^{l+1} - v_j^{l+1/2}}{T} + \frac{f}{2} u_j^{l+1/2} - \frac{k}{2} \Delta v^{l+1} = 0 \quad (5.67c)$$

$$\frac{u_j^{l+1} - u_j^{l+1/2}}{T} - \frac{f}{2} v_j^{l+1} - \frac{k}{2} \Delta u^{l+1} = 0 \quad (5.67d)$$

where $\Delta = \frac{\partial^2}{\partial z^2}$.

Introducing $u_j^{l+1/2}$ and $v_j^{l+1/2}$ from (5.67a) and (5.67b) into (5.67c) and (5.67d) the system of equations is obtained

$$u_j^{l+1} = \frac{kT}{2} \Delta(u^l + u^{l+1}) + \frac{fT}{2}(v_j^{l+1} + v_j^l) + u_j^l \quad (5.68a)$$

$$v_j^{l+1} = \frac{kT}{2} \Delta(v^l + v^{l+1}) + [1 - (fT)^2/2]v_j^l - \frac{fkT^2}{2} \Delta u^l - fTu_j^l \quad (5.68b)$$

which is much simpler than (5.67).

The stability of (5.68) if examined by expression (4.17) leads to the following roots of the characteristic equation

$$\lambda_{1,2} = (1 - s^2/2 - CN^2/4 \pm s \sqrt{CN^2/4 - 1 + s^4/4}) / (1 + CN/2)^2 \quad (5.69)$$

The result is a function of the two parameters

$$s = fT \text{ and } CN = \frac{kT4}{h^2} \sin^2 \sigma_1 \frac{h}{2}.$$

Considering the magnitudes of s and CN we can consider, first of all, the case $s < CN$. Equation (5.69) then simplifies to

$$\lambda_{1,2} = (1 - CN^2/4) / (1 + CN/2)^2 = (1 - CN/2) / (1 + CN/2) \quad (5.70)$$

and therefore stability is always assured.

If, on the other hand, $s \approx CN$, the inequality $CN^2 + s^2 < 4$ leads to the condition $|\lambda_{1,2}| < 1$.

Assuming in turn the dominance of the Coriolis term $s > CN$, equation (5.69) leads to a stable numerical scheme when

$$fT < 2 \quad (5.71)$$

We may conclude that the splitting method described by the system (5.67) is stable under a fairly wide variation in the physical parameters. Such a property seems to be very important, when, for example, the eddy-viscosity coefficient k is varying in the tide wave from zero up to $10^3 \text{ cm}^2/\text{sec}$. Thus, if the stability condition depends on this parameter k (as in the case of (5.62)), one may face insurmountable difficulties in satisfying stability. In this respect an application of a completely implicit numerical scheme saves us very often from such a surprise.

§9. A treatment of the boundary layer in the tide wave

The bottom boundary layer is the place where laminar flow is transferred into turbulent flow. The conditions under which a turbulent regime appears can be found in principle from the stability of a prescribed vertical distribution of velocity and density. An initial instability is confined to the region where gradients of velocity and density achieve a certain critical value. Usually such regions are situated in the vicinity of the bottom. A proper description of the boundary layer at the bottom can only be made by a suitable description of the transfer of momentum in the vertical direction. We shall suppose, therefore, that the eddy viscosity is an unknown variable and, to close the usual set of equations, an equation for the turbulent energy is added. Firstly, a simplified problem without density stratification will be treated. We shall use the set of equations already applied in chapter III, §9 to study the vertical distribution of the wind-driven current

$$\frac{\partial b^2}{\partial t} = k \left[\left(\frac{\partial u}{\partial z} \right)^2 + \left(\frac{\partial v}{\partial z} \right)^2 \right] + \alpha_b \frac{\partial}{\partial z} \left[k \frac{\partial b^2}{\partial z} \right] - \epsilon \quad (5.72)$$

where

$$k = c_0 l b \quad \text{and} \quad \epsilon = c_1 b^3 / l \quad (5.73a, b)$$

The parameter of the turbulence scale l occurring in this system is expressed by von Karman's formula

$$l = - \chi \frac{b/l}{\frac{\partial}{\partial z}(b/l)} \quad (5.74)$$

It is customary to solve the system (5.72), (5.73), but it is also possible to eliminate one variable from this set. Expressing the scale of turbulence from (5.73a) as $l = k/c_0 b$ and introducing this into (5.73b) we find

$$\epsilon = c_0 c_1 b^4 / k \quad (5.75)$$

Substituting l into (5.74) we obtain

$$\frac{dk}{dz} - k \frac{d(\ln b^2)}{dz} = \chi b c_0 \quad (5.76)$$

Clearly the overall solution may proceed through the system (5.72), (5.76), which does not contain the parameter l . To obtain a unique solution of this system the following boundary conditions are assumed

$$\alpha_b k \frac{\partial b^2}{\partial z} = 0 \quad \text{at } z = z_0 \quad \text{and } z = H \quad (5.77)$$

because a turbulent flow of energy disappears at the sea bottom and at the free surface.

The scale of turbulence at the bottom of roughness $z = z_0$ goes to the limiting value

$$l_0 = \chi z_0 \quad (5.78)$$

Thus the eddy viscosity coefficient from (5.73a) at $z = z_0$ is equal to

$$k = c_0 b \chi z_0 \quad (5.79)$$

In the considered boundary layer the source of instability was confined to the bottom roughness. When a density stratification is present it may combine with the current distribution to give a complicated pattern to the vertical stability properties. These can be estimated with the help of the Richardson number. To model this combined effect the equation of density conservation is added to the overall system of equations as

$$\frac{\partial \rho}{\partial t} + w \left(\frac{\partial \rho}{\partial z} - \frac{N^2}{g/\rho_0} \right) = \alpha_\rho \frac{\partial}{\partial z} \left(k \frac{\partial \rho}{\partial z} \right) \quad (5.80)$$

where we follow the notation of chapter III, §9.

Assuming that the flux of mass at the surface and at the bottom vanishes, then the relevant boundary condition for (5.80) is

$$\alpha_\rho k \frac{\partial \rho}{\partial z} = 0 \quad \text{at } z = z_0 \quad \text{and } z = H \quad (5.81)$$

In (5.80) and (5.81) ρ denotes the fluctuation of the density around a mean value ρ_0 . Therefore the density of water ρ_1 is expressed as follows

$$\rho_1 = \rho_0(z) + \rho(x, y, z, t) \quad (5.82)$$

In the case of a density-stratified medium an additional term is introduced on the right side of the energy balance equation (5.72) to describe the production or loss of turbulent energy due to the buoyancy force, namely

$$\alpha_{\rho} k \frac{g}{\rho_0} \left(\frac{d\rho}{dz} - \frac{N^2}{g/\rho_0} \right) \quad (5.83)$$

When the objective is to describe the boundary layer using the set of equations (5.72), (5.76) and (5.80), then clearly they should be linked to the system (5.60). We shall shortly consider the numerical treatment of this complicated set. Although an explicit approach is possible, we shall confine ourselves to a) an implicit numerical scheme and b) the splitting method.

Though we expect from the latter a higher order of approximation, the former method is not bounded by any stability criterion and therefore may be easily implemented. The best approach seems to be an application of several numerical schemes. Such a procedure may at least shed some light on the approximation errors in the different methods. If the implicit method is applied the set of equations, apart from equation (5.65), will contain a numerical analogue of the energy equation (5.72)

$$\begin{aligned} \frac{B^{l+1} - B^l}{T} = k^l \left(\left| \frac{\partial u^l}{\partial z} \right| \left| \frac{\partial u^{l+1}}{\partial z} \right| + \left| \frac{\partial v^l}{\partial z} \right| \left| \frac{\partial v^{l+1}}{\partial z} \right| \right) + \alpha_b \frac{\partial}{\partial z} \left(k \frac{\partial B^{l+1}}{\partial z} \right) \\ - c_0 c_1 B^l B^{l+1} / k^l \end{aligned} \quad (5.84)$$

where $B = b^2$.

Approximating B^2 in time as $B^l B^{l+1}$ we imply that in the course of the calculation $B \geq 0$.

The eddy viscosity occurring in (5.84) is derived from (5.76) by the following numerical scheme

$$\frac{1}{2h} (b_{j+1} + b_j) (k_{j+1} - k_j) - \frac{1}{h} (k_j + k_{j+1}) (b_{j+1} - b_j) = \chi b_j b_{j+1} c_0 \quad (5.85a)$$

thus

$$k_{j+1} = k_j (3b_{j+1} - b_j) / (3b_j - b_{j+1}) + 2hc_0 \chi b_j b_{j+1} / (3b_j - b_{j+1}) \quad (5.85b)$$

A more subtle approach is required if the splitting method is considered. It is also obvious that the proof of the numerical stability is impossible with conventional techniques due to the nonlinear properties of the energy equation.

In implementing the splitting method we shall follow the derivation in system (5.67). Corresponding to the first subset of equations, (5.67a) and (5.67b), the relevant form of the energy equation is

$$\frac{B^{1+1/2} - B^1}{T} = \frac{1}{2}\alpha_b \frac{\partial}{\partial z} (k^1 \frac{\partial B^1}{\partial z}) - \frac{1}{2} c_o c_1 B^1 B^{1+1/2} / k^1 + \frac{k^1}{2} \left\{ \left(\frac{\partial u^1}{\partial z} \right)^2 + \left(\frac{\partial v^1}{\partial z} \right)^2 \right\} \quad (5.86a)$$

and corresponding to the second subset (5.67c) and (5.67d) we have

$$\frac{B^{1+1} - B^{1+1/2}}{T} = \frac{1}{2}\alpha_b \frac{\partial}{\partial z} (k^{1+1/2} \frac{\partial B^{1+1}}{\partial z}) - \frac{1}{2} c_o c_1 B^{1+1/2} B^{1+1} / k^1 + \frac{1}{2} k^{1+1/2} \left\{ \left(\frac{\partial u^{1+1}}{\partial z} \right)^2 + \left(\frac{\partial v^{1+1}}{\partial z} \right)^2 \right\} \quad (5.86b)$$

The eddy viscosity in (5.86) is computed with the expression (5.85b). It does not require splitting since formally it is not a function of time.

REFERENCES

- Bogdanov, K.T.; Kim, K.V.; Magarik, V.A., 1964. Numerical Solution of Tide Hydrodynamic Equations on Electronic Computing Machine BESM-2 for the Pacific Ocean Basin. Tr. Inst. Okieanologii AN SSSR N. 75: 73 - 98.
- Bogdanov, K.T., 1975. Tides of the World Ocean. Nauka. Moskwa.
- Defant, A., 1919. Untersuchungen über die Gezeitenerscheinungen in Mittel- und Randmeeren, Buchten und Kanälen, Teil I: Die Methoden der Untersuchung. Denkschrift Wiener Akademie der Wissenschaften.
- Defant, A., 1924. Die Gezeiten des Atlantischen Ozeans und des Arktischen Meeres. Ann. Hydr. v. 52: 153-166 and 177-184.
- Defant, A., 1932. Die Gezeiten und inneren Gezeitenwellen des Atlantischen Ozeans. Wiss. Ergeb. Deutsch. Atl. Exp. "Meteor" 1925-1927 v. 7: 1-318.
- Defant, A., 1961. Physical Oceanography. Pergamon Press, v. 2.
- Hansen, W., 1949. Die halbtägigen Gezeiten im Nordatlantischen Ozean. Deutsch. Hydr. Zeit. Band 2: 44-61.
- Hansen, W., 1952. Gezeiten und Gezeitenströme der halbtägigen Hauptmondtide M_2 in der Nordsee. Deutsch. Hydr. Zeit. Erg.H. 1: 1-46.
- Hansen, W., 1956. Theorie zur Errechnung des Wasserstandes und der Strömungen in Randmeeren nebst Anwendungen. Tellus 8:287-300.
- Heaps, N., 1969. A Two-Dimensional Numerical Sea Model. Phil. Trans. Royal Soc. London, v. 265:93-137.

- Heaps, N., 1972. On the Numerical Solution of the Three-Dimensional Hydrodynamic Equations for Tides and Storm Surges. Mem. Soc. Royale des Sciences de Liège 6^e serie t.I: 143-180.
- Heiskanen, W., 1921. Über den Einfluß der Gezeiten auf die säkulare Acceleration des Mondes. Ann. Acad. Sci. Fennicae A.18, N.2: 1-84.
- Hendershott, M.C., 1977. Numerical Models of Ocean Tides. in: The Sea v. 6, Wiley-Interscience Publ., New York: 47-95.
- Jeffreys, H., 1921. Tidal Friction in Shallow Seas. Phil. Trans. Roy. Soc. London A 221: 239-264.
- Kagan, B.A., 1968. Hydrodynamic Models of Tidal Motion in the Sea. Gidrometeoizdat, Leningrad.
- Kagan, B.A., 1977. Global Interaction of Oceanic and Earth's Tides. Gidrometeoizdat, Leningrad.
- Kowalik, Z. and Nguyen Bich Hung, 1977. On the System of Hydrodynamic Equations for Certain Oceanographical Problems in the Region of the Earth's Pole and the Stability of its Solution. Oceanologia N.7:5-20.
- Kowalik, Z. and Untersteiner, N., 1978. A Study of the M_2 -Tide in the Arctic Ocean. Deutsch. Hydr. Zeit. (to be published).
- Lamb, H., 1945. Hydrodynamics. Dover Publ. New York.
- Lauwerier, H.A. and Damsté, B.R., 1963. North Sea Problem. A Numerical Treatment. Proc. Kon. Ned. Acad. Wetensch. A 66: 169-184.
- Marchuk, G.I.; Kagan, B.A.; Tamsalu, R.E., 1969. A Numerical Method to Calculate Tidal Motion in the Adjacent Sea. Izv. AN SSSR, Phys. Atmosph. Ocean N. 5: 694-703.
- Marchuk, G.; Gordeev, R.; Kagan, B.; Rivkind, W., 1972. Numerical Method to Solve Tidal Dynamics Equations and Results of its Testing. Publ. by Comput. Centre Novosybirsk.
- Marchuk, G.I. and Kagan B.A., 1977. Oceanic Tides. Gidrometeoizdat, Leningrad.
- Nekrasov, A.W., 1975. Tide Waves in the Adjacent Seas. Gidrometeoizdat, Leningrad.
- Oceanographic Atlas of the Polar Seas. Part II. U.S. Naval Oceanographic Office, Washington D.C., 1958.
- Pekeris, C.L. and Accad, Y., 1969. Solution of Laplace's Equations for the M_2 -Tide in the World Oceans. Phil. Trans. Roy. Soc. London A 265: 413-436.
- Racer-Ivanova, C.F., 1956. Study of the Free Oscillation of Diurnal and Semi-Diurnal Type in the Shallow Basins. Izv. AN SSSR, Ser. Geoph. N.1.
- Stretensky, L.N., 1947. Theory of the Long Period Tide. Izv. AN SSSR, Ser. Geoph. Geogr. v. 11, N. 3.
- Sverdrup, H.W., 1926. Dynamics of Tides on the North-Siberian Shelf. Geoph. Publ. Norske Viden - Akad. Oslo 4(5).
- Taylor, G.I., 1921. Tidal Oscillations in Gulfs and Rectangular Basins. Proc. London Math. Soc. s. 2, v. XX:148-181.
- Zahel, W., 1973. The Diurnal K_1 -Tide in the World Ocean - a Numerical Investigation. Pure and Applied Geophysics 109: 1819-1825.
- Zahel, W., 1977. A Global Hydrodynamic-Numerical 1^0 -Model of the Ocean Tides; the Oscillation System of the M_2 -Tide and its Distribution of Energy Dissipation. Annales de Geophysique T. 33: 31-40.

Chapter VI MODELS OF SHALLOW COASTAL AREAS AND TIDAL RIVERS

This chapter will be devoted to the modelling of the hydrodynamic processes in semi-enclosed seas, rivers and estuaries. Dynamic processes, as described by the general equations derived in chapter I, take a new and different form, due mainly to the one-directional character of flow in rivers and estuaries. In addition, in shallow water, where variations of the water level are of the same order as the depth, the nonlinear effects start to play an important rôle. Because of this, we shall reconsider certain results obtained in chapter I, especially those related to the bottom stress.

The model of storm surges in semi-enclosed seas is also discussed since it delivers a set of boundary conditions to the nested models of coastal oceanography.

To compute a dynamic phenomenon in small areas such as bays and estuaries, one is usually lacking the boundary condition on the open boundary, through which an external domain exerts an influence. The best solution is to use observed values, for example tide gauge data. This is not always possible. Therefore a chain of nested models on decreasing grids is usually constructed. The first step is a model of storm surge or tide which includes the mesoscale basins like the North Sea or the Baltic Sea. In the course of the work done by Hansen (1956, 1962, 1966), Platzman (1958, 1963), Uusitalo (1962), Jelesniansky (1965, 1966), Heaps (1969), Reid and Bodine (1968) and many others (i.e. Volcinger and Piaskovski, 1968), many important questions related to the physical and numerical problems of vertically-integrated equations were elucidated. The numerical reproduction of the tide and storm surge is now at a level where it can be used in a forecasting system, therefore we shall not dwell on such models. In studying the dynamic phenomena in shallow coastal waters and rivers we shall depend a great deal on the well-known model of the North Sea developed by Hansen (1956). The model with a grid distance of 37 km is very well suited to problems concerning large scale processes provided the topographic approximation is guaranteed. But as soon as more specific questions arise, due to the local vertical or horizontal nature, a refinement of the grid seems to be the best solution. One of the most promising applications of the small scale models is the prediction of dynamic processes in the areas of planned engineering constructions. A refinement of the grid is necessary there to reproduce in the model the optimum resemblance to nature. On the other hand, a numerical model of this kind is needed to forecast the storm surges and tides in basins screened from the open sea by

islands and sandbanks located at the end of narrow channels.

Of course when one has access to a computer of great memory size and the cost of computation is of no importance, the grid refinement problem may be solved to a large extent.

§1. Some remarks on one-dimensional models

In this chapter the dynamics of flow will be considered using the notion of the average velocity. The one-dimensional flow will be studied with the help of equations (1.52) and (1.54), namely

$$B \frac{\partial \zeta}{\partial t} + \frac{\partial (UQ)}{\partial x} = 0 \quad (6.1)$$

$$\frac{\partial U}{\partial t} + U \frac{\partial U}{\partial x} = -g \frac{\partial \zeta}{\partial x} + \frac{1}{H + \zeta} (\tau_s^{(x)} - \tau_b^{(x)}) \quad (6.2)$$

where B denotes the width of the channel, $Q = B(H + \zeta)$ is a cross-sectional area and $\tau_b^{(x)} = rU|U|$.

As is usual in estuaries, one cross-section is very different in its structure and magnitude from the next. As the slope of the river bed is not constant along the length of the river we can speak of an asymmetry of the profile which is due to changes in the geometry of the width, depth and cross-sectional area.

If the influence of this asymmetry on the flow is small compared with the friction of the bed, the nonlinear term $U \frac{\partial U}{\partial x}$ in (6.2) may be neglected. But generally this is not the case, especially in the middle and the upper parts of the river, where usually great changes occur in subsequent cross-sectional areas.

The convective term has to be considered as a measure of the asymmetry in the equation of motion. If the rate of change of cross-section $\frac{\partial Q}{\partial x}$ is great, it must be expected that the velocity changes substantially as well. To estimate its magnitude, $\frac{\partial U}{\partial x}$ has to be computed from the generally valid equation of continuity (6.1).

It follows from (6.1), that the advection term can be expressed as

$$U \frac{\partial U}{\partial x} = - \frac{\partial Q}{\partial x} \frac{U^2}{Q} - \frac{UB}{Q} \frac{\partial \zeta}{\partial t} \quad (6.3)$$

Introducing (6.3) into the equation of motion (6.2), where the term due to the surface stress $\tau_s^{(x)}$ is omitted, gives

$$\frac{\partial U}{\partial t} + g \frac{\partial \zeta}{\partial x} + U \left(\frac{r|U|}{H + \zeta} - \frac{\partial Q}{\partial x} \frac{U}{Q} - \frac{B \partial \zeta}{Q \partial t} \right) = 0 \quad (6.4)$$

We now investigate the term in parentheses

$$\frac{r|U|}{H+\zeta} - \frac{\partial Q}{\partial x} \frac{U}{Q} - \frac{B\partial\zeta}{Q\partial t} \quad (6.5)$$

as a generalised expression for the total resistance to motion. It can be seen that the share of $U\frac{\partial U}{\partial x}$ in the total resistance is always important. This is especially true in the case of great velocities $\frac{\partial\zeta}{\partial t}$, small depth and extended width, as well as in the case of pronounced changes of the cross-sectional area $\frac{1}{Q}\frac{\partial Q}{\partial x}$.

Since the terms $\frac{U}{Q}\frac{\partial Q}{\partial x}$ and $\frac{B}{Q}\frac{\partial\zeta}{\partial t}$ change their signs during one tidal period they influence the total resistance irregularly. $\frac{\partial\zeta}{\partial t}$ generally reaches its maximum shortly after low water and in this way reduces the relative influence of the friction term. Subsequently the reduction decreases, the change of the sign takes place roughly half way between high (hwt) and low water time (lwt), an increase of energy dissipation occurs accordingly.

The cross-sectional area diminishes up-stream. When U is greater than zero (flood), the term $\frac{U}{Q}\frac{\partial Q}{\partial x}$ increases the total resistance, while the negative sign of U at the ebb reduces it. It follows that both terms $\frac{U}{Q}\frac{\partial Q}{\partial x}$ and $\frac{B}{Q}\frac{\partial\zeta}{\partial t}$ have opposite signs outside the times between high water and the turning point K_f as well as between low water and turning point K_e . K_f and K_e denote in this instance the turning points between flood and ebb and between ebb and flood respectively.

Reduced friction forces cause higher velocities and, thus, a further increase in the water level. Therefore it can be concluded that the convective term $U\frac{\partial U}{\partial x}$ has its greatest influence between lwt and K_e , particularly, because Q then is minimum. Actually the real elevation of the water level cannot be approximated without including the term $U\frac{\partial U}{\partial x}$ during that period.

In the equation of one-dimensional motion the Coriolis force does not appear. However, it may play an important rôle in the case of flow in the mouth of a river.

If we set $v = 0$ in the hydrodynamic equations, we obtain the equation of geostrophical motion for one-directional flow from (1.22)

$$-fu = g\frac{\partial\zeta}{\partial y} \quad (6.6)$$

where $\frac{\partial\zeta}{\partial y}$ describes the lateral slope at the mouth. Taking approximate values of the parameters $g = 10 \text{ m/sec}^2$, $u = 1 \text{ m/sec}$ and $f = 10^{-4} \text{ sec}^{-1}$, and using a grid distance of $h = 10 \text{ km}$, we obtain from the difference

form of the geostrophic equation

$$- fu = g\Delta\zeta/h \quad (6.7)$$

the value of 10 cm for $\Delta\zeta$. From this result it may be concluded that the Coriolis force cannot be disregarded even in one-dimensional flow.

Finally let us consider the rôle of variable density (Heaps, 1972). Due to the influence the density gradient has on the distribution of the current in the area of the mouth of a river, the hydrodynamic differential equations of motion have to be specified in such a way that a simple relation between current and mass distribution will hold. These equations will only provide the average current velocities, i.e. it will not be possible to depict a vertical distribution, except through the application of the equation of continuity in a non-averaged form.

We may begin to account for the effects of variable density by using a simplified equation of motion (1.1)

$$\frac{\partial u}{\partial t} = - \frac{1}{\rho} \frac{\partial p}{\partial x} \quad (6.8)$$

where the terms which will not play a rôle in the following discussion are omitted from (1.1).

The pressure in (6.8) is calculated with the help of expression (1.28)

$$p = p_a + \rho_0 g(\zeta - z) + g \int_z^0 \rho_1 d\eta \quad (6.9)$$

As we saw in chapter I the density in (6.9) is a sum of an average part ρ_0 and a variable part ρ_1 .

To ascertain the mean vertical velocity, equation (6.8) is integrated from the bottom $-H$ to the sea surface ζ , thus

$$\frac{\partial U}{\partial t}(H+\zeta) = \frac{\partial p_a}{\partial x}(H+\zeta) + \rho_0 g \frac{\partial \zeta}{\partial x}(H+\zeta) + \int_{-H}^{\zeta} g \left(\frac{\partial}{\partial x} \int_z^0 \rho_1 d\eta \right) dz \quad (6.10)$$

The influence of the density distribution on the mean velocity along the longitudinal axis of river is stated in (6.10) by the term

$$\frac{1}{(H+\zeta)} \int_{-H}^{\zeta} g \left(\frac{\partial}{\partial x} \int_z^0 \rho_1 d\eta \right) dz \quad (6.11)$$

An investigation of the density term in the equation of motion shows that the mean flood-current velocity is naturally accelerated in the presence of a density gradient, while the ebb-current velocity is decelerated.

§2. River models

Further development will be based on the equations (6.1) and (6.2) in the form

$$\frac{\partial \zeta}{\partial t} + \frac{1}{B} \frac{\partial}{\partial x} \{BU(H+\zeta)\} = 0 \quad (6.12)$$

$$\frac{\partial U}{\partial t} + U \frac{\partial U}{\partial x} = -g \frac{\partial \zeta}{\partial x} - \frac{1}{H+\zeta} \tau_b^{(x)} \quad (6.13)$$

These equations form a hyperbolic system and in order to obtain a unique solution to the system we adjoin suitable boundary conditions. The boundary conditions for the channel problem can be formulated in the terms of sea-level, velocity or mass transport, namely

$$\zeta(x=0,t) = \alpha_1(t) \quad \zeta(x=L,t) = \alpha_2(t) \quad (6.14a)$$

$$U(x=0,t) = \beta_1(t) \quad U(x=L,t) = \beta_2(t) \quad (6.14b)$$

$$QU(x=0,t) = \gamma_1(t) \quad QU(x=L,t) = \gamma_2(t) \quad (6.14c)$$

Here L is the length of the channel and α , β and γ are given functions of time. The initial conditions, as was shown in chapter IV, depend on the type of equation. To demonstrate the equation-type of system (6.12), (6.13) it is first of all transformed to the standard form (4.124). To do this, we define a vector \vec{V} with co-ordinates U and $H+\zeta$. Assuming the width B to be constant, the above system is rewritten as a single vector equation

$$\frac{\partial \vec{V}}{\partial t} + A \frac{\partial \vec{V}}{\partial x} = \vec{\tau} \quad (6.15)$$

where

$$A = \begin{bmatrix} U & g \\ H_1 & U \end{bmatrix}; \quad \vec{\tau} = \begin{bmatrix} \tau_b^{(x)}/H_1 \\ 0 \end{bmatrix}; \quad H_1 = H + \zeta \quad (6.16)$$

To prove that (6.15) is of the hyperbolic type we introduce a determinant

$$\text{Det}(A - \lambda E) = 0 \tag{6.17}$$

which provides two eigenvalues $\lambda_{1,2} = U \pm \sqrt{gH_1}$.

Since both eigenvalues are different and real, in virtue of the theorem stated in chapter IV, the system of equations is hyperbolic. The number of initial conditions for the unique solution of the posed problem is equal to the number of negative eigenvalues. Assuming that $U < \sqrt{gH_1}$ it follows from the result above that one initial condition is satisfactory for a unique solution.

A numerical solution will be sought through equations (6.12) and (6.13) in a slightly changed form

$$\frac{\partial \zeta}{\partial t} + \frac{1}{B} \frac{\partial B}{\partial x} U(H+\zeta) + \frac{\partial}{\partial x} \{U(H+\zeta)\} = 0 \tag{6.18}$$

$$\frac{\partial U}{\partial t} + U \frac{\partial U}{\partial x} = -g \frac{\partial \zeta}{\partial x} - \frac{rU|U|}{h + \zeta} \tag{6.19}$$

This system will be transformed into a difference form with the help of the grid plotted in fig. 47.

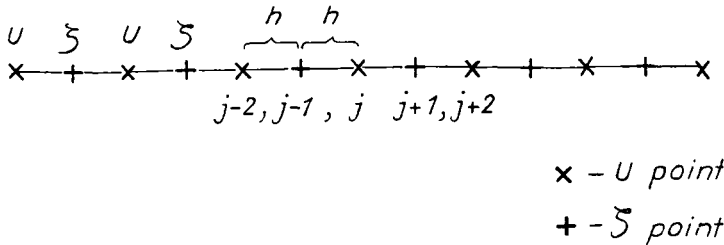


Fig. 47. GRID FOR A ONE-DIMENSIONAL PROBLEM.

The differential quotients in (6.18) and (6.19) are replaced with central differences to give

$$\begin{aligned} \frac{U_j^{1+1} - U_j^{1-1}}{2\tau} = & - U_j^{1-1} (U_{j+2}^{1-1} - U_{j-2}^{1-1}) \frac{1}{4h} - \frac{g}{2h} (\zeta_{j+1}^1 - \zeta_{j-1}^1) \\ & - r |U_j^{1-1}| U_j^{1-1} / \{H_j + 0.5(\zeta_{j+1}^1 + \zeta_{j-1}^1)\} \end{aligned} \tag{6.20}$$

$$\frac{\zeta_{j+1}^{1+2} - \zeta_{j+1}^1}{2T} = -\frac{1}{4hB_{j+1}}(U_{j+2}^{1+1} + U_j^{1+1})(H_{j+1} + \frac{1}{j+1})(B_{j+2} - B_j) \quad (6.21)$$

$$-\frac{1}{2h}\{U_{j+2}^{1+1}[H_{j+2} + 0.5(\zeta_{j+3}^1 + \zeta_{j+1}^1)] - U_j^{1+1}[H_j + 0.5(\zeta_{j+1}^1 + \zeta_{j-1}^1)]\}$$

If the geometry of the river is so complicated that the above approach leads to an erroneous result, a more complicated model of two-dimensional flow could be introduced easily through the system derived in chapter I

$$\frac{\partial U}{\partial t} = -g \frac{\partial \zeta}{\partial x} - \frac{1}{H+\zeta} rU \sqrt{U^2+V^2} + fV \quad (6.22)$$

$$\frac{\partial \zeta}{\partial t} + \frac{\partial}{\partial x}\{(H+\zeta)U\} + \frac{\partial}{\partial y}\{(H+\zeta)V\} = 0 \quad (6.23)$$

$$\frac{\partial V}{\partial t} = -g \frac{\partial \zeta}{\partial y} - \frac{1}{H+\zeta} rV \sqrt{U^2+V^2} - fU \quad (6.24)$$

The numerical form of (6.22) - (6.24) has to take into account the difference in the geometry of the one-dimensional flow. It leads first of all to different grids across the cross-section and along the main flow. Since for a proper reproduction of the motion a cross-sectional grid will have an extremely small step in space, this in turn will influence the magnitude of the time step. To avoid this obstacle an implicit form of the equations across the cross-sections will be introduced. From now on we shall direct an axis parallel to the cross-section. The numerical scheme of (6.22) - (6.24) will therefore be of an implicit form along the y direction and of explicit form along the x-axis. We shall work only with (6.23) and (6.24) to derive the implicit part of the overall system, because the explicit form has been developed already and was thoroughly discussed in chapter IV

$$\frac{V^{1+1} - V^{1-1}}{2T} = -\frac{g}{2} \left(\frac{\partial \zeta^{1+1}}{\partial y} + \frac{\partial \zeta^{1-1}}{\partial y} \right) - \frac{rV^1}{H+\zeta} \sqrt{U^2+V^2} - fU^1 \quad (6.25)$$

$$\frac{\zeta^{1+1} - \zeta^{1-1}}{2T} = -\frac{1}{2} \frac{\partial}{\partial y}\{(H+\zeta^{1-1})(V^{1+1}+V^{1-1})\} - \frac{\partial}{\partial x}\{(H+\zeta^{1-1})U^1\} \quad (6.26)$$

If the terms along the x-axis in the above equations are ignored for a moment, it is easily seen, with the help of (4.17), that the system is unconditionally stable. To derive an algorithm for a

numerical solution we collect on the left hand side of the equations the implicit terms, and on the right hand side, the explicit terms as follows

$$V_{j,k}^{l+1} + \frac{gT}{2h}(\zeta_{j,k+1}^{l+1} - \zeta_{j,k-1}^{l+1}) = -\frac{2rT}{H_{j,k} + \zeta_{j,k}^1} V_{j,k}^1 \sqrt{U^2 + V^2} - 2TfU_{j,k}^1$$

$$- \frac{gT}{2h}(\zeta_{j,k+1}^{l-1} - \zeta_{j,k-1}^{l-1}) + V_{j,k}^{l-1} = F_{1,j,k}^1 \quad (6.27)$$

$$\zeta_{j,k}^{l+1} + \frac{T}{2h}(H_{j,k+1}V_{j,k+1}^{l+1} - H_{j,k-1}V_{j,k-1}^{l+1}) = -\frac{T}{2h}(H_{j,k+1}V_{j,k+1}^{l-1}$$

$$- H_{j,k-1}V_{j,k-1}^{l-1}) - \frac{T}{h}(H_{j,k}U_{j,k}^1 - H_{j-1,k}U_{j-1,k}^1) + \zeta_{j,k}^{l-1} = F_{2,j,k}^1 \quad (6.28)$$

Comparing the method of approximation in this system with numerical forms (6.20) and (6.21) we may see that previously U and V were taken at different space points. Now the points U , V and ζ from the vicinity are brought together and placed under the same space index. This procedure will be explained later on.

The solution to the system (6.27) and (6.28) can be easily derived using the line factorization method as presented in chapter II. To apply the method we must reduce the system of equations to one equation of a three-point form. Starting with (6.28) we set

$$\zeta_{j,k+1}^{l+1} = -\frac{T}{2h}(H_{j,k+2}V_{j,k+2}^{l+1} - H_{j,k}V_{j,k}^{l+1}) + F_{2,j,k+1}^1 \quad (6.29)$$

$$\zeta_{j,k-1}^{l+1} = -\frac{T}{2h}(H_{j,k}V_{j,k}^{l+1} - H_{j,k-2}V_{j,k-2}^{l+1}) + F_{2,j,k-1}^1 \quad (6.30)$$

Next substituting it into (6.27)

$$V_{j,k}^{l+1} - \frac{gT^2}{4h^2}(H_{j,k-2}V_{j,k-2}^{l+1} + H_{j,k+2}V_{j,k+2}^{l+1} - 2H_{j,k}V_{j,k}^{l+1})$$

$$= \frac{gT}{2h}(F_{2,j,k-1}^1 - F_{2,j,k+1}^1) + F_{1,j,k}^1 \quad (6.31)$$

a three-point formula is obtained, suitable for treatment by the line-factorization method.

After the distribution of velocity has been derived we may proceed in two directions; either through (6.28) to perform the straightforward calculations of ζ or to set a three-point algorithm for ζ and after that performing the calculation.

It is obvious from chapter II that (6.31) will lead to a convergent solution if the diagonal terms prevail over the nondiagonal ones. The condition of convergence is expressed as

$$\frac{gT^2}{4h^2}(H_{j,k+2} + H_{j,k-2}) < 1 \quad (6.32)$$

therefore we again have to choose the time and space steps to comply with this inequality. As we know from chapter IV it is possible to bypass this obstacle using an implicit algorithm.

§3. A one-dimensional treatment of river flow: the multi-channel system

In this paragraph we shall return again to a one-dimensional description of the river flow because that approach, though not very sophisticated, may provide a fast and correct answer to a great number of dynamic problems. Let us consider the cross-section plotted in fig. 48. The overall cross-section can be split into two parts: the 'conveyance cross-section' and the 'reservoir'. The boundary line between these cross-sectional areas cannot be fixed without further consideration, but a tentative boundary can be drawn from the structure of the cross-section. For example, such a line can easily be drawn if a profile possesses the geometrical structure presented in fig. 49. Nevertheless, the procedure does not give any information about the real magnitude of either cross-section or of the flow through it, but it provides the range wherein conditions of flow or storage predominate

In equations (6.1) and (6.2) the velocity can be regarded as a mean value related to the cross-sectional area. Let us shortly consider the problems which appear as soon as we try to derive the velocity distribution due to the dual structure of the cross-section in the one-dimensional model.

Consider a rectangular cross-section of width B and depth H . Water flows through it with average velocity U .

Imagine that we add to this a cross-section of width b and depth h with the flow velocity u . In both longitudinal profiles the same surface gradient appears, therefore

$$rU^2/H = g\frac{\partial\zeta}{\partial x}; \quad ru^2/h = g\frac{\partial\zeta}{\partial x} \quad (6.33)$$

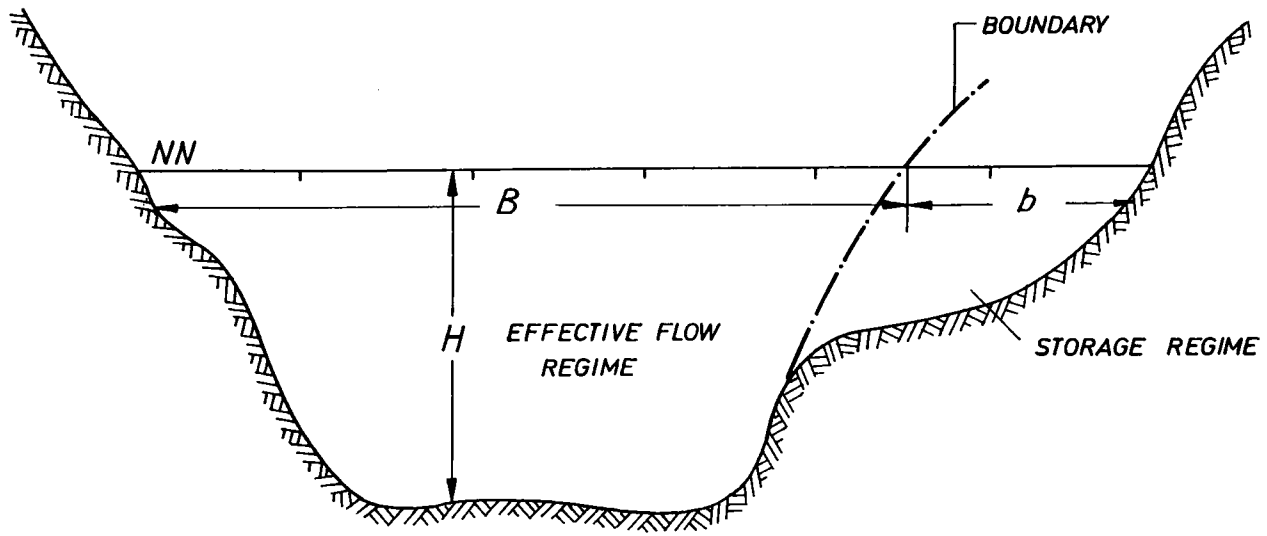


FIG. 48. CROSS-SECTION OF THE RIVER FLOW. B - WIDTH OF THE EFFECTIVE FLOW REGIME, b - WIDTH OF THE STORAGE REGIME.

The total amount of water flow is given by

$$F = BUH + buh \quad (6.34)$$

Setting $\frac{g}{r} \frac{\partial \zeta}{\partial x} = c^2$, $U = c\sqrt{H}$, $u = c\sqrt{h}$, $H/h = n$ and assuming for the sake of simplicity that $B = b$ we find

$$F = cBH^{3/2} (1 + 1/n^{3/2}) \quad (6.35)$$

If on the other hand the geometry of the cross-section is neglected and only its total area is considered, the mean value of depth $\bar{H} = (H+h)/2$ and velocity \bar{U} may be related to it. Thus in a similar way to (6.33) we find

$$r \cdot \bar{U}^2 / \left(\frac{H+h}{2}\right)^2 = g \frac{\partial \zeta}{\partial x} \quad (6.36)$$

and

$$\bar{U} = c\sqrt{(H+h)/2} \quad (6.37)$$

Setting again $B=b$ and $H/h = n$ we derive the total mean flow

$$\bar{F} = 2B\bar{U}(H+h)/2 \quad (6.38a)$$

and

$$\bar{F} = cB(H+h)^{3/2} (1 + 1/n^{3/2})/2^{3/2} \quad (6.38b)$$

In order to compare the possible magnitudes of F and \bar{F} we put $h = H/4$ and find

$$F = 1.14 \bar{F} \quad (6.39)$$

Therefore, the water transports are not necessarily equal when the cross-sectional areas are of the same magnitude. They only approach each other when h approaches H . The difference in transport is proportional to the difference in depth. From this it can be inferred that the flow dynamics are not only a function of the cross-sectional area but also of its morphological structure.

A special method has been developed to model the flow in rivers with complicated bottom topography, the multi-channel system (Ramming, 1971). For this purpose the cross-section is divided into a number of unequal vertical strips which form a lattice of grid points for the

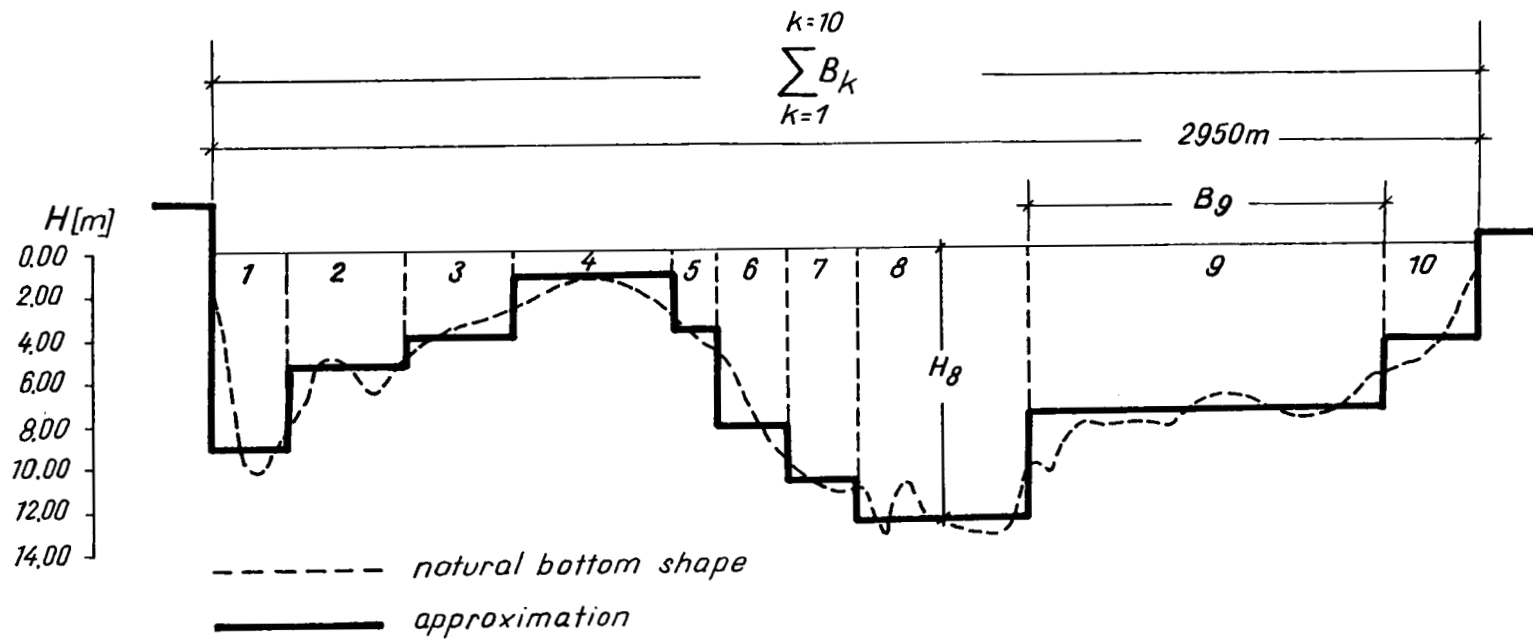


Fig. 49. CROSS-SECTIONAL AREA OF THE RIVER ELBE (678 km DOWNSTREAM), CLOSE TO GLÜCKSTADT.

numerical calculations. An example of such a calculation is shown in fig. 11 where the cross-section of the River Elbe at the point 678 km is considered as a sum of 10 strips. Now, introducing an index of enumeration k across the section and an index j of successive cross-sections along the river, we may write the expression for the transport of water in the form (see fig. 49)

$$Q = \sum_{k=1}^N B_{j,k} (H_{j,k} + \zeta_{j,k}^1) U_{j,k}^1 \quad (6.40)$$

This method was tested extensively on the River Eider (Ramming, 1971) where the flow is driven by the incoming tides from the North Sea. The river shows very irregular cross-sections and a remarkably variable depth distribution. In an early computation the cross-sectional areas were taken as a function of the water elevation and the depth was calculated as the ratio of the area over the width for an average water level. The numerical results obtained by this simplified method, when compared with the measured data, were far from satisfactory. In particular, we were not able to reproduce the steep part of the tidal curve during the flood tide. The computations took into account only an overall area for the cross-sections but not their complex geometry. Such a procedure mainly distorts the friction and nonlinear advective terms in the equations of motion and continuity which are responsible for the nonharmonic behaviour of tidal curves. Since the tidal range and depth can be of the same order, the nonlinear processes are of special importance for the very shallow part of a river.

To include in a model the effects described above we must include the fine structure of the depth distribution of the River Eider. To do this, the strips from one cross-section to another are connected together, forming parallel channels of different widths and depths. Having computed a transport for a single channel which passes through all cross-sections of the river, the total transport is determined as the sum of the transports in the adjacent channels. The overall procedure is explained in fig. 49. The cross-section of the River Eider on 93.45 km was divided into 10 strips (Fig. 50) of different widths and then the velocity pertinent to each strip is calculated. The greatest velocity occurs in the deepest part of the cross-section. The velocity in the very shallow part, though very small, changes in a highly nonlinear manner. The tidal curve on 96.46 km of the river as computed by this method (Fig. 51) shows a remarkable agreement with gauge observations.

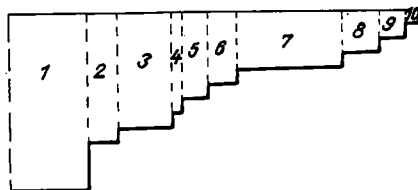
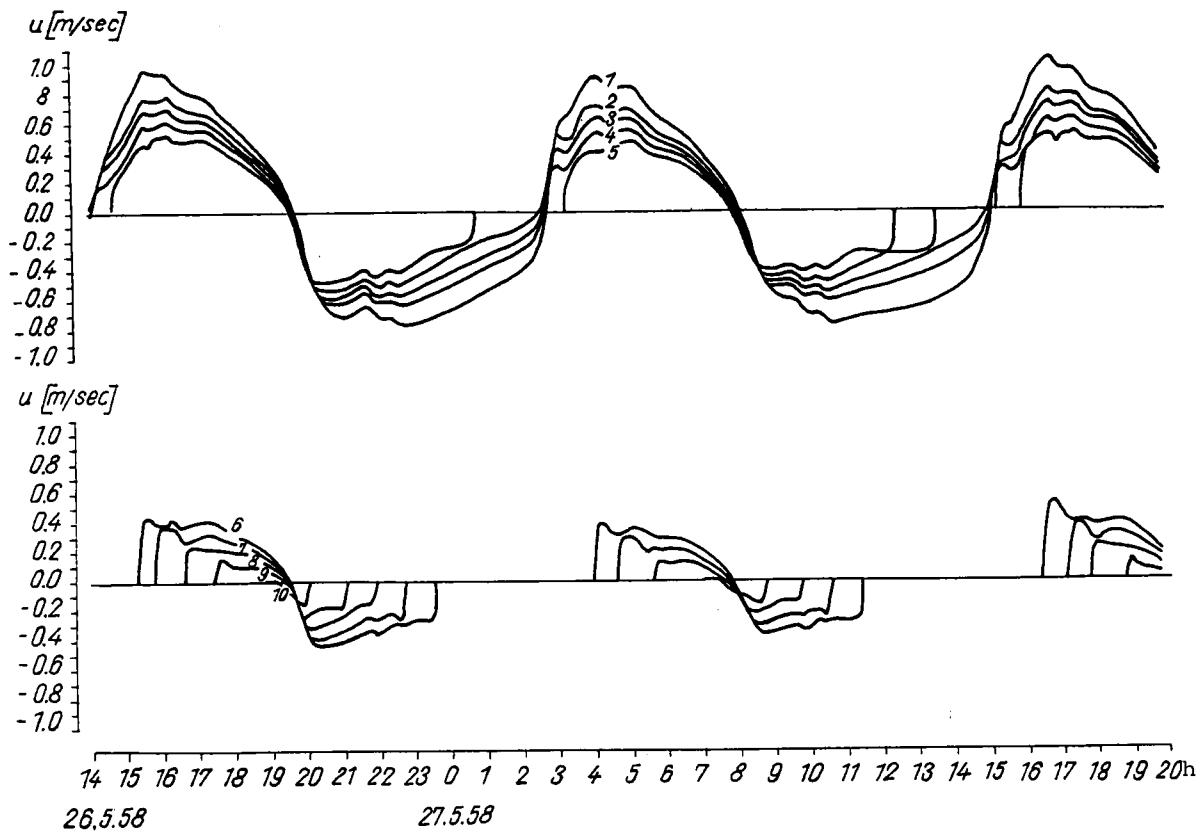


Fig. 50. VELOCITY DISTRIBUTION OF TIDAL CURRENTS, COMPUTED FOR EVERY STRIP OF A CROSS-SECTION OF THE RIVER EIDER ON 93.45 km , 26./27. MAY 1958.

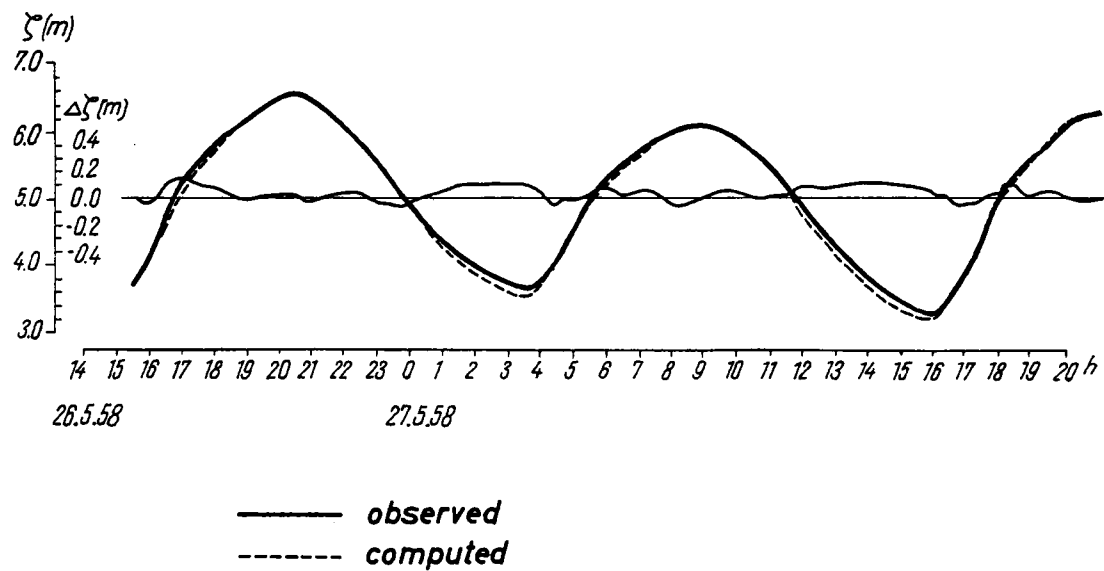


Fig. 51. WATER LEVEL IN THE RIVER EIDER (96.46 km DOWNSTREAM, 26./27. MAY 1958). THIN CONTINUOUS LINE - DIFFERENCE BETWEEN OBSERVED AND COMPUTED VALUES.

§4. A two-dimensional model of the River Elbe covering the area between Seemannshöft and Cuxhaven

A one-dimensional flow model as described by equations (6.18) and (6.19) with an adequate approximation of the cross-section may give an answer to many problems, see e.g. Ramming (1971). However, the depth varies considerably in the River Elbe and especially in the mouth of its complicated estuary. The islands in the Elbe, which certainly influence the currents, cannot be treated even by a network of channels with one-dimensional flow. The same is true of the drying banks which are characteristic of this estuarine region. In shallow water the influence of the nonlinear interactions on the dynamics of the boundary layers (at the bottom and surface) of the water column is of considerable importance.

A plot of water levels is very often extremely nonharmonic and the wave amplitudes may be of the same order as the depth. The water motion due to the very irregular bottom and coastal shape is rather complicated. Therefore, the channel approximation in a network model may reproduce this flow only up to the first order of approximation. Also, the Coriolis force and the cross-sectional component of velocity cannot be taken into account in a one-dimensional representation of the channel geometry.

It is evident that, in order to gain a deeper insight into the hydrodynamic processes, a two-dimensional system of equations and a grid with a small step size is required. This leads inevitably to an excessive demand on the storage capacity of the computer. To illustrate the situation let us take a grid spacing of $2h_x = 2h_y = 670$ m and a depth $H + \zeta = 24.2$ m. From the Courant-Friedrich-Lewy criterion (Chapter IV, 4.145) for an explicit numerical scheme we find

$$2T \leq 2h_x / \sqrt{2g(H + \zeta)} \quad (6.41)$$

and

$$T < 15 \text{ sec}$$

It would be necessary to use a grid of 36,000 points in the River Elbe to describe in a satisfactory manner all the geometrical irregularities of the river bed and banks.

Therefore a model has been developed which a) determines the water level ζ and the V component of velocity by means of an implicit diffe-

rence method described by equations (6.25) and (6.26), and b) calculates the U component of velocity by the usual explicit method. Since in the river the depth changes very rapidly across the river, a very fine mesh for water level and velocity has been chosen. The implicit forms of the equation were written along the same direction (here V is directed across the river).

The grid points in the direction of the main flow (U direction) were chosen with a much bigger step. Since the stability condition for the implicit method is less stringent than the condition for the explicit scheme, the overall time step was defined by the larger space distance along the main direction of flow in the river. Remarkable savings in computer time were achieved. Running times for the semi-implicit model were 1/5 to 1/10 of those for the fully explicit method.

Two-dimensional variables are usually placed in computer memory as a rectangular array with indices j,k. Such an approach makes very inefficient use of computer storage in our problem. To diminish the storage requirements we proceed as follows: First of all we organise ζ , U and V into triples even though they are defined at different grid points. Each triple is labelled as shown below.

One ζ -, U- and V-point each are forming a triple of the following form:

+ x M-K-1 .	+ x M-K .	+ x M-K+1 .	+ x M-K+2 .	+ x M-K+3 .
+ x M-1 .	+ x M .	+ x M+1 .	+ x M+2 .	+ x M+3 .
+ x M+L-1 .	+ x M+L .	+ x M+L+1 .	+ x M+L+2 .	+ x M+L+3 .

where

M	index of the actual triple	+	ζ -point
K	index-difference concerning the triple over M	x	u-point
L	index-difference concerning the triple below M	.	v-point

Next, we shall use, instead of two-dimensional indices, which lead to a large rectangular array with many points outside the river domain, one-dimensional enumeration, as will be described in chapter VIII, §3.

We shall enumerate all triples in succession along each line in the y direction starting at Cuxhaven. The point with label P will have the obvious numeration for the neighbouring points on the left and right hand side, but, in order to identify the triples above and below, information on a serial number of line and the overall number of triples in each line should be given.

The numerical solution of the flow problem in the River Elbe as presented by equations (6.28) and (6.31) can be carried out by the line-factorization method. As Ramming (1971) demonstrated, Banachiewicz's method (1938) is better than the line-factorization method.

§5. Approximation of the coast-line

The coast-line of the River Elbe, because of its complicated shape and enormous changes in river width, could hardly be approximated by a boundary with a grid step of several hundred meters. Such a boundary as presented in fig. 52 (upper part) does not reproduce a natural coast-line correctly. The rectangular grid region is either too large and includes a land area, or it is so small that part of the water region is neglected. Therefore, at the boundary, instead of a grid distance defined by $x = jh_x$, $y = kh_y$, where $j, k = 1, 2, \dots$, noninteger values of j, k will be taken. Usually j, k is taken as 0.25, 0.50 or 0.75. In this manner, the refined approximation of the coast line will be achieved. The parallel shifting of the boundary will cause a change of position of the U- and V-points at the margins. However, the modified grid distance between the points of velocity at the boundary and the nearest distance to the boundary points do not enter the equation, since the normal component of velocity disappears at the boundary. In the numerical computations equations (6.25) and (6.26) are used, though at the boundary the equation of continuity is set in a special form to account for the variable grid

$$\frac{\zeta_{j,k}^{1+1} - \zeta_{j,k}^{1-1}}{2T} = -\frac{1}{4h_y L_1} [(H + \zeta)_{j,k+1} (V_{j,k+1}^{1+1} + V_{j,k+1}^{1-1}) - (H + \zeta)_{j,k-1} (V_{j,k-1}^{1+1} + V_{j,k-1}^{1-1})] - [(H + \zeta)_{j+1,k} U_{j+1,k}^1 - (H + \zeta)_{j-1,k} U_{j-1,k}^1] \frac{1}{2h_x L_2} \quad (6.42)$$

where L_1 and L_2 are nondimensional numbers which take values smaller or greater than 1 when the grid distance at the boundary is smaller or greater than h_x and h_y respectively.

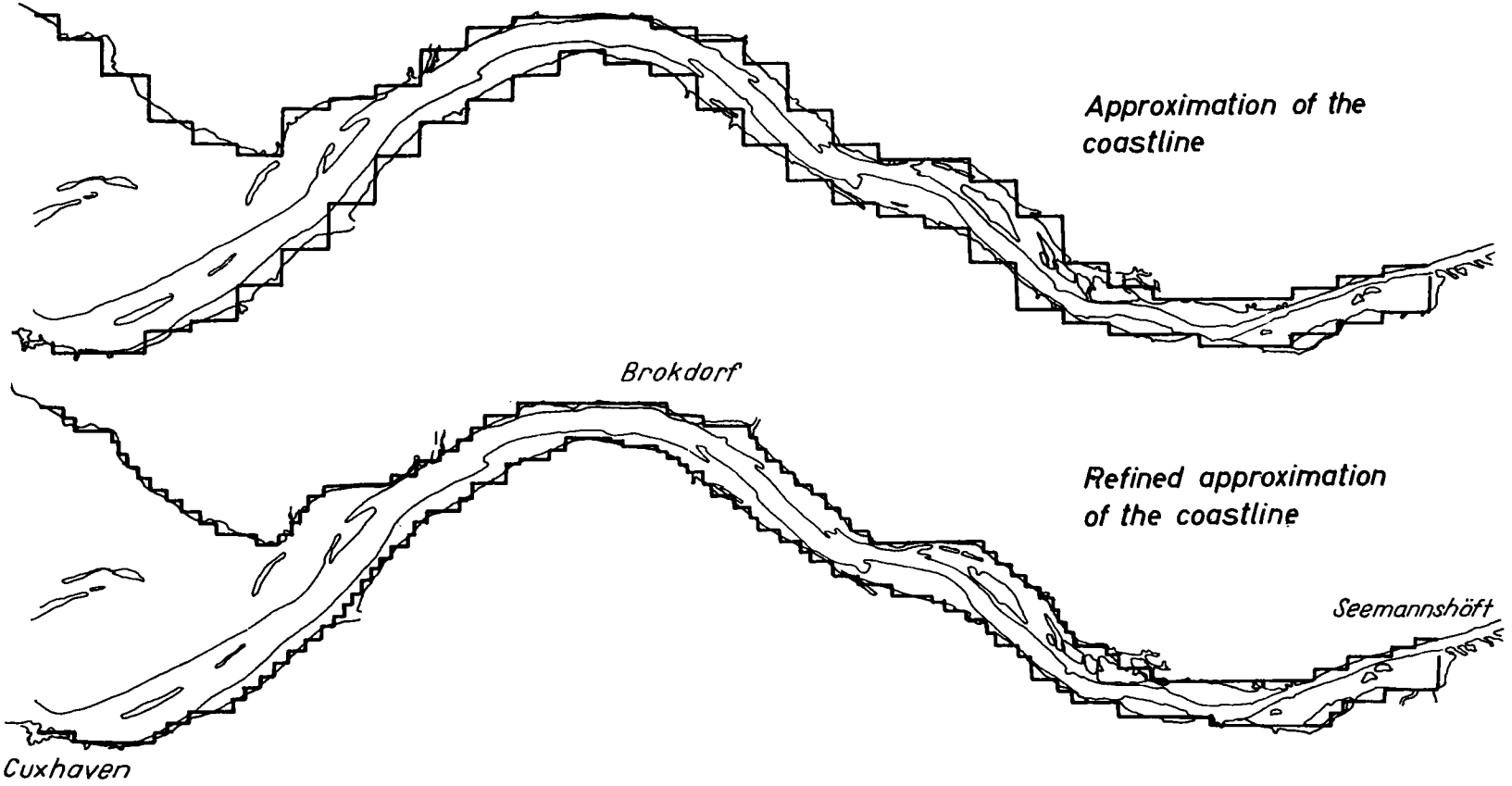


Fig. 52. MODEL OF THE RIVER ELBE BETWEEN CUXHAVEN AND SEEMANSHÖFT.

those grid points $H + \zeta > 0$. Again in the calculations a water level from the neighbouring point is implemented. In the above consideration it is assumed that the depth between the grid points is known. If this is not the case, we imply the linear variations of the depth.

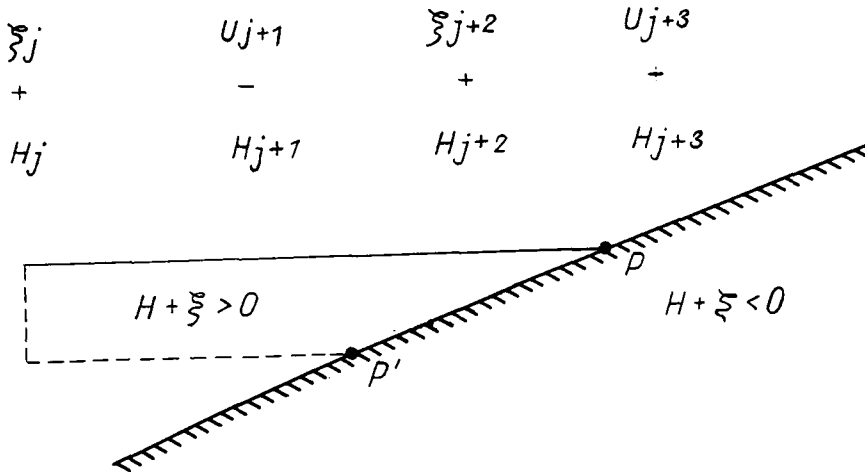


Fig. 53. A SKETCH TO ILLUSTRATE PROCESSES ON TIDAL FLATS.

With regard to this at each time step the water depth and the morphology of the neighbourhood of an actual grid point (U, V, ζ) must be proved concerning the physical possibility of transport directions. Furthermore, it must be observed that an overflowing or backflowing process of extreme shallow water is not dependent on the grid distance, but is proceeding according to physical laws and will be introduced into the numerical treatment by gathering the progress of the water-line.

In explanation regarding conditions to be set up the following sketch may be given

ζ (m)	U (m)	ζ (m+1)	U (m+1)
+	x	+	x
H_z (m)	H_U (m)	H_z (m+1)	H_U (m+1)

For the following examinations it must be observed that the depths H_U and H_z beyond the undisturbed sea surface must have a positive

Let us note that if the boundary is normal to the x-axis, the equation of motion at the boundary in the x direction simplifies to

$$fV = g \frac{\partial \zeta}{\partial x} \quad (6.43)$$

and the component of the slope at the boundary can be easily estimated from (6.43) at any time step on the assumption that the V component of velocity is known from the equation

$$\frac{\partial V}{\partial t} = -g \frac{\partial \zeta}{\partial y} - \frac{rV|V|}{H + \zeta} \quad (6.44)$$

On the other hand, if a section of the boundary is perpendicular to the y-axis, the equation of motion yields

$$fU = -g \frac{\partial \zeta}{\partial y} \quad (6.45)$$

$$\frac{\partial U}{\partial t} = -g \frac{\partial \zeta}{\partial x} - \frac{rU|U|}{H + \zeta} \quad (6.46)$$

The new (shifted) boundaries, when applied to the River Elbe, are plotted in fig. 52 (lower part).

§6. Modelling the flooding and uncovering of tidal flats

In areas of shallow water in the coastal zone the flooding and uncovering of islands, tidal flats and coast-lines is an important feature. The area under water varies with time in response to tide, wind, river flow and bottom topography. The edge or boundary of this area appears, expands, coalesces with its parts, contracts and disappears in a periodic fashion. Clearly, the topology of this feature can be very complex when considered as a continuum. However, when it is represented on a grid of points, it is simplified considerably.

To explain the procedure let us consider the one-dimensional case depicted in fig. 53. Point P on the coast divides the 'wet' region, where the water depth $H + \zeta$ is positive, from the 'dry' region with $H + \zeta < 0$. Point P is moving in time along the coast and its position can be found from equation $H + \zeta = 0$. Actually we do not know the value of ζ in point P and therefore the water level from the nearest grid point, i.e. ζ_{j+2} , is taken. If we intend to compute a current at the point U_{j+1} or U_{j+3} a check is first done to make sure that in

sign and below the undisturbed niveau down to the bottom it must have a negative sign.

$$(\zeta(m), \zeta(m+1))_{\min} > (Hz(m), Hz(m+1), HU(m))_{\max} \quad (6.47)$$

then $U(m)$ will be determined by the equation of motion, and the actual depth for the friction term will be ascertained by

$$(\zeta(m), \zeta(m+1))_{\max} - (Hz(m), Hz(m+1), HU(m))_{\max} \quad (6.48)$$

Multiplying this water depth determined by $U(m)$ the transport to be considered in the equation of continuity is gained. If the condition (6.47) is not fulfilled, then it has to be proved, whether

$$(Hz(m), Hz(m+1), HU(m))_{\max} > (\zeta(m), \zeta(m+1))_{\min} \quad (6.49)$$

If the maximum depth is larger or equal to the minimum of the two neighbouring sea-levels, in the first instance it follows that $U(m)=0$, however the possibility cannot be excluded that the depth of transport to set up as agreed upon

$$HT = (\zeta(m), \zeta(m+1))_{\max} - (Hz(m), Hz(m+1), HU(m))_{\max} > 0 \quad (6.50)$$

In this case the length of the water flow s_n has to be checked and whether the next grid point of the water-line has been reached in such a case.

If $s_n <$ grid distance, then s_n will be stored and added to the distance newly determined at the next time step. This addition will be repeated time step by time step until $s_n \geq$ grid distance. Only in this case $U(m)$ will be determined.

The appertaining direction of the velocity is resulting from the slope of the sea surface between the two neighbouring ζ points.

It is necessary to distinguish all thinkable cases, because it is possible that from time to time in some points there will be no water. One has to check the neighbourhood of each grid point from time step to time step with regard to the actual water depth, the depth distribution and the physical possibility of transports and directions of transports. It is also necessary to pay attention to the velocity of the overflow and the draining processes of extremely shallow water in order to make sure that the process in nature is in a good agreement with the process in the hydrodynamic-numerical model. The covered

distance of water is computed and it will be checked if the next grid point has been reached. With this simple method one can find out the motion of the water-line.

During the treatment of the continuity equation it should be checked whether $H + \zeta \leq 0$. It will be sensible to select 0.02 m as a coefficient datum. If $H + \zeta \leq 0.02$, then the area represented by this point will be considered as dry and $\zeta = -H$ is applied. The values $H + \zeta \leq 0.02$ will be stored by points and are then again transported to the point if $H + \zeta > 0.02$, i.e. if the actual water depth exceeds this value. Thus it will be possible that mass deviations may occur in time steps, but over a tidal cycle, the masses will be maintained.

Let us first consider a simplified example of a basin which is open at one side and has a bottom slope of 1.6 ‰ and is 13,200 m in length (Fig. 54). At the closed end of the basin the velocity vanishes and along the open boundary the water level is prescribed as

$$\zeta = 50.0 \cos \omega t \quad (\text{in cm}) \quad (6.51)$$

where $\omega = 2\pi/43200 \text{ sec}^{-1}$.

The grid distance is equal to 1200 m, and the equations (6.207) and (6.21) with $r = 3 \times 10^{-3}$ are applied. In fig. 54 the free surface shape in the vicinity of the coast at 0, 3, 6 and 9 hours is plotted.

The next example concerns the 'Neuwerker Watt', including the isle of 'Scharhörn', near the estuary of the River Elbe. The domain is shown in fig. 55 and is covered by a rectangular grid of step size 670 m. The depth distribution of this region is very complicated and the tidal amplitude reaches 3.0 m. The height of the dike near 'Neuwerk' is 5.4 m. From the observed sea-level data taken from gauge records at the points A, B and C in fig. 8, we chose the periods 29th September to 3rd October and 15th to 17th October 1967.

A comparison of the computed and observed sea-level as a function of time is presented in fig. 56. The differences in amplitude are less than ± 6 cm. Such a good reproduction of the tidal processes in the region of the 'Neuwerker Watt' and other derived results show that the hydrodynamic-numerical method is able to reproduce very complex hydrodynamic processes in extremely shallow areas with remarkable accuracy.

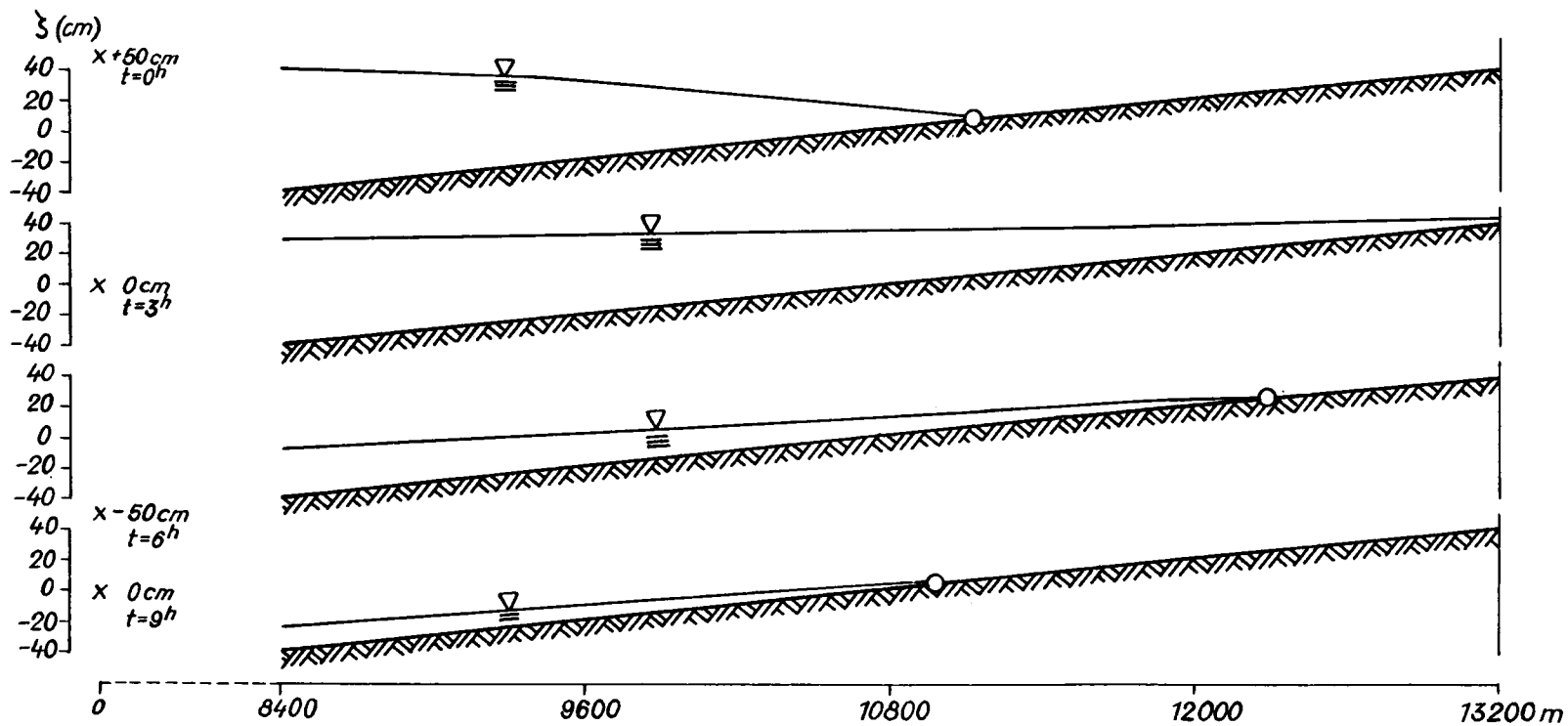


Fig. 54. WATER LEVEL DISTRIBUTION IN A CHANNEL WITH SLOPING BOTTOM.
 x - LEVEL AT THE OPEN BOUNDARY, o - POINT WHERE $\zeta = -H$.

OUTER ELBE



Fig. 55. LOCATION OF THE POINTS A,B AND C IN THE NEUWERKER WATT, WHERE MEASUREMENTS OF SFA-LEVEL WERE TAKEN

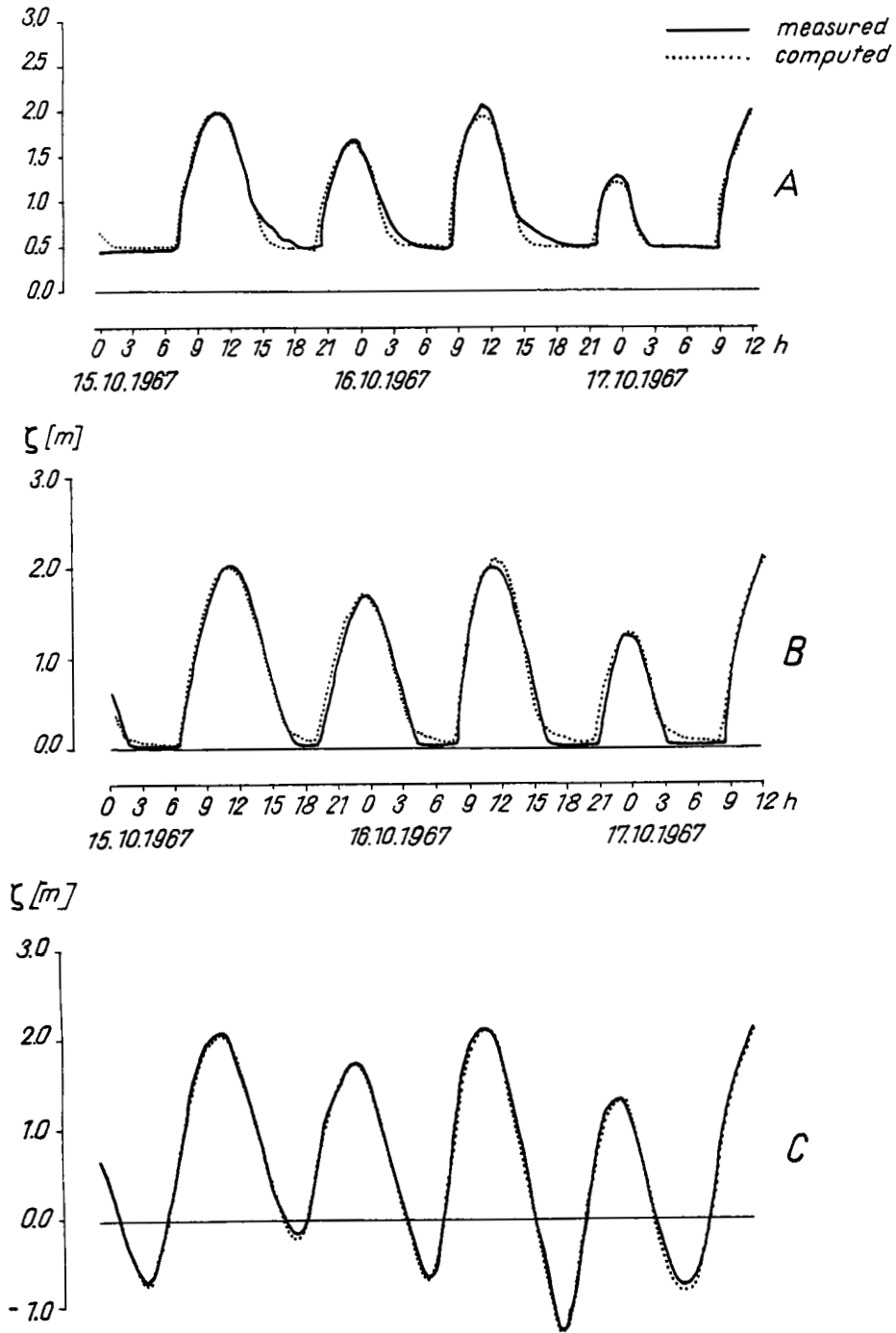


Fig. 56. OBSERVED AND COMPUTED SEA-LEVEL IN THE CENTRE OF THE NEUWERKER WATT (OUTER ELBE).

§7. A special treatment of the bottom friction in extremely shallow waters

The dependence of bottom stress on the velocity and depth is confirmed by a great deal of research under a variety of field conditions (Chapter I, §4). However in storm surges and in the behaviour of long waves knowledge of the bottom stress is still far from satisfactory. This situation is due entirely to the complicated hydrodynamics of turbulent flow in the bottom boundary layer, see e.g. Collins (1963), Kitajgorodski (1970). In the study of this problem the early work of Reid (1957) is also relevant. He assumed that the bottom stress is a function of surface stress with a nondimensional constant. Yamada (1959) derived an analogous expression

$$\tau_b = \frac{3k}{H^2} U - \tau_s/2 \quad (6.52)$$

In (6.52) knowledge of the vertical eddy viscosity k is presumed.

A general solution to the problem may be approached through the integration in time of the nonaveraged equations of motion and after that describing the bottom stress through the definition

$$\tau_b = -\rho k \frac{dU}{dz} .$$

This leads to a very complicated but not insoluble problem as was shown by Jelesnianski (1967). A recent attempt has been made by Nihoul (1977). An interesting relationship between the nonlinear and linear expressions of the stress in tidal flow was demonstrated by i.e. Provost (1974).

A new unresolved problem arises in very shallow areas when the free surface oscillations are of the same order as the depth. In these natural conditions a new modified expression for the bottom friction coefficient will be presented based on the comparison of observed and calculated water level and on numerical stability considerations. But, first, let us try to estimate the magnitude of the friction coefficient and its time fluctuation during one tidal period at an arbitrary place on the river. The following simplified method can be applied. With the help of water levels recorded by tide gauges and the known geometry of a cross-section the average velocity is calculated by cubature. Then the equation of motion (6.19) is used to present the friction coefficient in the form

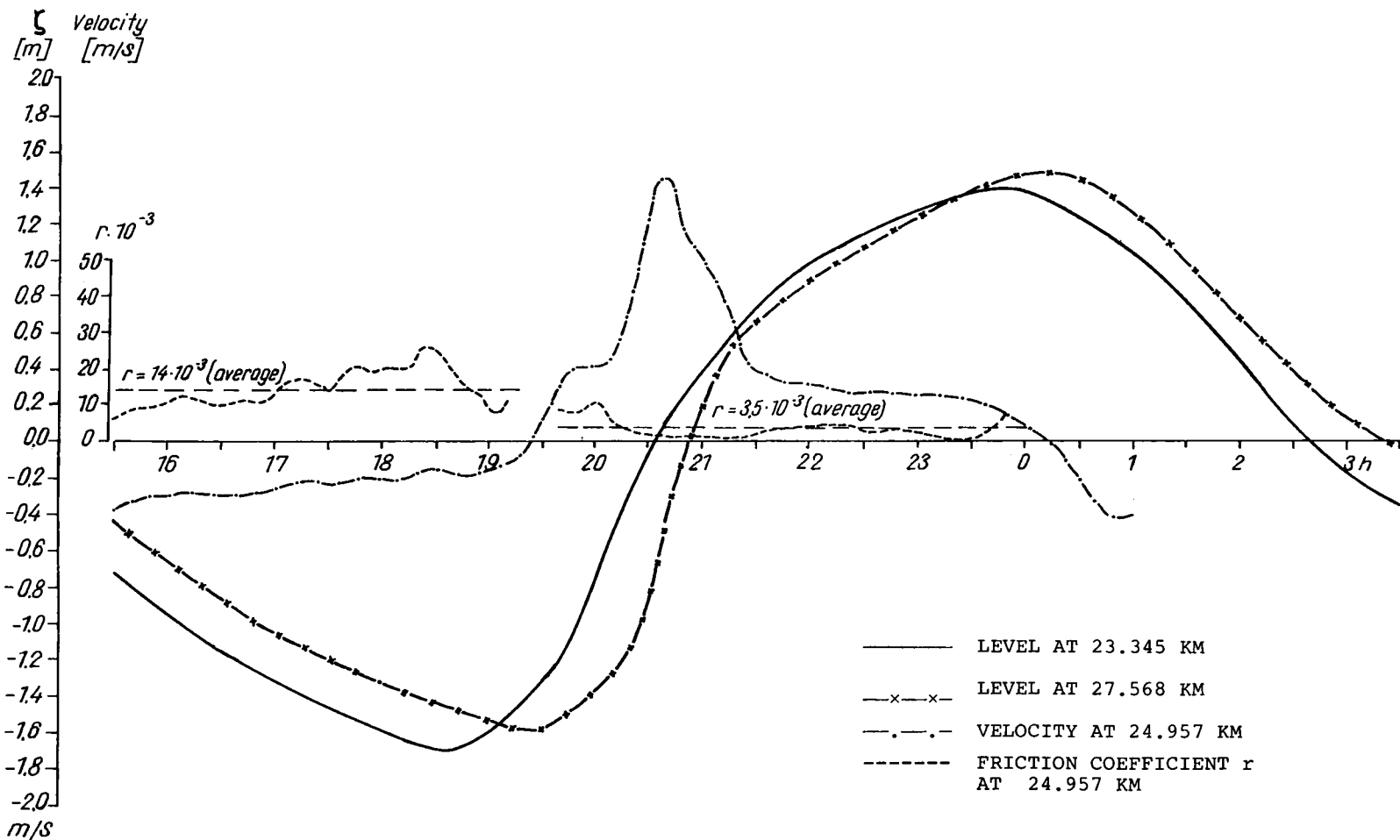


Fig. 57. FRICTION COEFFICIENT r CALCULATED BY EXPRESSION (6.59) BY MEANS OF RECORDED WATER LEVELS AND VELOCITIES DERIVED FROM THE EQUATION OF CONTINUITY.

$$r = \frac{1}{U|U|} \left(\frac{\partial U}{\partial t} + g \frac{\partial \zeta}{\partial x} \right) (H + \zeta) \quad (6.53)$$

With the possible exception of time intervals around the points K_e and K_f when the velocity U is zero, the true value of r is derived. The magnitude of r as calculated by this method is not constant throughout the tidal period, but it varies, mainly due to the unsteadiness of the river geometry. An example of the computed variation of the friction coefficient, together with the water level and calculated velocity for the cross-section of the River Eider near Friedrichstadt, is plotted in fig. 57.

It should be stressed that the overall value of the coefficient is an average of all existing coefficients, and sometimes it may be very far from a local condition. The possibility of such averaging depends strongly on the assumption of small variations of bottom roughness along the river length and that the effects of resistance due to the geometry of the river are considered by an additional term in the equation of motion.

Returning for the moment to fig. 57, it may be observed that a) the time of maximum velocity does not correspond exactly with the time of zero water level, and b) the time of zero velocity is not exactly in phase with the maximum (or minimum) water level. This phase difference α is due entirely to the bottom friction. The bottom stress can be defined in terms of α in the following manner (Ippen and Harleman, 1966)

$$\tau_b = \frac{2\pi}{T} U \tan 2\alpha \quad (6.54)$$

Let us now consider the numerical problems which arise in connection with shallow water dynamics. An application of the friction term in the equations of motion leads to proper results when the depth is more than 10 m. In shallow water with an actual depth of 3 - 4 m the stability of the numerical scheme is difficult to handle. To present the problem let us consider a one-dimensional system of equations

$$\frac{\partial U}{\partial t} + \frac{rU|U|}{h + \zeta} = -g \frac{\partial \zeta}{\partial x} \quad (6.55)$$

$$\frac{\partial \zeta}{\partial t} + \frac{\partial}{\partial x} [(H + \zeta)U] = 0 \quad (6.56)$$

The explicit mixed difference-differential form of (6.55) is

$$U^{l+1} = U^l (1 - rT|U|/(H+\zeta)) - gT \frac{\partial \zeta}{\partial x} \quad (6.57)$$

which shows that the first term on the right hand side of (6.57) describes a dissipation due to the bottom friction. The numerical stability is preserved if

$$1 - rT|U|/(H+\zeta) > 0 \quad (6.58)$$

Otherwise a flow of energy is present and this leads to numerical instability.

It is obvious that this important condition is violated in very shallow water, for instance when $H + \zeta = 0.1$ m and $U \neq 0$ m/sec. Therefore, the difference scheme has to be modified in such a way that the physical law of energy conservation is not violated in very shallow water.

The simplest ad-hoc solution is to set the friction term in an implicit form

$$U^{l+1} - U^l = - rT U^{l+1} |U|/(H+\zeta) \quad (6.59)$$

and thus

$$U^{l+1} = U^l / [1 + rT|U|/(H+\zeta)] \quad (6.60)$$

From (6.60) stability follows, but in the case of $(H + \zeta)$ being very small, the situation becomes obscure.

Analysing (6.57) one may come to the conclusion that whenever condition (6.58) is violated, the expression (6.57) can be reduced to

$$U^{l+1} = - gT \frac{\partial \zeta}{\partial x} \quad (6.61)$$

By means of the following arguments one can show that this neglect leads to a non-acceptable result:

- a) the neglect of the whole term is not correct, because in that case the velocity is only determined by the gradient term $g \frac{\partial \zeta}{\partial x}$ without consideration of the velocity in the time step before
- b) if we consider the equation of continuity (6.56) and substitute u by $g \frac{\partial \zeta}{\partial x}$ then it follows

$$\frac{\partial \zeta}{\partial t} + \frac{\partial}{\partial x} (g(H+\zeta) \frac{\partial \zeta}{\partial x}) = 0 \quad (6.62)$$

After some simple transformations and neglects of terms which have a second deviation it comes out the equation

$$\frac{\partial \zeta}{\partial t} + g \frac{\partial H \partial \zeta}{\partial x \partial x} \approx 0 \quad (6.63)$$

The variation of depth at the flats and sands is very small, that is equivalent to $\frac{\partial H}{\partial x} \approx 0$, and one can say as a first approximation

$$\frac{\partial \zeta}{\partial t} \approx 0 \quad (6.64)$$

This means a stop of the water motion at those areas or in those discrete points of the model where the bottom friction term had been neglected because of the small actual water depth. The sands and flats are not uncovered because the given condition is incorrect. The results obtained are not satisfactory. In nature these water masses flow with relatively high velocity into the narrow channels so-called 'Priele'. In the numerical model these water masses are missing, they are not present at other discrete points which now have a phase displacement.

It is also possible to solve an explicit numerical scheme by varying the time step in order to preserve the inequality in (6.58). To avoid such a complicated procedure the expression for the friction term will be modified in such a manner that stability will hold at an arbitrary depth.

The depth variation of the friction coefficient r can be inferred by setting $r = \frac{1}{32} (\log_{10} 14.8H/10.0)^{-2}$.

The latter follows from the logarithmic distribution of velocity (Chapter I) with an assumed size at the bottom equal to 0.1 mm.

Another approach consists of the introduction of a generalized function to describe the dependence of the bottom friction coefficient on depth (Ramming, 1976)

$$\tau_b = rU|U|/(H+\zeta) = rU|U|(H+\zeta+H_0 e^{-pH})/(H+\zeta+H_1) \quad (6.65)$$

The parameters H_0 and H_1 , which have the dimensions of depth, can be set in an arbitrary way. Numerical experimentation showed that the best results may be obtained with $H_0 = H_1 = 1$ m. The exponential parameter p is taken from the range 0.5, 1, 2, ..., 10. Usually $p = 1$ was taken.

A comparison of the different expressions for the dependence of

$$1) \frac{1}{H}$$

$$2) \frac{1}{H+H_1} \text{ with } H_1=1, H=h+\zeta$$

$$3) - 13) \frac{1}{(H+H_1)^2} \times (H+H_0 e^{-pH}) \text{ with } H_1 = H_0 = 1$$

$$p = 0.5; 1; 2; \dots \dots 10$$

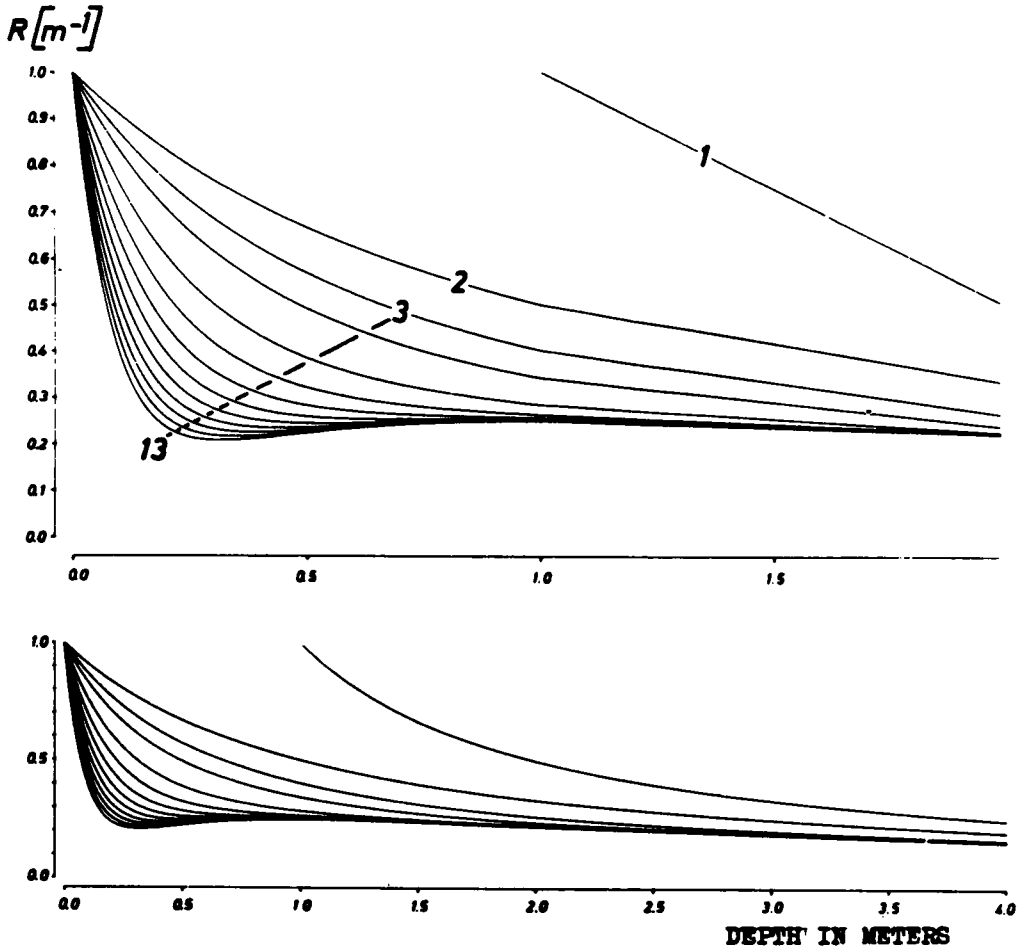


Fig. 58. THE DEPENDENCE OF DIFFERENT FRICTION TERMS ON DEPTH (I).

A : $R = \frac{f}{H}$

B : $R = \frac{r}{H+H_1}$

C : $R = \frac{r}{(H+H_1)^2} (H+H_0 e^{-H})$

D : $R = \frac{f}{8H}$

E : $R = \frac{f}{8(H+H_1)}$

F : $R = \frac{f}{8(H+H_1)^2} (H+H_0 e^{-H})$

$r = 0.003$

$H = h + \zeta$

$H_1 = H_0 = 1$

$f = \frac{1}{4} \left(\log_{10} \frac{14.8 H}{0.10} \right)^{-2}$

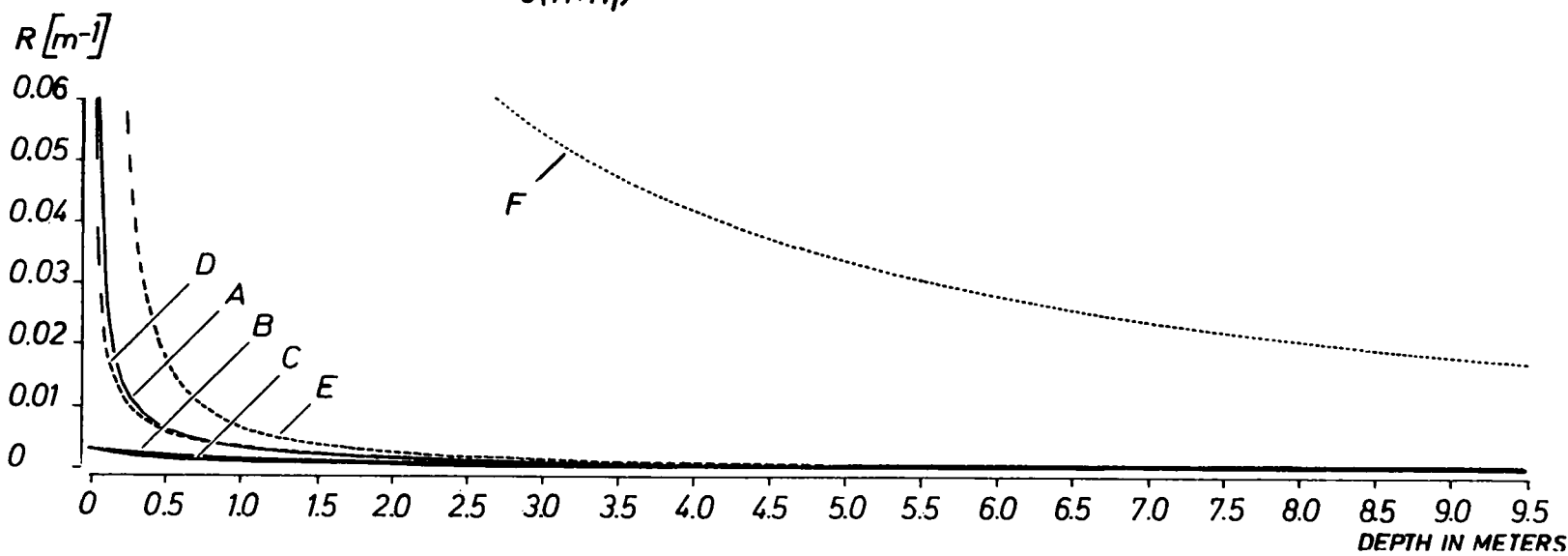


Fig. 59. THE DEPENDENCE OF DIFFERENT FRICTION TERMS ON DEPTH (II).

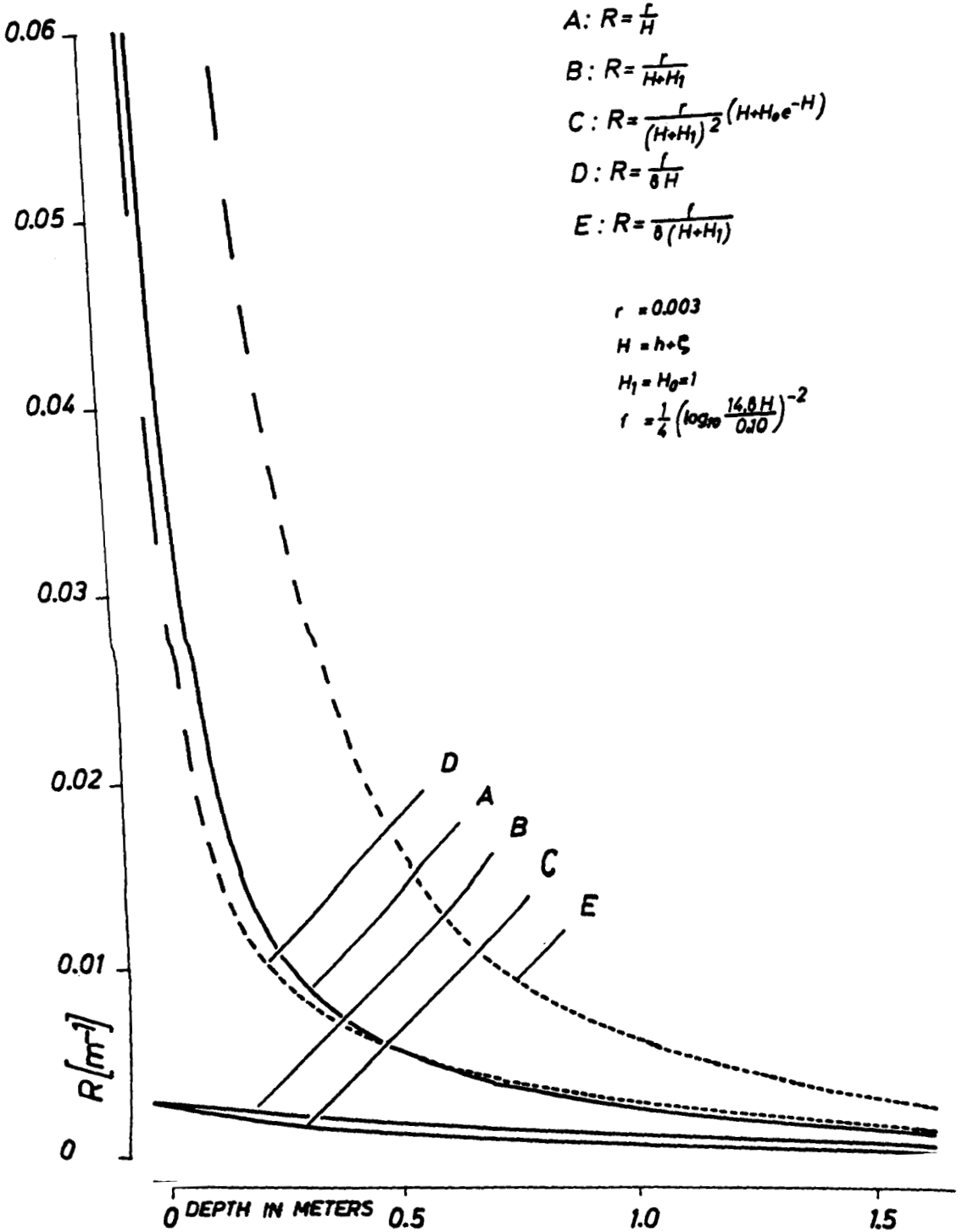


Fig. 60. THE DEPENDENCE OF DIFFERENT FRICTION TERMS ON DEPTH (II), SMALLER SCALE.

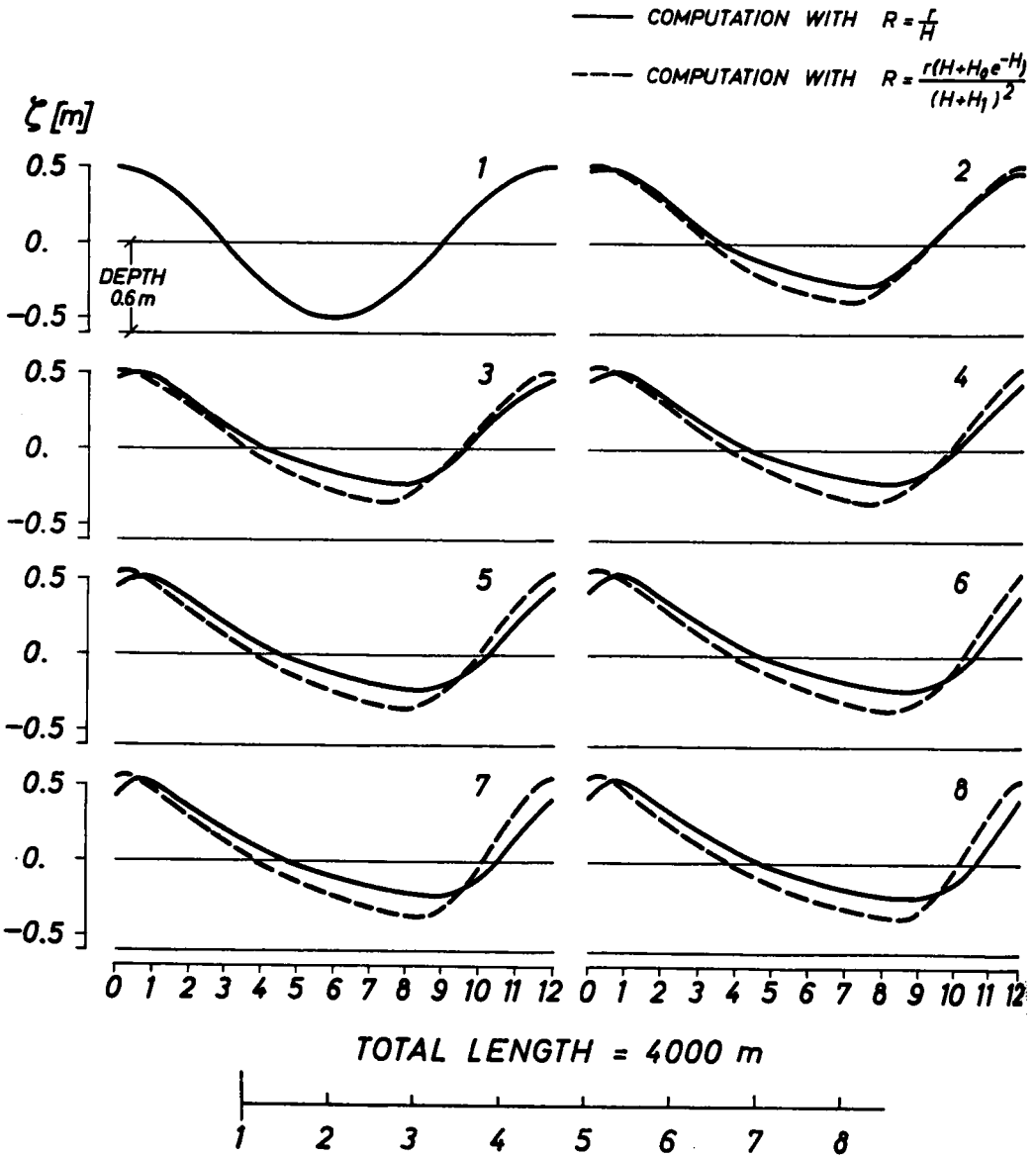


Fig. 61. COMPUTED SEA-LEVEL VARIATION AT DIFFERENT POINTS 1 - 8.

bottom stress on depth in very shallow water is given in figs. 58 - 60.

A uniform channel which is closed at one end (point 8) and forced sinusoidally at the other end (point 1) was used. The distance between the sections was 500m. The computed water levels at the eight points are shown in fig. 61.

To investigate the validity of (6.65) computations were performed with two different laws of bottom friction at 80 points in the German Bight. The results at two selected points are presented and compared with the tide gauge observations in fig. 62.

Generally, the new expression leads to a better description of amplitude and phase in the regions of high and low water. Returning for the moment to our starting point, i.e. to the condition (6.58) we may write it now as

$$1 - rT \left| U \left(\frac{H + \zeta + H_0 e^{-pH}}{H + \zeta + H_1} \right) \right| > 0 \quad (6.66)$$

Through a proper choice of H_0 , H_1 and p , (6.66) may hold for the arbitrary values of $H + \zeta$. It seems that further study is still required to clarify all the physical and mathematical aspects of this problem.

§8. Residual currents

When planning hydraulic works it may be of use to consider not only the periodic changes of current but also the possible existence of a residual value of current when the process is regarded over a tidal period. A residual circulation is formed when the nonlinear terms due to the bottom stress and advection are included in the equation. This kind of motion, presented for the North Sea by Nihoul (1976) and Maier-Reimer (1977), shows a good agreement with measurements. Although the overall current is rather small, it may influence the exchange of water masses and the motion of particles suspended in the water. The residual current or mean transport velocity is defined in the following manner for a one-dimensional case

$$u = \int_0^T (H + \zeta) u \, dt / \int_0^T (H + \zeta) \, dt \quad (6.67)$$

where T is the tidal period. Assuming that the tide wave propagates along the x direction, we take the velocity as

$$u = u_0 \cos \left(\frac{2\pi}{T}t - \frac{2\pi}{L}x \right) \quad (6.68)$$

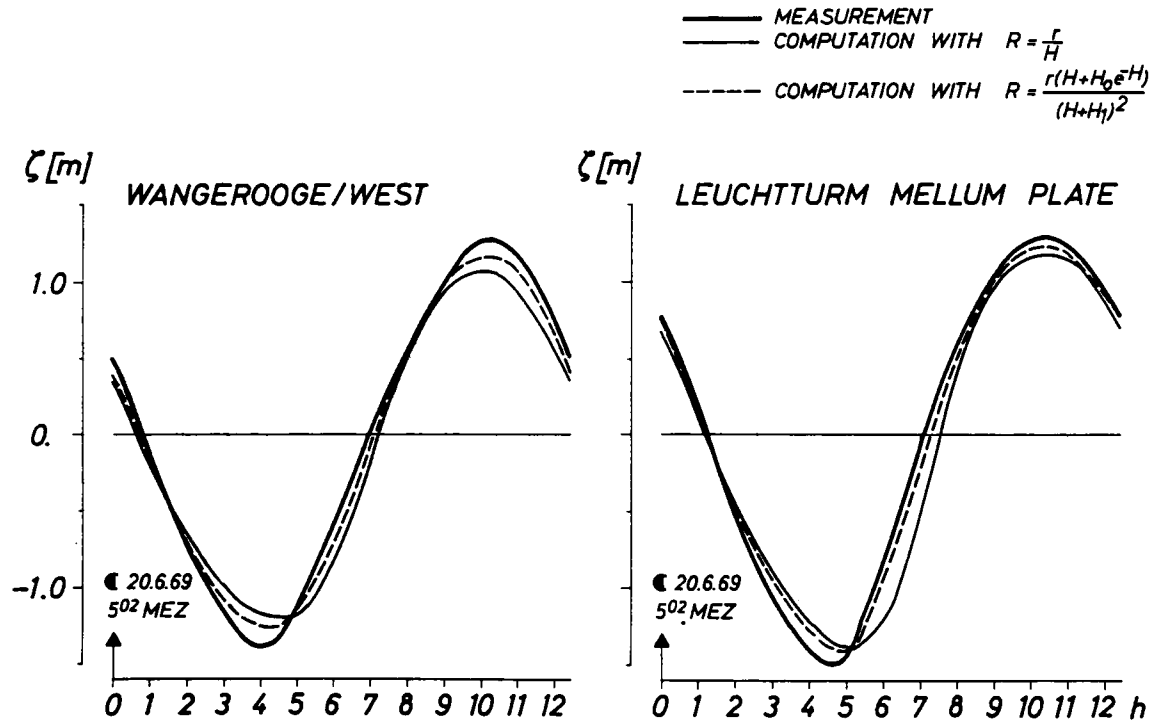


Fig. 62. COMPARISON BETWEEN MEASURED AND COMPUTED WATER LEVELS AT TWO SELECTED POINTS IN THE GERMAN BIGHT FOR TWO DIFFERENT LAWS OF BOTTOM FRICTION.

From the equation of continuity, expression (6.68) yields for the water level variations

$$\zeta = u_0 \frac{HT}{L} \cos\left(\frac{2\pi}{T}t - \frac{2\pi}{L}x\right) \quad (6.69)$$

Finally introducing (6.69) and (6.68) into (6.67), the following expression for the residual current is derived

$$u = u_0^2 / 2\sqrt{gH} \quad (6.70)$$

We shall apply equation (6.67) to produce a picture of residual current distribution in the German Bight (Ramming, 1978). The amplitude and current distribution were calculated for the normal-tide 1971. The residual current was estimated using expression (6.60). The results are plotted in fig. 63. The main features of the current distribution can be summarized as follows. Between Seemannshöft and Stadersand strong residual currents appear which are directed down-stream. The different directions of the residual flow in the region of Grauerort are possibly due to the influence of the islands. A remarkably high level of residual current (up to 30 cm/sec) occurs near Kolmar. In this part of the River Elbe pronounced slopes in the water surface as well as high velocities occur in the tide wave.

The region of negligible residual currents is situated between Glückstadt and Brunsbüttelkoog. This part of the river is marked by a turbidity zone and a zone of high seston concentration (Fig. 64).

In the navigable waters near Otterndorf and Cuxhaven the currents of 5 - 10 cm/sec are directed towards the estuary. Otherwise the distribution of current in this region is very varied, probably due to the complicated morphological structure. An extremely large value of current (30 - 40 cm/sec) is observed towards the north from Otterndorf and it may contribute to the permanent morphological variations in this part of the estuary.

The pattern of residual currents presented above suggests the possibility of a deeper insight into the dynamic processes which are modelled by the hydrodynamic-numerical method.

§9. The application of the grid refinement and the irregular grid

When the area of integration is a complex one, it is obvious that the topography cannot be approximated in a satisfactory manner, when the resolution of the grid is coarse. Details, like narrow channels,

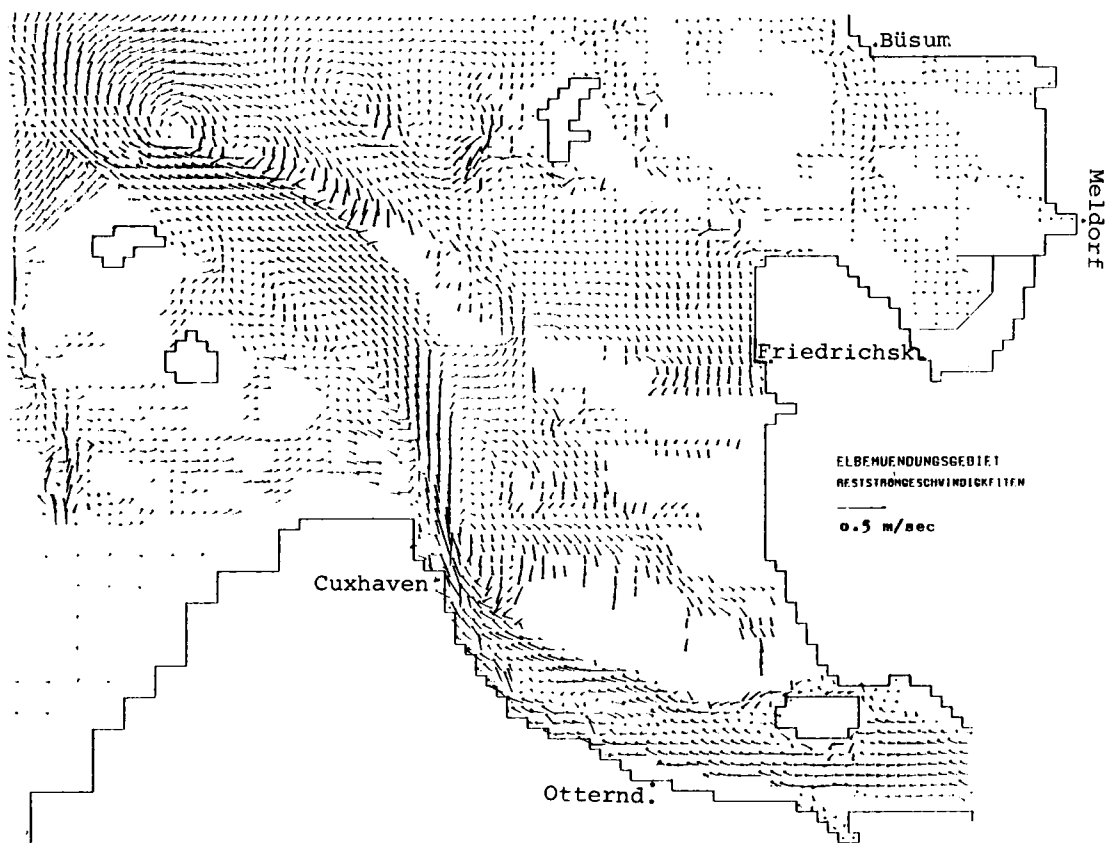


Fig. 63. ELBE ESTUARY, VELOCITY DISTRIBUTION OF RESIDUAL CURRENTS.

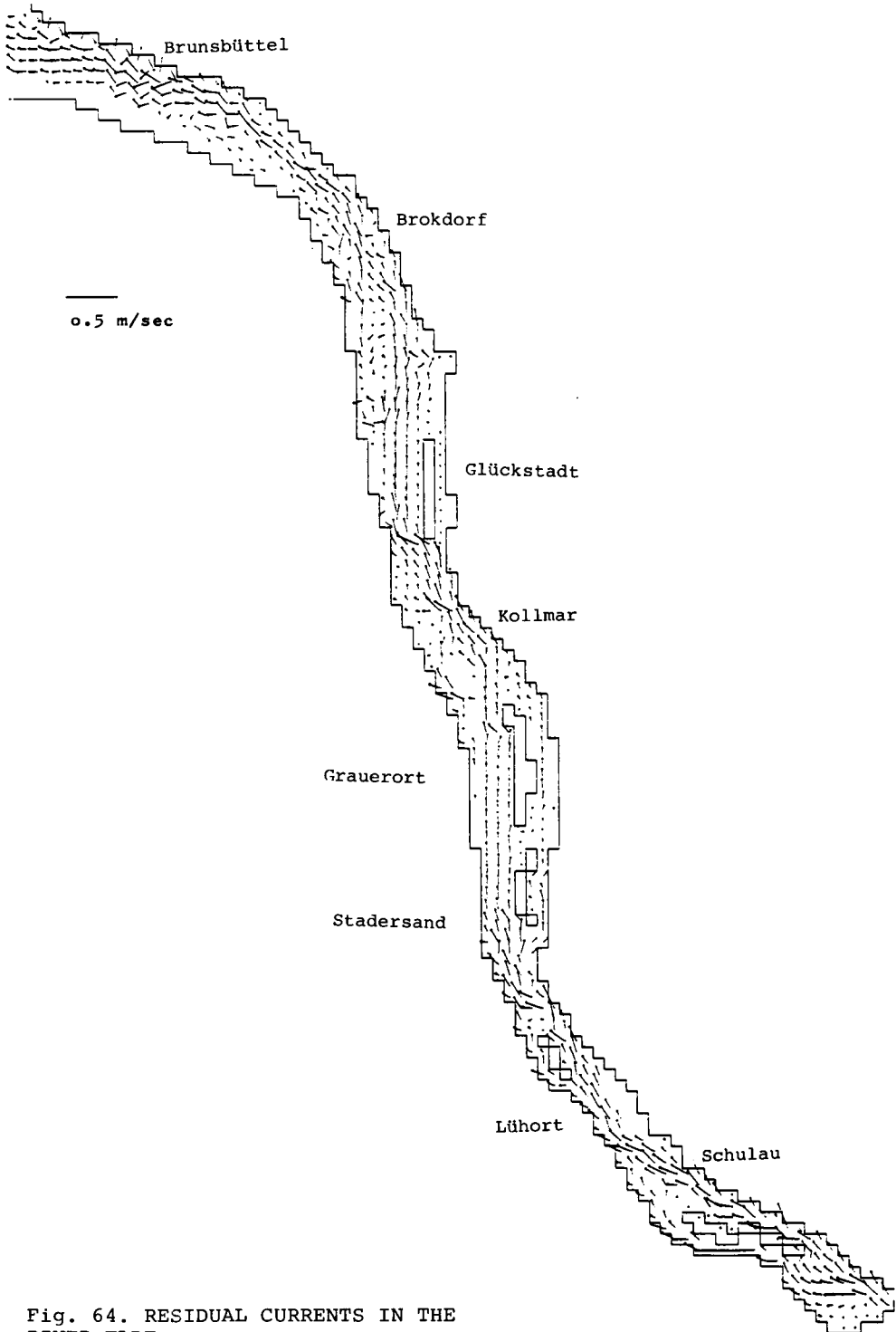


Fig. 64. RESIDUAL CURRENTS IN THE RIVER ELBE.

waterways, constructions influencing the velocity field and the exact location of water gauges in the shallow areas, will not be included in the model and the computations.

In this respect there exist several possible solutions, two of which will be presented here. Firstly, a coarse grid may be connected to a fine grid in the region where higher resolution is needed. Secondly, a grid with irregular steps may be employed, using the smallest grid distance in the region of primary interest while the grid size increases and accuracy decreases with increasing distance from the region of high resolution. We shall dwell upon the second approach. Let us consider three points situated in an irregular grid along the x-axis with the grid distances $x_1x_2 = h_1$, $x_2x_3 = h_2$ in fig. 65.



Fig. 65. IRREGULAR ONE-DIMENSIONAL GRID.

Starting from the expressions (2.5) and (2.6) we use the Taylor series to define the derivatives of the function $f(x)$ at the central point x_2 in fig. 65 as follows

$$f(x_1) = f(x_2) - \frac{\partial f}{\partial x} h_1 + \frac{\partial^2 f}{\partial x^2} \frac{h_1^2}{2} - O(h_1^3) \quad (6.71)$$

$$f(x_3) = f(x_2) + \frac{\partial f}{\partial x} h_2 + \frac{\partial^2 f}{\partial x^2} \frac{h_2^2}{2} + O(h_2^3) \quad (6.72)$$

Subtracting (6.71) from (6.72) yields the first derivative

$$\frac{f(x_3) - f(x_1)}{h_1 + h_2} + \frac{\partial^2 f}{\partial x^2} \frac{(h_2^2 - h_1^2)}{2} = \frac{\partial f}{\partial x} \quad (6.73)$$

If $\frac{\partial^2 f}{\partial x^2}$ is of bounded magnitude the above derivative approximates the differential form only up to first-order accuracy in relation to the grid distance. The second-order approximation is attained in (6.73) in an equidistant grid where $h_1 = h_2$. Substituting (6.66) and other similar expressions into (6.1) and (6.2) we derive the finite-difference analogue on an irregular grid.

The system is much more complicated when it is compared with the system of equations set on an equidistant grid. However, quite often, various spurious effects are generated, resulting from the poor approximation.

Therefore the distortion of the solution may remove all the advantages we expected by introducing the grid refinement. One possible way to remove this effect is using a method which assures smooth variation of the functions and their derivatives from one grid point to another. If, instead of an irregular grid, the coarse equidistant grid is considered, and in certain regions the fine grid is superimposed, we have to cope with transition phenomena from a fine to a coarse grid. A great number of numerical experiments show that the transition is related to distortion in a smooth variation of flow. Koss (1971) presented a vortex system which is due to numerical approximation. Generally speaking, the different grids act like different media; in this way waves passing through the transition zone are reflected and distorted.

Relating the process of propagation to the idea of characteristic and defining the characteristic direction as $\Delta x/\Delta t$, one may observe the change in $\Delta x/\Delta t$. It is quite obvious that the change will not occur if the time-space interval is changed on both sides of the transition zone accordingly, that is in the smooth way.

One of the best methods of fitting smooth curves or surfaces to a set of data is the method of splines. When the method is applied to a system of difference equations on an irregular grid, it results in a considerable increase in spatial accuracy.

In this way we not only gain a smoothing effect but also a tool for obtaining higher accuracy in numerical integration. Usually one works with cubic splines (Ahlberg et al., 1967). The cubic spline $S(x)$ is a cubic interpolation of the variable S_j given only at grid points $j = 1, 2, \dots, J$. Through an appropriate set of equations continuous values of $S'(x)$ and $S''(x)$ are ensured. In this way the transition effects at the boundary between coarse and fine grids are smoothed out since they are essentially due to the discontinuity in $S'(x)$ and $S''(x)$ at the grid points on the boundary.

Simpler methods than the spline technique very often provide quite satisfactory results. Ramming (1976) has presented a method of refining a grid using a factor of refinement $1/n$ where n is an odd number ($1/n = 1/3, 1/5, 1/7, \dots$). The so-called one-third refinement was found to be satisfactory. With this technique the transition between coarse and fine grids can be coped with numerically and additional refinements-if required - can be easily implemented in a nested sequence (see fig. 66). The left side of fig. 66 shows the grid when the neighbourhood points U, V and ζ are taken as one triple point. The system of node numbering used here is obtained by abandoning the two-dimensional

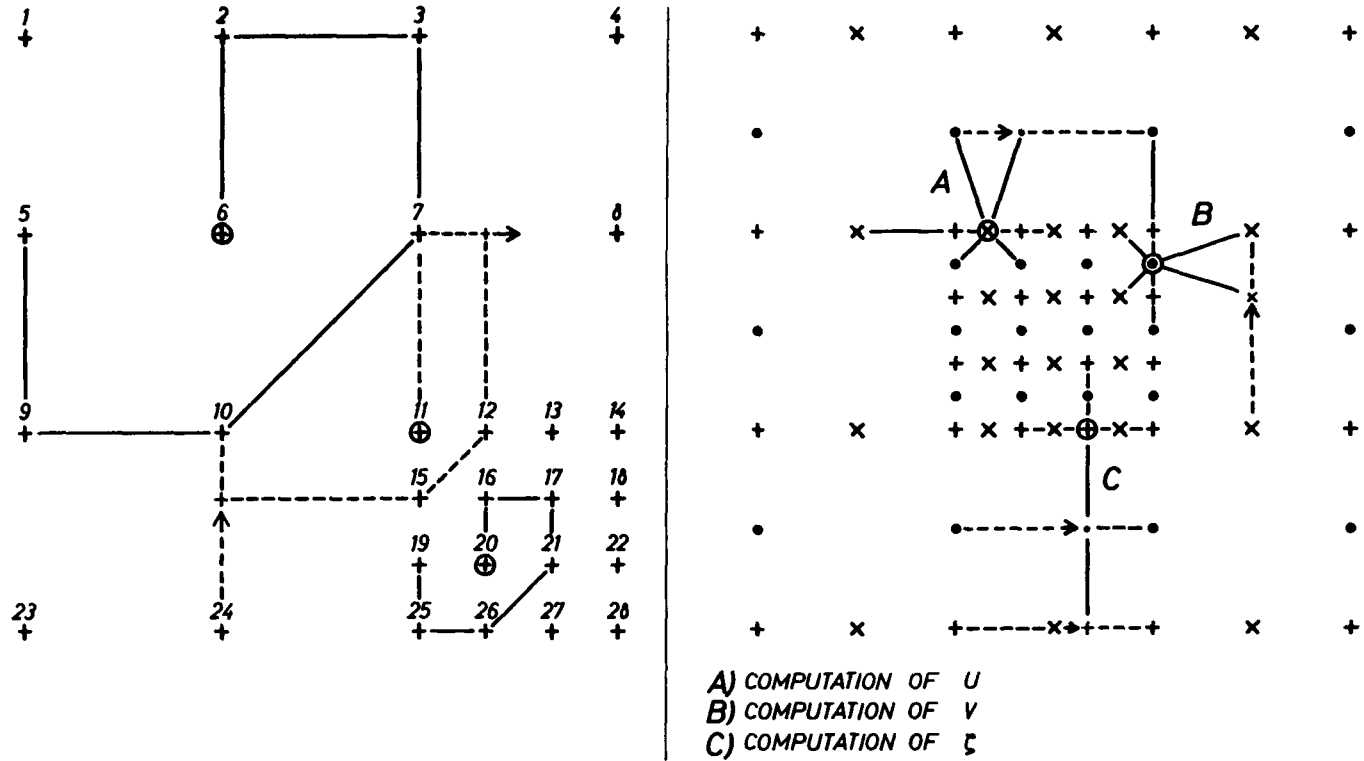


Fig. 66. INTERRELATION BETWEEN AREAS OF DIFFERENT GRID DISTANCES.

(j,k) co-ordinate system and replacing it with a one-dimensional numbering of points. Such an approach facilitates the use of the refinement technique and makes the model applicable to many different problems. The right hand side of fig. 66 shows each U, V and ζ point separately. The method of calculating each finite difference in the transition zone is also indicated. In order to calculate $\frac{\partial U}{\partial t}$ the values of V and ζ from the coarse grid and fine grid respectively should be taken into account. The first and second derivatives can be calculated at these points on the basis of (6.65) and (6.66). In numerical experiments with $n = 3$ the results obtained at the transition points were steady to within the limits of practical accuracy wherever they were analysed. Through the introduction of the following expression for the second derivative from (6.72)

$$\frac{\partial^2 f}{\partial x^2} = \frac{2}{h_2} (f(x_3) - f(x_2)) - \frac{2}{h_2} \frac{\partial f}{\partial x} + O(h_2) \quad (6.74)$$

into (6.71), we arrive at the numerical form for the first derivative

$$\begin{aligned} \frac{\partial f}{\partial x} = & \frac{h_1}{h_2(h_1 + h_2)} f(x_3) - \frac{h_2}{h_1(h_1 + h_2)} f(x_1) + \frac{h_2 - h_1}{h_1 h_2} f(x_2) \\ & + O(h_1^2) + O(h_1 h_2) + O(h_2^2) \end{aligned} \quad (6.75)$$

which is of the second order of approximation.

The addition of (6.74) and (6.75) results in the expression for the second derivative at the point x_2

$$\frac{\partial^2 f}{\partial x^2} = 2 \left\{ \frac{1}{h_1(h_1 + h_2)} f(x_1) - \frac{1}{h_1 h_2} f(x_2) + \frac{1}{h_2(h_1 + h_2)} f(x_3) \right\} \quad (6.76)$$

These finite expressions and the computation of the missing values of U, V and ζ by linear interpolation interrelate the two areas of coarse and fine resolution and guarantee the proper interaction of variables in the transition zone.

§10. Some results and conclusions derived from the nested model of the North Sea

The model was first tested in the area of the German Bight with a grid step $2h = 37$ km (Fig. 68). The boundary conditions at the open boundary were taken from the earlier calculations of tides for the

whole basin of the North Sea (the classical model developed by Hansen - see fig. 67). The results, when compared with the gauge observations, depict a maximum difference in phase up to 20 min. and in amplitude of up to 15 cm. This remarkable agreement opens the possibility of further applications of this model in engineering practice. Through the refining of the grid it is possible to include in the model minor variations in the bottom and coastal morphology and also planned coastal engineering constructions. The refinement procedure is feasible if the parts of the basin which are of interest are treated separately and provided the boundary conditions are known from previous calculations.

We begin with the uniform 37 km-grid which was used by Hansen in his treatment of the North Sea problem. Since we were interested in the fine scale motion of the River Elbe we expanded Hansen's grid into a telescopic nest of four subgrids in the coastal area of the German Bight and River Elbe. The final grid within the river had a grid spacing of $(1/3)^4 \times 37 \text{ km} = 457 \text{ m}$ (see fig. 68).

Fig. 69 displays the mean mass transport during one tidal cycle computed for the area of the German Bight with grid steps $2h = 12333 \text{ m}$ (area 2), $2h = 4111 \text{ m}$ (area 3) and $2h = 1370 \text{ m}$ (area 4) - see fig. 68 for the location of the respective areas.

In area 4 with the finest resolution, the details of the flow and the distribution of velocity in the Elbe estuary due to the fresh water input can be seen. While the areas 2 and 3 lack the necessary small scale detailment, they show stream-splitting, that is, the development of vorticity due to the merging of the river transport with the flow of the German Bight.

It is possible to check the appearance of the flow due to a small island and the existence of temporarily dry areas in proceeding from the large scale grid to small scale grid. In the areas of extremely shallow water where the nonlinear terms are of the greatest importance and where large horizontal differences in velocity are present we have introduced the advective terms and moving boundaries.

§11. Some examples of the application of hydrodynamic-numerical models on coastal engineering

In the planning considerations for engineering structures in tidal rivers or in coastal areas in general, a detailed knowledge on possible consequences of the changing dynamic processes are essential to arrive

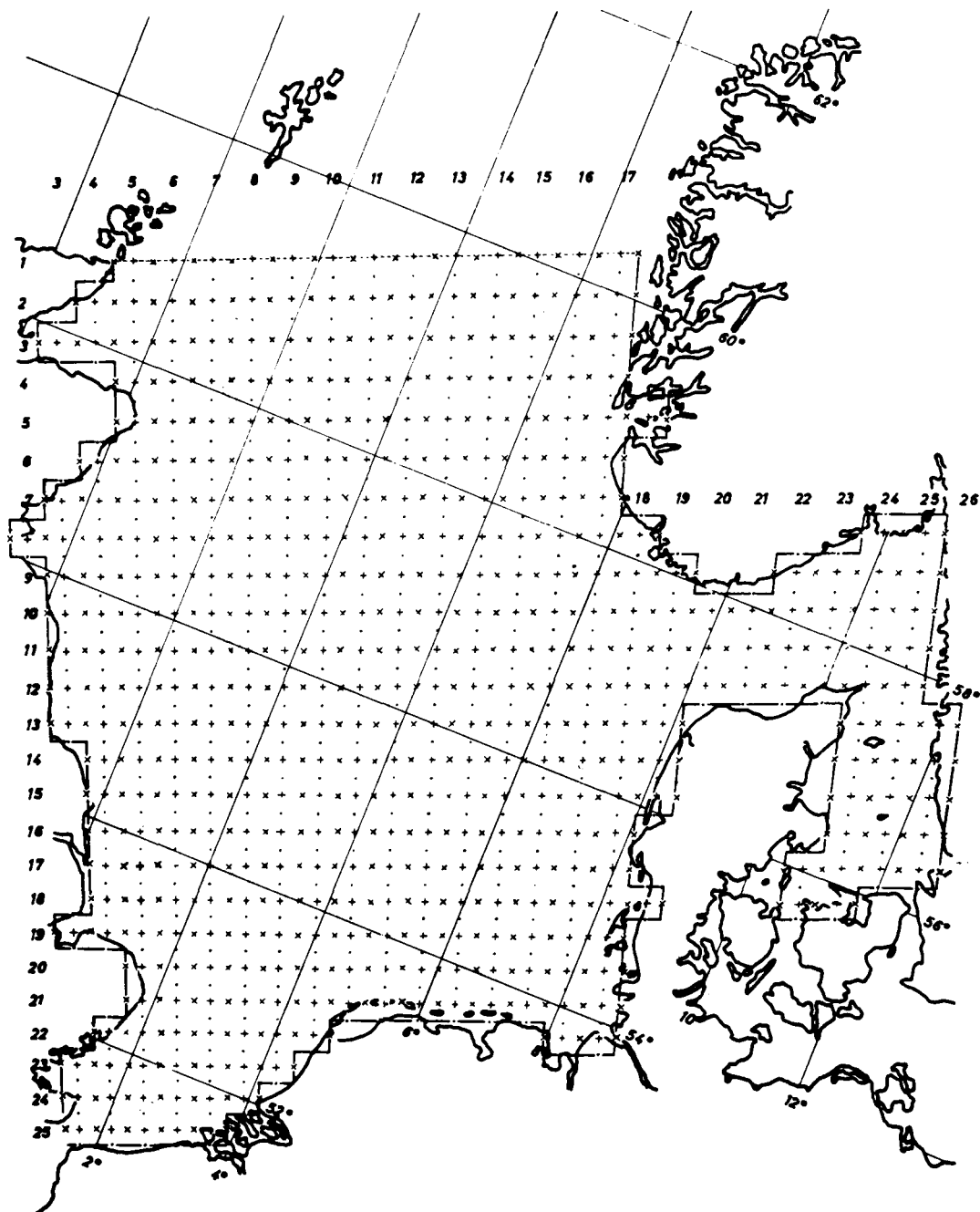


Fig. 67. GRID OF THE CLASSICAL NORTH SEA MODEL DEVELOPED BY HANSEN.

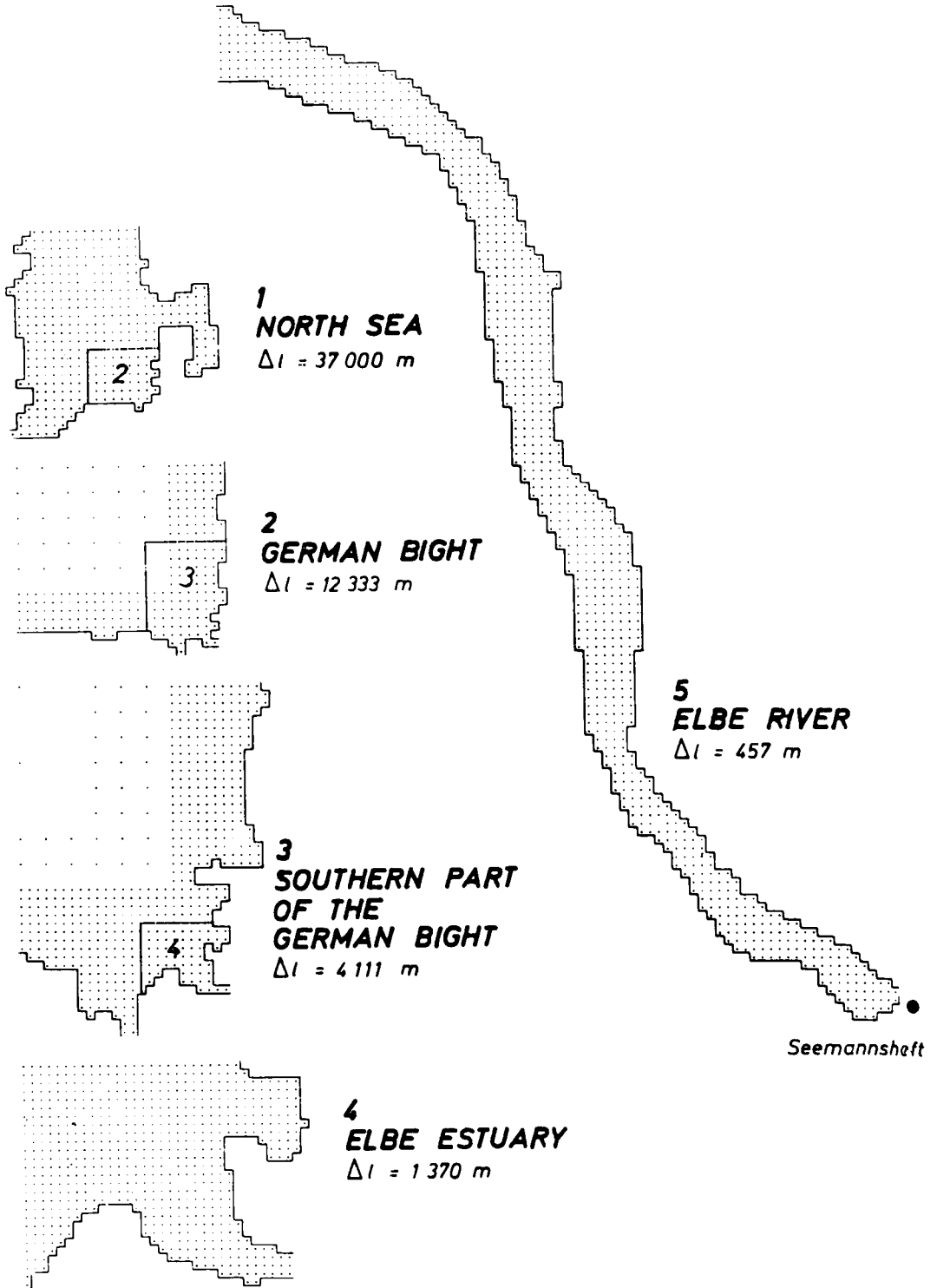


Fig. 68. FINE RESOLUTION OF THE NORTH SEA GRID IN COASTAL AREAS.

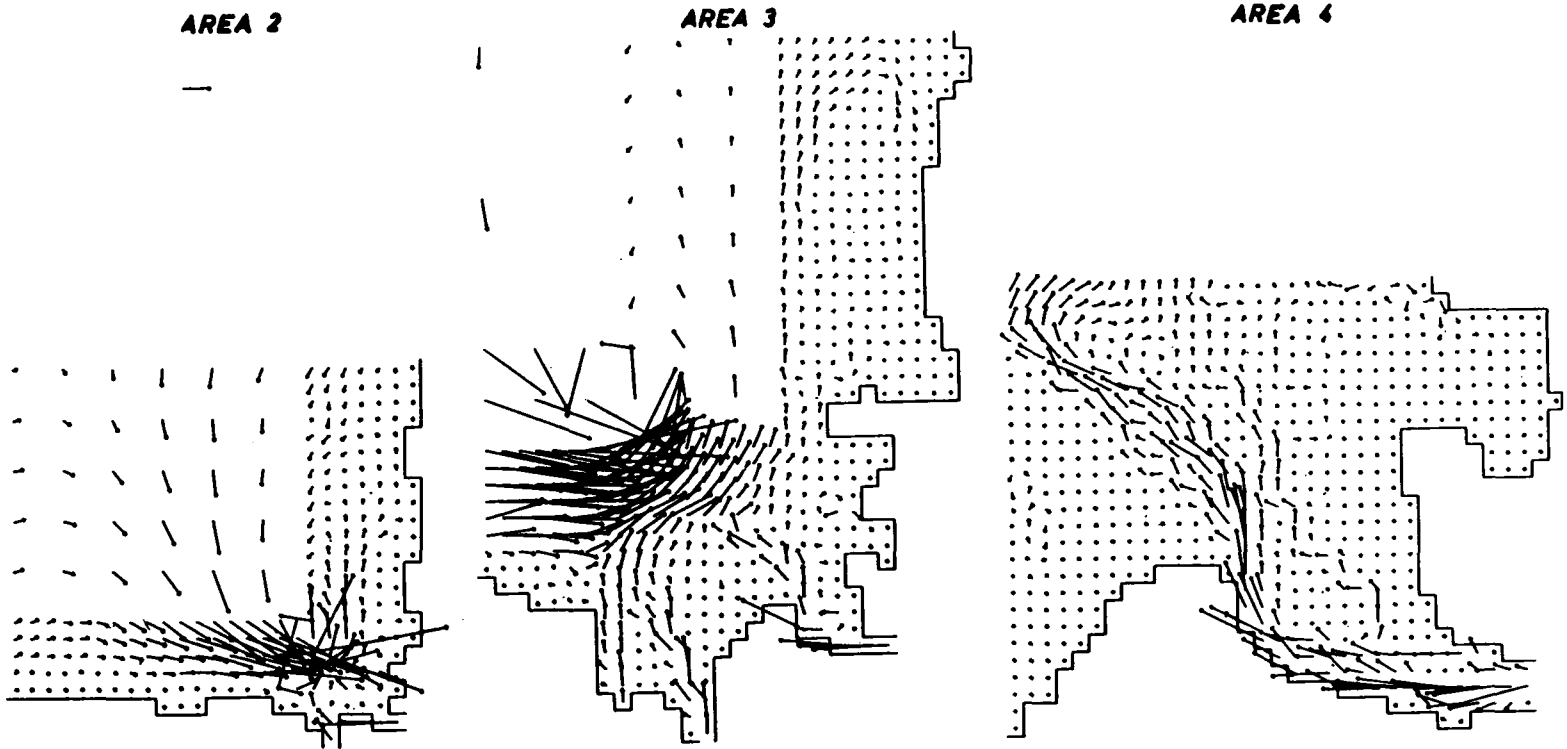


Fig. 69. MEAN MASS TRANSPORT OVER ONE TIDAL PERIOD (M_2) IN THE GERMAN BIGHT ON JUNE 20, 1969.

at optimum solutions. The model considered here is based on the equations of motion and continuity already described extensively in the preceding chapters; it enables the interested scientist to investigate possible influences of several structural changes at different locations at the same time. Accordingly it renders possible to examine whether the changes in the dynamic processes are caused by a certain engineering structure (such as breakwater, dike etc.) or by the interaction of different buildings. The knowledge of possible connections between large-scale motions and local changes in the coastal topography then may be of some assistance in the planning procedures, too.

A further development of the already very large and complicated numerical models depends heavily on the memory capacity and efficiency of the available computer. Furthermore, the necessary lucidity sets a certain limit to the 'improvement' of a computer program.

A The basic model

In the following a North-Sea-Model with an extensively refined grid in shallow water areas is presented as an example of the application on both coastal research and engineering, a section of which is shown in fig. 70. The refinement of the grid enables without difficulty the attachment of tidal rivers and their respective estuaries to deliver boundary conditions for local investigations in accordance with dynamic processes in the open sea. A better approximation of the coast line and the very complicated bottom topography may also be of some advantage for the research of scientific problems in the sea as a whole. The computation of sea-level variations and the mass transport in the extremely shallow parts almost totally depends on the quality of the approximation of tidal flats and drifting sandbanks, which have such an influence on the motion of water in coastal areas. Here the phenomenon of uncovering and flooding of extensive parts of the coast due to the existence of very intricate patterns in the tidal currents is simulated by a physically appropriate numerical technique.

The model, including the North Sea area, comprises 7216 point triples, i.e. 21648 points altogether, in each of which a mean water depth according to nautical charts approximates the existing bottom topography. In the Elbe estuary a grid refinement takes place from a distance between computation points of 4111 m to approximately 457 m (i.e. 1/9) towards the south and east respectively. In this way the grid is refined from the northern North Sea entrance (between Aberdeen and Bergen) with a grid distance of 37,000 m towards the German Bight by a factor of 1/81.

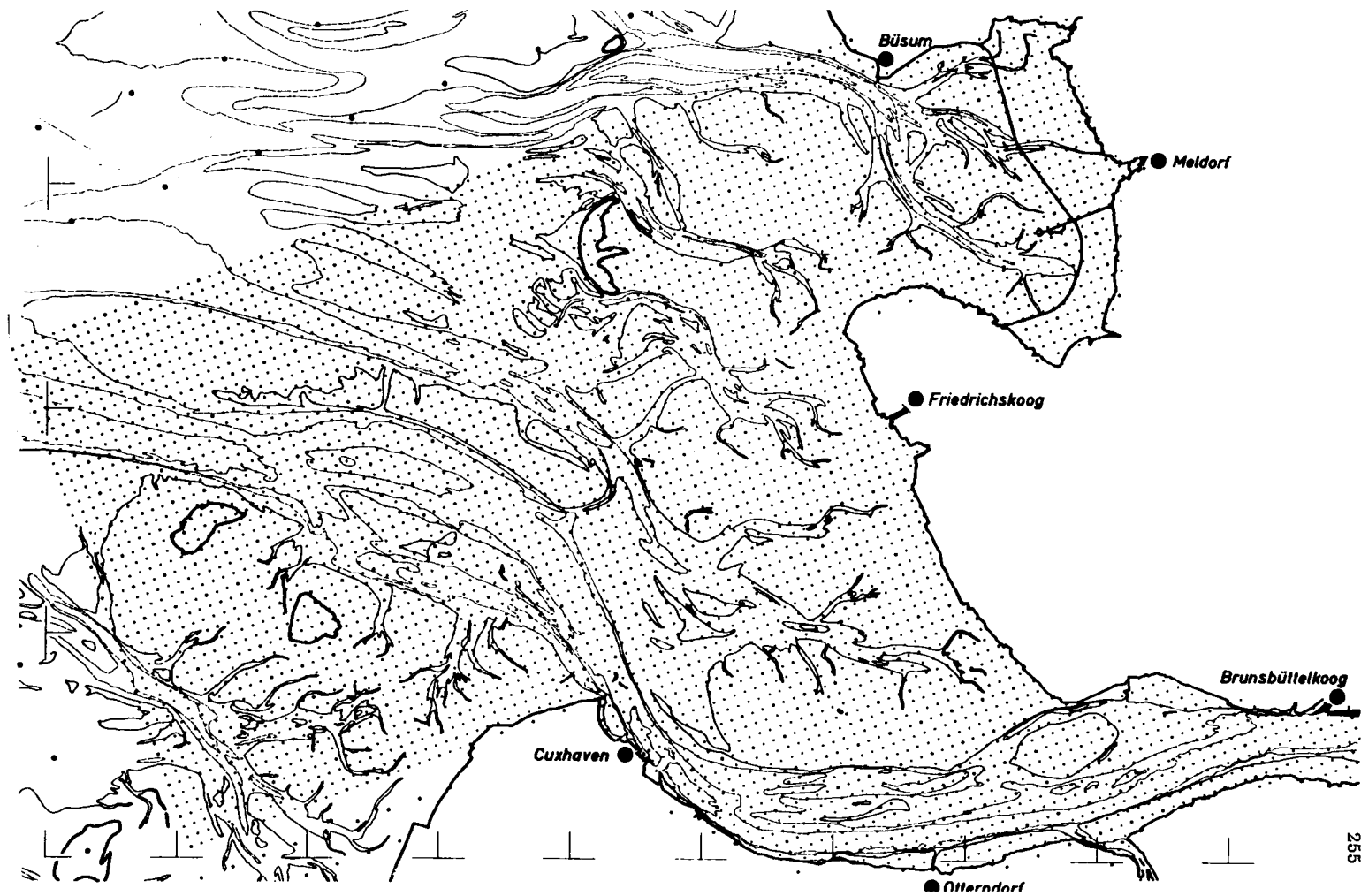


Fig. 70. SECTION OF THE BASIC MODEL (GERMAN BIGHT).

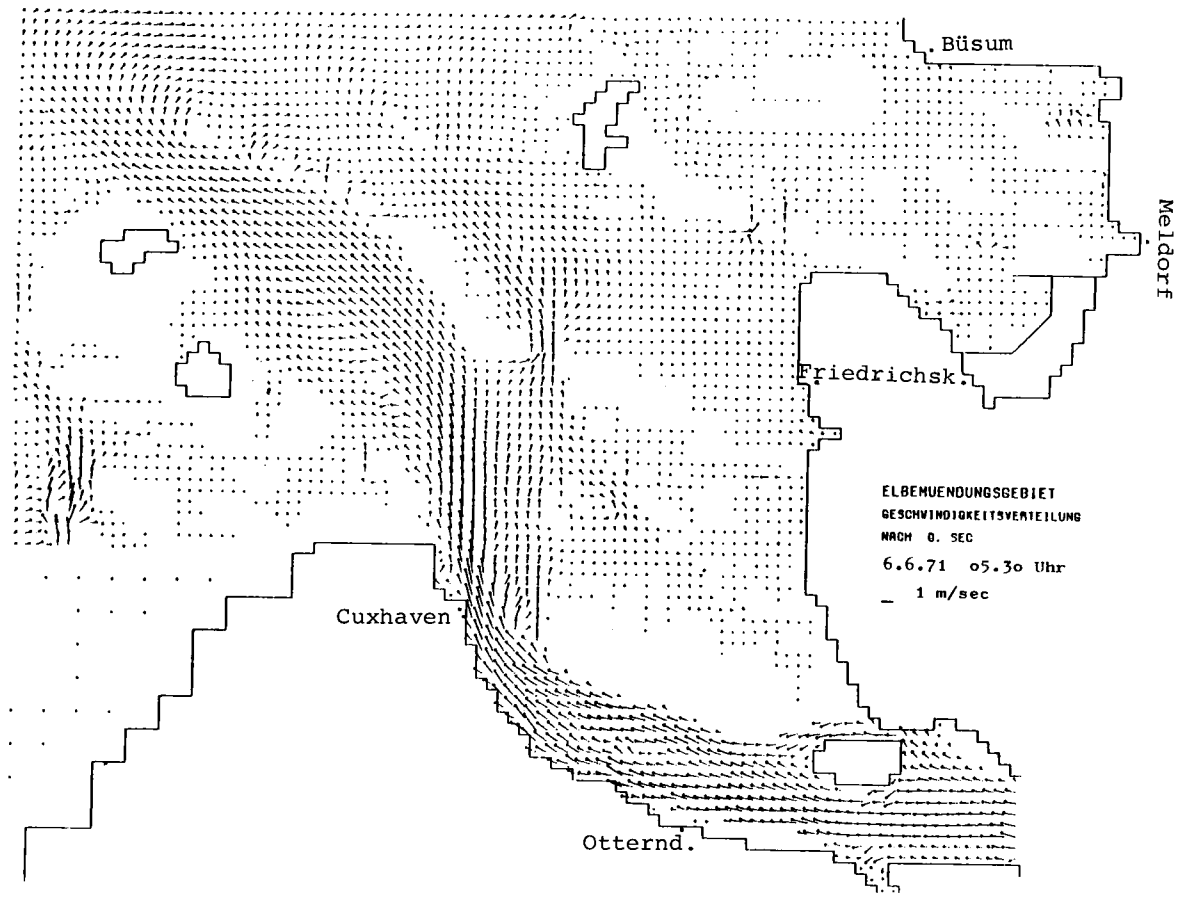


Fig. 71. VELOCITY DISTRIBUTION IN THE ELBE ESTUARY ON JUNE 6th, 1971, 05.30 M.E.T.

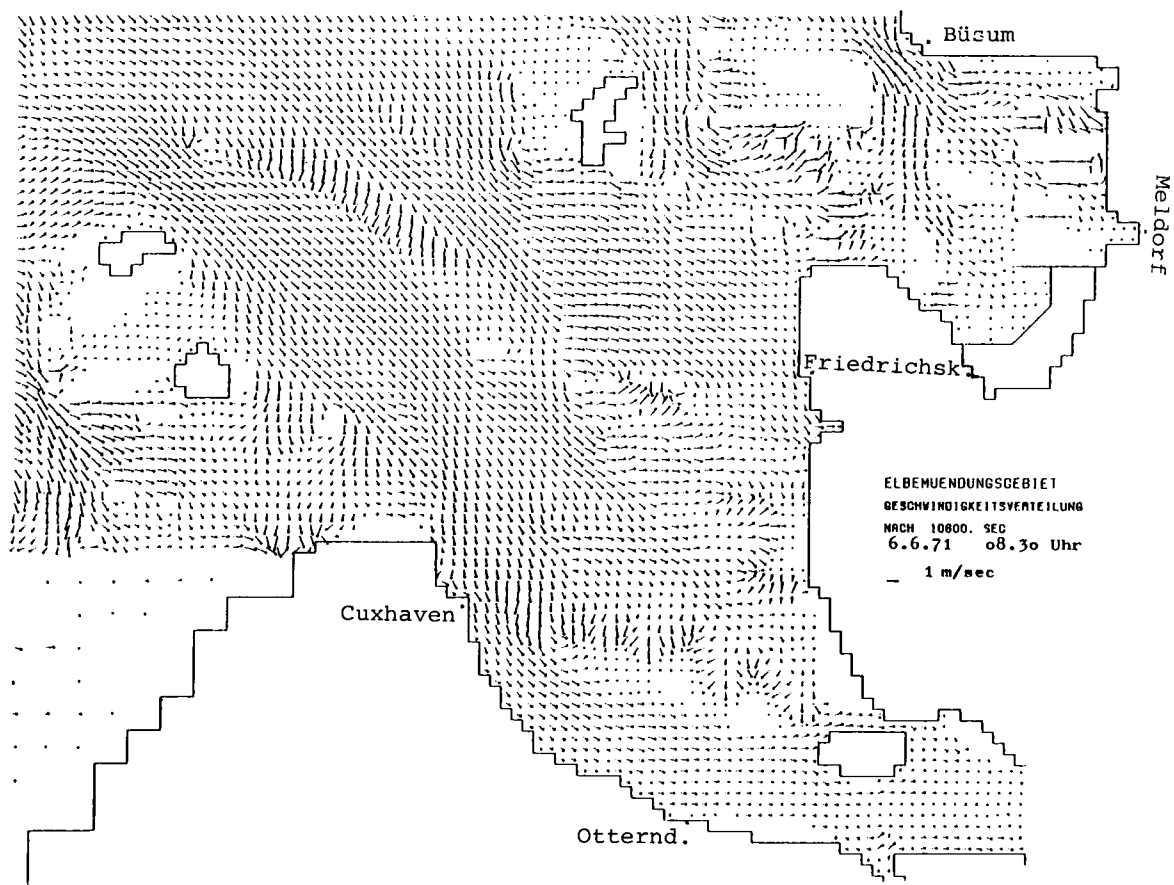


Fig. 72. VELOCITY DISTRIBUTION IN THE ELBE ESTUARY ON JUNE 6th, 1971, 08.30 M.E.T.

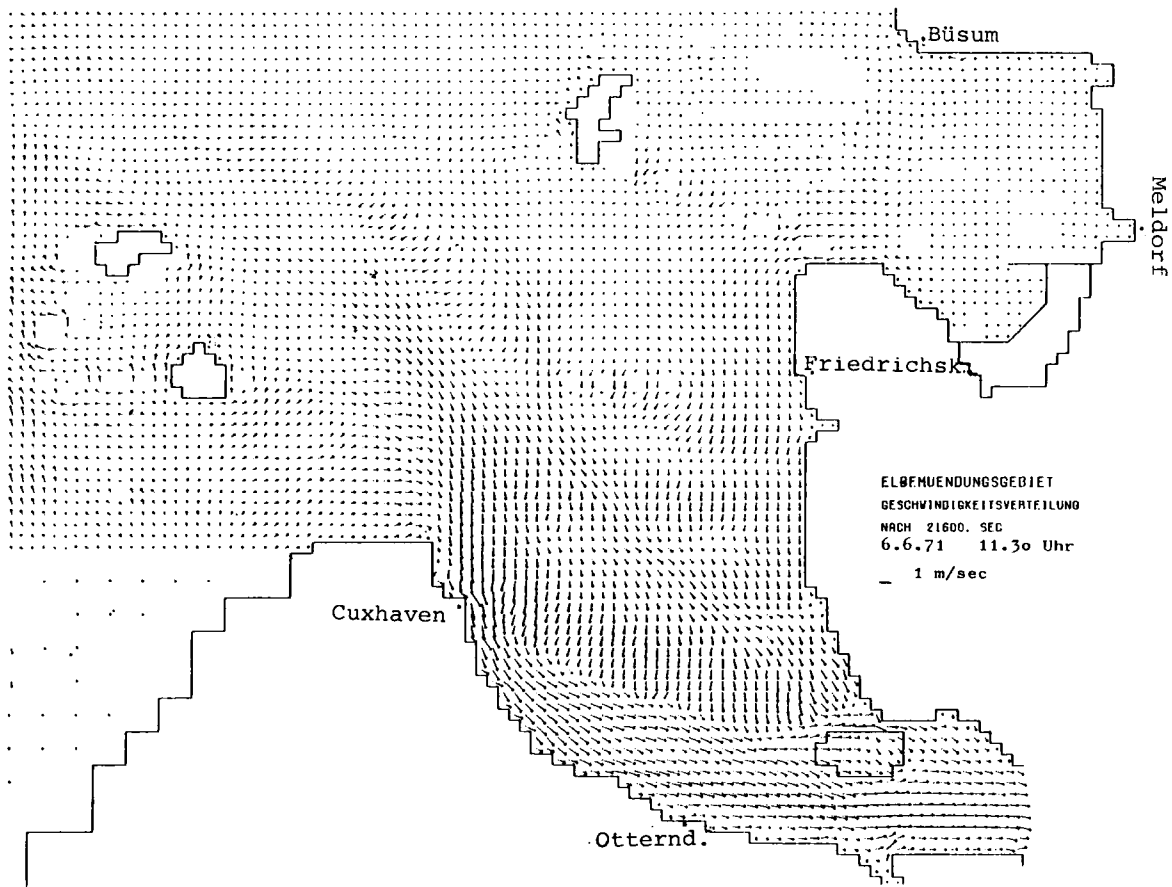


Fig. 73. VELOCITY DISTRIBUTION IN THE ELBE ESTUARY ON JUNE 6th, 1971, 11.30 M.E.T.

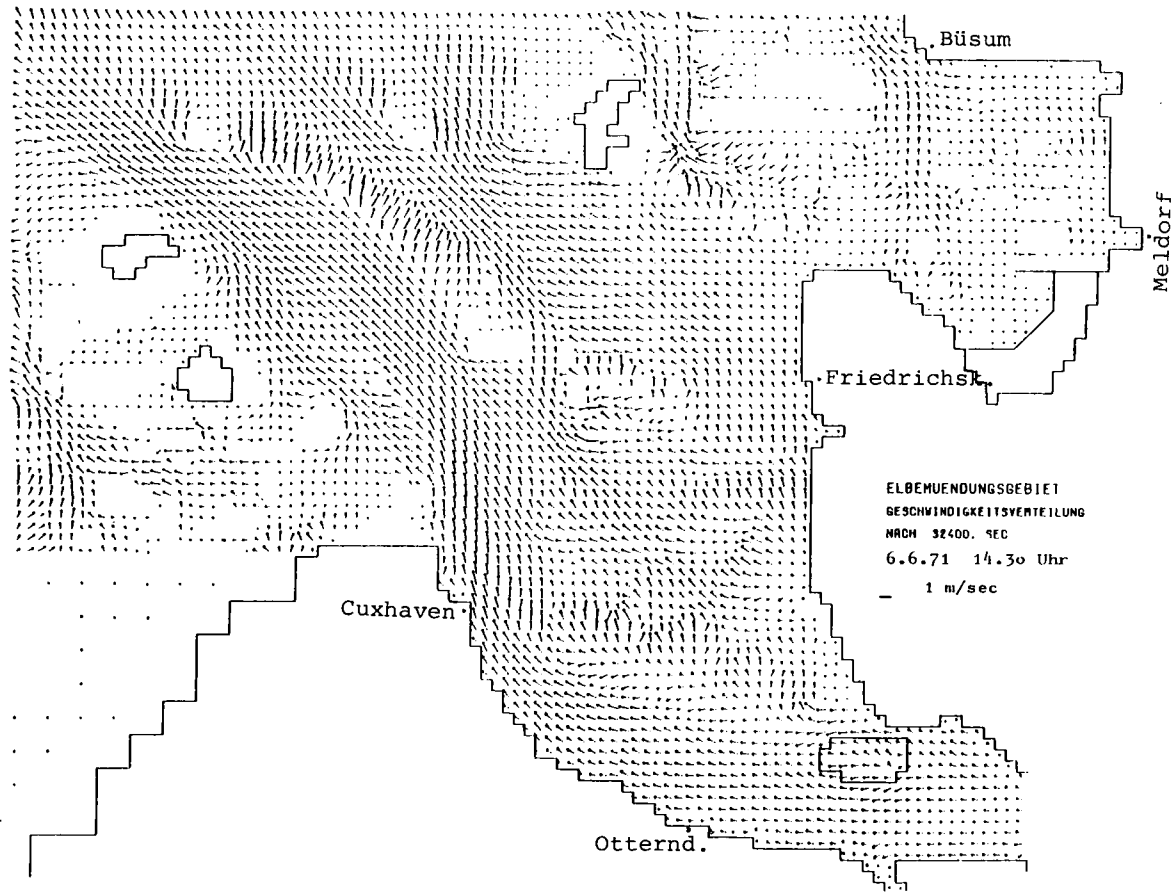


Fig. 74. VELOCITY DISTRIBUTION IN THE ELBE ESTUARY ON JUNE 6th, 1971, 14.30 M.E.T.

The similarity with dynamic processes in nature was checked by the comparison of computed and measured sea-level variations in the area taken on the 6th of June in 1971.

The horizontal and vertical motions are determined by the applied boundary conditions, the bottom topography and the choice of the parameters r and A_h respectively. The dimensionless coefficient of bottom friction r is taken as constant over the whole model as 2.5×10^{-3} . The horizontal eddy diffusion coefficient A_h is assumed to be representative for the influence of turbulent motion, which otherwise could not have been included in this model. A further calibration by variable parameters r and A_h in time and space did not take place in order to ensure a homogeneous treatment of all grid points.

A total agreement of the computations with observations or measurements cannot be expected in any case, since

1. the equations of motion deliver vertically integrated velocities;
2. the approximation of bottom topography is dependend on the grid. In coastal areas despite a grid distance of 457 m certain generalisations are indispensable.
3. the numerical model includes some built-in simplifications and parametrizations, which are only able to describe complex physical processes in nature in a linear and integrated form.

The following boundary conditions were applied:

- a) at the entrance to the northern North Sea and the English Channel

$$\zeta(m) = c(m) A(m) \cos(\sigma t - \phi(m)) \quad (3.77)$$

$$\frac{\partial u}{\partial x} = 0, \quad \frac{\partial v}{\partial y} = 0 \text{ normal to the open boundary} \quad (3.78)$$

- b) at the closed boundaries

$$u = 0 \quad \text{and} \quad v = 0 \text{ respectively} \quad (3.79)$$

where

A amplitude of the main lunar tide M_2
 σ frequency of the main lunar tide M_2
 ϕ phase of the main lunar tide M_2
 m space index
 c see explanation beneath.

The frequency and phase of the main lunar tide M_2 was not changed, however the corresponding amplitude $A(m)$ was multiplied by a factor $c(m) > 1$ in order to parametrize the time- and space-dependent amplitudes of other important tides. Apart from this, the water level variations at Seemannshöft in the River Elbe on 6th of June 1971 between 05.30 M.E.T. and 17.55 M.E.T. were taken as boundary conditions.

The application of the afore-mentioned boundary conditions is admissible for the reproduction of sea-levels and velocities as long as tides are concerned which are almost wholly undisturbed by wind action.

The considered model allows practically further refinements in every section of the coast line to investigate the influences of topographical changes, whether caused by natural or technical reasons, on the dynamic processes. However, although the elevations of sea-level could be reproduced fairly well in the check mentioned above, in a comparison with measurements of current meters, for some reason possible only in a qualitative way, a reproduction of the tendency of flow could only be achieved. The figs. 71 - 74 display the velocity distribution every three hours in the considered period at the 6th of June 1971 in the Elbe estuary. The uncovering and flooding of tidal flats, as well as the accordingly highly variable flow pattern around them, is clearly seen.

B First example: The effect of a structural change due to a breakwater on movement processes

The breakwater considered here is situated at the west coast of the island of Wangerooge and has an approximate length of 1400 m and present height of NN - 1.40 m. The breakwater, commonly called 'Buhne H' is a neuralgical point of the investigation area. The existence of this structure, its height and length as well as its direction determine considerably the course of the dynamic processes at the north of Wangerooge, in the Harle as well as in the tidal flats behind Spiekeroog and Wangerooge. It should be mentioned that possible morphological changes were not taken into consideration in these investigations.

The following three cases were investigated:

- Model I breakwater, actual state
- Model II breakwater, height NN + 1.50 m
- Model III breakwater, actual height, half length.

These marks are also valid for all figures within this paper.

Before starting the investigations it had to be checked firstly:

- a) How large should the model area be selected?
- b) How is a further screen-grid dissolution to be effected in accordance with the tasks of the investigation?
- c) How far can or should a reduction of the screen-grid distance be carried out so that the peculiarities of the morphology and the breakwater can be well approximated?
- d) How great will the time step be depending on the screen distance and the depth? Will such a caused computation expenditure be supportable?
- e) What tide should be selected for the investigations and what sort of boundary values will be available?

to a)

The size of the model area to be selected will depend at first on the numerical investigations to be carried out and upon the nature of the given questions. In the present case, the influence of a construction upon the dynamic processes must be investigated. It is also to be checked, which alterations of these vertical and horizontal movement processes will have to be expected in case of a possible constructional interference. Therefore, the size of the investigation area should be selected so that the open boundary of the numerical model cannot be influenced by the change of movement processes to be expected. Based on the available floating measures and the morphology north of Wangerooge and Spiekeroog, the model area was selected as shown in fig. 75.

From the later obtained results it can be seen that the open boundaries are sufficiently far away from the range influenced by the breakwater.

to b)

The selection of the screen grid and the degree of solution depends on the morphology and to the same extent upon the necessary accuracy of reproduction of the changes of movement to be expected.

Available was a part model with a mesh size of 457 m. The area north of Wangerooge offers itself for a further screen-grid solution. Changes in the dynamic processes can be expected for certain in the so-called remote range in relation to the breakwater because of constructional measures of the building which had to be investigated.

A screen distance of 153 m was selected in this part area. In this manner, the topography could be reproduced in a fineness which conforms to the available maps. This part area is illustrated in figs. 75 and 76

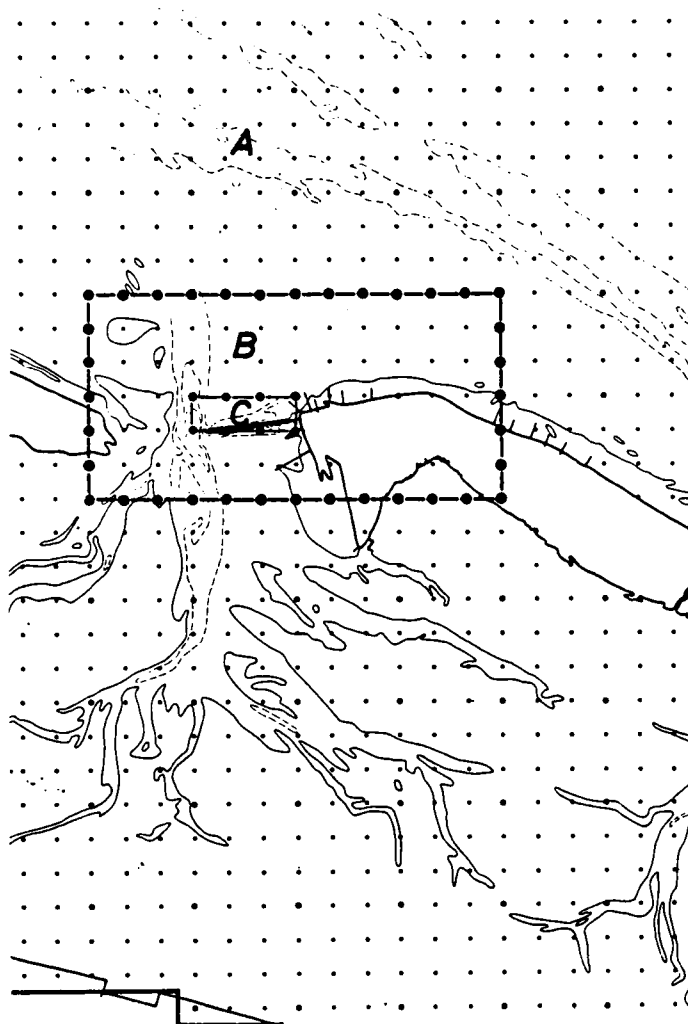


Fig. 75. AREAS A, B AND C WITH DIFFERENT GRID DISTANCES.

A further solution - the one-third-refinement method - was naturally required in the close range of the breakwater. A screen distance of 51 m between points of equal importance (ζ/ζ , u/u , v/v) has for the approximation of the morphology in the numerical model the consequence of a depth indication every 25.5 m since the ζ - as well as the u - and v -points are available. Unfortunately, the breakwater does not run parallel to the screen.

But the necessary deviations in the reproduction of the location in the numerical model should be considered as unimportant.
to c)

From the explanations under b) it can be concluded that the solution is an optimum one. The results which will be later explained add to this a multiple number of hints. In this connection it should be mentioned also, that to our knowledge, for investigations of this principal importance such extreme screen solutions have been applied for the first time and, apart from this, an interaction between areas of different grid distance was ensured.
to d)

The area with the lowest screen distance is bordered in the west by the breakwater's head. The further in the west situated deep channel has already a grid distance of 153 m. A further screen resolution in this range also would bring hardly better results and would lead to a not anymore supportable computation expenditure.

The condition of the numerical stability according to Courant, Friedrich and Lewy (1928)

$$2T \text{ (time step)} < 2h \text{ (smallest grid distance)} / \sqrt{2gH_{\max} \text{ (greatest depth)}}$$

leads because of the great depths in the above mentioned case to a very short time step.

From the given screen refinements and the morphological conditions follows the necessity for the numerical model to use a time step of 3 seconds. This means for a tidal period of 44700 sec = 12^h25 min an amount of 14900 time steps.

This computation expenditure is considered as supportable. The periodic stationarity was obtained after two computed periods, this, however, only because an approximated initial distribution was at our disposal. This model will be available for other possible investigations and is programmed to an optimum. The obtained results justify this computation expenditure.

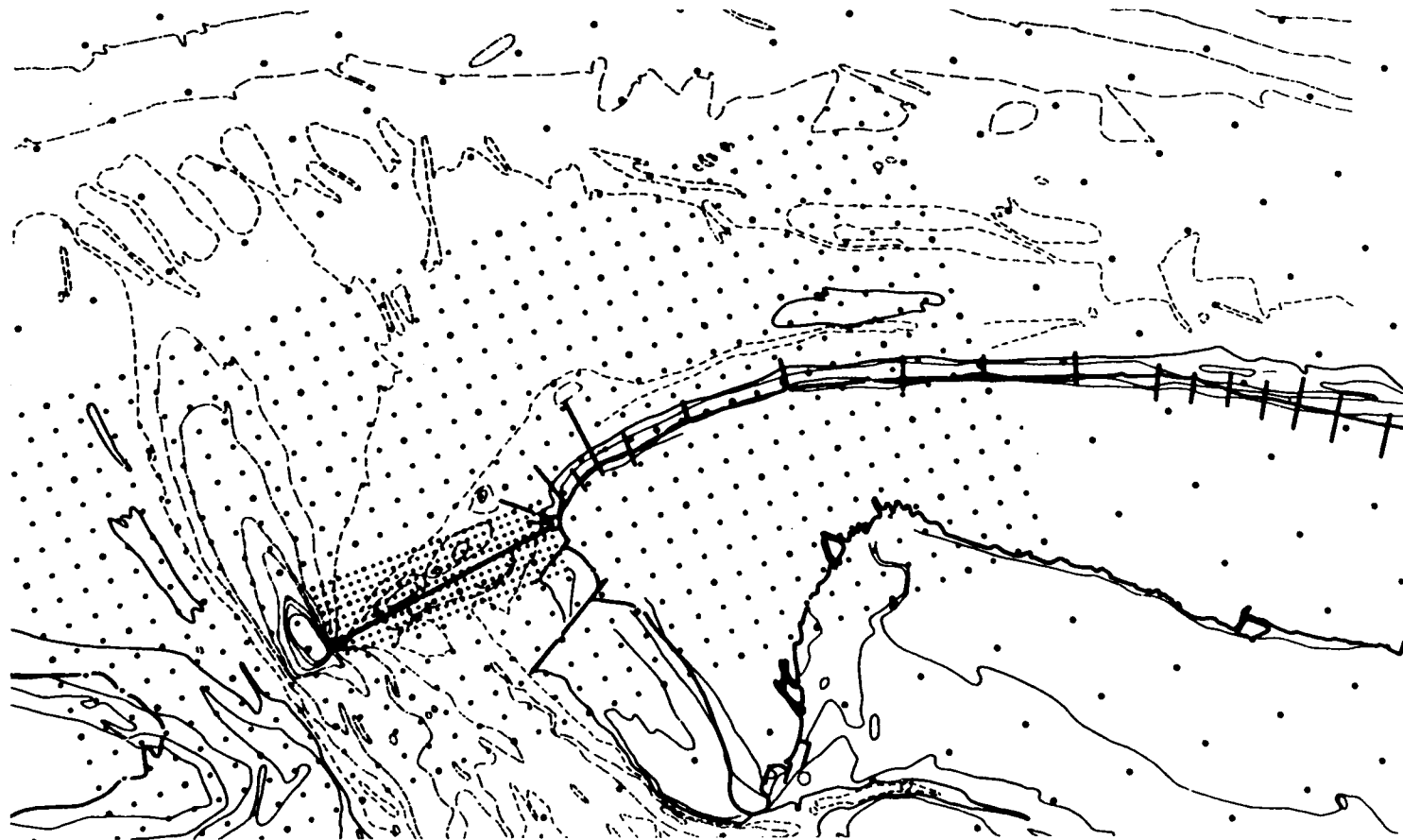


Fig. 76. LOCATION OF THE BREAKWATER AND THE APPLIED GRID RESOLUTION IN ITS VICINITY.

to e)

An extensively undisturbed, i.e. a not wind-influenced tidal period was selected for the investigations. The author has water level observations at various points from an investigation series from the June 20, 1969 at hand. Naturally, any other tide can be used, but it should be as free as possible from wind influence and the measuring period should not be in the range of the nipp- or spring-time.

Since this model area is a part of the North Sea model, by the aid of which the movement processes in the Weser-Jade-Regime were determined to a task-orientated screen resolution, the necessary water level values could be taken in the points at the open model boundary as $f(t)$ from the available model. After completing the timely linear interpolation and subsequently smoothing the curvature (this is absolutely permissible because of the very short time step), the water level values for the intermediate points were also obtained by linear interpolation (this is also permissible because of the short grid distance).

Model I

Here the remark should be permitted that the solution of the grid within this area - as far as illustrated in the area A - is insufficient. With a point distance of 457 m, the locally extremely complicated current movements cannot be reproduced satisfactorily. A nesting in the areas B (153 m) and C (51 m) will provide a much better information on the in- and overflowing processes (see fig. 75).

The duration of the tidal current v_f is usually longer than the duration of the low-tide current v_e . The high tidal current velocities with $v_{\max} \approx 1.8$ m/sec in the southern part of the Harle are worth noticing.

Model II

The velocities at the breakwater's head are greater and retain this order of magnitude also over a longer period in comparison to model I. The time of inflow is also longer. Both of the afore-mentioned processes are of importance for the interpretation of the numerically determined average transports of a tidal cycle and they will find here their confirmation.

Extremely high tidal current velocities (1.5 - 2.1 m/sec) occur in the Harle at the south of the breakwater, whereas the low-tide velocities appear to be low. These high velocities can - when the water is running up on the flat, i.e. with the occurrence of morphological barriers - lead to strong eddy formations and may change the morphological structure.

The water level changes in the points of the investigation area at the north of the breakwater and remains, when compared with those of model I, in the centimetre range. The high water, however, in the Harle and south of the breakwater lies at a phase difference of approximately 30 minutes clearly lower, about 25 to 30 cm. This influence is effective up to 3100 m south of the breakwater.

Model III

Apart from the changes which result solely on account of conditions - shortening of the breakwater by 50 % - there is a strong similarity between the results of model I and model III. This local change is obviously of no special importance for the total process - with the exception of one phenomenon to be mentioned: The through-current flows more uniformly as has been expected, but the turning of the current takes place further west in comparison with the present condition of the breakwater.

Model I, II, III

The effect of the alteration of the breakwater towards the position of the current dividing area is of special interest. From the lines of the directions of maximum velocity in each model the turning point can be located of the current path in the near vicinity of the island. The further this point moves to the east, the greater the strand-parallel running tide and low-tide velocities are, which cause simultaneously the transport of solid particles. The following result is on hand: By a rise of the breakwater to NN + 1.50 m, the turning point is displaced by 3500 m to the east and by shortening the breakwater by 50 % at the present height of NN - 1.40 m, it will be displaced by 1000 m to the west (Fig. 79).

The distribution of tidal currents in all three investigations permits the conclusion that in the case of a rise of the breakwater to NN + 1.50 m, the water masses in front of Wangerooge will shift at first very far to the east - further than at the present condition of the breakwater - and will be involved in the dynamic processes in front of the breakwater with large streams directed parallel to the strand and in the Harle (Fig. 77).

In a comparison of the average transports of a tidal cycle in the three cases to be investigated, the amounts should also be checked by measurements. Important for the judgements of the results, however, should be qualitative relations (Fig. 78).

In order to give a deeper insight in the applied models, some remarks on the horizontal turbulent eddy viscosity and the advective

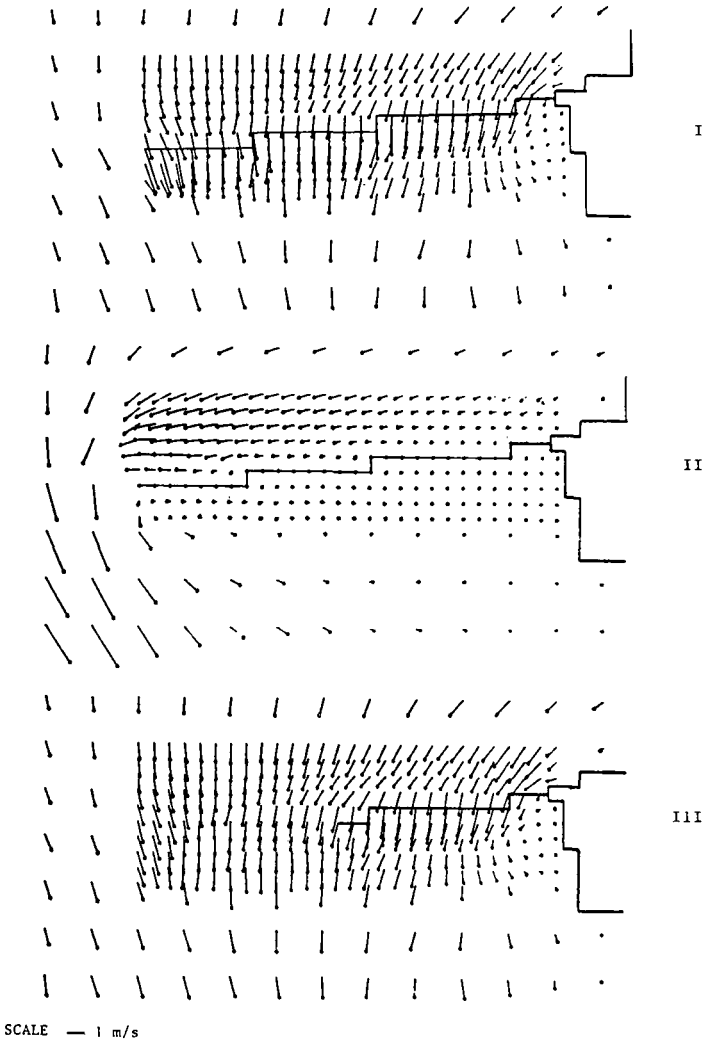


Fig. 77. AREA C - DISTRIBUTION OF VELOCITIES 9 HOURS AFTER MOON'S TRANSIT THROUGH THE MERIDIAN OF GREENWICH (20.6.79 - 14.02 h).

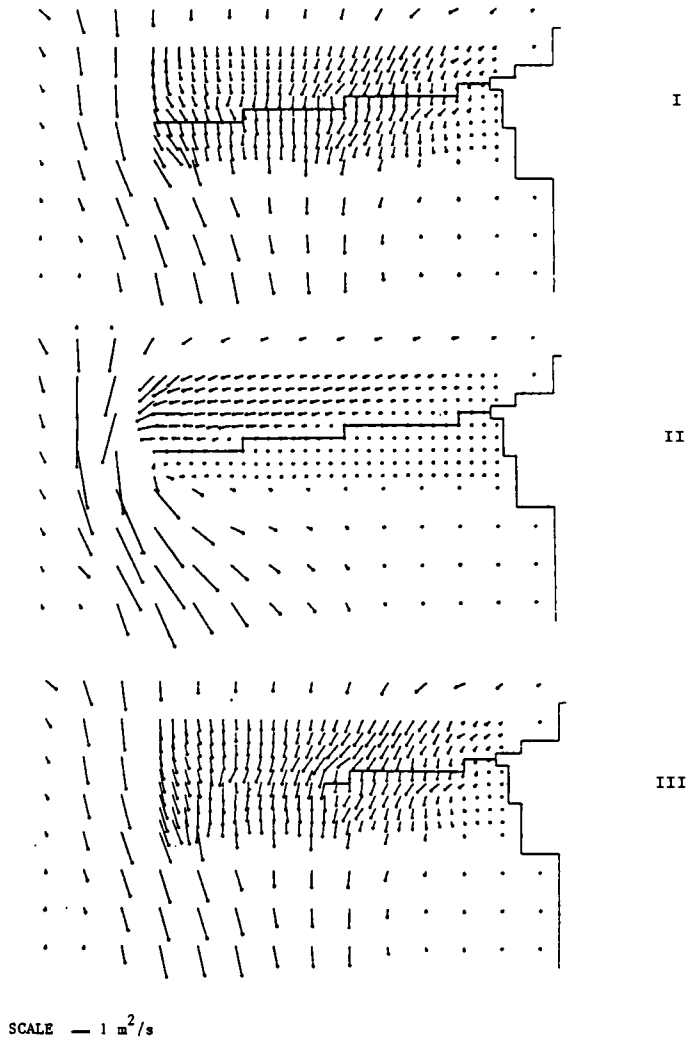


Fig. 78. AREA C - MEAN MASS TRANSPORT OVER ONE TIDAL CYCLE.

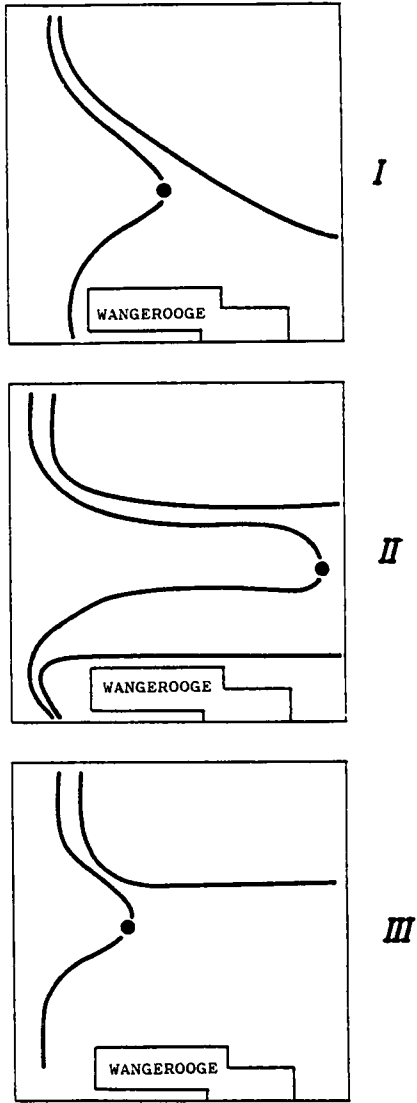


Fig. 79. DISPLACEMENT OF DIVERGENCE.

terms should be made. The advective terms as an important part of the description of dynamic processes in shallow water cannot be neglected in the numerical model. Unfortunately, they cause numerical disturbances in the model which have to be stabilised by using a time step and grid size dependent coefficient A_h , which describes the horizontal turbulent eddy viscosity.

Shoal areas are often cut through by a narrow channel with depths up to 5 m and more. On the grid points on the edges of such a channel as well as on points where the shallow water area borders on navigable channels or waterways respectively, instabilities occur on account of the large $\frac{\partial H}{\partial x}$. Here also, the coefficient mentioned above will have a stabilizing effect.

If one considers the following equation (Brettschneider, 1967)

$$A_h = \frac{1 - \alpha}{4} \frac{(2h)^2}{2T} \quad (3.80)$$

A_h can be generalized by a dependency to the bottom slope to

$$A_h = \frac{1}{4} (1 - \alpha e^{\Delta H/h}) \frac{(2h)^2}{2T} \quad (3.81)$$

and simplified to

$$A_h = \frac{1}{4} (1 - \alpha (1 - \frac{\Delta H}{h})) \frac{(2h)^2}{2T} \quad (3.82)$$

where $2h$ denotes the respective grid distance in x or y direction.

In the submitted investigations, the smoothing factor α was set equal to 0.98 and A_h takes up values between 2.5 to 170 m^2/sec according to grid distance. It is easily recognisable that by medium formation at a strong bottom slope a stronger dampening will occur.

The advective terms $u \frac{\partial u}{\partial x}$, $v \frac{\partial u}{\partial y}$, $v \frac{\partial v}{\partial y}$ and $u \frac{\partial v}{\partial x}$ will be treated on the boundaries of the numerical model as follows

$$\frac{\partial u}{\partial x} \text{ or } \frac{\partial v}{\partial y} = 0 \text{ on the open boundary.} \quad (3.83)$$

On the closed boundaries the terms $u \frac{\partial u}{\partial x}$ and $v \frac{\partial v}{\partial y}$ cause no difficulties. $v \frac{\partial u}{\partial y}$ and $u \frac{\partial v}{\partial x}$ are treated in the same way as in the centre of the area, since the components of velocity will disappear at the respective boundaries in accordance to the presuppositions, therefore, they will also be equal to zero outside the area.

C Second example: The influence of river normalization on the distribution of tidal currents in the River Elbe

The area under investigation between Brunsbüttel and Stadersand was taken as a numerical part model from a North-Sea-German-Bight-Elbe model developed during the last few years, with a very extensive screen-grid division of 37,000 m in the North Sea down to 457 m in the River Elbe (see part B of this chapter), and was prepared for the planned investigations (Figs.80a, 80b). Only numerical results obtained with the numerical model under different conditions compared with observations will be discussed here.

The investigation model has altogether 536 point triples, i.e. 536 ζ -points, in which the water level distribution is computed, and 536 u-points and 536 v-points, by which the time expiration of the velocity components is determined or given at the open boundaries.

On the open north west boundary and on the open south east boundary of the investigation area, the water levels as well as the velocities of components were given as $f(t)$ which were taken from the above described model, the natural similarity of which was examined ($2T = 20$ sec).

A possible transport of solids is not included in the numerical model. The point of departure is an unaltered morphology irrespective of the construction changes incorporated into the model.

It must be said beforehand that the area of the lower Elbe in the region of Rhinplatte, Schwarztonnensand and Pagensand certainly belongs to the critical zones which require special attention and observation. The flow cross-section bottle-necks to the north west and south east of the Schwarztonnensand contribute to relatively high velocities and, thereby, to an overall unstable dynamic equilibrium condition in this region and particularly in the river areas downstream. Possible morphological changes as further components remained unconsidered.

The following four investigations were carried out:

- 1) Reproduction of the time dependent movement (water levels and velocities) at the present condition, i.e. with the depth distribution of 1971 (Model 801).
- 2) Link-up of the Schwarztonnensand to the westbank with a simultaneous accretion to the level NN + 4.00 m with a water side slope to NN. The Schwarztonnensand lies roughly between Elbe-km 662 and 668, i.e. Grauerort and Glückstadt (Model 802).
- 3) The same model as 802 under 2) but with an additional high-water free area to NN + 4.00 m at the north west of the Schwarztonnensand -

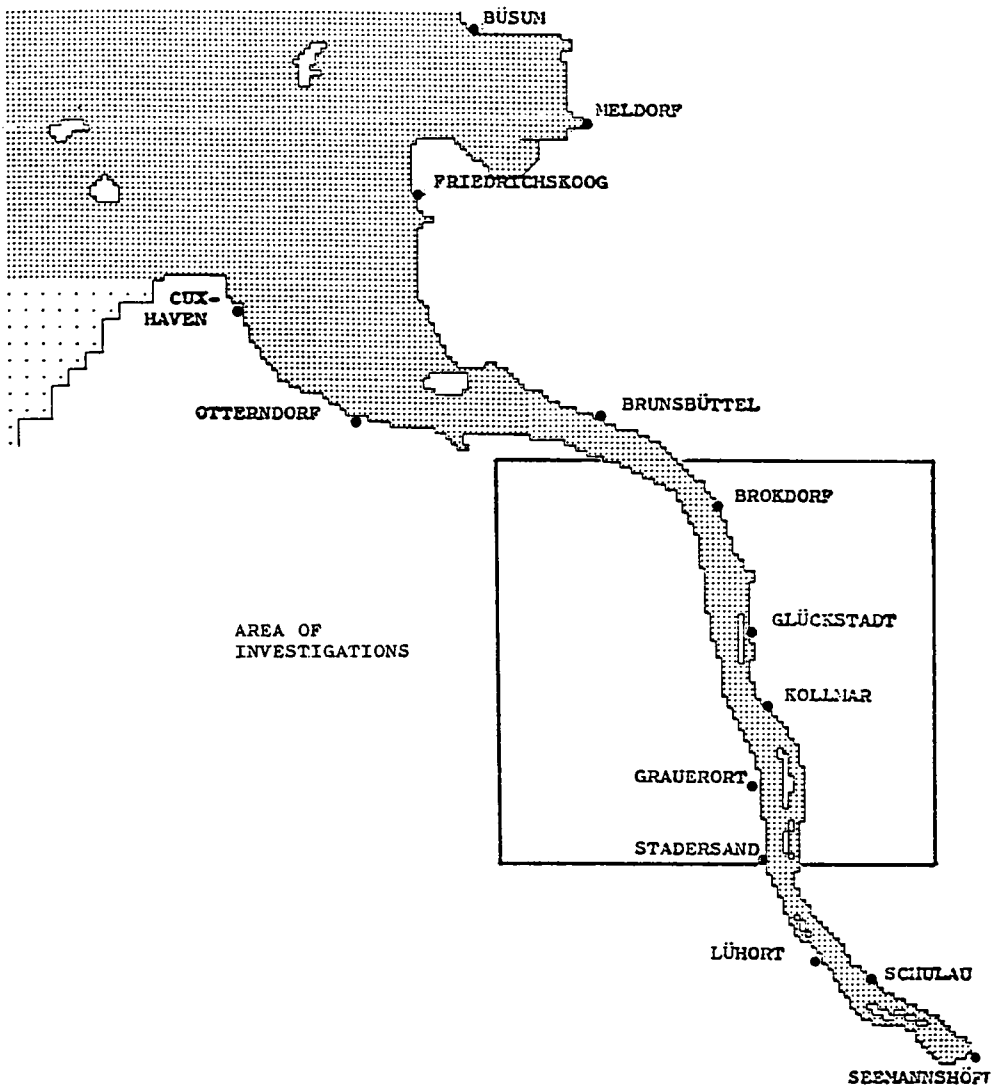


Fig. 80a. RIVER ELBE, ELBE ESTUARY AND THE AREA OF INVESTIGATIONS.

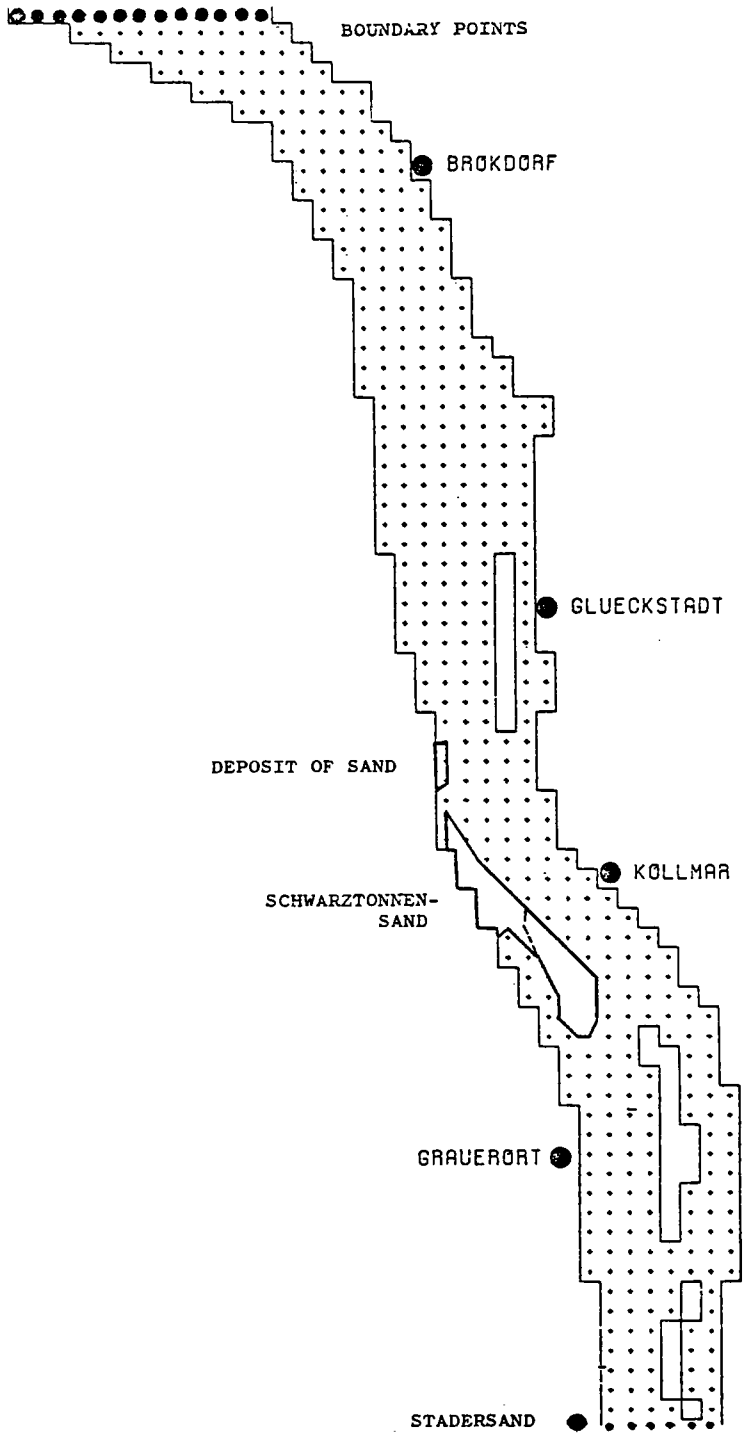


Fig. 8Ob. THE INVESTIGATION AREA, THE BOUNDARY POINTS, THE DEPOSIT OF SAND, THE SCHWARZTONNENSAND AND THE LINK-UP TO THE WEST RIVER BANK OF THE ELBE.

sealed from the Elbe side and built into the numerical model (Model 804).

- 4) The Schwarztonnensand accreted to a height of NN + 4.00 m but not linked to the west bank. The area free at high water at the north west of the Schwarztonnensand, however, remains (Model 805).

The investigations were necessary for examining the influence of the planned measures with regard to the dynamic occurrences. The Schwarztonnensand serves as a deposit for dredged material. Because of its favourable location as a natural sandbank it is well suited to take up the sand dredged by the continuous deepening of the waterway in the River Elbe.

The figures 80a and b show the lower Elbe with the investigation region. The sands and the shallow water area are fairly well approximated. The planned deposit of dredged material on the Schwarztonnensand as well as the high-water free accretion on the west bank are also fairly well reproduced.

The reproduction of natural similarity - the calibration of the numerical model - could be obtained without difficulty by the given boundary and initial values from an existing larger model. It is known that analytical solutions in a compact form cannot be provided for the system of partial differential equations used. Thus only a comparison by means of water level observations inside the model region remains.

The differences of high-water and low-water times within the investigation area were a maximum 10 minutes, the deviations in the water level 5 cm. If an accordance is obtained with water level measurements at discrete points, it can be supposed that the appropriate space and time distribution of the vertically integrated velocities also corresponds to the real conditions in nature.

For prognostic investigations the accordance is an irrevocable assumption, whereby the deviations must be permitted within the scope of the numerically possible accuracy. This will not exclude the fact, however, that there will quite often be critical areas which require closer investigation and examination.

For the reproduction of the separate movements in extremely shallow river bank areas and sometimes partly dry sandbanks, the onset already proved was used again for the bottom friction (Ramming, 1976).

The dynamic processes in the area at that time were determined by means of the model 801 and so well reproduced that further investigations are permissible and a comparison may result in realistic predictions.

A very remarkable result with regard to numerical reproductions of the average current velocities is that at discrete points relatively great values, partly more than 1.0 m/sec, were determined. This fact indicates high surface velocities such as have been measured by Lucht (1963). The time expiration of velocities with regard to a curve form (high-tidal break) is in good accordance with the determinations of Klein (1960) and Lucht (1963). Here it becomes evident how sensitively the velocities react upon the morphological structure of the river bed.

The description of the results is limited to significant features which must be considered as worth noticing, essential or also critical. Some of these results are so evident and also physically understandable that they require no special description.

- 1) Influence of the accretion of the Schwarztonnensand and its link-up to the western bank of the River Elbe. In the figures 81 to 83 the velocity fields of the models 801 and 805 are illustrated. The direction changes of the velocity vectors as a consequence of the building measures are partly considerable and amount not very seldom to 35° - 45° . Increases in the amounts are often up to 35 %. Particularly noticeable is the magnitude range or the size of the area in which such changes occur. The range of influence includes a sector of the lower Elbe which extends from the Rhinplatte up to the north of Grauerort. It can be concluded that this part of the River Elbe is a critical area which reacts sensitively to constructional changes. As a consequence, alterations of the dynamic balance may occur and particularly so if long periods of time are observed or if morphological changes are included. The influences in the near vicinity are already considerable. Here it should be particularly mentioned that already with a screen-grid resolution of 457 m eddy formation can be clearly recognized on the south-eastern point of the accreted Schwarztonnensand. Here and in the area between Schwarztonnensand and the west river bank phase delays will occur as this area is partly (at least) cut off from the present process of movement. The velocities at the east river bank near Kollmar and south of the Rhinplatte are also effected. The magnitude of the sector of influence remains almost unaltered during a tidal period. The figures 81 to 86 show clearly that even the Glückstadt waterway and the area at the east of the Rhinplatte show changes of velocities in amount and direction. The considerable changes in the high waters and low waters in the area between Schwarztonnensand and the west banks of the river are typical for regions which are only partially and with much delay involved in the total movement processes. If the ground

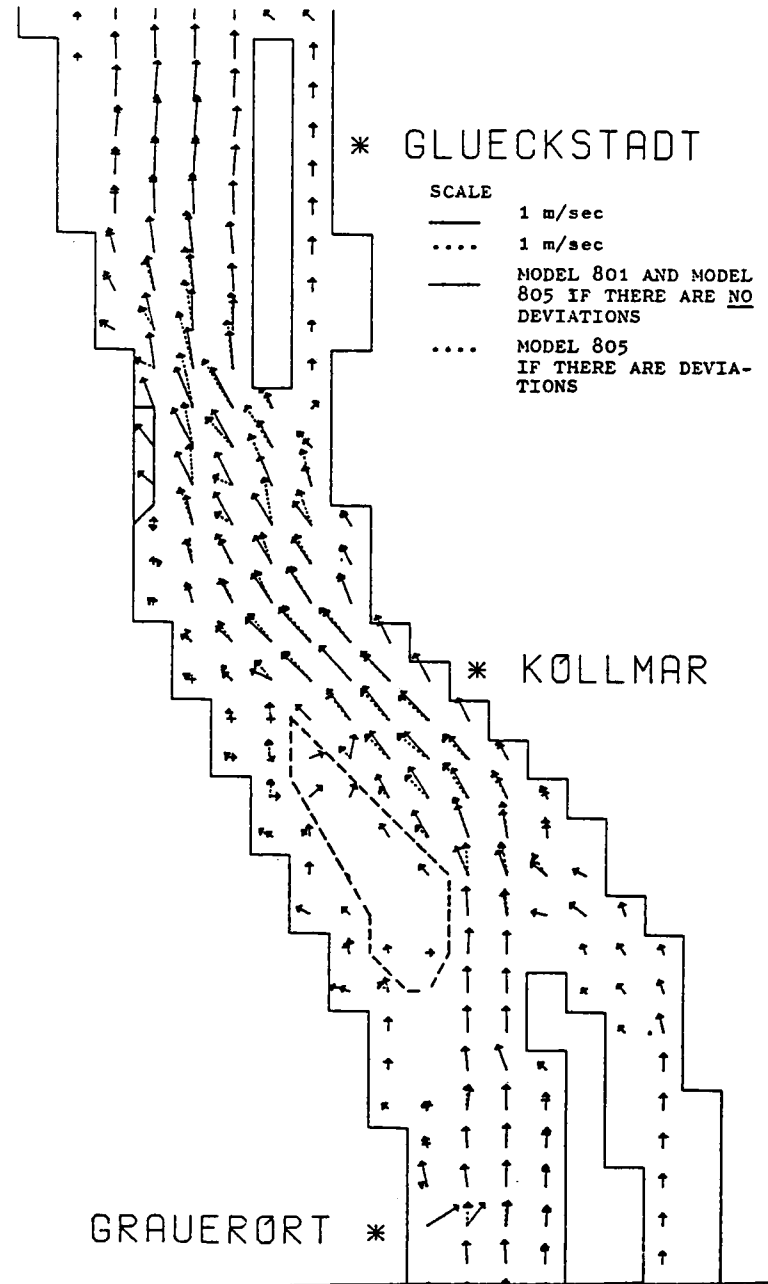


Fig. 81. DISTRIBUTION OF VELOCITIES AT MOON'S TRANSIT THROUGH THE MERIDIAN OF GREENWICH.

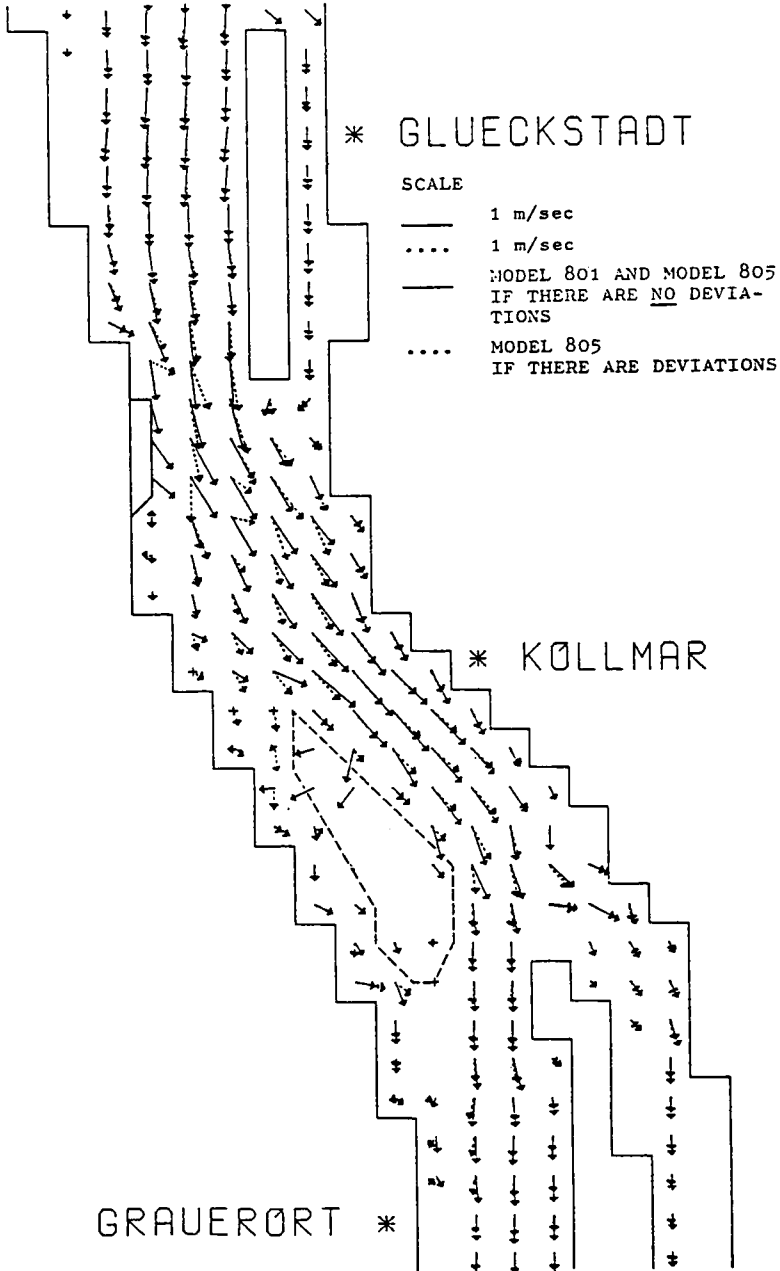


Fig. 82. DISTRIBUTION OF VELOCITIES 4 HOURS AFTER THE MOON'S TRANSIT THROUGH THE MERIDIAN OF GREENWICH.

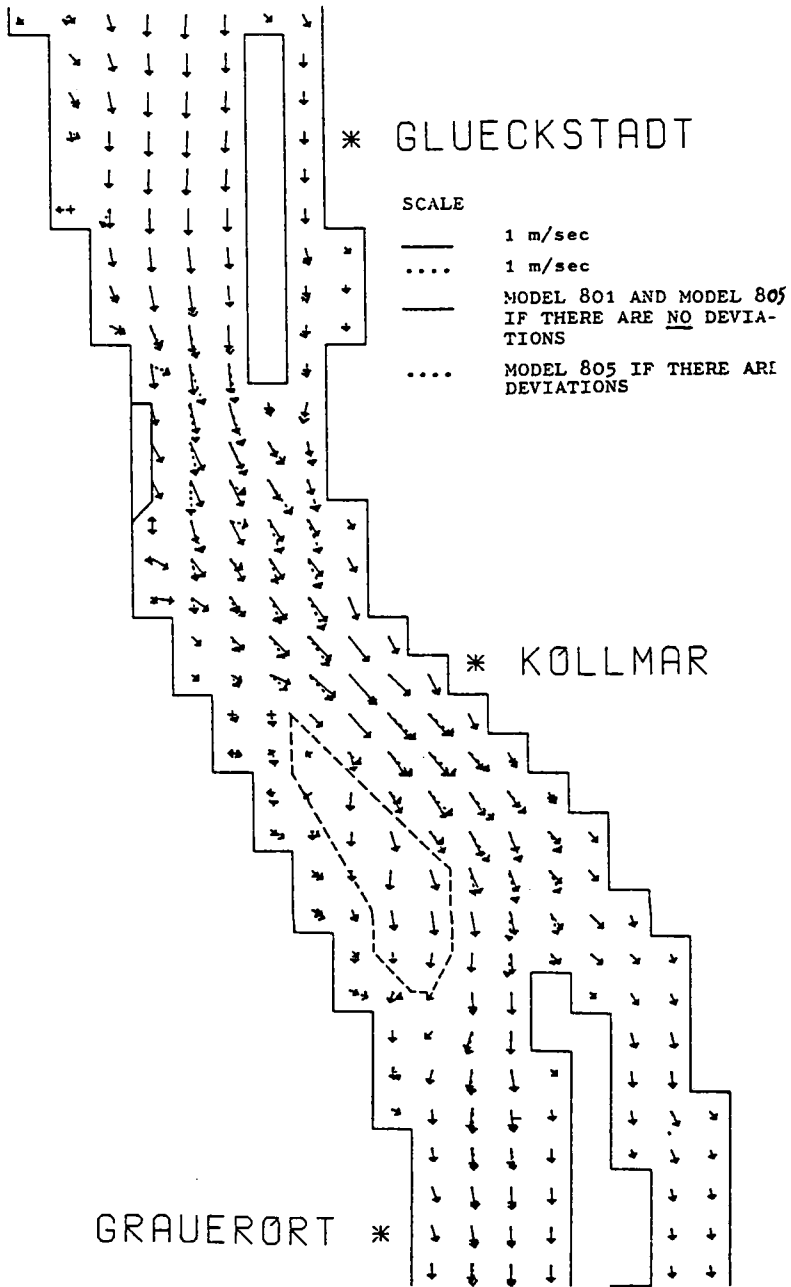


Fig. 83. DISTRIBUTION OF VELOCITIES 8 HOURS AFTER THE MOON'S TRANSIT THROUGH THE MERIDIAN OF GREENWICH.

conditions permit, morphological changes may occur here which will possibly permit a lessening of the strongly increased tidal rises.

- 2) Influence of an additional accretion of a flat surface free at high water on the west bank of the River Elbe. Even these seemingly insignificant construction measures may cause changes which can be worth noticing:
 - a) the velocities in the Glückstadt waterway to the east of the Rhinplatte will be influenced;
 - b) in the narrowed flow cross-section between the Rhinplatte and the accretion occur clearly recognizable higher velocities;
 - c) higher velocities occur also at the east river bank whereas the velocities at the west river bank are slightly reduced.

With regard to the water levels it should be noted that the range of influence extends from 1 km south east of Kollmar up to 4 km south east of Brokdorf and has a total extension of approx. 15 km. The maximum increase of the high water amounts to approx. 3 cm, north of the Rhinplatte still to 2 cm and south of the Rhinplatte to approx. 1 cm. If one adds to these values the lowering of the low water of 2 to 3 cm and the increase of the tidal rise as a consequence of the accretion and the link-up of the Schwarztonnensand of 8 cm, an increase of the tidal rise of approx. 12 to 14 cm will result. Even if these values indicate only a tendency and the order of magnitude, it remains to be taken into consideration that it is not only a change in a small sector of the River Elbe, but in an area of approx. 40 to 50 km² so that consequences with regard to the dynamic balance of the River Elbe cannot be avoided.

- 3) Consequences if no link-up of the Schwarztonnensand with the west river bank exists. The velocity vectors for the River Elbe region Glückstadt - Grauerort give an extensively homogeneous and physically clear picture in a confined investigation area. The area between the Schwarztonnensand and the west river bank takes part in the dynamic processes in so far as the morphology will permit. The eddy formations to the south and west of the Schwarztonnensand will therefore be strongly reduced - as far as reproducible by the selected screen distance. An increase in the high-tide and low-tide velocity between Glückstadt and Grauerort - the region of influence - is still to be understood as a consequence of the cross-section narrowing and the change of the dynamic balance. The current directions parallel to the bank of the Schwarztonnensand may contribute to the up-keep of waterway depth. By not linking the Schwarztonnensand to the

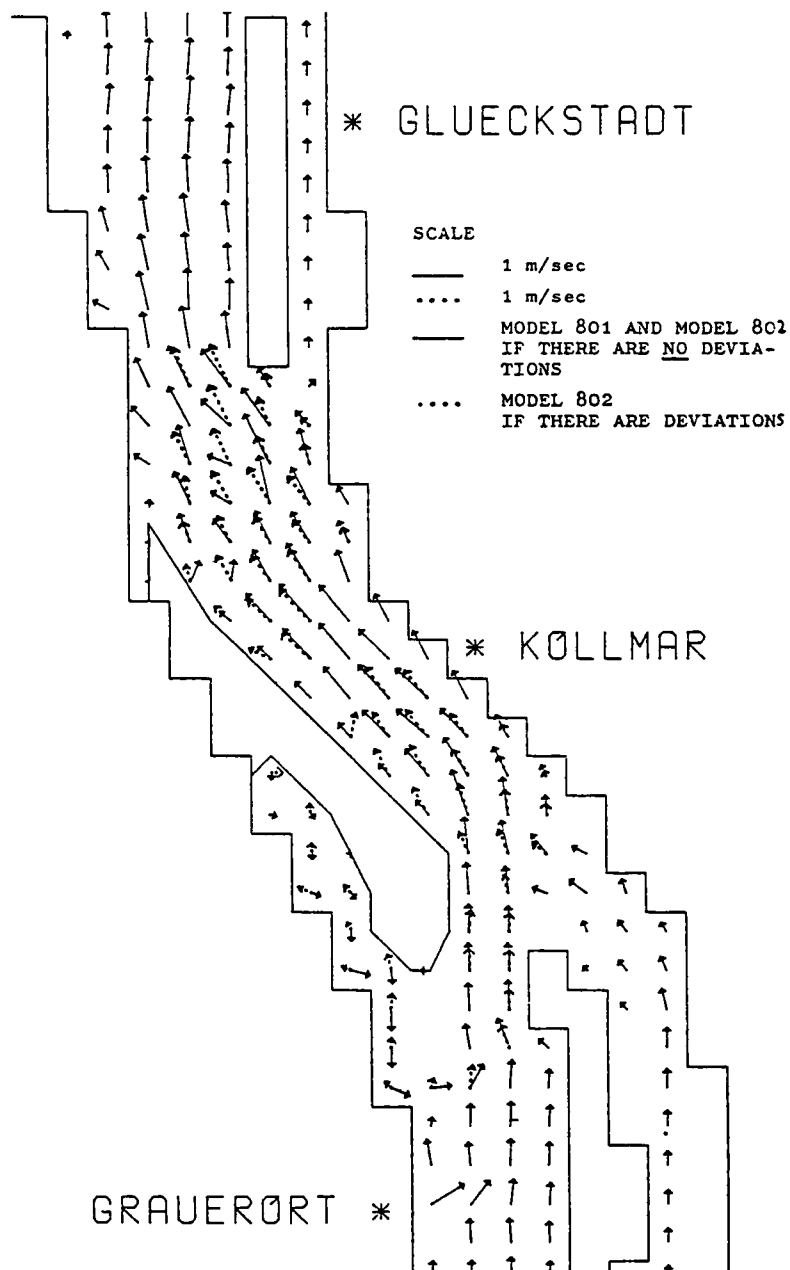


Fig. 84. DISTRIBUTION OF VELOCITIES AT MOON'S TRANSIT THROUGH THE MERIDIAN OF GREENWICH.

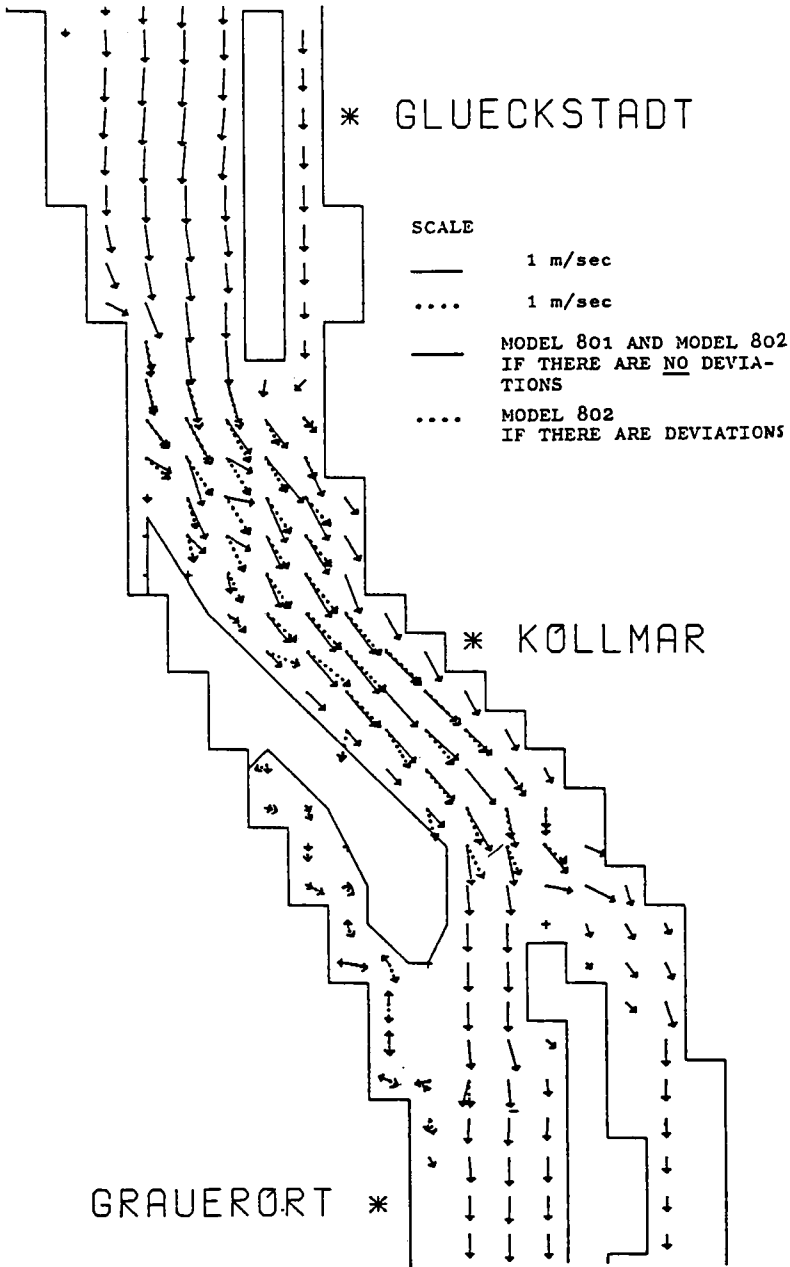


Fig. 85. DISTRIBUTION OF VELOCITIES 4 HOURS AFTER MOON'S TRANSIT THROUGH THE MERIDIAN OF GREENWICH

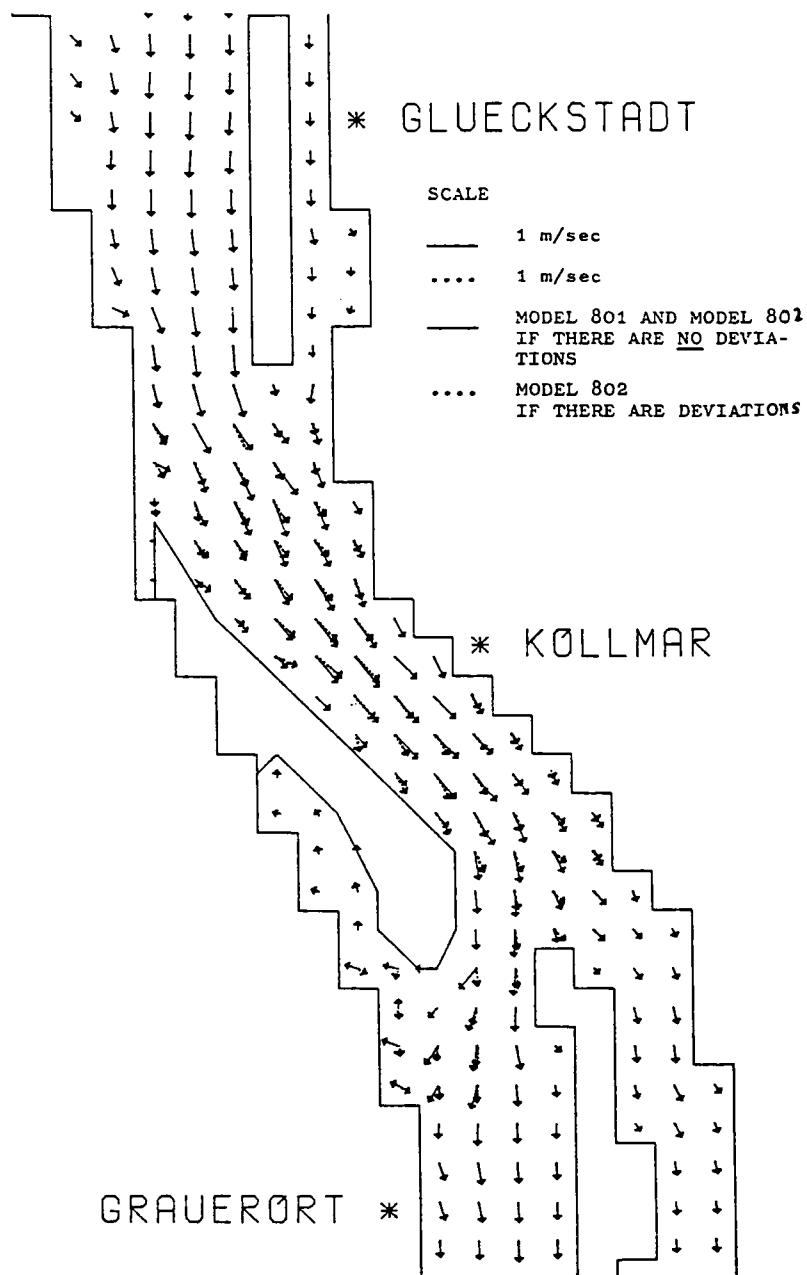


Fig. 86. DISTRIBUTION OF VELOCITIES 8 HOURS AFTER THE MOON'S TRANSIT THROUGH THE MERIDIAN OF GREENWICH.

west river bank, a reduction in the tidal rise will be obtained despite the insignificant high-water free accretion to the north west of the dredged material deposit. The region of influence will be only insignificantly altered. The impairment of the dynamic balance in model 805 is not so incisive as in model 804. The comparison between model 801 - present condition - and model 805 - no link-up but accretion to the north west of the deposit - shows that the construction change is naturally an interference which will effect the dynamic balance but a better adaptation to the present river current picture will be obtained.

From the results described above the following conclusions can be drawn:

- a) Before starting building-construction measures on or in tidal waters or rivers it will be sensible to carry out an investigation into the sphere of influence by using appropriate methods.
- b) The local influences within a close range as well as the imaginable changes over a more distant range and the effect of measures in other river sectors should also be considered in these investigations.
- c) The effect of interaction and the dynamic balance can only be dealt with by large-scale investigation (i.e. comprising the entire River Elbe). Particularly in rivers with a tidal character, the dynamic balance can be considerable disturbed by various construction measures which may not be adapted to each other. In this connection time is also an important component which must not be neglected.
- d) Cross-section narrowings as a consequence of construction measures in tidal rivers - although they are of great advantage to shipping - severely interfere with the balance of dynamic processes. Even with regard to tidal waves they should be carefully considered.
- e) In this example it has been demonstrated that a numerical model can be one device for investigating coastal engineering problems.

REFERENCES

- Ahlberg, J.H.; Nilson, E.N.; Walsh, J.L., 1967. The Theory of Splines and Their Applications. New York Academic Press.
- Banachiewicz, Th., 1938. Méthode de résolution numérique des équations linéaires. Bull. Intern. de l'Académie Polonaise d. Sciences et d. Lettres, N. 8 - 10 A.
- Collins, J.I., 1963. Inception of Turbulence at the Bed Under Periodic Gravity Waves. Jour. Geoph. Res. N. 68: 6007-6014.
- Hansen, W., 1956. Theorie zur Errechnung des Wasserstandes und der Strömungen in Randmeeren nebst Anwendungen. Tellus VIII: 287-300.

- Hansen, W., 1962. Hydrodynamical Methods Applied to Oceanographic problems. Mitt. d. Inst. f. Meeresk. d. Universität Hamburg I: 25-34.
- Hansen, W., 1966. Die Reproduktion der Bewegungsvorgänge im Meere mit Hilfe hydrodynamisch-numerischer Verfahren. Mitt. d. Inst. f. Meeresk. d. Univ. Hamburg V.
- Heaps, N.S., 1969. A Two-Dimensional Numerical Sea Model. Philos. Trans. Roy. Soc. of London v. 265, N. 1160: 93-137.
- Heaps, N.S., 1972. Estimation of Density Currents in the Liverpool Bay Area of the Irish Sea. Geoph. J.R. Astr. Soc. v. 30: 415-432.
- Iamada, H., 1959. Theoretical Estimation of Meteorological High Water. Rep. Res. Inst. Fluid Eng. Kyushu Univ. v. 6, N. 2: 27-44
- Ippen, A.T. and Harleman, R.D.F., 1966. Tidal Dynamics in Estuaries. In: Estuary and Coastline Hydrodynamics. McGraw-Hill, New York: 493-545.
- Jelesnianski, C.P., 1965. A Numerical Calculation of Storm Tides Introduced by a Tropical Storm Impinging on a Continental Shelf. Month. Weath. Rev. N. 93: 343-358.
- Jelesnianski, C.P., 1966. Numerical Computations of Storm Surges without Bottom Stress. Month. Weath. Rev. N. 9: 379-394.
- Jelesnianski, C.P., 1967. Numerical Computation of Storm Surges with Bottom Stress. Month. Weath. Rev. v. 95, N. 11: 740-756.
- Kitajgorodski, S.A., 1970. Physics of Atmosphere-Ocean Interaction. Gidrometeoizdat, Leningrad.
- Klein, H.-A., 1960. Strömungsverhältnisse und Wassermengen der Tideelbe. Mitt. d. WSD Hamburg Nr. 11.
- Koss, W.J., 1971. Numerical Integration Experiments with Variable Resolution Two-Dimensional Cartesian Grids Using the Box Method. Month. Weath. Rev. v. 99: 725-738.
- Le Provost, Ch., 1974. Contribution à l'étude des Marées dans les Mers littorales. Application à la Manche. Univ. Scien. et Medicale de Grenoble, Ph. D. Thesis.
- Lucht, F., 1963. Strömungsmessungen 1958/1961 im unteren Tidegebiet der Elbe. Mitt. d. WSD Hamburg, Nr. 15.
- Maier-Reimer, E., 1977. Residual Circulation in the North Sea due to the M_2 -Tide and Mean Annual Wind Stress. Deutsch. Hydr. Zeit. Heft 3: 69-80.
- Nihoul, J.C.J., 1976. Modélisation des systèmes marins. Université de Liège.
- Nihoul, J.C.J., 1977. Three-Dimensional Model of Tides and Storm Surges in a Shallow Well-Mixed Continental Sea. Dynamics of Atm. and Oceans N. 2: 29-47.
- Platzman, G.W., 1958. A Numerical Computation of the Surge of 26th June 1954 on Lake Michigan. Geophysica N. 6: 407-438.
- Platzman, G.W., 1963. The Dynamical Prediction of Wind Tides on Lake Erie. Met. Monogr. v. 4, N. 26.
- Ramming, H.-G., 1961. Gezeiten und Gezeitenströme in der Eider. Mitt. d. Inst. f. Meeresk.d.Univ. Hamburg, Heft I.
- Ramming, H.-G., 1971. Hydrodynamical-Numerical Investigations and Horizontal Dispersion of Seston in the Elbe River. Mémoires de la Société Royale des Sciences de Liège, TOME VI.

- Ramming, H.-G., 1977. Numerical Investigations of the Influence of Coastal Structures on the Hydrodynamic Off-Shore Process by Application of a Nested Tidal Model. In: Hydrodynamics of Estuaries and Fjords. Elsevier Publishing Company: 315 - 348.
- Ramming, H.-G., 1978. The Influence of River Normalization on the Distribution of Tidal Currents in the Elbe River. Proc. VII th Intern. Harbour Conference 1978, Antwerpen.
- Ramming, H.-G., 1978. Ein numerisches Nordsee-Modell mit hoher Gitternetzauflösung im Elbemündungsgebiet und in der Elbe. Mitt. d. Wasser- und Schifffahrtsdirektion Nord Nr. 23.
- Reid, R.O., 1957. Modification of the Quadratic Bottom-Stress Law for Turbulent Channel Flow in the Presence of Surface Wind Stress. Techn. Memo. 93. U.S. Army Corps of Eng. Beach Erosion Board.
- Reid, R.O. and Bodine, B.R., 1968. Numerical Model for Storm Surges in Galveston Bay. J. Waterways and Harbours Division PASCE N. 5805: 33-57.
- Rose, D., 1960. Über die quantitative Ermittlung der Gezeiten und Gezeitenströme in Flachwassergebieten mit dem Differenzenverfahren. Mitt. d. Franzius-Inst. für Grund- und Wasserbau d. Techn. Hochschule Hannover, Heft 18.
- Uusitalo, S., 1962. The Numerical Calculation of Wind Effect on the Sea Level Elevation. Mitt. d. Inst. f. Meereskunde d. Univ. Hamburg, Heft I: 245-256.
- Volcinger, N.E. and Piaskovski, R.v., 1968. Basic Oceanological Problems of the Shallow Water Theory. Gidrometeoizdat, Leningrad.

Chapter VII THE APPLICATION OF THE TRANSPORT EQUATIONS

§1. The basic concepts

A finely divided substance, released into a body of water, will immediately tend to spread out uniformly throughout the whole basin. This tendency, e.g. of salt or pollutants, to disperse is caused by different factors such as molecular and turbulent processes or advective motion. Turbulent dispersion is influenced by the velocity field and characterized by a more or less uniform spectrum extending from small scale motion of the order of a centimetre up to the largest scales of horizontal motion with dimensions equal to those of the ocean itself. It is customary to classify the turbulent motion by a set of eddies of different dimensions. Using Fourier analysis, time series of velocity at a certain point are decomposed. Then the ergodic hypothesis is involved in trying to extend the statistics spatially.

Observing a cloud of substance in the sea we find that those eddies of length greater than the dimensions of the cloud 'advect' it. In other words the cloud is transported or 'advected' as an integral object (a reversible process). On the other hand, those eddies with dimensions smaller than the cloud effect the 'dispersion' of the cloud itself (an irreversible process). As the size of a cloud of substance grows with time, the relative importance of dispersion and advection processes is constantly changing. Therefore we come to the conclusion that turbulent diffusion is a function of time and space. This contrasts sharply with molecular diffusion which has constant length and time scales.

The following equation which is based on the work of Fick (1855) is the usual expression for the rate of change of substance concentration due to molecular diffusion and advection:

$$\frac{\partial c}{\partial t} + \sum_{i=1}^3 \frac{\partial (u_i c)}{\partial x_i} = \sum_{i=1}^3 \frac{\partial}{\partial x_i} (D_i \frac{\partial c}{\partial x_i}) \quad (7.1)$$

where c is the concentration (defined by mass of substance per unit mass of water) and u_i are the components of velocity along the x_i co-ordinates (here $x_1 = x$, $x_2 = y$, $x_3 = z$). The molecular diffusion coefficient is taken as constant in each direction, i.e. $D_1 = D_2 = D_3 = D$. A solution of equation (7.1) is possible for constant values of u_i and a fairly wide range of initial and boundary conditions. The results of such computations, however, differ quite strongly from the observed

state in natural basins. Accordingly the constancy of u_i and the molecular diffusion concept as a whole were abandoned long ago as means of describing diffusion in the ocean. Turbulent diffusion shows a far more complicated pattern of variability. It is fairly obvious that such a situation calls for a statistical approach, since only the averaged values of variables are stable and meaningful.

Suppose that the velocity field can be described by a mean value \bar{u}_i and a varying (turbulent) component u'_i , i.e.

$$u_i = \bar{u}_i + u'_i \quad (7.2)$$

In the same way the concentration is taken as

$$c = \bar{c} + c' \quad (7.3)$$

We can introduce (7.2) and (7.3) into (7.1). Assuming that either $u(t)$ or $c(t)$ is only slowly varying with time, the Reynolds rules for averages (Hinze, 1959) can be applied. Averaging accordingly the resulting equation in time, we obtain the following equation which describes the mean concentration:

$$\frac{\partial \bar{c}}{\partial t} + \sum_{i=1}^3 u_i \frac{\partial \bar{c}}{\partial x_i} = \sum_{i=1}^3 - \frac{\partial \bar{u}'_i c'}{\partial x_i} + \sum_{i=1}^3 \frac{\partial}{\partial x_i} (D_i \frac{\partial \bar{c}}{\partial x_i}) \quad (7.4)$$

The averaged values of the varying components, e.g. \bar{u}'_i , are equal to zero. In (7.4) \bar{c} and \bar{u}_i are not steady values in time, since the averaging encompasses the finite span of time T , thus

$$\bar{c}(t, T) = \frac{1}{T} \int_{\tau=t-T/2}^{\tau=t+T/2} c(x_1, x_2, x_3, \tau) d\tau$$

$$\bar{u}_i(t, T) = \frac{1}{T} \int_{\tau=t-T/2}^{\tau=t+T/2} u_i(x_1, x_2, x_3, \tau) d\tau \quad (7.5)$$

Such an expression is commonly called a moving (with time) average.

In (7.4) the new expression $\bar{u}'_i c'$ describes the flux of substance due to turbulent motion. Mathematically it represents a new unknown quantity, therefore the problem is not closed and cannot be solved in a unique way. Using the Boussinesq hypothesis, Taylor (1915) and Schmidt (1917) assumed that the turbulent flux of a substance is

proportional to the gradient of the mean concentration

$$\overline{u_i'c'} = -K_{ij} \frac{\partial \bar{c}}{\partial x_j} \quad (7.6)$$

where K_{ij} is the eddy diffusivity tensor. This coefficient represents the participation of turbulence in the overall transport process and describes the intensity of turbulent mixing which is generally much greater than molecular diffusion D_i . Usually the nondiagonal terms of K_{ij} are assumed to be negligibly small (Monin and Jaglom, 1965). Therefore the general equation to describe transport phenomena in a turbulent medium is the following

$$\frac{\partial c}{\partial t} + u \frac{\partial c}{\partial x} + v \frac{\partial c}{\partial y} + w \frac{\partial c}{\partial z} = \frac{\partial}{\partial x} (K_x \frac{\partial c}{\partial x}) + \frac{\partial}{\partial y} (K_y \frac{\partial c}{\partial y}) + \frac{\partial}{\partial z} (K_z \frac{\partial c}{\partial z}) \quad (7.7)$$

From now on we omit the overbar denoting the mean value to simplify the notation.

A second approach to the same problem is also possible. Since turbulence is a random process, diffusive mixing can also be treated as a random process. To describe the transport of a particle Kolmogoroff (1931) derived the equation for the probability density $p(M, t | M_0, t_0)$ of the displacement of a particle from the point $M_0(x_0, y_0, z_0)$ to the point $M(x, y, z)$ in time $t - t_0$

$$\frac{\partial p}{\partial t} + \sum_{i=1}^3 \frac{\partial}{\partial x_i} (u_i p) = \sum_{i=1}^3 \sum_{j=1}^3 \frac{\partial^2}{\partial x_i \partial x_j} (K_{ij} p) \quad (7.8)$$

where

$$u_i = \frac{\partial}{\partial t} \int x_i p(M, t | M_0, t_0) dx_1 dx_2 dx_3 \quad (7.9)$$

$$K_{ij} = \frac{\partial}{\partial t} \int x_i x_j p(M, t | M_0, t_0) dx_1 dx_2 dx_3 \quad (7.10)$$

mean the average velocity and the eddy diffusion coefficient.

The concentration c in a turbulent cloud emitted from a point source and the probability density are connected as follows (Hinze, 1959)

$$c = Qp(M, t | M_0, t_0) \quad (7.11)$$

In (7.11) Q is the mass of substance released instantaneously from the source. Multiplying (7.8) by Q we arrive at an equation for the concentration c instead of the probability density p . When the coordinates of the particle being observed are changing in accordance with a Markov process, K_{ij} can be expressed in terms of the dispersion or variance of the displacement as follows

$$K_x = \frac{1}{2} \frac{d}{dt} \overline{[x(t) - x(t_0)]^2} \quad (7.12a)$$

$$K_y = \frac{1}{2} \frac{d}{dt} \overline{[y(t) - y(t_0)]^2} \quad (7.12b)$$

$$K_z = \frac{1}{2} \frac{d}{dt} \overline{[z(t) - z(t_0)]^2} \quad (7.12c)$$

These expressions often serve as a means of relating observed values of the dispersion rate of tagged particles with the eddy diffusion coefficient.

Taylor (1921) started the statistical approach by considering diffusion by continuous movement. When a tagged particle is observed in its movement, it possesses velocity u_t at time t and velocity $u_{t+\tau}$ at time $t+\tau$ respectively. The mean square displacement during time is specified as

$$\overline{x^2} = \overline{\left[\int_t^{t+\tau} u(\gamma) d\gamma \right]^2} \quad (7.13)$$

or

$$\overline{x^2} = \int_t^{t+\tau} \int_0^{t+\tau} \overline{u(\gamma_1)u(\gamma_2)} d\gamma_1 d\gamma_2 \quad (7.14)$$

Introducing the Lagrangian coefficient of correlation

$$R_L(\gamma_2 - \gamma_1) = \frac{1}{u^2} \overline{u(\gamma_1)u(\gamma_2)} = \frac{1}{u^2} \overline{u_t u_{t+\tau}} \quad (7.15)$$

(7.14) is changed to

$$\overline{x^2} = \overline{u^2} \int_t^{t+\tau} (\tau - \gamma) R_L d\gamma \quad (7.16)$$

where $\gamma_1 - \gamma_2 = \gamma$.

The eddy diffusion coefficient for the x-axis in agreement with (7.12) is set as

$$K_x = \overline{u^2} \int_t^{t+\tau} R_L(\gamma) d\gamma \quad (7.17)$$

The further development is wholly dependent on the coefficient of Lagrangian correlation (Hinze, 1959). Two obvious cases are apparent; for a small time step τ the coefficient $R_L(\tau)$ is very close to unity, therefore

$$\overline{x^2} = \overline{u^2} \tau^2 \quad (7.18)$$

It is reasonable to assume that velocities which are sufficiently far apart in time are uncorrelated and $R_L = 0$, thus

$$\overline{x^2} = 2K_x \tau \quad (7.19)$$

In addition to the approaches presented above, Richardson (1926) also introduced the concept of neighbour separation to represent the percentage of pairs of particles which are the same distance apart. The diffusion problem is described there in terms of the separation of particles and not of a concentration. Instead of the usual concept of the diffusion coefficient the neighbour diffusion coefficient $F(l)$ is introduced. If the probability density for the separation distance l between the pair of particles is $q(l)$, then

$$\frac{\partial q}{\partial t} = \frac{\partial}{\partial l} [F(l) \frac{\partial q}{\partial l}] \quad (7.20)$$

The concept of neighbour diffusion is still very popular for two reasons: firstly, it is a relatively simple way of performing experiments with tagged particles and secondly the dependence of F against distance as proposed by Richardson (1926)

$$F(l) = k l^{4/3} \quad (7.21)$$

holds also for the usual diffusion coefficient K . Following Ozmidov (1968) we set $F \approx 3K$.

§2. Two-dimensional turbulent diffusion

The process of turbulent diffusion is more or less non-isotropic depending on the scale being considered. Non-isotropy is indicated by different intensities of turbulent diffusion in the horizontal

and vertical directions. The observed horizontal orientation of turbulent motion is due mainly to

- a) big differences in the characteristic horizontal and vertical dimensions of natural basins (the typical ratio of these dimensions is 1000:1),
- b) the non-isotropic flow of energy out of the biggest eddies, which is the generating mechanism for establishing smaller eddies in agreement with the Kolmogoroff theory (Ozmidov, 1968).

Vertical diffusion, on the other hand, is dependent on the action of the Archimedian force, since due to the density stratification the vertical exchange of momentum and matter decays. A great number of publications has been devoted to the problem of vertical diffusion (e.g. Bowden, 1962; Zeidler, 1975). Vertical eddy diffusion is usually related to the Richardson number

$$R_i = - \frac{g \frac{\partial \rho}{\partial z}}{\rho \frac{\partial \bar{u}}{\partial z}} / \left(\frac{\partial \bar{u}}{\partial z} \right)^2 \quad (7.22)$$

For the vertical diffusion coefficient K_z Munk and Anderson (1948) proposed the following form

$$K_z = A_0 (1 + \beta R_i)^{-m} \quad (7.23)$$

where

$$\beta = 3.33$$

$$m = 3/2$$

$$A_0 = l_0^2 \left| \frac{d\bar{u}}{dz} \right| \quad (7.24)$$

l_0 is the mixing length (sometimes called 'scale of turbulence')

A_0 is the eddy diffusion coefficient when there is no density stratification ($R_i = 0$)

\bar{u} is the mean velocity.

The overall problem of vertical exchange may be solved through the application of the equation of turbulent energy and the similarity hypothesis of Kolmogoroff as stated in chapter III, equations (3.60), (3.61) and (3.62). It is seen from (3.61) that the eddy diffusion coefficient is related to the eddy viscosity by the constant parameter α_ρ . In the computation of the current we took $\alpha_\rho = 0.1$, while at the sea surface, where the well-mixed layer exists, the value $\alpha_\rho = 1$ is more probable. Therefore, in choosing a vertical

eddy diffusion coefficient we may start from the value of the eddy viscosity.

Very often, in the sea or in a river, a strong one-directional shear flow is observed which causes the advection of a substance and at the same time transverse dispersion or mixing. Transverse dispersion is a factor which can be related to the diffusion by expression (7.12). In general the dispersion (turbulent diffusion) coefficient depends on the shape of the cross-section (river, channel), the water depth and the mean velocity. We present some results for different flows of special types as follows

a) Steady pipe flow (Taylor, 1954)

$$K_z = 10.1 a \sqrt{\tau/\rho} \quad (7.25)$$

In this equation a is the pipe's radius and τ the shear stress at the wall (Hereafter all units are expressed in metres, seconds and grams).

b) Steady open-channel flow of a homogeneous fluid with constant depth (Elder, 1959)

$$K_z = 5.9 (H + \zeta) \sqrt{\tau/\rho} \quad (7.26)$$

Assuming that the stress at the bottom is given by $rU|U|$ it follows (Bowden, 1963)

$$K_z = 0.324 (H + \zeta) |U| \quad (7.27)$$

With the help of this relation, which considers both, the spatial as well as, implicitly, the time change of K_z , Bowden (1963) successfully investigated the diffusion processes in several estuaries. It is a great consolation that K_z as computed by (7.27) is close to the value obtained using a quite different approach, which considered the currents in a shallow sea (3.38).

c) Steady flow in an open channel (Fischer, 1967)

$$K_z = \frac{1}{A} \int_0^b q \left[\int_0^z E_z / H \cdot \left(\int_0^z q d\alpha \right) d\beta \right] dl \quad (7.28)$$

where

q rate of flow per unit width (m^2/sec)

b width of the channel

A cross-sectional area

E_z coefficient of diffusion given by $E_z = 0.234H\sqrt{\tau/\rho}$

Let us now consider horizontal mixing with an assumption of horizontal isotropy. The equation governing this process can be written in polar co-ordinates as

$$\frac{\partial c}{\partial t} = \frac{1}{r} \frac{\partial}{\partial r} (K_1 r \frac{\partial c}{\partial r}) \quad (7.29)$$

where r is a radius with its origin at the source. The horizontal eddy diffusion coefficient K_1 is a function of the radial distance (and of time).

Depending on the assumed functional dependence of K_1 on r , two solutions of (7.29) are possible. Joseph and Sender (1958) proposed a solution in which

$$K_1 = Pr/2 \quad (7.30)$$

P is called a diffusion velocity and is equal to 1 ± 0.5 cm/sec. This approach is based on the natural concept that the change in dispersion (7.13) should depend on a certain characteristic velocity.

Another approach is based on the concept of energy transfer by the turbulent eddies from big to small scales and the supposition that the turbulent diffusion takes place mainly in the inertial subrange where local isotropy exists. In this subrange all characteristics of turbulence depend on the rate of transfer of turbulent energy (Landau and Lifshitz, 1959), therefore

$$K_1 = k_1 r^{4/3} = k_2 \epsilon^{1/3} r^{4/3} \quad (7.31)$$

The dependence of the radial eddy diffusivity K_1 on the horizontal scale of the process r is presented in fig. 87. The data for this figure were gathered by Okubo and Ozmidov (1970). Their data cover different scales but were taken only in a surface layer which was well-mixed. Experiments in the deeper layers show that the intensity of horizontal mixing is smaller than that in the surface layer. Horizontal mixing in the thermocline was studied by Kullenberg (1970) and provides a typical value for the diffusion velocity P of 0.1 cm/sec compared with 1 cm/sec in the surface layer. It should be stressed that in the basins of limited depth, the intensity of horizontal diffusion decreases with depth. Ozmidov (1968) proposed on the basis of his own experiments a corrected expression for the neighbour diffusion coefficient (7.21)

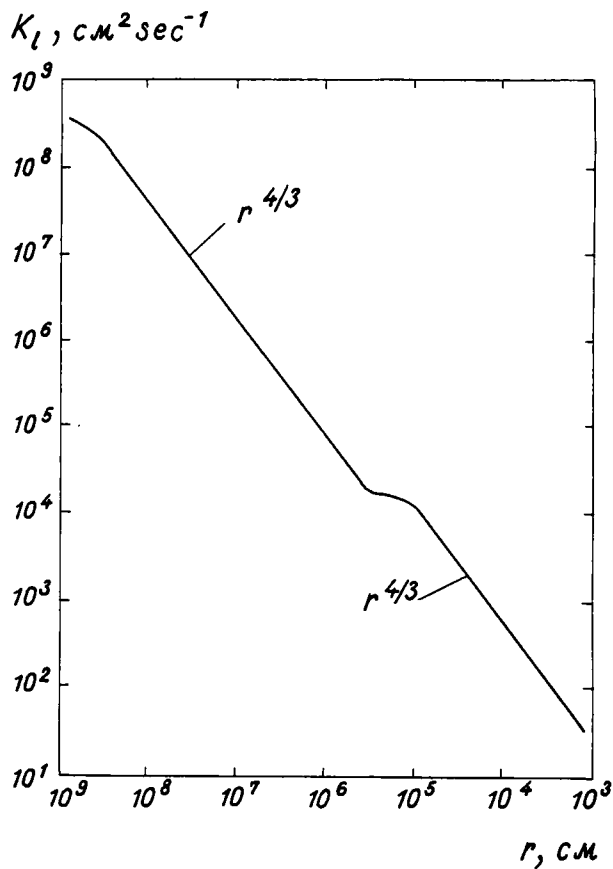


Fig. 87. DEPENDENCE OF HORIZONTAL EDDY DIFFUSION K_1 ON THE SCALE OF PHENOMENON r ACCORDING TO OKUBO AND OZMIDOV (1970).

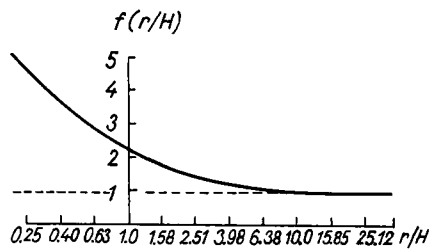


Fig. 88. CORRECTION $f(r/H)$ TO THE $4/3$ LAW FOR THE SMALL DEPTHS H ACCORDING TO OZMIDOV (1968).

$$F = k_1 r^{4/3} f(r/H) \quad (7.32)$$

The dependence of f on r/H is plotted in fig. 88.

Finally, we shall briefly describe the boundary and initial conditions. Initially, if the basin is free from any passive mixture, then $c(t=0, x, y) = 0$. It is also conceivable that when there is a background concentration the computed concentration can be related to the difference between this background concentration and the concentration of the mixture.

The boundary condition for the diffusion problem may be stated in the following general form

$$\alpha \frac{\partial c}{\partial n} + \beta c = Q(t) \quad (7.33)$$

where $Q(t)$ is a given function of time, n denotes a normal to the boundary and α and β are prescribed parameters.

If the source of the mixture is placed at the boundary, the following conditions are possible:

- a) Given that a quantity $Q_1(t)$ of a substance is released from a source, then at that fluid part of the boundary contour $\alpha \frac{\partial c}{\partial n} = Q_1(t)$ and at the coast (everywhere else) $\alpha \frac{\partial c}{\partial n} = 0$.
- b) Given a concentration at the boundary $Q_2(t)$, then $\beta c = Q_2(t)$ at the fluid contour and $\alpha \frac{\partial c}{\partial n} = 0$ at the coast.

It should be stressed that the boundary condition at the coast may depend to a large extent on the nature of the coast and its absorbing properties. The coastal properties as related to the given mixture are characterized by an absorption factor γ . In case of complete absorption the concentration vanishes at the coast, i.e. $c = 0$. Partial coastal absorption may be modelled by the expression

$$\frac{K}{\gamma} \frac{\partial c}{\partial n} + \beta c = 0 \quad (7.34)$$

where K denotes the eddy diffusion coefficient at the grid point nearest to the coast.

When the source is placed in the open basin the boundary condition expresses the requirement that the mixture vanishes with increasing distance from the point of release

$$c(t, x \rightarrow \infty, y \rightarrow \infty) = 0 \quad (7.35)$$

§3. Numerical methods of solving the transport equation

We shall start with the horizontal diffusion, neglecting the advection, thus

$$\frac{\partial c}{\partial t} = K \Delta c \quad (7.36)$$

The result obtained in chapter IV allows us to write (7.36) in a finite difference form with second-order accuracy in space and time. The time step T is divided into two substeps and the operator in (7.36) is split in the following way

$$\frac{1}{2} \frac{\partial c}{\partial t} = \frac{K}{2} \Delta c \quad (7.37a)$$

$$\frac{1}{2} \frac{\partial c}{\partial t} = \frac{K}{2} \Delta c \quad (7.37b)$$

For this system we can write down the mixed implicit-explicit form as follows

$$\frac{c^{l+1/2} - c^l}{T} = \frac{K}{2} \left(\frac{\partial^2 c^{l+1/2}}{\partial x^2} + \frac{\partial^2 c^l}{\partial y^2} \right) \quad (7.38a)$$

$$\frac{c^{l+1} - c^{l+1/2}}{T} = \frac{K}{2} \left(\frac{\partial^2 c^{l+1/2}}{\partial x^2} + \frac{\partial^2 c^{l+1}}{\partial y^2} \right) \quad (7.38b)$$

The computation at every time step can be performed with the help of the factorization method (Chapter II), along the x -axis for (7.38a) and along the y -axis for (7.38b).

The overall stability is a function of the stabilities of the individual substeps. To analyse the stability along with expression (4.17) we shall use a simplified form

$$c = c^l e^{i\sigma_1 j h} e^{i\sigma_2 k h} \quad (7.39)$$

Substituting (7.39) into (7.38a) we find after some manipulation that

$$\lambda_1 = c^{l+1/2}/c^l = \left[1 - \frac{2KT}{h^2} \sin^2 \left(\frac{1}{2} \sigma_2 h \right) \right] / \left[1 + \frac{2KT}{h^2} \sin^2 \left(\frac{1}{2} \sigma_1 h \right) \right] \quad (7.40)$$

From (7.38b) it follows that

$$\lambda_2 = c^{1+1}/c^{1+1/2} = [1 - \frac{2KT}{h^2} \sin^2(\frac{1}{2}\sigma_1 h)] / [1 + \frac{2KT}{h^2} \sin^2(\frac{1}{2}\sigma_2 h)] \quad (7.41)$$

Hence the overall stability parameter for the time step T is

$$\lambda = \lambda_1 \lambda_2 = c^{1+1}/c^1 \quad (7.42)$$

where

$$\lambda = \frac{[h^2 - 2KT \sin^2(\frac{1}{2}\sigma_2 h)][h^2 - 2KT \sin^2(\frac{1}{2}\sigma_1 h)]}{[h^2 + 2KT \sin^2(\frac{1}{2}\sigma_1 h)][h^2 + 2KT \sin^2(\frac{1}{2}\sigma_2 h)]} \quad (7.43)$$

Since the modulus of λ in (7.43) is always smaller than unity, the system (7.38) is unconditionally stable for an arbitrary choice of time and space steps. As we know from the considerations presented in chapter IV, the accurate reproduction of the physical phenomena limits the time step to a value which is close to that required for stability in the explicit method. On the other hand, as practical computations show, the time step in implicit schemes for transport phenomena may be taken to be much longer than that in the corresponding explicit schemes.

Let us consider now the explicit numerical scheme applied to (7.36)

$$\frac{c^{1+1} - c^1}{T} = K\Delta c^1 \quad (7.44)$$

Hence from (7.39) it follows that

$$\lambda = 1 - \frac{4KT}{h^2} [\sin^2(\frac{1}{2}\sigma_1 h) + \sin^2(\frac{1}{2}\sigma_2 h)] \quad (7.45)$$

The stability criterion $|\lambda| \leq 1$ provides the inequality

$$0 \leq T \leq h^2/4K \quad (7.46)$$

We may therefore state that the time step in the explicit method is a function of the diffusion coefficient K and the grid distance h.

We shall consider now a more complicated case of lateral transport while advection is present

$$\frac{\partial c}{\partial t} + u \frac{\partial c}{\partial x} + v \frac{\partial c}{\partial y} = K\Delta c \quad (7.47)$$

The simplest numerical scheme is, of course, the explicit one, but we have to take into account the variability of the coefficients u and v of the first derivatives. Such a numerical scheme has a rather weak approximation and, additionally, severely limits the time step. For this reason we shall seek more flexible numerical schemes. Firstly we introduce an implicit form which will be part of the general algorithm

$$\begin{aligned} \frac{c^{l+1} - c^l}{T} + \frac{u - |u|}{2} \nabla_x^+ c^{l+1} + \frac{u + |u|}{2} \nabla_x^- c^{l+1} + \frac{v - |v|}{2} \nabla_y^+ c^{l+1} \\ + \frac{v + |v|}{2} \nabla_y^- c^{l+1} = K \Delta c^{l+1} \end{aligned} \quad (7.48)$$

The stability parameter calculated with the help of (7.39) is equal to

$$\begin{aligned} \lambda = c^{l+1}/c^l = 1/\{1 + \frac{4KT}{h^2}[\sin^2(\frac{1}{2}\sigma_1 h) + \sin^2(\frac{1}{2}\sigma_2 h)] \\ + \frac{2T}{h}[|u|\sin^2(\frac{1}{2}\sigma_1 h) + |v|\sin^2(\frac{1}{2}\sigma_2 h)] \\ + \frac{iT}{h}[u \sin^2(\frac{1}{2}\sigma_1 h) + v \sin^2(\frac{1}{2}\sigma_2 h)]\} \end{aligned} \quad (7.49)$$

It follows from (7.49) that $|\lambda| \leq 1$ and therefore (7.48) is unconditionally stable, although the approximation is only of the first order in space and time. Now we propose a general algorithm which possesses partly the properties of an implicit algorithm but is a much better approximation than (7.48). Splitting (7.47) into a system of two equations we obtain

$$\begin{aligned} \frac{c^{l+1/2} - c^l}{T} + \frac{1}{2} \frac{(u - |u|)}{2} \nabla_x^+ c^{l+1/2} + \frac{1}{2} \frac{(u + |u|)}{2} \nabla_x^- c^{l+1/2} + \frac{1}{2} \nabla_y^+ c^l \\ = \frac{K}{2} \frac{\partial^2 c^{l+1/2}}{\partial x^2} + \frac{K}{2} \frac{\partial^2 c^l}{\partial y^2} \end{aligned} \quad (7.50)$$

$$\begin{aligned} \frac{c^{l+1} - c^{l+1/2}}{T} + \frac{1}{2} \nabla_x^+ c^{l+1/2} + \frac{1}{2} \frac{(v - |v|)}{2} \nabla_y^+ c^{l+1} + \frac{1}{2} \frac{(v + |v|)}{2} \nabla_y^- c^{l+1} \\ = \frac{K}{2} \frac{\partial^2 c^{l+1/2}}{\partial x^2} + \frac{K}{2} \frac{\partial^2 c^{l+1}}{\partial y^2} \end{aligned} \quad (7.51)$$

where ∇ , ∇^+ and ∇^{\sim} denote backward, forward and central differences respectively. The stability parameters of (7.50) and (7.51) are respectively

$$\lambda_1 = c^{1+1/2}/c^1 = [1 - \frac{2KT}{h^2} \sin^2(\frac{1}{2}\sigma_2 h) - \frac{ivT}{2h} \sin\sigma_2 h] / [1 + \frac{2KT}{h^2} \sin^2(\frac{1}{2}\sigma_1 h) + \frac{2|u|T}{h} + \frac{iuT}{2h} \sin\sigma_1 h] \quad (7.52)$$

$$\lambda_2 = c^{1+1}/c^{1+1/2} = [1 - \frac{2KT}{h^2} \sin^2(\frac{1}{2}\sigma_1 h) - \frac{iuT}{2h} \sin\sigma_1 h] / [1 + \frac{2KT}{h^2} \sin^2(\frac{1}{2}\sigma_2 h) + \frac{2|v|T}{h} + \frac{ivT}{2h} \sin\sigma_2 h] \quad (7.53)$$

The resulting overall stability is equal to $\lambda = \lambda_1 \lambda_2 = c^{1+1}/c^1$. Its absolute value is difficult to analyse in general, but it indicates stability for a much wider range of time-space steps than the explicit scheme (7.46). In the system of equations (7.50) and (7.51) second-order approximation in time $O(T^2)$ and in space $O(h^2)$ is obtained, but the advection term possesses an accuracy of the order of $O(h^{3/2})$.

Since the transport-diffusion equation satisfies the inequality (2.24), we may propose a stable algorithm of second-order accuracy in time and space. Using the method for approximating the operators given in chapter II, we get

$$\frac{c^{1+1/2} - c^1}{T} = \frac{1}{2}(L_1 c^{1+1/2} + L_2 c^1) \quad (7.54)$$

$$\frac{c^{1+1} - c^{1+1/2}}{T} = \frac{1}{2}(L_1 c^{1+1/2} + L_2 c^{1+1}) \quad (7.55)$$

where

$$L_1 c = \frac{1}{h^2} \{ (\sqrt{RF\bar{X}} + uh/4\sqrt{RF\bar{X}})^2 (c_{j+1,k} - c_{j,k}) - (\sqrt{RB\bar{X}} - uh/4\sqrt{RB\bar{X}})^2 (c_{j,k} - c_{j-1,k}) \} \quad (7.56)$$

$$L_2 c = \frac{1}{h^2} \{ (\sqrt{RF\bar{Y}} + vh/4\sqrt{RF\bar{Y}})^2 (c_{j,k+1} - c_{j,k}) - (\sqrt{RB\bar{Y}} - vh/4\sqrt{RB\bar{Y}})^2 (c_{j,k} - c_{j,k-1}) \} \quad (7.57)$$

$$\text{RFX} = \frac{1}{2}(K_{j+1,k} + K_{j,k}); \quad \text{RBX} = \frac{1}{2}(K_{j,k} + K_{j-1,k}) \quad (7.58)$$

$$\text{RFY} = \frac{1}{2}(K_{j,k+1} + K_{j,k}); \quad \text{RBY} = \frac{1}{2}(K_{j,k} + K_{j,k-1}) \quad (7.59)$$

The system of equations in (7.54) and (7.55) may also be represented as one equation in the Crank-Nicholson form

$$\frac{c^{l+1} - c^l}{T} = \frac{1}{2} L(c^l + c^{l+1}) \quad (7.60)$$

where $L = L_1 + L_2$.

A difficulty arises at once if the stability of (7.60) or both, (7.54) and (7.55), is analysed, since the operator L contains variable coefficients. We shall use instead the property of the positive-definite operator mentioned in chapter II. Assuming that the operator L is characterized by the set of eigenvalues $\lambda_n > 0$ and related eigenfunctions ψ_n , which are the solution of the problem (see chapter VIII),

$$L\psi + \lambda\psi = 0, \quad (7.61)$$

the dependent variable in (7.60) may therefore be expanded in terms of the eigenfunctions ψ_n

$$c^l = \sum_n C_n^l \psi_n \quad (7.62)$$

where C_n^l are the Fourier coefficients of the expansion. They can be found by substituting (7.62) in (7.60) to give

$$C_n^{l+1} = C_n^l - \frac{1}{2}\lambda_n T C_n^l - \frac{1}{2}\lambda_n T C_n^{l+1} \quad (7.63)$$

or rearranged in terms of the time index l

$$C_n^{l+1} = C_n^l (1 - \frac{1}{2}\lambda_n T) / (1 + \frac{1}{2}\lambda_n T) \quad (7.64)$$

Assuming that the first term in the above recurrence relation is bounded $C_n^0 = \phi < \infty$, the coefficient at time step l becomes

$$C_n^l = \phi (1 - \frac{1}{2}\lambda_n T)^l / (1 + \frac{1}{2}\lambda_n T)^l \quad (7.65)$$

The series is convergent on condition that

$$|(1 - \frac{1}{2}\lambda_n T) / (1 + \frac{1}{2}\lambda_n T)| < 1 \quad (7.66)$$

which leads to the inequality

$$0 < \lambda_n T \quad (7.67)$$

Since $\lambda_n > 0$ for the positive definite operator, the convergence of (7.65) follows from (7.67) and the unconditional stability of (7.60) is proved. In the same way the stability of the system (7.54) and (7.55) may be proved.

§4. The application of the transport equation in a multi-channel model

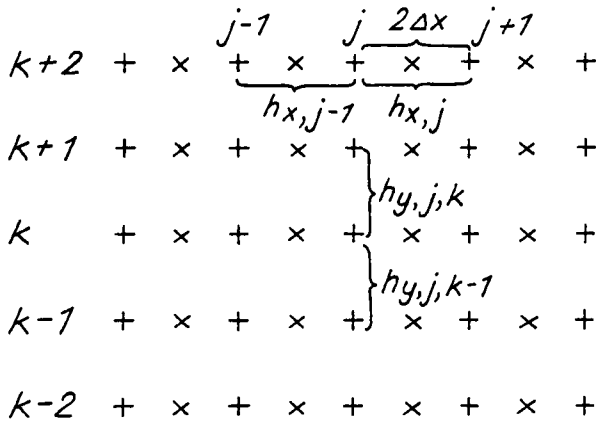
In the numerical examples which we shall now present we shall dwell mainly upon the diffusion processes in the River Elbe so as to illustrate the capabilities of the hydrodynamic-numerical model. These examples are not intended to yield a general knowledge of the complicated pattern of diffusion, dispersion and salt mixing processes which are encountered in rivers and estuaries (see e.g. Ippen, 1966). The hydrodynamics of a salt-water wedge and the mixing in such a region may necessitate a completely different approach to the eddy diffusion processes. The problems occurring at the interface between fresh and salt water in rivers needs further laboratory experiments and in-situ measurements (Ozturk, 1970) together with numerical computations.

The extremely high bottom velocity in rivers and estuaries leads to very intensive erosion and sedimentation processes and results in a fast rebuilding of the river cross-section, which in turn influences the hydrodynamics of river flow. To ascertain possible variations, Harleman and Ippen (1969) have presented the effects of salinity intrusion on shoaling in the different estuaries.

Due to the complicated pattern of flow in rivers and estuaries, as presented in §2, the expressions for the eddy diffusion coefficient which were derived for channels of simple geometry often failed when applied to natural conditions. Sooky (1969) attempted to improve the situation through the consideration of a complicated channel geometry.

Because in the domain of integration the initial and boundary conditions are very far from being analytical, the numerical method has been applied to the dispersion problem with some success, e.g. Harleman et al. (1968).

In our consideration of diffusion processes we shall depend a great deal on the multi-channel model derived in chapter VI.



+ = ζ -point

x = u-, H-, c-point

Fig. 89. A SECTION OF A GRID IN THE MULTI-CHANNEL MODEL

A section of the grid for the multi-channel model is plotted in fig. 89. Directing the x-axis along the longitudinal axis of the channel, assuming $K = K_x = K_y$ and transverse velocity $v = 0$, the equation (7.7) becomes

$$\frac{\partial c}{\partial t} + u \frac{\partial c}{\partial x} = K \left(\frac{\partial^2 c}{\partial x^2} + \frac{\partial^2 c}{\partial y^2} \right) \quad (7.68)$$

The handling of the general equations of transport to examine horizontal diffusion processes in seas and rivers is only possible when the hydrodynamic-numerical method is applied to the hydrodynamic equations. It allows us to consider the morphological structure as well as the shape of the shore and to give the velocity and water level as a function of place and time (see chapter VI).

Accordingly, the above equation is transformed into a difference equation. The partial derivative with respect to time is replaced with a forward difference, while the spatial derivatives are replaced with central differences. It is further assumed that the time step $T = 2\Delta T$ and the mesh spaces $2\Delta x = h_{x,j}$ and $2\Delta y = h_{y,j,k}$ need not necessarily be equal. Hence

$$\frac{\partial c}{\partial t} = \frac{c_{j,k}^{1+1} - c_{j,k}^1}{2\Delta T} \quad (7.69)$$

$$\frac{\partial c}{\partial x} = \frac{1}{2} \left\{ \frac{c_{j+1,k}^1 - c_{j,k}^1}{h_{x,j}} + \frac{c_{j,k}^1 - c_{j-1,k}^1}{h_{x,j-1}} \right\} \quad (7.70)$$

$$\frac{\partial^2 c}{\partial x^2} = \frac{2}{h_{x,j} + h_{x,j-1}} \left\{ \frac{c_{j+1,k}^1 - c_{j,k}^1}{h_{x,j}} - \frac{c_{j,k}^1 - c_{j-1,k}^1}{h_{x,j-1}} \right\} \quad (7.71)$$

$$\frac{\partial^2 c}{\partial y^2} = \frac{2}{h_{y,j,k} + h_{y,j,k-1}} \left\{ \frac{c_{j,k+1}^1 - c_{j,k}^1}{h_{y,j,k}} - \frac{c_{j,k}^1 - c_{j,k-1}^1}{h_{y,j,k-1}} \right\} \quad (7.72)$$

Considering the above expressions, the difference equation, solved for $c_{j,k}^{1+1}$, yields

$$\begin{aligned} c_{j,k}^{1+1} = & c_{j,k}^1 - 2\Delta T u_{j,k}^1 \left\{ \frac{c_{j+1,k}^1}{2h_{x,j}} + c_{j,k}^1 \frac{h_{x,j} - h_{x,j-1}}{2h_{x,j}h_{x,j-1}} - \frac{c_{j-1,k}^1}{2h_{x,j-1}} \right\} \quad (7.73) \\ & + 4\Delta TK \left\{ \frac{c_{j+1,k}^1}{(h_{x,j} + h_{x,j-1})h_{x,j}} - \frac{c_{j,k}^1}{h_{x,j}h_{x,j-1}} + \frac{c_{j-1,k}^1}{h_{x,j-1}(h_{x,j} + h_{x,j-1})} \right\} \\ & + 4\Delta TK \left\{ \frac{c_{j,k+1}^1}{(h_{y,j,k} + h_{y,j,k-1})h_{y,j,k}} - \frac{c_{j,k}^1}{h_{y,j,k}h_{y,j,k-1}} \right. \\ & \left. + \frac{c_{j-1,k}^1}{h_{y,j,k-1}(h_{y,j,k} + h_{y,j,k-1})} \right\} \end{aligned}$$

The coefficients of (7.73) are replaced by the following abbreviations

$$a_{j+1} = \frac{2\Delta T}{2h_{x,j}}; \quad a_j = \frac{2\Delta T(h_{x,j} - h_{x,j-1})}{2h_{x,j}h_{x,j-1}}; \quad a_{j-1} = \frac{2\Delta T}{2h_{x,j-1}}$$

$$b_{j+1} = \frac{4\Delta TK}{h_{x,j}(h_{x,j} + h_{x,j-1})}; \quad b_j = \frac{4\Delta TK}{h_{x,j}h_{x,j-1}}; \quad b_{j-1} = \frac{4\Delta TK}{h_{x,j-1}(h_{x,j} + h_{x,j-1})}$$

$$d_{j,k+1} = \frac{4\Delta TK}{h_{y,j,k}(h_{y,j,k} + h_{y,j,k-1})}; \quad d_{j,k} = \frac{4\Delta TK}{h_{y,j,k}h_{y,j,k-1}}$$

$$d_{j,k-1} = \frac{4\Delta TK}{h_{y,j,k-1}(h_{y,j,k} + h_{y,j,k-1})} \quad (7.74)$$

Applying the above notation the numerical form of (7.68) becomes

$$c_{j,k}^{l+1} = c_{j,k}^l - u_{j,k}^l (c_{j+1,k}^l a_{j+1} + c_{j,k}^l a_j - c_{j-1,k}^l a_{j-1})$$

$$+ c_{j+1,k}^l b_{j+1} - c_{j,k}^l b_j + c_{j-1,k}^l b_{j-1} + c_{j,k+1}^l d_{j,k+1} - c_{j,k}^l d_{j,k}$$

$$+ c_{j,k-1}^l d_{j,k-1} \quad (7.75)$$

The slight asymmetry in the notation is due to the fact that along the y-axis the grid distance h_x is constant, but h_y varies along the x-axis, so as to approximate the cross-section of the channel with greater accuracy.

According to Richtmyer (1957) the following criterion for the numerical stability is given, on condition that the advective term $u \frac{\partial c}{\partial x}$ is neglected,

$$\frac{2\Delta TK (h_x^2 + h_y^2)}{h_x^2 h_y^2} < 1 \quad (7.76)$$

For $h_y \ll h_x$ - as is the case in this model - the criterion simplifies to

$$\frac{2\Delta TK}{h_y^2} < 1 \quad (7.77)$$

Therefore the choice of the time step ΔT depends on the maximum eddy diffusion coefficient K and the smallest step along the width h_y . The calculation procedure starts with the equation of motion at time t in order to find the velocity distribution u which appears in the advective term. Then the water levels are computed from the equation of continuity and the concentration from the convective-diffusion equation. The condition for numerical stability of the explicit form of the equation of motion and continuity

$$\frac{2\Delta T \sqrt{gH_{\max}}}{h_x} < 1 \quad (7.78)$$

is often satisfied if (7.77) holds.

If the horizontal and vertical motions are periodical, it is advisable to calculate the periodic state at every inner point of the domain at first and then to treat the equation of exchange numerically for a convenient number of periods. But it has to be assumed that the effect of the horizontal exchange of the mixture on the water levels and velocities is negligibly small.

Let us check both criteria presented above in the case of the flow in the River Elbe, to which we have already applied the hydrodynamic-numerical method in chapter VI.

The minimum and maximum values of the geometrical quantities used in the Elbe model and the horizontal coefficient of exchange can be assumed to be $h_{x,\min} = 6000$ m, $h_{y,\min} = 10$ m, $H_{\max} = 25.6$ m and $K = 100$ m²/sec (Ramming, 1971). On the basis of these magnitudes the following upper bounds for the choice of $2\Delta T$ must be considered:

$$2\Delta T < 375 \text{ sec from (7.78) and}$$

$$2\Delta T < 1 \text{ sec from (7.77).}$$

Therefore, if an explicit method is applied, the time step is of the order of 1 sec. This essential restriction is due entirely to the shortest space step found in the grid domain, which is equal to 10 m. A time step of 1 sec demands a considerable amount of computer time to derive any meaningful results. The equations give short-term variations of water level and velocity which are of no importance to the overall phenomenon. In order to maintain all the information on the fine morphological structure of the multi-channel system and in order to be independent of the time step restriction, an implicit difference scheme was chosen instead in the direction of the y-axis. To compute the concentration in the x direction an explicit difference method was still applied.

We shall adapt the following implicit scheme for the convective-diffusion equation (7.68)

$$\frac{c^{l+1} - c^l}{2\Delta T} + u^l \frac{\partial c^l}{\partial x} = K \frac{\partial^2 c^l}{\partial x^2} + K \frac{\partial^2 c^{l+1}}{\partial y^2} \quad (7.79)$$

The terms depending on the time step l are grouped together and called R . Hence (7.79) yields

$$c^{l+1} - 2\Delta TK \frac{\partial^2 c^{l+1}}{\partial y^2} = R \quad (7.80)$$

By changing the partial derivatives to finite differences and taking into account the given coefficients as well as the boundary condition, (7.80) may be formulated as

$$c_{j,k}^{l+1} (1 + 2e_{j,k}) - c_{j,k+1}^{l+1} e_{j,k+1} - c_{j,k-1}^{l+1} e_{j,k-1} = R_{j,k}^l \quad (7.81)$$

The most suitable methods of solving this equation are the line factorization method presented in chapter II as well as the method of Banachiewicz (1938).

We observe that in (7.81) the elements of the coefficients' matrix possess the property of diagonal predominance over the nondiagonal elements, i.e.

$$1 + 2e_{j,k} > |e_{j,k+1}| + |e_{j,k-1}| \quad (7.82)$$

This leads, on the one hand, to the convergence of (7.81) in time, as was proved in chapter II, and, on the other hand, it is possible to choose the time step in a less restricting fashion.

Another implicit-explicit procedure can be initiated with the equation

$$\frac{c^{l+1} - c^l}{2\Delta T} + u^l \frac{\partial c^l}{\partial x} = K \frac{\partial^2 c^l}{\partial x^2} + \frac{K}{2} \left(\frac{\partial^2 c^l}{\partial y^2} + \frac{\partial^2 c^{l+1}}{\partial y^2} \right) \quad (7.83)$$

and by suitable manipulation we may obtain a numerical form similar to (7.81).

We have performed several numerical experiments in a geometrically simple model of a channel with the two methods described above (Ramming, 1971).

The two solutions differed from each other by at most 0.002% ϵ . In the problems which will be presented further on the first method will usually be applied. Generally, it allows us to increase the time step considerably as compared with the purely explicit method. At first glance this behaviour of the model is somewhat astonishing, because as can be seen from (7.79), the scheme is not completely implicit. The predominance of the implicit over the explicit properties follows

from the space discretization and the choice of $h_x \gg h_y$. Let us analyse this feature with the help of (7.79), neglecting the advective term

$$\frac{c_{j,k}^{l+1} - c_{j,k}^l}{2\Delta T} = K \frac{c_{j+1,k}^l + c_{j-1,k}^l - 2c_{j,k}^l}{h_x^2} + K \frac{c_{j,k+1}^{l+1} + c_{j,k-1}^{l+1} - 2c_{j,k}^{l+1}}{h_y^2} \quad (7.84)$$

Applying the expression (7.39) and taking into account the unequal steps along the x- and y-axes, we derive the following expression for the parameter of stability

$$\lambda = c^{l+1}/c^l = [1 - \frac{8K\Delta T}{h_x^2} \sin^2(\sigma_1 h_x)] / [1 + \frac{8K\Delta T}{h_y^2} \sin^2(\sigma_2 h_y)] \quad (7.85)$$

The overall stability depends on the relations between h_x , h_y , ΔT , $\sin^2(\sigma_1 h_x)$ and $\sin^2(\sigma_2 h_y)$. However, since $h_x \gg h_y$, λ will take values smaller than unity over a wide range of the above parameters. Actually the most unfavourable case arises when the denominator in (7.85) attains its smallest value, i.e. 1. This leads to the following condition for the time step

$$\Delta T < h_x^2 / 4K \quad (7.86)$$

§5. A comparison between an analytical and a numerical solution

The convective-diffusion equation is a differential equation of the parabolic type (unless $K = 0$). Generally, an analytical solution in the complete form cannot be given. Therefore, we shall investigate one special case to show whether the results of the difference method agree with the solution of the differential equation, or moreover, whether they lie in a certain range of accuracy. We start with the simple problem of a channel open at both ends; the velocity U and the cross-section are constant. As the volume is constant as well, the cross-sectional area may be omitted and the convective-diffusion equation becomes

$$\frac{\partial c}{\partial t} + U \frac{\partial c}{\partial x} = K \frac{\partial^2 c}{\partial x^2} \quad (7.87)$$

The following analytical solution can be derived subject to the boundary condition $\frac{\partial c}{\partial x} = 0$ at both open ends (Frank and von Mises, 1961)

$$c = c_1 \exp \left\{ -t \left(Kn^2 \frac{\pi^2}{L^2} + U^2/4K \right) + \frac{Ux}{2K} \left(\sin \frac{n\pi x}{L} - \frac{2K\pi n}{LU} \cos \frac{n\pi x}{L} \right) \right\} + c_2 \quad (7.88)$$

Where c_1 and c_2 are constants, n is any integer number ($n = 1, 2, \dots$) and L is the length of the channel.

To obtain a solution to the same problem by numerical means, the explicit difference form is introduced

$$c_j^{l+1} = c_j^l - \frac{U\Delta T}{\Delta x} (c_{j+1}^l - c_{j-1}^l) + \frac{K\Delta T}{2(\Delta x)^2} (c_{j+1}^l + c_{j-1}^l - 2c_j^l) \quad (7.89)$$

The initial and final distribution of the concentration is plotted in fig. 90. The initial distribution from the solution of the transport equation at $t = 0$ is found to be

$$c_0 = c_1 \exp \left\{ \frac{Ux}{2K} \left(\sin \frac{n\pi x}{L} - \frac{2K\pi n}{LU} \cos \frac{n\pi x}{L} \right) \right\} + c_2 \quad (7.90)$$

with the following values of parameters: $U = 0.1$ m/sec, $L = 10^4$ m, $c_1 = 100$ °/oo, $c_2 = 10$ °/oo, $n = 1$, $K = 100$ m²/sec. The number of grid points in the channel is equal to 101 and $\Delta x = 100$ m. When $t \rightarrow \infty$, the concentration is the same at each point of the channel as can be seen from the solution (7.88). For example, at the grid point 31 the expected solution $c = 10$ °/oo appears after 973 time steps according to the analytical solution. The difference scheme leads to a stationary concentration with $c = 9.569$ °/oo after 1056 time steps of integration. Hence the difference solution deviates 4.31 % from the differential solution. Checking not only point 31 but also point 61, as depicted in fig. 91, we reach the conclusion that the numerical treatment of the transport equation gives not only the solution to the stationary state, but also describes in a satisfactory manner the time-dependent course of the process.

This observation is of some importance for the problems to be handled later on, in natural channels, when, due to the absence of an analytical solution, the quality of the numerical investigation has to be judged by comparing predicted and measured concentrations. The proper reproduction of the transport processes by the numerical model gives us a tool with which to study a variety of problems related to the physical and geometrical properties of the model. We confine ourselves to the

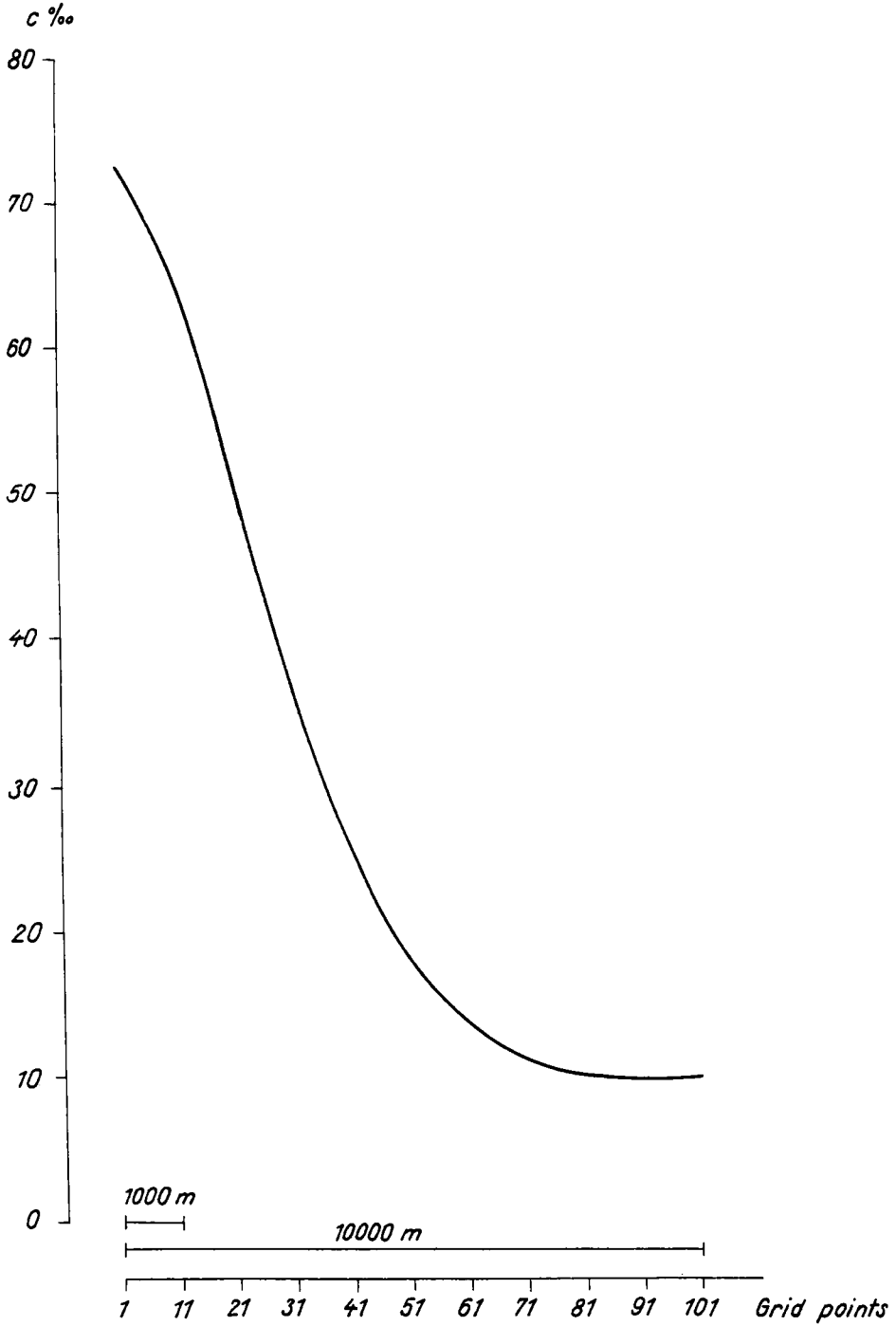


Fig. 90. INITIAL DISTRIBUTION OF CONCENTRATION IN THE CHANNEL.

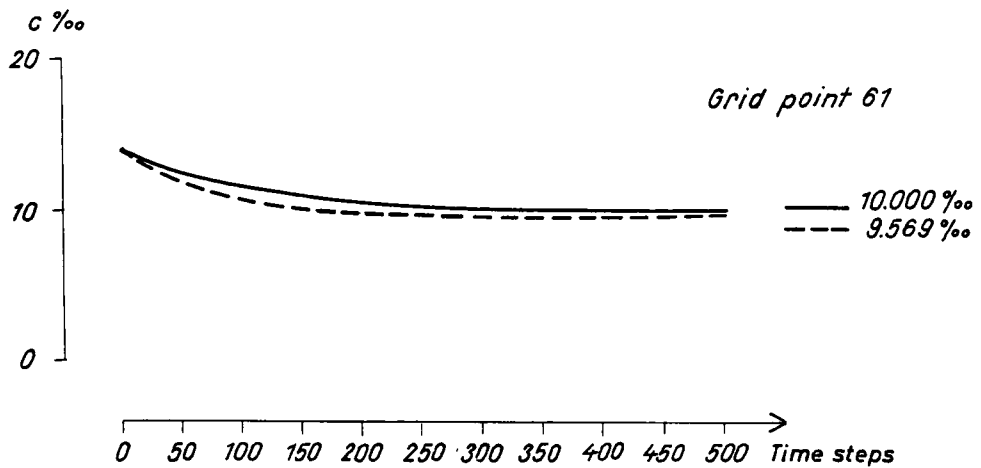
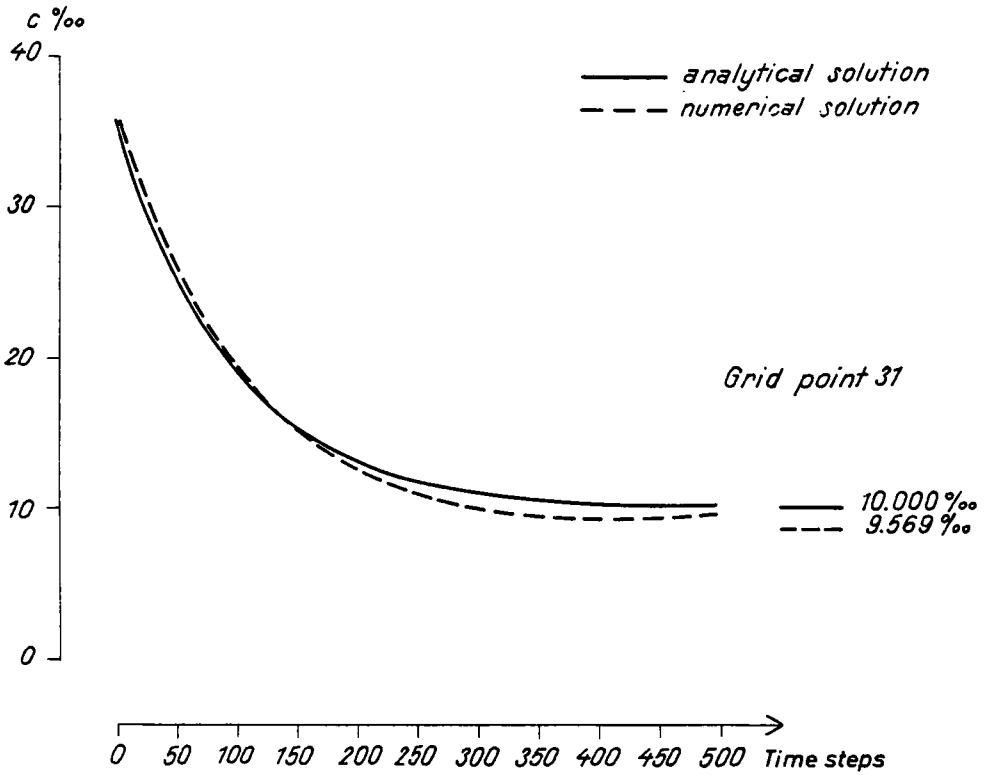


Fig. 91. COMPARISON OF ANALYTICAL AND NUMERICAL SOLUTIONS IN POINTS 31 AND 61 OF THE CHANNEL.

TABLE 7.1

Distribution of concentration along the channel after 0, 50, 100, 150 and 200 tidal periods of numerical integration

Periods	Grid point									
	1	2	3	4	5	6	7	8	9	10
Horizontal eddy viscosity $A = 10 \text{ m}^2/\text{sec}$										
0	0.00	0.00	0.00	0.00	0.00	0.00	10.00	35.00	35.00	0.00
50						0.65	7.92	32.50	36.61	0.00
100			0.01			0.37	5.53	30.16	37.49	0.00
150						0.07	2.95	27.79	37.78	0.00
200							2.91	25.43	37.54	0.00
Horizontal eddy viscosity $A = 50 \text{ m}^2/\text{sec}$										
0	0.00	0.00	0.00	0.00	0.00	0.00	10.00	35.00	35.00	0.00
50					0.11	2.20	12.97	25.21	32.01	0.00
100			0.01		0.30	3.22	12.38	21.84	27.53	0.00
150					0.40	3.71	11.65	19.34	23.94	0.00
200					0.45	3.89	10.89	17.32	21.10	0.00
Horizontal eddy viscosity $A = 100 \text{ m}^2/\text{sec}$										
0	0.00	0.00	0.00	0.00	0.00	0.00	10.00	35.00	35.00	0.00
50				0.05	1.16	6.40	14.33	21.93	26.84	0.00
100			0.01	0.32	2.60	7.52	13.24	18.01	21.00	0.00
150				0.47	3.32	7.63	11.96	15.32	17.42	0.00
200				0.60	3.54	7.34	10.80	13.36	14.95	0.00

study of an impact of a variable horizontal eddy viscosity on the distribution of concentration along the channel. We shall consider again the same channel but with grid steps ten times greater, i.e. instead of 101 points only 10 will be present. Three different values of the horizontal eddy viscosity will be taken: $10 \text{ m}^2/\text{sec}$, $50 \text{ m}^2/\text{sec}$ and $100 \text{ m}^2/\text{sec}$. In each case, the same initial distribution is taken with a maximum concentration at points 8 and 9 (see table 7.1) When the equation of transport is integrated in time over a sufficiently large number of tidal periods, i.e. several days, the increased magnitude of eddy viscosity leads to two characteristic phenomena. Firstly, the maximum concentration diminishes with increasing eddy viscosity (the case of $10 \text{ m}^2/\text{sec}$ shows a small increase of concentration), and secondly, the concentration of the mixture is dispersed over a greater number of grid points when compared to the initial spread.

§6. The turbidity zone of the River Elbe

Starting with the transport equation in the form

$$\frac{\partial c}{\partial t} + u \frac{\partial c}{\partial x} + v \frac{\partial c}{\partial y} = K_x \frac{\partial^2 c}{\partial x^2} + K_y \frac{\partial^2 c}{\partial y^2} \quad (7.91)$$

the horizontal dispersion of suspended matter in the River Elbe was investigated.

The phenomenon of horizontal dispersion is a turbulent transport process which depends on the bottom topography and on the motion of water in the horizontal as well as in the vertical direction. Due to the high velocities, the water in the river can be assumed to be well-mixed in the vertical direction, and therefore the processes governed by the vertical stratification are of negligible importance. In such a case, as we have seen in §2 of this chapter, the coefficient of eddy diffusion may be identified with the coefficient of eddy viscosity. In the following calculations expression (7.27) will be applied.

It is assumed that the mixture - which, in our case, is the seston - is dispersed equally from the bottom to the surface and remains in suspension all the time. The mixture is of such a quantity that it does not essentially change the water density. The investigated concentrations reproduce the averaged distribution of the material at the grid points. Together with the numerical form of equation (7.91), the two-dimensional model of the River Elbe described in chapter VI was applied. Observed water levels and the time-dependent concentration

of suspended material as given by the measurements of Nöthlich (1967) are used as the boundary conditions at the open boundary near Cuxhaven. Nöthlich specified the average quantity of seston during these measurements as 28.6 mg/l of dry weight at high water and 56.4 mg/l of dry water weight at low water at one point within the Elbe estuary. The boundary condition taken as

$$c = 0.0424 + 0.0141 \cos \frac{2\pi}{T}t \quad (7.92)$$

reproduces the above values at high and low water with insignificant errors. It was assumed that (7.92) is valid for the whole cross-section at the mouth of the river. The computations were started at low water and the tide averaged over the years 1951 - 1955 (normal-tide) was used. Because simultaneous measurements were unavailable it was only possible to compare the numerical results with measurements from the year 1967.

It is well known that the dispersion of suspended matter in tidal rivers varies with the seasons and depends on meteorological factors, the fresh water input and the salinity of the incoming water to the estuary. We have proceeded on the assumption that, as a first approximation, the main components of the transport of suspended material during the time when the measurements were made were the same as during the normal-tide 1951/55.

A comparison between a computed and a measured mean concentration of seston in five sections of the River Elbe is shown in figure 92. It must be noted that the measurements were made at several places and at different tidal phases. Therefore, while reproducing the numerical data, at the grid points situated near the observational points, we have always specified maximum and minimum concentration.

The essential numerical results are presented in figs. 93 and 94. They show the distribution of seston due to the dynamic processes in the River Elbe between Otterndorf and Stadersand. In the first figure, the distribution during the time of maximum seston concentration, and in the second figure, the distribution during the time of minimum seston concentration in Cuxhaven is shown. At high water as well as at low water at Cuxhaven, a zone of high seston concentration (about 200 mg/l) exists near Brunsbüttel. During high water this zone is broader than at low water while there is no essential difference in the length of the zone. This turbidity zone is a typical phenomenon in the River Elbe and results from the interaction of several processes. Relying upon the qualitative reproduction of this turbidity zone by means of

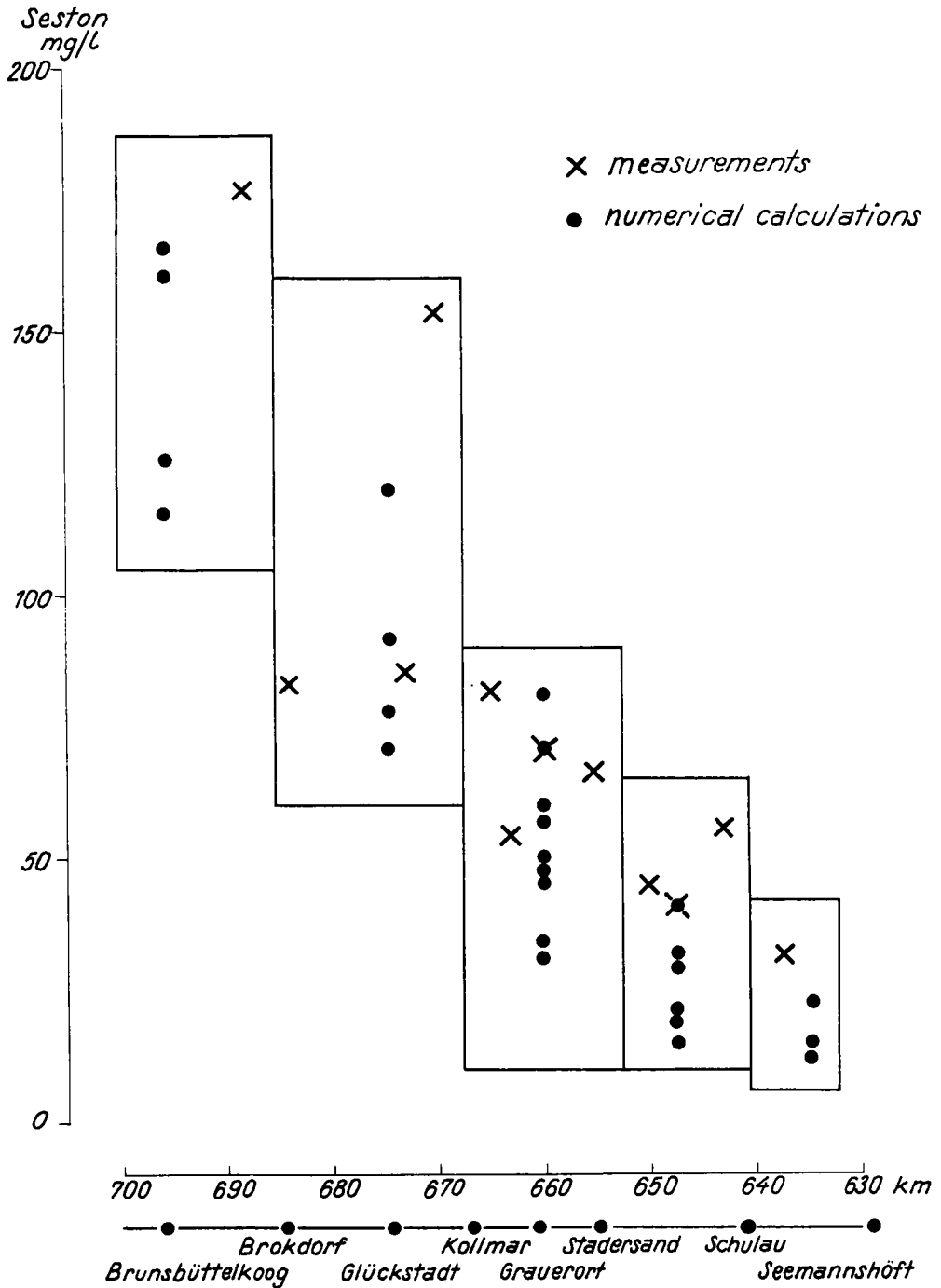


Fig. 92. COMPARISON OF COMPUTED AND MEASURED MEAN CONCENTRATION OF SESTON IN FIVE SECTIONS OF THE RIVER ELBE.

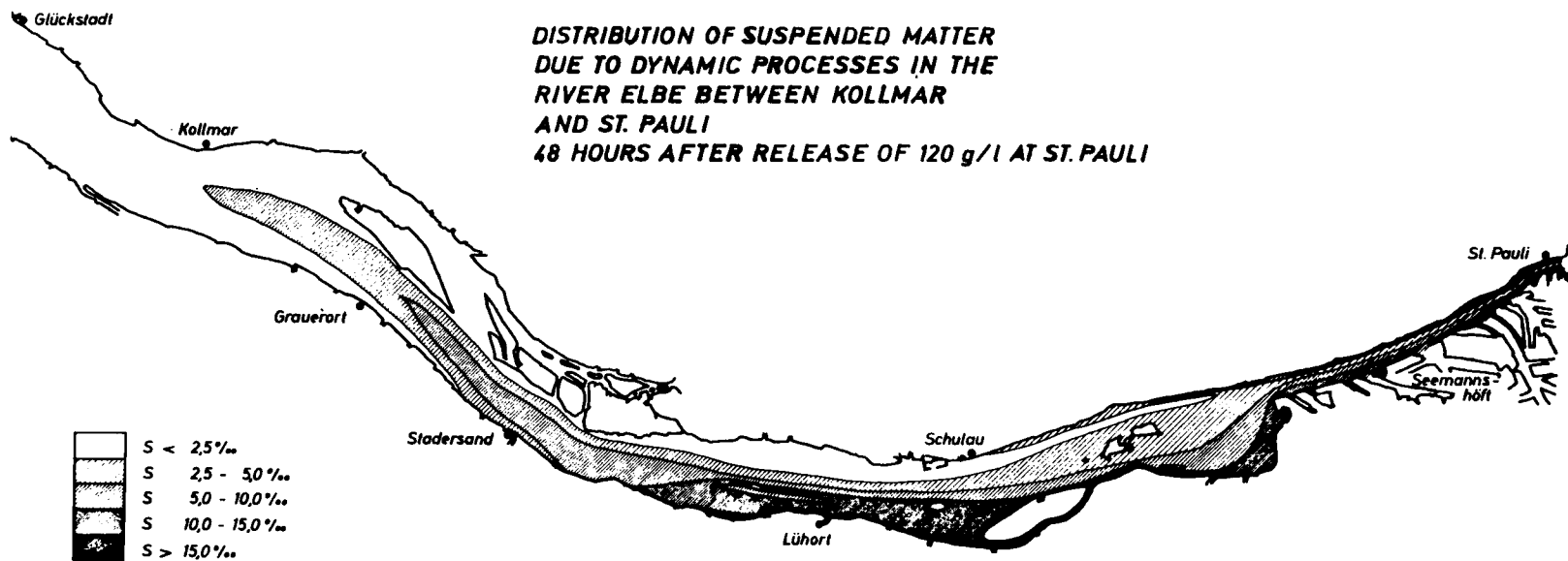


Fig. 93. DISTRIBUTION OF SUSPENDED MATTER DUE TO DYNAMIC PROCESSES IN THE RIVER ELBE BETWEEN KOLLMAR AND ST. PAULI - 48 HOURS AFTER RELEASE OF 120 g/l AT ST. PAULI.

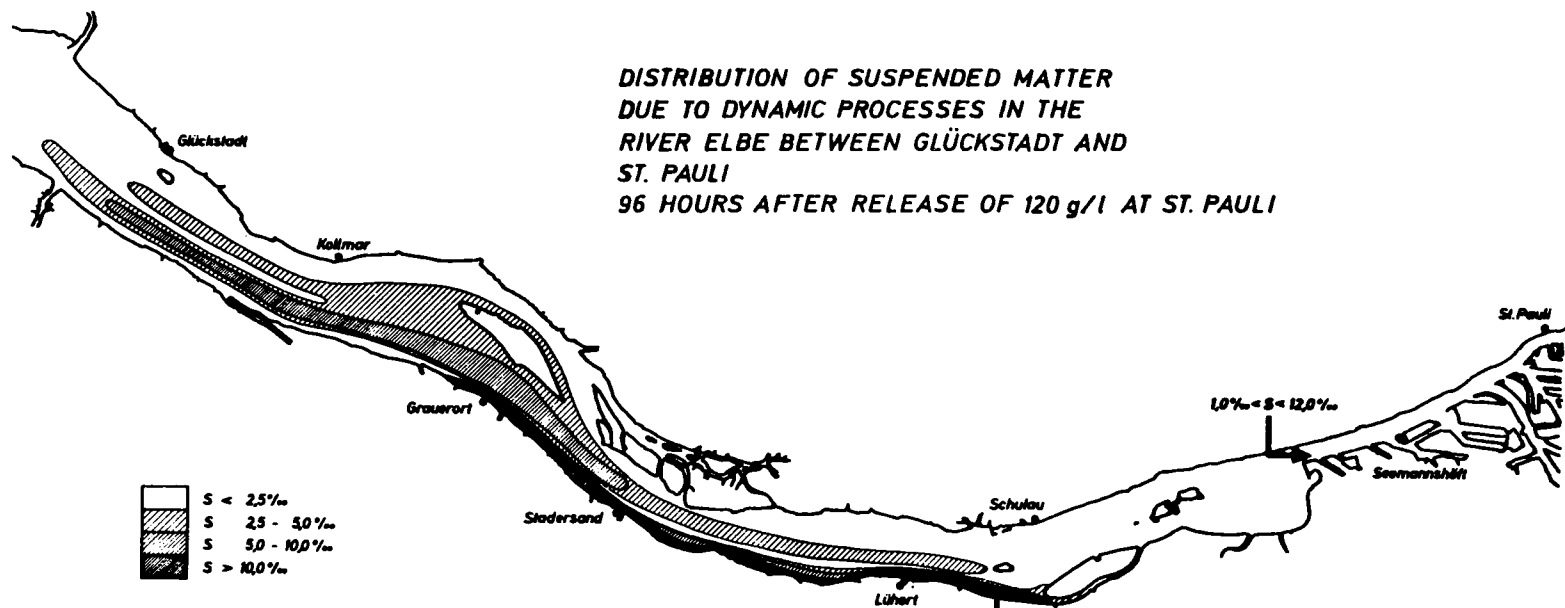


Fig. 94. DISTRIBUTION OF SUSPENDED MATTER DUE TO DYNAMIC PROCESSES IN THE RIVER ELBE BETWEEN GLÜCKSTADT AND ST. PAULI - 96 HOURS AFTER RELEASE OF 120 g/l AT ST. PAULI.

the hydrodynamic-numerical method as presented in chapter VI, it can be concluded that the existence of this zone is determined mainly by the hydrodynamics of the river. In this section of the estuary the residual currents are very small. These results suggest various possibilities for the application of the numerical method, and they contribute to the development of a model which can be extended to include other, e.g. hydrobiological, components. It is also possible to use models of this kind for the problems of pollution. The first example of such an application is the location of the turbidity zone in the River Elbe due to the exceptionally small residual currents. Small values of the residual currents in a stretch of the estuary also imply a large residence time for wastes in this area. It is therefore important in certain coastal engineering projects not only to compute the velocities and their directions but also to consider the variation in the residual currents.

§7. The transport of pollutants

Based upon the results of the preceding chapter it is possible to handle practical and actual problems of pollution. For that purpose the equation of transport (7.7) together with the system of hydrodynamic-numerical equations derived in the previous chapters are applied. To show the capacity of this approach to handle the problem of pollutant dispersion, a pollutant is released at $t=0$ which gives rise immediately to a uniform concentration of 20 ‰ between Brunsbüttelkoog and Brokdorf (Fig. 95). With the help of the above equations the process of dispersion of this cloud of material was computed for a period of 144 hours, using the normal-tides of 1951/55. The run of the lines $c = 0$ gives the extension of the area in which the released amount of matter is located. At first, the material disperses quickly because of the steep gradient due to the initial distribution. But after 24 - 72 hours there is no essential change in the limitation of the area as is shown in fig. 95. Even when a time-dependent increase of material in the source area is assumed at the beginning of the investigations, the extension and location of the dispersion area corresponds to the one shown in fig. 95. This long residence time of the pollutant, as we know, is mainly due to the negligible residual currents in the area of Brunsbüttel. After 120 - 144 hours the area grows, especially in the direction of Cuxhaven and mainly in the water way, and expands insignificantly upstream. This small example of the many investigations performed shows that the dynamically-conditioned distribution of sus-

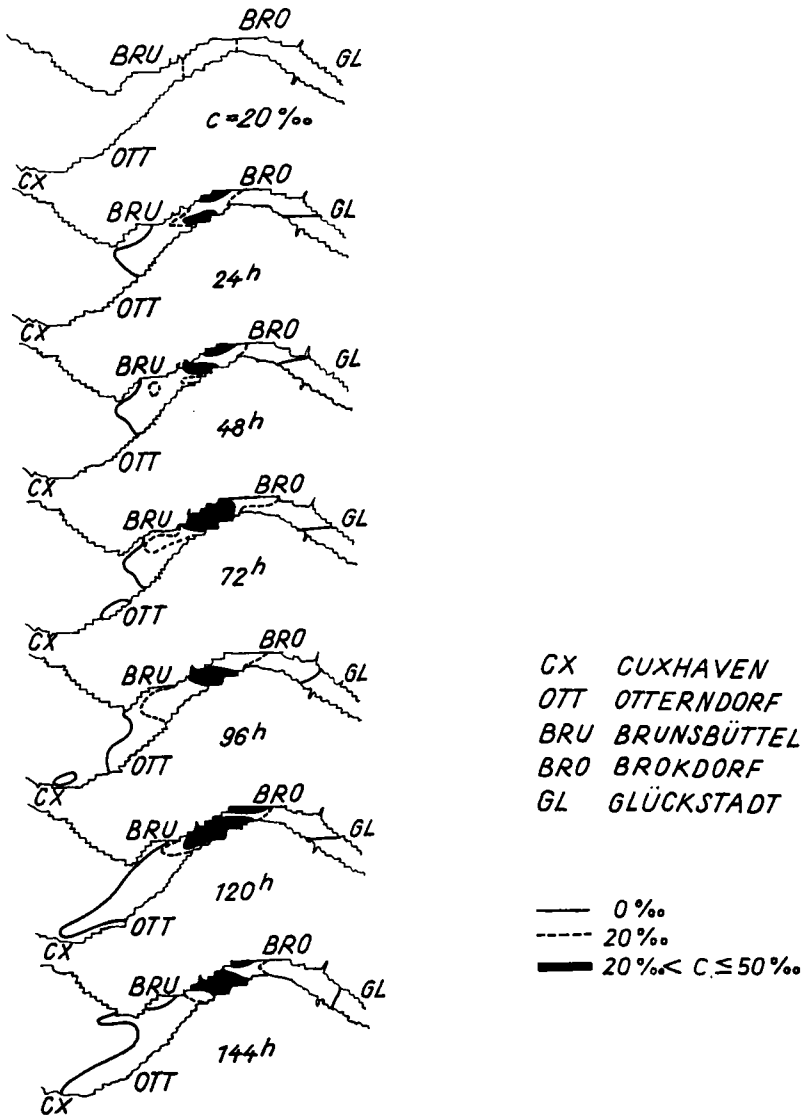


Fig. 95. TIME DEPENDENT PROCESS OF SPREADING MATTER IN THE RIVER ELBE WITH THE INITIAL CONCENTRATION 20 ‰ AND A SOURCE FUNCTION AS COMPUTED BY THE HYDRODYNAMIC-NUMERICAL MODEL.

pended matter and its transport can be examined numerically with a model, provided that the above conditions are fulfilled. These results may help to solve certain problems in coastal engineering.

REFERENCES

- Banachiewicz, T., 1938. Méthode de resolution numérique des équations linéaires du calcul des déterminants et des inverses et de réduction des formes quadratiques. Bulletin International de l'Académie Polonaise des Sciences et des Lettres, Série A, N. 8-10.
- Bowden, K.F., 1962. Turbulence. In: The Sea, v. 1. Interscience Publishers, New York, London:802-825.
- Bowden, K.F., 1963. The Mixing Processes in a Tidal Estuary. Int.J. Air Water Pollution N. 7.
- Elder, J.W., 1959. The Dispersion of Marked Fluid in Turbulent Shear Flow. Jour. Fluid Mech., N. 5:544-560.
- Fick, A., 1855. Über Diffusion. Ann. Physik. Chem. 2, 94:59-86.
- Fisher, H.B., 1967. The Mechanics of Dispersion in Natural Streams. Proc. ASCE, 93 (HY6): 187-216.
- Frank, Ph. and von Mises, R., 1961. Die Differentialgleichungen und Integralgleichungen der Mechanik und Physik. Band II.
- Harleman, D.R.F.; Lee, C.H.; Hall, L.C., 1968. Numerical Studies of Unsteady Dispersion in Estuaries. Proc. ASCE, 94 (SA5): 897-911.
- Harleman, D.R.F. and Ippen, A.T., 1969. Salinity Intrusion Effects in Estuary Shoaling. Proc. ASCE, 95 (HY1): 9-27.
- Hinze, J.O., 1959. Turbulence. McGraw-Hill Book Co., New York.
- Ippen, A.T., 1966. Salinity Intrusion in Estuaries. In: Estuary and Coastline Hydrodynamics. McGraw-Hill Book Co., New York:598-629.
- Joseph, J. and Sendner, H., 1958. Über die horizontale Diffusion im Meere. Deutsch. Hydr. Zeit. 11: 49-77.
- Kolmogoroff, A.N., 1931. Über die analytischen Methoden in der Wahrscheinlichkeitsrechnung. Math. Ann. v. 104.
- Kullenberg, G., 1970. Measurement of Horizontal and Vertical Diffusion in Coastal Waters. Kungl. Vetenskaps - och Vitterhets-Samhället, Göteborg. Series Geophysica v. 2.
- Landau, L.D. and Lifshitz, E.M., 1959. Fluid Mechanics. Pergamon Press, London.
- Monin, A.S. and Jaglom, A.M., 1965. Statistical Hydromechanics, v. 1. Nauka, Moscow.
- Munk, W.H. and Anderson, E.R., 1948. Note on the Theory of the Thermocline. Journ. of Marine Res. v. 7, N. 3: 276-295.
- Nöthlich, I., 1967. Untersuchungen über die Beziehungen zwischen Strömung und Schwebstoffgehalt in der Unterelbe. Unveröffentl. Bericht d. Wasser- und Schifffahrtsdirektion Hamburg.
- Okubo, A. and Ozmidov, R.V., 1970. Empirical Dependence of the Coefficient of Horizontal Turbulent Diffusion in the Ocean on the Scale of Phenomenon in Question. Izv. Atmosph. Ocean. Phys. v. 6, N. 5.

- Ozmidov, R.V., 1968. Horizontal Turbulence and Turbulent Exchange in the Ocean. Nauka, Moscow.
- Ozturk, Y.F., 1970. Seawater Intrusion Length in Stratified Estuaries. Water Res. N. 4: 477-484.
- Ramming, H.G., 1971. Hydrodynamisch-numerische Untersuchungen über strömungsabhängige Horizontalausbreitung von Stoffen in Modellflüssen mit Anwendungen auf die Elbe. Mitteilungen d. Inst. f. Meereskunde d. Univ. Hamburg XVIII.
- Ramming, H.G., 1973. Reproduktion physikalischer Prozesse in Küstengebieten. Die Küste, Heft 22.
- Richardson, L.F., 1926. Atmospheric Diffusion Shown on a Distance-Neighbour Graph. Proc. Roy. Soc. London A 110: 709-727.
- Richtmyer, R.D., 1957. Difference Methods for Initial-Value Problems. Inter. Publishers, New York.
- Schmidt, W., 1917. Der Massenaustausch bei der ungeordneten Strömung in freier Luft und seine Folgen. Sitzungsber. Acad. Wiss. Wien, Math.-nat. kl. (2a), Band 126, N. 6: 757-804.
- Sooky, A.A., 1969. Longitudinal Dispersion in Open Channels. Proc. ASCE 95 (HY4): 1327-1346.
- Taylor, G.I., 1915. Eddy Motion in the Atmosphere. Phil. Trans. Roy. Soc. A 215: 1-26.
- Taylor, G.I., 1921. Diffusion by Continuous Movements. Proc. London Math. Soc. A 20.
- Taylor, G.I., 1954. The Dispersion of Matter in Turbulent Flow Through a Pipe. Proc. Roy. Soc. A 223: 446-468.
- Zeidler, R., 1975. Hydromechanics of the Waste- and Heated Water Discharge to the Marine Environment and Related Problems. Oceanologia, N. 5.

Chapter VIII PERIODIC MOTION

§1. Introduction

The study of oscillatory motion in natural basins can be separated into two interconnected fields:

1. The spectral method of analysis, when a proper time series of the parameter of interest has been recorded.
2. The solution of differential (or difference) equations which describe the set of eigenvalues and eigenfunctions.

We shall study an oscillatory motion in a sea by the latter method, since the first one is generally connected with the technical problem of obtaining a satisfactorily long and stationary series of data (Bendat and Piersol, 1971). Our primary aim is to describe a seiche-like motion in closed and semi-enclosed basins with the set of equations

$$\frac{\partial M_x}{\partial t} - fM_y = -gH \frac{\partial \zeta}{\partial x} \quad (8.1)$$

$$\frac{\partial M_y}{\partial t} + fM_x = -gH \frac{\partial \zeta}{\partial y} \quad (8.2)$$

$$\frac{\partial \zeta}{\partial t} + \frac{\partial M_x}{\partial x} + \frac{\partial M_y}{\partial y} = 0 \quad (8.3)$$

This is the linearized form of (1.32), (1.33) and (1.41), assuming that the external forces can be neglected. The condition at a rigid boundary states that the component of mass transport normal to the coast must vanish

$$M_n = (HU)_n = 0 \quad (8.4)$$

For the case of an open boundary, the necessary condition will be introduced later on.

We start by considering one differential equation from the above system and discuss eventual obstacles in the way of obtaining a solution. Assuming that the variables which appear in the equations change periodically, like the function $e^{i\omega t}$, we arrive by means of cross-differentiation of (8.1) and (8.2) and by virtue of the continuity

equation (8.3) at

$$(\omega^2 - f^2) \frac{ifg}{\omega} J(H, \zeta) + g\nabla(H\nabla\zeta) = 0 \quad (8.5)$$

The boundary condition (8.4) ought also to be expressed with the help of the sea-level variation. By introducing the angle α between the vector \vec{n} (normal to the coast) and the x-axis and the angle β between \vec{n} and the y-axis, (8.4) becomes

$$M_x \cos \alpha + M_y \cos \beta = 0 \quad (8.6)$$

Next, from (8.1) and (8.2) the components of mass transport are expressed in terms of the sea-level

$$M_x = \frac{gH}{\omega^2 - f^2} (f \frac{\partial \zeta}{\partial y} + i\omega \frac{\partial \zeta}{\partial x}) \quad (8.7)$$

$$M_y = \frac{gH}{\omega^2 - f^2} (i\omega \frac{\partial \zeta}{\partial y} - f \frac{\partial \zeta}{\partial x}) \quad (8.8)$$

Finally substituting (8.7) and (8.8) into (8.6) the appropriate boundary condition for (8.5) is derived

$$(f \frac{\partial \zeta}{\partial y} + i\omega \frac{\partial \zeta}{\partial x}) \cos \alpha + (i\omega \frac{\partial \zeta}{\partial y} - f \frac{\partial \zeta}{\partial x}) \cos \beta = 0 \quad (8.9)$$

Thus the study of the natural oscillations can be carried out using the system of primary equations (8.1), (8.2) and (8.3) or by consulting the equation of second order (8.5).

This approach to the problem of oscillatory motion has been known for many years. The history of the problem and valuable partial solutions can be found in Lamb's 'Hydrodynamics' or in 'Physical Oceanography' by Defant.

Our aim is to give a description of the recent numerical methods worked out by Platzman (1972), Rao and Shwab (1976) and others. Generally speaking, two classes of oscillatory motion can be discovered in equation (8.5).

Firstly, when the Earth's rotation is neglected ($f=0$), equation (8.5) simplifies to

$$\omega^2 \zeta + g\nabla(H\nabla\zeta) = 0 \quad (8.10)$$

which characterizes the long gravitational waves.

Secondly, in the case of rotational motion, another class of periodic oscillations appears and, as follows from (8.5), it is strongly influenced by the coupling between depth and sea-level due to the Jacobian expression $J(H, \zeta)$.

Let us study now the properties of (8.10) assuming a periodic solution $\zeta_n = \bar{\zeta}_n \exp(i\omega_n t)$. Here $\bar{\zeta}_n$ is an eigenfunction related to the eigenfrequency ω_n . Introducing this form of solution into (8.10) we obtain

$$-\omega_n^2 \bar{\zeta}_n = g \nabla (H \nabla \bar{\zeta}_n) \quad (8.11)$$

which together with (8.9) describes the set of eigenfrequencies $\{\omega_n\}$ and the set of eigenfunctions $\{\bar{\zeta}_n\}$. From the practical point of view the most important oscillations are those with the longest period ($\omega \rightarrow 0$). Obviously the existence of periodic oscillations in (8.11) is assured when ω_n^2 are both real and positive numbers. This property can be easily proved by the fact that, in the absence of rotation, (8.9) simplifies to $\frac{\partial \zeta}{\partial n} = 0$. Multiplying (8.11) by $\bar{\zeta}_n$ and subsequently integrating over the domain $\bar{D} = \{0 \leq x \leq l_1; 0 \leq y \leq l_2\}$, we have

$$-\omega_n^2 \int_0^{l_1} \int_0^{l_2} \bar{\zeta}_n \bar{\zeta}_n \, dx \, dy = \int_0^{l_1} \int_0^{l_2} \bar{\zeta}_n g \nabla (H \nabla \bar{\zeta}_n) \, dx \, dy \quad (8.12)$$

which is transformed by elementary manipulation of the right hand side of (8.12) to give

$$\omega_n^2 = g \int_0^{l_1} \int_0^{l_2} H \left[\left(\frac{\partial \bar{\zeta}_n}{\partial x} \right)^2 + \left(\frac{\partial \bar{\zeta}_n}{\partial y} \right)^2 \right] dx \, dy / \int_0^{l_1} \int_0^{l_2} (\bar{\zeta}_n)^2 dx \, dy \quad (8.13)$$

This expression, often called Rayleigh's form, is used to calculate the frequency when the eigenfunctions of the problem are known. When the domain of integration D is simple, for example a rectangular basin with constant depth, the solution of (8.11) is easy. A set of natural eigenperiods possesses an infinite (but countable) number of periods T_n in the range of $T_{\max} > T_n \geq 0$. A basin with a complicated geometry cannot be treated in such an analytical way. We start the numerical approach to the problem by analysing one-dimensional motion. In this case (8.11) simplifies to

$$-\omega_n^2 \zeta = g \frac{\partial}{\partial x} (H \frac{\partial \zeta}{\partial x}) \quad (8.14)$$

However, in the more complicated cases only the iterative methods can provide the required solution.

§2. The general properties of eigenvalues

Before we embark on a deeper analysis of the problem, let us recall the basic properties of a matrix A and the parameter λ involved in the eigenvalue problem. The elements of the matrix A will be denoted as a_{jk} (j stands for the row number and k for the column number). Let us recall the following theorem (Ralston, 1965):

If the coefficients of A are both symmetrical ($a_{jk} = a_{kj}$) and real, all eigenvalues and eigenvectors related to A are real. Eigenvectors related to the different eigenvalues are mutually orthogonal. As regards equation (8.10) certain parts of the theorem have already been proved. Assuming that the eigenvectors $\vec{\zeta}_1$ and $\vec{\zeta}_m$ are related to the eigenvalues λ_1 and λ_m , we have the two equations

$$A \vec{\zeta}_1 = \lambda_1 \vec{\zeta}_1 \quad (8.19)$$

and

$$A \vec{\zeta}_m = \lambda_m \vec{\zeta}_m \quad (8.20)$$

Next, multiplying (as a scalar) (8.19) by $\vec{\zeta}_m$ and (8.20) by $\vec{\zeta}_1$, we obtain

$$(\vec{\zeta}_m, A \vec{\zeta}_1) = \lambda_1 (\vec{\zeta}_m, \vec{\zeta}_1) \quad (8.21)$$

$$(\vec{\zeta}_1, A \vec{\zeta}_m) = \lambda_m (\vec{\zeta}_1, \vec{\zeta}_m) \quad (8.22)$$

Observe that the multiplication is performed on the left hand side. This is important due to the fact that this property is not commutative in general.

A is symmetrical due to the above theorem, that is $\vec{\zeta}_1^T A = A^T \vec{\zeta}_1 = A \vec{\zeta}_1$. Thus we may change the order of multiplication in (8.22) in this way

$$(\vec{\zeta}_m, A \vec{\zeta}_1) = \lambda_m (\vec{\zeta}_m, \vec{\zeta}_1) \quad (8.23)$$

Here A^T is a transposed matrix (one with coefficients a_{kj}).

Subtracting (8.23) from (8.21) we obtain

$$(\lambda_1 - \lambda_m) (\vec{\zeta}_m, \vec{\zeta}_1) = 0 \quad (8.24)$$

which shows that if $\lambda_1 \neq \lambda_m$, $\vec{\zeta}_m \neq 0$ and $\vec{\zeta}_1 \neq 0$, the eigenvectors $\vec{\zeta}_m$ and $\vec{\zeta}_1$ are orthogonal.

Let us now prove that the eigenvalues related to the matrix A are real (Faddeeva, 1959).

First the conjugate values $\vec{\zeta}_1^*$ and λ_1^* are introduced. In the case of

$$A\vec{\zeta}_1 = \lambda_1\vec{\zeta}_1 \quad (8.25)$$

and

$$A\vec{\zeta}_1^* = \lambda_1^*\vec{\zeta}_1^* \quad (8.26)$$

and if the same operations as above are performed with the assumption that $\vec{\zeta}_1 \neq 0$, the following expression is derived

$$(\lambda_1 - \lambda_1^*) (\vec{\zeta}_1^*, \vec{\zeta}_1) = 0 \quad (8.27)$$

This shows that

$$\lambda_1 = \lambda_1^* \quad (8.28)$$

and implies that λ_1 is a real quantity.

In the case of positive-definite operators (matrices), which play such a special rôle in the development of numerical methods, it can easily be deduced that the eigenvalues are real and positive. Multiplying (as scalars) both sides of (8.19) by $\vec{\zeta}_1$, it follows that

$$(A\vec{\zeta}_1, \vec{\zeta}_1) = \lambda (\vec{\zeta}_1, \vec{\zeta}_1) \quad (8.29)$$

and hence

$$\lambda = (A\vec{\zeta}_1, \vec{\zeta}_1) / (\vec{\zeta}_1, \vec{\zeta}_1) \quad (8.30)$$

The definition of a positive-definite operator $(A\vec{\zeta}_1, \vec{\zeta}_1) > 0$ and the fact that the scalar multiplication $(\vec{\zeta}_1, \vec{\zeta}_1) > 0$ establishes that $\lambda > 0$ in expression (8.30).

Considering a matrix A with its elements complex and symmetrical (in the sense that $a_{jk} = a_{kj}$), we shall prove that the eigenvalues related to this matrix are real.

Starting from the equation

$$A\vec{\zeta}_k = \lambda_k \vec{\zeta}_k \quad (8.31)$$

and

$$A^{T*}\vec{\zeta}^* = \lambda_k^* \vec{\zeta}_k^*, \quad (8.32)$$

multiplying (8.31) by $\vec{\zeta}_k^*$ and (8.32) by $\vec{\zeta}_k$, subtracting the resulting equations from each other and taking next into account that $A = A^{T*}$ and $(\vec{\zeta}_k, \vec{\zeta}_k^*) > 0$, we obtain

$$(\lambda_k - \lambda_k^*) (\vec{\zeta}_k, \vec{\zeta}_k^*) = 0 \quad (8.33)$$

On condition that $\vec{\zeta}_k \neq 0$, $\vec{\zeta}_k^* \neq 0$ it follows from (8.33) that $\lambda_k = \lambda_k^*$ and λ is a real number.

Finally, we would like to pay particular attention to some special questions of a general nature. The computational methods for eigenvalues and eigenfunctions form a large part of linear algebra, and the best presentation of these is given in Wilkinson's treatise (1965). For this problem a certain optimum approach is needed, since it is possible for a given differential equation to construct different numerical forms and consequently different matrices. Among the set of matrices, the symmetrical ones are to be preferred. This is due to a relatively easy way of solving symmetrical determinants and partly due to the possibility of saving computer memory, for it is sufficient to store in only half of a symmetrical matrix. Furthermore we intend to provide a method of constructing symmetrical matrices which will describe two-dimensional oscillations.

§3. Eigenvalues in two-dimensional oscillations: The construction of a symmetrical matrix

Equation (8.10) describes the gravitational oscillation in a two-dimensional domain. If a suitable numerical form on a finite difference grid is given for it, we may seek a solution to the eigenvalue problem. Introducing, as usual, a grid step h and indices along the x - and y -axes j and k respectively, we derive the symmetrical nume-

rical form based on the expression (2.15)

$$\begin{aligned} & \frac{g}{2h^2} [(H_{j+1,k} + H_{j,k}) (\zeta_{j+1,k} - \zeta_{j,k}) - (H_{j,k} + H_{j-1,k}) (\zeta_{j,k} - \zeta_{j-1,k}) \\ & + (H_{j,k+1} + H_{j,k}) (\zeta_{j,k+1} - \zeta_{j,k}) - (H_{j,k} + H_{j,k-1}) (\zeta_{j,k} - \zeta_{j,k-1})] \\ & + \omega^2 \zeta_{j,k} = 0 \end{aligned} \quad (8.34)$$

(8.34) can be rearranged in the form

$$\begin{aligned} & \frac{g}{2h^2} [(H_{j+1,k} + H_{j,k}) \zeta_{j+1,k} + (H_{j,k} + H_{j-1,k}) \zeta_{j-1,k} + (H_{j,k+1} + H_{j,k}) \zeta_{j,k+1} \\ & + (H_{j,k} + H_{j,k-1}) \zeta_{j,k-1}] + [\omega^2 - \frac{g}{2h^2} (4H_{j,k} + H_{j+1,k} + H_{j-1,k} \\ & + H_{j,k+1} + H_{j,k-1})] \zeta_{j,k} = 0 \end{aligned} \quad (8.34b)$$

It is easy to observe that (8.34) and (8.34b) cannot be written as the product of a matrix by a vector in the same way as (8.17) or (8.18). Nevertheless, to use the methods of linear algebra we are compelled to introduce a vector-matrix notation. In order to do this, we construct from the two-dimensional enumeration (j,k) a one-dimensional enumeration in which every grid point will have a consecutive number. We shall present this new method of enumeration in equation (8.34b). The numerical grid is plotted in fig. 96. It shows, together with the (j,k) -enumeration, the new one-dimensional enumeration. When the latter is considered, the boundary points are disregarded, since it follows from the condition $\frac{\partial \zeta}{\partial n} = 0$ that all points adjacent to the boundary possess the same values of the sea-level as points on the boundary. Additionally, we set $H = 0$ at all boundary grid points. In the net in fig. 96 there are 6 internal grid points. To seek a solution for the eigenvalues and eigenvectors we write down at every grid point a difference equation, namely

$$\zeta_2 (H_2 + H_1) + \zeta_1 H_1 + \zeta_4 (H_4 + H_1) + \zeta_1 H_1 + \zeta_1 (2h^2 \omega^2 / g - (4H_1 + H_2 + H_4)) = 0$$

$$\zeta_3 (H_3 + H_2) + \zeta_1 (H_1 + H_2) + \zeta_5 (H_2 + H_5) + \zeta_2 H_2 + \zeta_2 (2h^2 \omega^2 / g - (4H_2 + H_3 + H_1 + H_5)) = 0$$

$$\zeta_3 H_3 + \zeta_2 (H_2 + H_3) + \zeta_6 (H_3 + H_6) + \zeta_3 H_3 + \zeta_3 (2h^2 \omega^2 / g - (4H_3 + H_2 + H_6)) = 0$$

$$\zeta_5 (H_4+H_5) + \zeta_4 H_4 + \zeta_4 H_4 + \zeta_1 (H_1+H_4) + \zeta_4 (2h^2\omega^2/g - (4H_4+H_5+H_1)) = 0$$

$$\zeta_6 (H_5+H_6) + \zeta_4 (H_4+H_5) + \zeta_5 H_5 + \zeta_2 (H_2+H_5) + \zeta_5 (2h^2\omega^2/g - (4H_5+H_6+H_4+H_2)) = 0$$

$$\zeta_6 H_6 + \zeta_5 (H_5+H_6) + \zeta_6 H_6 + \zeta_3 (H_3+H_6) + \zeta_6 (2h^2\omega^2/g - (4H_6+H_5+H_3)) = 0$$

These equations we rearrange in a vector-matrix form, since it helps to analyse the property of the coefficients' matrix.

$$\begin{bmatrix}
 \frac{2h^2\omega^2}{g} - 2H_1 & ; & H_2+H_1 & ; & 0 & ; & H_1+H_4 & ; & 0 & ; & 0 \\
 -H_2-H_4 & & & & & & & & & & \\
 H_2+H_1 & ; & \frac{2h^2\omega^2}{g} - 3H_2 & ; & H_2+H_3 & ; & 0 & ; & H_2+H_5 & ; & 0 \\
 & & -H_3-H_1-H_5 & & & & & & & & \\
 0 & ; & H_2+H_3 & ; & \frac{2h^2\omega^2}{g} - 2H_3 & ; & 0 & ; & 0 & ; & H_3+H_6 \\
 & & & & -H_2-H_6 & & & & & & \\
 H_1+H_4 & ; & 0 & ; & 0 & ; & \frac{2h^2\omega^2}{g} - 2H_4 & ; & H_4+H_5 & ; & 0 \\
 & & & & -H_5-H_1 & & & & & & \\
 0 & ; & H_2+H_5 & ; & 0 & ; & H_4+H_5 & ; & \frac{2h^2\omega^2}{g} - 3H_5 & ; & H_6+H_5 \\
 & & & & & & -H_2-H_4-H_6 & & & & \\
 0 & ; & 0 & ; & H_3+H_6 & ; & 0 & ; & H_5+H_6 & ; & \frac{2h^2\omega^2}{g} - 2H_6 \\
 & & & & & & & & & & -H_3-H_5
 \end{bmatrix}
 \begin{bmatrix}
 \zeta_1 \\
 \zeta_2 \\
 \zeta_3 \\
 \zeta_4 \\
 \zeta_5 \\
 \zeta_6
 \end{bmatrix}
 =
 \begin{bmatrix}
 0 \\
 0 \\
 0 \\
 0 \\
 0 \\
 0
 \end{bmatrix}
 \tag{8.35}$$

Analysing the matrix of coefficients it is obvious at once that all the elements are real and that the property of symmetry holds, because $a_{jk} = a_{kj}$. This form of matrix is closely related with the symmetrical form of the difference equation discussed in chapter II or, speaking more generally, to the self-adjoint properties of difference operators.

In order to obtain a symmetrical matrix, special precautions should be taken at the boundary grid points, i.e.

1. The one-dimensional enumeration does not include the boundary grid points.
2. Apart from the boundary condition, the depth is always set equal to zero at the boundary.

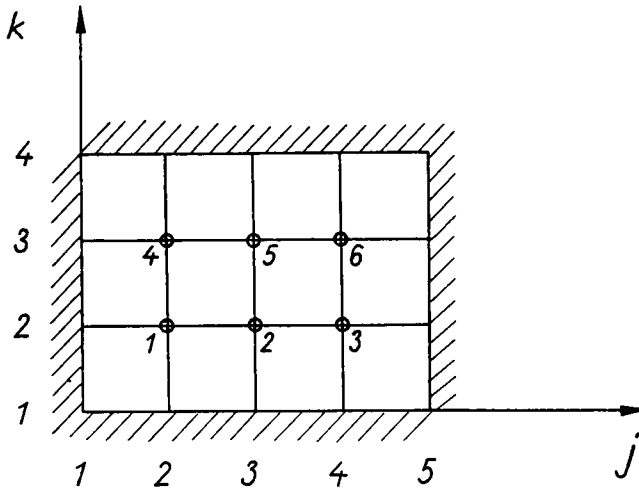


Fig. 96. PLACING OF POINTS TO CONSTRUCT ONE-DIMENSIONAL ARRAY IN TWO-DIMENSIONAL PLANE

The method presented above of ensuring symmetry is somewhat like the method proposed by Loomis (1973). The further derivation of a set of eigenvalues and eigenfunctions consists simply in the application of standard procedures for solving a symmetrical matrix for example the Jacobi method (Ralston, 1965).

§4. Galerkin's method and its application to the problem of eigenvalues and eigenvectors

Let us consider a linear boundary problem (the following method may also be applied to nonlinear problems):

$$L\zeta = f(x) \quad (8.36)$$

with the boundary condition

$$L_1\zeta = 0 \quad (8.37)$$

Here L_1 and L denote differential operators and x the co-ordinate. Introducing a system of functions $\phi_j(x)$, $j=1,2,\dots,m$ (often called

basic functions) which are linearly independent and part of the complete set of functions, we may represent the function ζ , the solution of (8.36), as a linear combination of ϕ_j with the coefficients a_j

$$\zeta = \sum_{j=1}^m a_j \phi_j(x) \quad (8.38)$$

In addition it is assumed that the functions ϕ_j satisfy the boundary condition (8.37). Referring to the known theorem on the orthogonality of arbitrary continuous functions (given in the domain $[a, b]$) to the complete set of functions ϕ_j (Collatz, 1964) we may seek the unknown coefficients a_j from the orthogonality condition

$$((L\zeta - f(x)), \phi_k) = 0 \quad (8.39)$$

$$k = 1, 2, \dots, m.$$

Here the brackets and commata denote scalar multiplication in the sense

$$\int_a^b (L\zeta - f(x)) \phi_k dx = 0 \quad (8.40)$$

Taking into account the expression for ζ (8.38) the condition of orthogonality is stated as

$$\sum_{j=1}^m (a_j L\phi_j, \phi_k) = (f(x), \phi_k); \quad k = 1, 2, \dots, m \quad (8.41)$$

Therefore a system of m equations which determines the m unknown coefficients a_j is obtained. When these coefficients are introduced into (8.38), the function ζ is determined as the solution of the boundary problem (8.36), (8.37). If equation (8.36) is set for an eigenvalue problem

$$L\zeta = \lambda \zeta \quad (8.42)$$

then the eigenvalues and eigenfunctions can be found using Galerkin's method (Kantorovich and Krylov, 1958; Kaliski, 1966). Substituting (8.42) in the orthogonality condition (8.41)

$$\sum_{j=1}^m (a_j L\phi_j, \phi_k) = \lambda(\phi_j, \phi_k) ; k = 1, 2, \dots, m \quad (8.43)$$

again a system of m algebraic equations is obtained. The vanishing of the determinant of this homogeneous system, under condition that $a_j \neq 0$ (a consequence of the assumption that the set of ϕ_j is a complete one), provides the set of eigenvalues. When the eigenvalues have all been found, the coefficients a_j can be determined from (8.43) and then from (8.38) the eigenvectors may be obtained.

Before applying Galerkin's method in the general case, a simplified numerical example will be considered to illustrate the ideas stated above. Let us suppose that gravitational oscillations are observed in a one-dimensional basin of length $l = 50$ km along the x -axis. The depth varies linearly as $H = H_0 + kx$, so $H(x=0) = 50$ m and $H(x=l)=55$ m.

The differential equation which yields the eigenvalues and eigenfunctions is given by (8.14)

$$g \frac{\partial}{\partial x} (H \frac{\partial \zeta}{\partial x}) + \omega^2 \zeta = 0 \quad (8.44)$$

Substituting into (8.44) the depth dependence and the new variable y defined by the expression $H_0 + kx = Wy$, we find

$$\frac{\partial}{\partial y} (y \frac{\partial \zeta}{\partial y}) + \omega^2 W \zeta / gk^2 = 0 \quad (8.45)$$

The solution of this equation is easily formulated in terms of Bessel's functions J_0 and N_0 (Mc Lachlan, 1948)

$$\zeta = A J_0 (2 \frac{\omega}{k} \sqrt{yW/g}) + B N_0 (2 \frac{\omega}{k} \sqrt{yW/g}) \quad (8.46)$$

Next, by utilizing the boundary condition $\frac{\partial \zeta}{\partial y} = 0$, the eigenfrequencies ω_k are defined.

In seeking a solution of (8.44) by Galerkin's method the basic functions ϕ_j have to be chosen first. Here we shall use the characteristic properties of these functions, i.e. completeness and fulfilment of the boundary condition. For equation (8.44) the functions $\phi_j(x) = \cos \frac{j\pi x}{l}$ are chosen since they satisfy the above properties and in the computations we take $j = 1, 2$, so that (8.38) is taken in the following form

$$\zeta = a_1 \cos \frac{\pi x}{l} + a_2 \cos \frac{2\pi x}{l} \quad (8.47)$$

Substituting (8.47) into (8.43) we obtain the system of two equations

$$\int_0^1 \left\{ \sum_{j=1}^2 a_j g \frac{\partial}{\partial x} ((H_0 + kx) \frac{\partial}{\partial x} \phi_j) + \omega^2 a_j \phi_j \cos \frac{\pi x}{l} \right\} dx = 0 \quad (8.48a)$$

$$\int_0^1 \left\{ \sum_{j=1}^2 a_j g \frac{\partial}{\partial x} ((H_0 + kx) \frac{\partial}{\partial x} \phi_j) + \omega^2 a_j \phi_j \cos \frac{2\pi x}{l} \right\} dx = 0 \quad (8.48b)$$

and by integration it becomes

$$a_1 g k \cdot 16/9 + a_2 (l\omega^2/2 - 2\pi^2 H_0 g/l - kg\pi^2) = 0 \quad (8.49a)$$

$$a_1 (\omega^2 l/2 - H_0 g \pi^2/2l - gk\pi^2/4) + a_2 kg \cdot 64/9 = 0 \quad (8.49b)$$

These equations provide two values for the eigenvalues or for the periods of oscillation $T_1 = 2\pi/\omega_1 = 4900.75$ sec and $T_2 = 2\pi/\omega_2 = 2216.12$ sec. As a comparison we calculate the two longest periods by the usual expression for a one-dimensional basin with constant depth H_0 (Defant, 1961)

$$T_1 = 2l/\sqrt{gH_0} = 4515.23 \text{ sec} ; \quad T_2 = T_1/2 = 2257.61 \text{ sec.}$$

The final numerical problem of Galerkin's method is the system of equations (8.43) (or in the considered example (8.49)) from which, through the vanishing of a determinant, the set of eigenvalues is calculated. On the other hand, the direct method of determining the eigenvalues from a difference equation as presented in the previous paragraph also leads to a determinant. The following question may be asked: Why use Galerkin's method instead of the direct method? The answer is that Galerkin's method leads to a much faster solution than the direct method. This follows from the fact that in the difference method we have to consider, in the one-dimensional case, around 100 grid points, that is 100 equations or a determinant with 100 unknowns. Using Galerkin's method we can quite often obtain the same answer by choosing a small number ($m=2$ to 5) of suitable basic functions and by solving 2 to 5 equations.

Let us direct our attention now to the major problem, i.e. to the description of two-dimensional free oscillations on the rotating Earth.

The main difficulty in applying Galerkin's method here lies in the construction of a set of orthogonal functions in two-dimensional space which satisfies the boundary condition, since this condition in the general case (8.9) is quite complicated.

In addition the problem, as defined by (8.5), is posed in a complex space. All these obstacles compel us to study the eigenoscillations through the system of primary equations (8.1), (8.2) and (8.3) instead of using one equation of higher order (8.5).

In the following two methods of solving the eigenvalue problem, using the primary system of equations, will be presented, namely Platzman's (1972) method and Galerkin's method.

Firstly, we shall describe Galerkin's method. The major question is the construction of an orthogonal set of functions. This problem was solved by Rao and Shwab (1976). The velocity field (mass transport \vec{M}) is split into a potential component \vec{M}^ϕ and a rotational component \vec{M}^ψ . In this way $\vec{M} = \vec{M}^\phi + \vec{M}^\psi$. Next, recalling the definition of a stream function ψ and a potential function ϕ , we may write

$$M_x^\phi = -H \frac{\partial \phi}{\partial x} \quad M_x^\psi = - \frac{\partial \psi}{\partial y} \quad (8.50)$$

$$M_y^\phi = -H \frac{\partial \phi}{\partial y} \quad M_y^\psi = \frac{\partial \psi}{\partial x}$$

Employing (8.50) the rotor and divergence of the vector \vec{M} can be expressed by the second-order differential equations

$$\text{div } \vec{M} = -\nabla(H\nabla\phi) \quad (8.51)$$

$$\text{rot } \vec{M}/H = \nabla(H^{-1}\nabla\psi) \quad (8.52)$$

If the mass transport \vec{M} is known, (8.51) and (8.52) can be solved as a nonhomogeneous elliptical problem (at every instant). However the problem is usually the reversed, i.e. since \vec{M} is unknown, the solution will be constructed as a sum related to the set of orthogonal functions ψ and ϕ . With this aim in mind (8.51) and (8.52) will be solved as homogeneous equations. The two derived sets of eigenfunctions will establish two sets of orthogonal or basic functions for Galerkin's solution. The boundary conditions for the problem are obvious and follow from (8.4)

$$(\vec{M} \cdot \vec{n}) = (\vec{M}^\phi + \vec{M}^\psi) \cdot \vec{n} = 0 \text{ and therefore } \vec{M}^\phi \cdot \vec{n} = 0 \text{ and } \vec{M}^\psi \cdot \vec{n} = 0 \quad (8.53)$$

The same condition may be expressed with the help of the stream and potential functions as

$$H \frac{\partial \phi}{\partial n} = 0 \quad \text{and} \quad \psi = 0 \quad (8.54)$$

The homogeneous part of (8.51) and (8.52) together with the boundary conditions (8.54) have a unique solution, but it seems that this is only true in a simply connected domain. Let us therefore start by considering the equations for the eigenproblems. By virtue of (8.51) and (8.52) it follows that

$$L_1 \phi_\alpha = \nabla (H \nabla \phi_\alpha) = -\phi_\alpha \lambda_\alpha \quad (8.55)$$

and

$$L_2 \psi_\alpha = \nabla (H^{-1} \nabla \psi_\alpha) = -\psi_\alpha \mu_\alpha \quad (8.56)$$

Here ϕ_α and ψ_α denote the eigenfunctions and λ_α and μ_α the corresponding eigenvalues. The operators in (8.55) and (8.56) are self-adjoint. Thus all the eigenvalues are real and the eigenfunctions ϕ_α and ψ_α belong to two complete and orthogonal sets of functions. The condition of orthogonality may be stated in the following way

$$\int_{\bar{D}} \phi_\beta L_1 \phi_\alpha \, dD = -\lambda_\alpha \int_{\bar{D}} \phi_\alpha \phi_\beta \, dD = J_1 \delta_{\alpha\beta} \quad (8.57)$$

Taking into account (8.51),

$L_1 \phi_\alpha = -\nabla \vec{M}_\alpha^\phi$ and $\int \phi_\beta L_1 \phi_\alpha \, dD = -\int \phi_\beta \nabla \vec{M}_\alpha^\phi \, dD = \int \vec{M}_\alpha^\phi \nabla \phi_\beta \, dD$ are derived. Using the expression (8.50), the condition becomes

$$\int_{\bar{D}} 1/H \cdot \vec{M}_\alpha^\phi \cdot \vec{M}_\beta^\phi \, dD = \lambda_\alpha \int_{\bar{D}} \phi_\alpha \cdot \phi_\beta \, dD = J_1 \delta_{\alpha\beta} \quad (8.58)$$

Here D denotes the domain of integration and

$$\delta = \begin{cases} 1 & \text{if } \alpha = \beta \\ 0 & \text{if } \alpha \neq \beta \end{cases}$$

A similar orthogonality condition may be defined for the rotational component \vec{M}^ψ

$$\int_{\bar{D}} 1/H \cdot \vec{M}_\alpha \cdot \vec{M}_\beta \, dD = \mu_\alpha \int_{\bar{D}} \psi_\alpha \cdot \psi_\beta \, dD = J_2 \delta_{\alpha\beta} \quad (8.59)$$

We now can prove that the problems (8.55) and (8.56), with boundary condition (8.54), are characterized by real and positive eigenvalues, and that the eigenfunctions are mutually orthogonal. For two different eigenfunctions, (8.55) yields

$$\nabla (H\nabla\phi_\alpha) = -\lambda_\alpha \phi_\alpha \quad (8.60)$$

and

$$\nabla (H\nabla\phi_\beta) = -\lambda_\beta \phi_\beta \quad (8.61)$$

Multiplying (8.60) by ϕ_β and (8.61) by ϕ_α , subtracting the equations from each other and integrating the result over the domain $\bar{D}(x,y)$, we find

$$\int_{\bar{D}} [\phi_\beta \nabla(H\nabla\phi_\alpha) - \phi_\alpha \nabla(H\nabla\phi_\beta)] \, dD = (\lambda_\alpha - \lambda_\beta) \int_{\bar{D}} \phi_\alpha \phi_\beta \, dD \quad (8.62)$$

To prove that ϕ_α and ϕ_β are orthogonal to each other it is sufficient to show that the left hand side of (8.62) is equal to zero when $\lambda_\alpha \neq \lambda_\beta$. We shall now rearrange the left hand side of (8.62) with the help of the boundary condition (8.54) to yield

$$\begin{aligned} \int_{\bar{D}} [\nabla(\phi_\beta H\nabla\phi_\alpha) - H\nabla\phi_\beta \nabla\phi_\alpha - \nabla(\phi_\alpha H\nabla\phi_\beta) + H \nabla\phi_\alpha \nabla\phi_\beta] \, dD \\ = \int_{\bar{D}} [\nabla(\phi_\beta H\nabla\phi_\alpha) - \nabla(\phi_\alpha H\nabla\phi_\beta)] \, dD = 0 \end{aligned}$$

With the orthogonality condition it is easy to show that $\lambda_\alpha > 0$. Again through the multiplication of (8.55) by ϕ_α we have

$$(L_1\phi_\alpha, \phi_\alpha) = -\lambda_\alpha (\phi_\alpha, \phi_\alpha) = \int_{\bar{D}} \phi_\alpha \nabla(H\nabla\phi_\alpha) \, dD = - \int_{\bar{D}} H \nabla\phi_\alpha \nabla\phi_\alpha \, dD$$

and therefore

$$\lambda_\alpha = \int_{\bar{D}} H (\nabla\phi_\alpha)^2 \, dD / \int_{\bar{D}} (\phi_\alpha)^2 \, dD \quad (8.63)$$

Let us return again to the problem of eigenoscillation of free standing waves in a basin of arbitrary shape. The set of eigenfunctions

defined by (8.55) and (8.56) allows us to construct the solution for the vector of mass transport as a linear combination in the same way as (8.38) was constructed, namely

$$\vec{M}^\phi = \sum_{\alpha} P_{\alpha}(t) \vec{M}_{\alpha}^{\phi}(x, y) \quad (8.64)$$

$$\vec{M}^{\psi} = \sum_{\alpha} Q_{\alpha}(t) \vec{M}_{\alpha}^{\psi}(x, y) \quad (8.65)$$

The sea-level variations are set in a similar form

$$\zeta = \sum_{\alpha} R_{\alpha}(t) \zeta_{\alpha}(x, y) \quad (8.66)$$

As can be deduced from the continuity equation, ζ_{α} is closely related to the eigenfunctions ϕ_{α} , since

$$\zeta_{\alpha} = \phi_{\alpha} \sqrt{\lambda/g} \quad (8.67)$$

To find the unknown expansion coefficients P_{α} , Q_{α} and R_{α} the primary equations and orthogonality conditions will be employed. Expressing the equations of motion and continuity (8.1) - (8.3) in the vector form

$$\frac{\partial \vec{M}}{\partial t} - [\vec{f} \times \vec{M}] = -gH \nabla \zeta \quad (8.68)$$

$$\frac{\partial \zeta}{\partial t} + \nabla \cdot \vec{M} = 0 \quad (8.69)$$

we insert (8.64), (8.65) and (8.66) into (8.68). Hence

$$\begin{aligned} \sum_{\beta} \vec{M}_{\beta}^{\phi} \frac{\partial P_{\beta}}{\partial t} + \sum_{\beta} \vec{M}_{\beta}^{\psi} \frac{\partial Q_{\beta}}{\partial t} - \sum_{\beta} P_{\beta} [\vec{f} \times \vec{M}_{\beta}^{\phi}] - \sum_{\beta} Q_{\beta} [\vec{f} \times \vec{M}_{\beta}^{\psi}] &= -gH \sum_{\beta} R_{\beta} \nabla \zeta_{\beta} \\ &= -\sqrt{g\lambda} H \sum_{\beta} R_{\beta} \nabla \phi_{\beta} = \sqrt{\lambda g} \sum_{\beta} R_{\beta} \vec{M}_{\beta}^{\phi} \end{aligned} \quad (8.70)$$

Multiplying (8.70) by \vec{M}_{α}^{ϕ} using scalar products and next by \vec{M}_{α}^{ψ} , two equations are obtained which define the coefficients

$$J_1 \frac{dP_{\alpha}}{dt} - \sum_{\beta} A_{\alpha\beta} P_{\beta} - \sum_{\beta} B_{\alpha\beta} Q_{\beta} = J_1 R \sqrt{g\lambda} \alpha \quad (8.71)$$

$$J_2 \frac{dQ_{\alpha}}{dt} - \sum_{\beta} C_{\alpha\beta} P_{\beta} - \sum_{\beta} D_{\alpha\beta} Q_{\beta} = 0 \quad (8.72)$$

A third equation is derived from the continuity equation (8.69) through multiplication by \vec{M}_β^ϕ

$$\frac{dR_\alpha}{dt} + P_\alpha \sqrt{g\lambda_\alpha} = 0 \quad (8.73)$$

The nonlinear terms in the preceding equations are expressed in this way

$$A_{\alpha\beta} = \int \frac{1}{D} 1/H \cdot \vec{M}_\alpha^\phi [\vec{f} \times \vec{M}_\beta^\phi] dD \quad (8.74)$$

$$B_{\alpha\beta} = \int \frac{1}{D} 1/H \cdot \vec{M}_\alpha^\phi [\vec{f} \times \vec{M}_\beta^\psi] dD \quad (8.75)$$

$$C_{\alpha\beta} = \int \frac{1}{D} 1/H \cdot \vec{M}_\alpha^\psi [\vec{f} \times \vec{M}_\beta^\phi] dD \quad (8.76)$$

$$D_{\alpha\beta} = \int \frac{1}{D} 1/H \cdot \vec{M}_\alpha^\psi [\vec{f} \times \vec{M}_\beta^\psi] dD \quad (8.77)$$

These coefficients possess intrinsically the property of symmetry, namely

$$A_{\alpha\beta} = -A_{\beta\alpha}; B_{\alpha\beta} = -C_{\alpha\beta}; D_{\alpha\beta} = -D_{\beta\alpha} \quad (8.78)$$

We introduce a new notation in order to write down equations (8.71) - (8.73) in vector-matrix form setting

$$J_1 = J_2 = J; \quad 1/J \cdot \sum_{\beta} A_{\alpha\beta} = A; \quad 1/J \cdot \sum_{\beta} B_{\alpha\beta} = B; \quad 1/J \cdot \sum_{\beta} C_{\alpha\beta} = C; \quad 1/J \cdot \sum_{\beta} D_{\alpha\beta} = D$$

$$\vec{S} = \begin{bmatrix} P_\alpha \\ Q_\alpha \\ R_\alpha \end{bmatrix} \quad (8.79)$$

The equations (8.71) - (8.73) may be written simply as one vector equation

$$\frac{d\vec{S}}{dt} = -a \vec{S} \quad (8.80)$$

$$\text{where } a = \begin{bmatrix} -A & -B & -v \\ -C & -D & 0 \\ v & 0 & 0 \end{bmatrix} \quad (8.81)$$

Assuming that the periodic oscillation is of the form $\vec{S} = \vec{S}_1 e^{i\omega t}$, equation (8.80) becomes

$$(ia - \omega) \vec{S}_1 = 0 \quad (8.82)$$

The element of the complex matrix ia satisfies the symmetry condition, since $a_{jk} = a_{kj}^*$. Therefore (8.33) leads to the conclusion that all eigenvalues are real. When the eigenvalues have been found, (8.82) may be employed to determine the components of \vec{S} . Subsequently P_α , Q_α and R_α will be inserted into (8.64), (8.65) and (8.66) to find the distribution of the sea-level and the mass transport in the basin being considered.

§5. A method of resonance iterations

In 1972 Platzman presented a method to solve the eigenvalue problem which is related to a method proposed much earlier by Lanczos (1956). The method itself is rather time consuming but on the other hand quite simple and may be generalized easily to solve many other problems.

The method is based on the observation that resonance will only occur in a dynamic system, if the period of an applied force is equal to any eigenperiod of the system. Hence a fictitious external force is introduced into the system of equations which describes the motion of a sea basin. The system is then integrated in time.

After a certain interval of time has elapsed (usually one period), the integration is stopped and the frequency of oscillation is computed from the distribution of U , V and ζ with the help of Rayleigh's formula (8.13). The new frequency value is introduced into the expression for the external force and again the system of equations is integrated in time. The iterative process of fitting the frequency of the external force in this way ensures convergence to the eigenfrequency of the dynamic system.

Let us again consider the primitive set of equations (8.1) - (8.3) without the friction term. To simplify the problem the Coriolis force is also omitted. Introducing new dependent variables

$$M_x/H = U = u_1 \sqrt{gH}; \quad M_y/H = V = v_1 \sqrt{gH}; \quad \zeta = \zeta_1 \quad (8.83)$$

we make the system of equations more symmetrical

$$\frac{\partial \zeta_1}{\partial t} = - \frac{\partial}{\partial x} (u_1 \sqrt{gH}) - \frac{\partial}{\partial y} (v_1 \sqrt{gH}) \quad (8.84)$$

$$\frac{\partial u_1}{\partial t} = -\sqrt{gH} \frac{\partial \zeta_1}{\partial x} \quad (8.85)$$

$$\frac{\partial v_1}{\partial t} = -\sqrt{gH} \frac{\partial \zeta_1}{\partial y} \quad (8.86)$$

The same system in the vector-matrix form becomes

$$\frac{\partial \vec{\zeta}_1}{\partial t} = iB \vec{\zeta}_1 \quad (8.87)$$

where

$$S_1 = \begin{bmatrix} \zeta_1 \\ u_1 \\ v_1 \end{bmatrix} \quad B = i \begin{bmatrix} 0 & \frac{\partial}{\partial x} \sqrt{gH} & \frac{\partial}{\partial y} \sqrt{gH} \\ \sqrt{gH} \frac{\partial}{\partial x} & 0 & 0 \\ \sqrt{gH} \frac{\partial}{\partial y} & 0 & 0 \end{bmatrix} \quad (8.88)$$

We recall the notation of the scalar product which shall be used later on

$$(\vec{\zeta}_1, \vec{\zeta}_1^T) = \int \int_D (u_1^2 + v_1^2 + \zeta_1^2) dx dy = \int \int_D ([U^2 + V^2] / \sqrt{gH} + \zeta^2) dx dy \quad (8.89)$$

The vector $\vec{\zeta}_1^T$ is transposed to $\vec{\zeta}_1$, that is a row vector.

Seeking an oscillatory solution in the form $\vec{\zeta}_1 = \vec{\zeta} e^{i\omega t}$, by insertion in (8.87) we find

$$i\omega \vec{\zeta} = iB \vec{\zeta} \quad (8.90)$$

Multiplying (8.90) by the vector $\vec{\zeta}^{*T}$ (conjugated and transposed to $\vec{\zeta}$), an expression analogous to Rayleigh's formula (8.13) is obtained

$$\omega^2 = (\vec{\zeta}^{*T}, B \vec{\zeta}) / (\vec{\zeta}^{*T}, \vec{\zeta}) \quad (8.91)$$

We introduce finite differences into the system (8.84) - (8.86) to obtain the symmetrical numerical form

$$\frac{\zeta_1^1 - \zeta_1^{1-1}}{T} = -\frac{\partial}{\partial x}(u_1^{1-1/2}\sqrt{gH}) - \frac{\partial}{\partial y}(v_1^{1-1/2}\sqrt{gH}) \quad (8.92)$$

$$\frac{u_1^{1+1/2} - u_1^{1-1/2}}{T} = -\sqrt{gH}\frac{\partial \zeta_1^1}{\partial x} \quad (8.93)$$

$$\frac{v_1^{1+1/2} - v_1^{1-1/2}}{T} = -\sqrt{gH}\frac{\partial \zeta_1^1}{\partial y} \quad (8.94)$$

We rewrite this difference-differential equation in the vector-matrix form in order to reveal an intrinsic property of the transition operator from time step $l-1$ to l

$$\frac{\vec{S}_1^1 - \vec{S}_1^{1-1}}{T} = -D\vec{S}_1^{1-1} + D^+\vec{S}_1^1 \quad (8.95)$$

where

$$S_1^1 = \begin{bmatrix} \zeta_1^1 \\ u_1^{1+1/2} \\ v_1^{1+1/2} \end{bmatrix} \quad (8.96)$$

$$D = \begin{bmatrix} 0 & \frac{\partial}{\partial x}\sqrt{gH} & \frac{\partial}{\partial y}\sqrt{gH} \\ 0 & 0 & 0 \\ 0 & 0 & 0 \end{bmatrix} \quad D^+ = \begin{bmatrix} 0 & 0 & 0 \\ \sqrt{gH}\frac{\partial}{\partial x} & 0 & 0 \\ \sqrt{gH}\frac{\partial}{\partial y} & 0 & 0 \end{bmatrix} \quad (8.97)$$

With this notation we can express the transition operator as

$$H = (1 - DT)(1 - D^+T)^{-1} \quad (8.98)$$

and (8.95) becomes

$$\vec{S}_1^1 = H \vec{S}_1^{1-1} \quad (8.99)$$

Now we shall take the second step in seeking the solution, namely we construct an analogous equation to (8.99) when an external force is present. The expression $S_1'(t)$ for a fictitious force is added to equation (8.99)

$$\vec{S}_1'(t) = \begin{bmatrix} \zeta_1'(t) \\ u_1'(t) \\ v_1'(t) \end{bmatrix} \quad (8.100)$$

The non-homogeneous equation corresponding to (8.99) is therefore written in the form

$$\vec{S}_1^{l+1} = H\vec{S}_1^{l-1} + \vec{S}_1^{l'} \quad (8.101)$$

Now we can return to the scalar form of (8.101) which is suitable for a numerical treatment

$$\zeta_1^{l+1} = \zeta_1^{l-1} - T \frac{\partial}{\partial x} (u_1^{l-1/2} \sqrt{gH}) + T \frac{\partial}{\partial y} (v_1^{l-1/2} \sqrt{gH}) + \zeta_1^{l'} \quad (8.102)$$

$$u_1^{l+1/2} = u_1^{l-1/2} - T \sqrt{gH} \frac{\partial}{\partial x} (\zeta_1^l - \zeta_1^{l'}) + u_1^{l+1/2'} \quad (8.103)$$

$$v_1^{l+1/2} = v_1^{l-1/2} - T \sqrt{gH} \frac{\partial}{\partial y} (\zeta_1^l - \zeta_1^{l'}) + v_1^{l+1/2'} \quad (8.104)$$

The external force is taken as periodic in time

$$\vec{S}_1^{l'} = \vec{S}' \exp(i2\pi t/T_1) = \vec{S}' \exp(i2\pi lT/T_1) \quad (8.105)$$

where l is a time index, $l = 0, 1, 2, \dots, n$; T denotes the time step of integration and T_1 is the period of oscillation. T_1 is set initially in an arbitrary way but in the vicinity of the presumed period. We can start with the computation of the above system of equations, but we are still lacking the numerical form of (8.91). The vector $\vec{S}_1^{l'} = \vec{S}' e^{i\omega t}$ with $t = lT$, when introduced into the homogeneous equation (8.99), yields

$$\vec{S} e^{i\omega lT} = H\vec{S} e^{i\omega(l-1)T} \quad (8.106)$$

Multiplying both sides by \vec{S}^{*T} , (8.106) becomes

$$(\vec{S}^{*T}, \vec{S} e^{i\omega T}) = (\vec{S}^*, \vec{S}) \quad (8.107)$$

Inserting (8.98) in (8.107), we define the frequency of free oscillation

$$e^{i\omega T} = (\vec{S}^{*T}, (1-TD)\vec{S}) / (\vec{S}^{*T}, (1-TD^+)\vec{S}) \quad (8.108)$$

The scalar products appearing in (8.108) can be described as a sum taken over all grid points

$$(\vec{S}^{*T}, \vec{S}) = \sum_j \sum_k (\zeta_1^* \zeta_1 + u_1^* u_1 + v_1^* v_1) h^2 \quad (8.109)$$

$$(\vec{S}^{*T}, D\vec{S}) = (\zeta_1^*, u_1^*, v_1^*) \begin{bmatrix} \frac{\partial}{\partial x}(u_1 \sqrt{gH}) + \frac{\partial}{\partial y}(v_1 \sqrt{gH}) \\ 0 \\ 0 \end{bmatrix} \\ = \sum_j \sum_k \zeta_1^* \left[\frac{\partial}{\partial x}(u_1 \sqrt{gH}) + \frac{\partial}{\partial y}(v_1 \sqrt{gH}) \right] h^2 \quad (8.110)$$

$$(S^{*T}, D^+S) = - \sum_j \sum_k (u_1^* \sqrt{gH} \frac{\partial \zeta_1^*}{\partial x} + v_1^* \sqrt{gH} \frac{\partial \zeta_1^*}{\partial y}) \quad (8.111)$$

The overall calculation of a set of eigenvectors and eigenfrequencies will be performed by the following system of equations: (8.102), (8.103), (8.104) and (8.108).

Taking an arbitrary value of amplitude \vec{S}' and period T_1 of the external force vector in (8.105) at the initial moment $t=0$, the system of equations (8.102) - (8.104) can be integrated in time from 0 to t . In this way the vector $\vec{S}_1(t)$ is derived. If in the next calculations $\vec{S}_1(t)$ is taken as the amplitude of the external force \vec{S}'_1 and the new period is obtained by (8.108), then the components of the external force approach the set of eigenvalues.

Assuming that the approximate value of the eigenperiod T is known, the number of integration steps in time can be taken as $T_1/T = L$. The arbitrary external force (with a period T_1) involved in the system (8.102) - (8.104) is integrated L -times until the value \vec{S}_1^L is obtained. This value is used to calculate from (8.108) ω_1^L and T_1^L . Changing in

(8.105) T_1 to T_1^L and \vec{S}' to \vec{S}_1^L we again perform integration. The repetition of this procedure leads to exact values of eigenvalues and eigenperiods.

§6. A method of computing the longest period of free oscillation

Let us begin by considering the system of equations (4.1), (4.2) and (4.3) with $f = 0$. The variables in this system will be presented in the form $f(t) e^{i(\sigma_1 x + \sigma_2 y)}$, therefore only the time dependent part of the solution is unknown and the equations (4.1) - (4.3) can be stated as

$$\frac{\partial M_x}{\partial t} + RM_x + igH\sigma_1 \zeta = \tau_x \quad (8.112)$$

$$\frac{\partial M_y}{\partial t} + RM_y + igH\sigma_2 \zeta = \tau_y \quad (8.113)$$

$$\frac{\partial \zeta}{\partial t} + i\sigma_1 M_x + i\sigma_2 M_y = 0 \quad (8.114)$$

or in the vector-matrix form

$$\frac{\partial \vec{S}}{\partial t} + B\vec{S} = \vec{\tau} \quad (8.115)$$

where σ_1 and σ_2 denote the wave numbers along the x- and y-axes respectively.

The formal solution to (8.115) is

$$\vec{S} = \vec{S}_0 e^{-At} + \vec{\tau} \int_0^t e^{pA} dp \quad (8.116)$$

where \vec{S}_0 is the initial value. Depending on the properties of the eigenvalues of the matrix A, different solutions are possible. We are interested in a solution for an external force constant in time, then (8.116) becomes

$$\vec{S} = \vec{S}_0 e^{-At} + \vec{\tau} \int_0^t e^{pA} dp \quad (8.117)$$

and

$$\vec{S} = \vec{S}_0 e^{-At} + \vec{\tau}/A \cdot (1 - e^{-At}) \quad (8.118)$$

The solution to (8.118) attains a steady state if each of the eigenvalues possesses a negative real part.

The eigenvalues of A are equal to

$$\lambda_1 = -R; \quad \lambda_{2,3} = -\frac{1}{2}(R \pm \sqrt{R^2 - 4H^2gH}) \quad (8.119)$$

Here $H^2 = \sigma_1^2 + \sigma_2^2$.

If at the initial moment $t=0$ the force $\vec{\tau}$, which is constant in time, begins to act, then the dynamic system will need a certain period of time to reach a new equilibrium. Three forms of solution are possible there:

1. The sea-level variations take place from $\zeta = 0$ to the steady state level ζ_{st} , without any periodic oscillations (Fig. 97).
2. The change of sea-level from $\zeta = 0$ to $\zeta = \zeta_{st}$ occurs with oscillations which diminish in time.
3. The sea-level does not attain a steady state and it changes periodically around the mean value.

The first case is realised if the friction in a dynamic system is large ($R \rightarrow \infty$). The second case appears when R is rather small. When $R \rightarrow 0$, then, in agreement with (8.119), the motion is dependent on the matrix whose eigenvalues are

$$\lambda = \pm iH\sqrt{gH} \quad (8.120)$$

Let us study thoroughly the solution of system (8.112) - (8.114) for the case $R = 0$ by rearranging the system to one equation in terms of the sea-level

$$\frac{\partial^2 \zeta}{\partial t^2} + gHH^2 \zeta = F(t) \quad (8.121)$$

Assuming as before that the expression $F(t)$ which is related to an external force is constant in time and that the initial value of the sea-level is $\zeta(t=0) = 0$, the solution of (8.121) is

$$\zeta(t) = F(t) (1 - \cos H_1 t) / H_1^2 \quad (8.122)$$

which corresponds to case 3 in fig. 97.

It is obvious that the frequencies of oscillation are equal to $H_1 = H\sqrt{gH}$. Therefore H_1 represents the set of frequencies and (8.122) the solutions related to them. Among all possible external forces the

system responds to the one of greatest amplitude $F(t)/H^2$.

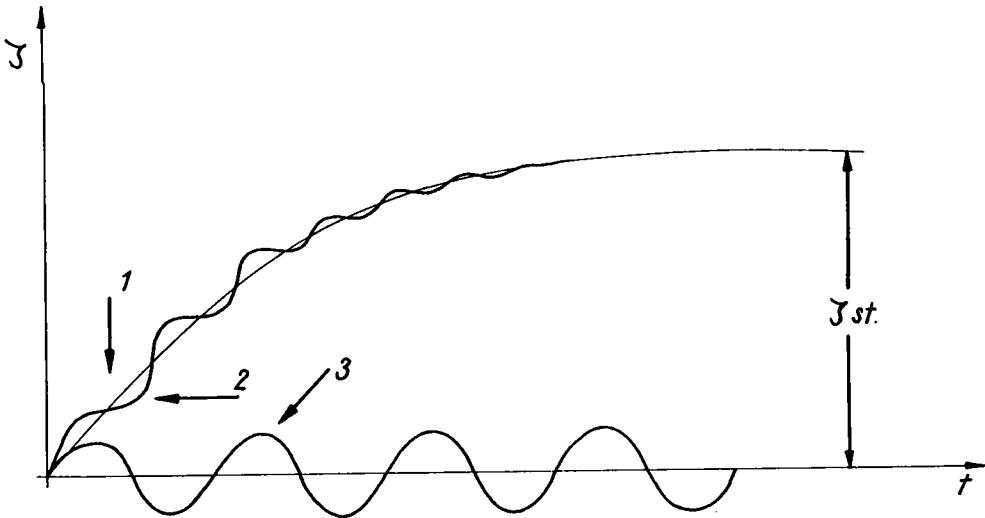


Fig. 97. THREE CHARACTERISTIC CASES OF RESPONSE OF A MECHANICAL SYSTEM UNDER THE ACTION OF A TIME-INDEPENDENT FORCE

Because the parameter $H_1^2 = H^2 gH = gH(2\pi/L)$ is smallest for the longest wave ($L \rightarrow \infty$), it follows that the greatest amplitude is due to the longest wave: that is, the one with the longest period. Finally, we may state that the system, in which friction forces are negligible, oscillates with the longest characteristic period of the dynamic system or with the longest eigenperiod under the influence of a constant external force.

§7. A method of computing a set of eigenperiods

The approach presented above will now be generalized to the set of eigenperiods so as to describe an oscillatory system in a complete way. We shall begin by reconsidering the solution (8.115) expressing it through a set of eigenvalues and eigenfrequencies. Starting with the solution to the homogeneous system (Hurewicz, 1966)

$$\vec{s} = \vec{s}_0 e^{-At} \quad (8.123)$$

we set it in the form

$$S = U e^{t\Lambda} \quad (8.124)$$

where

$$\Lambda = \begin{bmatrix} \lambda_1 & & & & \\ & \lambda_2 & & & \\ & & \cdot & & \\ & & & \cdot & \\ & 0 & & & \\ & & & & \lambda_n \end{bmatrix} \quad (8.125)$$

is the matrix composed of the set of eigenvalues λ_i . Inserting (8.124) into the homogeneous part of (8.115) yields

$$\vec{U}\Lambda + \Lambda\vec{U} = 0 \quad (8.126)$$

From this equation, through multiplication on the right hand side by \vec{U}^T , the matrix Λ is obtained as a function of the eigenvectors \vec{U} , \vec{U}^T and the matrix Λ

$$\Lambda = -\vec{U}\Lambda\vec{U}^T \quad (8.127)$$

In the above the identity $(\vec{U}, \vec{U}^T) = I$ is implied. Finally, inserting (8.127) into (8.123), we derive the required solution

$$S = e^{\vec{U}\Lambda\vec{U}^T} \cdot \vec{S}_0 = \vec{U} e^{\Lambda t} \vec{U}^T \vec{S}_0 \quad (8.128)$$

In order to make this process very clear we shall obtain the same solution by a somewhat different approach. Suppose the matrix Λ in (8.123) possesses n different eigenvalues λ_i , $i = 1, 2, \dots, n$. Expressing the solution (8.123) as a linear combination of n partial solutions

$$\vec{S} = \sum_i \vec{u}_i e^{\lambda_i t} \quad (8.129)$$

where \vec{u}_i is an eigenvector related to λ_i , and then substituting (8.129) into the homogeneous part of (8.115) we have

$$\sum_i (\vec{u}_i \lambda_i + \Lambda \vec{u}_i) = 0 \quad (8.130)$$

To find the matrix A we again multiply (8.130) by \vec{u}_i^T

$$A = - \sum_i \vec{u}_i \lambda_i \vec{u}_i^T \quad (8.131)$$

Finally, substituting (8.131) into (8.123) a solution which is analogous to (8.128) is derived

$$\vec{S} = (\vec{u}_1 e^{\lambda_1 t} \vec{u}_1^T + \dots + \vec{u}_n e^{\lambda_n t} \vec{u}_n^T) \vec{S}_0 = \vec{U} e^{\Lambda t} \vec{U}^T \vec{S}_0 \quad (8.132)$$

where

$$e^{\Lambda t} = \begin{bmatrix} e^{\lambda_1 t} & & & & \\ & e^{\lambda_2 t} & & & \\ & & \cdot & & \\ & & & \cdot & \\ & & & & e^{\lambda_n t} \end{bmatrix} \quad (8.133)$$

The solution of the homogeneous problem expressed either as (8.128) or (8.132) vanishes in time, when all the eigenvalues λ_i possess negative real parts. If the nonhomogeneous part of (8.115) is included, then the overall solution is

$$\vec{S} = \int_0^t e^{(t-p)A} \vec{r}(p) dp \quad (8.134)$$

Let us assume that the external force in (8.134) is periodic in time and consists of a random superposition of the frequencies σ_k

$$\vec{r}(x,y,t) = \sum_k e^{i\sigma_k t} \cdot \vec{r}_0(x,y) \quad (8.135)$$

In this case the explicit solution of (8.134) yields

$$\vec{S} = \sum_k \int_0^t e^{A(t-p)} i\sigma_k p \vec{r}_0(x,y) dp = \sum_k \vec{r}_0(x,y) (e^{i\sigma_k t} - e^{At}) / (i\sigma_k - A) \quad (8.136)$$

Analysing (8.136) we obtain the general result that resonance will occur when any eigenvalue of A coincides with an arbitrary forcing frequency σ_k . This can be confirmed by the inversion of the matrix $(i\sigma_k - A)$ in terms of the eigenvalues and eigenfunctions of the homogeneous problem. Firstly, by multiplying the denominator of (8.136) by the left and right

eigenvector, we find

$$\vec{U}^T (I\sigma_k - A) \vec{U} = I\sigma_k + \Lambda \quad (8.137)$$

Then inverting both sides of (8.137) yields

$$\vec{U}^T (I\sigma_k - A)^{-1} \vec{U} = (I\sigma_k + \Lambda)^{-1}$$

and finally multiplying by \vec{U} on the left and by \vec{U}^T on the right hand side, the inversion is completed to discover that

$$(I\sigma_k - A)^{-1} = \vec{U} (I\sigma_k + \Lambda)^{-1} \vec{U}^T \quad (8.138)$$

where the matrix $(I\sigma_k + \Lambda)^{-1}$ possesses the diagonal form

$$(I\sigma_k + \Lambda)^{-1} = \begin{bmatrix} (\sigma_k + \lambda_1)^{-1} & & & & \\ & (\sigma_k + \lambda_2)^{-1} & & & \\ & & \cdot & & \\ & & & \cdot & \\ & & & & (\sigma_k + \lambda_k)^{-1} \end{bmatrix} \quad (8.139)$$

Therefore the right hand side of (8.138) leads to (Lancaster, 1966)

$$\sum_{i=1}^n f_i / (\sigma_k + \lambda_i) \quad (8.140)$$

where $f_i = (\vec{u}_i, \vec{u}_i^T)$.

The solution of the nonhomogeneous problem (8.136) takes the following final form

$$S = \sum_k (e^{I\sigma_k t} - e^{At}) \sum_{i=1}^n \vec{T}_0(x, y) f_i / (\sigma_k + \lambda_i) \quad (8.141)$$

Due to the random value of σ_k the coincidence of σ_k with λ_i will cause resonance. If the friction is present, it will cause only an increase in the amplitude. A random force acting on a physical system will eventually lead to a random steady state in which the vector \vec{S} has strongly resonant characteristics in the neighbourhood of the eigenperiods. Treating the obtained solution as a stationary time series, the spectral method can be applied to define the set of eigenperiods (Bendat and Piersol, 1971).

Generally speaking, sea-level and velocity should be treated separately. Certain modes of oscillation are more pronounced in the variations in sea-level due to the greater magnitude of potential energy. Other methods can be better ascertained in velocity spectra due to the greater magnitude of kinetic energy.

Seiche-like motion is usually characterized by high potential energy and a rotational mode of oscillation, which is present in (8.5) through the Jacobian operator, is described by increased kinetic energy when compared to the gravitational mode, see e.g. Platzman (1972).

§8. The influence of friction and small variations of frequency

Until now, we have not mentioned the influence of friction in altering the eigenfrequencies of the oscillating system. The problem, when formulated in all its complexity, leads to the so-called lambda matrices (Lancaster, 1966). We shall present the influence of friction by a simplified version of the perturbation method (see e.g. Lanczos, 1956). Taking as a starting point the set of equations (8.1) - (8.3) in the vector-matrix form

$$\frac{\partial \vec{S}}{\partial t} = A \vec{S} \quad (8.142)$$

where

$$S = \begin{bmatrix} M_x \\ M_y \\ \zeta \end{bmatrix}; \quad A = \begin{bmatrix} 0 & f & -gH \frac{\partial}{\partial x} \\ -f & 0 & -gH \frac{\partial}{\partial y} \\ \frac{\partial}{\partial x} & \frac{\partial}{\partial y} & 0 \end{bmatrix} \quad (8.143)$$

Assuming that the dependent variables in (8.142) are changing in time according to $\vec{S} = \vec{S}_0 e^{i\Omega t}$, it yields

$$\vec{S}_0 i\Omega = A \vec{S}_0 \quad (8.144)$$

From (8.144) the matrix of eigenfrequencies is easily obtained

$$\Omega = i(\vec{S}_0^{*T}, A\vec{S}_0) / (\vec{S}_0^{*T}, \vec{S}_0) \quad (8.145)$$

It may be assumed that due to small variations in the parameters in (8.142), Ω is also subject to small variations. A general approach to

this problem, the so-called perturbation method, may be found in Lancaster (1966). To explain the idea behind this method we shall consider a simplified problem and shall assume that the variations are due entirely to the bottom friction. This force can easily be inserted into (8.142) by the mere addition of

$$\delta A \vec{S} = \begin{bmatrix} R & 0 & 0 \\ 0 & R & 0 \\ 0 & 0 & 0 \end{bmatrix} \begin{bmatrix} M_x \\ M_y \\ \zeta \end{bmatrix} \tag{8.146}$$

The expression for the eigenfrequency (8.145) changes to

$$\Omega + \delta\Omega = [-i(\vec{S}_0^{*T}, A\vec{S}_0) + i(\vec{S}_0^{*T}, A\vec{S}_0)] / (\vec{S}_0^{*T}, \vec{S}) \tag{8.147}$$

Since the variables considered are of a complex character, \vec{S}_0^{*T} in (8.147) is transposed and the conjugate value taken to give \vec{S}_0^* , i.e.

$$\vec{S}_0^{*T} = (M_x^*, M_y^*, \zeta^*) \tag{8.148}$$

From (8.146), by virtue of the scalar product definition (5.155), we derive the expression for the perturbed frequency

$$\delta\Omega = i [\iint R(M_x^2 + M_y^2) dx dy] / [\iint (M_x^2 + M_y^2) dx dy] \tag{8.149}$$

This result may be clarified if one considers (8.149) as a product

$$\delta\Omega_n = \frac{i(M_x^*, M_y^*, \zeta^*) \begin{bmatrix} +R & 0 & 0 & M_x \\ 0 & +R & 0 & M_y \\ 0 & 0 & 0 & \zeta \end{bmatrix}}{\begin{bmatrix} M_x \\ M_y \\ \zeta \end{bmatrix}} \tag{8.150}$$

related to all N grid points of the two-dimensional net (j,k). Accumulating (8.150) over all grid points, yields

$$\delta\Omega = \sum_{n=1}^N \delta\Omega_n = i \sum_{n=1}^N R_n (M_{x,n}^2 + M_{y,n}^2) / \sum_{n=1}^N (M_{x,n}^2 + M_{y,n}^2) \tag{8.151}$$

Since $\delta\Omega$ is a real value, it follows from (8.151) that the small changes of frequency are not related to the bottom friction. On the other hand, observations have shown that seiche periods change in the presence of friction.

Clearly something is wrong in this approach. The assumption that the bottom friction has a constant and real value cannot be taken as a proven fact. Taking the friction coefficient in (8.151) as a real value excludes the possibility that the bottom velocity and stress are out of phase. Observations confirm this phenomenon. To express this fact, one may put (Thijsse, 1965)

$$R = R_1 + iR_2 \quad (8.152)$$

Inserting (8.152) into (8.151), yields

$$\delta\Omega = - \frac{\sum_{n=1}^N R_{2,n} (M_{x,n}^2 + M_{y,n}^2)}{\sum_{n=1}^N (M_{x,n}^2 + M_{y,n}^2)} \quad (8.153)$$

This expression (8.153) indicates that bottom friction reduces the frequency or increases the period of free oscillation. Hence we have successfully resolved the paradox created by an incorrect assumption.

§9. Numerical schemes describing frictionless motion

We shall now consider certain numerical schemes for describing the general motion in a medium where friction is usually of no importance, since oscillatory motion in such a medium has already been considered in this chapter.

The numerical schemes presented will be strictly related to those derived in chapter IV. We shall start with a numerical analogue of the differential equations (8.1), (8.2) and (8.3) which uses the explicit scheme (4.128), (4.129) and (4.130). Putting the horizontal and vertical friction terms equal to zero, we derive a scheme which has a second-order approximation in space but the approximation in time is distorted due to the Coriolis term. It is possible to build a fully symmetrical scheme in space and time by averaging the Coriolis term in time as $\frac{f}{2}(M^{l+1} + M^{l-1})$. This term is now centred in time around the moment l , and a second-order approximation is achieved. But if the practical realization of such an approach is dealt with, it may be quite difficult to follow. The Coriolis force in the staggered net is taken as a mean value of the four neighbouring points and therefore when this term is taken in the implicit form it will demand an inversion of the

two-dimensional operator. The operator, for example along the x-axis, possesses the form, according to (4.132)

$$\square M_Y^1 = 0.25 (M_{Y,j+2,k+1}^{1-1} + M_{Y,j+2,k-1}^{1-1} + M_{Y,j,k+1}^{1-1} + M_{Y,j,k-1}^{1-1}) \quad (8.154)$$

Platzman (1972) in his numerical development used an even more complicated box operator

$$\square M_Y = 0.5 \sum_{k=1}^4 (q_o + q_k) M_{Y,k} / 4q_o \quad (8.155)$$

Here, the index o refers to the central grid point and $k = 1, 2, 3, 4$ to the neighbouring points; $q = f/H$. It is of interest to understand what the box operator does to the frictionless numerical scheme. When the stability of the explicit scheme was analysed, in the matrix (4.142) the Coriolis term was expressed as

$$b = 2Tf \cos\sigma_1 h \cos\sigma_2 h \quad (8.156)$$

Therefore along the x and y directions the box operator results in a cosine filter and its rôle is explained in fig. 89. The length of the wave in the numerical system changes in the range $4h \leq L \leq \infty$. Therefore the amplitude of the shortest waves ($L = 4h$) is strongly suppressed and the long waves pass through the filter practically without any distortion. The conclusion is simple enough, and though there is no 'physical' friction in the dynamic system, the box operator produces a similar effect due to the attenuation of the short wave oscillations.

Now using the splitting method presented in chapter IV, §12, we shall build a numerical scheme on the grid in fig. 34.

$$\frac{M_x^{1+1/2} - M_x^1}{T} - \frac{f}{2} \square M_Y^1 = -\frac{1}{2} gH \frac{\partial \zeta^1}{\partial x} \quad (8.157a)$$

$$\frac{M_Y^{1+1/2} - M_Y^1}{T} + \frac{f}{2} \square M_X^{1+1/2} = -\frac{1}{2} gH \frac{\partial \zeta^1}{\partial y} \quad (8.157b)$$

$$\frac{M_Y^{1+1} - M_Y^{1+1/2}}{T} + \frac{f}{2} \square M_X^{1+1/2} = -\frac{1}{2} gH \frac{\partial \zeta^{1+1}}{\partial y} \quad (8.157c)$$

$$\frac{M_x^{1+1} - M_x^{1+1/2}}{T} - \frac{f}{2} \square M_Y^{1+1} = -\frac{1}{2} gH \frac{\partial \zeta^{1+1}}{\partial x} \quad (8.157d)$$

$$\frac{\zeta^{1+1} - \zeta^1}{\Delta t} = -\frac{1}{2} \frac{\partial M_x^{1+1}}{\partial x} + \frac{\partial M_x^1}{\partial x} - \frac{1}{2} \frac{\partial M_y^{1+1}}{\partial y} + \frac{\partial M_y^1}{\partial y} \quad (8.157e)$$

Let us check the numerical stability of system (8.157). To do this we insert (8.157a) into (8.157d) and (8.157b) into (8.157c) and thus we arrive at the system

$$\frac{M_x^{1+1} - M_x^1}{\Delta t} - \frac{f}{2} \Delta x (M_y^{1+1} + M_y^1) = -\frac{1}{2} gH \frac{\partial}{\partial x} (\zeta^{1+1} + \zeta^1) \quad (8.158a)$$

$$\frac{M_y^{1+1} - M_y^1}{\Delta t} + \frac{f}{2} \Delta x (M_x^{1+1} + M_x^1) = -\frac{1}{2} gH \frac{\partial}{\partial y} (\zeta^{1+1} + \zeta^1) \quad (8.158b)$$

$$\frac{\zeta^{1+1} - \zeta^1}{\Delta t} = -\frac{1}{2} \frac{\partial}{\partial x} (M_x^{1+1} + M_x^1) - \frac{1}{2} \frac{\partial}{\partial y} (M_y^{1+1} + M_y^1) \quad (8.157e) = (8.158c)$$

In the above equations the space derivatives will be approximated with central differences.

Now assuming that each dependent variable changes in the manner described by (4.17) we derive a characteristic equation for the stability parameter

$$(\lambda - 1)M_x^* - (\lambda + 1)\frac{f}{2}\Delta x \cos \sigma_1 h \cos \sigma_2 h M_y^* + \frac{gH\Delta t}{2h}(\lambda + 1) i \sin \sigma_1 h \zeta^* = 0 \quad (8.159a)$$

$$(\lambda - 1)M_y^* + (\lambda + 1)\frac{f}{2}\Delta x \cos \sigma_1 h \cos \sigma_2 h M_x^* + \frac{gH\Delta t}{2h}(\lambda + 1) i \sin \sigma_2 h \zeta^* = 0 \quad (8.159b)$$

$$(\lambda - 1)\zeta^* + (\lambda + 1)\frac{i\Delta t}{2h}(\sin \sigma_1 h M_x^* + \sin \sigma_2 h M_y^*) = 0 \quad (8.159c)$$

A nontrivial solution to this homogeneous set of equations exists on condition that the determinant vanishes, and this leads to the equation

$$(\lambda - 1)^2 + (\lambda + 1)^2 (\phi + s)^2 = 0 \quad (8.160)$$

where

$$\phi = gH\Delta t^2 (\sin^2 \sigma_1 h + \sin^2 \sigma_2 h) / 2h^2$$

$$s = \frac{f\Delta t}{2} \cos \sigma_1 h \cos \sigma_2 h$$

The solution of (8.160) is $|\lambda| = 1$. Therefore the numerical system of (8.157) is unconditionally stable. The system of equations (8.158) follows the so-called Crank-Nicholson approach. With such a system

numerical calculations are extremely difficult to perform, since the system is implicit along both, the x- and the y-axis. Now let us observe a possible way around this obstacle. Firstly, the two equations in the system (8.157) are explicit and thus their calculation is straightforward. Coming to the third equation it is found that the value of $\partial \zeta^{l+1} / \partial y$ is unknown, so it must be expressed somehow through the variables on the l and l-1 time steps. The same is true for (8.157d). In these equations we set the new form of

$$\frac{\partial \zeta^{l+1}}{\partial y} \text{ and } \frac{\partial \zeta^{l+1}}{\partial x}$$

using the equation of continuity in two equivalent ways. To obtain the first derivative we put

$$\frac{\zeta^{l+1} - \zeta^l}{T} = - \frac{\partial M_x^{l+1/2}}{\partial x} - \frac{1}{2} \frac{\partial}{\partial y} (M_y^l + M_y^{l+1}) \quad (8.161a)$$

and to obtain the second derivative we put

$$\frac{\zeta^{l+1} - \zeta^l}{T} = - \frac{1}{2} \frac{\partial}{\partial x} (M_x^l + M_x^{l+1}) - \frac{\partial M_y^{l+1/2}}{\partial y} \quad (8.161b)$$

Now inserting ζ^{l+1} from (8.161a) into (8.157c) yields

$$\frac{M_y^{l+1} - M_y^{l+1/2}}{T} + \frac{f}{2} \square M_x^{l+1/2} = -gH \frac{1}{2} \left(\frac{\partial \zeta}{\partial y} \right)^l - T \frac{\partial^2 M_x^{l+1/2}}{\partial y \partial x} - \frac{T}{2} \frac{\partial^2 M_y^{l+1}}{\partial y^2} - \frac{T}{2} \frac{\partial^2 M_y^l}{\partial y^2} \quad (8.162)$$

Rearranging (8.162) in the form

$$\begin{aligned} M_y^{l+1} - \frac{1}{4gHT^2} \frac{\partial^2 M_y^{l+1}}{\partial y^2} &= M_y^{l+1/2} - \frac{f}{2T} \square M_x^{l+1/2} - \frac{1}{2gHT} \frac{\partial \zeta^l}{\partial y} + \frac{1}{2gHT^2} \left(\frac{\partial^2 M_x^{l+1/2}}{\partial x \partial y} \right. \\ &\quad \left. + \frac{1}{2} \frac{\partial^2 M_y^l}{\partial y^2} \right) \end{aligned} \quad (8.163)$$

the solution of (8.163) may be derived by factorization along the y-axis.

With the help of (8.161b) equation (8.157d) can be brought to a similar form

$$\begin{aligned}
 M_x^{l+1} - \frac{1}{4}gHT^2 \frac{\partial^2 M_x^{l+1}}{\partial x^2} &= M_x^{l+1/2} + \frac{f}{2T} \square M_y^{l+1/2} - \frac{gHT}{2} \frac{\partial \zeta^l}{\partial x} \\
 &+ \frac{1}{2}gHT^2 \left(\frac{\partial^2 M_y^{l+1/2}}{\partial x \partial y} + \frac{\partial^2 M_x^l}{2 \partial x^2} \right) \quad (8.164)
 \end{aligned}$$

The solution of (8.164) can also be derived by the factorization method, but this time along the x-axis. In this way the construction of the numerical scheme is achieved. The overall solution proceeds through equations (8.157a), (8.157b), (8.163), (8.164) and (8.157e). The application of the factorization method saves us from the inversion of the two-dimensional operators, which usually takes a great deal of computer time. The speed of computation in the presented scheme is comparable to that of an explicit method.

As we have shown the stability of the system (8.157) is unconditional, i.e. the scheme is stable for an arbitrary choice of time-space steps. In that sense, the method is more flexible than one in which the choice of time-space steps is restricted by a stability condition. Such conditions impose usually a very short time step. When dealing with gravity waves one can describe them within a reasonable amount of computer time. If, on the other hand, the aim is to study long-period phenomena, a very short time step may cause an unnecessary lengthening of computation time.

Let us now construct a numerical scheme related to fig. 33, where M_x and M_y are computed at the same grid point. In this case there is no need to introduce the box operator, therefore

$$\frac{M_x^{l+1} - M_x^{l-1}}{T} - \frac{f}{2}(M_y^{l+1} + M_y^{l-1}) = -gH \frac{\partial \zeta^l}{\partial x} \quad (8.165a)$$

$$\frac{M_y^{l+1} - M_y^{l-1}}{T} + \frac{f}{2}(M_x^{l+1} + M_x^{l-1}) = -gH \frac{\partial \zeta^l}{\partial y} \quad (8.165b)$$

$$\frac{\zeta^{l+2} - \zeta^l}{T} = - \frac{\partial M_x^{l+1}}{\partial x} - \frac{\partial M_y^{l+1}}{\partial y} \quad (8.165c)$$

The numerical scheme above possesses second-order accuracy in time as well as in space. The only obstacle when it comes to practical computation is the implicit form of the Coriolis term. To solve this problem one can write (8.165a) as

$$M_x^{l+1} - fTM_y^{l+1} = F_1 \quad (8.166a)$$

and (8.165b) as

$$M_y^{l+1} + fTM_x^{l+1} = F_2 \quad (8.166b)$$

where F_1 and F_2 contain only the dependent variables calculated at the l and $l-1$ time steps.

Substituting M_y^{l+1} from (8.166b) into (8.166a) and M_x^{l+1} from (8.166a) into (8.166b) we find

$$M_x^{l+1} = (F_1 + fTF_2)/(1 + f^2T^2) \quad (8.167a)$$

$$M_y^{l+1} = (F_2 - fTF_1)/(1 + f^2T^2) \quad (8.167b)$$

The computation algorithm includes therefore the expressions (8.167a), (8.167b) and (8.165c).

The computational stability of the system (8.165) studied on the basis of (4.17) leads to the following characteristic equation

$$(\lambda-1)^2 + S^2(\lambda^2+1)^2 + \phi^2\lambda^2 = 0 \quad (8.168)$$

where $S = fT$ and $\phi^2 = gHT^2(\sin^2\sigma_1h\cos^2\sigma_2h + \sin^2\sigma_2h\cos^2\sigma_1h)/h^2$. Setting $\lambda^2 = \delta$, brings (8.168) to the form

$$\delta^2(1+S^2) + \delta\{2(S^2-1) + \phi^2\} + 1 + S^2 = 0 \quad (8.169)$$

The roots of (8.169) are

$$\delta_{1,2} = \{-[2(S^2-1)+\phi^2] \pm \sqrt{[2(S^2-1)+\phi^2]^2 - 4(1+S^2)^2}\} / 2(1+S^2) \quad (8.170)$$

which provides $|\delta_{1,2}| = 1$ if

$$4(1+S^2)^2 > [2(S^2-1)+\phi^2]^2 \quad (8.171)$$

Denoting the minimum value of $(\sin^2\sigma_1h\cos^2\sigma_2h + \sin^2\sigma_2h\cos^2\sigma_1h)$ as W , the above inequality gives the following relationship between the time and space steps for a stable numerical calculation

$$\frac{T}{h}\sqrt{gH}W < 2 \quad (8.172)$$

In the range of the shortest waves in the system ($\sigma_1 h = \pi/2$, $\sigma_2 h = \pi/2$) $W = 0$ and therefore (8.172) is always true and the unconditional stability is achieved.

REFERENCES

- Bendat, J.S. and Piersol, A.G., 1971. Random Data: Analysis and Measurement Procedures. Wiley Interscience, New York.
- Collatz, L., 1964. Funktionalanalysis und numerische Mathematik. Springer-Verlag, Berlin.
- Connor, J.J. and Brebia, C.A., 1976. Finite Element Techniques for Fluid Flow. Newnes-Butterworths, London, Boston.
- Defant, A., 1961. Physical Oceanography, v.II. Pergamon Press, Oxford.
- Faddeeva, V.N., 1959. Computational Methods of Linear Algebra. Dover Publications Inc., New York.
- Hurewicz, W., 1966. Lectures on Ordinary Differential Equations. MIT-Press, Cambridge.
- Kaliski, S., 1966. Vibrations and Waves (in Polish). PWN, Warszawa.
- Kantorovich, L.V. and Krylov, V.I., 1958. Approximate Methods of Higher Analysis. Wiley Interscience, New York.
- Lamb, H., 1932. Hydrodynamics. Cambridge University Press.
- Lancaster, P., 1966. Lambda-Matrices and Vibrating Systems. Pergamon Press (Int. Ser. of Monor. in Pure and App. Math. v. 94).
- Lanczos, C., 1956. Applied Analysis. Prentice-Hall, Englewood Cliffs, New York.
- Loomis, H.G., 1973. A New Method for Determining Normal Modes of Irregular Bodies of Water with Variable Depth. Hawaii Institute of Geophysics, University of Hawaii.
- Mc Lachlan, N.W., 1948. Bessel Functions for Engineers. Oxford Univ. Press, London, New York.
- Platzman, G.W., 1972. Two-Dimensional Free Oscillations in Natural Basins. Journal of Physical Oceanography N. 2.
- Ralston, A., 1965. A First Course in Numerical Analysis. McGraw-Hill, New York.
- Rao, D.B. and Shwab, D.J., 1976. Two-Dimensional Normal Modes in Arbitrary Enclosed Basins on a Rotating Earth: Application to Lakes Ontario and Superior. Phil. Trans. Roy. Soc. A, London: 63-96.
- Thijsse, J.Th., 1965. Theory of Tides. Inter. Course in Hydraulic Engineering. Delft, Netherlands.
- Wilkinson, J.H., 1965. The Algebraic Eigenvalue Problem. Clarendon Press, Oxford.

LIST OF FIGURES

	page
Chapter I	
1 Co-ordinate system	3
2 Comparison of the observed current profile in the tidal wave with the logarithmic and potential law	14
3 Flow geometry in the channel	15
4 Coefficient of aerodynamic resistance against wind velocity	20
Chapter II	
no figures	
Chapter III	
5 Sea-level variations under the action of wind in one-dimensional geometry	48
6 Slope of the sea surface under the action of wind	49
7 Integration contour in the multiply-connected domain	54
8 Streamlines of the vertically integrated horizontal mass transport of the wind-driven circulation in a rectangular basin with constant depth	60
9 Surface current corresponding to fig. 8	61
10 Current velocity as a function of depth at one point in figs. 8 and 9	62
11 Streamlines of the vertically integrated horizontal mass transport of the wind-driven circulation in a rectangular basin with nonuniform depth	63
12 Surface current corresponding to fig. 11	64
13 Current velocity as a function of depth at one point in figs. 11 and 12	65
14 Streamlines of the vertically integrated horizontal mass transport of the wind-driven circulation in the rectangular sea with an island	66
15 Surface current corresponding to fig. 14	67
16 Current velocity as a function of depth at one point in figs. 14 and 15	69
17 Streamlines of the vertically integrated horizontal mass transport in the central and southern Baltic with a constant wind blowing towards the east	70
18 Surface current corresponding to fig. 17	71
19 Current against depth at three points in figs. 17 and 18	72
20 Streamlines of the vertically integrated horizontal mass transport in the central and southern Baltic with a constant wind blowing towards the south	74
21 Surface current corresponding to fig. 20	75
22 Current against depth at two points in figs. 20 and 21	76

	page
23 Absolute values of current velocities against depth at two points in figs. 20 and 21	77
24 A simplified summer density distribution at one point in the Baltic Sea	81
25 Current distribution at the same point as in fig.24	82
26 Calculated sea-levels in the Baltic Sea	86
27 Observed sea-levels in the Baltic Sea	87
28 Wind- and density-driven currents at the sea surface	88
29 Distribution of velocity, square root of energy and eddy viscosity against depth	102
30 Distribution of eddy viscosity in the two- and one-layer model	106
31 Distribution of velocity, square root of energy, eddy viscosity and dissipation against depth	108
 Chapter IV	
32 A symmetrical computational grid	115
33 Staggered grid	115
34a The order of computations in time on the staggered grid	116
34b The computational grid from fig. 34a placed in the x,y-plane	117
35 Characteristics of the implicit scheme	129
36 The method to construct the angular derivatives	136
37 Amplitude response due to the application of a time filter to a periodic function	139
38 Phase shift due to the application of a time filter to a periodic function	139
39 Amplification factors for the different filter parameters	141
40 Streamfunction computed by the explicit method	162
 Chapter V	
41 Stereographic projection	174
42 Co-tidal lines of the M_2 -tide in the Arctic Ocean	186
43 Co-range lines of the M_2 -tide in the Arctic Ocean	187
44 Principal axes of the M_2 tidal ellipses in the Arctic Ocean	190
45 Maximum absolute values of velocity divergence in the Arctic Ocean	192
46 Divergence of horizontal energy flux in the Arctic Ocean	193

Chapter VI	page
47 Grid distribution for a one-dimensional problem	211
48 Cross-section of the river flow	215
49 Cross-sectional area of the River Elbe	217
50 Velocity distribution of tidal currents computed for every strip of a cross-section of the River Eider	219
51 Water level in the River Eider	220
52 Model of the River Elbe between Cuxhaven and Seemannshöft	224
53 A sketch to illustrate processes on tidal flats	225
54 Water level distribution in a channel with sloping bottom	229
55 Location of points A, B and C in the Neuwerker Watt	230
56 Observed and computed sea-level in the centre of the Neuwerker Watt	231
57 Friction coefficient r calculated by means of recorded water level and velocity derived from the equation of continuity	233
58 The dependence of different friction terms on depth (I)	237
59 The dependence of different friction terms on depth (II)	238
60 The dependence of different friction terms on depth as in fig. 59, illustration in a smaller scale	239
61 Computed sea-level variation at different points	240
62 Comparison between measured and computed water levels at two selected points in the German Bight for two different laws of bottom friction	242
63 Residual currents in the Elbe estuary	244
64 Residual currents in the River Elbe	245
65 Irregular one-dimensional grid	246
66 Interrelation between areas of different grid sizes	248
67 Grid of the classical North Sea model	251
68 Fine resolution of the North Sea model in coastal areas	252
69 Mass transport averaged over one tidal period (M_2) in the German Bight	253
70 Section of the basic model (German Bight)	255
71 Velocity distribution in the Elbe estuary (I)	256
72 Velocity distribution in the Elbe estuary (II)	257
73 Velocity distribution in the Elbe estuary (III)	258
74 Velocity distribution in the Elbe estuary (IV)	259
75 Areas A, B and C with different grid distances	263
76 Location of the breakwater and the applied grid resolution in its vicinity	265
77 Area C - distribution of velocity 9 hours after the moon's transit through the meridian of Greenwich	268

	page
78 Area C - mean mass transport over one tidal cycle	269
79 Displacement of divergence	270
80a River Elbe, Elbe estuary and the area of investigation	273
80b The investigation area, the boundary points, the deposit of sand, the Schwarztonnensand and the link-up to the west river bank of the Elbe	274
81 Distribution of velocities at the moon's transit through the meridian of Greenwich	277
82 Distribution of velocities 4 hours after the moon's transit through the meridian of Greenwich	278
83 Distribution of velocities 8 hours after the moon's transit through the meridian of Greenwich	279
84 Distribution of velocities at the moon's transit through the meridian of Greenwich	281
85 Distribution of velocities 4 hours after the moon's transit through the meridian of Greenwich	282
86 Distribution of velocities 8 hours after the moon's transit through the meridian of Greenwich	283

Chapter VII

87 Dependence of horizontal eddy viscosity on the scale phenomenon r according to Okubo and Ozmidov	295
88 Correction $f(r/H)$ to the $4/3$ law for the small depths	295
89 A section of a grid in the multi-channel model	303
90 Initial distribution of concentration in the channel	310
91 Comparison of analytical solution with the numerical solution in grid points 31 and 61 of the channel	311
92 Comparison of computed and measured mean concentration of seston in five sections of the River Elbe	315
93 Distribution of suspended matter in the River Elbe (I)	316
94 Distribution of suspended matter in the River Elbe (II)	317
95 Time dependent process of spreading matter in the River Elbe as computed by the model	319

Chapter VIII

96 Location of points to construct a one-dimensional array in a two-dimensional space	331
97 Three characteristic cases of the response of a mechanical system under the action of a constant force	347

SUBJECT INDEX

Acceleration of convergence of iterational processes	165
Advection processes	287
Aerodynamic resistance	19
Alternating direction method	42
Amphidromic point	185
Amplification matrix	123
Basic functions	331
Bottom roughness	100
Boundary conditions	31, 52, 54, 144, 154, 296, 322
Boundary layer	89, 96, 201
Box operator	354
Channel motion	13, 45, 207, 214, 302
Commutative property of a scalar product	326
Consistency of difference and differential equations	118
Co-ordinate system	2
Coriolis force	
- method of approximation in a numerical scheme	149
Coriolis parameter	2
Crank-Nicholson method	133
Critical latitude	173
Current	
- ,bottom influence on	62, 69
- in the Baltic Sea	68
- ,influence of stratification on	78, 83
Density current	8, 209
Derivative	
- ,backward	24
- , central	25
- , forward	24
- in an irregular grid	246
Diagonal dominance condition	34, 38, 40
Diffusion	287, 289
Dimensional analysis	5
Dispersion processes	287
Dissipation equation	106
Drift current	50
Drying banks	226
Eddy viscosity coefficient	
- , horizontal	144

Eddy viscosity coefficient	
- , vertical	57,78,94,96,101
Eigenfrequency	324,347
Eigenfunctions	145,324
Eigenvalue	
- of a matrix	123,326
- of an operator	327
Eigenvectors	327
Ekman equations	51
Ekman solution	
- deep sea	95
- general	52
- shallow sea	92
Equation	
- of continuity	3,53
- of diffusion	287
- of motion	2
- of motion in a spherical co-ordinate system	171
Error of a solution	30,37
Explicit-implicit method	161
Explicit method	113
Explicit numerical scheme	148,161
Factorization (line inversion) method	39
Filters to modify a numerical scheme	137
Flux of momentum	91
Friction (Ekman) depth	77,91
Friction, influence on oscillations	351
Friction velocity	89
Galerkin's method	331
Gauss - Seidel method	38
Geostrophical wind	21
Geostrophic equation	7
Grid step in an elliptical problem	29
Horizontal diffusion	297
Horizontal diffusion, coefficient of	294
Hyperbolic equations	147,210
Ice motion due to tide	194
Implicit method	113
Implicit numerical scheme	121,124,129,154,161,299
Initial conditions	145
Instability of a numerical scheme at shortest waves	137,151,160

Irregular grid	246
Iteration method	37
Iteration process	
- , condition of convergence	36
Karman hypothesis	97
Kolmogoroff hypothesis	79,97
Length scale of turbulence	97,98,100,104
Line inversion method	39
Logarithmic boundary layer	104
Logarithmic distribution	13,100,103
Longest period of free oscillations	345
Love numbers	172
Mass transport, equation of	9,52,113
Mean velocity	11
Methods to study oscillatory motion	322
Monin-Obukchov length	109
Multi-channel system	302
Multiply-connected domain	54
Neighbour diffusivity	291
Nested model	249
Neutral flow	99
Nondimensional numbers	90,109
Nonlinear equations	132
Norm	
- of a matrix	37
- of an operator	117
Numerical friction	29,149
Numerical (false) solution	130,136
Optimum value of an iterative parameter	166
Order of approximation	25,118
Orthogonal functions	332,335
Oscillatory motion	324
Positive definite operator	33,152,327
Potential component of velocity	335
Probability density	289
Rayleigh's quotient	324,341
Residual currents	241
Resonance iteration	340
Reynolds number	90
River flow	210,232
Rossby number	90

Rotational component of velocity	335
Routh-Hurwitz condition	160
Scale of turbulence	79
Self-adjoint operator	34
Slope current	50, 76
Spline method	247
Split up method	43, 125, 163, 297
Stability	
- condition for the explicit numerical scheme	151, 181, 298
- of a numerical solution	119, 121
- parameter	120
Stereographic projection	174
Streamfunction	93
Stress	
- at the bottom	17, 232
- at the surface	19
- components	10
Subgrid-scale dissipation	144
Symmetrical matrix	325, 328
Tidal	
- ellipse	191
- energy	194
- energy-rate of dissipation	196
- problem	169
Tide	
- in the Arctic Ocean	185
- motion of the bottom	172
- potential	171
Transport equation	97
Transposed matrix	326
Turbidity zone	314
Turbulent	
- diffusion	289
- energy	78, 97
Universal constants	79, 98, 99
Vector norm	37
Velocity at the surface	94, 96
Vertical diffusion	293
Vertical distribution of current	
- numerical schemes	197

Viscosity (pseudo) in a numerical scheme	143
Wave	
- celerity	127
- deformation by a numerical scheme	128,183
Western intensification	62
Wind-driven circulation	68
Wind factor	93